Studien zur anodischen N-X-Bindungsbildung in intramolekularen Cyclisierungsreaktionen

Dissertation zur Erlangung des Grades

„Doktor der Naturwissenschaften“

im Promotionsfach Chemie

am Fachbereich Chemie, Pharmazie, Geographie und Geowissenschaften

der Johannes Gutenberg- Universität Mainz

vorgelegt von

ANTON KEHL

geb. in Malokanowka

Mainz, Juni 2020

Dekan:	Personenbezogene Daten
Erster Gutachter:	Personenbezogene Daten
Zweiter Gutachter:	Personenbezogene Daten
Datum der mündlichen Prüfung:	Personenbezogene Daten

Die vorliegende Arbeit wurde in der Zeit vom Dezember 2016 bis Juni 2020 im Department für Chemie der Johannes Gutenberg-Universität Mainz unter der Anleitung von Prof. Dr. Siegfried R. Waldvogel angefertigt.

Ich versichere, dass ich diese Arbeit eigenständig verfasst und keine anderen als die angegebenen Hilfsmittel (Literatur, Apparaturen, Materialien) verwendet sowie Zitate kenntlich gemacht habe.

_____

Anton Kehl

Danksagung

Personenbezogene Daten

Inhaltsverzeichnis

1 Einleitung

1.1 Stickstoff-Heterocyclen

Heterocyclische Motive sind bedeutsam und aufgrund ihrer Anwendungsvielfalt aus unserer modernen Gesellschaft nicht mehr wegzudenken. NJARDARSON *et al.* haben im Jahr 2014 eine Übersicht über Wirkstoffe, die die FDA (*Food and Drug Administration*) zugelassen hat, basierend auf zwölf typischen Krankheitskategorien erfasst. Die Kategorien umfassen unter anderem Desinfektionsmittel, sowie Mittel für onkologische, kardiovaskuläre und dermatologische Anwendungsgebiete, etc.[1,2] Hierbei wurde festgestellt, dass etwa 59% der zugelassenen Wirkstoffe Stickstoff-Heterocyclen aufweisen. In Abbildung 1 ist ein Teil der „Top 25“ Liste dargestellt (d. h. die 25 am häufigsten vertretenen „Wirkstoffgerüste“ innerhalb der zwölf gewählten Krankheitskategorien). Des Weiteren wurden im Jahr 2019 48 Wirkstoffe von der FDA zugelassen, von denen über 50% N-heterocyclische Strukturmuster auswiesen.[3]

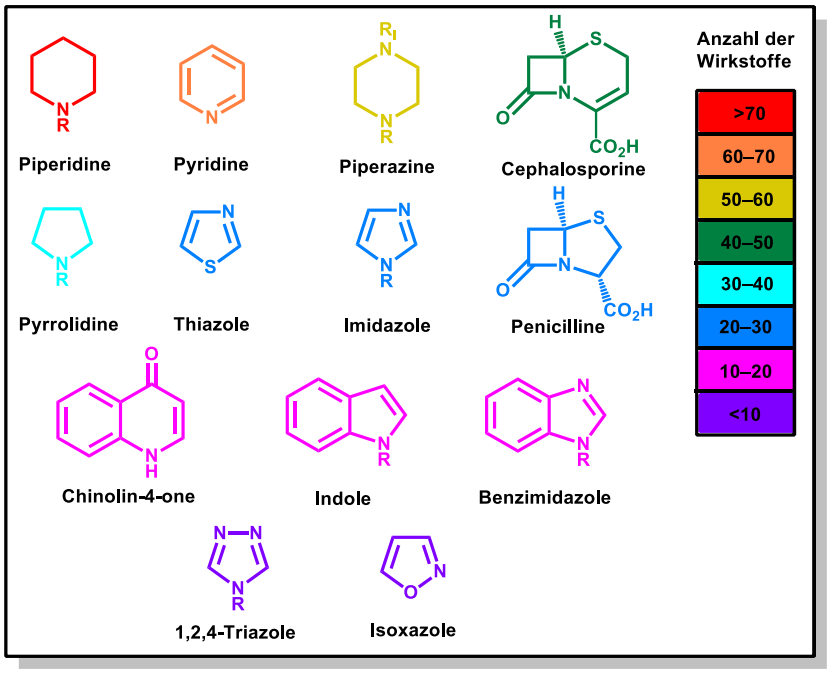

Abbildung 1: Übersicht von relevanten und der FDA zugelassenen Wirkstoffen, welche N-heterocyclische Strukturmotive beinhalten (Stand 2014). Die Farbskala gibt an, wie hoch die Anzahl der Wirkstoffe ist, die das jeweilige heterocyclische Motiv enthalten.[1]

Neben der Verbreitung im medizinischen Sektor, kommt der Einsatz von N-Heterocyclen auch in der Materialwissenschaft zum Tragen (Abbildung 2). So finden beispielsweise Polyvinylcarbazole (PVK), Polyphenyloxadiazole (PPOD) in Form eines Co-Polymers,

Polyphenylchinoxaline (PPQ) oder Schichten aus niedermolekularen Strukturen wie 1,3,4-Oxadiazolen und 1,2,4-Triazolen in organischen licht-emittierenden Dioden (OLED) Anwendung.[4,5] Weiterhin können diverse niedermolekularen Strukturen und Polymere, die Stickstoffheterocyclen enthalten, als Komponenten in organischen Feldeffekttransistoren (OFET)[6] oder in Photovoltaikzellen[7] eingesetzt werden.

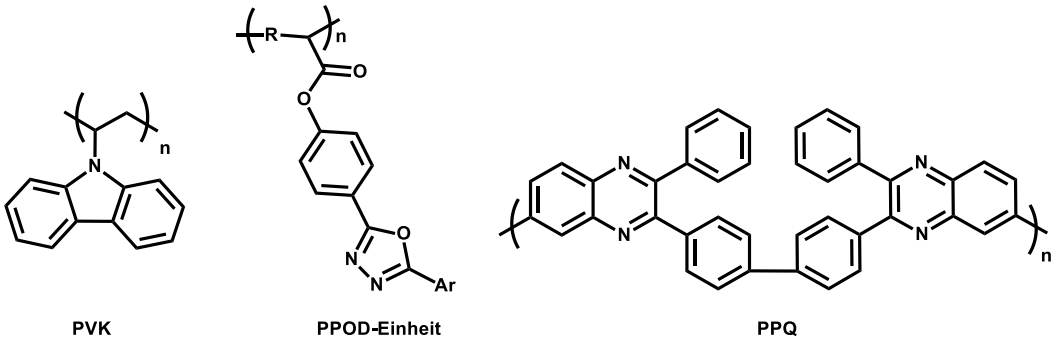

Abbildung 2: Beispiele für Polymere, die in OLED's Anwendung finden und heterocyclische Motive enthalten.

Als letztes Beispiel soll die Verwendung von N-Heterocyclen in Farben und Pigmenten dienen. Ein von VON BAEYER erstmals hergestellter klassischer Farbstoff, der Indolin-3-on- oder Isatin-basiert ist, ist Indigo.[8] Zudem werden diverse heterocyclische Motive in Azofarbstoffen verwendet, welche unter anderem zur Textilfärbung[9] (wie auch Indigo)[10] geeignet sind. (Abbildung 3). Als Beispiel sei das von J. H. ZIEGLER hergestellte Tartrazin angeführt,[11] welches zudem auch als Lebensmittelzusatzstoff fungiert.[12]

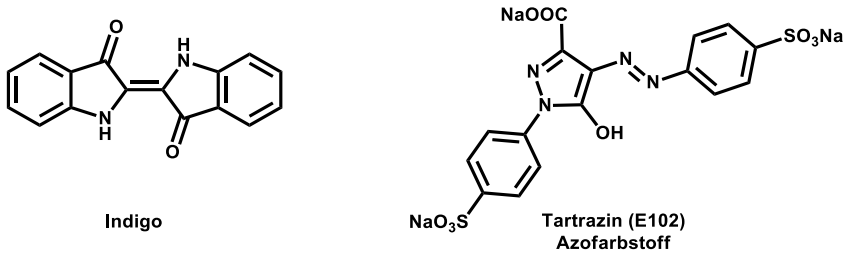

Abbildung 3: Farbstoffe mit Anwendungsmöglichkeiten, die Heterocyclen enthalten.

Aufgrund der Verbreitung von Heterocyclen im Alltag, ist ein möglichst einfacher, günstiger und auch nachhaltiger Zugang zu diesen wichtigen Verbindungsklassen dringend erforderlich. Die in diesem Kapitel vorgestellten Strukturmuster offenbaren die Relevanz von 5- und 6-gliedrigen heterocyclischen Systemen.

1.2 Oxidative Cyclisierungsreaktionen

Eine bedeutsame Synthesestrategie für Heterocyclen besteht darin, die Redoxchemie für Cyclisierungsreaktionen, in denen ein oder mehrere Heteroatome involviert sind, einzusetzen (Schema 1).[13] Ein wesentlicher Nachteil der reduktiven Varianten ist vor allem in der notwendigen Präfunktionalisierung verankert. Meist sind mehrstufige Prozesse zur Herstellung der Substrate notwendig, wodurch sich Abfälle und Kosten akkumulieren.[14] Zudem werden teilweise toxische Übergangsmetalle (z. B. Kupfer oder Nickel) für die Katalyse verwendet.[15–17]

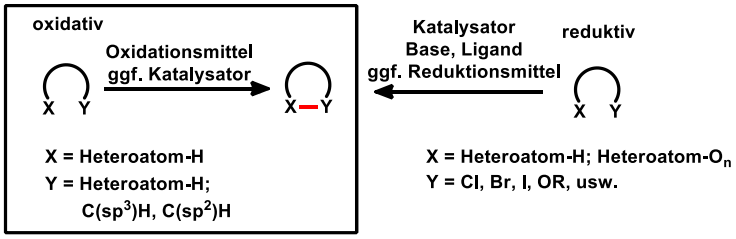

Schema 1: Allgemeine Darstellung einer Cyclisierungsreaktion unter oxidativen (links) und reduktiven (rechts) Bedingungen.

Bei intermolekularen Cyclisierungen muss zusätzlich eine C,C-Bindung aufgebaut werden, wodurch weitere Abgangsgruppen und/oder Reagenzien wie Metallorganyle erforderlich sind.[16,18] Daher ist die dehydrierende oxidative Herangehensweise eine attraktivere Alternative, da die oben erwähnten Nachteile teilweise oder ganz vermieden werden können. Allerdings vermag es diese Variante nicht den Reagenzabfall durch mindestens stöchiometrische Mengen an Oxidationsmittel und teilweise notwendigen Katalysatoren zu verhindern. Nichtsdestoweniger spart die direkte Natur der Reaktion die sonst notwendigen Funktionalisierungsschritte ein und sorgt dadurch für eine deutlich bessere Atomökonomie. Im weiteren Verlauf dieser Arbeit wird der Fokus auf die oxidativen Methoden gelenkt. Im Folgenden werden N-N-, C-O-, und C-N-Bindungsbildungen vorgestellt.

1.2.1 Oxidative N-N-,C-O- und C-N-Bindungsknüpfung

Der Aufbau von N-N-, C-O- und C-N-Bindungen gemäß klassischer oxidativer Methoden (metall-vermittelt und metallfrei) ist in Schema 2 in vereinfachter Form dargestellt.[19,20] Die wesentlichen Reagenzien zur Herstellung der entsprechenden N-N-, C-O- oder C-N-Bindungsknüpfung sind ebenfalls aufgeführt. Zur besseren Übersicht, sind die Verbindungslinien zwischen Reagenzien und Produkten farblich differenziert: N-N: schwarz; C-O: blau; C-N: orange.

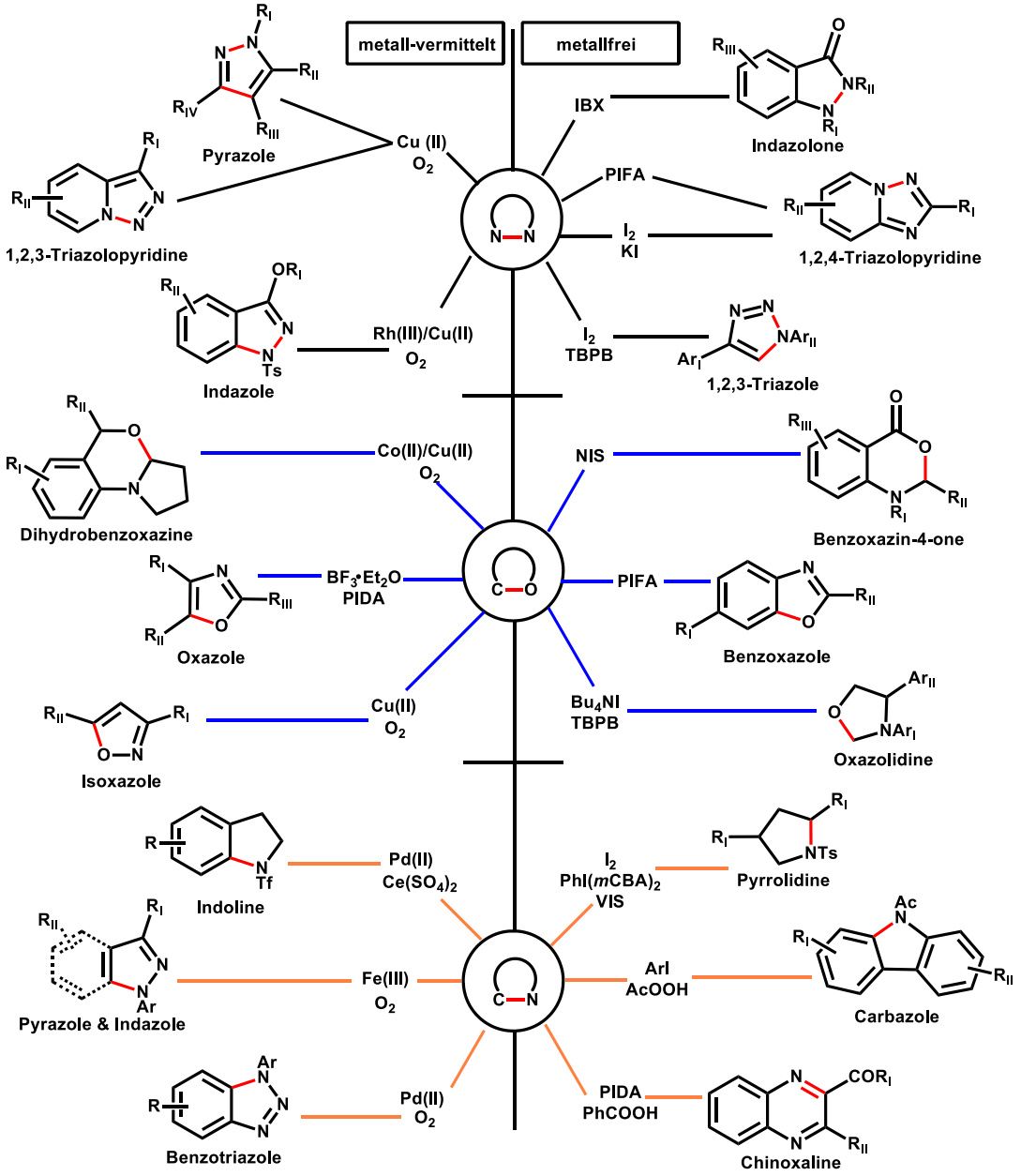

Schema 2: Auswahl an Stickstoffheterocyclen die durch klassische oxidative Methoden (metall-vermittelt (links) und metallfrei (rechts)) zugänglich sind (neu gebildete Bindungen sind rot markiert). [18-35] Abkürzungen: IBX: 2 Iodoxybenzoesäure; PIFA: Bis(trifluoracetoxy)iodbenzol; PIDA: Bis(acetoxy)iodbenzol; TBPB: *tert*-Butylperoxybenzoat; NIS: *N*-Iodsuccinimid; PhI(*m*CBA)$_2$: Bis(3-Chlorbenzoat)iodbenzol ; VIS: ca. 400–800 nm; ArI: 2,2'-Diiod-4,4',6,6'-tetramethylbiphenyl.

So sind sowohl einzelne als auch kondensierte Systeme zugänglich und können intramolekular oder intermolekular aufgebaut werden. Bei den intermolekularen Reaktionen handelt es sich um Kaskadenreaktionen, die eine zusätzliche Bindung aufbauen. Somit werden neben den N-N-Bindungen auch eine C-C-Bindung im Falle der Pyrazol-Synthese via Cu(II)[21] und eine C-N-Bindung für den Zugang zu Indazolen via Rh(III)/Cu(II)[22] geknüpft. Die metall-vermittelten Reaktionen greifen hauptsächlich auf Übergangsmetallverbindungen zurück, welche auf Kupfer,[21,22,23,24] Rhodium,[22] Kobalt,[24] Palladium,[25,26] Eisen[27] oder Bor,[28] in manchen Fällen auf co-katalysierten Systemen (Rh(III)/Cu(II)[22] und Co(II)/Cu(II)[24]), basieren. Zudem benötigen diese Reaktionen zusätzlich ein Oxidationsmittel zur Regeneration oder Aktivierung des Katalysators, welches für die jeweiligen Beispiele in Schema 2 angegeben ist. Somit können beispielsweise Nitrile und Enamin-Sturkturen mit $Cu(OAc)_2$ in einer Sauerstoffatmosphäre und unter hohen Temperaturen von 110 °C in DMF (*N*,*N*-Dimethylformamid) oder DCE (1,2-Dichlorethan) zur Synthese von Pyrazolen in Ausbeuten von 30–84% anhand einer C-C- und N-N-Bindungsbildungskaskade genutzt werden.[21] Hochsubstituierte Oxazole können durch den Aufbau einer C-O-Bindung ausgehend von *β*-Acylaminketonen in guten bis sehr guten Ausbeuten bis zu 84% erhalten werden. Die Cyclisierung gelingt unter Zuhilfenahme von PIDA als Oxidationsmittel in Kombination mit $BF_3{\cdot}Et_2O$ als LEWIS-Säure in DCM (Dichlormethan).[28] Die Verwendung von $Pd(OAc)_2$ mit $Ce(SO_4)_2$ als Oxidationsmittel hingegen ermöglicht eine C,N-Bindungsknüpfung, bei der geschützte Indoline in Ausbeuten von 40–80% resultieren.[25]

Die metallfreien Varianten verwenden häufig mindestens stöchiometrische Mengen Iod-basierte Oxidationsmittel wie 2-Iodoxybenzoesäure (IBX),[29] Bis(trifluoracetoxy)iodbenzol (PIFA),[30,31] Bis(acetoxy)iodbenzol (PIDA),[32] *N*-Iodsuccinimid (NIS),[33] sowie elementares Iod.[34] In manchen Fällen ist der Einsatz von Iod,[35] Iodsalzen (z. B. Bu_4NI)[36] oder Iodaromaten (z. B. 2,2'-Diiod-4,4',6,6'-tetramethylbiphenyl)[37] als Mediator in substöchiometrischen Mengen (< 30%) und eines Oxidationsmittels (Bis(3-Chlorbenzoat)iodbenzol ($PhI(mCBA)_2$), Peroxyessigsäure (AcOOH) oder TBPB) für die Transformation erforderlich. Beispielsweise können Indazolone ausgehend von *N*-Aryl-2-(alkylamin)benzamiden durch Behandlung mit IBX und Trifluoressigsäure in DCE und bei ca. 25 °C mittels einer N-N-Bindungsbildung in Ausbeuten von bis zu 53% erhalten werden.[29] Mit NIS wiederum gelingt ein C-O-Bindungsaufbau, indem *N*-Alkyl-*N*-arylanthranilsäuren zu entsprechenden 3,1-Benzoxazin-4-onen durch die Generierung eines Iminiumintermediats in

Ausbeuten von 41–93% umgesetzt werden.[33] Des Weiteren lassen sich Carbazole durch C-N-Bindungsbildung in Ausbeuten von 46–86% realisieren, indem 2-Acetaminbiphenyle mit 2,2'-Diiod-4,4',6,6'-tetramethylbiphenyl als Mediator und AcOOH als Oxidans in HFIP (1,1,1,3,3,3-Hexafluorisopropanol)/DCM bei ca. 25 °C umgesetzt werden.[37]

1.3 Amidylradikale und Amidylkationen

In Kapitel 1.2 wurde dargelegt, dass es viele Möglichkeiten der N-N-, C-O- und C-N-Bindungsbildung gibt, um N-Heterocyclen herzustellen. Dabei sind die Reaktionszentren sehr unterschiedlich und der Schlüsselschritt der Cyclisierung über diverse Reaktionspfade möglich. Die Amidfunktion ist dahingehend besonders, dass diese die Vielfalt durch den N-N-, C-O- und C-N-Bindungsaufbau ebenfalls ermöglicht. Daher stellt die Generierung von Amidylradikalen, welche auf oxidative[38–50] oder reduktive[15,44,45,51–58] Weise erzeugt werden können (Schema 3, oben), und Amidylkationen ein wichtiges und vielseitiges Instrument für Ringschlussreaktionen dar. Hierbei sei angemerkt, dass auf die reduktive Variante (Schema 3, links) nicht weiter eingegangen wird, sondern allein der Vollständigkeit dient. In den 1970er Jahren nutzten THOMSON *et al.* Kaliumperoxodisulphat zur Synthese von Phenanthridin-6-onen[38] mittels einer oxidativen dehydrierenden Ringschlussreaktion (Schema 3).

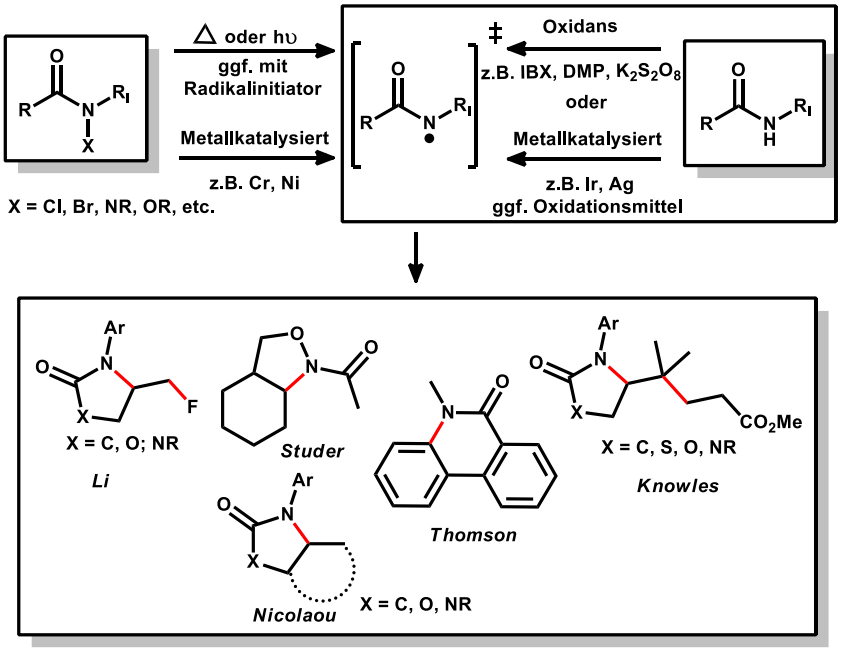

Schema 3: Erzeugung von Amidyl-Radikalen über klassische oxidative Methoden (oben rechts)[38–50] und ein ausgewähltes Produktspektrum (unten); reduktive Methoden (oben links).[15,44,45,51–58] DMP: DESS-MARTIN-Periodinan.

Allerdings ist die Produktvielfalt dieser Methode aufgrund der drastischen Bedingungen (hohe Temperaturen und hohe Oxidationskraft des Peroxodisulfats[59]) eingeschränkt. Vor ca. 20 Jahren gelang NICOLAOU *et al.* ein eleganterer Zugang zu diversen heterocyclischen Struktureinheiten mit IBX, darunter Pyrrolidin-2-one in Ausbeuten von 70–93%, indem aus Amiden oxidativ Amidylradikale generiert wurden und eine intramolekulare Hydroaminierung an einer Alkenfunktion vorgenommen wurde.[46–48] Aufgrund der hohen Reaktivität, des elektrophilen Charakters und der atomökonomisch günstigen Erzeugbarkeit der Amidylradikale, wurden über die Zeit einige Varianten entwickelt: Neben klassischen Oxidationsmitteln (IBX und DMP (Dess-Martin-Periodinan)) wie von NICOLAOU *et al.* und STUDER *et al.* demonstriert,[46–49] beschrieben LI *et al.* den Einsatz von Silbersalzen[41] in Kombination mit Oxidationsmitteln wie Selectfluor™ in einer Aminofluorierung und KNOWLES *et al.* eine photolytische Methode[40] mit einem Iridiumkatalysator und einer Phosphatbase, die die Synthese von diversen heterocyclischen Motiven in einer Carboaminierung gewähren (Schema 3, unten).

Die erste Herstellung von Amidylkationen gelang HAQUE *et al.* durch die Verwendung von LEWIS-Säuren wie $AgBF_4$ an *N*-Chloramiden in Anellierungsreaktionen, bei der durch eine Dehalogenierung des Amids AgCl und ein Amidylkation resultierten.[60] GLOVER *et al.* adaptierte diese Methode zur Herstellung von Benzoxazinen und Benzoxazepinen.[61] Die notwendigen stöchiometrischen Mengen an Silbersalzen sowie die notwendige Präfunktionalisierung machen diesen Zugang jedoch wirtschaftlich unattraktiv. Eine Verbesserung brachte die Oxidation von Amiden durch hypervalente Iod-Verbindungen wie PIFA (Schema 4).[20,62,63] Durch die obsolet werdende Präfunktionalisierung des Amids und die vergleichsweise einfache Darstellung der hypervalenten Iod-Verbindungen[64] konnte die Methode von HAQUE *et al.* abgelöst werden.

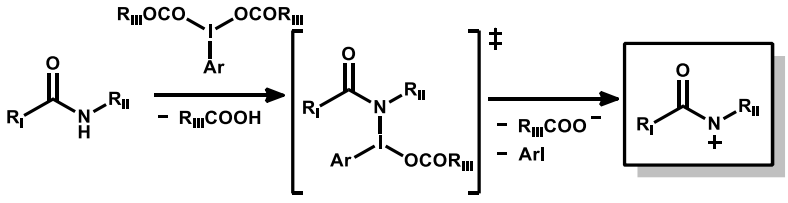

Schema 4: Eine allgemeine Darstellung von Amidylkationen mittels hypervalenten Iod-Reagenzien.[20]

In solchen Fällen ist es keine triviale Aufgabe eine Aussage über die Natur (Radikal oder Kation) eines Intermediats zu treffen, da hypervalente Iod-Verbindungen ionische und radikale Reaktionsführungen ermöglichen.[20,42,65] Analyseansätze wie beispielsweise die ESR-Spektroskopie und Kontrollexperimente, etwa mit Radikalfängern, gestatten es Hinweise auf

die vorliegende Reaktionsspezies zu sammeln und somit eine fundiertere Aussage zu treffen. Unabhängig davon, ob ein radikalischer oder kationischer Pfad vorherrscht, erlauben hypervalente Iod-Reagenzien durch die Oxidation von Amiden einen Zugang zu einigen heterocyclischen Grundbausteinen, die mittels N-N-, C-O- und C-N-Bindungen aufgebaut werden können (Schema 5). Zur Veranschaulichung können die folgenden Synthesen herangezogen werden: Benzimidazolin-2-one lassen sich durch die notwendigen Harnstoffvorläufer und den Einsatz von PIFA in DCM bei ca. 25 °C in Ausbeuten bis 84% überführen.[66] Unter ähnlichen Bedingungen sind Furopyrimidinone in Ausbeuten von 17–65% aus BIGINELLI-Addukten zugänglich.[67] Die Synthese der Phenanthridin-6-one basiert auf der Umsetzung von *N*-Methoxybiphenylcarboxamiden mit Iodbenzol und Peroxyessigsäure (AcOOH) in HFIP und ermöglicht Ausbeuten von 42–89%.[68]

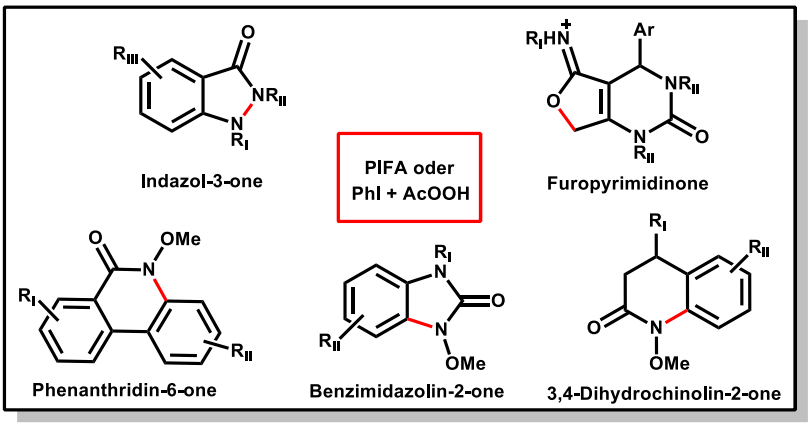

Schema 5: Synthese von diversen Heterocyclen mittels N-N-, C-O- oder C-N-Bindungsknüpfung mittels hypervalenten Iod(III)-Reganzien ausgehend von Amidstrukturen.[62,63,66–68]

Die Nachteile der in Kapitel 1.2 dargestellten Methoden ergeben sich einerseits aus den metall-vermittelten Methoden, vor allem jedoch durch die toxischen Eigenschaften (von Kupfer- und Kobaltreagenzien) und teilweise sehr hohen Kosten der entsprechenden Metallverbindungen (Palladium und Rhodium), wodurch ein Einsatz in der Synthese von Wirkstoffen unattraktiv wird. Zudem sind die Transformationen oftmals an gewisse Substratstrukturen gebunden (Enamine, Oxime, Hydrazone, etc.), die zunächst eingeführt werden müssen. Die Vorteile der Amide sind in diesem Fall der leichte Zugang durch Kondensationsreaktionen und die Reaktionsträgheit,[69] wodurch etwaige Modifikationen (z. B. nukleophile Angriffe, Reduktionen mit Natriumborhydrid, etc.) des Rückgrats in Anwesenheit von Amiden leichter realisierbar sind.

Allerdings ist die Verwendung von AcOOH aufgrund von explosionsartiger Zersetzung (> 20%) auf geringere Konzentrationen beschränkt.[70] Des Weiteren schaffen es die vorgestellten

Methoden ebenfalls nicht, eine „grüne“ Alternative zu bieten, da bei besagten Reaktionen Reagenzabfall in mindestens stöchiometrischen Mengen anfällt. Zudem übernehmen teure Übergangsmetalle (Ag oder Ir) in manchen Reaktionen nach wie vor eine tragende Rolle. Dieser Herausforderung stellt sich die organische Elektrochemie, die in den folgenden Kapiteln näher beleuchtet wird.

1.4 Elektroorganische Synthese

Die Elektrochemie wurde lange Zeit hauptsächlich für die Herstellung von Grundchemikalien genutzt. Die prominentesten Prozesse sind zum einen die Chlor-Alkali-Elektrolyse (oxidativ) sowie der BAIZER-Prozess (Adiponitrilsynthese), als reduktives Pendant.[71] In den vergangenen Jahren erfuhr die Elektrosynthese eine Art Renaissance und ist seitdem ein wichtiges Synthesewerkzeug, welches die Herstellung von Feinchemikalien zum Ziele hat und Gegenstand aktueller Forschung ist.[72,73] Dabei können die Bedingungen auf vielfältige Weise angepasst werden. Zu den grundlegenden Parametern zählen die folgenden:

- galvanostatische (Zwei-Elektroden-Aufbau) und potentiostatische (Drei-Elektroden-Aufbau) Bedingungen
- Zellgeometrie (ungeteilt; geteilt: Anoden- und Kathodenraum durch einen Separator getrennt; quasi-geteilt: der Aufbau ist ungeteilt, die Gegenelektrode besitzt ein möglichst kleines Volumen (z. B. ein Draht), um etwaige Nebenreaktion zu verringern)
- Reaktionsvermittlung (direkt an der Elektrode oder indirekt, d. h. durch einen Mediator (organisch, metallorganisch oder anorganisch), welcher an der Elektrode generiert und regeneriert wird)

Idealerweise – um ein möglichst einfaches, kostengünstiges und nachhaltiges System bereitstellen zu können – werden die Bedingungen so gewählt, dass ein ungeteiltes, galvanostatisches und direktes System resultiert. Dieser Aufbau kommt dem klassischen Bild einer organischen Reaktion sehr nahe (Abbildung 4).

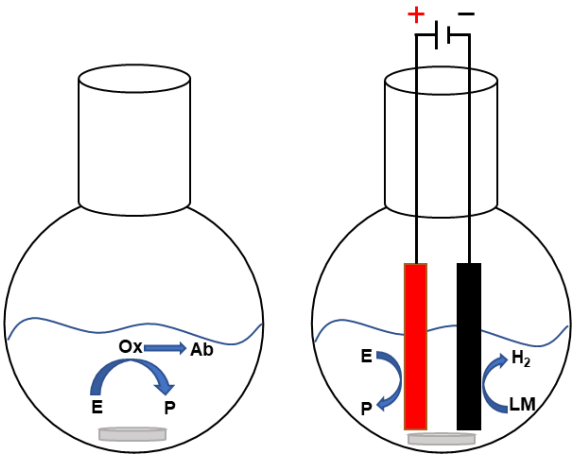

Abbildung 4: Links: Konventionelle organische Oxidation in einem Kolben. E = Edukt; P = Produkt; Ox = Oxidationsmittel; Ab = Reagenzabfall. Rechts: Anodische, direkte Transformation in einer ungeteilten Zelle unter galvanostatischen Bedingungen; Anodereaktion: E wird zu P oxidiert; Kathodenreaktion: Bildung von (idealerweise) Wasserstoff mittels Beteiligung eines protisches Lösungsmittels bzw. einer Protonenquelle (LM).

Darüber hinaus wirken Parameter wie Elektrodenmaterial, Leitsalz, Ladungsmenge und Stromdichte als weitere Stellschrauben und üben neben klassischen Einflussgrößen wie Lösungsmittel, Temperatur, Konzentration einen wichtigen Einfluss auf den Reaktionsverlauf aus. Eigenschaften wie der minimierte Reagenzienabfall durch den Einsatz von elektrischem Strom als terminales Oxidations- oder Reduktionsmittel, die inhärente Sicherheit (etwa durch Unterbrechung des Stroms) und der Verzicht auf toxische, instabile oder teure Ingredienzien zeichnen diese Methode als eine „grüne“ Alternative[74] zur klassischen organischen Synthese und als Konkurrenten zur Photochemie aus.

1.4.1 Anodische Cyclisierungsreaktionen

Innerhalb der letzten 20–30 Jahren wurde das Syntheseportfolio für anodische Ringschlussreaktionen erweitert.[73,75,76] Sowohl direkte als auch indirekte Methoden erlauben einen Zugang zu heterocyclischen Motiven mittels C,O- oder C,N-Bindungsaufbau (Schema 6).[77,78,79–82] So sind Isoxazole durch direkte Oxidation unter galvanostatischen Bedingungen in Ausbeuten bis zu 77% zugänglich. Einfache Bedingungen sowie günstige Elektrodenmaterialien (Anode: Graphit; Kathode: Eisenstab) in einem Perchlorat/Methanol-System zeichnen diese Methode aus.[82] Falls potentiostatische Bedingungen erwogen werden, so gelingt die Herstellung von 1,3,4-Oxadiazolen aus *N*-Aroylhydrazonen in Ausbeuten von 47–95%. Durch den Einsatz von Platinelektroden und einer Calomel-Referenzelektrode sowie einem Perchlorat/Methanol-System können diese Verbindungen mit herbiziden Eigenschaften aufgebaut werden.[81]

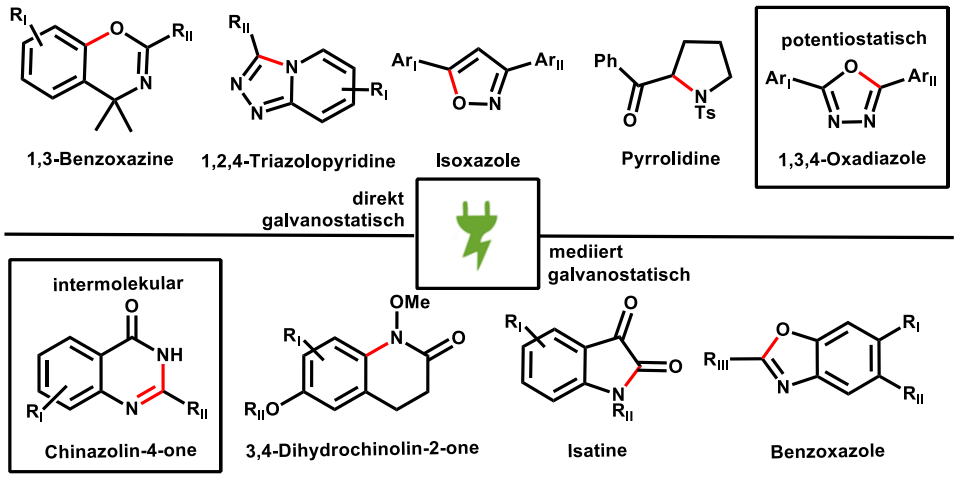

Schema 6: Zugang zu einer Auswahl an Heterocyclen mittels direkter und indirekter Methoden.

Mediierte Elektrosynthesen haben die Besonderheit, dass sie beispielweise in einem Zwei-Phasen-System[80] oder *ex cell* (nur Herstellung des Reagenzes unter elektrochemischen Bedingungen)[77,79] betrieben werden können. Auf diese Weise können Benzoxazole über ein Iod-mediiertes Zwei-Phasen-System in Ausbeuten von 70–91% erhalten werden. Ferner können Chinolin-2-one mittels *ex cell* generierten hypervalenten Iod(III)-Aromaten hergestellt werden.[80] Systeme, die unter direkten und metallfreien Bedingungen operieren, sind aufgrund ihrer Einfachheit deutlich vorteilhafter, vor allem im Hinblick auf eine potenzielle Anwendung, die über den Labormaßstab hinausgeht. Der Einsatz von mediierten Systemen mit Übergangsmetall-haltigen Komponenten[76] erfordert zusätzliche Aufreinigungsmaßnahmen, da vor allem in der Wirkstoffsynthese etwaige Übergangsmetallkontaminationen einen Störfaktor darstellt.

1.4.2 Anodisch generierte Amidylradikale

Wie in Kapitel 1.3 gezeigt, sind Amide und deren reaktive Intermediate vielseitig in Ringschlussreaktionen einsetzbar. Ein atomökonomischer Zugang zu den Amidylradikalen ist durch eine dehydrierende Oxidation möglich. Die klassischen Methoden verwenden allerdings Edelmetalle und/oder stöchiometrische Mengen an Oxidationsmitteln, die nicht so leicht mit dem Nachhaltigkeitsgedanken zu vereinbaren sind. Elektroorganische Synthese – als „grüne“ Alternativtechnologie – ermöglicht die Generierung von Amidylradikalen in Cyclisierungen und verzichtet zudem auf stöchiometrische Mengen an Oxidationsmittel. Auf diesem Gebiet haben MOELLER *et al.* Pionierarbeit geleistet (Schema 7, links).

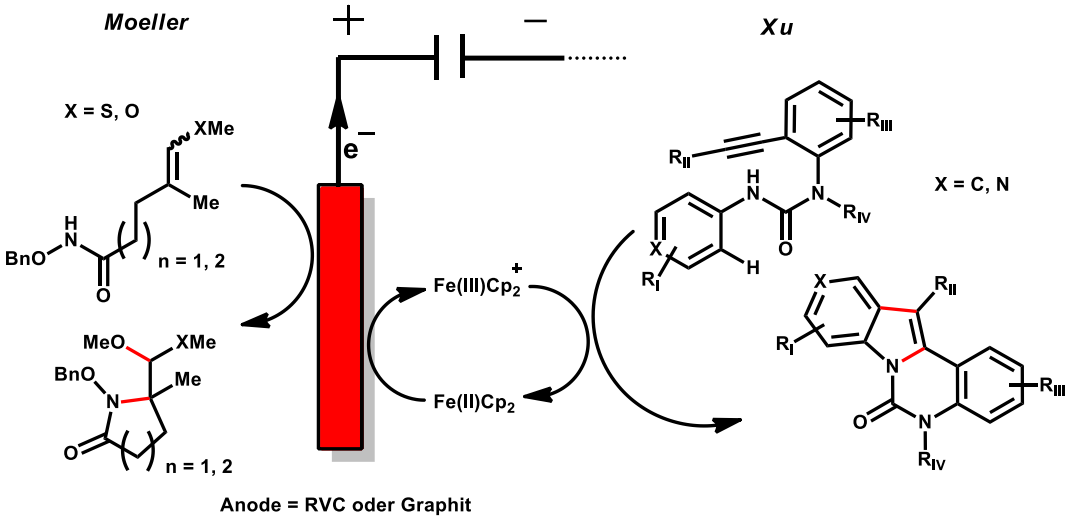

Schema 7: Anodisch generierte Amidyl-Radikale. Links: Direkt an der Anode zur Synthese von Pyrrolidin-2-onen und Piperidin-2-onen.[83] Rechts: Mediiert mit Ferrocen zur Darstellung von Indolen.[84]

Sie berichteten über eine Möglichkeit der direkten Generierung von Amidylradikalen an RVC-Anoden (*reticulated vitreous carbon*/ Glaskohlenstoffschaum) zur Lactamisierung.[83] Hierbei konnte die Cyclisierung an Vinylthioethern und Enolethern in überwiegend moderaten bis guten Ausbeuten von bis zu 60% gezeigt werden. XU *et al.* nutzten ein indirektes, mediiertes System, mit dessen Hilfe sie hochsubstituierte Indole und Azaindole in Ausbeuten von 45–94% mittels einer intramolekularen Kaskadenreaktion herstellen konnten (Schema 7, rechts). Ausgehend von einem *N*-Aryl-*N*'-(2-alkinphenyl)-harnstoff fand mittels Ferrocen als Mediator, eine Oxidation des Amids statt, wodurch ein Amidylradikal generiert wurde. Des Weiteren fand die Reaktion unter Rückfluss (80 °C) statt.[84]

Die bisherigen Cyclisierungsstrategien sahen den Angriff eines sp^2- oder sp-Zentrum vor und konzentrierten sich vor allem auf C-N-Bindungsknüpfungen. Aus diesem Grund war der erste elektrochemische Zugang zu Pyrazolidin-3,5-dionen via N-N-Bindungsbildung (zudem die erste elektrochemische und intramolekulare N-N-Bildung) aus der Arbeitsgruppe WALDVOGEL sehr interessant (Schema 8).[85]

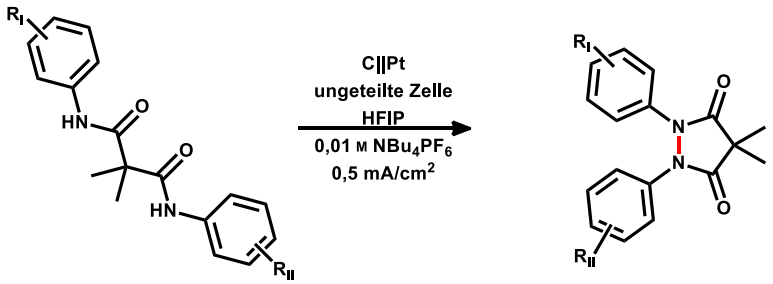

Schema 8: Synthese von Pyrazolidin-3,5-dionen mittels elektrochemischer N-N-Bindungsknüpfung.

Hierbei konnte durch eine direkte, anodische Reaktionsführung unter milden und galvanostatischen Bedingungen ein eleganter Weg zur N-N-Bindungsknüpfung in Ausbeuten von bis zu 89% etabliert werden.[85] Die simple, ungeteilte Zellgeometrie sowie die Stabilisierungseigenschaften von HFIP[86,87] tragen hier zur Generierung des gewünschten Cyclisierungsprodukts bei. Diese Stabilisierungseigenschaften des HFIP zeichnen sich vor allem durch eine hohe elektrochemische Stabilität,[88] Wasserstoffbrückenbindungs-eigenschaften,[89] eine geringere Nukleophilie (verglichen mit Isopropanol)[86] und der Fähigkeit mikroheterogene Strukturen[90] auszubilden aus. Die erwähnten Charakteristika des HFIP sowie die Möglichkeit der fast vollständigen Rückgewinnung machen den Einsatz des Lösungsmittels in der organischen Elektrosynthese attraktiv. Die Annahme zum Mechanismus der Pyrazolidin-3,5-dion-Synthese via N-N-Bindungsknüpfung stützt sich auf einen diradikalischen Pfad. Somit würde an der Anode durch Oxidation beider Amidfunktionen jeweils ein Amidylradikal gebildet werden. Allerdings konnte ein kationischer Mechanismus aufgrund der Datenlage nicht gänzlich ausgeschlossen werden. Eine präzisere mechanistische Überlegung bezüglich der Erzeugung von Amidylradikalen und Amidylkationen wird im nachfolgenden Kapitel thematisiert.

1.4.3 Reaktionspfade von anodisch generierten Amidylintermediaten

Wie in Kapitel 1.4.2 erwähnt, können bei der Oxidation von Amiden grundsätzlich zwei verschiedene Intermediate für den Verlauf der Reaktion verantwortlich sein. Analog zu klassischen Reaktionen,[20,65] können sowohl ein radikalischer oder ein kationischer Mechanismus auftreten (siehe Kap. 1.3). Der generelle Ablauf (Schema 9) sieht vor, dass zunächst eine Oxidation (Einelektronentransfer (SET)) des Stickstoffatoms zum Radikalkation erfolgt. Das entstandene Radikalkation ist um einige Größenordnungen acider als das korrespondierende Amid,[91] wodurch eine Deprotonierung im nachfolgenden Schritt erleichtert wird. Eine Base oder ein an der Kathode deprotoniertes Lösungsmittelmolekül könnten zur Deprotonierung des Amid-Radikalkations dienen.[85] Alternativ könnte auch ein Protonengekoppelter Energietransfer (PCET) auftreten. Bei diesem Szenario würden die Oxidation (SET) durch die Anode und die Deprotonierung durch eine BRØNSTED-Base konzertiert ablaufen.[92] Bei einem radikalischen Pfad steht nach dem Deprotonierungsschritt das Amidylradikal für eine Reaktion zur Verfügung (Schema 9, Pfad A). Im Falle eines

kationischen Pfades wird durch einen zweiten Oxidationsschritt (SET) aus dem Amidylradikal das Amidylkation gebildet (Schema 9, Pfad B).

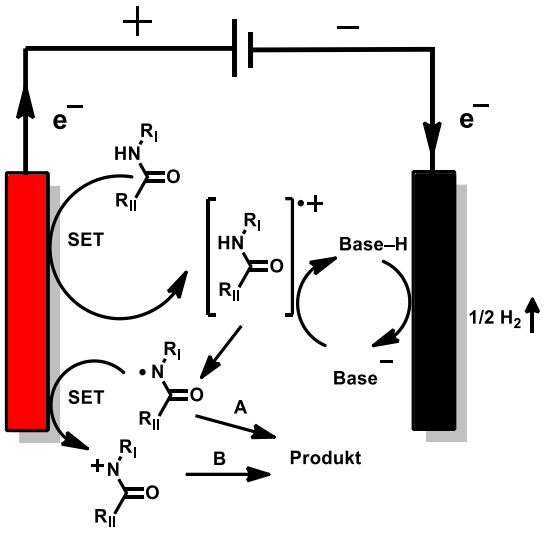

Schema 9: Potenzielle Reaktionspfade für die direkte Oxidation von Amiden, die im Amidylradikal oder Amidylkation resultieren. Die Deprotonierung des Amid-Wasserstoffs erfolgt exemplarisch durch eine Base.

2 Aufgabenstellung

Bisher konnte eindrucksvoll demonstriert werden, dass die elektrochemische Oxidation ein nützliches Synthesewerkzeug für die Herstellung unterschiedlicher Heterocyclen sein kann. Neben der N-N-Bindungsbildung zur Herstellung von 5-Ringheterocyclen soll nun im Rahmen dieser Arbeit die Ringgröße erweitert werden. Hierfür wird auf die elektrochemische Oxidation von Amiden zurückgegriffen (Schema 10).

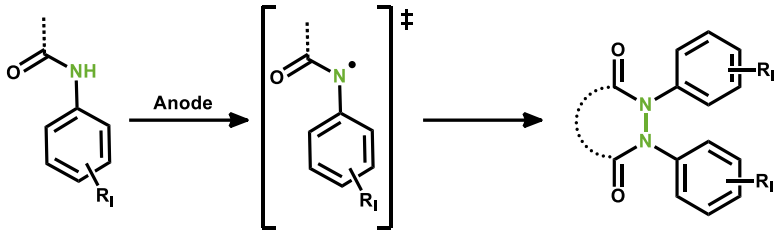

Schema 10: Elektrochemische Oxidation von Amiden zur Synthese von N-N-Heterocyclen mit unterschiedlichen Ringgrößen via einem postulierten radikalischen Mechanismus.

Weiterhin sollen hinreichende Untersuchungen vorgenommen werden, um mit fundierten Daten eine Aussage zum Mechanismus der N-N-Bindungsbildung zu treffen. Zur Debatte stehen ein radikalischer oder ein kationischer Mechanismus (Schema 11).

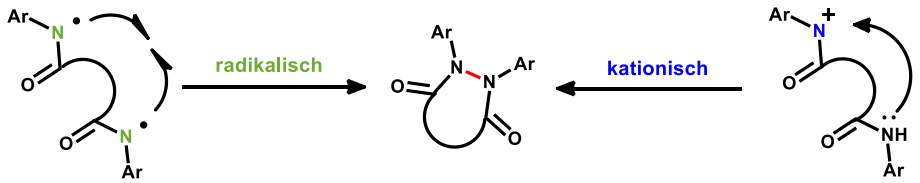

Schema 11: Denkbare Reaktionspfade.

Ein Verständnis für das Reaktionsverhalten hilft dabei weitere Syntheserouten für wichtige Bausteine zu entdecken und etablierte Routen durch „grüne“ elektrochemische Alternativen zu ergänzen oder abzulösen. Folglich soll das Konzept der Amid-Oxidation auf die Bildung von N-X-Bindungen ausgeweitet und somit weitere heterocyclische Strukturen zugänglich gemacht werden (Schema 12).

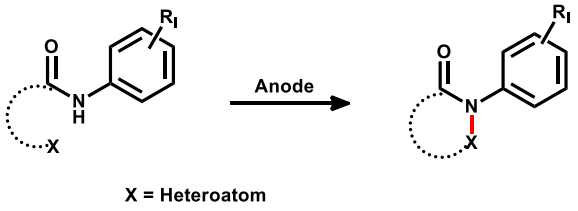

Schema 12: Cyclisierungsreaktion mit N-Heteroatom-Bindung.

3 Ergebnisse und Diskussion

3.1 Anwendung von Amidylradikalen in der elektrochemischen Synthese von Benzoxazolen

Das Manuskript zu diesem Kapitel wurde bereits publiziert.

T. Gieshoff, A. Kehl, D. Schollmeyer, K. D. Moeller, S. R. Waldvogel, *Electrochemical Synthesis of Benzoxazoles from Anilides – A New Approach to Employ Amidyl Radical Intermediates, Chem. Commun.* **2017**, *53*, 2974–2977.

Hintergrund

Die erfolgreiche Herstellung von Pyrazolidin-3,5-dionen via N-N-Bindungsbildung[85] durch Oxidation von Malonsäuredianiliden gab Anlass, die Methode auf die Bildung von 6-Ringen zu adaptieren. Die anfänglichen Versuche erlaubten ausgehend von Bernsteinsäuredianiliden zwar die Produktbildung, allerdings war die Ausbeute ausbaufähig und darüber hinaus konnte das Auftreten von Benzoxazolen beobachtet werden, welche durch eine C-O-Bindungknüpfung zustande kamen (Schema 13).

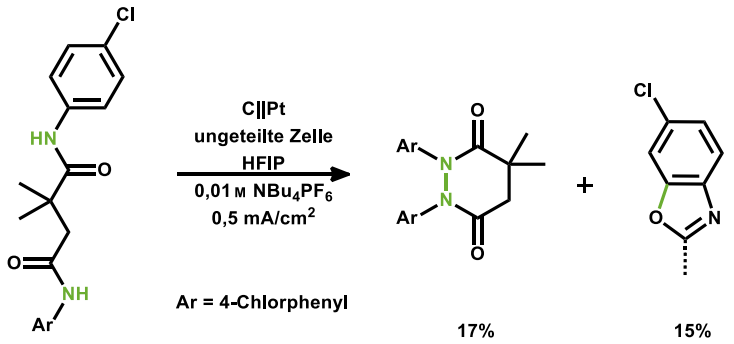

Schema 13: Übertragung der direkten anodischen N-N-Bindungsmethode auf ein Bernsteinsäuregerüst.

Diese interessante Beobachtung wurde genutzt, um durch eine Modulation der Bedingungen und einer Modifikation der Substrate die Bildung von Benzoxazolen in einer 5-endo-trig Cyclisierung selektiv zu steuern. Da dieser Heterocyclus in der Natur vorkommt und eine pharmakologische Relevanz aufweist,[93] ist ein einfacher und nachhaltiger Zugang wünschenswert. Konventionelle Synthesen stützen sich hierbei auf 2-Aminphenole, die mit aktivierten Säuren oder Aldehyden unter oxidativen Bedingungen umgesetzt werden,[94] oder Anilide, die mittels Metallkatalyse (CuO-Nanopartikel) und Abgangsgruppen zur Zielstruktur

überführt werden.[95] Zudem kann PIFA mit TMSOTf (Trifluormethansulfonsäuretrimethylsilylester) als Additiv dazu genutzt werden, um Anilide mittels einer C-O-Bindungsbildung zu anellieren.[31]

Der Vorteil der anodischen Umsetzung liegt vor allem in den Einsparungen von Reagenzien und dem resultierenden Abfall, der sich so vermeiden lässt.

Ergebnisse

Um Produktgemische zu vermeiden, wurden fortwährend für die anodische C-O-bindungsbildende Cyclisierung Monoanilide als Substrate eingesetzt, da auf diese Weise die Nebenreaktion der N-N-Bindungsbildung verhindert werden kann (Schema 13). Die entsprechende Eduktsynthese konnte durch Kondensation mit den gewünschten Anilinen und Säurechloriden in einer Stufe und hohen Ausbeuten erfolgen. Es wurden zudem zwei gängige Reaktionsanordnungen untersucht, um lediglich zu überprüfen, ob diese elektrochemische Reaktion bei drastischen Parameteränderungen (wie Elektroden- sowie Zellgeometrie und den Elektrodenanordnung) ebenfalls funktioniert und ob zwei verschiedene Herangehensweisen Vorteile bergen. Bei Anordnung A (Abbildung 5, links) handelt es sich um eine quasi-geteilte Zelle, bestehend aus einem 25 mL Drei-Hals-Kolben, einem gewinkelten Elektrodenarrangement aus RVC (Anode) und einem Platin-Draht (Kathode).[83] Anordnung B (Abbildung 5, rechts) ist der Standard-Aufbau: Eine ungeteilte 5 mL Teflon-Zelle mit parallel zueinander ausgerichteten Elektroden (Anode: isostatisches Graphit; Kathode: Platin-Blech).

Abbildung 5: Reaktionsanordnungen A (links) und B (rechts).

Die beiden Anordnungen wurden an zwei Substraten (Schema 14) untersucht. Hierbei wurden ein Anilid mit einem vergleichsweise schwach elektronenschiebenden (R = Cl) und einem elektronenschiebenden (R = OMe) Rest eingesetzt. Dabei stellte sich heraus, dass die Reaktion, unabhängig vom Aufbau (Abbildung 5), grundsätzlich möglich ist und die Produktbildung beider Derivate erlaubt. Weiterhin wurde ermittelt, dass das Substrat mit der

elektronenschiebenden Methoxygruppe höhere Ausbeuten (86%) unter Verwendung der Anordnung A ermöglicht. Mit Anordnung B hingegen konnte nur eine Ausbeute von 55% erzielt werden (Schema 14). Dies könnte mit der stark erhöhten Oberfläche zusammenhängen, die die Glaskohlenstoffschaumanode bietet (Anordnung A). Bei dem Derivat mit dem schwach elektronenschiebenden Chlorsubstituenten lag die Ausbeute mit Aufbau A bei 56% während Aufbau B diese mit 66% übertraf. Aufgrund der unterschiedlichen Reaktionsanordnungen ist ein direkter Vergleich schwierig, allerdings lässt sich ein Trend erkennen: Sobald ein *para*-Methoxyanilin verwendet wurde, waren die Ausbeuten (ca. 80%) mit Konzept A durchgehend höher, unabhängig von der eingesetzten Benzoesäure. Bei schwach elektronenschiebenden (-Cl) oder elektronenziehenden Resten (-OTf) an der 4-Anilinposition fielen die Ausbeuten (ca. 60%) mit Aufbau A tendenziell niedriger aus. Selbstverständlich können neben den Unterschieden im Aufbau (A und B) weitere Faktoren eine Rolle spielen, etwa der Elektrodenabstand, die Diffusion, etc. Daher bieten diese unterschiedlichen Ansätze auch die Möglichkeit eine Reaktion oder Derivate, die scheinbar nicht unter den gegebenen Bedingungen funktionieren, durch eine Veränderung des Aufbaus zu optimieren und dabei Bedingungen wie Lösungsmittel, Leitsalz und Elektrodenmaterialien konstant zu lassen.

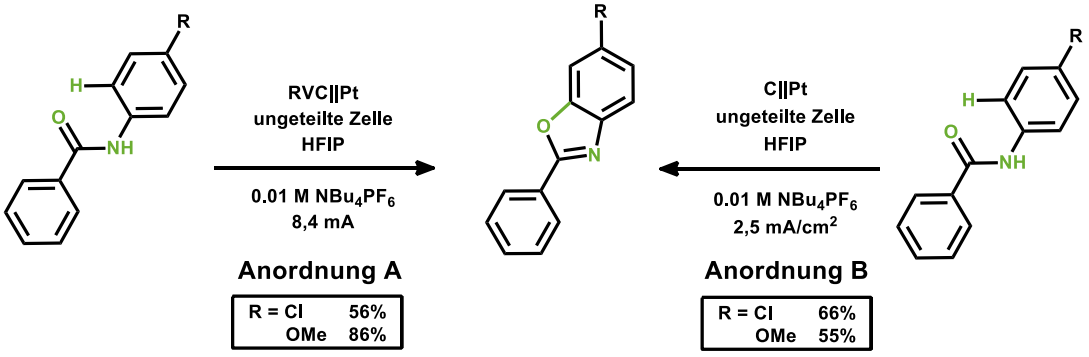

Schema 14: Reaktionsbedingungen der Konfigurationen A und B zur Synthese von Benzoxazolen.

Zunächst ging man bei dieser Reaktion von einem radikalischen Mechanismus aus. Die ersten Zweifel kamen mit der unerwarteten Reaktion von *N*-(4-Methylphenyl)benzamid, bei der ein HFIP-Ether entstanden war (Schema 15). Daher wurden weitere Untersuchungen unternommen (Kap. 3.3).

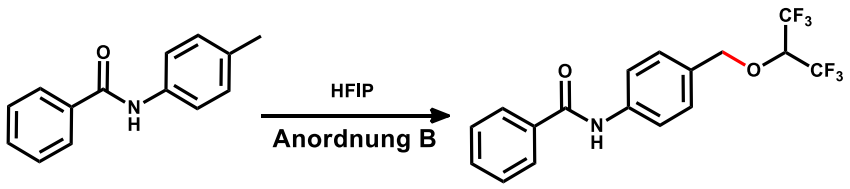

Schema 15: HFIP-Etherbildung als Nebenreaktion.

Erklärung meines Beitrages:

Personenbezogene Daten

3.2 Elektrochemische Umwandlung von Phthalsäuredianiliden zu Phthalatzin-1,4-dionen mittels dehydrierender N-N-Bindungsbildung

Das Manuskript zu diesem Kapitel wurde bereits publiziert.

A. Kehl, T. Gieshoff, D. Schollmeyer, S. R. Waldvogel, *Electrochemical Conversion of Phthaldianilides to Phthalazin-1,4-diones by Dehydrogenative N-N Bond Formation*, *Chem. Eur. J.* **2018**, *24*, 590–593.

Hintergrund

Phthalazin-1,4-dion-Strukturen können aufgrund ihrer biologischen Aktivität in medizinischen Produkten Anwendung finden.[96] So sollten sie in diesem Projekt mittels anodischer dehydrierender N-N-Bindungsbildung, ausgehend von Phthalsäuredianiliden, hergestellt werden. Zuvor wurde versucht das N-N-Verknüpfungs-Konzept auf Bernsteinsäuredianilide zu übertragen, um 6-Ringheterocyclen herstellen zu können. Allerdings erwies sich diese Transformation als äußerst langsam, u. a. weil der Thorpe-Ingold-Effekt, der bei dem modifizierten Malonsäuregerüst deutlich stärker zum Tragen kam,[85,97] in diesem Fall deutlich weniger beitragen konnte. Als Konsequenz war die Ausbeute des erwarteten Produkts niedrig. Daher wurde eine andere Strategie gewählt, die die Vorkoordination deutlich stärker in den Vordergrund rückte. Bei einem Phthalsäuregerüst wird durch die an sp^2-Zentren gebundenen Amide eine gute Vorkoordination und somit eine höhere Reaktionswahrscheinlichkeit beider Amide miteinander gewährleistet.

Ergebnisse

Die Substrate ließen sich auf einfache Weise herstellen. Waren etwa symmetrische Phthalsäuredianilide gewünscht, so konnte eine Kondensation mit dem gut erhältlichen Säuredichlorid und dem entsprechenden Anilin durchgeführt werden. Bei anspruchsvollen, nicht-symmetrischen Derivaten hingegen wurde eine andere Syntheseroute entwickelt, die von einem Phthalsäureanhydrid ausging (Schema 16): Zunächst konnte ein Monoanilid durch eine simple Kondensation mit dem notwendigen Anhydrid gebildet werden, welches durch Behandlung mit Trifluoressigsäureanhydrid in ein Isoimid überführt wurde. In einem letzten Schritt wurde schließlich das zweite Anilin hinzugegeben und in einer Ringöffnungsreaktion

das gewünschte nicht-symmetrische Phthalsäuredianilid in Ausbeuten von bis zu 50% über drei Stufen erhalten.

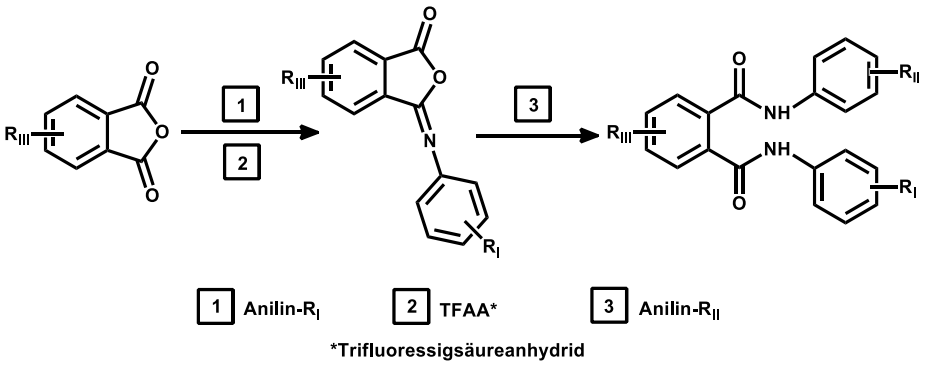

Schema 16: Synthesesequenz für nicht-symmetrische Vorläufermoleküle ausgehend vom Anhydrid (links) über ein Isoimid (mittig) hin zum Phthalsäuredianilid (rechts).

Bei dem Versuch Diamide mit heterocyclischen Aminen aufzubauen, konnte jedoch nur das thermodynamisch stabile Phthalimid erhalten werden.

Die Elektrosynthese lieferte 15 Derivate, die in Ausbeuten von bis zu 89% erhalten wurden (Schema 17). Dabei konnten durch die hochmodulare Vorläufersynthesesequenz symmetrische, nicht-symmetrische sowie Dianilide mit substituiertem Phthalsäuregerüst untersucht werden. Diese Methode toleriert Gruppen (z. B. -Chlor, -Brom, -Cyano, -Triflyl), die sich für diverse Weiterreaktionen eignen und somit eine zusätzliche Modifikation der gewünschten Zielstrukturen erlauben. Aniline mit freier *para*-Position bargen niedrige Ausbeuten von unter 40%, da hier Überoxidationen und/oder Zersetzungsreaktionen auftraten.[85]

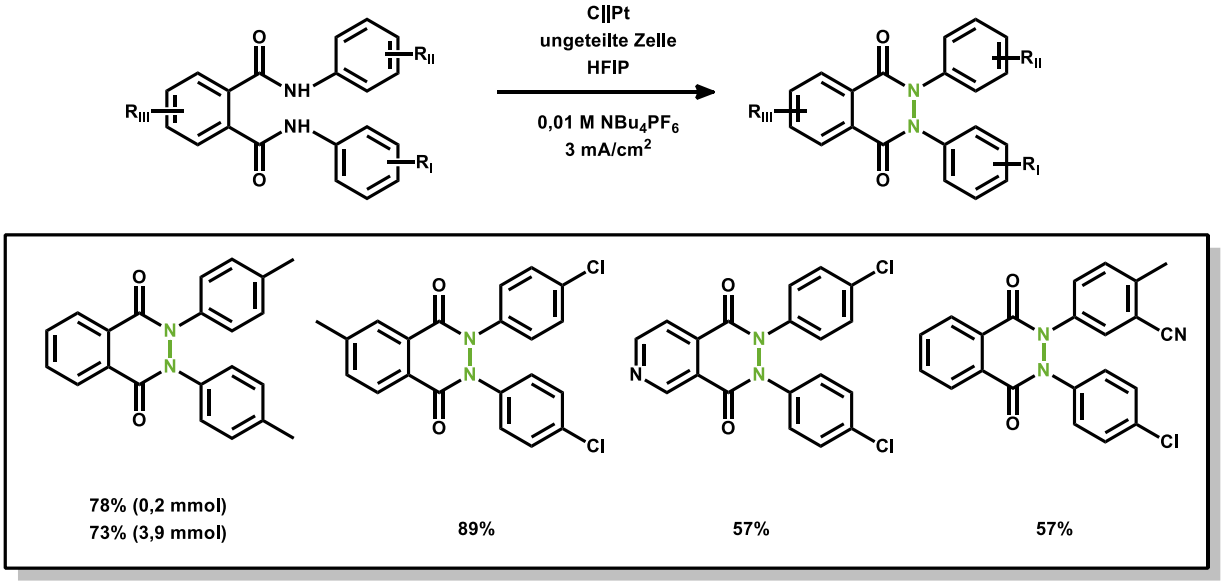

Schema 17: Reaktionsbedingungen und ausgewählte Derivate der Phthalazion-1,4-dion-Synthese.

Elektronenziehende funktionelle Gruppen (z. B. -Fluor, -Cyano, -Triflyl) hingegen, die am Anilinkörper eingeführt wurden, reagierten ähnlich gut. Zudem wurde die Reaktion an einem Beispiel in einer 80 mL Becherglaszelle im größeren Maßstab (3,9 mmol statt 0,2 mmol) erfolgreich durchgeführt, womit die Möglichkeit einer Hochskalierung nachgewiesen werden konnte.

Die cyclovoltammetrischen (CV) Studien bestätigten die Vermutung, dass es sich bei dieser Reaktion überwiegend um eine radikalische Bindungsknüpfung handeln muss, da die beiden Oxidationssignale, die jeweils im Cyclovoltammogramm zu sehen waren, der Amid-Funktion zugeordnet werden konnten. In Kapitel 3.3 werden die dazu notwendigen Informationen näher ausgeführt. An dieser Stelle sei die Rolle des Lösungsmittels HFIP kurz erläutert: Aufgrund der Annahme, dass die Reaktion einem radikalischen Mechanismus folgt, sind N-zentrierte σ- oder π-Radikale denkbar.[38] Bei dieser Reaktion wird die Herstellung von π-Radikalen vermutet. Im Falle der Bildung von π-Radikalen ist HFIP dazu in der Lage durch Wasserstoffbrückenbindungen und den elektronenziehenden Charakter die Aufenthaltswahrscheinlichkeit des Radikals am Carbonylsauerstoff, durch die Konjugationsmöglichkeit zwischen Stickstoff und Carbonylsauerstoff, zu unterdrücken. Weiterhin spricht die geringe Ausbeute der Derivate mit einer freien para-Position eher für die Bildung von π-Radikalen (verwendete Aniline: unsubstituiert: 17% N-N-Produkt; 3-*tert*-Butyl-Anilin: 34% N-N-Produkt). Durch den π-Charakter des Radikals ist eine Wechselwirkung mit dem π-System des Anilinkörpers möglich, wodurch eine Delokalisation des Radikals denkbar ist. Als Konsequenz treten Zersetzungsprozesse auf. Für die Generierung von π-Radikalen sprechen ebenfalls die Resultate aus den Untersuchungen von *N*-*tert*-Butoxyamidylradikalen durch ESR-Spektroskopie, allerdings sei darauf hingewiesen, dass diese Exemplare reduktiv erzeugt wurden (beispielsweise durch Dehalogenierung einer *N*-Chloramid-Spezies).[98]

Erwähnenswert ist in diesem Zusammenhang die Möglichkeit, die gebildete N-N-Bindung in Form eines Azobenzols aus dem Phthalsäuregerüst mittels Hydrazins in einer Ausbeute von 88% herauszulösen (Schema 18).

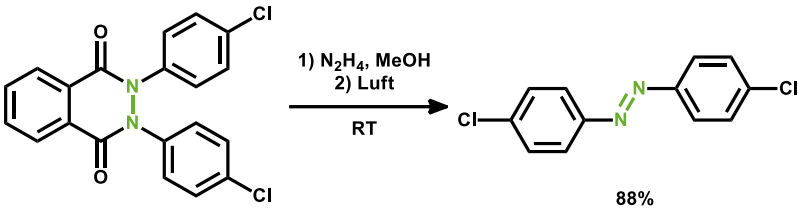

Schema 18: Freisetzung von 4,4'-Dichlorazobenzol mittels Hydrazins.

Erklärung meines Beitrages:

Personenbezogene Daten

3.3 Einsicht in den Mechanismus der anodischen N-N- und C-O-Bindungsbildung ausgehend von Aniliden mittels dehydrierender Kupplung

Das Manuskript zu diesem Kapitel wurde bereits publiziert.

T. Gieshoff, A. Kehl, D. Schollmeyer, K. D. Moeller, S. R. Waldvogel, *Insights into the Mechanism of the Anodic N-N Bond Formation by Dehydrogenative Coupling*, *J. Am. Chem. Soc.* **2017**, *139*, 12317–12324.

Hintergrund

Zusätzlich zu den Arbeiten an den Phthalazin-1,4-dionen (Kapitel 3.2), war die Frage nach dem Reaktionsmechanismus der vorangegangenen Themen (Kapitel 3.1 und die Kapitel 1.4.2 Schema 8) interessant. Wie bereits erläutert, traten bei der elektrochemischen Oxidation eines Bernsteinsäuredianilides zwei unterschiedliche Produkte auf (Schema 19). Durch die Verwendung eines Phthalsäuregerüst anstatt des der Bernsteinsäure konnte das N-N-Produkt selektiv erhalten werden. Für das C-O-Produkt wurden Monoanilide genutzt und somit Benzoxazole generiert. Somit konnte die Möglichkeit der Einflussnahme auf den Reaktionsverlauf in den Kapiteln 3.1 und 3.2 demonstriert werden.

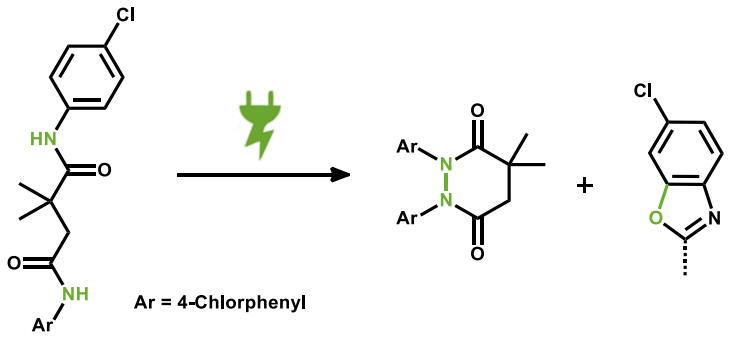

Schema 19: Konkurrenzreaktion zwischen N-N- und C-O-Bindungsbildung.

Was die Transformation in Schema 19 verdeutlicht, ist die folgende Fragestellung: Verlaufen beide Transformationen nach dem gleichen Mechanismus? Falls nicht: Welcher Mechanismus ist jeweils für welche Transformation verantwortlich? Um einen Einblick in die mechanistischen Details zu erhalten, wurden CV-Messungen und eine synthetische Beweisführung eingesetzt.

Ergebnisse

Zunächst wurde der Mechanismus der N-N-Bindungsbildung betrachtet (Schema 20): Nach einem SET und einer anschließenden Deprotonierung des gebildeten Radikalkations (beispielsweise durch eine kathodisch generiertes HFIP-Anion) wird ein Amidylradikal gebildet. Dem gebildeten Radikal stehen zwei Möglichkeiten zur Verfügung: Das zweite Amid wird der gleichen Reaktion unterworfen, woraufhin ein Diradikal entsteht, welches in einer Rekombination die N-N-Bindung aufbaut (**I**, grün) oder das entstandene Radikal wird an der Anode erneut oxidiert und bildet ein Kation, welches nukleophil von dem zweiten Amid angegriffen wird, wodurch die N-N-Bindung zustande kommt (**II**, blau). Fortwährend wird für die Generierung eines Kations eine blaue Farbkodierung und für die Radikale eine grüne Farbkodierung verwendet (siehe Schema 20).

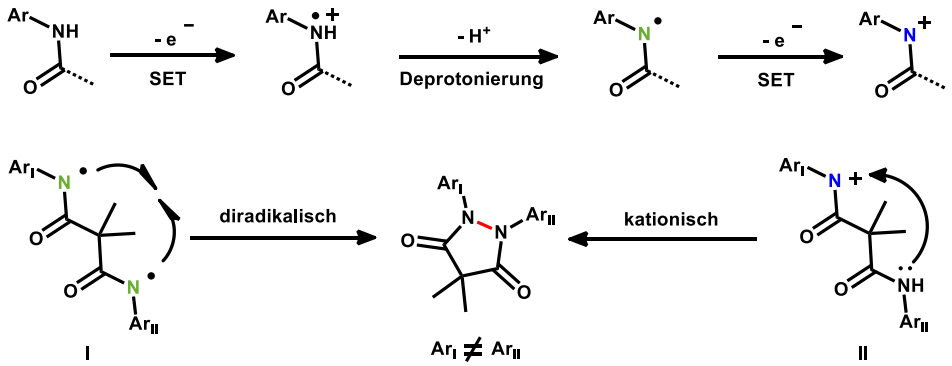

Schema 20: Plausible mechanistische Schritte mit radikalischer (**I**) und kationischer (**II**) N-N-Bindungsbildung.

Damit eine Unterscheidung dieser Pfade möglich ist, ist es wichtig zu wissen, welche Oxidationspotentiale beteiligt sind. Um die Oxidationspotentiale eindeutiger bestimmen zu können, wurden Modelsubstrate (*N*-Pivaloylaniline) mit nur einer Anilidstruktur hergestellt und CV-Studien durchgeführt. Die Absicht dieses Unterfangens war es die Oxidationspotentiale (Radikal und Kation) für individuelle Anilide zu ermitteln (siehe Schema 20, obere Zeile). Nach erfolgten CV-Messungen konnten fast allen Aniliden zwei Oxidationspotentiale zugeordnet werden (Abbildung 6). In diesen Fällen handelte es sich um die Oxidation zum Radikal ($E_{Ox,1}$) und die Folgeoxidation zum Kation ($E_{Ox,2}$), welche sich untereinander im Substitutionsmuster sowie den Substituenten unterschieden. Anschließend wurden Malonsäuredianilide anhand folgender Kriterien hergestellt (Ar_I und Ar_{II} im Schema 20):

- Es sollen nichtsymmetrische, d. h. mit zwei unterschiedlichen Anilinen, Substrate sein, denen idealerweise beide Oxidationspotentiale ($E_{Ox,1}$ für die Bildung des Radikals und $E_{Ox,2}$ für die Bildung des Kations) eindeutig zugeordnet werden können.

- Fall (**I**): Ar_I ($E_{Ox,1}$) & Ar_{II} ($E_{Ox,1}$) < Ar_I ($E_{Ox,2}$) & Ar_{II} ($E_{Ox,2}$)
- Fall (**II**): Ar_I ($E_{Ox,1}$ & $E_{Ox,2}$) < Ar_{II} ($E_{Ox,1}$ & $E_{Ox,2}$)

Somit lassen sich folgende Annahmen für die N-N-Bindungsbildung formulieren:

Fall (I): Falls die Oxidationspotentiale für die Radikalbildung von Anilid A & B (Ar_I und Ar_{II}) ähnlich bzw. die Abstände zu den korrespondierenden Oxidationspotentialen der Kationionenbildung groß genug sind, dann sollte die Diradikalbildung wahrscheinlicher sein.

Fall (II): Wenn die Oxidationspotentiale des Anilids A niedriger sind als die des Anilids B, so ist zu erwarten, dass Anilid A tendenziell zum Kation oxidiert wird und folglich ein kationischer Mechanismus wahrscheinlicher ist.

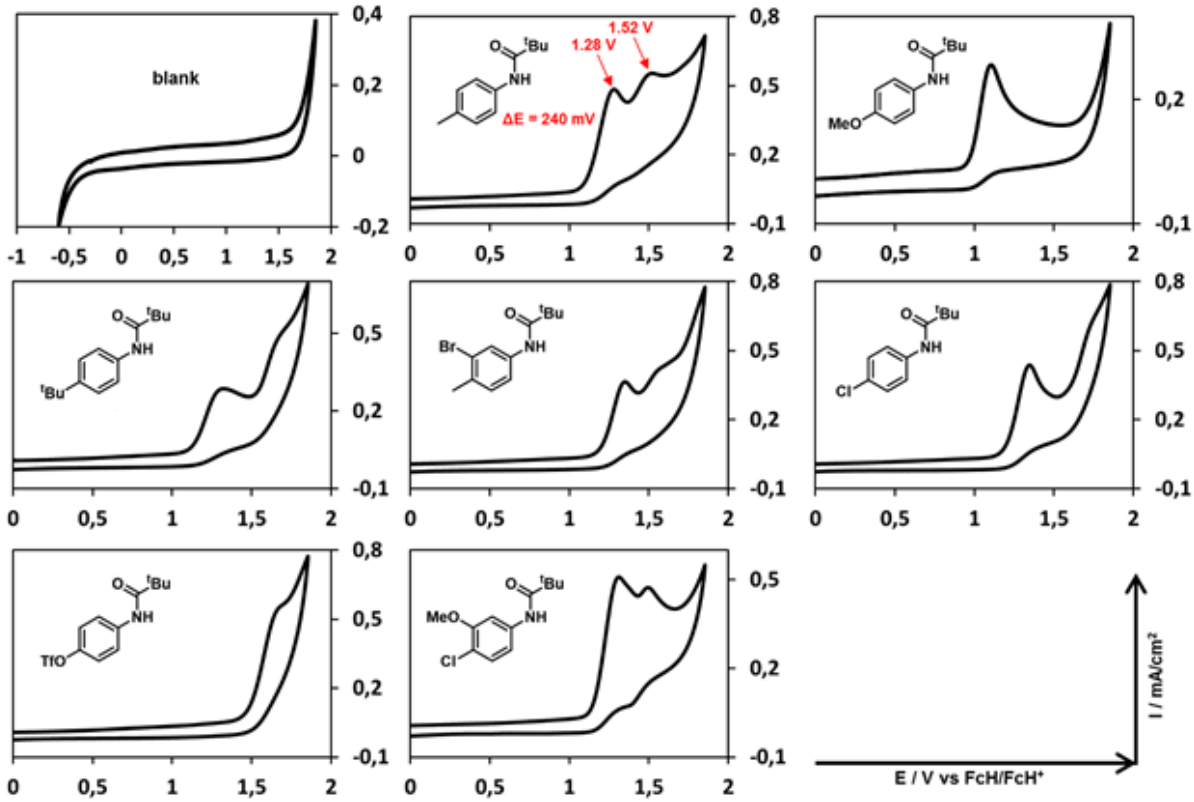

Abbildung 6: Cyclovoltammetische Studien der *N*-Pivaloylanilide zur jeweiligen Bestimmung der Oxidationspotentiale $E_{Ox,1}$ und $E_{Ox,2}$. (Bedingungen: 1 mM Edukt in 0.1 M NBu_4PF_6 (5 mL), Arbeitselektrode und Gegenelektrode: Glaskohlenstoff, Referenzelektrode: Ag/AgCl in gesättigter. LiCl in EtOH, Scangeschwindigkeit: 200 mV/s), finale Referenzierung vs. FcH/FcH+. FcH: Ferrocen.

Es wurde vermutet, dass die N,N-Bindungsbildung diradikalisch abläuft und somit Substrate, die gemäß **Fall I** hergestellt wurden, das gewünschte Produkt ergeben würden. Die Elektrolyseprodukte der gemischten Malonsäuredianilide konnten eindrucksvoll darlegen, dass die getroffenen Vorhersagen richtig waren. Die Substrate, die gemäß **Fall I** hergestellt wurden, resultierten in dem N,N-Produkt als Hauptprodukt. Entsprechend kamen bei den Substraten nach **Fall II** Derivate mit „solvent trapping“ hervor, bei denen hauptsächlich

Protonen am Anilingerüst oder in benzylischer Stellung durch HFIP-Moleküle substituiert wurden (Schema 21).

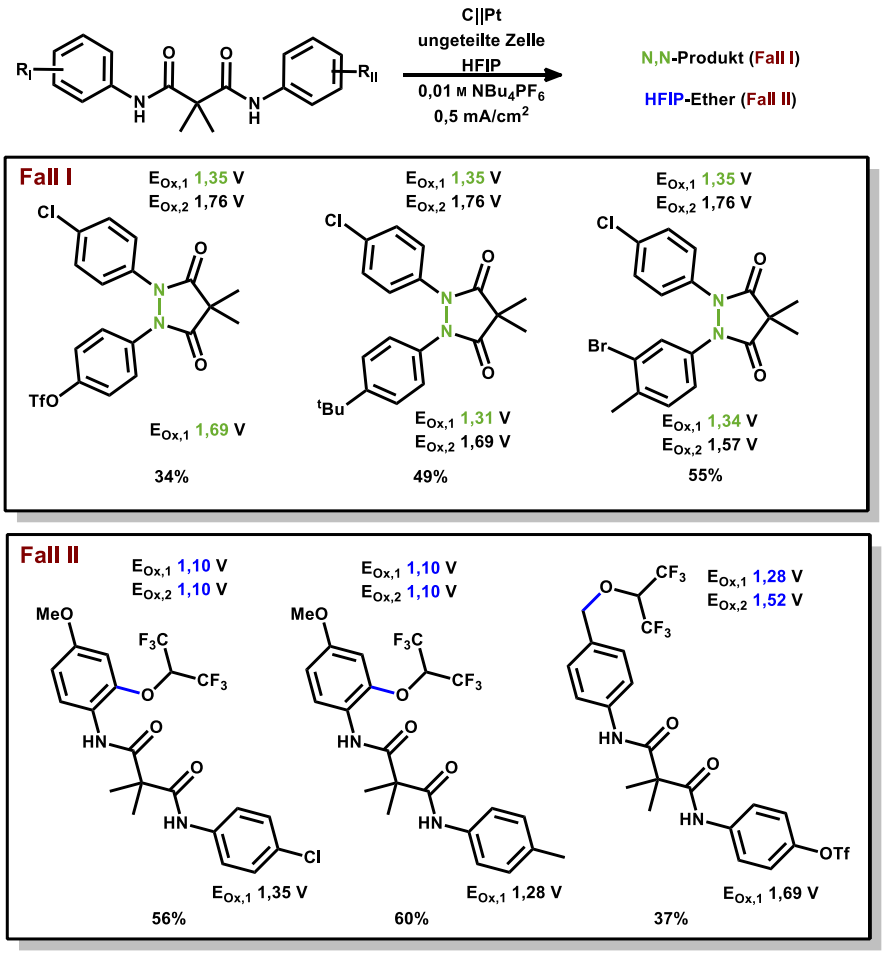

Schema 21: Produkte der Elektrolysen, die gemäß Fall I und II konzipiert wurden. Die ausschlaggebenden Oxidationspotentiale, die im Fall I zur Diradikalbildung und in Fall II zur Kationbildung führten, sind jeweils oben und unten für die entsprechenden Anilide angegeben und grün (radikalisch) oder blau (kationisch) markiert.

Weiterhin wurden diese Erkenntnisse dazu verwendet, um den Mechanismus der Benzoxazolbildung näher zu beleuchten. Während den Arbeiten an der Benzoxazolsynthese brachte eine unerwartete Beobachtung einen wichtigen Hinweis, die die Untersuchung für den Mechanismus anregte. Bei einem *para*-Methylanilid, kam es bevorzugterweise zu der Bildung von HFIP-Ethern, vergleichbar mit den Beispielen für **Fall II** in Schema 21. Das erwartete Benzoxazol ist bei dieser Reaktion nicht entstanden. Dieser Umstand führte zu der Annahme, dass bei der Benzoxazolbildung wahrscheinlich ein kationisches Intermediat vorliegt (Schema 22). Hierbei kann das Amidylkation (**III**) zu einer Deprotonierung in benzylischer Position führen, wodurch ein Azochinonmethid (**IV**) entsteht und anschließend eine nukleophile Addition des Lösungsmittels stattfindet. Daher erscheint die Annahme, dass

Benzoxazole wahrscheinlich über ein Amidylkation gebildet werden, nachdem das Kation eine oxa-NAZAROV-ähnliche Cyclisierung vollzogen hat, plausibel (Schema 22).

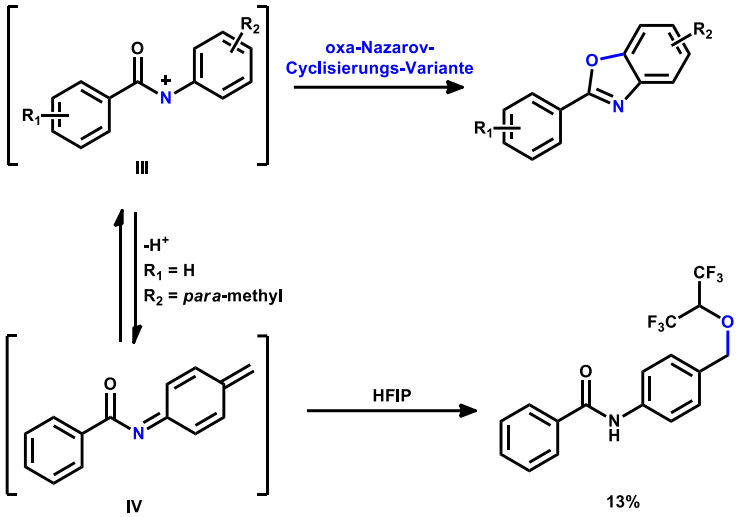

Schema 22: Kationisches Intermediat für die Benzoxazol-Synthese und das "solvent trapping".

Werden Schema 21 Fall II und Schema 22 verglichen, fällt auf, dass das „solvent trapping“ bei der Synthese der Benzoxazole kein Problem darstellt, wie es bei den N-N-Bindungsreaktionen der Dianilide der Fall ist. Dieses Verhalten ist wahrscheinlich darauf zurückzuführen, dass bei den Dianiliden die Bildung der Benzoxazole und die Lösungsmittelreaktion in Konkurrenz stehen. Die Wahrscheinlichkeit für einen Angriff des Carbonylsauerstoffs zur Bildung des Benzoxazols wird herabgesetzt, wenn Dianilide eingesetzt werden. Es scheint, dass durch die Ausbildung von Wasserstoffbrückenbindungen zwischen dem Carbonylsauerstoff und der zweiten Anilidfunktion die Nukleophilie des Carbonylsauerstoffs verringert und folglich der Angriff durch HFIP begünstigt wird.

Erklärung meines Beitrages:

Personenbezogene Daten

3.4 Elektrochemische Synthese von 5-Arylphenanthridin-6-onen durch dehydrierende C-N-Bindungsbildung

Das Manuskript zu diesem Kapitel wurde bereits publiziert.

A. Kehl, V. M. Breising, D. Schollmeyer, S. R. Waldvogel, *Electrochemical Synthesis of 5-Aryl-phenanthridin-6-one by Dehydrogenative N,C Bond Formation*, *Chem. Eur. J.* **2018**, *24*, 17230–17233.

Hintergrund

Nach der erfolgreichen Synthese von heterocyclischen Strukturmotiven via N-N- (Kapitel 3.2) und C-O-Bindungsknüpfung (Kapitel 3.1), wurden weitere Möglichkeiten erwogen, um den vielseitigen Einsatz der Methode durch die Verwendung von Amidylradikalen zu demonstrieren. Erste Untersuchungen bezüglich einer Oxidation von Biphenylcarboxamiden ergaben, dass die Synthese von 5-Arylphenanthridin-6-onen mittels einer 6-endo-trig Cyclisierungsreaktion, die aus der Oxidation einer Amidfunktionalität hervorgeht, möglich ist (Schema 23).

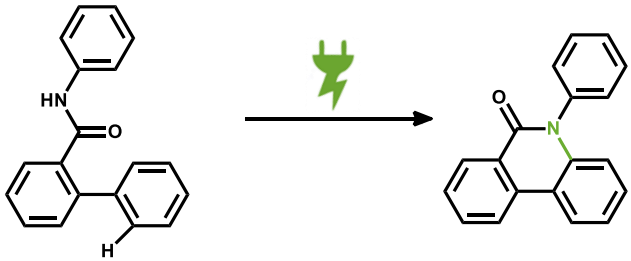

Schema 23: Elektrochemisch induzierte 6-endo-trig Cyclisierung von Biphenylcarboxamiden mittels einer C-N-Bindungsbildung.

Dadurch ist neben der N-N-Bindung auch eine C-N-Bindungsreaktion über die Amidylradikale zugänglich. Im Allgemeinen kommen Phenanthridin-6-one in Naturstoffen vor und besitzen biologische Aktivität.[99]

Der erste elektrochemische Zugang zu Phenanthridin-6-onen wurde in den 1970er Jahren von GRIMSHAW und MANNUS realisiert und bediente sich einer intramolekularen reduktiven C-C-Bindungsknüpfung zwischen zwei Arenen.[100] Durch wenige Beispiele, die notwendige Abgangsgruppe, den teuren (Platin) sowie giftigen (Quecksilber) Elektroden, einem potentiostatischen Aufbau mit einer geteilten Zellgeometrie war der Ansatz allerdings nur wenig attraktiv. ZHANG *et al.* griffen auf Biphenyl-2-carboxamide als Substrate zurück, jedoch

beschränkten sich die Amide auf *N*-acyloxy- oder *N*-pivaloyloxy-geschützte Substrate.[101] Es wurde ein Brom-mediiertes System in einer ungeteilten Zelle unter galvanostatischen Bedingungen verwendet. Jedoch leidet dieser Ansatz unter einer niedrigen Stromausbeute von 40% und der Notwendigkeit für 100–200 mol% an Mediator (NaBr).

Ergebnisse

Die Herstellung der Substrate konnte in nur zwei unkomplizierten Schritten erfolgen: Zunächst wurde ein Benzanilid mittels Oxalyldichlorid und einer anschließenden Kondensation mit einem Anilin vorbereitet, welches anschließend in einer nachgelagerten SUZUKI-Kupplung mit substituierten 2-Brombenzoesäure umgesetzt wurde (Schema 24).

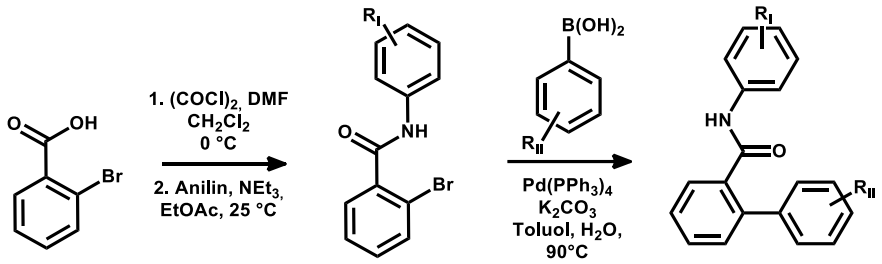

Schema 24: Synthesestrategie der *N*-Arylbiphenyl-2-carboxamide über Benzanilide (mittig) als Zwischenstufe.

Nach der Eduktsynthese wurde der elektrochemische Schlüsselschritts optimiert. Hierbei stachen isostatisches Graphit (Anode) und Nickel (Kathode) (Ausbeute: 85%) als günstige und effektive Elektrodenmaterialien heraus. Sollte eine metallfreie Umgebung gefordert sein, kann die Nickelkathode problemlos und ohne großen Ausbeuteverlust durch isostatisches Graphit ersetzt werden. Die optimierten Bedingungen dienten zur Synthese einiger Derivate, die überwiegend gute bis sehr gute Ausbeuten von bis zu 85% erzielten (Schema 25). Zudem wurde die Reaktion an einem Beispiel in einer 80 mL Glasbecherzelle im Gramm-Maßstab erfolgreich durchgeführt, womit die Möglichkeit einer Hochskalierung nachgewiesen werden konnte. Schwach elektronenschiebende (z. B. -Chlor, -Brom, -Iod) und stark elektronenziehende Gruppen (z. B. -Cyano, -Nitro und -Ester) lassen sich problemlos und in Ausbeuten bis 85% herstellen (Schema 25). Stark elektronenschiebende funktionelle Gruppen wie -Methoxy, die am Anilinkörper eingeführt wurden, reagierten unter Zersetzung und zeigten keinerlei Produktbildung. Benzylische Positionen am Biphenylgerüst sorgten für ein komplexes Produktgemisch, darunter auch HFIP-Ether.

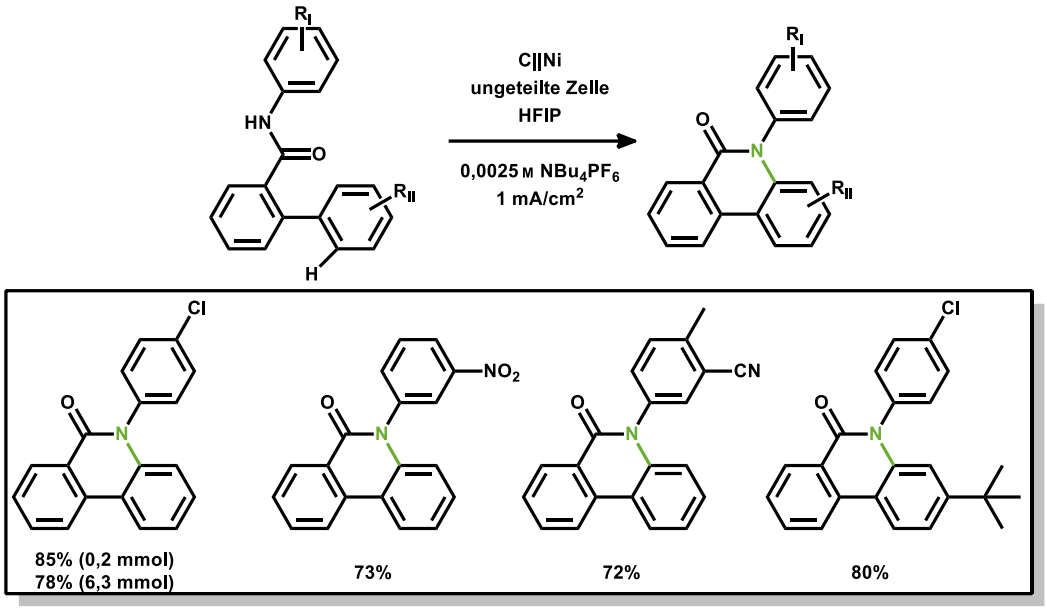

Schema 25: Synthese von 5-Arylphenanthridin-6-onen und einer Auswahl an Derivaten.

Die Oxidation von Alkylamiden, die bei deutlich höheren Oxidationspotentialen zu erwarten sind,[102] resultierte in einer C-O-Bindungsbildung, welche nach der Standardaufarbeitung 6*H*-benzo[c]chromen-6-on ergab (Schema 26). Allerdings genügte die Standardaufarbeitung nicht, um das resultierende Lacton vollständig zu isolieren, da es sich auf dem Säulenmaterial langsam zersetzte und dadurch ein Produktgemisch erhalten wurde. Allerdings konnten saubere Fraktionen mit 35% Produkt erhalten werden. Da es sich hierbei immer um das gleiche Lacton handelte, wurde auf eine erneute Isolierung mit den anderen Amidresten verzichtet. Diese Reaktion könnte das Ergebnis einer Oxidation des Biphenylgerüsts und eines darauffolgenden nukleophilen Angriffs des Carbonylsauerstoffs am Aromaten sein.

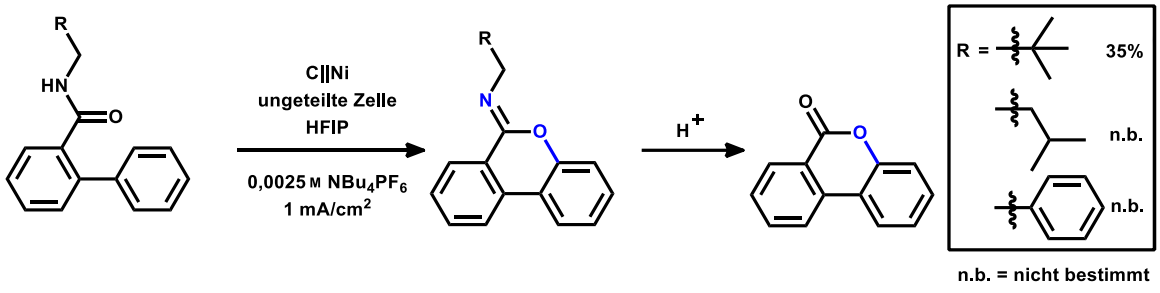

Schema 26: Beobachtete Limitierung der untersuchten Substratbreite der Alkylamide.

CV-Untersuchungen legen die Vermutung nahe, dass sich diese Reaktion ebenfalls auf eine radikalische Bindungsknüpfung stützt, da die beiden Oxidationssignale, die jeweils im CV zu sehen sind, der Amidfunktion (aufgrund einiger Übereinstimmungen mit den Daten aus Kapitel 3.3) zugeordnet werden können. Aufgrund des erfolgreichen Umsatzes von

Substraten mit stark elektronenziehenden Substituenten, wodurch eine Oxidation erschwert wird, ist eine Oxidation des Biphenyls als initiierender Schritt unwahrscheinlich.

Erklärung meines Beitrages:

Personenbezogene Daten

3.5 Elektrochemische Synthese von Carbazolen mittels einer dehydrierenden Kupplungsreaktion

Das Manuskript zu diesem Kapitel wurde bereits publiziert.

A. Kehl, N. Schupp, V. M. Breising, D. Schollmeyer, S. R. Waldvogel, *Electrochemical Synthesis of Carbazoles by Dehydrogenative Coupling Reaction*, *Chem. Eur. J.* **2020**, *in press*.

Hintergrund

In diesem Projekt ging es darum das Syntheseportfolio der etablierten Methode unter Ausnutzung von anodisch generierten Amidylradikalen auf die Synthese von Carbazolen auszuweiten. Inspiriert durch die Transformation von Biphenyl-2-carboxamiden zu 5-Arylphenanthridin-6-onen (Schema 25), wurde ein leichter Zugang zu Carbazolen erkannt und ein geeigneter Syntheseweg entwickelt (Abbildung 7). Carbazole sind wertvolle Strukturbausteine, die in Naturstoffen vorkommen,[103,104] biologische Aktivität aufweisen und damit pharmakologische Anwendung finden,[105] sowie im technischen Sektor beispielsweise in Form von Polymeren als Lochleitungsschicht in OLEDs ihre Berechtigung genießen.[4,106] Über die Zeit wurden etliche Synthesestrategien entwickelt, die auf die unterschiedlichsten Vorläufermoleküle zurückgreifen.[104] Der für unsere Zwecke dienliche Schlüsselschritt bestand in der N-C-Bindungsbildung, ausgehend von einer 2-Aminbiphenylstruktur. (Abbildung 7).

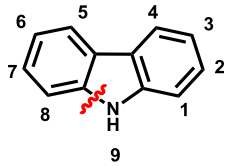

Abbildung 7: Retrosynthetischer Ansatz für den Schlüsselschritt zur Carbazol-Synthese.

Bisher ist noch kein direkter elektrochemischer Zugang zu dieser Verbindungsklasse bekannt. Hierbei spielt die Labilität von Carbazolen bezüglich elektrochemischer Bedingungen eine wichtige Rolle. Grundsätzlich sind die Positionen 3, 6 und 9 oxidationslabil und folglich an diesen Stellen Nebenreaktionen (Dehydrodimerisierung, etc.) zu erwarten.[107] Um diese Nebenreaktionen zu vermeiden, bediente sich der erste elektrochemische Ansatz dieser

Reaktion, welcher von NISHIYAMA *et al.* entwickelt wurde, eines *ex cell*-Konzepts.[79] Hierbei wurden durch elektrochemische Oxidation hypervalente Iod(III)-Spezies generiert und anschließend dem Substrat zugegeben. Der abreagierte Iodaromat konnte isoliert werden und stand somit für die nächste Oxidation bereit. FRANCKE *et al.* verfeinerten dieses Konzept und kombinierten das Leitsalz und die Iod-Spezies zu einer Struktur.[77] POWERS *et al.* gingen noch einen Schritt weiter, indem sie das Iodaromat-Konzept aufgriffen und eine mediierte potentiostatische Synthesemethode vorstellten.[108] In dieser Methode wurde die hypervalente Iod(III)-Spezies *in situ* hergestellt und eine Überoxidation des Produkts durch die potentiostatischen Bedingungen unterdrückt. Die oben erwähnten Methoden haben entscheidende Nachteile, die eine Verwendung über den Labormaßstab hinaus unwahrscheinlich machen (*ex cell*-Konzept, Mediator, teure Elektrodenmaterialien und/oder einen potentiostatischen Aufbau). Der nächste Entwicklungsschritt, der einen Großteil der Nachteile eliminieren soll, sieht den Übergang zur direkten anodischen Oxidation vor.

Resultate

Die Vorläufermoleküle können über eine hochmodulare Syntheseroute erstellt werden: Hierbei kann das gewünschte Substitutionsmuster eingeführt und dabei auf breite kommerziell verfügbare Grundbausteine zurückgegriffen werden. Ausgehend von 2-Bromanilinen wurde in einer SUZUKI-Kupplung das Biphenylgerüst aufgebaut und in einer nachgeschalteten Kondensationsreaktion mit Benzoylchlorid die Amingruppe zum Amid funktionalisiert, überwiegend mit Ausbeuten von ca. 80% in zwei Stufen.

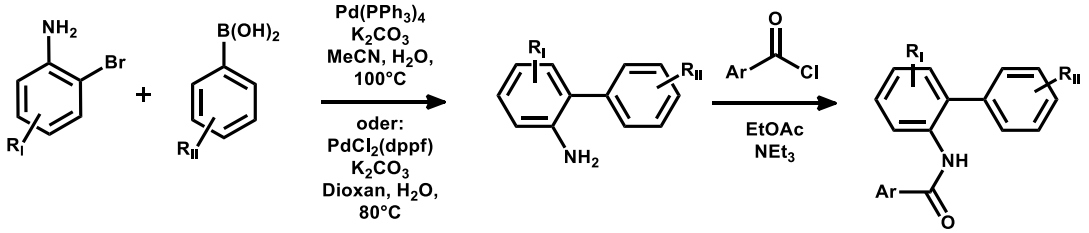

Schema 27: Syntheseroute für die Vorläufermoleküle.

Zur Optimierung des Schlüsselschritts, der eine 5-endo-trig Cyclisierung mittels einer C-N-Bindungsbildung zum Carbazol vorsieht, wurden zunächst die Bedingungen der Phenanthridin-6-one (Kapitel 3.4) herangezogen. Die Reaktion wurde im Hinblick auf den Einfluss von Lösungsmitteln, Leitsalzen, Elektrodenmaterialien und Stromdichten untersucht. Es wurde zunächst ein Lösungsmittelgemisch [a] HFIP mit 15% H_2O verwendet, um einen vollständigen Umsatz bei möglichst geringer Ladungsmenge zu erzielen. Eine geringe

Ladungsmenge, die sich nahe der theoretischen Ladungsmenge befindet, ist wichtig, da auf diesem Wege die Überoxidation des Produkts auf ein Minimum reduziert werden kann und die Stromausbeute erhöht wird. Zudem wurde mit der Zugabe des Wassers eine Absenkung des Oxidationspotentials in CV-Studien beobachtet, was zu einer Erklärung des besseren Umsatzes beiträgt (siehe Anhang A245 und A246). Unter Applizierung der zuvor optimierten Bedingungen wurden 16 unterschiedliche Substrate für die elektrochemische Synthese der entsprechenden Carbazole initiiert, welche in Ausbeuten von bis zu 86% hergestellt werden konnten.

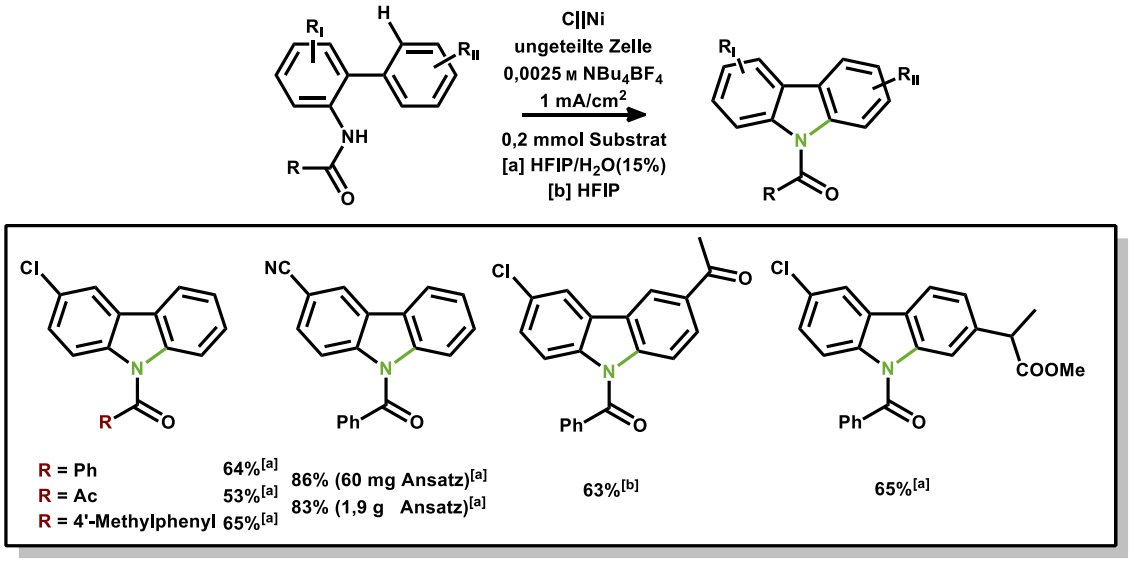

Schema 28: Auswahl an Derivaten (inklusive des N-geschützten Wirkstoffs Carprofen (1. von rechts), die mittels dehydrierender C-N-Bindungsbildung erfolgreich hergestellt wurden.

Es konnte beobachtet werden, dass bei manchen Substraten der Wasserzusatz von 15% mit Umsatzeinbrüchen einherging. Dies konnte vermieden werden, indem auf den Wasserzusatz verzichtet wurde (Einsatz von [b] HFIP). Des Weiteren konnten die CV-Daten in Kombination mit synthetischen Bemühungen einen guten Einblick dahingehend verschaffen, dass die Bildung des Amidylradikals eine wichtige Rolle bei dem Umsatz des Substrats spielt. Denn beim Einsatz von stark elektronenziehenden Komponenten, wie etwa einem Pyridingerüsts anstelle des Anilinkörpers, konnte keine Oxidation unter den angelegten Bedingungen festgestellt und das Edukt fast vollständig zurückgewonnen werden (Schema 29). Das Cyclovoltammogramm dieser Verbindung bestätigt diesen Sachverhalt, indem kein Oxidationssignal in dem untersuchten Potentialfenster beobachtet werden konnte.

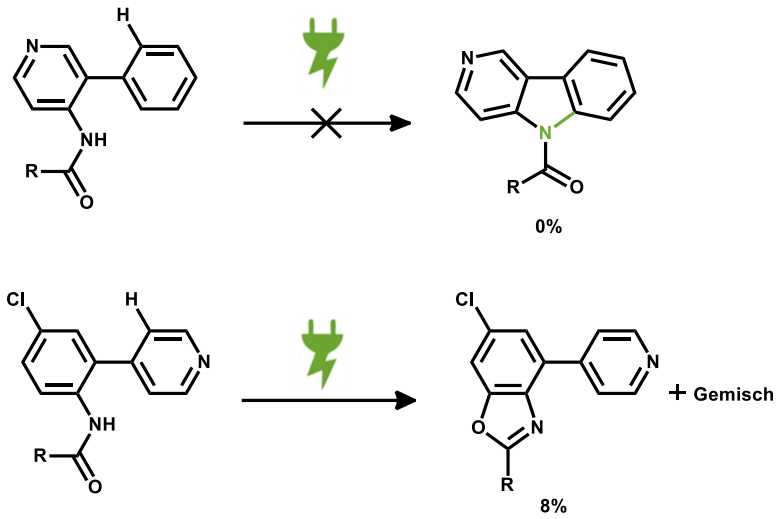

Schema 29: Stark desaktivierende Substrate, die direkt mit der Amidfunktion verbunden sind, verhindern die Oxidation des Amids (oben). Stark desaktivierende Funktionen am benachbarten Ring ermöglichen die Oxidation des Amids, verhindern allerdings die Bildung des Carbazols bzw. *β*-Carbolins (unten).

Weiterhin konnte in manchen Fällen eine Konkurrenzreaktion in Form einer Benzoxazolbildung beobachtet werden. Dies trat immer dann auf, wenn der Umsatz unzureichend und langsam verlief (teilweise bei Substraten, die ohne Wasserzusatz keinen vollständigen Umsatz zeigten oder stark desaktiviert sind (Schema 29, unten)). Dieses Verhalten spricht dafür, dass die Transformation zum Carbazol vor allem radikalisch ablaufen sollte, da die Benzoxazolbildung mit hoher Wahrscheinlichkeit einem kationischen Mechanismus folgt. Ferner wurde die Skalierbarkeit der Reaktion in einer 80 mL Becherglaszelle demonstriert. Zudem erlaubt diese Methode die Herstellung von wertvollen Verbindungen wie dem geschützten Naturstoff Glycozolin (40%) oder dem nichtsteroidalen Antiphlogistikum Carprofen (Elektrolyse: 65%; Deblockierung: 92%, Gesamtausbeute über drei Stufen 56%). Die Entschützung erfolgt einfach und schnell durch Erhitzen unter Rückfluss in Methanol und Zugabe von Natriumhydroxid. Somit konnte eine direkte elektrochemische Methode entwickelt werden, die Carbazole auf einfachem Wege zugänglich macht, ohne hypervalente Iodreagenzien auskommt und durch den simplen Aufbau potenziell für größere Maßstäbe eingesetzt werden kann.

Erklärung meines Beitrages:

Personenbezogene Daten

4 Zusammenfassung

Im Rahmen dieser Arbeit konnten Syntheserouten für diverse heterocyclische Strukturen wie Benzoxazolen, Pyrazolidin-1,4-dionen, Phenanthridin-6-onen und Carbazolen gefunden werden. Zudem konnte zur Aufklärungsarbeit bezüglich der mechanistischen Vorgänge beigetragen werden. Die ursprüngliche Herangehensweise an die N-N-Bindungsknüpfung für 6-Ringheterocyclen erlaubte es mittels einer unerwarteten C-O-Bindungbildung über eine 5-endo-trig Cyclisierung Benzoxazole zu generieren. Nach einer gezielten Modifikation der Substrate konnten die entsprechenden Monoanilide in zwei unterschiedlichen Elektrolyse-Konfigurationen (paralleler und gewinkelter Elektrodenaufbau) selektiv zum gewünschten Produkt umgesetzt werden (Schema 30).

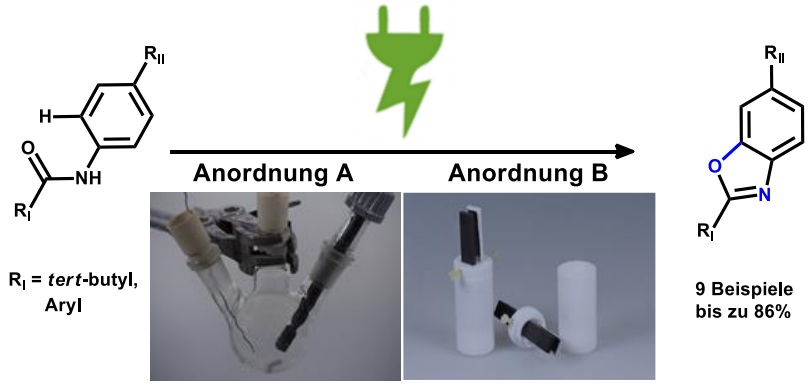

Schema 30: Synthese von Benzoxazolen mittels anodischer C-O-Bindungsknüpfung.

Die Herstellung von 6-gliedrigen N-Heterocyclen gelang anschließend, indem ein Gerüst mit sp^2-Charakter (Phthalsäuregerüst) und damit einer Vorkoordination gewählt wurde, wodurch eine Vielzahl an Phthalazin-1,4-dion-Derivaten zugänglich waren (Schema 31).

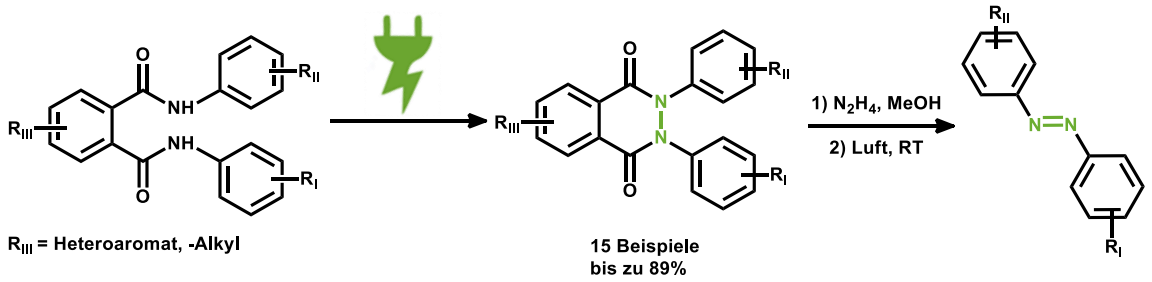

Schema 31: Elektrochemische Synthese von Phthalazin-1,4-dionen mit optionaler Weiterreaktion zur Freisetzung von Azobenzolen.

Dadurch sind symmetrische, nicht-symmetrische sowie Dianilide mit substituiertem Phthalsäuregerüst zugänglich. Zusätzlich kann eine Azobenzoleinheit aus dem erzeugten

Produkt freigesetzt werden, wenn in einem gesondertem Schritt Hydrazin als Nukleophil einsetzt wird.

Gleichzeitig wurde eine Mechanismusaufklärung am Beispiel der Pyrazolidin-3,5-dion-Derivate vorangetrieben, bei der CV-Studien und Synthese zur Aufklärung der N-N-Bindungsbildung kombiniert wurden. Dabei zeigte sich, dass die N-N-Bindung überwiegend über einen diradikalischen Mechanismus erfolgen muss (Schema 32, grüner Pfad). Darüber hinaus ließen die Resultate Rückschlüsse auf den Mechanismus der Benzoxazolbildung zu, gemäß denen die C-O-Bindungsknüpfung aller Wahrscheinlichkeit nach auf einem kationischen Mechanismus mit einer nachgelagerten oxa-NAZAROV-ähnlichen Cyclisierung beruht (Schema 32, blauer Pfad).

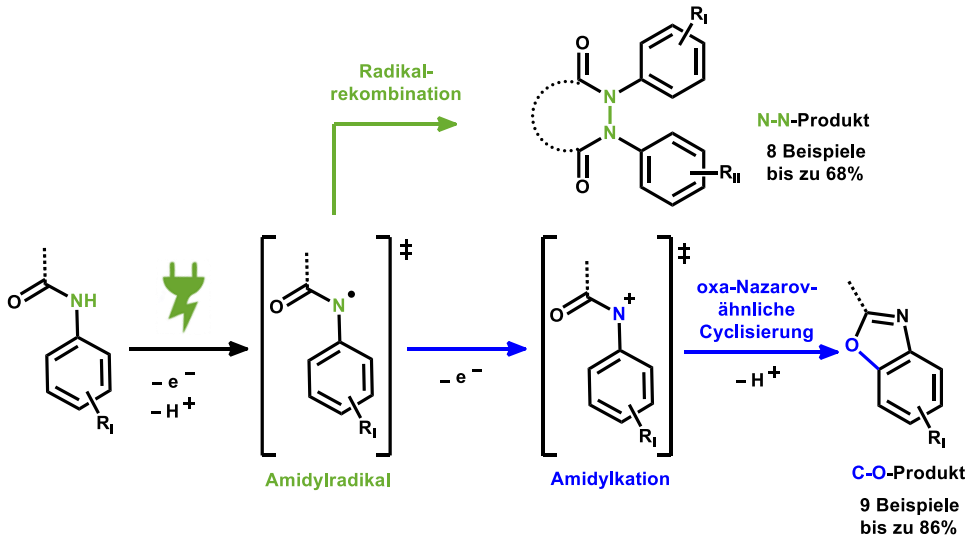

Schema 32: Wahrscheinliche Reaktionspfade für N-N- und C-O-Bindungsknüpfungen.

Nach den erworbenen Erkenntnissen wurden Möglichkeiten zur C-N-Bindungsknüpfung untersucht. Dabei stellte sich heraus, dass durch die Oxidation von *N*-Aryl-2-carboxamiden durch eine 6-endo-trig Cyclisierung 5-Arylphenanthridin-6-one in Ausbeuten von bis zu 85% aufgebaut werden können (Schema 33).

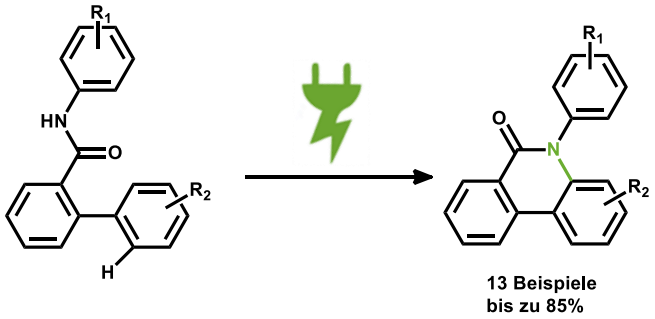

Schema 33: Elektrochemischer Zugang zu 5-Arylphenanthridin-6-onen.

CV-Untersuchungen und die Erfahrung aus den mechanistischen Studien legen die Vermutung nahe, dass es sich bei dieser Reaktion überwiegend um eine radikalische Bindungsknüpfung handelt.

Schließlich wurde, inspiriert durch die vorangegangene C-N-Bindungsknüpfung, eine Möglichkeit zur Synthese von Carbazolen entwickelt. Ausgehend von 2-Benzamidbiphenylen kann durch anodische Oxidation in Ausbeuten von bis zu 86% die Synthese von N-geschützten Carbazolen über eine 5-endo-trig Cyclisierung erfolgen (Schema 34). Zudem ist die Skalierbarkeit mühelos durchführbar und der Zugang zu den freien Carbazolen dank einer simplen und kostengünstigen Entschützungsmöglichkeit (Schema 34) gegeben. Dadurch sind Naturstoffe wie Glycozolin oder Wirkstoffe wie Carprofen (Elektrosynthese: 65%; Entschützung: 92%) durch diese unkomplizierte Methode darstellbar. Auch hier konnten CV-Studien einen radikalischen Reaktionsmechanismus bekräftigen.

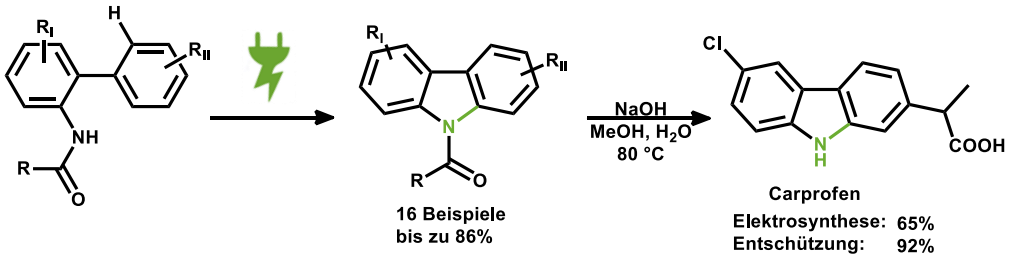

Schema 34: Carbazol-Synthese mittels anodischer Oxidation von Amiden und der Entschützungsschritt.

5 Ausblick

Auf der Grundlage der in dieser Arbeit vorgestellten synthetischen Zugänge, ergeben sich weitere Ansatzpunkte für heterocyclische Strukturen. Ein vielversprechender 5-Ringheterocyclus ist Indolin-2-on, welches in Naturstoffen oder in Pharmaka vertreten ist.[109] Die entsprechenden Säuren sind kommerziell erhältlich und können mühelos in die gewünschten Anilide überführt werden. Alternativ können die Säuren durch elektrochemische Carboxylierung von Benzylhalogeniden hergestellt werden, um damit auch die Praktikabilität der organischen Elektrosynthese zu unterstreichen.[110]

Eine denkbare Herangehensweise beruht auf den 2-Arylethansäureamiden. Durch eine C-N-Bindungsbildung (5-endo-trig Cyclisierung) könnte dabei das gewünschte Indolin-2-on entstehen (Schema 35, links). Alternativ wäre der Zugang basierend auf 2-Aryl-2-methylpropansäureamiden möglich, da die beiden Methylgruppen erfahrungsgemäß durch den Thorpe-Ingold-Effekt zur Vorkoordination beitragen und Nebenreaktionen in Benzylstellung verhindern (Schema 35, rechts).

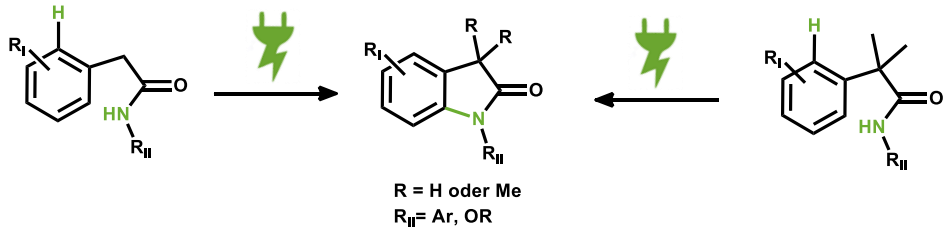

Schema 35: Denkbare Zugänge zu Indolin-2-on-Derivaten.

Die elektrochemische Amidylradikal-induzierte 6-endo-dig Cyclisierung biete eine Möglichkeit der Chinolin-2-on-Synthese (Schema 36). Chinolinone sind wertvolle Strukturen, die durch ihre bioaktiven Eigenschaften vor allem als Wirkstoffe in Pharmaka Anwendung finden können.[111] Durch den Einsatz von den kommerziell verfügbaren Zimtsäuren oder deren Herstellung mittels einer KNOEVENAGEL-Reaktion (DOEBNER-Variante), können mittels Thionylchlorid und anschließender Kondensation mit einem Anilin in das Zimtsäureamid transformiert werden.

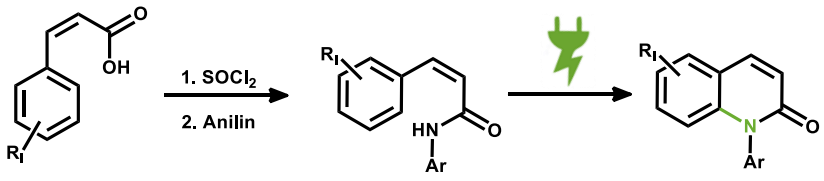

Schema 36: Synthesepfad zu Chinolin-2-on-Derivaten.

Basierend auf den Kenntnissen aus der Synthese von Phenanthridin-6-onen wäre eine Cyclisierung von Amidylradikalen an sp^3-Zentren interessant, um so Isoindolinone zu erhalten. Dieses Strukturmotiv zeigt biologische Aktivität, weshalb ein leichter Zugang wertvoll wäre.[112] Vor dieser 5-endo-tet Cyclisierung könnte ein 1,5-Wasserstoffatomtransfer (1,5-HAT) erfolgen (Schema 37).[101,113] Die Benzoesäure-basierten Derivate könnten etwa durch eine KUMADA- oder NEGISHI-Kupplung bereitgestellt werden. Eine Vielzahl an Derivaten ist auch kommerziell erhältlich. Alternativ ist auch eine Synthese via einem 1-Brom-2-alkylbenzol mit CO_2 und *n*-Butyllithium denkbar.[114]

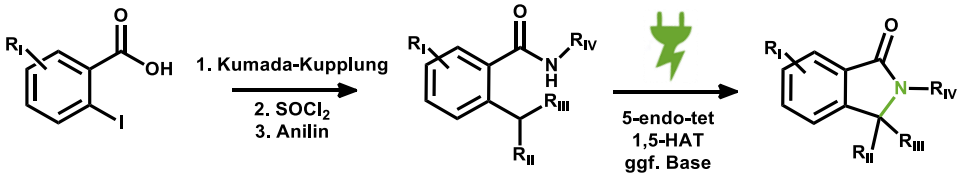

Schema 37: Synthesepfad zu Isoindolinon-Derivaten.

Benzodiazepine sind bekannte Strukturen und finden als pharmazeutische Wirkstoffe Anwendung.[115] Die Erweiterung der elektrochemischen Methode um die Bildung von 7-gliedrigen Heterocyclen wäre dadurch möglich. Ein vielversprechender Ansatz basiert auf der Funktionalisierung eines Benzophenons und/oder eines Benzophenonimins. Die entsprechende Synthesesequenz sähe hierbei einen Transiminierungsschritt am Benzophenonimin mit einem Aminosäureester/-amid vor (Schema 38).[116] Sollte das Amid nicht direkt einführbar sein, so kann es durch nachfolgende Funktionalisierung geschehen. Anschließend kann eine 7-endo-trig Cyclisierung durch eine anodische C-N Bindungsbildung erfolgen (Schema 38).

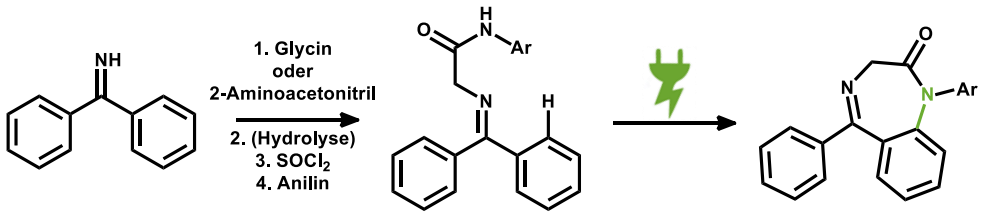

Schema 38: Syntheseroute zu Benzodiazepinen.

Aus den Resultaten der Carbazole ging hervor, dass sich unter den verwendeten Bedingungen kein *β*-Carbolin bilden ließ. Die cyclovoltammetrischen Studien haben allerdings gezeigt, dass eine Oxidation des entsprechenden Substrates möglich ist. Durch angepasste Bedingungen könnte eine Route zu den *β*-Carbolinen mittels einer 5-endo-trig Cyclisierung gefunden

werden (Schema 39). Viele Alkaloide beinhalten diese Struktur und zeigen oft biologische Aktivität.[117]

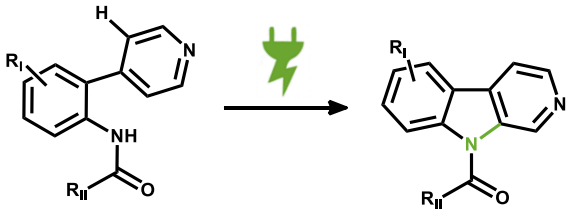

Schema 39: Mögliche Syntheseroute zu *β*-Carbolin-Strukturen.

Abschließend ist zu erwähnen, dass neben der Erweiterung der Produktpalette der elektrochemischen Methode auch eine allgemeine Untersuchung von anderen N-Schutzgruppen, die die Generierung von N-zentrierten Amidylkationen erlauben, durchgeführt werden soll. So diente in dem Fall von ZHANG *et al.* eine Acetyloxy- oder Pivaloyloxy-Funktion als Schutzgruppe für das Amid zur Bildung von Phenanthridin-6-on-Derivaten.[101] Diese Gruppen haben den Vorteil, dass sie eine Benzoxazolbildung strukturbedingt verhindern (da kein Aromat bzw. Olefin für eine oxa-NAZAROV-ähnliche Cyclisierung zur Verfügung steht) und dadurch einen kationischen Pfad, zumindest theoretisch erlauben. Der somit frei zugängliche kationische Pfad wäre auf vielfältige Weise einsetzbar und nicht mehr auf oxa-NAZAROV-Variante beschränkt (Schema 32, blauer Pfad). So ließe sich das leere p-Orbital des Amidylkations, auch mit besetzten nichtbindenden Orbitalen von benachbarten Heteroatomen (z. B. Methoxy-, Acetyloxy- oder Pivaloyloxygruppen) stabilisieren.[20] Daher sollte eine Eignung solcher Schutzgruppen auf die direkte anodische Oxidation überprüft werden. Eine Schwierigkeit könnte darin liegen, diese funktionellen Gruppen (aufgrund eines hohen Oxidationspotentials) zur Oxidation zu bewegen, weshalb in der Literatur Mediatoren verwendet werden.[20,101,118] Jedoch kann dieses Problem durch eine geeignete Wahl der Elektroden, Elektrolyte, etc. überwunden werden.

6 Literatur

[1] E. Vitaku, D. T. Smith, J. T. Njardarson, *J. Med. Chem.* **2014**, *57*, 10257–10274.

[2] E. A. Ilardi, E. Vitaku, J. T. Njardarson, *J. Chem. Educ.* **2013**, *90*, 1403–1405.

[3] A. Mullard, *Nat. Rev. Drug Discov.* **2020**, *19*, 79–84.

[4] S. K. Schrader, *Proc. SPIE* **2003**, *4991*, 45−63.

[5] a) M. Thelakkat, H.-W. Schmidt, *Polym. Adv. Technol.* **1998**, *9*, 429–442; b) W. Li, J. Li, M. Wang, *Isr. J. Chem.* **2014**, *54*, 867–884.

[6] a) B. Lucas, T. Trigaud, C. Videlot-Ackermann, *Polym. Int.* **2012**, *61*, 374–389; b) Q. Miao, *Adv. Mater.* **2014**, *26*, 5541–5549; c) W. Zhang, Y. Liu, G. Yu, *Adv. Mater.* **2014**, *26*, 6898–6904; d) B. J. Jung, N. J. Tremblay, M.-L. Yeh, H. E. Katz, *Chem. Mater.* **2011**, *23*, 568–582; e) Z. Yi, S. Wang, Y. Liu, *Adv. Mater.* **2015**, *27*, 3589–3606.

[7] a) C. Liu, K. Wang, X. Gong, A. J. Heeger, *Chem. Soc. Rev.* **2016**, *45*, 4825–4846; b) Q. Li, Z. Jiang, J. Qin, Z. Li, *Aust. J. Chem.* **2012**, *65*, 1203.

[8] A. Baeyer, V. Drewsen, *Ber. Dtsch. Chem. Ges.* **1882**, *15*, 2856–2864.

[9] a) G. H. Elgemeie, M. H. Helal, H. M. El-Sayed, *Pigment. Resin Technol.* **2001**, *30*, 210–228; b) M. A. Weaver, L. Shuttleworth, *Dyes Pigm.* **1982**, *3*, 81–121; c) A. D. Towns, *Dyes Pigm.* **1999**, *42*, 3–28.

[10] a) J. Seixas de Melo, A. P. Moura, M. J. Melo, *J. Phys. Chem. A* **2004**, *108*, 6975–6981; b) Jose-Yacaman, Rendon, Arenas, P. M. C. Serra, *Science* **1996**, *273*, 223–225.

[11] J. H. Ziegler, M. Locher, *Ber. Dtsch. Chem. Ges.* **1887**, *20*, 834–840.

[12] "Regulation (EC) No 1333/2008 of the European Parliament and of the council of 16 December 2008 on food additives (OJ L 354 31.12.2008, p. 16)", http://data.europa.eu/eli/reg/2008/1333/2020-03-25 (Aufgerufen am 18.06.2020).

[13] a) P. Ruiz-Castillo, S. L. Buchwald, *Chem. Rev.* **2016**, *116*, 12564–12649; b) M. Kaur, R. Kumar, *ChemistrySelect* **2018**, *3*, 5330–5340; c) F. Ferretti, D. R. Ramadan, F. Ragaini, *ChemCatChem* **2019**, *11*, 4450–4488; d) A. Y. Sukhorukov, *Front. Chem.* **2020**, *8*, 215; e) P. Thansandote, M. Lautens, *Chem. Eur. J.* **2009**, *15*, 5874–5883; f) X.-X. Guo, D.-W. Gu, Z. Wu, W. Zhang, *Chem. Rev.* **2015**, *115*, 1622–1651.

[14] a) J. Yamaguchi, A. D. Yamaguchi, K. Itami, *Angew. Chem. Int. Ed.* **2012**, *51*, 8960–9009; *Angew. Chem.* **2012**, *124*, 9092–9142; b) W. R. Gutekunst, P. S. Baran, *Chem. Soc. Rev.* **2011**, *40*, 1976–1991; c) L. McMurray, F. O'Hara, M. J. Gaunt, *Chem. Soc. Rev.* **2011**, *40*,

1885–1898; d) J. D. Hayler, D. K. Leahy, E. M. Simmons, *Organometallics* **2019**, *38*, 36–46.

[15]L. Angelini, J. Davies, M. Simonetti, L. Malet Sanz, N. S. Sheikh, D. Leonori, *Angew. Chem. Int. Ed.* **2019**, *58*, 5003–5007; *Angew. Chem.* **2019**, *131*, 5057–5061.

[16]M. Taillefer, D. Ma, *Amination and Formation of sp2 C-N Bonds*, Springer-Verlag, Berlin/Heidelberg, **2013**.

[17]G. Altenhoff, F. Glorius, *Adv. Synth. Catal.* **2004**, *346*, 1661–1664.

[18]D.-Y. Goo, S. K. Woo, *Org. Biomol. Chem.* **2016**, *14*, 122–130.

[19]a) P. J. Borpatra, B. Deka, M. L. Deb, P. K. Baruah, *Org. Chem. Front.* **2019**, *6*, 3445–3489; b) Q. Guo, Z. Lu, *Synthesis* **2017**, *49*, 3835–3847; c) T.-S. Mei, L. Kou, S. Ma, K. M. Engle, J.-Q. Yu, *Synthesis* **2012**, *44*, 1778–1791; d) M. Zhang, A.-Q. Zhang, Y. Peng, *J. Organomet. Chem.* **2013**, *723*, 224–232; e) Z. Zheng, D. Zhang-Negrerie, Y. Du, K. Zhao, *Sci. China Chem.* **2014**, *57*, 189–214.

[20]S. Maiti, M. T. Alam, A. Bal, P. Mal, *Adv. Synth. Catal.* **2019**, *361*, 4401–4425.

[21]M. Suri, T. Jousseaume, J. J. Neumann, F. Glorius, *Green Chem.* **2012**, *14*, 2193.

[22]D.-G. Yu, M. Suri, F. Glorius, *J. Am. Chem. Soc.* **2013**, *135*, 8802–8805.

[23]a) T. Hirayama, S. Ueda, T. Okada, N. Tsurue, K. Okuda, H. Nagasawa, *Chem. Eur. J.* **2014**, *20*, 4156–4162; b) Y. Sun, A. Abdukader, H. Zhang, W. Yang, C. Liu, *RSC Adv.* **2017**, *7*, 55786–55789.

[24]X.-J. Shang, Z.-Q. Liu, *Synthesis* **2017**, *49*, 4693–4697.

[25]T.-S. Mei, X. Wang, J.-Q. Yu, *J. Am. Chem. Soc.* **2009**, *131*, 10806–10807.

[26]R. K. Kumar, M. A. Ali, T. Punniyamurthy, *Org. Lett.* **2011**, *13*, 2102–2105.

[27]T. Zhang, W. Bao, *J. Org. Chem.* **2013**, *78*, 1317–1322.

[28]S. S. Chavan, B. D. Rupanawar, R. B. Kamble, A. M. Shelke, G. Suryavanshi, *Org. Chem. Front.* **2018**, *5*, 544–548.

[29]S. W. Park, H. Choi, J.-H. Lee, Y.-J. Lee, J.-M. Ku, S. Y. Lee, T.-G. Nam, *Arch. Pharm. Res.* **2016**, *39*, 302–309.

[30]Z. Zheng, S. Ma, L. Tang, D. Zhang-Negrerie, Y. Du, K. Zhao, *J. Org. Chem.* **2014**, *79*, 4687–4693.

[31]Z. Yu, L. Ma, W. Yu, *Synlett* **2012**, *23*, 1534–1540.

[32]H. Zhang, J. Shen, Z. Yang, X. Cui, *RSC Adv.* **2019**, *9*, 7718–7722.

[33]Le Liu, L. Du, D. Zhang-Negrerie, Y. Du, *RSC Adv.* **2015**, *5*, 29774–29781.

[34]L. Song, X. Tian, Z. Lv, E. Li, J. Wu, Y. Liu, W. Yu, J. Chang, *J. Org. Chem.* **2015**, *80*, 7219–7225.

[35]a) Z.-J. Cai, X.-M. Lu, Y. Zi, C. Yang, L.-J. Shen, J. Li, S.-Y. Wang, S.-J. Ji, *Org. Lett.* **2014**, *16*, 5108–5111; b) C. Martínez, K. Muñiz, *Angew. Chem. Int. Ed.* **2015**, *54*, 8287–8291; *Angew. Chem.* **2015**, *127*, 8405–8409.

[36]V. Satheesh, M. Sengoden, T. Punniyamurthy, *J. Org. Chem.* **2016**, *81*, 9792–9801.

[37]A. P. Antonchick, R. Samanta, K. Kulikov, J. Lategahn, *Angew. Chem. Int. Ed.* **2011**, *50*, 8605–8608; *Angew. Chem.* **2011**, *123*, 8764–8767.

[38]A. R. Forrester, A. S. Ingram, R. H. Thomson, *J. Chem. Soc., Perkin Trans. 1* **1972**, 2847.

[39]D. C. Miller, G. J. Choi, H. S. Orbe, R. R. Knowles, *J. Am. Chem. Soc.* **2015**, *137*, 13492–13495.

[40]G. J. Choi, R. R. Knowles, *J. Am. Chem. Soc.* **2015**, *137*, 9226–9229.

[41]Z. Li, L. Song, C. Li, *J. Am. Chem. Soc.* **2013**, *135*, 4640–4643.

[42]S. H. Cho, J. Yoon, S. Chang, *J. Am. Chem. Soc.* **2011**, *133*, 5996–6005.

[43]J. Jia, Y. A. Ho, R. F. Bülow, M. Rueping, *Chem. Eur. J.* **2018**, *24*, 14054–14058.

[44]M. D. Kärkäs, *ACS Catal.* **2017**, *7*, 4999–5022.

[45]S. Z. Zard, *Chem. Soc. Rev.* **2008**, *37*, 1603–1618.

[46]K. C. Nicolaou, P. S. Baran, Y.-L. Zhong, H.-S. Choi, W. H. Yoon, Y. He, K. C. Fong, *Angew. Chem. Int. Ed.* **1999**, *38*, 1669–1675; *Angew. Chem.* **1999**, *111*, 1781–1784.

[47]K. C. Nicolaou, Y.-L. Zhong, P. S. Baran, *Angew. Chem. Int. Ed.* **2000**, *39*, 625–628; *Angew. Chem.* **2000**, *112*, 636–639.

[48]K. C. Nicolaou, P. S. Baran, Y.-L. Zhong, S. Barluenga, K. W. Hunt, R. Kranich, J. A. Vega, *J. Am. Chem. Soc.* **2002**, *124*, 2233–2244.

[49]B. Janza, A. Studer, *J. Org. Chem.* **2005**, *70*, 6991–6994.

[50]M. Wasa, J.-Q. Yu, *J. Am. Chem. Soc.* **2008**, *130*, 14058–14059.

[51]J. H. Horner, O. M. Musa, A. Bouvier, M. Newcomb, *J. Am. Chem. Soc.* **1998**, *120*, 7738–7748.

[52]P. Mackiewicz, R. Furstoss, B. Waegell, R. Cote, J. Lessard, *J. Org. Chem.* **1978**, *43*, 3746–3750.

[53]J. Lessard, R. Cote, P. Mackiewicz, R. Furstoss, B. Waegell, *J. Org. Chem.* **1978**, *43*, 3750–3756.

[54]R. Göttlich, *Synthesis* **2000**, *32*, 1561–1564.

[55]G. Heuger, S. Kalsow, R. Göttlich, *Eur. J. Org. Chem.* **2002**, *2002*, 1848–1854.

[56]X. Hoang-Cong, B. Quiclet-Sire, S. Z. Zard, *Tetrahedron Lett.* **1999**, *40*, 2125–2126.

[57]H. Lu, C. Li, *Tetrahedron Lett.* **2005**, *46*, 5983–5985.

[58]F. Gagosz, C. Moutrille, S. Z. Zard, *Org. Lett.* **2002**, *4*, 2707–2709.

[59]A. F. Holleman, E. Wiberg, N. Wiberg, *Anorganische Chemie*, Walter de Gruyter, Berlin/New York, **2016**.

[60]O. E. Edwards, D. Vocelle, J. W. ApSimon, F. Haque, *J. Am. Chem. Soc.* **1965**, *87*, 678–679.

[61]S. A. Glover, A. Goosen, C. W. McCleland, J. L. Schoonraad, *J. Chem. Soc., Perkin Trans. 1* **1984**, 2255.

[62]A. Correa, I. Tellitu, E. Domínguez, R. Sanmartin, *J. Org. Chem.* **2006**, *71*, 3501–3505.

[63]Y. Kikugawa, M. Kawase, *Chem. Lett.* **1990**, *19*, 581–582.

[64]a) J. G. Sharefkin, H. Saltzman, *Org. Synth.* **1963**, *43*, 62; b) D. B. Dess, J. C. Martin, *J. Am. Chem. Soc.* **1991**, *113*, 7277–7287.

[65]X. Wang, A. Studer, *Acc. Chem. Res.* **2017**, *50*, 1712–1724.

[66]A. G. Romero, W. H. Darlington, E.J. Jacobsen, J. W. Mickelson, *Tetrahedron Lett.* **1996**, *37*, 2361–2364.

[67]I. Couto, I. Tellitu, E. Domínguez, *J. Org. Chem.* **2010**, *75*, 7954–7957.

[68]D. Liang, D. Sersen, C. Yang, J. R. Deschamps, G. H. Imler, C. Jiang, F. Xue, *Org. Biomol. Chem.* **2017**, *15*, 4390–4398.

[69]S. A. Ruider, N. Maulide, *Angew. Chem. Int. Ed.* **2015**, *54*, 13856–13858; *Angew. Chem.* **2015**, *127*, 14062–14064.

[70]a) "Tätigkeiten mit Peressigsäure. Arbeitssicherheitsinformation (ASI) 8.03", https://www.bgn.de/?storage=3&identifier=%2F450531&eID=sixomc_filecontent&hmac=0765f61802a31f97ee875a6e07c8b45865390739 (Aufgerufen am 28.06.2020); b) "Peroxyessigsäure", http://gestis.itrust.de/nxt/gateway.dll/gestis_de/039230.xml?f=templates$fn=default.htm$3.0 (Aufgerufen am 28.06.2020); c) B. Phillips, P. S. Starcher, B. D. Ash, *J. Org. Chem.* **1958**, *23*, 1823–1826.

[71]H. Lund, O. Hammerich, *Organic Electrochemistry*, Marcel Dekker, New York, **2001**.

[72]a) R. Francke, R. D. Little, *Chem. Soc. Rev.* **2014**, *43*, 2492–2521; b) S. Möhle, M. Zirbes, E. Rodrigo, T. Gieshoff, A. Wiebe, S. R. Waldvogel, *Angew. Chem. Int. Ed.* **2018**, *57*, 6018–6041; *Angew. Chem.* **2018**, *130*, 6124–6149; c) J. L. Röckl, D. Pollok, R. Franke, S. R.

Waldvogel, *Acc. Chem. Res.* **2020**, *53*, 45–61; d) S. R. Waldvogel, S. Lips, M. Selt, B. Riehl, C. J. Kampf, *Chem. Rev.* **2018**, *118*, 6706–6765; e) A. Wiebe, T. Gieshoff, S. Möhle, E. Rodrigo, M. Zirbes, S. R. Waldvogel, *Angew. Chem. Int. Ed.* **2018**, *57*, 5594–5619; *Angew. Chem.* **2018**, *130*, 5694–5721; f) M. Yan, Y. Kawamata, P. S. Baran, *Chem. Rev.* **2017**, *117*, 13230–13319.

[73]Y. Jiang, K. Xu, C. Zeng, *Chem. Rev.* **2018**, *118*, 4485–4540.

[74]a) B. A. Frontana-Uribe, R. D. Little, J. G. Ibanez, A. Palma, R. Vasquez-Medrano, *Green Chem.* **2010**, *12*, 2099; b) H. J. Schäfer, *C. R. Chim.* **2011**, *14*, 745–765.

[75]a) R. Francke, *Beilstein J. Org. Chem.* **2014**, *10*, 2858–2873; b) N. Sbei, A. V. Listratova, A. A. Titov, L. G. Voskressensky, *Synthesis* **2019**, *51*, 2455–2473; c) Z. Ye, F. Zhang, *Chin. J. Chem.* **2019**, *37*, 513–528.

[76]A. V. Listratova, N. Sbei, L. G. Voskressensky, *Eur. J. Org. Chem.* **2020**, *2020*, 2012–2027.

[77]T. Broese, R. Francke, *Org. Lett.* **2016**, *18*, 5896–5899.

[78]a) K. Inoue, Y. Ishikawa, S. Nishiyama, *Org. Lett.* **2010**, *12*, 436–439; b) D.-Z. Lin, Y.-L. Lai, J.-M. Huang, *ChemElectroChem* **2019**, *6*, 4188–4193; c) P. Qian, J.-H. Su, Y. Wang, M. Bi, Z. Zha, Z. Wang, *J. Org. Chem.* **2017**, *82*, 6434–6440; d) F. Xu, X.-Y. Qian, Y.-J. Li, H.-C. Xu, *Org. Lett.* **2017**, *19*, 6332–6335; e) H.-C. Xu, K. D. Moeller, *J. Am. Chem. Soc.* **2008**, *130*, 13542–13543; f) Z. Ye, M. Ding, Y. Wu, Y. Li, W. Hua, F. Zhang, *Green Chem.* **2018**, *20*, 1732–1737.

[79]D. Kajiyama, K. Inoue, Y. Ishikawa, S. Nishiyama, *Tetrahedron* **2010**, *66*, 9779–9784.

[80]W.-C. Li, C.-C. Zeng, L.-M. Hu, H.-Y. Tian, R. D. Little, *Adv. Synth. Catal.* **2013**, *355*, 2884–2890.

[81]S. Singh, L. K. Sharma, A. Saraswat, I. R. Siddiqui, H. K. Kehri, R. K. P. Singh, *RSC Adv.* **2013**, *3*, 4237.

[82]H.-L. Xiao, C.-C. Zeng, H.-Y. Tian, L.-M. Hu, R. D. Little, *J. Electroanal. Chem* **2014**, *727*, 120–124.

[83]H.-C. Xu, J. M. Campbell, K. D. Moeller, *J. Org. Chem.* **2014**, *79*, 379–391.

[84]Z.-W. Hou, Z.-Y. Mao, H.-B. Zhao, Y. Y. Melcamu, X. Lu, J. Song, H.-C. Xu, *Angew. Chem. Int. Ed.* **2016**, *55*, 9168–9172; *Angew. Chem.* **2016**, *128*, 9314–9318.

[85]T. Gieshoff, D. Schollmeyer, S. R. Waldvogel, *Angew. Chem. Int. Ed.* **2016**, *55*, 9437–9440; *Angew. Chem.* **2016**, *128*, 9587–9590.

[86]I. Colomer, A. E. R. Chamberlain, M. B. Haughey, T. J. Donohoe, *Nat. Rev. Chem.* **2017**, *1*.

[87]a) A. Kirste, M. Nieger, I. M. Malkowsky, F. Stecker, A. Fischer, S. R. Waldvogel, *Chem. Eur. J.* **2009**, *15*, 2273–2277; b) T. Dohi, N. Yamaoka, Y. Kita, *Tetrahedron* **2010**, *66*, 5775–5785; c) L. Eberson, M. P. Hartshorn, O. Persson, *J. Chem. Soc., Perkin Trans. 2* **1995**, 1735; d) S. K. Sinha, T. Bhattacharya, D. Maiti, *React. Chem. Eng.* **2019**, *4*, 244–253.

[88]R. Francke, D. Cericola, R. Kötz, D. Weingarth, S. R. Waldvogel, *Electrochim. Acta* **2012**, *62*, 372–380.

[89]a) M. J. Kamlet, J. L. M. Abboud, M. H. Abraham, R. W. Taft, *J. Org. Chem.* **1983**, *48*, 2877–2887; b) J.-P. Bégué, D. Bonnet-Delpon, B. Crousse, *Synlett* **2004**, 18–29.

[90]O. Hollóczki, A. Berkessel, J. Mars, M. Mezger, A. Wiebe, S. R. Waldvogel, B. Kirchner, *ACS Catal.* **2017**, *7*, 1846–1852.

[91]E. Baciocchi, H. Møllendal, D. W. Aksnes, T. Brekke, K. Maartmann-Moe, H. H. Tønnesen, T. Tokii, *Acta Chem. Scand.* **1990**, *44*, 645–652.

[92]a) L. Q. Nguyen, R. R. Knowles, *ACS Catal.* **2016**, *6*, 2894–2903; b) E. C. Gentry, R. R. Knowles, *Acc. Chem. Res.* **2016**, *49*, 1546–1556.

[93]a) J. P. Davidson, E. J. Corey, *J. Am. Chem. Soc.* **2003**, *125*, 13486–13489; b) M.-J. Don, C.-C. Shen, Y.-L. Lin, W.-J. Syu, Y.-H. Ding, C.-M. Sun, *J. Nat. Prod.* **2005**, *68*, 1066–1070; c) L. Leventhal, M. R. Brandt, T. A. Cummons, M. J. Piesla, K. E. Rogers, H. A. Harris, *Eur. J. Pharmacol.* **2006**, *553*, 146–148; d) J. Nishiu, M. Ito, Y. Ishida, M. Kakutani, T. Shibata, M. Matsushita, M. Shindo, *Diabetes Obes. Metab.* **2006**, *8*, 508–516; e) A. D. Rodríguez, C. Ramírez, I. I. Rodríguez, E. González, *Org. Lett.* **1999**, *1*, 527–530; f) S. Sato, T. Kajiura, M. Noguchi, K. Takehana, T. Kobayashi, T. Tsuji, *J. Antibiot.* **2001**, *54*, 102–104; g) L.-Q. Sun, J. Chen, K. Takaki, G. Johnson, L. Iben, C. D. Mahle, E. Ryan, C. Xu, *Bioorg. Med. Chem. Lett.* **2004**, *14*, 1197–1200; h) M. Ueki, K. Ueno, S. Miyadoh, K. Abe, K. Shibata, M. Taniguchi, S. Oi, *J. Antibiot.* **1993**, *46*, 1089–1094; i) S. Yoshida, S. Shiokawa, K.-i. Kawano, T. Ito, H. Murakami, H. Suzuki, Y. Sato, *J. Med. Chem.* **2005**, *48*, 7075–7079; j) X. Zhang, X. Fang, M. Xu, Y. Lei, Z. Wu, X. Hu, *Angew. Chem. Int. Ed.* **2019**, *58*, 7845–7849; *Angew. Chem.* **2019**, *131*, 7927–7931.

[94]M. S. Mayo, X. Yu, X. Zhou, X. Feng, Y. Yamamoto, M. Bao, *J. Org. Chem.* **2014**, *79*, 6310–6314.

[95]N. Khatun, S. Guin, S. K. Rout, B. K. Patel, *RSC Adv.* **2014**, *4*, 10770.

[96]a) F. Al'-Assar, K. N. Zelenin, E. E. Lesiovskaya, I. P. Bezhan, B. A. Chakchir, *Pharm. Chem. J.* **2002**, *36*, 598–603; b) R. P. Jain, J. C. Vederas, *Bioorg. Med. Chem. Lett.* **2004**, *14*,

3655–3658; c) A. M. Khalil, M. A. Berghot, M. A. Gouda, S. A. El Bialy, *Monatsh. Chem.* **2010**, *141*, 1353–1360; d) X.-J. Liu, H.-J. Zhang, Z.-S. Quan, *Med. Chem. Res.* **2017**, *26*, 1935–1946; e) M. F. Zayed, R. R. Ayyad, *Drug Res.* **2012**, *62*, 532–536.

[97] R. M. Beesley, C. K. Ingold, J. F. Thorpe, *J. Chem. Soc., Trans.* **1915**, *107*, 1080–1106.

[98] a) P. Tordo, E. Flesia, G. Labrot, J.-M. Surzur, *Tetrahedron Lett.* **1972**, *13*, 1413–1416; b) T. Koenig, J. A. Hoobler, W. R. Mabey, *J. Am. Chem. Soc.* **1972**, *94*, 2514–2515.

[99] a) D. Bellocchi, A. Macchiarulo, G. Costantino, R. Pellicciari, *Bioorg. Med. Chem.* **2005**, *13*, 1151–1157; b) T. A. Grese, M. D. Adrian, D. L. Phillips, P. K. Shetler, L. L. Short, A. L. Glasebrook, H. U. Bryant, *J. Med. Chem.* **2001**, *44*, 2857–2860; c) M. He, C. Qu, O. Gao, X. Hu, X. Hong, *RSC Adv.* **2015**, *5*, 16562–16574; d) J. Ishida, K. Hattori, H. Yamamoto, A. Iwashita, K. Mihara, N. Matsuoka, *Bioorg. Med. Chem. Lett.* **2005**, *15*, 4221–4225; e) Z. Jin, *Nat. Prod. Rep.* **2011**, *28*, 1126–1142; f) S. Patil, S. Kamath, T. Sanchez, N. Neamati, R. F. Schinazi, J. K. Buolamwini, *Bioorg. Med. Chem.* **2007**, *15*, 1212–1228; g) S. D. Shnyder, P. A. Cooper, N. J. Millington, J. H. Gill, M. C. Bibby, *J. Nat. Prod.* **2008**, *71*, 321–324; h) Z. Tu, W. Chu, J. Zhang, C. S. Dence, M. J. Welch, R. H. Mach, *Nucl. Med. Biol.* **2005**, *32*, 437–443; i) D. Weltin, V. Picard, K. Aupeix, M. Varin, D. Oth, J. Marchal, P. Dufour, P. Bischoff, *Int. Immunopharmacol.* **1995**, *17*, 265–271.

[100] J. Grimshaw, D. Mannus, *J. Chem. Soc., Perkin Trans. 1* **1977**, 2456.

[101] S. Zhang, L. Li, M. Xue, R. Zhang, K. Xu, C. Zeng, *Org. Lett.* **2018**, *20*, 3443–3446.

[102] A. Adenier, M. M. Chehimi, I. Gallardo, J. Pinson, N. Vilà, *Langmuir* **2004**, *20*, 8243–8253.

[103] a) T.-S. Wu, S.-C. Huang, P.-L. Wu, C.-M. Teng, *Phytochemistry* **1996**, *43*, 133–140; b) N. Wongthet, N. Sanevas, J. Schinnerl, K. Valant-Vetschera, M. Bacher, S. Vajrodaya, *Biochem. Syst. Ecol.* **2018**, *80*, 84–90; c) T. Sripisut, S. Laphookhieo, *J. Asian Nat. Prod. Res.* **2010**, *12*, 614–617.

[104] A. W. Schmidt, K. R. Reddy, H.-J. Knölker, *Chem. Rev.* **2012**, *112*, 3193–3328.

[105] a) S. Sellamuthu, G. Gutti, D. Kumar, S. Kumar Singh, *Mini-Rev. Org. Chem.* **2018**, *15*, 498–507; b) A. Zall, D. Kieser, N. Höttecke, E. C. Naumann, B. Thomaszewski, K. Schneider, D. T. Steinbacher, R. Schubenel, S. Masur, K. Baumann et al., *Bioorg. Med. Chem.* **2011**, *19*, 4903–4909; c) S. Thiratmatrakul, C. Yenjai, P. Waiwut, O. Vajragupta, P. Reubroycharoen, M. Tohda, C. Boonyarat, *Eur. J. Med. Chem.* **2014**, *75*, 21–30; d) F.-F. Zhang, L.-L. Gan, C.-H. Zhou, *Bioorg. Med. Chem. Lett.* **2010**, *20*, 1881–1884; e) P.

Rajakumar, K. Sekar, V. Shanmugaiah, N. Mathivanan, *Eur. J. Med. Chem.* **2009**, *44*, 3040–3045; f) M. Saravanabhavan, K. Sathya, V. G. Puranik, M. Sekar, *Spectrochim. Acta A* **2014**, *118*, 399–406; g) G. Surineni, P. Yogeeswari, D. Sriram, S. Kantevari, *Med. Chem. Res.* **2015**, *24*, 1298–1309; h) C. Börger, C. Brütting, K. K. Julich-Gruner, R. Hesse, V. P. Kumar, S. K. Kutz, M. Rönnefahrt, C. Thomas, B. Wan, S. G. Franzblau et al., *Bioorg. Med. Chem.* **2017**, *25*, 6167–6174; i) L. Sun, Y. Wu, Y. Liu, X. Chen, L. Hu, *Bioorg. Med. Chem. Lett.* **2017**, *27*, 261–265; j) A. Caruso, D. Iacopetta, F. Puoci, A. R. Cappello, C. Saturnino, M. S. Sinicropi, *Mini-Rev. Med. Chem.* **2016**, *16*, 630–643.

[106] N. Blouin, A. Michaud, D. Gendron, S. Wakim, E. Blair, R. Neagu-Plesu, M. Belletête, G. Durocher, Y. Tao, M. Leclerc, *J. Am. Chem. Soc.* **2008**, *130*, 732–742.

[107] a) J. F. Ambrose, R. F. Nelson, *J. Electrochem. Soc.* **1968**, *115*, 1159–1164; b) J. F. Ambrose, L. L. Carpenter, R. F. Nelson, *J. Electrochem. Soc.* **1975**, *122*, 876–894; c) K. Karon, M. Lapkowski, *J Solid State Electrochem* **2015**, *19*, 2601–2610.

[108] A. Maity, B. L. Frey, N. D. Hoskinson, D. C. Powers, *J. Am. Chem. Soc.* **2020**, *142*, 4990–4995.

[109] M. Kaur, M. Singh, N. Chadha, O. Silakari, *Eur. J. Med. Chem.* **2016**, *123*, 858–894.

[110] S. Bazzi, E. Schulz, M. Mellah, *Org. Lett.* **2019**, *21*, 10033–10037.

[111] a) C. Bonnefous, J. E. Payne, J. Roppe, H. Zhuang, X. Chen, K. T. Symons, P. M. Nguyen, M. Sablad, N. Rozenkrants, Y. Zhang et al., *J. Med. Chem.* **2009**, *52*, 3047–3062; b) G. Claassen, E. Brin, C. Crogan-Grundy, M. T. Vaillancourt, H. Z. Zhang, S. X. Cai, J. Drewe, B. Tseng, S. Kasibhatla, *Cancer Lett.* **2009**, *274*, 243–249; c) J. M. Kraus, H. B. Tatipaka, S. A. McGuffin, N. K. Chennamaneni, M. Karimi, J. Arif, C. L. M. J. Verlinde, F. S. Buckner, M. H. Gelb, *J. Med. Chem.* **2010**, *53*, 3887–3898; d) Z.-J. Ni, P. Barsanti, N. Brammeier, A. Diebes, D. J. Poon, S. Ng, S. Pecchi, K. Pfister, P. A. Renhowe, S. Ramurthy et al., *Bioorg. Med. Chem. Lett.* **2006**, *16*, 3121–3124; e) J. Pedron, C. Boudot, S. Hutter, S. Bourgeade-Delmas, J.-L. Stigliani, A. Sournia-Saquet, A. Moreau, E. Boutet-Robinet, L. Paloque, E. Mothes et al., *Eur. J. Med. Chem.* **2018**, *155*, 135–152; f) M. Reyes-Batlle, M. B. Freijo, A. López-Arencibia, J. Lorenzo-Morales, G. McNaughton-Smith, J. E. Piñero, T. Abad-Grillo, *Bioorg. Chem.* **2020**, *99*, 103791.

[112] a) Y. Kato, M. Takemoto, K. Achiwa, *Chem. Pharm. Bull.* **1993**, *41*, 2003–2006; b) T. Yao, R. C. Larock, *J. Org. Chem.* **2005**, *70*, 1432–1437; c) E. C. Taylor, P. Zhou, L. D. Jennings, Z. Mao, B. Hu, J.-G. Jun, *Tetrahedron Lett.* **1997**, *38*, 521–524; d) J. G. Pierce, D.

L. Waller, P. Wipf, *J. Organomet. Chem.* **2007**, *692*, 4618–4629; e) L. Shi, L. Hu, J. Wang, X. Cao, H. Gu, *Org. Lett.* **2012**, *14*, 1876–1879.

[113] N. Goswami, D. Maiti, *Isr. J. Chem.* **2020**, *60*, 303–312.

[114] S. Kitagaki, K. Sugisaka, C. Mukai, *Org. Biomol. Chem.* **2015**, *13*, 4833–4836.

[115] a) J. Schüttler, H. Schwilden, *Modern Anesthetics*, Springer-Verlag, Berlin, Heidelberg, **2008**; b) S. G. Smith, R. Sanchez, M.-M. Zhou, *Chem. Biol.* **2014**, *21*, 573–583.

[116] M. J. O'Donnell, R. L. Polt, *J. Org. Chem.* **1982**, *47*, 2663–2666.

[117] R. Cao, W. Peng, Z. Wang, A. Xu, *Curr. Med. Chem.* **2007**, *14*, 479–500.

[118] F. Wang, S. S. Stahl, *Angew. Chem. Int. Ed.* **2019**, *58*, 6385–6390; *Angew. Chem.* **2019**, *131*, 6451–6456.

7 Publikationen-Anhang

Anhang-Inhaltsverzeichnis der vorgestellten Publikationen:

Journal Name

COMMUNICATION

Electrochemical Synthesis of Benzoxazoles from Anilides – A New Approach to Employ Amidyl Radical Intermediates

Received 00th January 20xx,
Accepted 00th January 20xx

DOI: 10.1039/x0xx00000x

www.rsc.org/

Tile Gieshoff,[a,b,c] Anton Kehl,[a] Dieter Schollmeyer,[a] Kevin D. Moeller[c] and Siegfried R. Waldvogel*[a,b]

A novel electrochemical method for the synthesis of benzoxazoles from readily available anilides is reported. Various functionalities are tolerated and good yields can be achieved. By employing common electrode materials and a simple constant current protocol, this method is an attractive new alternative to conventional pathways.

Benzoxazoles represent an important structure in heterocyclic chemistry and are key motifs of several natural products, pharmaceuticals, and biologically active compounds.[1] Thus, they are a significant topic of contemporary research, and efficient synthetic strategies starting from simple starting materials are highly desired. Traditionally, benzoxazoles have been synthesized by treating 2-aminophenols with activated acids or aldehydes under oxidative conditions.[2] In recent years, this approach has been complemented by methods capitalizing on anilide or benzoxazole core scaffolds that can be employed as substrates in a variety of coupling reactions. Coupling strategies using substrates prefunctionalized with a leaving group and capitalizing on CH-activation have been reported.[3]

The use of electrochemistry can offer a mechanistically distinct and significantly sustainable approach to benzoxazoles.[4] In addition, this method can be considered as inherently safe. In an electrochemical reaction, electric current serves as an inexpensive and potentially renewable reagent that avoids the need to a stoichiometric redox reagent. This both minimizes the waste produced in the reaction and removes the limitations on redox potential associated with every chemical reagent. This later point is important because it enables electrochemical reactions to readily access extraordinary reaction pathways.[5,6] This combination of sustainability and mechanistic opportunity has led to the recent development of a variety of valuable electrolysis protocols.[5,7,8–10]

Here, we report the first direct, reagent-free electroorganic synthesis of benzoxazoles based on alkyl and aryl anilides in a simple electrochemical set-up cell (Scheme 1). The reaction employs easily accessible starting materials, inexpensive electrode materials, and a low concentration of supporting electrolyte. The result is a synthetically attractive alternative to conventional methods for synthesizing the target structure. We anticipate that amidyl radicals act as intermediates, which are directly generated at the anode.[5,10] The efficient formation of amidyl radicals has been of great interest for the chemical community.[11] Their structure and reactivity has been mostly explored in the context of rearrangements and hydroamination reactions.[8,12]

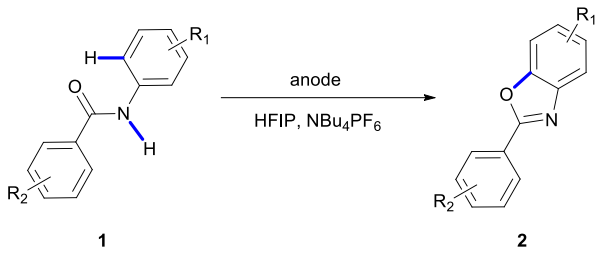

1 2

Scheme 1 Electrochemical synthesis of benzoxazoles.

The transformation illustrated in Scheme 1 was discovered in the course of our studies concerning the electrochemical formation of N,N bonds.[5] The addition of an amidyl radical to a neighbouring aryl ring was observed in cases wherein the desired N,N bond formation was slow. In these cases, a mixture of N,N bond coupling and the formation of benzoxazoles was obtained. The mixture issue was quickly resolved by using monoanilides in order to exclude the intramolecular N,N bond formation.

N-(4-Chlorophenyl)benzamide (**1a**) was then chosen as a test substrate for optimization studies. The aromatic substitution

[a] *Institute of Organic Chemistry, Johannes Gutenberg University Mainz, Duesbergweg 10-14, D-55128 Mainz, Germany. E-mail: waldvogel@uni-mainz.de*
[b] *Graduate School Materials Science in Mainz, Staudingerweg 9, D-55128 Mainz, Germany.*
[c] *Department of Chemistry, Washington University in St. Louis, St. Louis, Missouri 63130, United States.*
† Footnotes relating to the title and/or authors should appear here.
Electronic Supplementary Information (ESI) available: [details of any supplementary information available should be included here]. See DOI: 10.1039/x0xx00000x

pattern was known to afford high yields for reactions leading to N,N bond formation,[5] a scenario that suggested the systems compatibility with the formation of a reactive amidyl radical. When the reaction was screened for its compatibility with different electrolyte systems,[13] only the use of hexafluoroisopropyl alcohol (HFIP) as a solvent enabled the desired formation of the benzoxazole. Methanol and other solvents commonly applied in electrochemical transformations lead to degradation of the anilides, even though conventional and electrochemical reactions of amidyl radicals in methanol are described in literature.[8–10,14] This result suggested that the cyclization was slow and thus required sufficient stabilization by the solvent. HFIP is able to effectively stabilize radical intermediates.[15] The almost quantitative recovery of this particular solvent (b.p. 56 °C) allows minimization of the fluorine footprint.[5,16] By employing a low concentration of tetrabutylammonium hexafluorophosphate (0.01 M) as supporting electrolyte, the atom economy and work-up are significantly improved.

Electrochemical reactions are usually sensitive to the current density applied and the electrode geometry.[10] Hence, we optimized the applied current for the two most commonly used laboratory scale electrochemical set-ups. Set-up A relies on a 25 mL three-necked flask, wherein a reticulated vitreous carbon (RVC) anode and a platinum wire cathode are placed angular to each other. Set-up B is a beaker-type cell with a flat isostatic graphite anode and a platinum plate cathode, which are orientated parallel to each other.[5] The latter provides a more defined and homogenous electric field. More detailed information about both reaction setups can be found within the supporting information.

Table 1 Optimization of electrolysis parameters

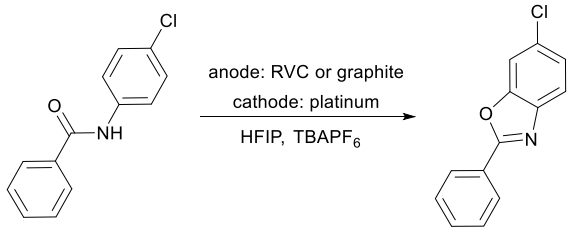

1a **2a**

Entry	Set-up[a]	j [mA/cm²]	I [mA]	Isolated yield [%]
1	A	-	1.1	31
2	A	-	4.1	54
3	A	-	8.4	56
4	A	-	12.4	49
5	B	1.3	-	50
6	B	1.9	-	53
7	B	2.5	-	66
8	B	5.0	-	57

[a] Set-up **A**: 25 mL three-necked flask, RVC (100 PPI) anode, platinum wire cathode, 0.4 mmol substrate, 0.01 M $TBAPF_6$ in 10 mL HFIP, amount of charge = 2 F; Set-up **B**: beaker-type cell, isostatic graphite anode, platinum cathode, 8 cm^2 electrode surface, 1.0 mmol substrate, 0.01 M $TBAPF_6$ in 25 mL HFIP, 2 F amount of charge.

With the optimized electrolysis conditions in hand, the scope of this electrosynthetic method was elucidated.

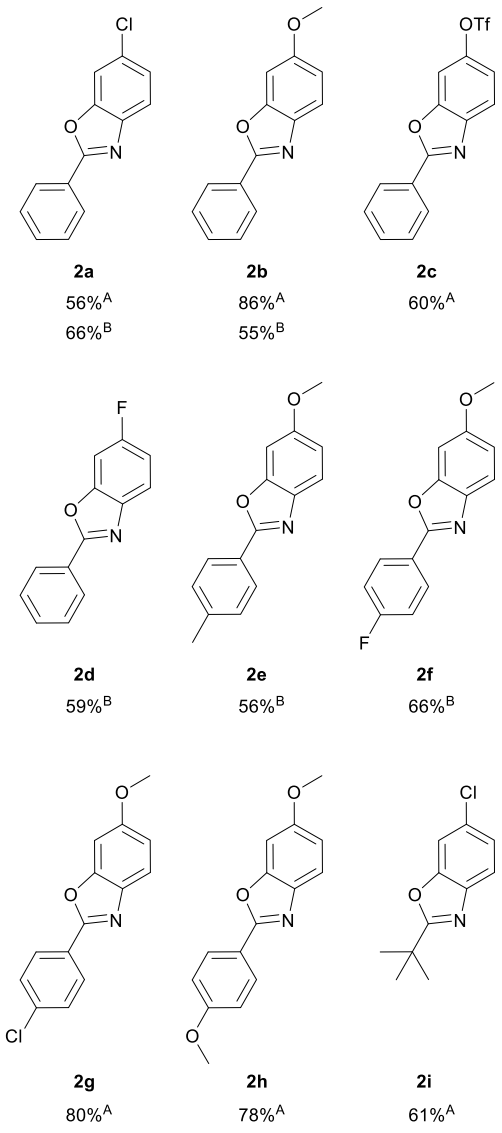

2a 56%[A] 66%[B] **2b** 86%[A] 55%[B] **2c** 60%[A]

2d 59%[B] **2e** 56%[B] **2f** 66%[B]

2g 80%[A] **2h** 78%[A] **2i** 61%[A]

Scheme 2 Scope. A: Set-up A, B: Set-up B.

Several valuable functionalities are tolerated by the method leading to the synthesis of a variety of benzoxazoles in good to very good yield. Electron donating substituents on either the amide or the anilide part of the substrate have a beneficial effect onto the yield (**2b**, **2g** and **2h**). In addition, typical leaving group functionalities are also tolerated. In particular, chloro and triflate moieties are compatible with the reactions opening up the opportunity to further functionalize and diversify the scaffolds make using an assortment of subsequent transformations, i.e. cross-coupling reactions. On the amide part of the substrate, aromatic systems and quaternary alkyls are tolerated, while α hydrogens lead to unselective degradation processes. The different anilides were converted with both electrolysis set-ups **A** and **B**. The respective yields for these set-ups were compared using substrates **1a** and **1b**. The formation of **2a** afforded a higher yield using set-up **B**, while the

A2

formation of **2b** proceeded better with set-up **A**. Two points about this finding deserve comment. First, note that both setups generated product and could be used to determine the synthetic potential of the reaction. So, for exploratory purposes the nature of the reaction setup is not important. However, when optimizing the reactions the observations underscore the need to pay attention to electrochemical conditions. Electrochemical reactions depend not only on how the reactive intermediates are generated, but also on how those intermediates interact with the chemical environment immediately surrounding the electrode, diffuse away from the electrode involved in their generation, and the gradient of chemical environments encountered during that diffusion process. All of these things depend on the nature of the electrochemical field in the cell, a field that relies on electrode configuration, spacing, etc. The point is simple. If the yield of a desired electrochemical reaction is lower than one might prefer, then one should look at alterations of the electrolysis set-up and the electrode geometry as one means of influencing that yield.

Regarding the mechanism of the transformations observed, we propose that oxidation of the substrate leads to an amidyl radical that is stabilized by the neighboring aromatic ring by resonance.[17] This first oxidation step might be facilitated by deprotonation of the amide via in-situ generated alcoholate anions derived from HFIP at the cathode. Bond formation between the amidic oxygen and the ortho carbon of the aromatic ring leads to the formation of a heterocyclic radical. A second oxidation followed by the loss of a proton then completes product formation. It is also possible that the reaction proceeds through a second oxidation that occurs prior to the cyclization followed by an electrocyclic oxa-Nazarov-type reaction.[18]

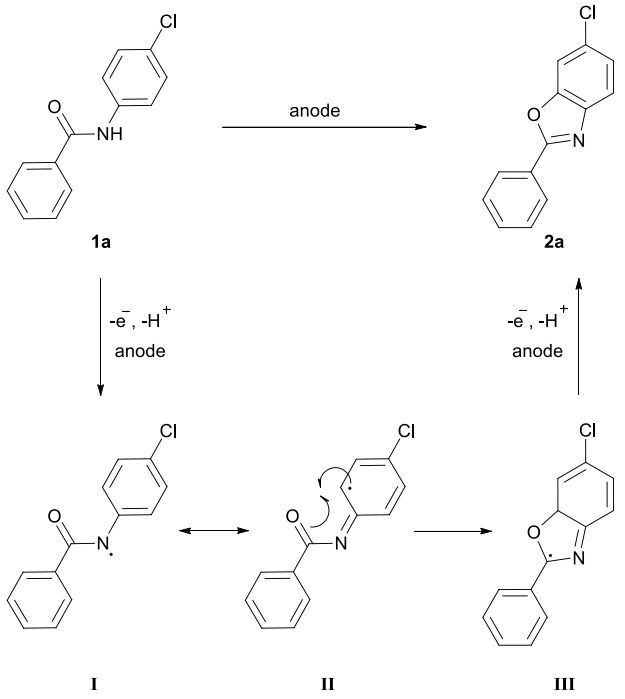

Scheme 3 Proposed mechanism.

The proposed mechanism suggests that the aromatic ring has substantial radical nature. This observation is supported by experimental data. An aryl radical would be expected to undergo significant coupling chemistry at the position *para* to the amidyl group. In practice, this occurs, and a substituent is required at the *para*-position of the N-substituted aryl-ring in order to prevent side reactions at this position. [5] The mechanism also explains why electron-releasing substituents on the ring favor the observed reaction since they both aid in the oxidation steps and stabilize the intermediate radical. Interestingly, if an *ortho* position is blocked by a substituent in the substrate, no product is formed. Evidently, a substituent in this position prevents rotation along the carbon nitrogen bond to generate the planar orientation required for resonance of the N-based radical into the aromatic ring.[19]

In conclusion, we have developed a straightforward and sustainable electrochemical synthesis for the direct construction of benzoxazoles from easy accessible anilides. A variety of functional groups are tolerated by the reaction, and these groups a well-positioned to enable further synthetic manipulation of the products. The comparison of the two most commonly used electrolysis set-ups in synthetic labs demonstrate that the method can be readily adopted by others.

T.G. is a recipient of a DFG fellowship by the Excellence Initiative by the Graduate School Materials Science in Mainz (GSC 266). The work done in the labs of KDM was supported by the US National Science Foundation (CHE-1463913).

Notes and references

1 a) L. Leventhal, M. R. Brandt, T. A. Cummons, M. J. Piesla, K. E. Rogers and H. A. Harris, *Eur. J. Pharmacol.*, 2006, **553**, 146; b) J. Nishiu, M. Ito, Y. Ishida, M. Kakutani, T. Shibata, M. Matsushita and M. Shindo, *Diabetes, Obes. & Metab.*, 2006, **8**, 508; c) M.-J. Don, C.-C. Shen, Y.-L. Lin, W.-J. Syu, Y.-H. Ding and C.-M. Sun, *J. Nat. Prod.*, 2005, **68**, 1066; d) S. Yoshida, S. Shiokawa, K.-i. Kawano, T. Ito, H. Murakami, H. Suzuki and Y. Sato, *J. Med. Chem.*, 2005, **48**, 7075; e) T. Bradshaw and A. Westwell, *CMC*, 2004, **11**, 1009; f) L.-Q. Sun, J. Chen, K. Takaki, G. Johnson, L. Iben, C. D. Mahle, E. Ryan and C. Xu, *Bioorg. Med. Chem. Lett.*, 2004, **14**, 1197; g) J. P. Davidson and E. J. Corey, *J. Am. Chem. Soc.*, 2003, **125**, 13486; h) S. Sato, T. Kajiura, M. Noguchi, K. Takehana, T. Kobayashi and T. Tsuji, *J. Antibiot.*, 2001, **54**, 102; i) A. D. Rodríguez, C. Ramírez, I. I. Rodríguez and E. González, *Org. Lett.*, 1999, **1**, 527; j) M. Ueki, K. Ueno, S. Miyadoh, K. Abe, K. Shibata, M. Taniguchi and S. Oi, *J. Antibiot.*, 1993, **46**, 1095; k) W. S. Saari, J. M. Hoffman, J. S. Wai, T. E. Fisher, C. S. Rooney, A. M. Smith, C. M. Thomas, M. E. Goldman and J. A. O'Brien, *J. Med. Chem.*, 1991, **34**, 2922.

2 M. S. Mayo, X. Yu, X. Zhou, X. Feng, Y. Yamamoto and M. Bao, *J. Org. Chem.*, 2014, **79**, 6310.

3 a) N. Khatun, S. Guin, S. K. Rout and B. K. Patel, *RSC Adv.*, 2014, **4**, 10770; b) W.-C. Li, C.-C. Zeng, L.-M. Hu, H.-Y. Tian and R. D. Little, *Adv. Synth. Catal.*, 2013, **355**, 2884; c) L.-S. Kang, H.-l. Xiao, C.-C. Zeng, L.-M. Hu and R. D. Little, *J. Electroanal. Chem.*, 2016, **767**, 13; d) T. Morofuji, A. Shimizu

and J.-i. Yoshida, *Chem. Eur. J.*, 2015, **21**, 3211; e) H. Salehzadeh, D. Nematollahi and H. Hesari, *Green Chem.*, 2013, **15**, 2441; f) G. Altenhoff and F. Glorius, *Adv. Synth. Catal.*, 2004, **346**, 1661; g) S. Ueda and H. Nagasawa, *J. Org. Chem.*, 2009, **74**, 4272; h) S. Ueda and H. Nagasawa, *Angew. Chem. Int. Ed.*, 2008, **47**, 6411; *Angew. Chem.,* 2008, **120,** 6511–6513; i) K. Yang, X. Chen, Y. Wang, W. Li, A. A. Kadi, H.-K. Fun, H. Sun, Y. Zhang, G. Li and H. Lu, *J. Org. Chem.*, 2015, **80**, 11065; j) S. K. Alla, P. Sadhu and T. Punniyamurthy, *J. Org. Chem.*, 2014, **79**, 7502; k) R. D. Viirre, G. Evindar and R. A. Batey, *J. Org. Chem.*, 2008, **73**, 3452.

4 a) E. J. Horn, B. R. Rosen and P. S. Baran, *ACS Central Science*, 2016, **2**, 302; b) B. A. Frontana-Uribe, R. D. Little, J. G. Ibanez, A. Palma and R. Vasquez-Medrano, *Green Chem.*, 2010, **12**, 2099; c) J.-i. Yoshida, K. Kataoka, R. Horcajada and A. Nagaki, *Chem. Rev.*, 2008, **108**, 2265; d) S. R. Waldvogel and S. Möhle, *Angew. Chem. Int. Ed.*, 2015, **54**, 6398; *Angew. Chem.,* 2015, **127,** 6496–6497; e) O. Hammerich and B. Speiser, eds., *Organic electrochemistry*, CRC Press, Boca Raton, Fla., 5th edn., 2016; f) R. Francke and R. D. Little, *J. Am. Chem. Soc.*, 2014, **136**, 427; g) S. R. Waldvogel and B. Janza, *Angew. Chem. Int. Ed.*, 2014, **53**, 7122; *Angew. Chem.,* 2014, **126,** 7248–7249; h) S. R. Waldvogel and M. Selt, *Angew. Chem. Int. Ed.*, 2016, **55**, 12578; *Angew. Chem.,* 2016, **128,** 12766–12768.

5 T. Gieshoff, D. Schollmeyer and S. R. Waldvogel, *Angew. Chem. Int. Ed.*, 2016, **55**, 9437; *Angew. Chem.,* 2016, **128,** 9587–9590.

6 a) S. Lips, A. Wiebe, B. Elsler, D. Schollmeyer, K. M. Dyballa, R. Franke and S. R. Waldvogel, *Angew. Chem. Int. Ed.*, 2016, **55**, 10872; *Angew. Chem.,* 2016, **128,** 11031–11035; b) A. Wiebe, D. Schollmeyer, K. M. Dyballa, R. Franke and S. R. Waldvogel, *Angew. Chem. Int. Ed.*, 2016, **55**, 11801; *Angew. Chem.,* 2016, **128,** 11979–11983; c) B. Elsler, D. Schollmeyer, K. M. Dyballa, R. Franke and S. R. Waldvogel, *Angew. Chem. Int. Ed.*, 2014, **53**, 5210; *Angew. Chem.,* 2014, **126,** 5311–5314; d) B. R. Rosen, E. W. Werner, A. G. O'Brien and P. S. Baran, *J. Am. Chem. Soc.*, 2014, **136**, 5571; e) E. J. Horn, B. R. Rosen, Y. Chen, J. Tang, K. Chen, M. D. Eastgate and P. S. Baran, *Nature*, 2016, **533**, 77; f) C. Gütz, M. Selt, M. Bänziger, C. Bucher, C. Römelt, N. Hecken, F. Gallou, T. R. Galvão and S. R. Waldvogel, *Chem. Eur. J.*, 2015, **21**, 13878; g) S. Herold, S. Möhle, M. Zirbes, F. Richter, H. Nefzger and S. R. Waldvogel, *Eur. J. Org. Chem.*, 2016, **2016**, 1274; h) H.-C. Xu and K. D. Moeller, *J. Am. Chem. Soc.*, 2008, **130**, 13542; i) T. Morofuji, A. Shimizu and J.-i. Yoshida, *J. Am. Chem. Soc.*, 2013, **135**, 5000; j) H. Wu and K. D. Moeller, *Org. Lett.*, 2007, **9**, 4599; k) J. Mihelcic and K. D. Moeller, *J. Am. Chem. Soc.*, 2003, **125**, 36.

7 a) R. Francke, *Beilstein J. Org. Chem.*, 2014, **10**, 2858; b) H.-B. Zhao, Z.-W. Hou, Z.-J. Liu, Z.-F. Zhou, J. Song and H.-C. Xu, *Angew. Chem. Int. Ed.*, 2017, **56**, 587; *Angew. Chem.,* 2017, **129,** 602–605.

8 L. Zhu, P. Xiong, Z.-Y. Mao, Y.-H. Wang, X. Yan, X. Lu and H.-C. Xu, *Angew. Chem. Int. Ed.*, 2016, **55**, 2226; *Angew. Chem.,* 2016, **128,** 2266–2269.

9 Z.-W. Hou, Z.-Y. Mao, H.-B. Zhao, Y. Y. Melcamu, X. Lu, J. Song and H.-C. Xu, *Angew. Chem. Int. Ed.*, 2016, **55**, 9168; *Angew. Chem.,* 2016, **128,** 9314–9318.

10 H.-C. Xu, J. M. Campbell and K. D. Moeller, *J. Org. Chem.*, 2014, **79**, 379.

11 a) K. C. Nicolaou, P. S. Baran, Y.-L. Zhong, S. Barluenga, K. W. Hunt, R. Kranich and J. A. Vega, *J. Am. Chem. Soc.*, 2002, **124**, 2233; b) B. Janza and A. Studer, *J. Org. Chem.*, 2005, **70**, 6991; c) S. Maity and N. Zheng, *Angew. Chem. Int. Ed.*, 2012, **51**, 9562; d) X.-Q. Hu, J.-R. Chen, Q. Wei, F.-L. Liu, Q.-H. Deng, A. M. Beauchemin and W.-J. Xiao, *Angew. Chem. Int. Ed.*, 2014, **53**, 12163; *Angew. Chem.,* 2014, **126,** 12359–12363; e) G. J. Choi and R. R. Knowles, *J. Am. Chem. Soc.*, 2015, **137**, 9226.

12 a) S. Z. Zard, *Chem. Soc. Rev.*, 2008, **37**, 1603; b) C. Moutrille and S. Z. Zard, *Chem. Commun.*, 2004, 1848; c) N. Fuentes, W. Kong, L. Fernández-Sánchez, E. Merino and C. Nevado, *J. Am. Chem. Soc.*, 2015, **137**, 964.

13 C. Gütz, B. Klöckner and S. R. Waldvogel, *Org. Process Res. Dev.*, 2016, **20**, 26.

14 a) A. Redden, R. J. Perkins and K. D. Moeller, *Angew. Chem. Int. Ed.*, 2013, **52**, 12865; *Angew. Chem.,* 2013, **125,** 13103–13106; b) K. J. Frankowski, R. Liu, G. L. Milligan, K. D. Moeller and J. Aube, *Angew. Chem. Int. Ed.*, 2015, **54**, 10555; *Angew. Chem.,* 2015, **127,** 10701–10704; c) H.-C. Xu and K. D. Moeller, *Angew. Chem. Int. Ed.*, 2010, **49**, 8004; *Angew. Chem.,* 2010, **122,** 8176–8179.

15 L. Eberson, M. P. Hartshorn and O. Persson, *J. Chem. Soc., Perkin Trans. 2*, 1995, 1735.

16 a) R. Francke, D. Cericola, R. Kötz, D. Weingarth and S. R. Waldvogel, *Electrochim. Acta*, 2012, **62**, 372; b) A. Kirste, G. Schnakenburg, F. Stecker, A. Fischer and S. R. Waldvogel, *Angew. Chem. Int. Ed.*, 2010, **49**, 971; *Angew. Chem,* 2010, **122,** 983–987; c) B. Riehl, K. Dyballa, R. Franke and S. Waldvogel, *Synthesis*, 2016, **49**, 252.

17 P. Naumov, Y. Topcu, M. Eckert-Maksic, Z. Glasovac, F. Pavosevic, M. Kochunnoonny and H. Hara, *J. Phys. Chem. A*, 2011, **115**, 7834.

18 M. J. Di Grandi, *Org. Biomol. Chem.*, 2014, **12**, 5331.

19 S. Böhm and O. Exner, *Chem. Eur. J.*, 2000, **6**, 3391.

A4

Electronic Supplementary Material (ESI) for ChemComm.

TABLE OF CONTENTS

General information

All reagents were used in analytical grades and were obtained from commercial sources. Solvents were purified by standard methods.[1] For electrochemical reactions, different electrode materials were used: isostatic graphite electrodes were obtained from SGL carbon, Bonn, Germany.

Column chromatography was performed on silica gel 60 M (0.040-0.063 mm, Macherey-Nagel GmbH & Co, Düren, Germany) with a maximum pressure of 2.0 bar. Either a glass column or a preparative chromatography system (Büchi-Labortechnik GmbH, Essen, Germany) were used with a Büchi Control Unit C-620, an UV detector Büchi UV photometer C-635, Büchi fraction collector C-660 and two Pump Modules C-605 for adjusting the solvent mixtures. Mixtures of hexane and ethyl acetate (7:1) or cyclohexane and ethyl acetate (10:1) were used as eluents. Silica gel 60 sheets on aluminium (F254, Merck, Darmstadt, Germany) were employed for thin layer chromatography.

Gas chromatography was performed on a Shimadzu GC-2025 (Shimadzu, Japan) using a Zebron ZB-5MSi column (Phenomenex, USA; length: 30 m, inner diameter: 0.25 mm, film: 0.25 µm, pre-column: 5 m, carrier gas: hydrogen). GC-MS measurements were carried out on a Shimadzu GC-2010 (Shimadzu, Japan) using a Zebron ZB-5MSi column (Phenomenex, USA; length: 30 m, inner diameter: 0.25 mm, film: 0.25 µm, pre-column: 5 m, carrier gas: helium) combined with a GCMS-QP2010.

Microanalysis was performed by a VarioMICRO cube (Elementar Analysesysteme, Hanau, Germany).

Melting points were determined by a Melting Point Apparatus SMP3 (Stuart Scientific, Staffordshire, U.K.) and are uncorrected.

Spectroscopy and Spectrometry: ^{1}H NMR, ^{13}C NMR and ^{19}F spectra were recorded at 25 °C by using a Bruker Avance II 400 or a Bruker Avance III HD 400 (Analytische Messtechnik, Karlsruhe, Germany). Chemical shifts (δ) are reported in parts per million (ppm) relative to TMS as internal standard or traces of $CHCl_3$ or DMSO in the corresponding deuterated solvent. For the ^{19}F spectra, α-trifluortoluene served as external standard (δ = –63.9 ppm).[2] Mass spectra and high resolution mass spectra were obtained by using a QTof Ultima 3 (Waters, Milford, Massachusetts) apparatus employing ESI+.

X-ray analysis: All data were collected on a STOE IPDS2T diffractometer (Oxford Cryostream 700er series, Oxford Cryosystems) using graphite monochromated Mo K_α radiation (λ= 0.71073 Å). Intensities were measured using fine-slicing ω and φ-scans and corrected for background, polarization and Lorentz effects. The structures were solved by direct methods and refined anisotropically by the least-squares procedure implemented in the SHELX program system.[3]

The supplementary crystallographic data for this paper can be obtained free of charge from The Cambridge Crystallographic Data Center via www.ccdc.cam.ac.uk/data_request/cif. Deposition numbers and further details are given with the individual characterization data.

[1] W. L. F. Armarego and C. L. L. Chai, *Purification of laboratory chemicals*, Butterworth-Heinemann, Amsterdam, 5th ed., **2003**.

[2] S. Berger, S. Braun, H.-O. Kalinowski, *NMR-Spektroskopie von Nichtmetallen*, Thieme, Stuttgart, **1994**.

[3] G. M. Sheldrick, *SHELXS97* and *SHELXL97: Programm for the Refinement of Crystal Structures;* Dept. of Structural Chemistry, University of Göttingen: Germany, **1997**.

Electrolysis protocols

General electrolysis protocol A in 25 mL three-necked flasks

A solution of 0.4 mmol anilide derivative and 38 mg tetrabutylammonium hexafluorophosphate (0.01 M) in 10 mL hexafluoroisopropanol (HFIP) is placed in a 25 mL three-necked round-bottom flask. A reticulated vitreous carbon (100 PPI) anode and a platinum wire cathode is placed in the solution and sonicated for 30 s. The solution is electrolyzed with a constant current of 8.4 mA until 2 F are applied. Full conversion is checked by TLC. After electrolysis, the solvent is removed via distillation and product is isolated via column chromatography with mixtures of hexanes and ethyl acetate.

Figure 1: Electrochemical set-up in a three-necked flask (electrolysis protocol A) and the 25 mL beaker-type glass cell (electrolysis protocol B).

General electrolysis protocol B in 25 mL glass cells

Undivided 25 mL glass electrolysis cells were used (Figure 1). A solution of 1.0 mmol anilide derivative and 97 mg tetrabutylammonium hexafluorophosphate is electrolyzed with a current density of 2.5 mA/cm^2 using an isostatic graphite anode and a platinum cathode, until 2 F are applied. Full conversion is checked via TLC. For optimization studies, different currents were applied. The electrode area in solution is 8.0 cm^2 After electrolysis, the solvent is recovered by distillation and the product is isolated via column chromatography with mixtures of cyclohexane and ethyl acetate.

Tested solvents and non-convertible anilides

Table 1: Tested solvents and their applicability for the conversion.

Solvent	Applicability
HFIP	✓
acetonitrile	product traces
methanol	no product formation

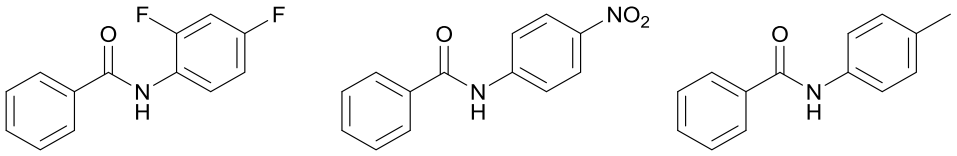

Scheme 1: Non-convertible anilides.

Synthesis of starting materials

Substituted Benzanilides and pivalanilides were prepared from acid chlorides and corresponding anilines according to the literature.[4]

N-(4-Trifluoromethansulfonylphenyl)benzamide

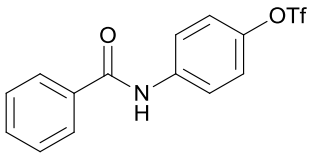

To a solution of 426 mg *N*-(4-hydroxyphenyl)benzamide (2 mmol) in 10 mL pyridine was added 404 µL trifluoromethansulfonic anhydride (2.4 mmol) dropwise at 0 °C. The mixture was allowed to stir at 0 °C for 10 minutes and 12 h at room temperature. 20 mL ethyl acetate was added and the organic layer was washed with aqueous 1 M $CuSO_4$ solution (3 x 20 mL) and water (1 x 40 mL). The organic layer was dried with $MgSO_4$ and the solvent was removed under reduced pressure the yield 654 mg of the pure triflate as orange solid (yield: 95%, 1.89 mmol)

^{1}H NMR (400 MHz, DMSO-d_6) δ = 10.53 (s, 1H), 7.99 – 7.92 (m, 4H), 7.64 – 7.59 (m, 1H), 7.58 – 7.52 (m, 2H), 7.52 – 7.48 (m, 2H).

^{13}C NMR (101 MHz, DMSO-d_6) δ = 165.84, 144.50, 139.58, 134.51, 131.85, 128.45, 127.73, 121.78, 121.75, 118.26 (q, *J* = 321.1 Hz).

^{19}F NMR (377 MHz, DMSO-d_6) δ = -73.90.

HRMS for $C_{14}H_{10}F_3NO_4S$ (ESI+) [M+Na^+]: calc.: 368.0180, found: 368.0172.

Synthesis of benzoxazoles (2a-i)

Some benzoxazoles were prepared according to electrolysis protocol A and electrolysis protocol B. For these compounds, only one protocol is named.

6-Chloro-2-phenyl-1,3-benzoxazole (2a)

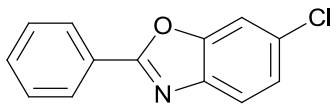

According to electrolysis protocol B, 232 mg *N*-(4-chlorophenyl)benzamide (1.0 mmol) are electrolyzed until 2 F are applied. Column chromatography yielded 152 mg product as colorless solid (yield: 66%, 0.66 mmol).

^{1}H NMR (400 MHz, $CDCl_3$) δ = 8.23 – 8.20 (m, 2H), 7.66 (d, J = 8.5 Hz, 1H), 7.58 (d, J = 2.0 Hz, 1H), 7.54 – 7.50f (m, 3H), 7.32 (dd, J = 8.5, 2.0 Hz, 1H).

[4] a) W. M. Seganish, P. DeShong, *J. Org. Chem.*, 2004, **69**, 1137; b) F. Buckingham, S. Calderwood, B. Checa, T. Keller, M. Tredwell, T. L. Collier, I. M. Newington, R. Bhalla, M. Glaser, V. Gouverneur, *J. Fluorine Chem.* 2015, **180**, 33.

^{13}C NMR (101 MHz, $CDCl_3$) δ = 163.64, 150.86, 140.84, 131.76, 130.62, 128.93, 127.61, 126.65, 125.24, 120.42, 111.20.

HRMS for $C_{13}H_8ClNO$ (ESI+) [M+H$^+$]: calc.: 230.0373, found: 230.0373.

MP: 102.0–103.0 °C (CH_2Cl_2)

6-Methoxy-2-phenyl-1,3-benzoxazole (2b)

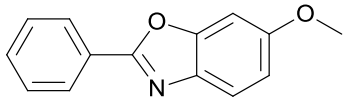

According to electrolysis protocol A, 227 mg *N*-(4-chlorophenyl)benzamide (0.4 mmol) are electrolyzed until 2 F are applied. Column chromatography yielded 77 mg product as colorless solid (yield: 86%, 0.34 mmol).

^{1}H NMR (400 MHz, $CDCl_3$) δ = 8.27 – 8.11 (m, 2H), 7.62 (d, *J* = 8.8 Hz, 1H), 7.55 – 7.38 (m, 3H), 7.05 (d, *J* = 2.4 Hz, 1H), 6.92 (dd, *J* = 8.8, 2.4 Hz, 1H), 3.81 (s, 3H).

^{13}C NMR (101 MHz, $CDCl_3$) δ = 162.01, 158.11, 151.46, 135.71, 130.88, 128.69, 127.01, 119.80, 112.64, 95.24, 55.72.

HRMS for $C_{14}H_{11}NO_2$ (ESI+) [M+H$^+$]: calc.: 226.0868, found: 226.0867.

MP: 66.0–67.0 °C (CH_2Cl_2)

6-Trifluormethansulfonat-2-phenyl-1,3-benzoxazole (2c)

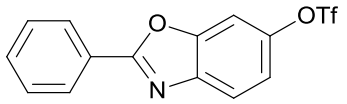

According to electrolysis protocol B, 138 mg *N*-(4-trifluormethansulfonylphenyl)benzamide (0.4 mmol) are electrolyzed until 2 F are applied. Column chromatography yielded 82 mg product as colorless solid (yield: 60%, 0.24 mmol).

^{1}H NMR (400 MHz, $CDCl_3$) δ = 8.37 – 8.17 (m, 2H), 7.81 (d, *J* = 8.7 Hz, 1H), 7.65 – 7.47 (m, 4H), 7.30 (dd, *J* = 8.7, 2.4 Hz, 1H).

^{13}C NMR (101 MHz, $CDCl_3$) δ = 165.22, 150.33, 146.31, 141.98, 132.24, 129.08, 127.82, 126.31, 120.65, 118.76 (q, J = 321.0 Hz), 118.23, 105.06.

^{19}F NMR (377 MHz, $CDCl_3$) δ = -73.67.

HRMS for $C_{14}H_8F_3NO_4S$ (ESI+) [M+H$^+$]: calc.: 344.0204, found: 344.0207.

MP: 92.0–93.0 °C (EtOH)

Anal. Calcd for $C_{14}H_8F_3NO_4S$: C, 48.99; H, 2.35; N, 4.08; S, 9.34. Found: C, 49.03; H, 2.30; N, 4.10; S, 9.80

Crystal structure determination of 2c (CCDC 1530094): $C_{14}H_8F_3NO_4S$, M_r = 343.2 g/mol, colorless block (0.09 x 0.33 x 0.42 mm^3), P $2_1/c$ (monoklin), a = 16.5356 Å, b = 7.3275 Å, c = 11.8114 Å, V = 1364.76 $Å^3$, Z = 4, F(000) = 696, ρ = 1.669 g/cm^3, μ = 0.290 mm^{-1}, Mo-Kα graphite monochromator (0.71073 Å), 120 K, 107.5 °, 7371 reflections, 3288 independent reflections, wR_2 = 0.0843, R_1 = 0.0338, 0.37 e/$Å^3$, –0.33 e/$Å^3$, GoF = 1.021

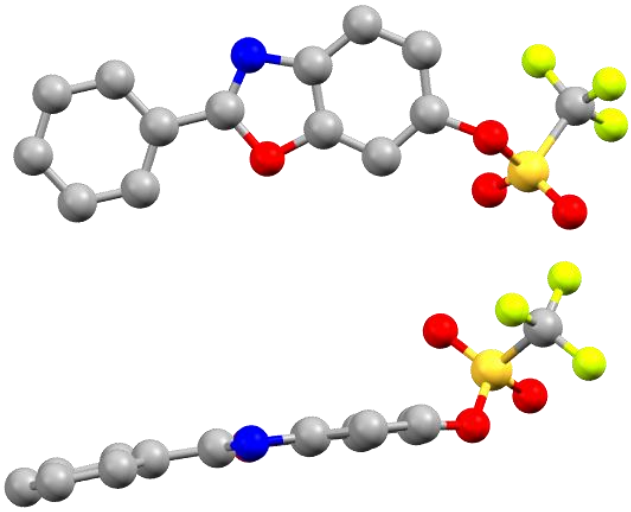

Figure 2: Molecular structure of derivative 2c by X-ray analysis (up: top view; down: side view).

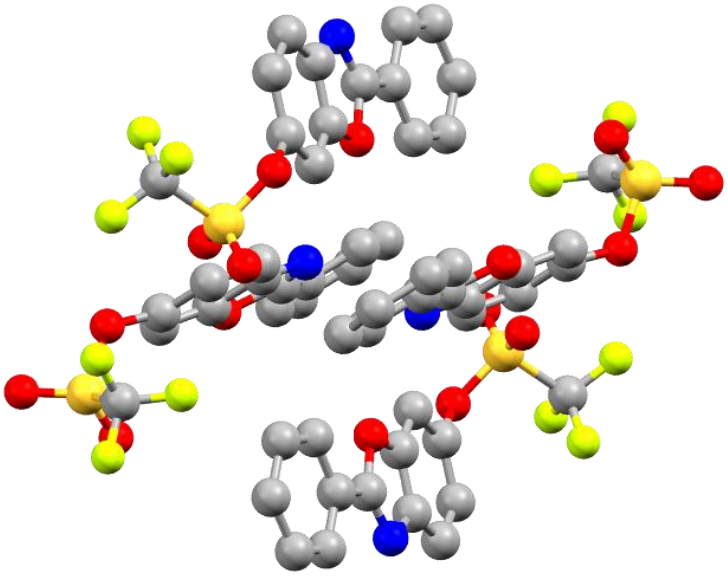

Figure 3 Packing of 2c in the solid state.

Single crystals for structure determination were obtained by recrystallization from ethanol at room temperature. In the packing, a significant π- π interaction between the benzoxazole and phenyl moieties is present.

6-Fluoro-2-phenyl-1,3-benzoxazole (2d)

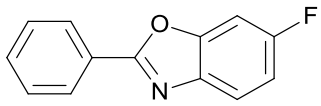

According to electrolysis protocol B, 215 mg *N*-(4-fluorophenyl)benzamide (1.0 mmol) are electrolyzed until 2 F are applied. Column chromatography yielded 125 mg product as colorless solid (yield: 59%, 0.59 mmol).

^{1}H NMR (400 MHz, $CDCl_3$) δ = 8.25 – 8.19 (m, 2H), 7.70 (dd, *J* = 8.7, 4.9 Hz, 1H), 7.58 – 7.49 (m, 3H), 7.31 (dd, *J* = 7.9, 2.4 Hz, 1H), 7.11 (ddd, *J* = 9.6, 8.7, 2.4 Hz, 1H).

^{13}C NMR (101 MHz, $CDCl_3$) δ = 163.69 (d, J = 3.4 Hz), 160.65 (d, J = 244.1 Hz), 150.69 (d, J = 14.7 Hz), 138.40 (d, J = 1.9 Hz), 131.59, 128.94, 127.46, 126.87, 120.23 (d, J = 10.2 Hz), 112.53 (d, J = 24.7 Hz), 98.67 (d, J = 28.3 Hz).

^{19}F NMR (377 MHz, $CDCl_3$) δ = -116.22.

HRMS for $C_{13}H_8FNO$ (ESI+) [$M+H^+$]: calc.: 214.0668, found: 214.0660.

MP: 105.0–106.0 °C (CH_2Cl_2)

6-Methoxy-2-(4-methylphenyl)-1,3-benzoxazole (2e)

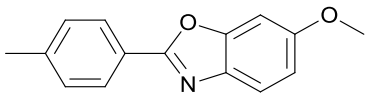

According to electrolysis protocol B, 241 mg 4-Methyl-*N*-(4-methoxyphenyl)benzamide (1.0 mmol) are electrolyzed until 2 F are applied. Column chromatography yielded 134 mg product as colorless solid (yield: 56%, 0.56 mmol).

^{1}H NMR (400 MHz, DMSO) δ = 8.12 – 8.06 (m, 2H), 7.62 (d, *J* = 8.7 Hz, 1H), 7.33 – 7.28 (m, 2H), 7.10 (d, *J* = 2.3 Hz, 1H), 6.94 (dd, *J* = 8.7, 2.4 Hz, 1H), 3.87 (s, 3H), 2.43 (s, 4H).

^{13}C NMR (101 MHz, DMSO) δ = 162.47, 158.07, 151.51, 141.50, 135.90, 129.57, 127.12, 124.56, 119.76, 112.58, 95.41, 55.91, 21.58.

HRMS for $C_{15}H_{13}NO_2$ (ESI+) [$M+H^+$]: calc.: 240.1025, found: 240.1025.

MP: 90.0–91.0 °C (CH_2Cl_2)

2-(4-Fluorophenyl)-6-methoxy-1,3-benzoxazole (2f)

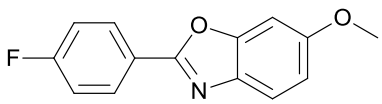

According to electrolysis protocol B, 245 mg 4-Fluoro-*N*-(4-methoxyphenyl)benzamide (1.0 mmol) are electrolyzed until 2 F are applied. Column chromatography yielded 160 mg product as colorless solid (yield: 66%, 0.66 mmol).

^{1}H NMR (400 MHz, $CDCl_3$) δ = 8.22 – 8.15 (m, 2H), 7.62 (d, *J* = 8.7 Hz, 1H), 7.23 – 7.14 (m, 2H), 7.10 (d, *J* = 2.3 Hz, 1H), 6.96 (dd, *J* = 8.7, 2.4 Hz, 1H), 3.88 (s, 3H).

^{13}C NMR (101 MHz, $CDCl_3$) δ = 165.75, 162.29 (d, *J* = 191.3 Hz), 158.27, 151.63, 135.79, 129.32 (d, *J* = 8.8 Hz), 123.68 (d, *J* = 3.4 Hz), 119.93, 116.10 (d, *J* = 22.2 Hz), 112.82, 95.43, 55.94.

^{19}F NMR (376 MHz, $CDCl_3$) δ = –109.38.

HRMS for $C_{14}H_{10}FNO_2$ (ESI+) [M+H$^+$]: calc.: 244.0774, found: 244.0776.

MP: 105.0–106.0 °C (CH_2Cl_2)

2-(4-Chlorophenyl)-6-methoxy-1,3-benzoxazole (2g)

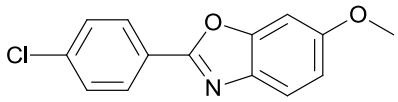

According to electrolysis protocol A, 105 mg 4-Chloro-*N*-(4-methoxyphenyl)benzamide (0.4 mmol) are electrolyzed until 2 F are applied. Column chromatography yielded 83 mg product as colorless solid (yield: 80%, 0.32 mmol).

^{1}H NMR (400 MHz, $CDCl_3$) δ = 8.09 – 8.03 (m, 2H), 7.59 (d, *J* = 8.7 Hz, 1H), 7.45 – 7.40 (m, 2H), 7.04 (d, *J* = 2.4 Hz, 1H), 6.93 (dd, *J* = 8.7, 2.4 Hz, 1H).

^{13}C NMR (101 MHz, $CDCl_3$) δ = 161.07, 158.33, 151.52, 137.08, 135.65, 129.07, 128.26, 125.72, 119.95, 112.90, 95.28, 55.82.

HRMS for $C_{14}H_{10}ClNO_2$ (ESI+) [M+H$^+$]: calc.: 260.0478, found: 260.0475.

MP: 134.0–135.0 °C (CH_2Cl_2)

6-Methoxy-2-(4-methoxyphenyl)-1,3-benzoxazole (2h)

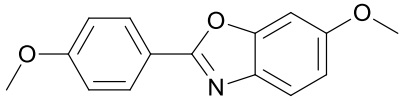

According to electrolysis protocol A, 103 mg 4-Methoxy-*N*-(4-methoxyphenyl)benzamide (0.4 mmol) are electrolyzed until 2 F are applied. Column chromatography yielded 80 mg product as colorless solid (yield: 78%, 0.31 mmol).

^{1}H NMR (400 MHz, $CDCl_3$) δ = 8.15 – 8.06 (m, 2H), 7.58 (d, *J* = 8.7 Hz, 1H), 7.05 (d, *J* = 2.4 Hz, 1H), 7.01 – 6.94 (m, 2H), 6.91 (dd, *J* = 8.7, 2.4 Hz, 1H), 3.84 (s, 6H).

^{13}C NMR (101 MHz, $CDCl_3$) δ = 162.27, 161.86, 157.81, 151.40, 135.93, 128.80, 119.82, 119.44, 114.19, 112.31, 95.36, 55.82, 55.30.

HRMS for $C_{15}H_{13}NO_3$ (ESI+) [M+Na$^+$]: calc.: 278.0793, found: 278.0797.

MP: 108.5–109.5 °C (CH_2Cl_2)

2-(2,2-Dimethylethyl)-6-methoxy-1,3-benzoxazole (2i)

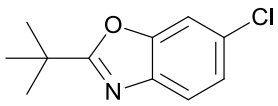

According to electrolysis protocol A, 85 mg *N*-(4-chlorophenyl)pivalamide (0.4 mmol) are electrolyzed until 2 F are applied. Column chromatography yielded 51 mg product as colorless liquid (yield: 61%, 0.24 mmol).

^{1}H NMR (400 MHz, DMSO) δ = 7.59 (dd, *J* = 8.4, 0.5 Hz, 1H), 7.50 (dd, *J* = 2.0, 0.5 Hz, 1H), 7.27 (dd, *J* = 8.4, 1.9 Hz, 1H), 1.48 (s, 9H)

^{13}C NMR (75 MHz, DMSO) δ = 174.23, 151.00, 139.99, 130.01, 124.61, 120.15, 111.02, 34.24, 28.38.

HRMS for $C_{11}H_{12}ClNO$ (ESI+) [$M+H^+$]: calc.: 210.0686, found: 210.0696.

NMR spectra

N-(4-Trifluoromethansulfonylphenyl)benzamide

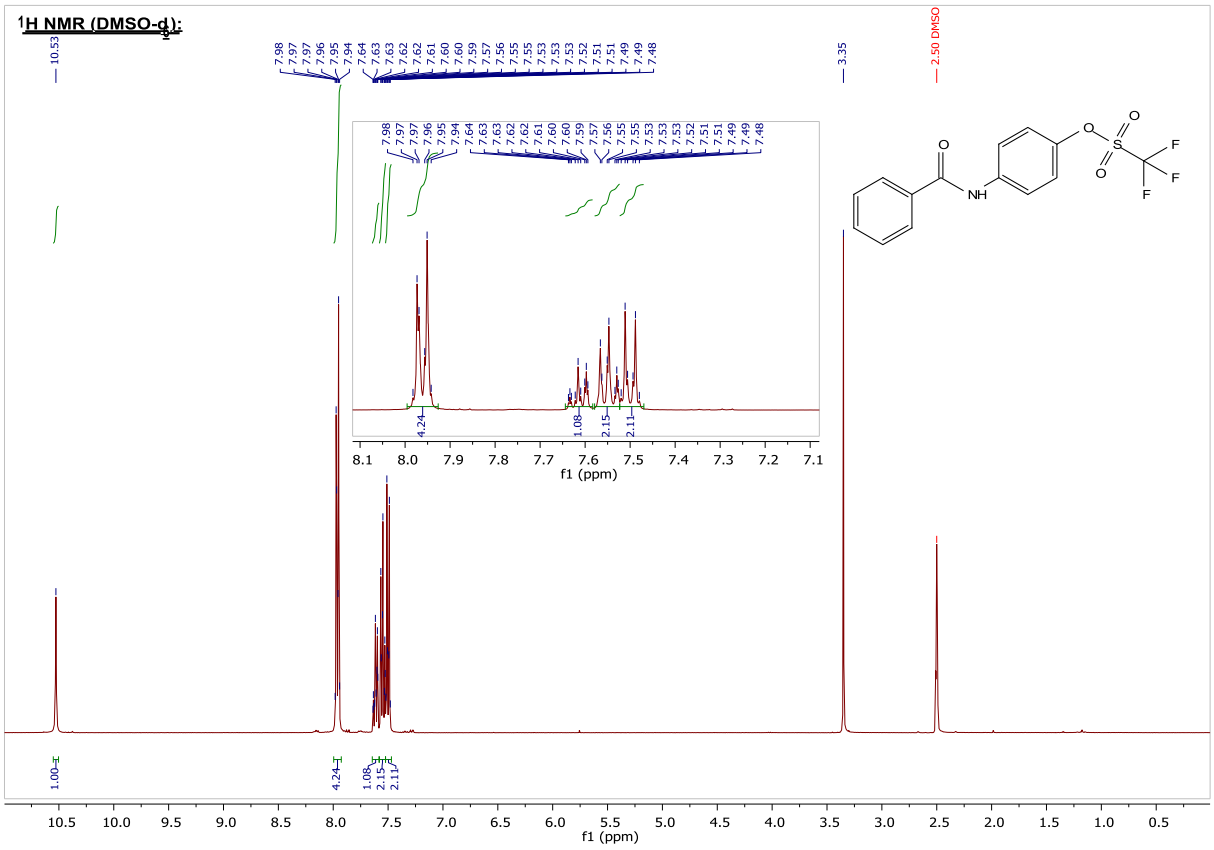

^{13}C NMR (DMSO-d$_6$):

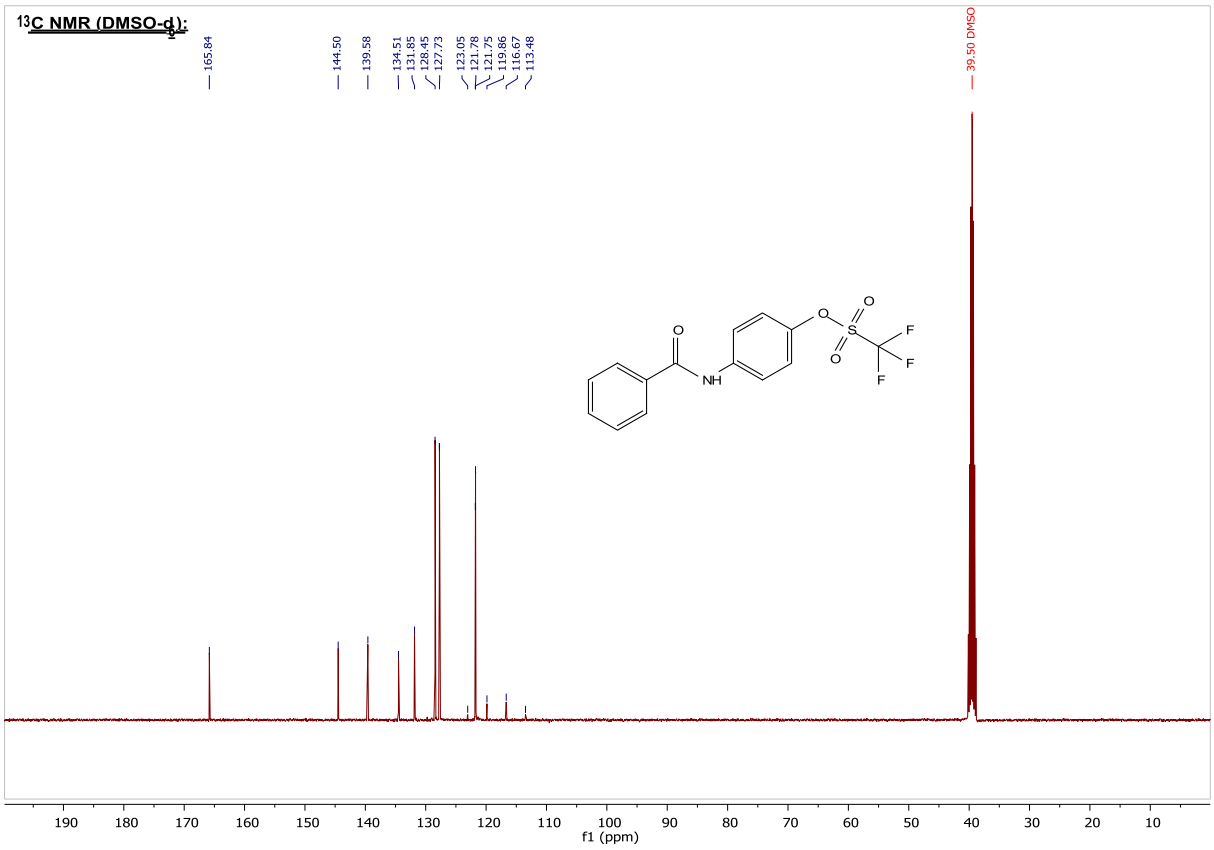

^{19}F NMR (DMSO-d$_6$):

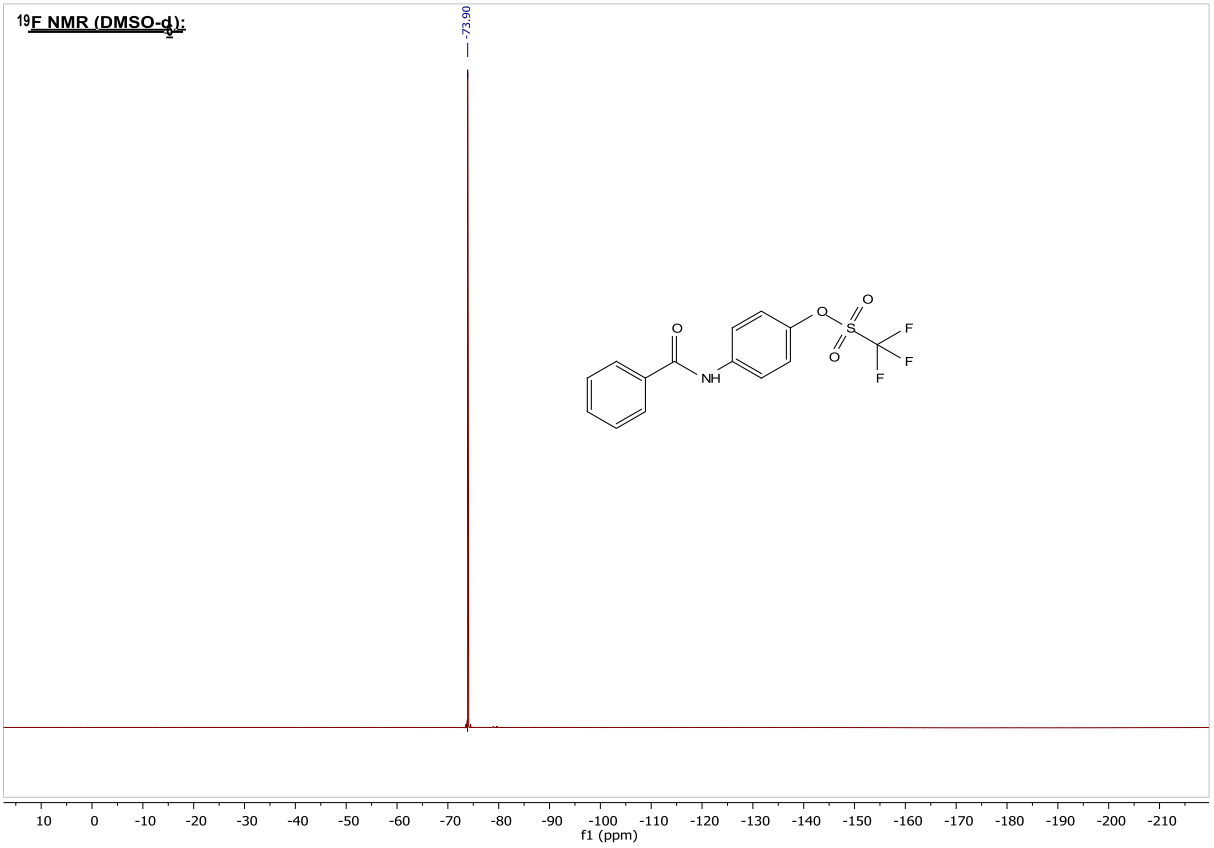

6-Chloro-2-phenyl-1,3-benzoxazole (2a)

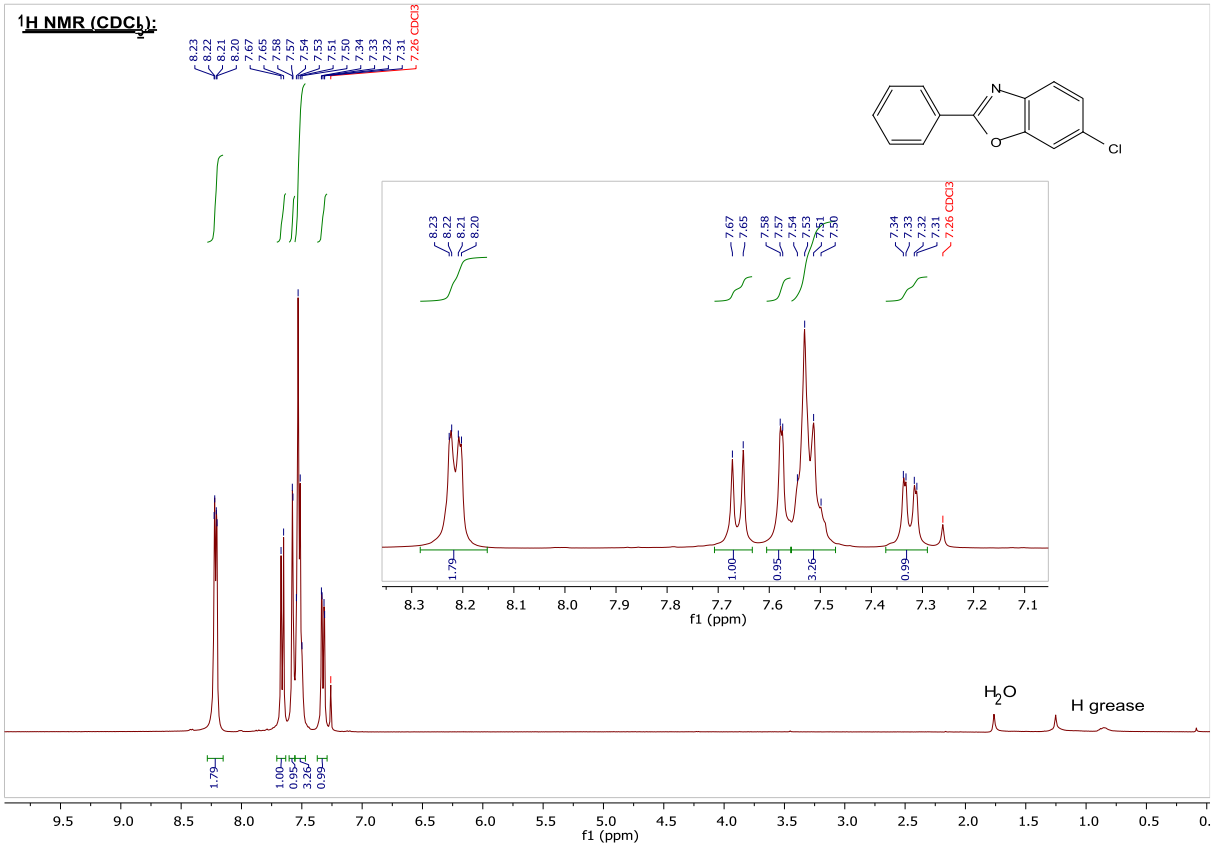

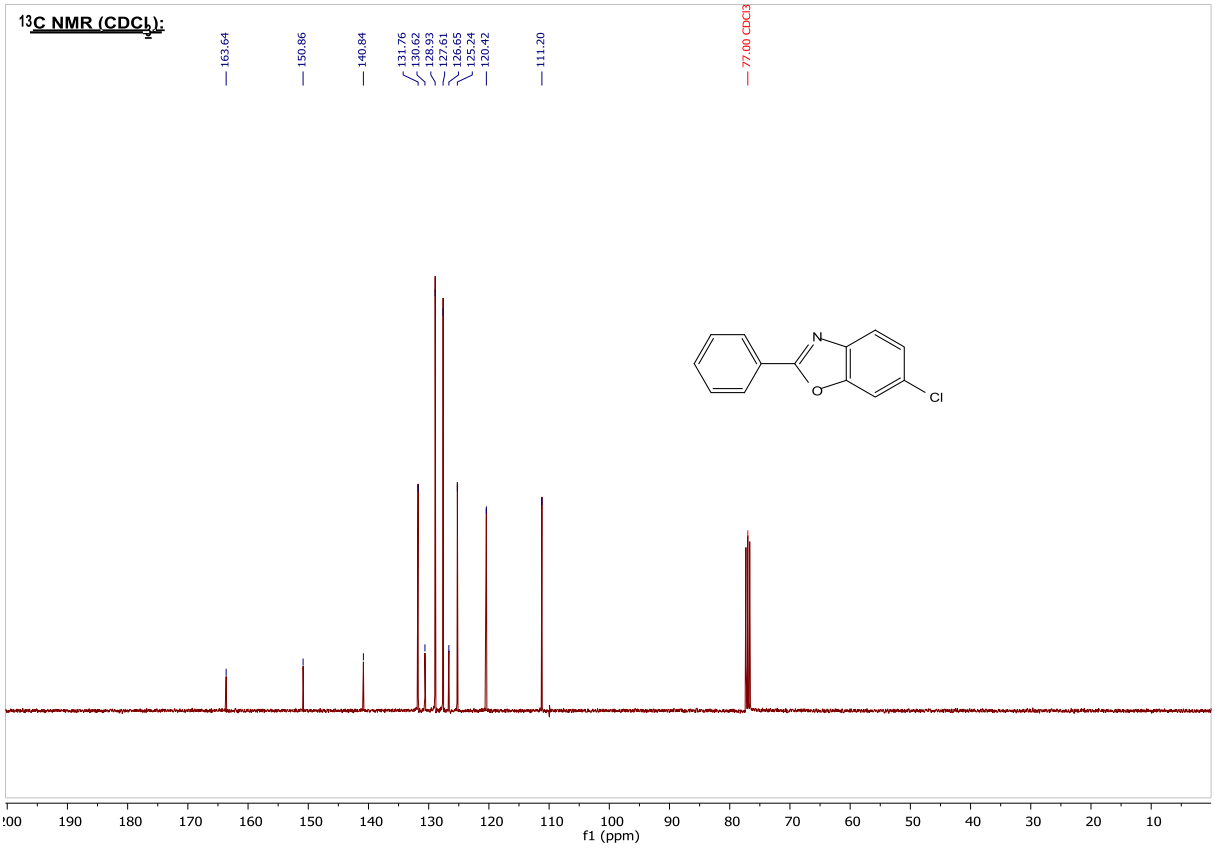

6-Methoxy-2-phenyl-1,3-benzoxazole (2b)

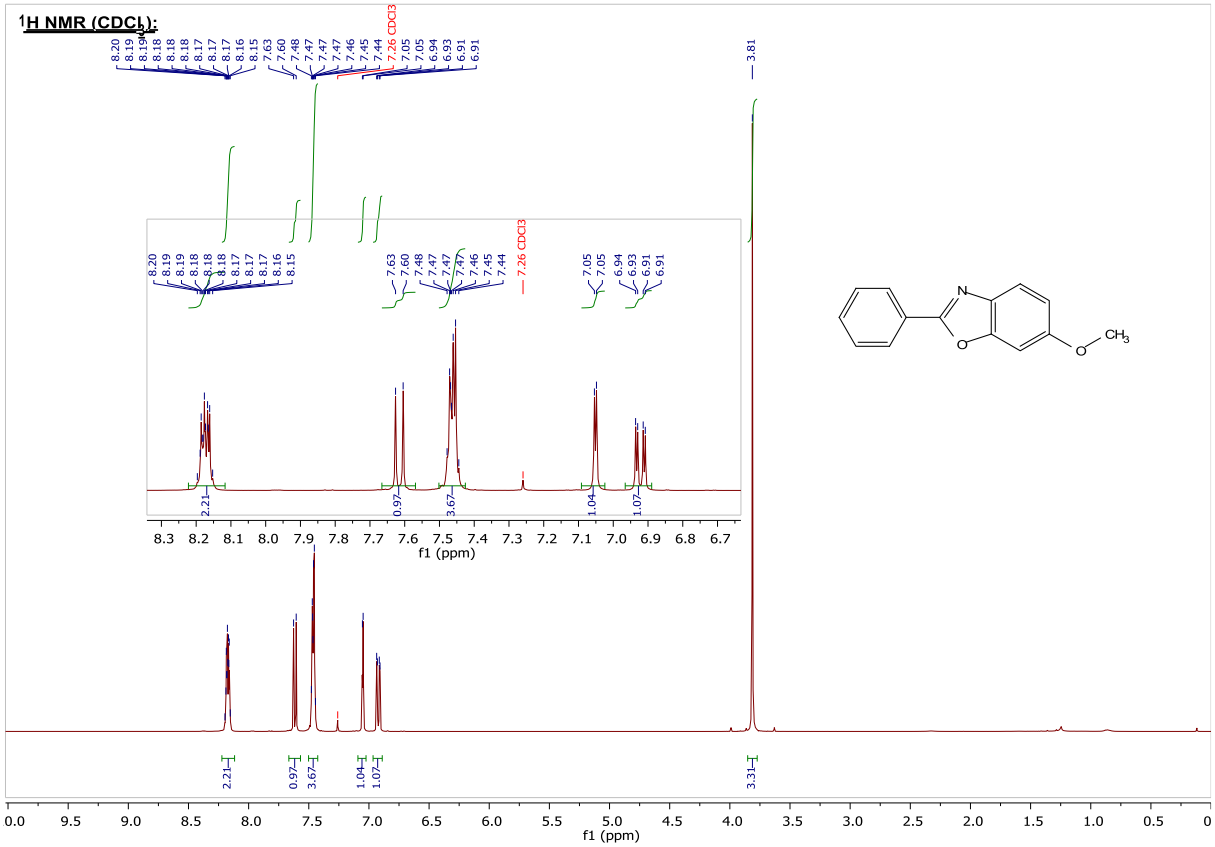

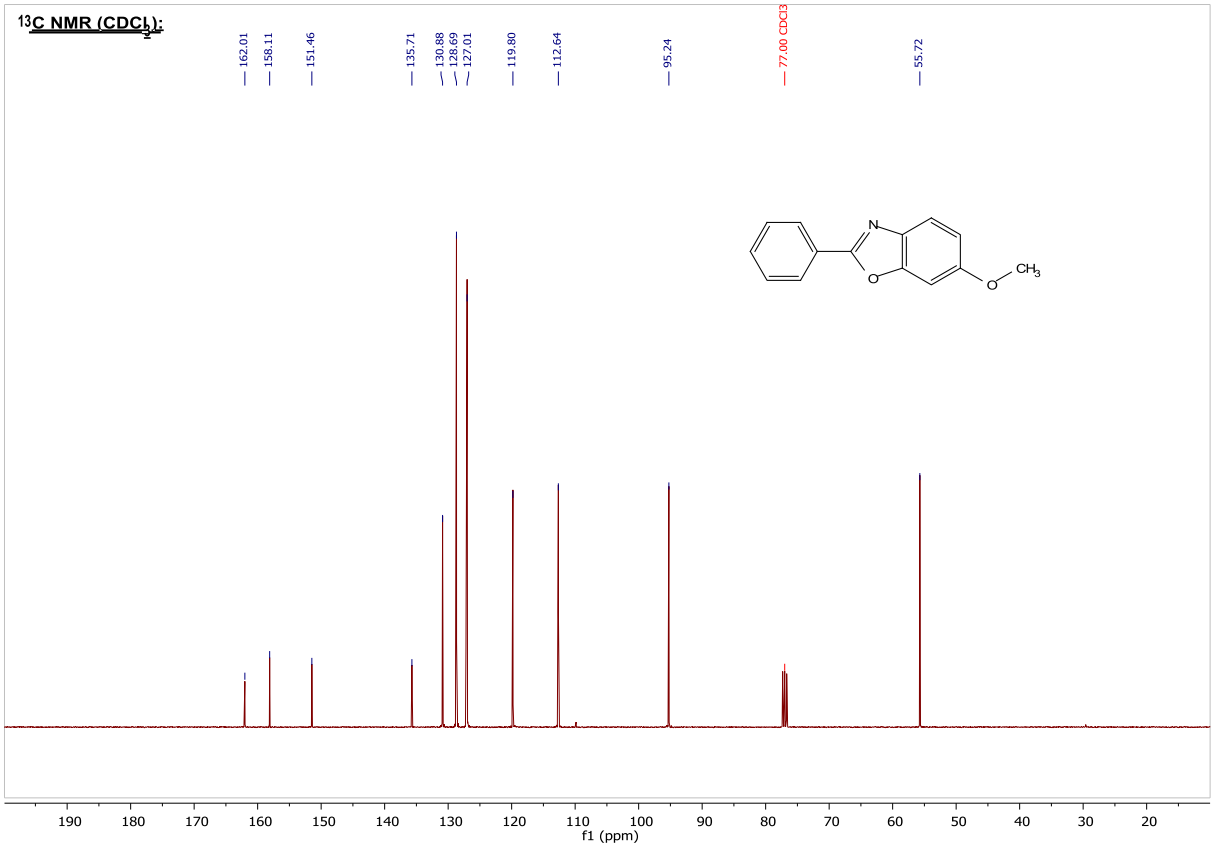

6-Trifluormethansulfonat-2-phenyl-1,3-benzoxazole (2c)

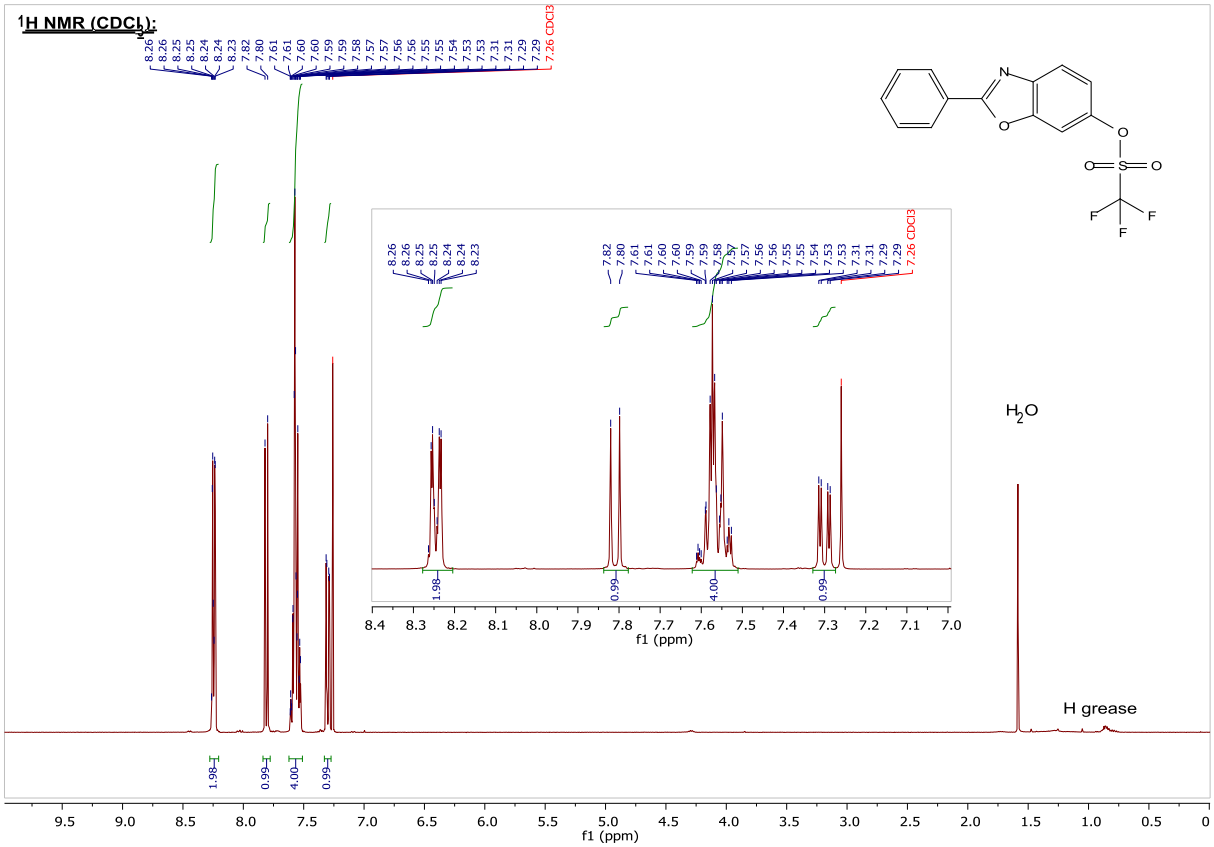

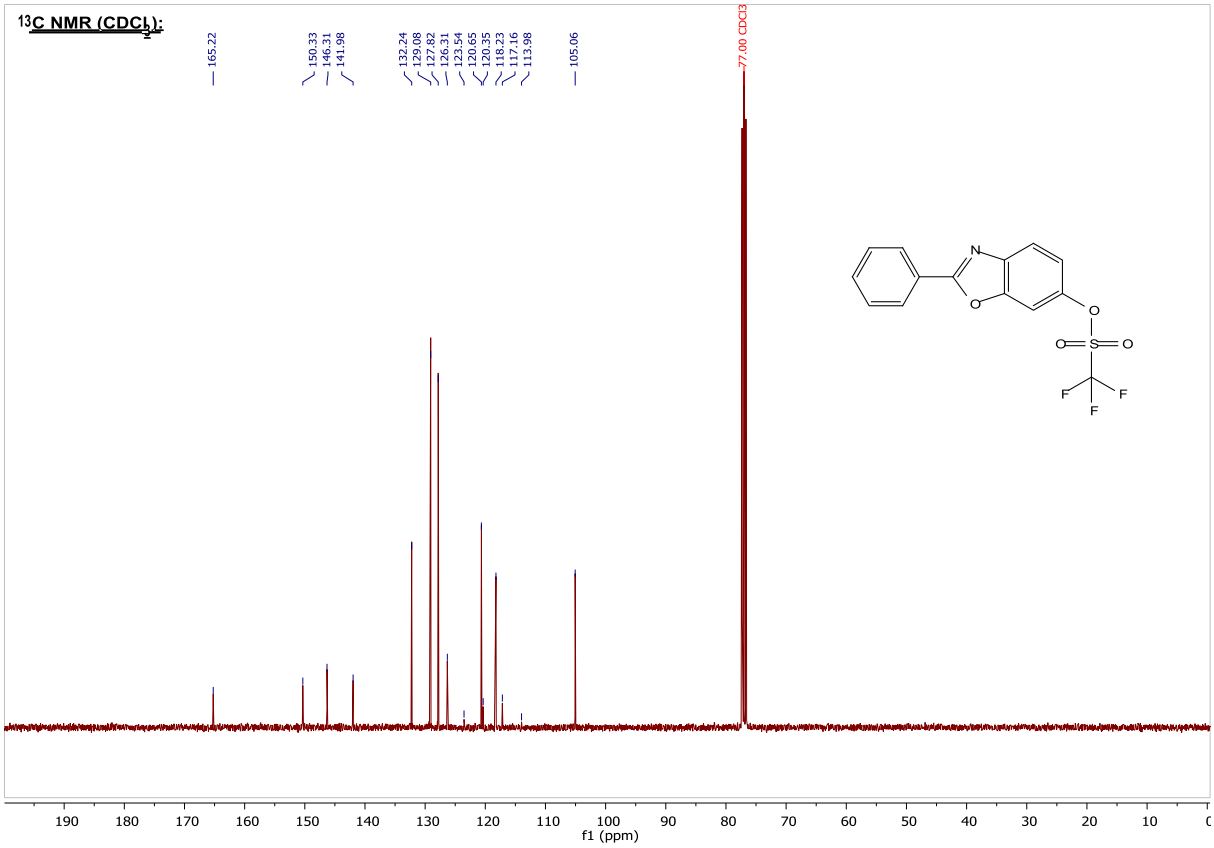
13C NMR (CDCl3):
165.22
150.33
146.31
141.98
132.24
129.08
127.82
126.31
123.54
120.65
120.35
118.23
117.16
113.98
105.06
77.00 CDCl3
f1 (ppm)

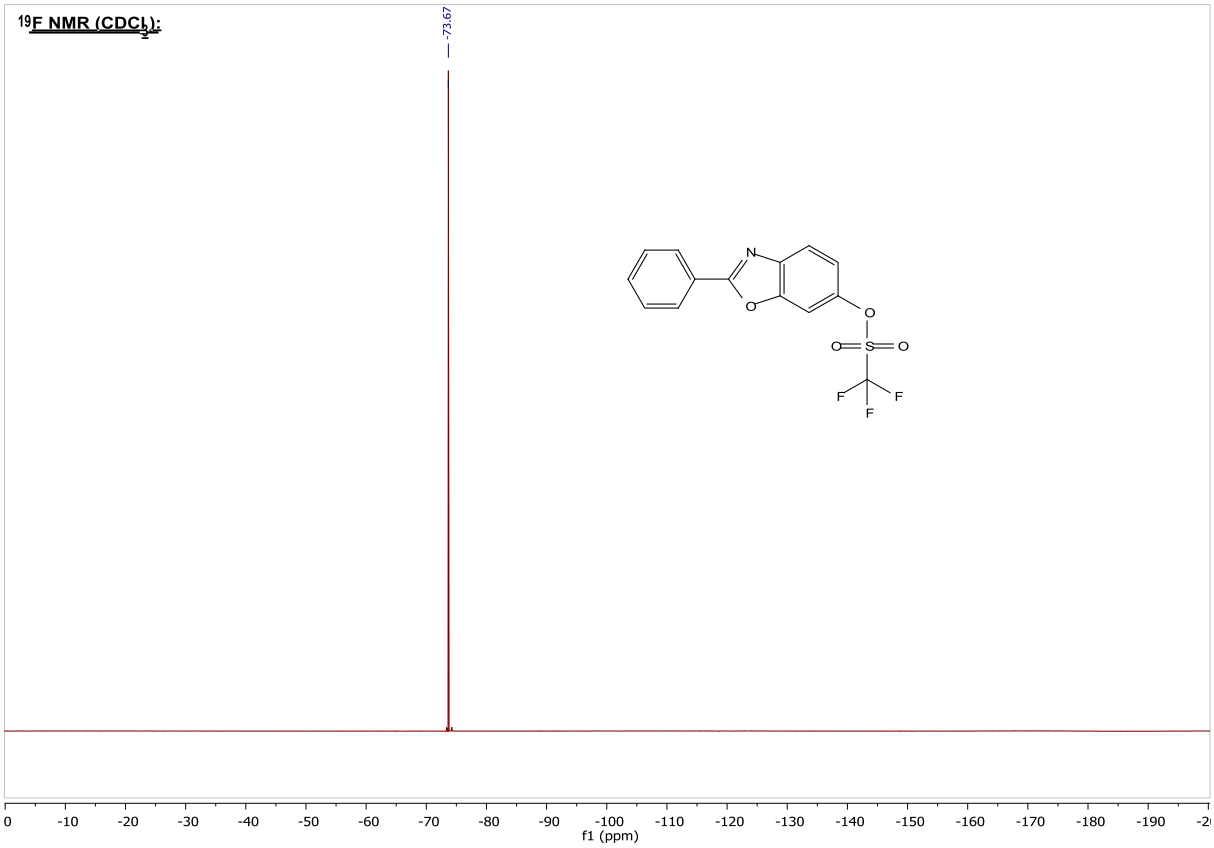
19F NMR (CDCl3):
-73.67
f1 (ppm)

6-Fluoro-2-phenyl-1,3-benzoxazole (2d)

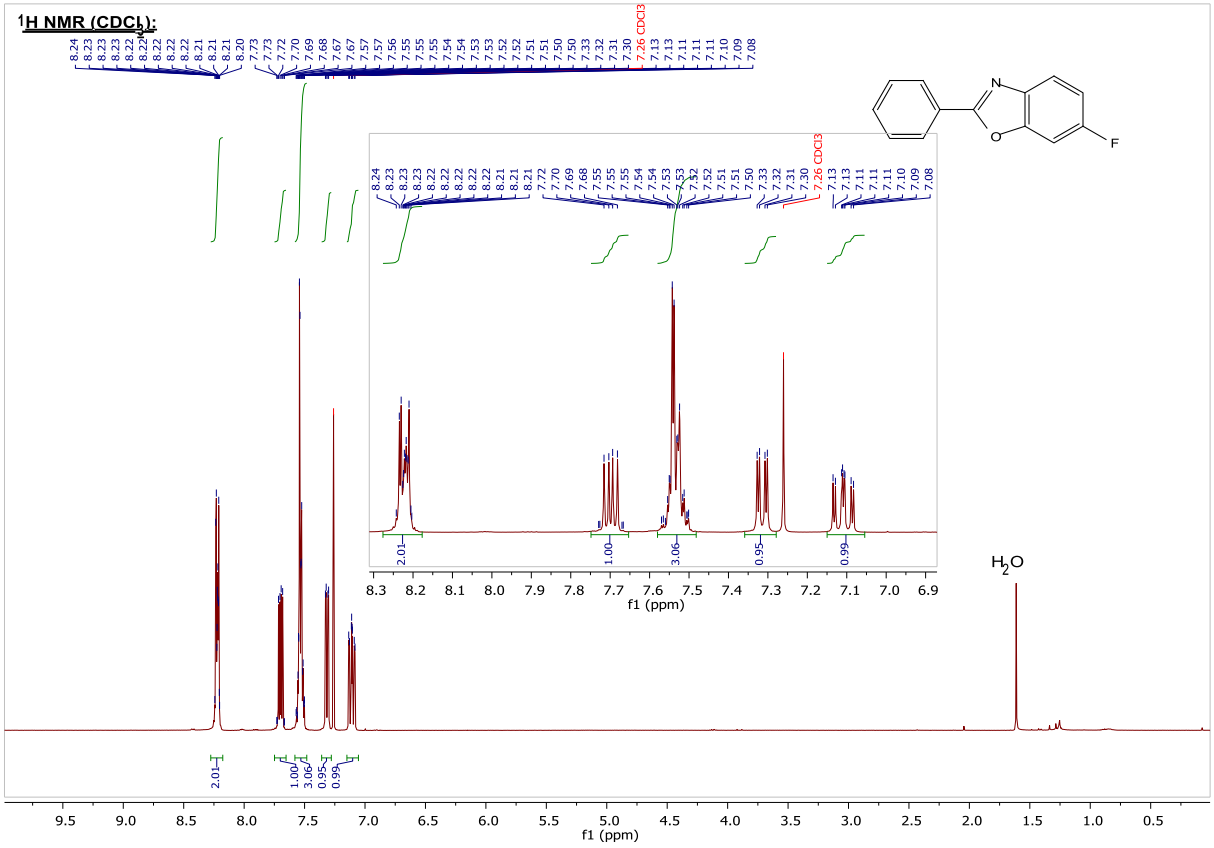

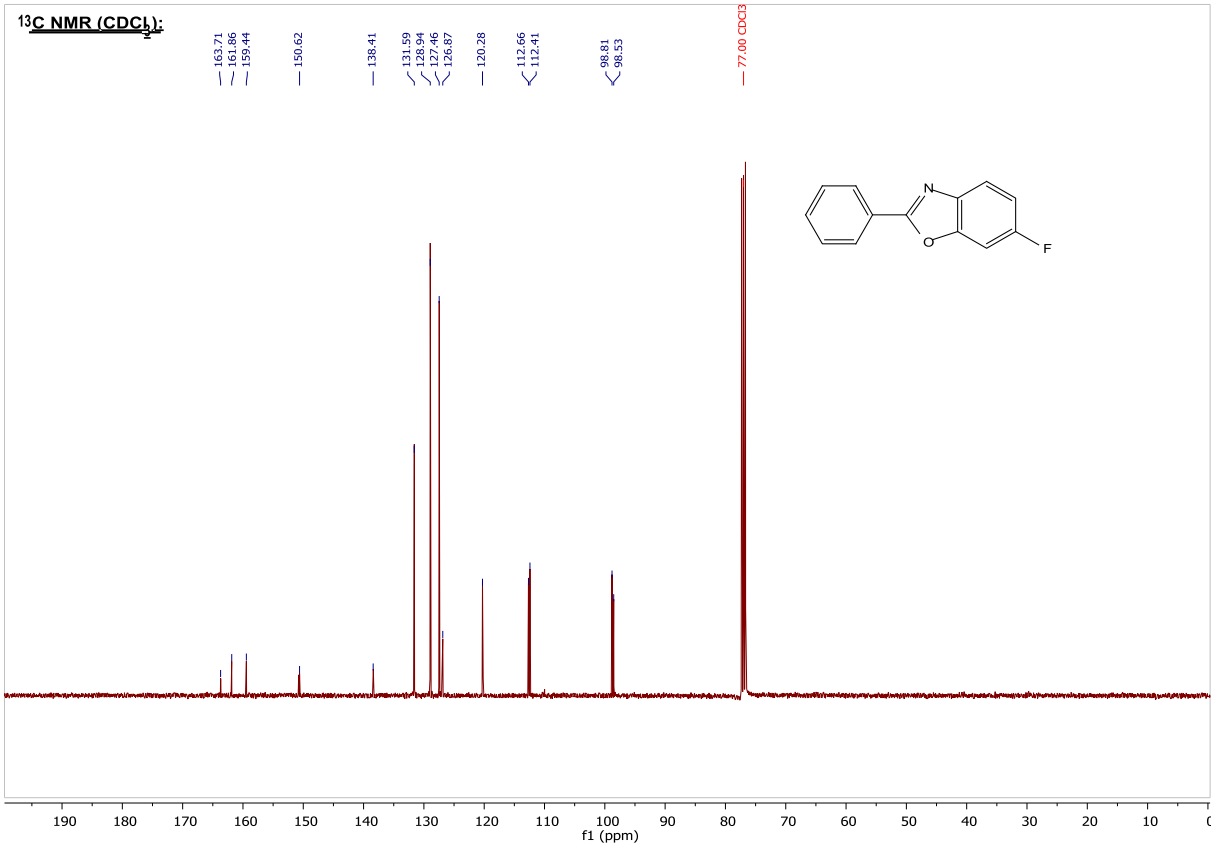
13C NMR (CDCl3):
163.71
161.86
159.44
150.62
138.41
131.59
128.94
127.46
126.87
120.28
112.66
112.41
98.81
98.53
77.00 CDCl3
N
O
F
190 180 170 160 150 140 130 120 110 100 90 80 70 60 50 40 30 20 10
f1 (ppm)

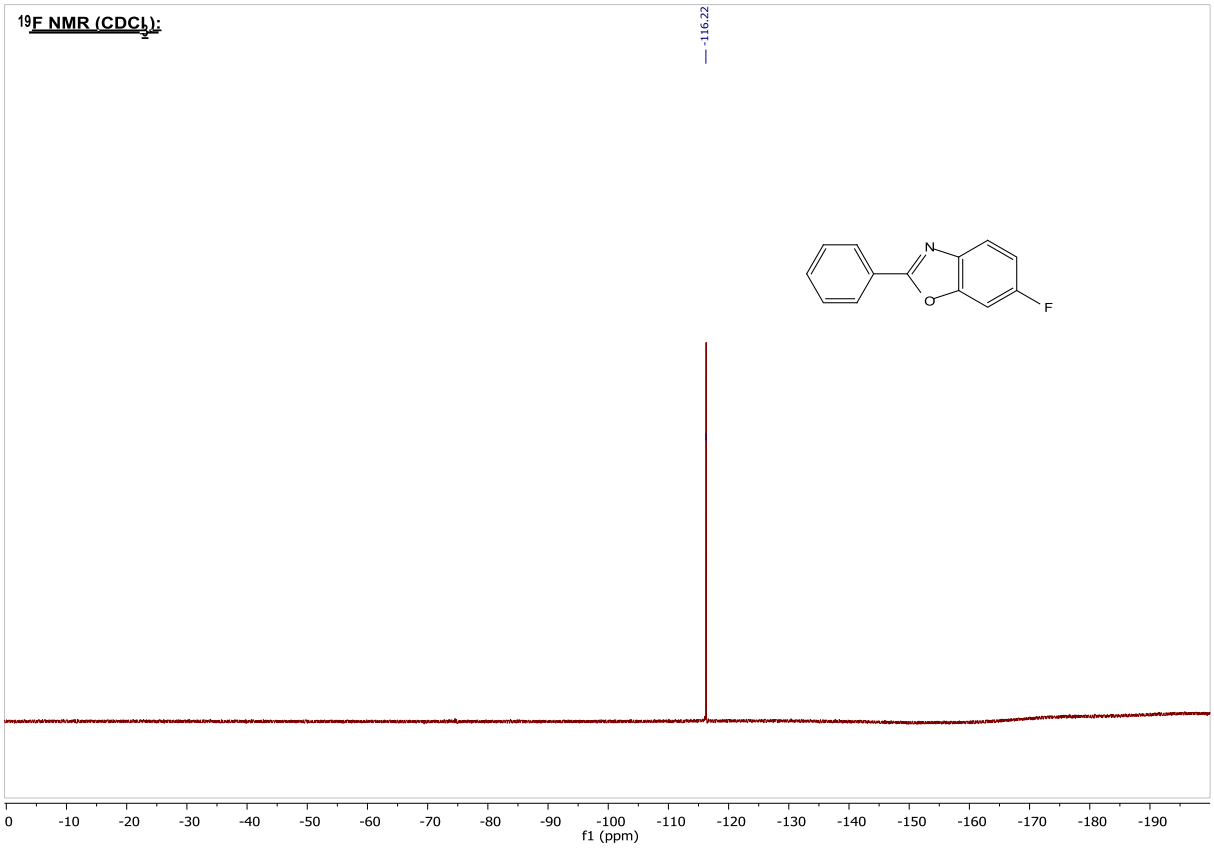
19F NMR (CDCl3):
-116.22
N
O
F
0 -10 -20 -30 -40 -50 -60 -70 -80 -90 -100 -110 -120 -130 -140 -150 -160 -170 -180 -190
f1 (ppm)

6-Methoxy-2-(4-methylphenyl)-1,3-benzoxazole (2e)

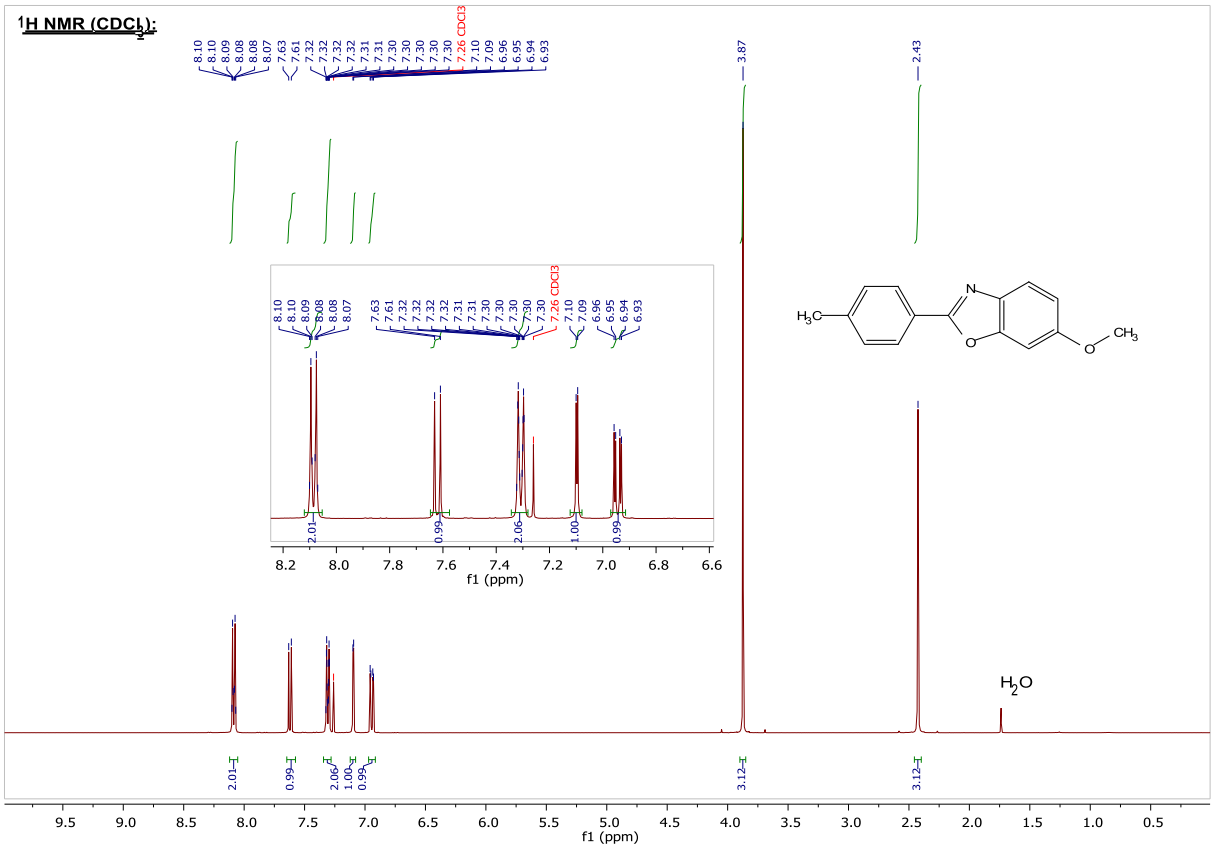

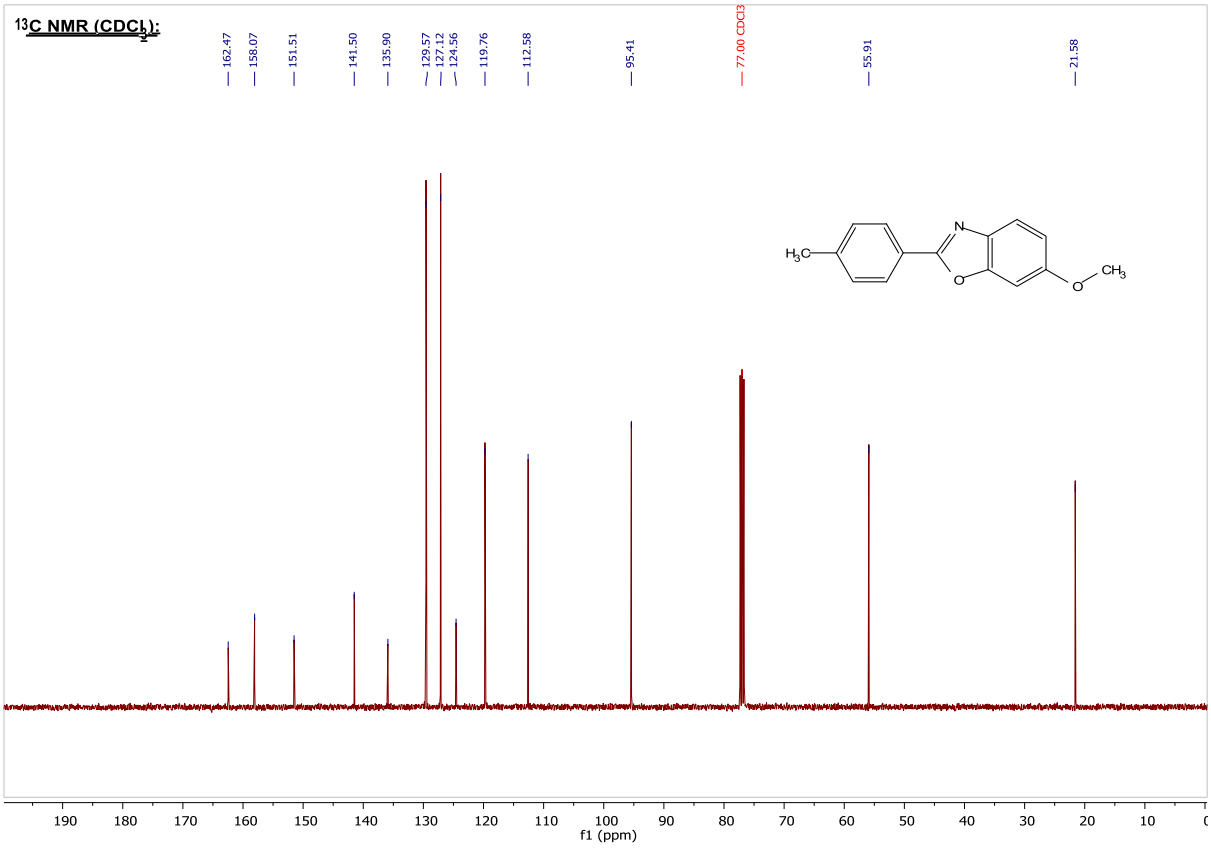

2-(4-Fluorophenyl)-6-methoxy-1,3-benzoxazole (2f)

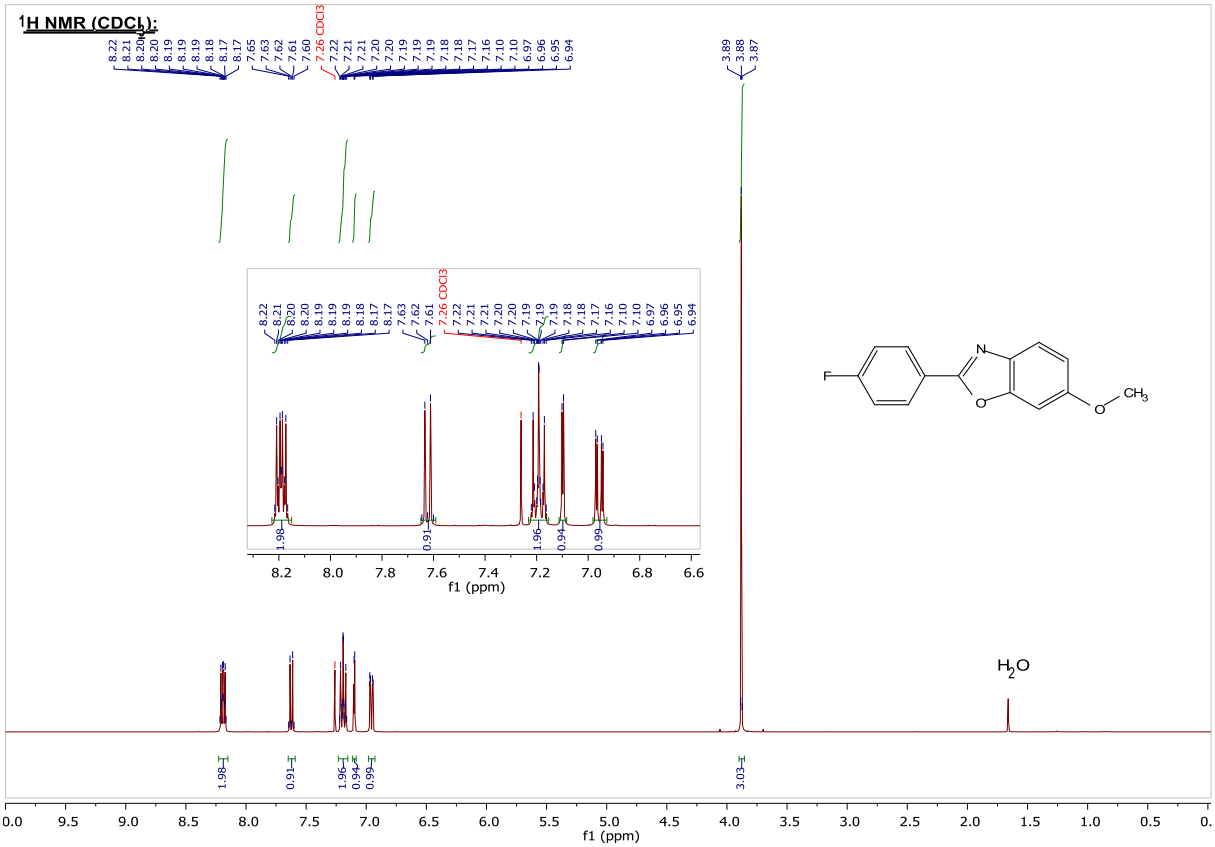

^{13}C NMR ($CDCl_3$):

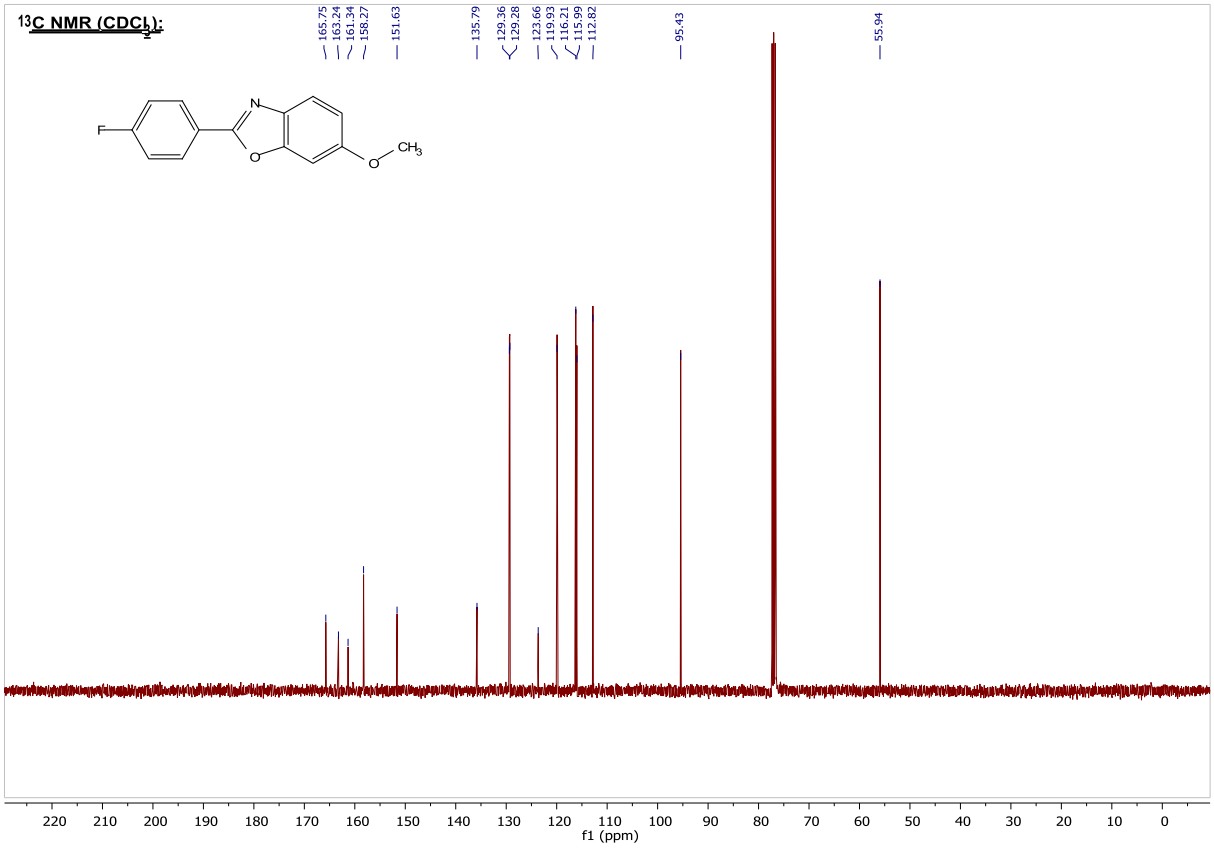

^{19}F NMR ($CDCl_3$):

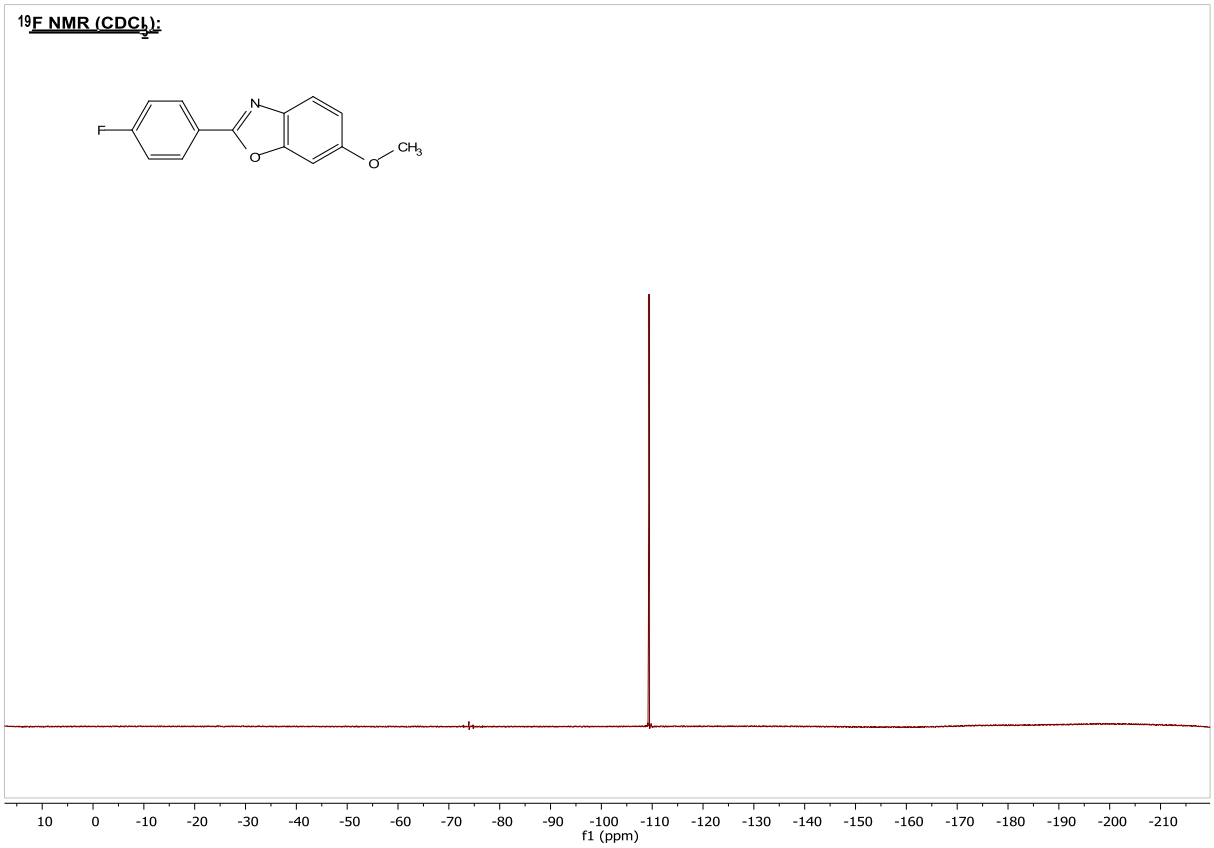

2-(4-Chlorophenyl)-6-methoxy-1,3-benzoxazole (2g)

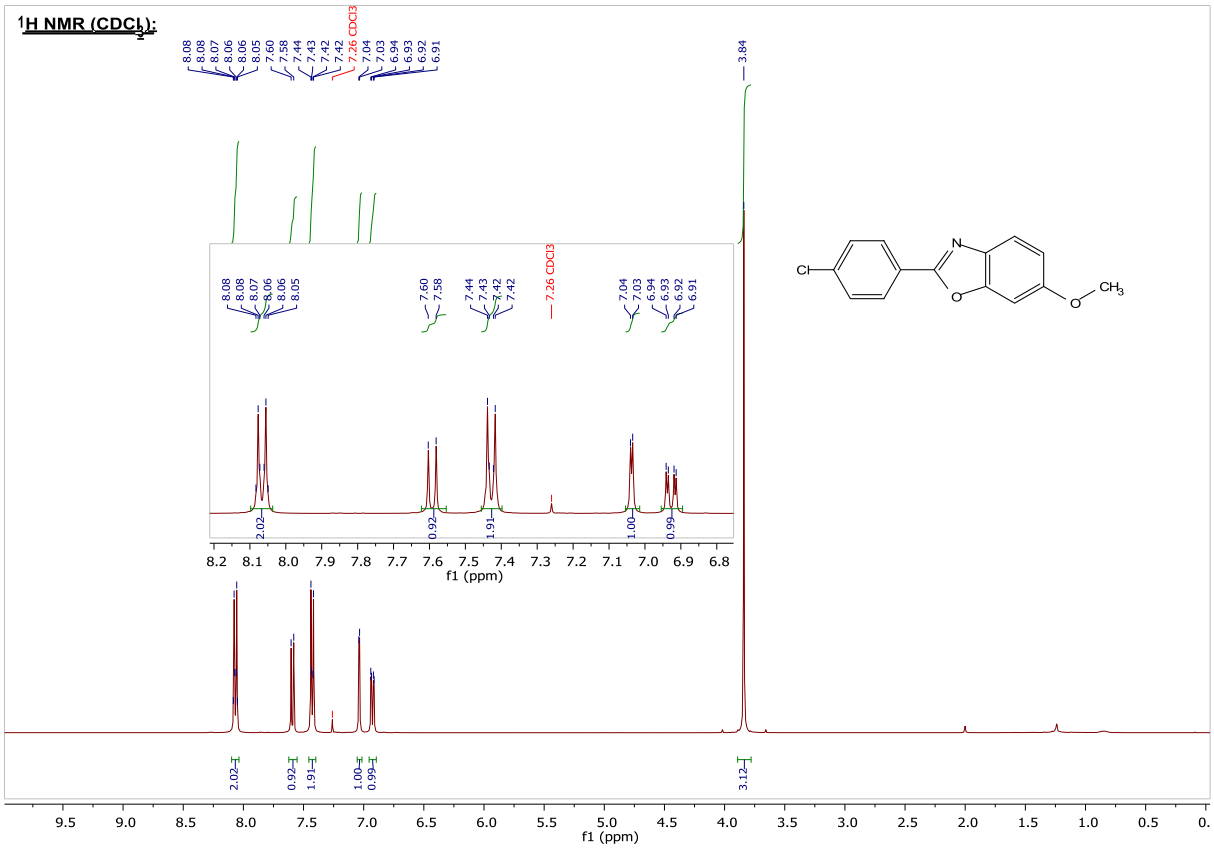

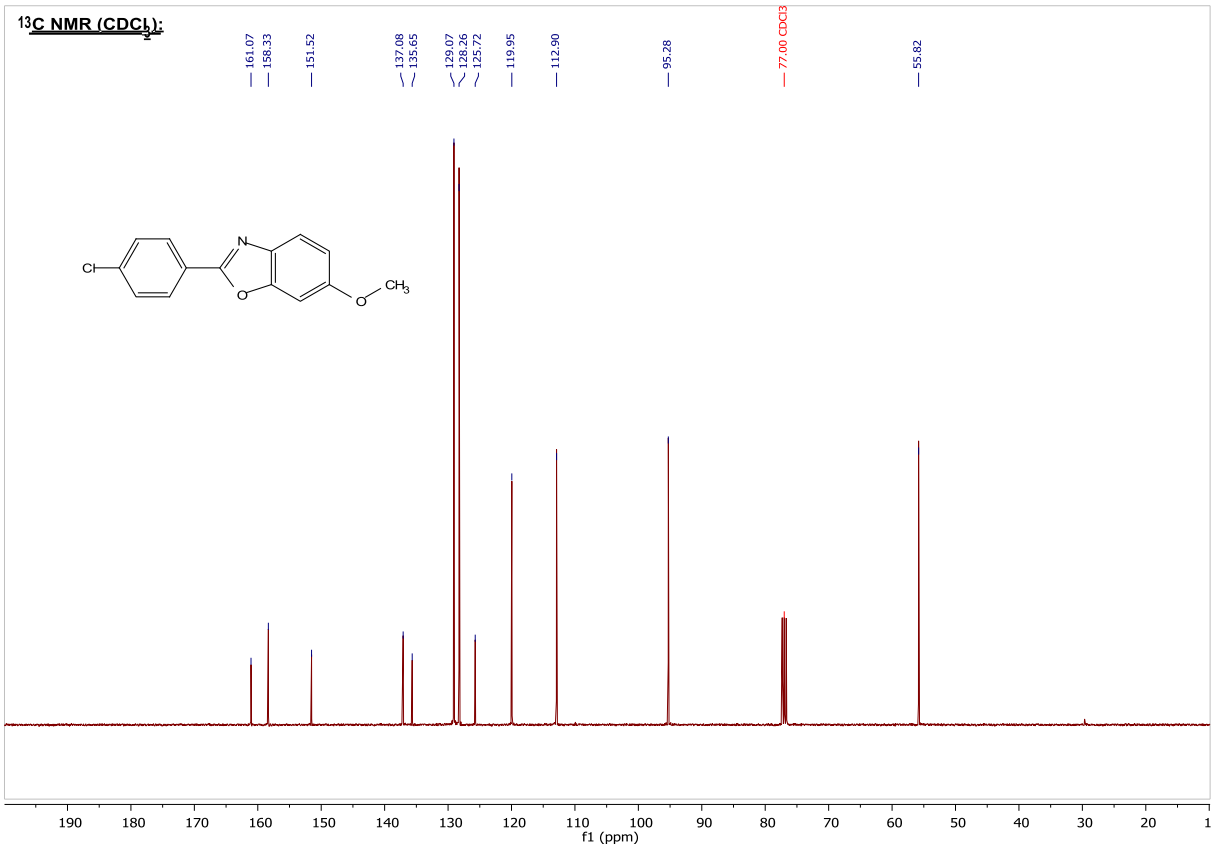

6-Methoxy-2-(4-methoxyphenyl)-1,3-benzoxazole (2h)

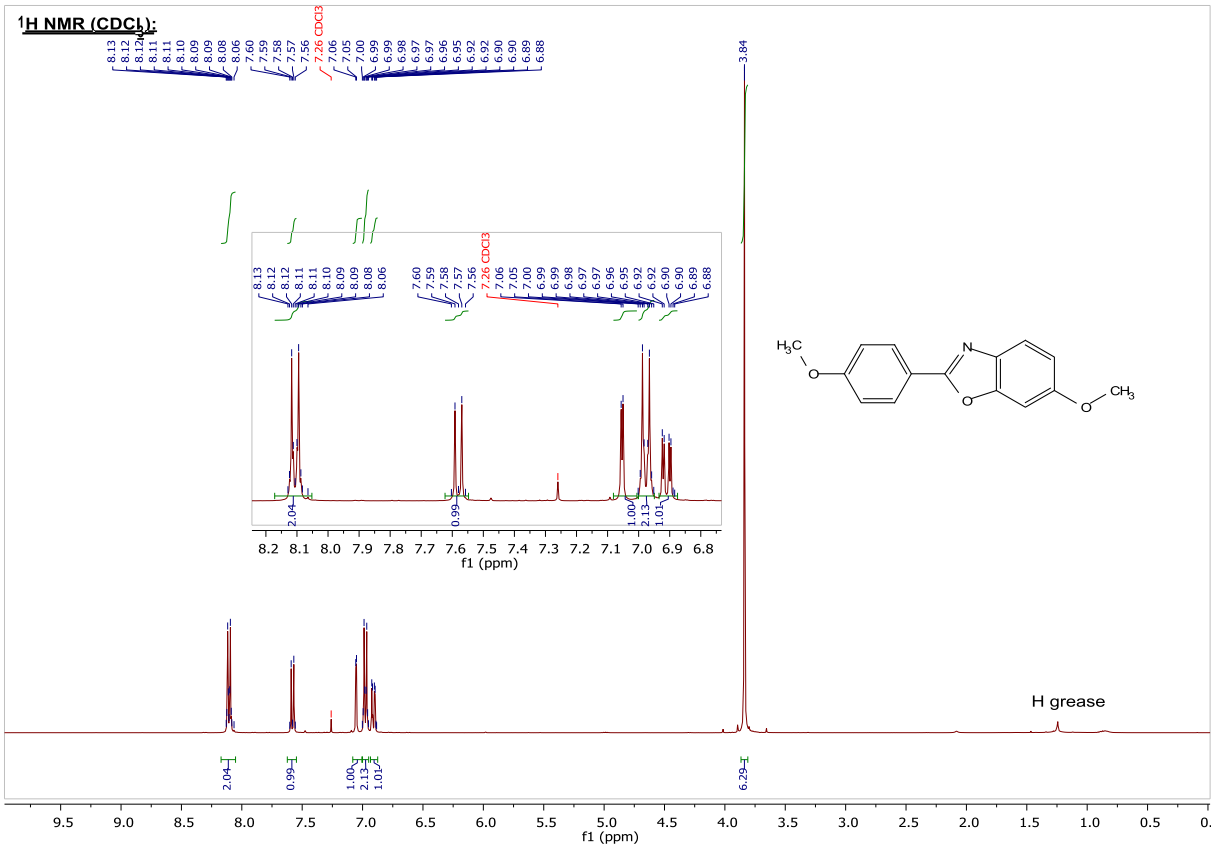

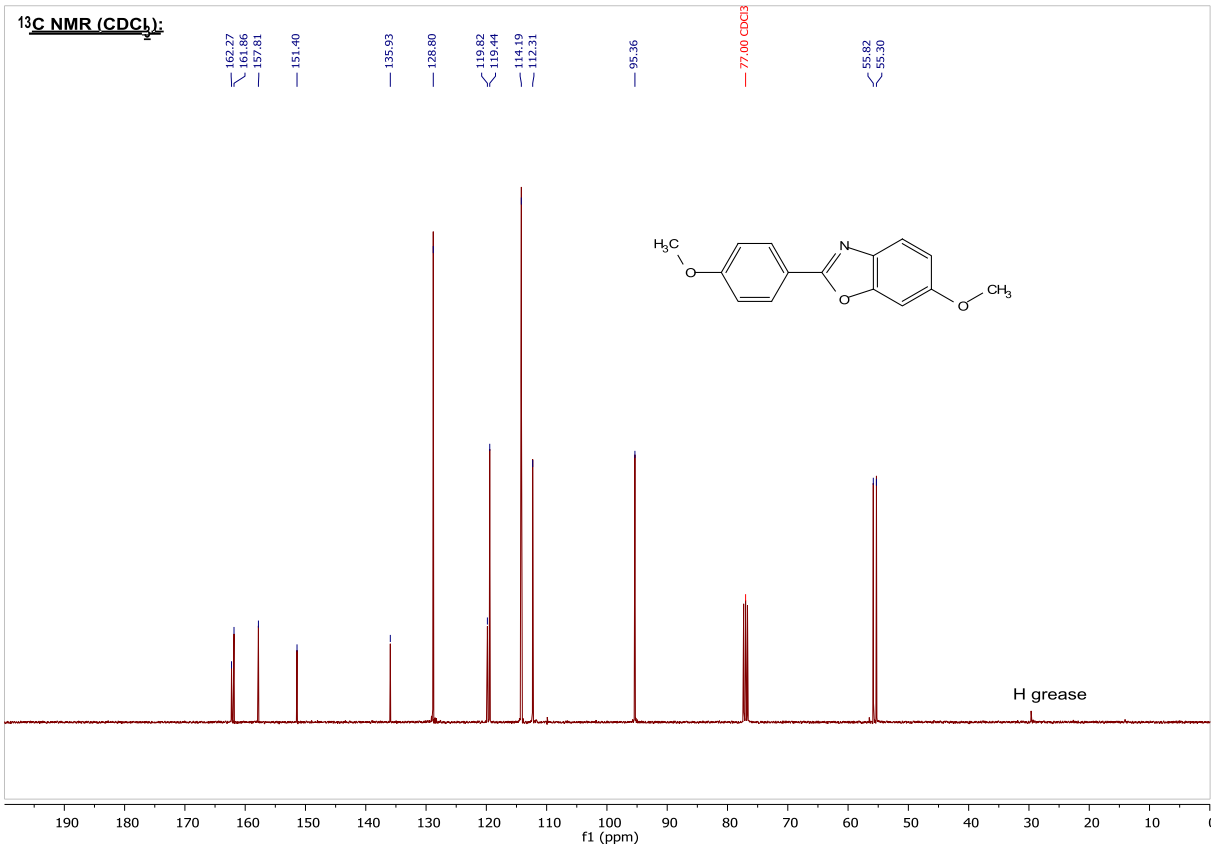

2-(2,2-Dimethylethyl)-6-methoxy-1,3-benzoxazole (2i)

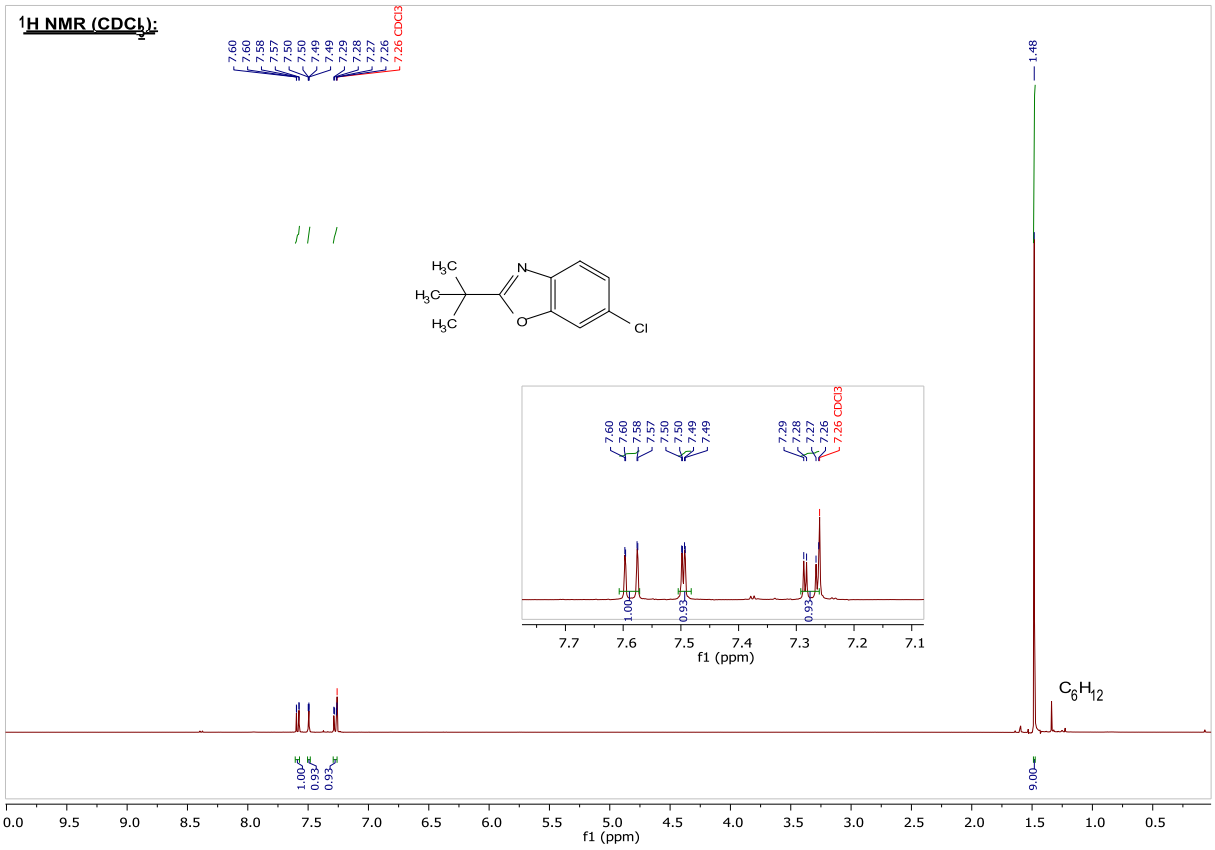

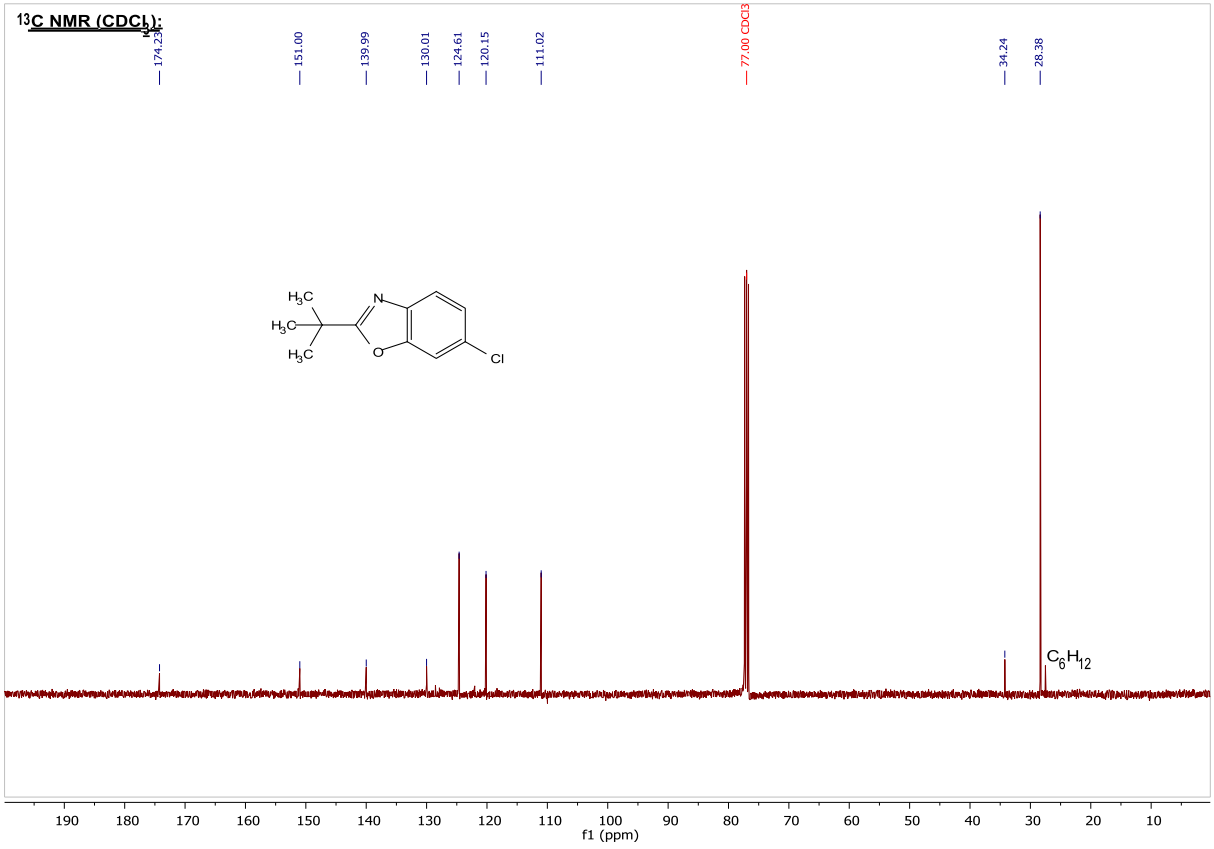

Electrochemistry

Electrochemical Conversion of Phthaldianilides to Phthalazin-1,4-diones by Dehydrogenative N–N Bond Formation

Anton Kehl,[a] Tile Gieshoff,[a, b] Dieter Schollmeyer,[a] and Siegfried R. Waldvogel*[a, b]

Abstract: The electrochemical synthesis of 6-membered rings via anodic dianilide N–N coupling is challenging due to concurring benzoxazole co-formation. The rigidity of the a phthalic acid backbone allows a novel access to phthalazin-1,4-diones by N–N bond formation using anodically generated amidyl radicals. Since conventional synthetic routes to phthalazin-1,4-diones require the use of toxic *N,N'*-diarylhydrazines and generate reagent waste, a safer and more sustainable approach is required. Easy accessible starting materials, a broad scope of applicable functional groups, promising yields, and a very simple set-up elevate this sustainable method.

Phthalazin-1,4-dione derivatives were investigated by Kaufmann during his pharmaceutical studies in 1927.[1] During the 1950's, industrial research confirmed the anesthetic properties of these derivatives and developed more efficient access to medicinal chemistry applications based on phthalazin-1,4-diones with a functionalized phthalic acid backbone in order to replace the barbiturate based anesthetics with their side effects.[2] Nowadays, phthalazin-1,4-diones are not used as anesthetic drugs. However, the heterocyclic motif is apparent in various compounds with anti-inflammatory, analgesic, anti-pyretic, anti-hypoxant,[3a] anti-convulsant,[3b] and anti-bacterial[3c] properties. Furthermore, these derivatives can also be used as precursors for the synthesis of pharmaceutically relevant structures.[4]

The general synthetic approach for phthalazin-1,4-diones usually includes a condensation reaction of activated phthalic acid derivatives and *N,N'*-diarylhydrazines (Scheme 1, upper part). General strategies for N–N bond formation involve Cu,[5a] Ni^{II}/Ni^{III},[5b] Rh^{III}/Cu^{II},[5c] and Pd complexes[5d] or hypervalent iodine reagents (e.g. [bis(trifluoroacetoxy)iodo]benzene (PIFA)[5e]). Major drawbacks accompany these two synthetic strategies: Hydrazine derivatives are highly toxic and carcinogenic.[6] Furthermore, the diversity of commercially available starting materials is limited and thus upstream reactions are necessary to achieve more complex substitution patterns. When metal complexes or stoichiometric amounts of oxidizers or leaving groups are necessary, this has negative effects onto atom economy and ecological aspects due to the generation of reagent waste. Hence, improvements with regards to these distinct drawbacks are highly desired. A way to meet those requirements is electro-organic chemistry as a green alternative.[7] By employing electric current as inexpensive and sustainable reducing or oxidizing agent, the amount of waste is tremendously reduced and the employment of toxic starting materials can be avoided. Besides, electrochemistry as synthetic tool is inherently safe and extraordinary reaction pathways are accessible.[8]

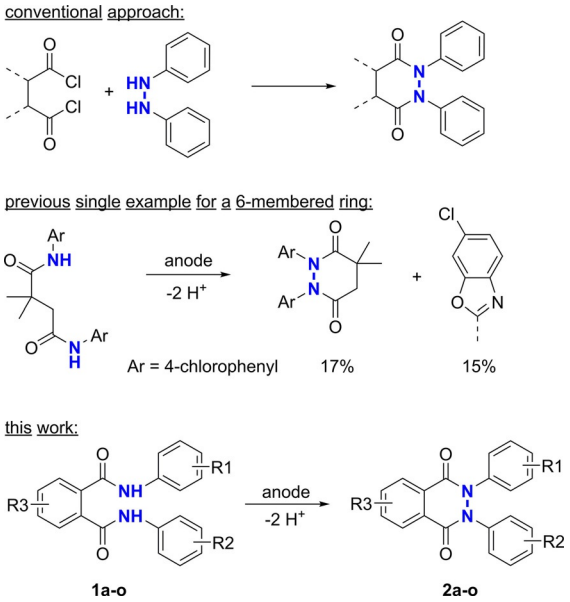

Scheme 1. Strategies for the synthesis of N–N bonds in 6-membered rings and our novel approach for phthalazin-1,4-diones.

Until now, only few electrochemical N–N coupling reactions are reported.[9] Baran and co-workers developed a potentiostatic electrolysis protocol in an undivided cell for the dehydrodimerization of carbazole derivatives.[10] Recently, we reported an electrolytic synthesis to pyrazolidin-3,5-diones.[11] The formation of 6-membered rings is challenging compared to 5-membered rings. In initial studies, the co-formation of benzoxazoles due to a slower N–N bond formation is the major obstacle (Scheme 1, middle part).[11b,12] The targeted 6-membered ring

[a] A. Kehl, T. Gieshoff, Dr. D. Schollmeyer, Prof. Dr. S. R. Waldvogel
Institut für Organische Chemie
Duesbergweg 10–14, 55128 Mainz (Germany)
E-mail: waldvogel@uni-mainz.de
Homepage: http://www.chemie.uni-mainz.de/OC/AK-Waldvogel/
[b] T. Gieshoff, Prof. Dr. S. R. Waldvogel
Graduate School Materials Science in Mainz
Staudingerweg 9, 55128 Mainz (Germany)
Supporting information and the ORCID identification number(s) for the author(s) of this article can be found under https://doi.org/10.1002/chem.201705578.

was only isolated in a low yield in a single example. Due to the orientation of the anilide moieties bound to a phthalic acid backbone, which capitalizes on the rigidity due to its sp^2-character, the requirements for a successful N–N bond formation are present. Based on these findings, we report a new synthetic route to phthalazin-1,4-diones (Scheme 1, lower part), combining a new access to 6-membered rings via N–N bond formation with the installation of an unsaturated backbone.

Easily accessible phthaldianilides as starting materials, an inexpensive anode material, and a constant current protocol demonstrates the general and simple applicability of this approach. The established methodology is applied to a scope of different phthaldianilides in order to demonstrate its generality on the one hand, and to get access to various phthalazin-1,4-dione derivatives on the other hand. This concept relies on the formation of amidyl radicals as intermediates, which subsequently form the N–N bond.[11] The application of amidyl radicals is well-studied in the context of hydroaminations,[13a] rearrangements,[13b] and cyclization reactions.[13b,14]

The symmetric precursors can be easily prepared in good yields by treatment of phthalic dichloride with a corresponding aniline derivative.[15] Compared to *N*,*N*′-diarylhydrazines, much more aniline derivatives are commercially available. When aniline derivatives with strong electron withdrawing or releasing properties are used, phthalic imide can be the major product. This issue can be effectively circumvented by using a synthetic route that also enables access to non-symmetric phthalic dianilides (Scheme 2; further details in Supporting Information).[16] Starting with commercially available phthalic anhydride, the aniline induced ring opening proceeds smoothly. Subsequent formation of the isoimide and ring opening with the second aniline enables a facile access to phthalic dianilides in good yields without further purification steps.

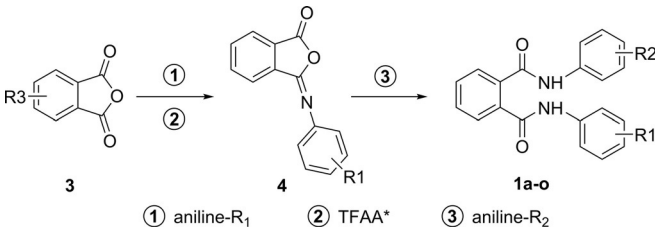

Scheme 2. Synthetic route to non-symmetric precursors. *TFAA = trifluoroacetic anhydride.

The electrolysis conditions for the N–N cyclization were determined by screening studies, whereby the protocol for the synthesis of pyrazolidin-3,5-diones served as a starting point. 1,1,1,3,3,3-Hexafluoroisopropanol (HFIP) exclusively enables an effective conversion. This key function is due to its radical stabilizing properties.[17] HFIP is recovered almost entirely by distillation, thus a low fluorine footprint can be maintained. Additionally, isostatic graphite as inexpensive anode material and platinum as long-lasting cathode material show best results. We also tested glassy carbon and boron-doped diamond as anode materials (Supporting Information), but their performance was inferior to the established graphite anode. Remarkably, low concentrations of supporting electrolyte (0.01 M NBu_4PF_6) are sufficient. For a general and easy applicability, a simple set-up employing an undivided cell rounds the methodology off. Critical parameters in electro-organic conversions, which demand further optimization, are current density and the amount of applied charge. *N*,*N*′-Di(4-chlorophenyl)phthaldiamide (**1d**) was chosen as test substrate, since this particular anilide moiety is already proven to achieve high yields in N–N cyclization reactions.[11a] The optimization reactions were carried out in Teflon cells (reaction volume: 5 mL), which enable a time-efficient parameter screening.[18] Since we observed variations in the isolated yield in the course of our scale-up studies, we decided to optimize these parameters in a 25 mL beaker-type preparative cell as well (Table 1).

Table 1. Influence of the current density onto the yield of **2d**.

Entry	5 mL Teflon cell[a] Current density [mA cm^{-2}]	Yield [%]	25 mL beaker-type cell[b] Current density [mA cm^{-2}]	Yield [%]
1	0.5	56	1	39
2	1	62	2	55
3	1.5	60	3	65
4	2	63	4	33
5	3	59	5	35

[a] 0.2 mmol substrate **1d**, 0.01 M NBu_4PF_6, anode: graphite, cathode: platinum, solvent: HFIP, 2.2 F, undivided Teflon cell (5 mL); [b] 1.0 mmol substrate **1d**, 0.01 M NBu_4PF_6, anode: graphite, cathode: platinum, solvent: HFIP, 2.2 F, undivided beaker-type cell (25 mL).

The best results were achieved by applying a current density of 3 mA cm^{-2} in a beaker-type set-up. Compared to the N–N bond formation in pyrazolidin-3,5-dione synthesis, whereby 0.5 mA cm^{-2} had to be applied, this results in a shorter reaction time.[11b,13] Applying the optimized parameters to various phthaldianilide substrates, we were able to establish a scope of phthalazin-1,4-dione derivatives with various functional groups and substitution patterns at the aromatic ring and the phthalic acid backbone (Scheme 3).

The majority of compounds were synthesized in moderate to good yields, tolerating chloro- (**2d**, **2i**, **2j**, **2l**, **2m**, **2n**, **2o**), bromo- (**2j**, **2k**, **2n**), triflate- (**2i**), or nitrile (**2l**) functionalities, which allow subsequent reactions. The highest yield of 89% was achieved at the generation of compound **2o**, which contains a methyl substitution of the phthalic acid backbone. The formation of the N–N coupled product was confirmed via X-ray structure analysis of a suitable single crystal of **2d** (Scheme 3). Electron-releasing (**2g**) as well as electron-withdrawing moieties (**2e**, **2f**, **2i**, **2l**) are also compatible and give promising yields. The possibility to convert non-symmetric dianilides (**1h**, **1i**, **1j**, **1k**, **1l**) displays the significant value of this methodology. Moreover, substitutions like bromo (**2n**) or methyl (**2o**) are tolerated at the phthalic acid backbone, whereby further functionalizations are possible. With regards to heterocyclic moieties, the use of pyridine as backbone function is tolerated.

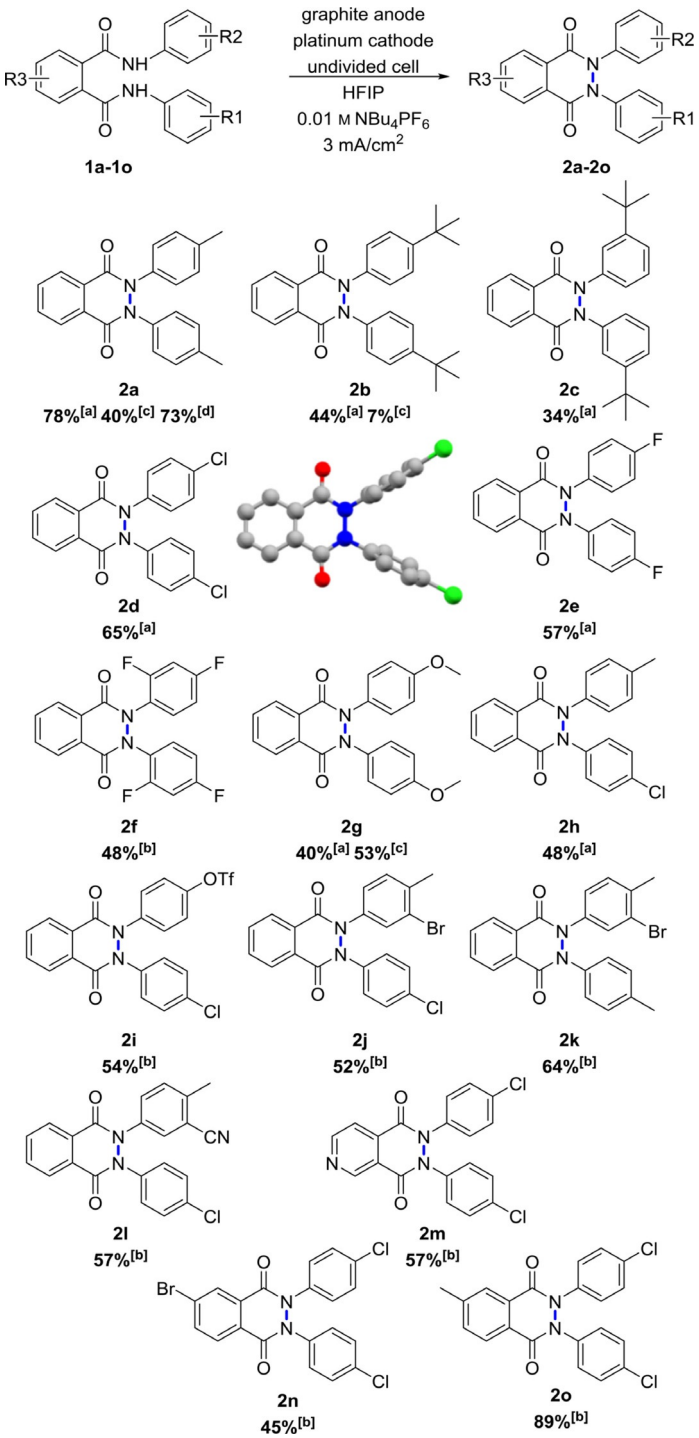

Scheme 3. Optimized parameters for the electrochemical N–N cyclization and the scope. [a] 25 mL beaker-type cell, 1 mmol substrate; [b] 5 mL Teflon cell, 0.2 mmol substrate; [c] 50 mL three-necked flask with RVC anode in an angular orientation, 0.6 mmol substrate; [d] 80 mL beaker-type cell, 3.9 mmol substrate.

Compound **2m** was synthesized in 57% yield. When employing anilides with an electron-rich moiety (**1b**, **1c**, **1g**), no complete conversion was observed during the electrolysis. Increasing the amount of charge did not improve the yield. An over-oxidation of the product is unlikely due to the high potential difference of approximately 300 mV compared to the precursors (cyclic voltammograms in Supporting Information). Furthermore, **2c** exhibits a free *para*-position, which is also likely to contribute to the lower yield due to side reactions (see Supporting Information, compound **2p**). Interestingly, **1a**, a substrate with an exposed benzylic position, achieved comparably high yields within this scope. Although one would expect that radicals can be stabilized in the benzylic position and thus facilitate side reactions. This substrate also gave similar yields on an almost gram-scale procedure, proving the general applicability of the method in different set-ups and at different scales. Alkyl amides are generally not convertible due to a lack of radical stabilization and high oxidation potentials. We tested this upon our studies of the electrochemical pyrazolidin-3,5-dione synthesis.

To further improve the yields, we tested another commonly used set-up which contains a three-necked flask employing a reticulated vitreous carbon (RVC) anode and a platinum wire cathode oriented angular to each other for some substrates (**1a**, **1b**, **1g**).[12] For **2g**, an increased yield of 53% was observed. Derivatives **2a** and **2b**, on the other hand, are less suitable for this electrode arrangement. The difference in the influence of this set-up to the reaction outcome reveals a significant optimization potential (further details in Supporting Information). If a specific conversion should be addressed, changes of the set-up can further improve yields and performance. Moreover, these results imply that first investigations can be conducted in very simple electrode and cell arrangements. In terms of the mechanism, it is likely that the cyclization derives from a diradical intermediate. We recently demonstrated that this possibility is most likely for the electrochemical formation of pyrazolidin-3,5-diones.[11b]

Interestingly, the liberation of the substituted hydrazobenzene is possible. With an excess of hydrazine (3 equiv.), this is an easy and mild access to azobenzene derivatives as well as to 2,3-dihydrophthalazin-1,4-dione in excellent yields (Scheme 4). The nucleophilic nature of hydrazine is sufficient in order to facilitate a substitution reaction at ambient conditions. The emerging hydrazobenzene is unstable and undergoes oxidation to yield the azobenzene derivative. This methodology might be an alternative to conventional azobenzene synthesis, if functional groups are neither tolerated nor accessible.

We established a new and sustainable access to phthalazin-1,4-diones with avoiding highly toxic and carcinogenic

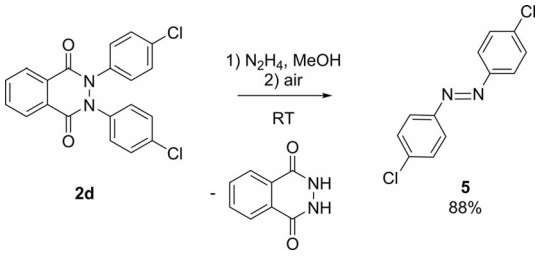

Scheme 4. Liberation of 4,4′-dichloroazobenzene from **2d**.

hydrazine compounds by employing electrochemical synthesis. This methodology is a valuable alternative to the conventional synthetic route having the advantage of easily accessible and inexpensive starting materials. A very simple set-up, metal catalyst- and oxidizer-free conditions as well as scalable and long-lasting electrode materials provide a straightforward and sustainable access to this class of substrates. A variety of derivatives is possible, valuable functionalities, which enable subsequent reactions, are tolerated, and non-symmetrical products are accessible by this method.

Acknowledgements

T. G. is a recipient of a DFG fellowship by the Excellence Initiative by the Graduate School Materials Science in Mainz (GSC 266). The support by The Advanced Lab for Electrochemistry and Electrosynthesis—ELYSION (Carl Zeiss Stiftung) and the DFG (WA 1276/17-1) is highly appreciated.

Conflict of interest

The authors declare no conflict of interest.

Keywords: electrochemistry · green chemistry · heterocyclic chemistry · N,N coupling · phthalazin-1,4-diones

[1] H. P. Kaufmann, *Angew. Chem.* **1927**, *40*, 69 – 79.

[2] a) H. Ruschig, R. Fugmann, H. Eggert, E. Fischer II, E. Lindner, DE956044, **1957**; b) H. Ruschig, R. Fugmann, E. Lindner, DE1029379, **1958**; c) H. Ruschig, R. Fugmann, H. Eggert, E. Fischer II, E. Lindner, US2874156, **1959**.

[3] a) F. Al-Assar, K. N. Zelenin, E. E. Lesiovskaya, I. P. Bezhan, B. A. Chakchir, *Pharm. Chem. J.* **2002**, *36*, 598 – 603; b) M. F. Zayed, R. R. Ayyad, *Arzneim.-Forsch.* **2012**, *62*, 532 – 536; c) A. M. Khalil, M. A. Berghot, M. A. Gouda, S. A. El Bialy, *Monatsh. Chem.* **2010**, *141*, 1353 – 1360.

[4] a) R. P. Jain, J. C. Vederas, *Bioorg. Med. Chem. Lett.* **2004**, *14*, 3655 – 3658; b) B. Dam, M. Saha, R. Jamatia, A. K. Pal, *RSC Adv.* **2016**, *6*, 54768 – 54776; c) X.-J. Liu, H.-J. Zhang, Z.-S. Quan, *Med. Chem. Res.* **2017**, *26*, 1935 – 1946.

[5] a) C. – *y.* Chen, G. Tang, F. He, Z. Wang, H. Jing, R. Faessler, *Org. Lett.* **2016**, 18, 1690 – 1693; b) J. B. Diccianni, C. Hu, T. Diao, *Angew. Chem. Int. Ed.* **2016**, *55*, 7534 – 7538; *Angew. Chem.* **2016**, *128*, 7660 – 7664; c) D.-G. Yu, M. Suri, F. Glorius, *J. Am. Chem. Soc.* **2013**, *135*, 8802 – 8805; d) Q.-Z. Zheng, P. Feng, Y.-F. Liang, N. Jiao, *Org. Lett.* **2013**, *15*, 4262 – 4265; e) A. Correa, I. Tellitu, E. Dominguez, R. SanMartin, *J. Org. Chem.* **2006**, *71*, 3501 – 3505.

[6] a) National Toxicology Program, *Carcinog. Tech. Rep. Ser.- U.S., Natl. Cancer Inst.* **1978**, *92*, 1 – 123; b) D. E. Dodd, L. J. Pluta, M. A. Sochaski, H. G. Wall, R. S. Thomas, *Int. J. Toxicol.* **2012**, *31*, 564 – 571.

[7] a) H. J. Schäfer, *C. R. Chim.* **2011**, *14*, 745 – 765; b) B. A. Frontana-Uribe, R. D. Little, J. G. Ibanez, A. Palma, R. Vasquez-Medrano, *Green Chem.* **2010**, *12*, 2099 – 2119.

[8] a) Yan, M.; Kawamata, Y.; Baran, P. S. *Chem. Rev.* **2017**, https://doi.org/10.1021/acs.chemrev.7b00397; b) C. Gütz, M. Selt, M. Bänziger, C. Bucher, C. Römelt, N. Hecken, F. Gallou, T. R. Galvão, S. R. Waldvogel, *Chem. Eur. J.* **2015**, *21*, 13878 – 13882; c) J. Chen, W.-Q. Yan, C. M. Lam, C.-C. Zeng, L.-M. Hu, R. D. Little, *Org. Lett.* **2015**, *17*, 986 – 989; d) S. Herold, S. Moehle, M. Zirbes, F. Richter, H. Nefzger, S. R. Waldvogel, *Eur. J. Org. Chem.* **2016**, 1274 – 1278; e) T. Morofuji, A. Shimizu, J.-i. Yoshida, *J. Am. Chem. Soc.* **2013**, *135*, 5000 – 5003; f) R. Francke, R. D. Little, *J. Am. Chem. Soc.* **2014**, *136*, 427 – 435; g) S. R. Waldvogel, M. Selt, *Angew. Chem. Int. Ed.* **2016**, *55*, 12578 – 12580; *Angew. Chem.* **2016**, *128*, 12766 – 12768; h) S. Moehle, S. R. Waldvogel, *Angew. Chem. Int. Ed.* **2015**, *54*, 6398 – 6399; *Angew. Chem.* **2015**, *127*, 6496 – 6497; i) A. Wiebe, D. Schollmeyer, K. M. Dyballa, R. Franke, S. R. Waldvogel, *Angew. Chem. Int. Ed.* **2016**, *55*, 11801 – 11805; *Angew. Chem.* **2016**, *128*, 11979 – 11983; j) S. Lips, A. Wiebe, B. Elsler, D. Schollmeyer, K. M. Dyballa, R. Franke, S. R. Waldvogel, *Angew. Chem. Int. Ed.* **2016**, *55*, 10872 – 10876; *Angew. Chem.* **2016**, *128*, 11031 – 11035.

[9] a) R. Bauer, H. Wendt, *Angew. Chem. Int. Ed. Engl.* **1978**, *17*, 202 – 203; *Angew. Chem.* **1978**, *90*, 214; b) R. Bauer, H. Wendt, *Angew. Chem. Int. Ed. Engl.* **1978**, *17*, 370 – 371; *Angew. Chem.* **1978**, *90*, 390.

[10] a) B. R. Rosen, E. W. Werner, A. G. O'Brien, P. S. Baran, *J. Am. Chem. Soc.* **2014**, *136*, 5571 – 5574; b) S. R. Waldvogel, B. Janza, *Angew. Chem. Int. Ed.* **2014**, *53*, 7122 – 7123; *Angew. Chem.* **2014**, *126*, 7248 – 7249.

[11] a) T. Gieshoff, D. Schollmeyer, S. R. Waldvogel, *Angew. Chem. Int. Ed.* **2016**, *55*, 9437 – 9440; *Angew. Chem.* **2016**, *128*, 9587 – 9590; b) T. Gieshoff, A. Kehl, D. Schollmeyer, K. D. Moeller, S. R. Waldvogel, *J. Am. Chem. Soc.* **2017**, *139*, 12317 – 12324.

[12] T. Gieshoff, A. Kehl, D. Schollmeyer, K. D. Moeller, S. R. Waldvogel, *Chem. Commun.* **2017**, *53*, 2974 – 2977.

[13] a) S. Z. Zard, *Chem. Soc. Rev.* **2008**, *37*, 1603 – 1618; b) N. Fuentes, W. Kong, L. Fernández-Sánchez, E. Merino, C. Nevado, *J. Am. Chem. Soc.* **2015**, *137*, 964 – 973.

[14] a) K. C. Nicolaou, P. S. Baran, Y.-L. Zhong, S. Barluenga, K. Hunt, R. Kranich, J. A. Vega, *J. Am. Chem. Soc.* **2002**, *124*, 2233 – 2244; b) Y.-F. Wang, H. Chen, X. Zhu, S. Chiba, *J. Am. Chem. Soc.* **2012**, *134*, 11980 – 11983; c) B. Janza, A. Studer, *J. Org. Chem.* **2005**, *70*, 6991 – 6994; d) S. Maity, N. Zheng, *Angew. Chem. Int. Ed.* **2012**, *51*, 9562 – 9566; *Angew. Chem.* **2012**, *124*, 9700 – 9704; e) X.-Q. Hu, J.-R. Chen, Q. Wei, F.-L. Liu, Q.-H. Deng, A. M. Beauchemin, W.-J. Xiao, *Angew. Chem. Int. Ed.* **2014**, *53*, 12163 – 12167; *Angew. Chem.* **2014**, *126*, 12359 – 12363; f) G. J. Choi, R. R. Knowles, *J. Am. Chem. Soc.* **2015**, *137*, 9226 – 9229; g) C. Moutrille, S. Z. Zard, *Chem. Commun.* **2004**, 1848 – 1849; h) L. Zhu, P. Xiong, Z.-Y. Mao, Y.-H. Wang, X. Yan, X. Lu, H.-C. Xu, *Angew. Chem. Int. Ed.* **2016**, *55*, 2226 – 2229; *Angew. Chem.* **2016**, *128*, 2266 – 2269; i) H.-C. Xu, J. M. Campbell, K. D. Moeller, *J. Org. Chem.* **2014**, *79*, 379 – 391.

[15] F. L. Dunlap, F. W. Cummer, *J. Am. Chem. Soc.* **1903**, *25*, 612 – 621.

[16] a) C. J. Perry, Z. Parveen, *J. Chem. Soc. Perkin Trans. 2* **2001**, 512 – 521; b) G. D. de Toranzo, J. A. Brieux, *J. Am. Chem. Soc.* **1967**, *10*, 982 – 983; c) W. R. Roderick, P. L. Bathia, *J. Org. Chem.* **1963**, *28*, 2018 – 2024.

[17] a) A. Kirste, M. Nieger, I. M. Malkowsky, F. Stecker, A. Fischer, S. R. Waldvogel, *Chem. Eur. J.* **2009**, *15*, 2273 – 2277; b) A. Kirste, G. Schnakenburg, F. Stecker, A. Fischer, S. R. Waldvogel, *Angew. Chem. Int. Ed.* **2010**, *49*, 971 – 975; *Angew. Chem.* **2010**, *122*, 983 – 987; c) R. Francke, D. Cericola, R. Kötz, D. Weingarth, S. R. Waldvogel, *Electrochim. Acta* **2012**, *62*, 372 – 380; d) O. Hollóczki, A. Berkessel, J. Mars, M. Mezger, A. Wiebe, S. R. Waldvogel, B. Kirchner, *ACS Catal.* **2017**, *7*, 1846 – 1852; e) B. Elsler, D. Schollmeyer, K. M. Dyballa, R. Franke, S. R. Waldvogel, *Angew. Chem. Int. Ed.* **2014**, *53*, 5210 – 5213; *Angew. Chem.* **2014**, *126*, 5311 – 5314; f) B. Elsler, A. Wiebe, D. Schollmeyer, K. M. Dyballa, R. Franke, S. R. Waldvogel, *Chem. Eur. J.* **2015**, *21*, 12321 – 12325.

[18] C. Gütz, B. Klöckner, S. R. Waldvogel, *Org. Process Res. Dev.* **2016**, *20*, 26 – 32.

Manuscript received: November 23, 2017

Accepted manuscript online: November 24, 2017

Version of record online: December 14, 2017

CHEMISTRY
A European Journal

Supporting Information

Electrochemical Conversion of Phthaldianilides to Phthalazin-1,4-diones by Dehydrogenative N—N Bond Formation

Anton Kehl,[a] Tile Gieshoff,[a, b] Dieter Schollmeyer,[a] and Siegfried R. Waldvogel*[a, b]

chem_201705578_sm_miscellaneous_information.pdf

TABLE OF CONTENTS

General information

All reagents were used in analytical grades and were obtained from commercial sources. Solvents were purified by standard methods.[1] For electrochemical reactions, different electrode materials were used: isostatic graphite electrodes were obtained from SGL carbon, Bonn, Germany.

Column chromatography was performed on silica gel 60 M (0.040-0.063 mm, Macherey-Nagel GmbH & Co, Düren, Germany) with a maximum pressure of 2.0 bar. A preparative chromatography system (Büchi-Labortechnik GmbH, Essen, Germany) was used with an Büchi Control Unit C-620, an UV detector Büchi UV photometer C-635, Büchi fraction collector C-660 and two Pump Modules C-605 for adjusting the solvent mixtures. Mixtures of cyclohexane and ethyl acetate were used as eluents. Silica gel 60 sheets on aluminium (F254, Merck, Darmstadt, Germany) were employed for thin layer chromatography.

Gas chromatography was performed on a Shimadzu GC-2025 (Shimadzu, Japan) using a Zebron ZB-5MSi column (Phenomenex, USA; length: 30 m, inner diameter: 0.25 mm, film: 0.25 µm, pre-column: 5 m, carrier gas: hydrogen). GC-MS measurements were carried out on a Shimadzu GC-2010 (Shimadzu, Japan) using a Zebron ZB-5MSi column (Phenomenex, USA; length: 30 m, inner diameter: 0.25 mm, film: 0.25 µm, pre-column: 5 m, carrier gas: helium) combined with a GCMS-QP2010.

Melting points were determined by a Melting Point Apparatus SMP3 (Stuart Scientific, Staffordshire, U.K.) or M-565 (Büchi, Flawil, Switzerland) and are uncorrected.

Spectroscopy and spectrometry: ^{1}H NMR, ^{13}C NMR and ^{19}F spectra were recorded at 25 °C by using a Bruker Avance II 400 or a Bruker Avance III HD 400 (Analytische Messtechnik, Karlsruhe, Germany). Chemical shifts (δ) are reported in parts per million (ppm) relative to TMS as internal standard or traces of $CHCl_3$ or DMSO-d_5 in the corresponding deuterated solvent. For the ^{19}F spectra, α-trifluortoluene served as external standard (δ = –63.9 ppm).[2] Mass spectra and high resolution mass spectra were obtained by using a QTof Ultima 3 (Waters, Milford, Massachusetts) apparatus employing ESI+.

Electrode materials: Highly isostatic graphite Sigrafine™ V2100 was obtained from SGL Carbon, Bonn, Germany. The geometries were machined from a big block. BDD electrode with a DIACHEM® 15 µM diamond layer on silica were obtained from *CONDIAS GmbH*, Itzehoe, Germany.

X-ray analysis: All data were collected on a STOE IPDS2T diffractometer (Oxford Cryostream 700er series, Oxford Cryosystems) using graphite monochromated Mo K_α radiation (λ= 0.71073 Å). Intensities were measured using fine-slicing ω and φ-scans and corrected for background, polarization and Lorentz effects. The structures were solved by direct methods and refined anisotropically by the least-squares procedure implemented in the SHELX program system.[3]

The supplementary crystallographic data for this paper can be obtained free of charge from The Cambridge Crystallographic Data Center via www.ccdc.cam.ac.uk/data_request/cif. Deposition numbers and further details are given with the individual characterization data.

General procedures

General protocol for the synthesis of symmetric phthaldianilide derivatives A[4]

To a solution of 40 mmol of an aniline derivative in 50 mL diethyl ether a solution consisting of 2.0 g (1.4 mL, 10 mmol) *o*-phthaloyl dichloride in 50 mL anhydrous diethyl ether was added dropwise at room temperature within 40 minutes. The mixture was stirred overnight (ca. 16 h). The precipitated solid was filtered off and washed with 200 mL water and 50 mL diethyl ether. If further purification was required, the solid was recrystallized from ethanol unless otherwise stated.

A1: In the case of a poor solubility in ethanol, recrystallization was omitted and the solid was purified by refluxing in 50 mL cyclohexane for 1 h, filtration and drying.

General protocol for the synthesis of symmetric phthaldianilide derivatives B

To a solution of 20 mmol of an aniline derivative and 20 mmol NEt_3 in 50 mL diethyl ether a solution consisting of 2.0 g (1.4 mL, 10 mmol) *o*-phthaloyl dichloride in 50 mL anhydrous diethyl ether was added dropwise at 0 °C within 40 minutes. The mixture was stirred overnight (ca. 16 h). The precipitated solid was filtered off and washed with 200 mL water and 50 mL diethyl ether. If further purification was required, the solid was recrystallized from ethanol unless otherwise stated.

General protocol for the synthesis of non-symmetric phthaldianilide derivatives C [5, 6]

C1: Synthesis of phthalmonoanilides[5]

To a solution of 50 mmol of an aniline derivative in 100 mL chloroform a suspension consisting of 50 mmol phthalic anhydride in 100 mL anhydrous chloroform was added in portions at room temperature within 2 minutes. The mixture was stirred overnight (ca. 16 h). The precipitated solid was filtered off, washed with 50 mL chloroform and used without further purification.

C2: Synthesis of non-symmetric phthaldianilides

The synthesis of non-symmetric phthaldianilides was performed in accordance to a modified procedure of Roderick and Bathia[7] / Toranzo and Brieux.[6] To a solution of 5 mmol of a phthalmonoanilide and 15 mmol NEt_3 in 18 mL anhydrous 1,4-dioxane under argon atmosphere, trifluoroacetic anhydride was added. After the mixture was stirred for 1.5 h at room temperature, it was poured on water. The precipitated isoimide was filtered off and washed consecutively with 50 mL water, 50 mL saturated $NaHCO_3$, and 50 mL water. Remains of water were removed at reduced pressure. To a solution of 2.5 mmol isoimide derivative in 50 mL THF, a solution consisting of 2.5 mmol aniline derivative in 50 mL THF was added dropwise at room temperature within 30 minutes. The mixture was stirred for 3 h. After removal of the solvent under reduced pressure, the product was obtained as solid, which was purified by refluxing in 50 mL cyclohexane for 1 h, filtration and drying unless otherwise stated.

General protocol for the electrochemical synthesis of phthalazin-1,4-dione derivatives D

D1: Application of undivided screening cells (5mL)

A solution of 0.2 mmol phthaldianilide and 19,6 mg (0.01 M) tetrabutylammonium hexafluorophosphate (NBu_4PF_6) in 5 mL 1,1,1,3,3,3-hexafluoroisopropanol (HFIP) employing a graphite anode and a platinum cathode was electrolyzed. The electrolysis was performed

under constant current conditions (current density j = 3 mA/cm^2, active surface 1.5 cm^2). After completion of the reaction according to TLC analysis, HFIP was recycled by distillation at reduced pressure (200-90 mbar, 50 °C). The purification of the product was conducted by column chromatography with the following gradient sequence: 2 minutes 100% cyclohexane; elevation of the ethyl acetate portion 0-10% within 30 minutes; if not stated otherwise.

D2: Application of beaker-type glass cells (25 mL)

Procedure D2 equates to procedure D1 with the following modifications: 1.0 mmol of substrate and 98 mg (0.01 M) NBu_4PF_6 are dissolved in 25 mL HFIP (current density j = 3 mA/cm^2, active surface 7.5 cm^2)

D3: Application of a 50 mL three-necked flask (15 mL)

Procedure D3 equates to procedure D1 with the following modifications: 0.6 mmol of the precursor with 58 mg (0.01 M) NBu_4PF_6 are dissolved in 15 mL HFIP and electrolyzed. The set-up consists of a reticulated vitreous carbon (100 PPI) anode and a platinum wire cathode arranged angular to each other. A current of 10 mA was applied.

D4: Application of beaker-type glass cells (80 mL)

Procedure D4 equates to procedure D1 with the following modifications: 3.9 mmol of substrate and 378 mg (0.01 M) NBu_4PF_6 are dissolved in 80 mL HFIP (current density j = 3 mA/cm^2, active surface 7.5 cm^2)

Electrolysis set-ups and electrode materials screening

Set-ups with electrodes in a parallel orientation were either conducted in a 5 mL Teflon cell[8] (Figure 1, left) with 7 cm x 1 cm electrodes or in a 25 mL beaker-type cell[9] (Figure 1, right) with 2 cm x 6 cm x 3 mm electrodes. Electrolysis with electrodes in an angular orientation were conducted in a 50 mL three-necked flask (Figure 1, middle). 100 ppi RVC electrodes were attached to a graphite rod and a platinum wire was used. Terminal voltage in 25 mL in glass cells typically is around 12 V.

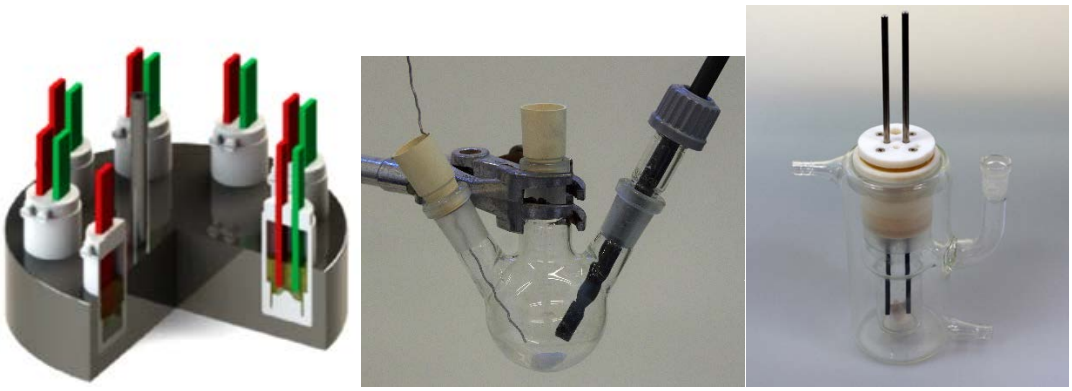

Figure 1: left: 5 mL Teflon cells;[8] middle: 50 mL three-necked flask with electrodes in an angular orientation; right 25 mL beaker-type cell.

In the course of our optimization studies, we also tested glassy carbon, boron-doped diamond, and reticulated vitreous carbon (RVC) as anode materials with *N,N'*-diphenylphthalamide a substrate, generally converting in low yields. The performance of all three materials was inferior to the established graphite anode (Table 1).

Table 1: Tested anode materials under optimized conditions for *N,N'*-diphenylphthalamide.[a]

Entry	Anode material	Isolated yield [%]
1	graphite	17
2	glassy carbon	5
3	Boron-doped diamond (BDD)	5

[a] 0.01 M NBu_4PF_6 in HFIP, cathode: platinum, 2.2 F, undivided Teflon cell (5 mL).

Synthesis of phthaldianilides

N,N'-Di(4-methylphenyl)phthaldiamide (1a)

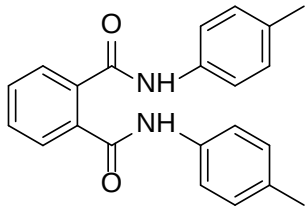

According to procedure A, 4.29 g (40 mmol, 4 eq.) of 4-methylaniline and 2.01 g (10 mmol, 1 eq.) of *o*-phthalic dichloride yielded 2.00 g (yield: 58%; 5.8 mmol) product as colorless crystalline solid. Product was recrystallized from ethanol.

^{1}H NMR (400 MHz, DMSO-d_6) δ [ppm] = 10.33 (s, 2H, N-H), 7.67–7.56 (m, 8H), 7.12 (d, *J* = 8.2 Hz, 4H), 2.27 (s, 6H).

^{13}C NMR (100 MHz, DMSO-d_6) δ [ppm] = 166.6, 136.9, 136.8, 132.3, 129.7, 129.0, 127.8, 119.6, 20.5.

HRMS for $C_{22}H_{20}N_2O_2$ (ESI+) $[M+H]^+$: calc.: 345.1603, found: 345.1603.

MP: 184.8–187.5 °C (decomposition).

N,N'-Bis(4-(1,1-dimethylethyl)phenyl)phthaldiamide (1b)

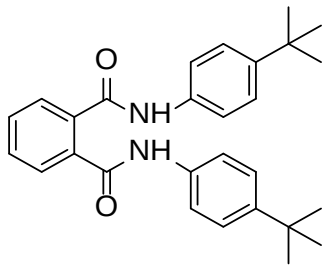

According to the procedure B, 1.49 g (10 mmol, 2 eq.) of 4-(1,1-dimethylethyl) aniline, 1.01 g (10 mmol, 2 eq.) of NEt_3, and 1.02 g (5 mmol, 1 eq.) of *o*-phthalic dichloride yielded 0.75 g (yield: 35%; 1.8 mmol) of product as colorless crystalline solid. Product was recrystallized from methanol.

^{1}H NMR (400 MHz, DMSO-d_6) δ [ppm] = 10.33 (s, 2H, N-H), 7.66–7.57 (m, 8H), 7.32 (d, *J* = 8.7 Hz, 4H), 1.26 (s, 18H).

^{13}C NMR (100 MHz, DMSO-d_6) δ [ppm] = 166.6, 145.7, 136.9, 129.6, 127.8, 125.2, 119.4, 34.0, 31.2.

HRMS for $C_{28}H_{32}N_2O_2$ (ESI+) $[M+H]^+$: calc.: 429.2542, found: 429.2239.

MP: 225.4–228.1 °C.

***N,N'*-Bis(3-(1,1-dimethylethyl)phenyl)phthaldiamide (1c)**

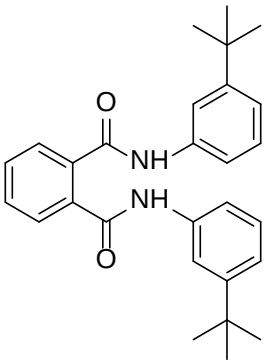

According to the procedure B, 1.01 g (6.7 mmol, 2 eq.) of 3-(1,1-dimethylethyl)aniline, 0.68 g (6.7 mmol, 2 eq.) of NEt_3 and 0.68 g (3.4 mmol, 1 eq.) of *o*-phthalic dichloride yielded 0.65 g (yield: 45%; 1.5 mmol) of product as colorless crystalline solid. Product was recrystallized from ethanol.

^{1}H NMR (400 MHz, DMSO-d_6) δ [ppm] = 10.34 (s, 2H, N-H), 7.72–7.64 (m, 4H), 7.63–7.56 (m, 4H), 7.23 (t, *J* = 7.9 Hz, 2H), 7.11 (d, *J* = 7.9 Hz, 2H), 1.26 (s, 18H).

^{13}C NMR (100 MHz, DMSO-d_6) δ [ppm] = 166.8, 151.2, 139.2, 136.8, 129.7, 128.2, 127.9, 120.5, 116.9, 116.7, 34.5, 31.1.

HRMS for $C_{28}H_{32}N_2O_2$ (ESI+) $[M+H]^+$: calc.: 429.2542, found: 429.2531.

MP: 168.9–171.7 °C (decomposition).

***N,N'*-Di(4-chlorophenyl)phthaldiamide (1d)**

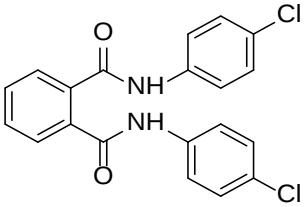

According to the procedure A1, 5.10 g (40 mmol, 4 eq.) of 4-chloroaniline and 2.02 g (10 mmol, 1 eq.) of *o*-phthalic dichloride yielded 2.88 g (yield: 75%; 7.5 mmol) of product as colorless crystalline solid.

^{1}H NMR (400 MHz, DMSO-d_6) δ [ppm] = 10.59 (s, 2H, N-H) 7.75–7.67 (m, 6H), 7.62 (dd, *J* = 5.5, 3.3 Hz, 2H), 7.38 (d, *J* = 8.9 Hz, 4H).

^{13}C NMR (100 MHz, DMSO-d_6) δ [ppm] = 167.3 138.7, 136.9, 130.4, 129.0, 128.3, 127.5, 121.7.

HRMS for $C_{20}H_{14}{}^{35}Cl_2N_2O_2$ (ESI+) $[M+Na]^+$: calc.: 407.0330, found: 407.0341.

MP: 203.8–205.3 °C (decomposition).

***N,N'*-Di(4-fluorophenyl)phthaldiamide (1e)**

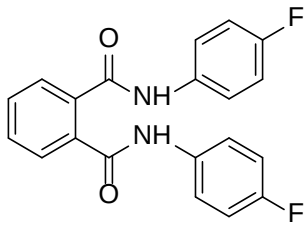

According to the procedure A1, 4.44 g (40 mmol, 4 eq.) of 4-fluoroaniline and 2.02 g (10 mmol, 1 eq.) of *o*-phthalic dichloride yielded 3.04 g (yield: 86%; 8.6 mmol) of product as colorless crystalline solid.

^{1}H NMR (400 MHz, DMSO-d_6) δ [ppm] = 10.49 (s, 2H, N-H), 7.73–7.60 (m, 8H), 7.16 (t, *J* = 8.9 Hz, 4H).

^{13}C NMR (100 MHz, DMSO-d_6) δ [ppm] = 166.7, 158.1 (d, *J* = 239.9 Hz), 136.6, 135.7, 129.8, 128.8, 121.4 (d, *J* = 7.8 Hz), 115.2 (d, *J* = 22.2 Hz).

^{19}F NMR (377 MHz, DMSO) δ [ppm] = -120.26.

HRMS for $C_{20}H_{14}F_2N_2O_2$ (ESI+) $[M+H]^+$: calc.: 353.1102, found: 353.1094.

MP: 218.8–227.9 °C.

***N,N'*-Bis(2,4-difluorophenyl)phthaldiamide (1f)**

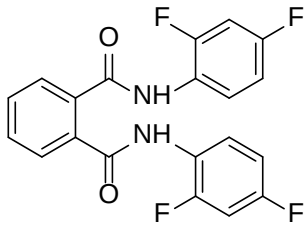

According to the procedure A, 1.30 g (10 mmol, 4 eq.) of 2,4-difluoroaniline and 0.51 g (2.5 mmol, 1 eq.) of *o*-phthalic dichloride yielded 0.27 g (yield: 28%; 0.7 mmol) of product as colorless crystalline solid. The reaction mixture was stirred only for 5 hours. Product was recrystallized from ethanol.

^{1}H NMR (400 MHz, DMSO-d_6) δ [ppm] = 10.20 (s, 2H, N-H), 7.72–7.63 (m, 6H), 7.33 (d, *J* = 9.2 Hz, 2H), 7.11 (d, *J* = 9.2 Hz, 2H).

^{13}C NMR (100 MHz, DMSO-d_6) δ [ppm] = 166.9, 159.1 (d, *J* = 244.0 Hz), 155.0 (d, *J* = 249.6 Hz), 135.8, 130.1, 128.0, 127.1 (d, *J* = 11.7 Hz), 122.5 (d, *J* = 12.3 Hz), 104.3 (m), 111.1 (d, *J* = 22.1 Hz).

^{19}F NMR (377 MHz, DMSO-d_6) δ [ppm] = -115.17, -118.69.

HRMS for $C_{20}H_{12}F_4N_2O_2$ (ESI+) $[M+Na]^+$: calc.: 411.0733, found: 411.0736.

MP: 200.2–203.1 °C (decomposition).

***N,N'*-Di(4-methoxyphenyl)phthaldiamide (1g)**

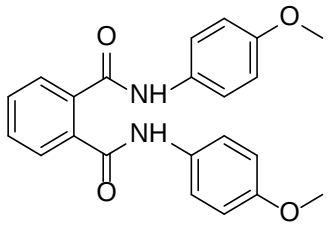

According to the procedure A1, 4.93 g (40 mmol, 4 eq.) of 4-methoxyaniline and 2.01 g (10 mmol, 1 eq.) of *o*-phthalic dichloride yielded 2.96 g (yield: 79%; 7.9 mmol) of product as colorless crystalline solid.

^{1}H NMR (400 MHz, DMSO-d_6) δ [ppm] = 10.26 (s, 2H, N-H), 7.68–7.54 (m, 8H), 6.89 (d, *J* = 9.0 Hz, 4H), 3.73 (s, 6H).

^{13}C NMR (75 MHz, DMSO-d_6) δ [ppm] = 166.9, 155.8, 137.3, 133.0, 130.0, 128.2, 121.6, 114.2, 55.6.

HRMS for $C_{22}H_{20}N_2O_4$ (ESI+) $[M+H]^+$: calc.: 377.1501, found: 377.1509.

MP: 187.1–191.7 °C (decomposition).

The analytical data matchs the reported data.[10]

***N*-(4-Chlorophenyl)-*N'*-(4-methylphenyl)phthaldiamide (1h)**

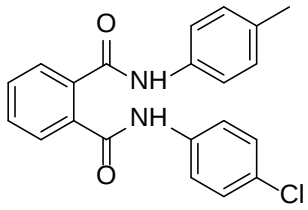

According to the procedure C1, 7.41 g (50 mmol, 1 eq.) of phthalic anhydride and 6.38 g (50 mmol, 1 eq.) of 4-chloroaniline yielded 10.14 g (yield: 73%; 37 mmol) of phthalic monoanilide as colorless solid, which was used without further purification. According to the procedure C2, 1.38 g (5 mmol, 1 eq.) of phthalic monoanilide, 1.52 g (15 mmol, 3 eq.) of NEt_3, and 1.58 g (7.5 mmol 1.5 eq.) of trifluoroacetic anhydride in 18 mL 1,4-dioxane yielded 1.19 g (yield: 93%; 4.6 mmol) of phthalic isoimide as yellow solid, which was used without further purification. 0.30 g (2.8 mmol, 1.2 eq.) of 4-methylaniline were dissolved in 25 mL of tetrahydrofuran. 0.60 g (2.3 mmol, 1 eq.) of the phthalic isoimide was suspended in 10 mL of tetrahydrofuran and added to the aniline solution to yield 0.52 g (1.42 mmol, 62%) of the product as colorless crystalline solid.

^{1}H NMR (600 MHz, DMSO-d_6) δ [ppm] = 10.59 (s, 1H), 10.39 (s, 1H), 7.73 (d, *J* = 8.8 Hz, 2H), 7.68 (m, 2H), 7.60 (m, 2H), 7.57 (d, *J* = 8.2 Hz, 2H), 7.38 (d, *J* = 8.8 Hz, 2H), 7.12 (d, *J* = 8.2 Hz, 2H), 2.26 (s, 3H).

^{13}C NMR (150 MHz, DMSO-d_6) δ [ppm] = 167.1, 166.5, 138.4, 136.9, 136.7, 132.4, 129.9, 129.0, 128.6, 127.9, 127.0, 121.2, 119.7, 20.6.

HRMS for $C_{21}H_{17}{}^{35}ClN_2O_2$ (ESI+) $[M+H]^+$: calc.: 365.1057, found: 365.1065.

MP: 168.9–171.7 °C (decomposition).

***N*-(4-Chlorophenyl)-*N'*-(4-trifluoromethylsulfonyloxyphenyl)phthaldiamide (1i)**

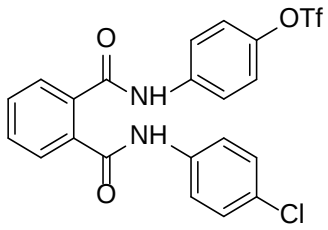

According to the procedure C1, 7.41 g (50 mmol, 1 eq.) of phthalic anhydride and 6.38 g (50 mmol, 1 eq.) of 4-chloroaniline yielded 10.14 g (yield: 73%; 37 mmol) of phthalic monoanilide as colorless solid, which was used without further purification. According to the procedure C2, 1.38 g (5 mmol, 1 eq.) of phthalic monoanilide, 1.52 g (15 mmol, 3 eq.) of NEt_3, and 1.58 g (7.5 mmol 1.5 eq.) of trifluoroacetic anhydride in 18 mL 1,4-dioxane yielded 1.19 g (yield: 93%; 4.6 mmol) of phthalic isoimide as yellow solid, which was used without further purification. 0.42 g (1.7 mmol, 1 eq.) of 4-trifluoromethylsulfonylaniline were dissolved in 25 mL of tetrahydrofuran. 0.45 g (1.7 mmol, 1 eq.) of the phthalic isoimide was suspended in 10 mL of tetrahydrofuran and added to the aniline solution to yield 0.47 g (0.9 mmol, 55%) of the product as colorless crystalline solid. Instead of refluxing in cyclohexane for 1 h, the crystalline solid was washed with 40 mL of dichloromethane.

^{1}H NMR (400 MHz, DMSO-d_6) δ [ppm] = 10.76 (s, 1H), 10.61 (s, 1H), 7.86 (d, *J* = 8.8 Hz, 2H), 7.74–7.62 (m, 6H), 7.47 (d, *J* = 8.6 Hz, 2H), 7.38 (d, *J* = 8.6 Hz, 2H).

^{13}C NMR (100 MHz, DMSO-d_6) δ [ppm] = 167.1, 166.7, 144.4, 139.7, 138.3, 136.4, 131.9, 130.0, 128.6, 127.9, 127.1, 127.0, 121.9, 121.2, 121.1, 120.9, 118.4 (q, *J* = 321.2 Hz).

^{19}F NMR (377 MHz, DMSO-d_6) δ [ppm] = -73.87.

HRMS for $C_{21}H_{14}{}^{35}ClF_3N_2O_5S$ (ESI+) $[M+Na]^+$: calc.: 521.0156, found: 521.0155.

MP: 153.9–156.2 °C (decomposition).

***N*-(3-Bromo-4-methylphenyl)-*N'*-(4-chlorophenyl)phthaldiamide (1j)**

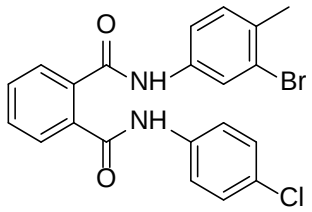

According to the procedure C1, 7.41 g (50 mmol, 1 eq.) of phthalic anhydride and 6.38 g (50 mmol, 1 eq.) of 4-chloroaniline yielded 10.14 g (yield: 73%; 37 mmol) of phthalic monoanilide as colorless solid, which was used without further purification. According to the procedure C2, 0.60 g (2.2 mmol, 1 eq.) of phthalic monoanilide, 668 mg (6.6 mmol, 3 eq.) of NEt_3, and 695 mg (3.3 mmol 1.5 eq.) of trifluoroacetic anhydride in 18 mL 1,4-dioxane yielded 500 mg

(yield: 83%; 1.9 mmol) of phthalic isoimide as yellow solid, which was used without further purification. 390 mg (2.1 mmol, 1 eq.) of 3-bromo-4-methylaniline were dissolved in 25 mL of tetrahydrofuran. 500 mg (1.9 mmol, 1 eq.) of the phthalic isoimide was suspended in 10 mL of tetrahydrofuran and added to the aniline solution to yield 368 mg (0.83 mmol, 44%) of the product as colorless crystalline solid. Instead of refluxing in cyclohexane for 1 h, the crystalline solid was washed with cyclohexane.

^{1}H NMR (400 MHz, DMSO-d_6) δ [ppm] = 10.59 (s, 1H), 10.53 (s, 1H), 8.06 (dd, *J* = 6.6, 1.8 Hz, 1H), 7.75 – 7.67 (m, 4H), 7.65 – 7.59 (m, 2H), 7.53 – 7.46 (m, 1H), 7.40 – 7.36 (m, 2H), 7.30 (d, *J* = 8.3 Hz, 1H), 2.30 (s, 3H).

^{13}C NMR (100 MHz, DMSO-d_6) δ [ppm] = 166.8, 166.8, 138.5, 138.3, 136.5, 136.4, 131.9, 130.9, 130.9, 130.0, 128.6, 127. 9, 127.9, 127.0, 123.7, 122.7, 121.2, 118.8, 21.8.

HRMS for $C_{21}H_{16}{}^{78}Br^{35}ClN_2O_2$ (ESI+) $[M+Na]^+$: calc.: 464.9976, found: 464.9972.

MP: 165.0–166.4 °C (decomposition).

***N*-(3-Bromo-4-methylphenyl)-*N'*-(4-methylphenyl)phthaldiamide (1k)**

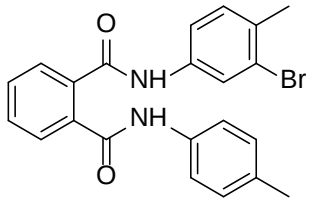

According to the procedure C1, 1.00 g (6.8 mmol, 1 eq.) of phthalic anhydride and 0.72 g (6.8 mmol, 1 eq.) of 4-methylaniline yielded 1.05 g (yield: 60%; 4.2 mmol) of phthalic monoanilide as colorless solid, which was used without further purification. According to the procedure C2, 0.39 g (1.5 mmol, 1 eq.) of phthalic monoanilide, 0.63 mL (4.5 mmol, 3 eq.) of NEt_3, and 0.33 mL (1.5 mmol 1.5 eq.) of trifluoroacetic anhydride in 18 mL 1,4-dioxane yielded 996 mg (yield: 100%; 4.2 mmol) of phthalic isoimide as yellow solid, which was used without further purification. 781 mg (4.2 mmol, 1 eq.) of 3-bromo-4-methylaniline were dissolved in 25 mL of tetrahydrofuran. 500 mg (1.9 mmol, 1 eq.) of the phthalic isoimide was suspended in 15 mL of tetrahydrofuran and added to the aniline solution to yield 936 mg (2.2 mmol, 53%) of the product as colorless crystalline solid. Instead of refluxing in cyclohexane for 1 h, the crystalline solid was washed with 2-propanole and dichloromethane.

^{1}H NMR (400 MHz, DMSO-d_6) δ [ppm] = δ 10.51 (s, 1H), 10.36 (s, 1H), 8.07 (d, *J* = 2.2 Hz, 1H), 7.71–7.64 (m, 2H), 7.63–7.56 (m, 4H), 7.52 (dd, *J* = 8.3, 2.2 Hz, 1H), 7.30 (d, *J* = 8.4 Hz, 1H), 7.13 (d, *J* = 8.3 Hz, 2H), 2.31 (s, 3H), 2.27 (s, 3H).

^{13}C NMR (100 MHz, DMSO-d_6) δ [ppm] = 167.4, 166.9, 139.0, 137.3, 137.2, 137.0, 132.8, 132.3, 131.3, 130.3, 130.2, 129.4, 128.3, 128.3, 124.1, 123.1, 120.1, 119.2, 22.2, 21.0.

HRMS for $C_{22}H_{19}{}^{78}BrN_2O_2$ (ESI+) $[M+H]^+$: calc.: 423.0703, found: 423.0711.

MP: 152.8–154.8 °C (decomposition).

***N*-(4-Chlorophenyl)-*N'*-(3-cyano-4-methylphenyl)phthaldiamide (1l)**

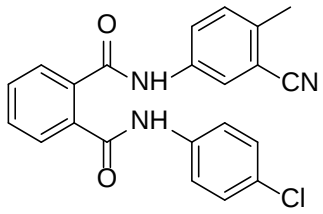

According to the procedure C1, 7.41 g (50 mmol, 1 eq.) of phthalic anhydride and 6.38 g (50 mmol, 1 eq.) of 4-chloroaniline yielded 10.14 g (yield: 73%; 37 mmol) of phthalic monoanilide as colorless solid, which was used without further purification According to the procedure C2, 0.60 g (2.2 mmol, 1 eq.) of phthalic monoanilide, 668 mg (6.6 mmol, 3 eq.) of NEt_3, and 695 mg (3.3 mmol 1.5 eq.) of trifluoroacetic anhydride in 18 mL 1,4-dioxane yielded 500 mg (yield: 83%; 1.9 mmol) of phthalic isoimide as yellow solid, which was used without further purification. 258 mg (1.9 mmol, 1 eq.) of 5-amino-2-methylbenzonitrile were dissolved in 15 mL of tetrahydrofuran. 500 mg (1.9 mmol, 1 eq.) of the phthalic isoimide was suspended in 15 mL of tetrahydrofuran and added to the aniline solution to yield 398 mg (1.02 mmol, 52%) of the product as colorless crystalline solid. Instead of refluxing in cyclohexane for 1 h, the crystalline solid was washed with dichloromethane.

^{1}H NMR (400 MHz, DMSO-d_6) δ [ppm] 10.71 (s, 1H), 10.61 (s, 1H), 8.09 (d, *J* = 2.3 Hz, 1H), 7.81 (dd, *J* = 8.4, 2.3 Hz, 1H), 7.75–7.67 (m, 4H), 7.66–7.61 (m, 2H), 7.43 (d, *J* = 8.5 Hz, 1H), 7.43–7.34 (m, 2H), 2.44 (s, 3H).

^{13}C NMR (100 MHz, DMSO-d_6) δ [ppm] = 167.1, 166.7, 138.3, 137.7, 136.5, 136.2, 136.2, 130.9, 130.1, 130.0, 128.6, 127.9, 127.9, 127.1, 124.3 122.4, 121.2, 117.9, 111.7, 19.3.

HRMS for $C_{22}H_{16}{}^{35}ClN_3O_2$ (ESI+) $[M+Na]^+$: calc.: 412.0823, found: 412.0813.

MP: 199.2–202.5 °C (decomposition).

***N*,*N'*-Di(4-chlorophenyl)-pyridine-3,4-diamide (1m)**

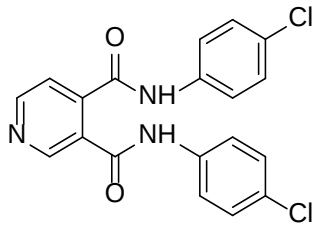

According to the procedure C1, 1.00 g (6.7 mmol, 1 eq.) of pyridine-3,4-pyridine-dicarboxylic acid anhydride and 0.84 g (6.7 mmol, 1 eq.) of 4-chloroaniline yielded 1.78 g (yield: 95%; 6.4 mmol) of the corresponding monoanilide isomers as colorless solid, which were used without further purification. According to the procedure C2, 1.00 g (3.6 mmol, 1 eq.) of monoanilides, 1.10 g (10.8 mmol, 3 eq.) of NEt_3, and 1.14 g (5.4 mmol 1.5 eq.) of trifluoroacetic anhydride in 18 mL 1,4-dioxane yielded 0.93 g (yield: 100%; 3.6 mmol) of isoimide as yellow solid, which was used without further purification. 0.46 g (3.6 mmol, 1 eq.) of 4-chlorolaniline were dissolved in 30 mL of tetrahydrofuran. 0.93 g (3.6 mmol, 1 eq.) of the isoimide was suspended in 10 mL of tetrahydrofuran and added to the aniline solution to yield 716 mg (1.85 mmol, 51%) of the product as colorless crystalline solid. Instead of refluxing in cyclohexane for 1 h, the crystalline solid was washed with 40 mL of dichloromethane.

^{1}H NMR (400 MHz, DMSO-d_6) δ [ppm] = 10.79 (s, 2H), 9.00–8.80 (m, 2H), 7.91–7.55 (m, 5H), 7.53–7.19 (m, 4H).

^{13}C NMR (100 MHz, DMSO-d_6) δ [ppm] = 165.0, 164.5, 151.7, 148.5, 143.5, 137.9, 137.8, 130.5, 128.7, 128.7, 127.6, 127.5, 121.9, 121.4, 121.1.

HRMS for $C_{19}H_{13}{}^{35}Cl_2N_3O_2$ (ESI+) $[M+Na]^+$: calc.: 408.0277, found: 408.0280.

MP: 180.9–182.7 °C (decomposition).

4-Bromo-*N*,*N'*-di(4-chlorophenyl)phthaldiamide (1n)

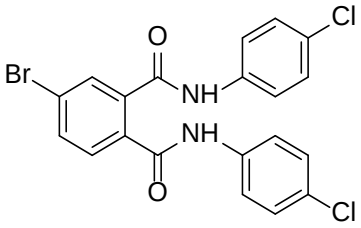

According to the procedure C1, 1.00 g (4.4 mmol, 1 eq.) of phthalic anhydride and 0.56 g (4.4 mmol, 1 eq.) of 4-chloroaniline yielded 1.40 g (yield: 89%; 4.0 mmol) of phthalic monoanilide as colorless solid, which was used without further purification. According to the procedure C2, 1.40 g (3.95 mmol, 1 eq.) of phthalic monoanilide, 1.20 g (11.9 mmol, 3 eq.) of NEt_3, and 1.24 g (5.9 mmol 1.5 eq.) of trifluoroacetic anhydride in 18 mL 1,4-dioxane yielded 1.33 g (yield: 100%; 3.95 mmol) of phthalic isoimide as yellow solid, which was used without further purification. 0.50 g (3.95 mmol, 1 eq.) of 4-chloroaniline were dissolved in 35 mL of tetrahydrofuran. 1.33 g (3.95 mmol, 1 eq.) of the phthalic isoimide was suspended in 10 mL of tetrahydrofuran and added to the aniline solution to yield 767 g (1.65 mmol, 42%) of the product as colorless crystalline solid. Instead of refluxing in cyclohexane for 1 h, the crystalline solid was washed with 40 mL of dichloromethane.

^{1}H NMR (400 MHz, DMSO-d_6) δ [ppm] = 10.66 (s, 1H), 10.63 (s, 1H), 7.92 (d, *J* = 1.9 Hz, 1H), 7.85 (dd, *J* = 8.2, 1.8 Hz, 1H), 7.72 – 7.68 (m, 4H), 7.66 (d, *J* = 8.2 Hz, 1H), 7.41 – 7.36 (m, 4H).

^{13}C NMR (100 MHz, DMSO-d_6) δ [ppm] = 165.9, 165.1, 138.4, 138.0, 138.0, 135.5, 132.7, 130.6, 130.6, 129.9, 128.6, 127.3, 127.2, 123.1, 121.3, 121.2.

HRMS for $C_{20}H_{13}{}^{78}Br^{35}Cl_2N_2O_2$ (ESI+) $[M+Na]^+$: calc.: 484.9430, found: 484.9433.

MP: 176.2–178.8 °C (decomposition).

***N*,*N'*-Di(4-chlorophenyl)-4-methyl-phthaldiamide (1o)**

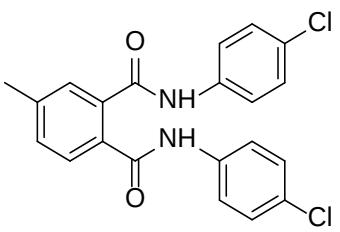

According to the procedure C1, 1.00 g (6.7 mmol, 1 eq.) of phthalic anhydride and 0.85 g (6.2 mmol, 1 eq.) of 4-chloroaniline yielded 1.68 g (yield: 94%; 5.8 mmol) of phthalic monoanilide as colorless solid, which was used without further purification. According to the procedure C2, 1.68 g (5.8 mmol, 1 eq.) of phthalic monoanilide, 1.75 g (17.4 mmol, 3 eq.) of NEt_3, and 1.82 g (8.7 mmol 1.5 eq.) of trifluoroacetic anhydride in 18 mL 1,4-dioxane yielded 1.58 g (yield: 100%; 5.8 mmol) of phthalic isoimide as yellow solid, which was used without further purification. 0.74 g (5.8 mmol, 1 eq.) of 4-trifluoromethylsulfonylaniline were dissolved in 25 mL of tetrahydrofuran. 1.58 g (5.8 mmol, 1 eq.) of the phthalic isoimide was suspended in 10 mL of tetrahydrofuran and added to the aniline solution to yield 977 mg (2.45 mmol, 42%) of the product as colorless crystalline solid. Instead of refluxing in cyclohexane for 1 h, the crystalline solid was washed with 40 mL of dichloromethane.

^{1}H NMR (300 MHz, DMSO-d_6) δ [ppm] = 10.55 (s, 1H), 10.51 (s, 1H), 7.75 – 7.68 (m, 4H), 7.61 (d, J = 7.8 Hz, 1H), 7.50 (s, 1H), 7.44 – 7.34 (m, 5H), 2.43 (s, 3H).

^{13}C NMR (100 MHz, DMSO-d_6) δ [ppm] = δ 167.0, 166.6, 140.0, 138.4, 136.8, 136.8, 133.5, 130.1, 128.5, 128.4, 127.9, 127.9, 127.0, 121.2, 121.2, 121.1, 20.8.

HRMS for $C_{21}H_{16}{}^{35}Cl_2N_2O_2$ (ESI+) $[M+Na]^+$: calc.: 421.0481, found: 421.0484.

MP: 222.6–224.8 °C (decomposition).

***N,N'*-Diphenylphthaldiamide (1p)**

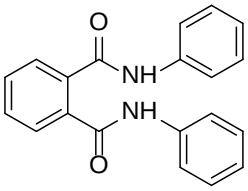

According to the procedure A, 3.73 g (40 mmol, 4 eq.) of aniline and 2.00 g (10 mmol, 1 eq.) of *o*-phthalic dichloride yielded 2.48 g (yield: 78%; 7.8 mmol) of product as colorless crystalline solid. Product was recrystallized from tetrahydrofuran.

^{1}H NMR (400 MHz, DMSO-d_6) δ [ppm] = 10.43 (s, 2H, N-H), 7.73–7.58 (m, 8H), 7.31 (t, *J* = 7.4 Hz, 4H), 7.07 (t, *J* = 7.4 Hz, 2H).

^{13}C NMR (100 MHz, DMSO-d_6) δ [ppm] = 166.8, 139.4, 136.8, 129.8, 128.6, 127.9, 123.5, 119.7.

HRMS for $C_{20}H_{16}N_2O_2$ (ESI+) $[M+H]^+$: calc.: 317.1290, found: 317.1298.

MP: 235.1–238.3 °C.

Synthesis of phthalazin-1,4-diones

2,3-Di(4-methylphenyl)-2,3-dihydrophthalazin-1,4-dione (2a)

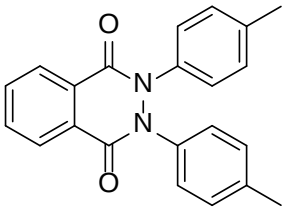

Small scale: According to procedure D2, 345 mg (1 mmol, 1 eq.) of **1a** and 97 mg NBu_4PF_6 in 25 mL HFIP were electrolyzed in a 25 mL beaker-type cell. An amount of 2.2 F of electric charge was applied to afford 269 mg (yield: 78%; 0.78 mmol) of greyish crystalline solid.

Large scale: According to procedure D3, 1.33 g (3.9 mmol, 1 eq.) of **1a** and 377 mg NBu_4PF_6 in 25 mL HFIP were electrolyzed in a 80 mL beaker-type cell. An amount of 2.4 F of electric charge was applied to afford 960 mg (yield: 72%; 2.80 mmol) of greyish crystalline solid.

^{1}H NMR (300 MHz, $CDCl_3$) δ [ppm] = 8.40 (m, 2H), 7.85 (m, 2H), 7.15 (d, *J* = 8.4 Hz, 4H), 7.06 (d, *J* = 8.1 Hz, 4H), 1.26 (s, 6H).

^{13}C NMR (75 MHz, $CDCl_3$) δ [ppm] = 158.5, 138.5, 135.1, 133.9, 129.7, 129.6, 128.7, 128.3, 21.3.

HRMS for $C_{22}H_{18}N_2O_2$ (ESI+) $[M+H]^+$: calc.: 343.1447, found: 343.1444.

MP: 178.6–179.8 °C (cyclohexane/ethylacetate).

The analytical data matches the reported data.[11]

2,3-Bis(4-(1,1-dimethylethyl)phenyl)-2,3-dihydrophthalazin-1,4-dione (2b)

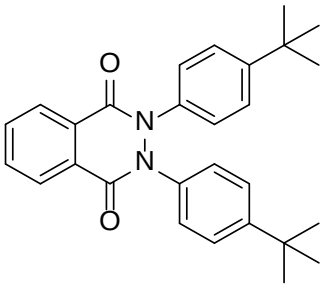

According to procedure D2, 429 mg (1 mmol, 1 eq.) of **1b** and 97 mg NBu_4PF_6 in 25 mL HFIP were electrolyzed in a 25 mL beaker-type cell. An amount of 3.0 F of electric charge was applied to afford 188 mg (yield: 44%; 0.44 mmol) of brownish crystalline solid.

^{1}H NMR (300 MHz, $CDCl_3$) δ [ppm] = 8.43 (m, 2H), 7.87 (m, 2H), 7.23 (d, *J* = 8.8 Hz, 4H), 7.13 (d, *J* = 8.8 Hz, 4H), 1.19 (s, 18H).

^{13}C NMR (75 MHz, $CDCl_3$) δ [ppm] = 158.3, 151.6, 134.7, 133.9, 129.8, 128.8, 128.3, 125.7, 34.7, 31.2.

HRMS for $C_{28}H_{30}N_2O_2$ (ESI+) $[M+H]^+$: calc.: 427.2386, found: 427.2392.

MP: 186.2–189.4 °C (cyclohexane/ethylacetate).

2,3-Bis(3-(1,1-dimethylethyl)phenyl)-2,3-dihydrophthalazin-1,4-dione (2c)

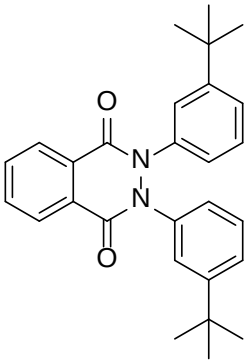

According to procedure D2, 429 mg (1 mmol, 1 eq.) of **1c** and 97 mg NBu_4PF_6 in 25 mL HFIP were electrolyzed in a 25 mL beaker-type cell. An amount of 2.7 F of electric charge was applied to afford 143 mg (yield: 34%; 0.34 mmol) of brown crystalline solid.

^{1}H NMR (400 MHz, $CDCl_3$) δ [ppm] = 8.43 (m, 2H), 7.86 (m, 2H), 7.20–7.13 (m, 8H), 1.19 (s, 18H).

^{13}C NMR (100 MHz, $CDCl_3$) δ [ppm] = 158.2, 152.0, 137.3, 133.8, 129.7, 128.3, 128.2, 126.3, 125.8, 125.4, 34.7, 31.1.

HRMS for $C_{28}H_{30}N_2O_2$ (ESI+) $[M+Na]^+$: calc.: 449.2199, found: 449.219.

MP: 126.6–128.7 °C (cyclohexane/ethylacetate).

2,3-Di(4-chlorophenyl)-2,3-dihydrophthalazin-1,4-dione (2d)

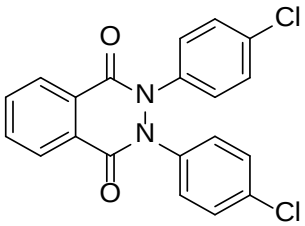

According to procedure D2, 385 mg (1 mmol, 1 eq.) of **1d** and 97 mg NBu_4PF_6 in 25 mL HFIP were electrolyzed in a 25 mL beaker-type cell. An amount of 2.2 F of electric charge was applied to afford 248 mg (yield: 65%; 0.65 mmol) of colorless crystalline solid.

^{1}H NMR (400 MHz, $CDCl_3$) δ [ppm] = 8.40 (m, 2H), 7.89 (m, 2H), 7.27 (s, 8H).

^{13}C NMR (75 MHz, $CDCl_3$) δ [ppm] = 158.6, 136.2, 134.3, 134.3, 129.5, 129.4, 129.3, 128.5.

HRMS for $C_{20}H_{12}{}^{35}Cl_2N_2O_2$ (ESI+) $[M+H]^+$: calc.: 383.0354, found: 383.0345.

MP: 178.5–179.2 °C (cyclohexane/ethylacetate).

2,3-Di(4-fluorophenyl)-2,3-dihydrophthalazin-1,4-dione (2e)

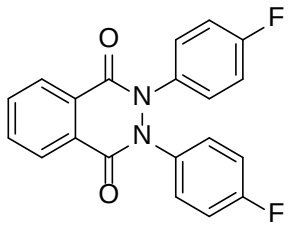

According to procedure D2, 352 mg (1 mmol, 1 eq.) of **1e** and 97 mg NBu_4PF_6 in 25 mL HFIP were electrolyzed in a 25 mL beaker-type cell. An amount of 2.2 F of electric charge was applied to afford 201 mg (yield: 57%; 0.57 mmol) of greyish crystalline solid.

^{1}H NMR (300 MHz, $CDCl_3$) δ [ppm] = 8.40 (m, 2H), 7.88 (m, 2H), 7.33–7.20 (m, 4H), 7.02–6.94 (m, 4H).

^{13}C NMR (75 MHz, $CDCl_3$) δ [ppm] = 162.0 (d, *J* = 249.9 Hz), 158.6, 134.3, 133.5 (d, *J* = 3.3 Hz), 130.7 (d, *J* = 8.9 Hz), 129.5, 128.4, 116.2 (d, *J* = 23.1 Hz).

^{19}F NMR (377 MHz, DMSO-d_6) δ [ppm] = -112.47.

HRMS for $C_{20}H_{12}F_2N_2O_2$ (ESI+) $[M+H]^+$: calc.: 351.0945, found: 351.0944.

MP: 170.8–172.2 °C (cyclohexane/ethylacetate).

2,3-Bis(2,4-difluorophenyl)-2,3-dihydrophthalazin-1,4-dione (2f)

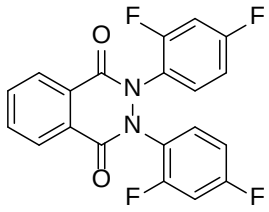

According to procedure D1, 78 mg (0.2 mmol, 1 eq.) of **1f** and 20 mg NBu_4PF_6 in 5 mL HFIP were electrolyzed in a 5 mL Teflon cell. An amount of 2.2 F of electric charge was applied to afford 36 mg (yield: 48%; 0.1 mmol) of colorless crystalline solid.

^{1}H NMR (300 MHz, $CDCl_3$) δ [ppm] = 8.41 (m, 2H), 7.90 (m, 2H), 7.32 (s, 2H), 6.82 (td, *J* = 5.9, 3.3 Hz, 4H).

^{13}C NMR (75 MHz, $CDCl_3$) δ [ppm] = 163.5 (d, *J* = 253.8 Hz), 157.9, 134.3, 131. 8 (d, *J* = 10.0 Hz), 129.2, 128.5, 120.9 (d, *J* = 11.6 Hz), 112.3 (d, *J* = 22.7 Hz), 105.1 (t, *J* = 22.7 Hz).

^{19}F NMR (377 MHz, DMSO-d_6) δ = -105.60, -113.96.

HRMS for $C_{20}H_{10}F_4N_2O_2$ (ESI+) $[M+H]^+$: calc.: 387.0757, found: 387.0744.

MP: 161.5–162.7 °C (cyclohexane/ethylacetate).

2,3-Di(4-methoxyphenyl)-2,3-dihydrophthalazin-1,4-dione (2g)

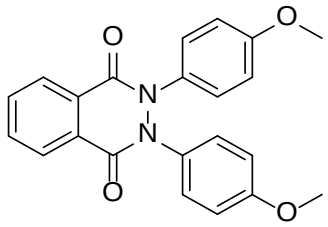

According to procedure D2, 375 mg (1 mmol, 1 eq.) of **1g** and 97 mg NBu_4PF_6 in 25 mL HFIP were electrolyzed in a 25 mL beaker-type cell. An amount of 3.0 F of electric charge was applied to afford 150 mg (yield: 40%; 0.40 mmol) of purple crystalline solid.

^{1}H NMR (300 MHz, $CDCl_3$) δ [ppm] = 8.40 (m, 2H), 7.65 (m, 2H), 7.14 (d, *J* = 9.0 Hz, 4H), 6.77 (d, *J* = 9.0 Hz, 4H), 1.26 (s, 18H).

^{13}C NMR (75 MHz, $CDCl_3$) δ [ppm] = 159.3, 158.5, 133.8, 130.6, 130.1, 129.7, 128.3, 114.27, 55.5.

HRMS for $C_{22}H_{18}N_2O_2$ (ESI+) $[M+H]^+$: calc.: 375.1345, found: 375.1339.

MP: 166.5–167.3 °C (cyclohexane/ethylacetate).

2-(4-Chlorophenyl)-3-(4-methylphenyl)-2,3-dihydrophthalazin-1,4-dione (2h)

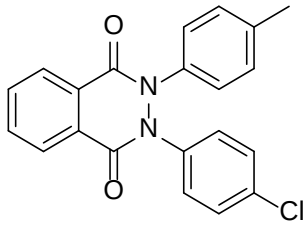

According to procedure D2, 365 mg (1 mmol, 1 eq.) of **1h** and 97 mg NBu_4PF_6 in 25 mL HFIP were electrolyzed in a 25 mL beaker-type cell. An amount of 2.2 F of electric charge was applied to afford 173 mg (yield: 48%; 0.48 mmol) of slightly orange crystalline solid.

^{1}H NMR (300 MHz, $CDCl_3$) δ [ppm] = 8.39 (m, 2H), 7.90–7.79 (m, 2H), 7.24 (s, 4H), 7.16 (d, *J* = 8.4 Hz, 2H), 7.08 (d, *J* = 8.2 Hz, 2H), 2.27 (s, 3H).

^{13}C NMR (75 MHz, $CDCl_3$) δ [ppm] = 158.5, 138.8, 136.3, 135.1, 134.1 (d, *J* = 9.2 Hz), 129.9, 129.8, 129.7, 129.4, 129.1, 128.4 (d, *J* = 7.2 Hz), 128.3, 21.3.

HRMS for $C_{21}H_{15}{}^{35}ClN_2O_2$ (ESI+) $[M+H]^+$: calc.: 363.0900, found: 363.0912.

MP: 172.5–174.0 °C (cyclohexane/ethylacetate).

2-(4-Chlorophenyl)-3-(4-trifluoromethylsulfonyloxyphenyl)-2,3-dihydrophthalazin-1,4-dione (2i)

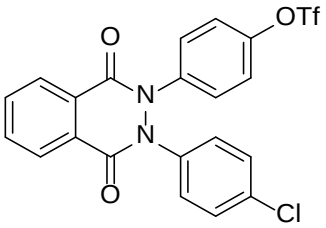

According to procedure D1, 100 mg (0.2 mmol, 1 eq.) of **1i** and 20 mg NBu_4PF_6 in 5 mL HFIP were electrolyzed in a 5 mL Teflon cell. An amount of 2.2 F of electric charge was applied to afford 54 mg (yield: 54%; 0.11 mmol) of grey crystalline solid.

^{1}H NMR (400 MHz, $CDCl_3$) δ [ppm] = 8.42–8.36 (m, 2H), 7.93–7.88 (m, 2H), 7.44 (d, *J* = 9.0 Hz, 2H), 7.26 (s, 4H), 7.22 (d, *J* = 9.0 Hz, 2H).

^{13}C NMR (100 MHz, $CDCl_3$) δ [ppm] = 158.7, 158.7, 148.3, 137.7, 136.3, 134.6, 134.5, 134.4, 129.9, 129.9, 129.4, 129.2, 129.2, 128.6, 128.6, 122.0, 119.5 (q, J = 321.5 Hz).

^{19}F NMR (377 MHz, $CDCl_3$) δ = -73.83.

HRMS for $C_{21}H_{14}{}^{35}ClF_3N_2O_5S$ (ESI+) $[M+H]^+$: calc.: 497.0108, found: 497.0186.

MP: 178.8–180.7 °C (cyclohexane/ethylacetate).

2-(3-Bromo-4-methylphenyl)-3-(4-chlorophenyl)-2,3-dihydrophthalazin-1,4-dione (2j)

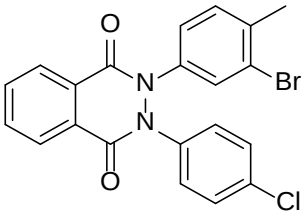

According to procedure D1, 89 mg (0.2 mmol, 1 eq.) of **1j** and 20 mg NBu_4PF_6 in 5 mL HFIP were electrolyzed in a 5 mL Teflon cell. An amount of 3.8 F of electric charge was applied to afford 46 mg (yield: 52%; 0.10 mmol) of brownish oil.

^{1}H NMR (400 MHz, $CDCl_3$) δ [ppm] = 8.41–8.33 (m, 2H), 7.89–7.83 (m, 2H), 7.52 (d, *J* = 1.8 Hz, 1H), 7.30–7.27 (m, 4H), 7.19–7.09 (m, 2H), 2.30 (s, 3H).

^{13}C NMR (100 MHz, $CDCl_3$) δ [ppm] = 158.5, 158.4, 138.5, 136.1, 136.1, 134.1, 134.0, 131.7, 131.7, 130.6, 130.6, 129.4, 129.2, 129.1, 128.3, 128.3, 126.8, 124.5, 22.6.

HRMS for $C_{21}H_{14}{}^{78}Br^{35}ClN_2O_2$ (ESI+) $[M+H]^+$: calc.: 441.0000, found: 441.0000.

2-(3-Bromo-4-methylphenyl)-3-(4-methylphenyl)-2,3-dihydrophthalazin-1,4-dione (2k)

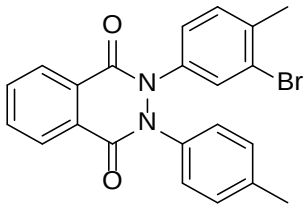

According to procedure D1, 85 mg (0.2 mmol, 1 eq.) of **1k** and 20 mg NBu_4PF_6 in 5 mL HFIP were electrolyzed in a 5 mL Teflon cell. An amount of 3.5 F of electric charge was applied to afford 54 mg (yield: 64%; 0.12 mmol) of brownish solid.

^{1}H NMR (400 MHz, $CDCl_3$) δ [ppm] = 8.43–8.36 (m, 2H), 7.90–7.82 (m, 2H), 7.50 (d, *J* = 2.0 Hz, 1H), 7.20–7.05 (m, 6H), 2.29 (s, 3H), 2.27 (s, 3H).

^{13}C NMR (100 MHz, $CDCl_3$) δ [ppm] = 158.4, 158.4, 138.6, 138.3, 136.1, 134.9, 133.0, 133.9, 132.1, 130.5, 129.6, 129.6, 129.3, 128.3, 128.2, 128.2, 127.3, 124.3, 22.6, 21.2.

HRMS for $C_{22}H_{17}{}^{78}BrN_2O_2$ (ESI+) $[M+H]^+$: calc.: 421.0546, found: 421.0543.

2-(4-Chlorophenyl)-3-(3-cyano-4-methylphenyl)-2,3-dihydrophthalazin-1,4-dione (2l)

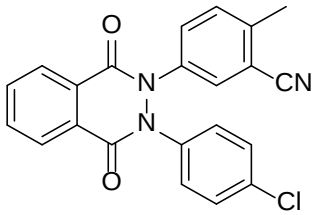

According to procedure D1, 78 mg (0.2 mmol, 1 eq.) of **1l** and 20 mg NBu_4PF_6 in 5 mL HFIP were electrolyzed in a 5 mL Teflon cell. An amount of 3.5 F of electric charge was applied to afford 44 mg (yield: 57%; 0.11 mmol) of brownish solid.

^{1}H NMR (400 MHz, $CDCl_3$) δ [ppm] = 8.37–8.31 (m, 2H), 7.89–7.83 (m, 2H), 7.60 (d, *J* = 2.3 Hz, 1H), 7.43 (dd, *J* = 8.3, 2.3 Hz, 1H), 7.29 – 7.26 (m, 4H), 7.23 (d, *J* = 8.4 Hz, 1H), 2.46 (s, 3H).

^{13}C NMR (100 MHz, $CDCl_3$) δ [ppm] = 158.4, 158.4, 142.0, 136.0, 135.8, 134.3, 134.2, 134.1, 131.8, 131.5, 130.8, 129.2, 129.1, 129.0, 128.9, 128.3, 128.3, 116.7, 113.4, 20.1.

HRMS for $C_{22}H_{14}{}^{35}ClN_3O_2$ (ESI+) $[M+H]^+$: calc.: 388.0847, found: 388.0846.

2,3-Di(4-chlorophenyl)-pyrido-[3,4-d]-2,3-dihydropyridazin-1,4-dion (2m)

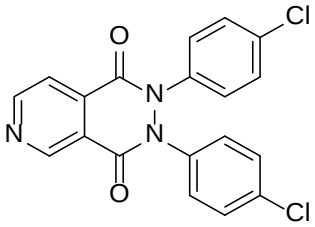

According to procedure D1, 77 mg (0.2 mmol, 1 eq.) of **1m** and 20 mg NBu_4PF_6 in 5 mL HFIP were electrolyzed in a 5 mL Teflon cell. An amount of 4.4 F of electric charge was applied to afford 44 mg (yield: 57%; 0.11 mmol) of brownish oil.

^{1}H NMR (400 MHz, $CDCl_3$) δ [ppm] = 9.66 (s, 1H), 9.15 (d, *J* = 5.2 Hz, 1H), 8.18 (d, *J* = 5.2 Hz, 1H), 7.34–7.26 (m, 4H), 7.27–7.23 (m, 4H).

^{13}C NMR (100 MHz, $CDCl_3$) δ [ppm] = 157.1, 156.7, 154.6, 151.1, 135.5, 135.5, 135.2, 135.2, 134.7, 134.7, 129.5, 129.4, 129.3, 123.1, 120.2.

HRMS for $C_{19}H_{11}{}^{35}Cl_2N_3O_2$ (ESI+) $[M+H]^+$: calc.: 384.0301, found: 384.0317.

6-Bromo-2,3-di(4-chlorophenyl) -2,3-dihydrophthalazin-1,4-dione (2n)

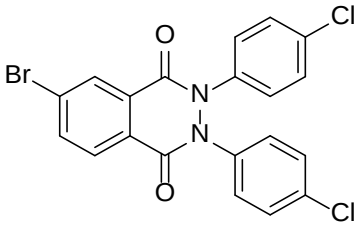

According to procedure D1, 93 mg (0.2 mmol, 1 eq.) of **1n** and 20 mg NBu_4PF_6 in 5 mL HFIP were electrolyzed in a 5 mL Teflon cell. An amount of 6.0 F of electric charge was applied due to solubility issues to afford 42 mg (yield: 45%; 0.09 mmol) of brownish oil.

^{1}H NMR (400 MHz, $CDCl_3$) δ [ppm] = 8.51 (d, *J* = 1.9 Hz, 1H), 8.23 (d, *J* = 8.4 Hz, 1H), 7.98 (dd, *J* = 8.4, 2.0 Hz, 1H), 7.30 – 7.21 (m, 8H).

^{13}C NMR (100 MHz, $CDCl_3$) δ [ppm] = 157.9, 157.2, 137.5, 135.8, 135.8, 134.4, 134.4, 131.2, 130.6, 130.1, 129.7, 129.4, 129.4, 129.3, 129.3, 128.0.

HRMS for $C_{20}H_{11}{}^{78}Br^{35}Cl_2N_2O_2$ (ESI+) $[M+H]^+$: calc.: 460.9454, found: 460.9434.

2,3-Di(4-chlorophenyl)-6-methyl-2,3-dihydrophthalazin-1,4-dione (2o)

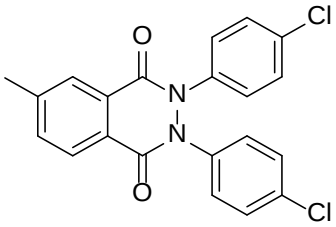

According to procedure D1, 79 mg (0.2 mmol, 1 eq.) of **1o** and 20 mg NBu_4PF_6 in 5 mL HFIP were electrolyzed in a 5 mL Teflon cell. An amount of 2.2 F of electric charge was applied to afford 71 mg (yield: 89%; 0.18 mmol) of brownish oil.

^{1}H NMR (400 MHz, $CDCl_3$) δ [ppm] = 8.28 (d, *J* = 8.0 Hz, 1H), 8.19 – 8.18 (m, 1H), 7.71 – 7.67 (m, 1H), 7.31 – 7.24 (m, 8H), 2.59 (s, 3H).

^{13}C NMR (100 MHz, $CDCl_3$) δ [ppm] = 158.8, 158.8, 145.7, 145.7, 136.4, 135.4, 135.4, 134.2, 134.2, 129.4, 129.3, 129.3, 128.6, 128.5, 126.9, 126.9, 22.1.

HRMS for $C_{21}H_{14}{}^{35}Cl_2N_2O_2$ (ESI+) $[M+Na]^+$: calc.: 419.0325, found: 419.0331.

2,3-Bisphenyl-2,3-dihydrophthalazin-1,4-dione (2p)

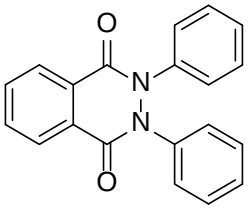

According to procedure D2, 316 mg (1 mmol, 1 eq.) of **1p** and 97 mg NBu_4PF_6 in 25 mL HFIP were electrolyzed in a 25 mL beaker-type cell. An amount of 2.5 F of charge was applied to afford 54 mg (yield: 17%; 0.17 mmol) of colorless crystalline solid.

^{1}H NMR (400 MHz, $CDCl_3$) δ [ppm] = 8.39 (m, 2H), 7.85 (m, 2H), 7.33–7.21 (m, 8H), 7.15 (t, *J* = 7.1 Hz, 2H).

^{13}C NMR (75 MHz, DMSO-d_6) δ [ppm] = 158.5, 137.7, 134.0, 129.7, 128.9, 128.8, 128.4, 128.4.

HRMS for $C_{20}H_{14}N_2O_2$ (ESI+) $[M+H]^+$: calc.: 315.1134, found: 315.1133.

MP: 170.2–171.5 °C (cyclohexane/ethylacetate).

The analytical data matchs the reported data.[11]

4,4‘-Dichloroazobenzene (5)

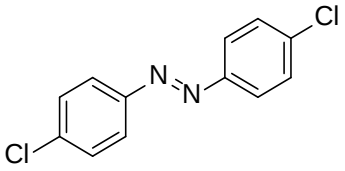

140 mg (0.370 mmol, 1 eq.) of **2d** were dissolved in 40 mL methanol and then 44 mg (1.1 mmol, 3.eq) of a hydrazine solution (80%) were added After stirring for 4 days at ambient conditions, the azobenzene was extracted with cyclohexane (3x 40 mL). The organic layer was washed with 1 M hydrochloride acid solution (1x 50 mL), water (1x 50 mL), and brine (1x 50 mL). After drying with $MgSO_4$ the solvent was removed under reduced pressure to yield 81 mg (88%, 0.324 mmol) as orange crystals.

^{1}H NMR (400 MHz, $CDCl_3$) δ [ppm] = 7.88–7.85 (m, 4H), 7.51–7.47 (m, 4H).

In addition the other analytical data match with reported ones.[12]

Crystallographic data

Crystal structure determination of **1d** (CCDC 1568132): $C_{20}H_{14}Cl_2N_2O_2$, M_r = 385.2 g/mol, colorless needle (0.040 x 0.110 x 0.92 mm^3), I a (monoklin), a = 14.880 Å, b = 9.5503 Å, c = 25.8277 Å, V = 3525.8 $Å^3$, Z = 8, F(000) = 1584, ρ = 1.451 g/cm^3, μ = 0.39 mm^{-1}, Mo-Kα graphite monochromator, -80 °C, 23749 reflections, 8657 independent reflections, wR_2 = 0.1972, R_1 = 0.0655, 0.92 e/$Å^3$, –0.41 e/$Å^3$, GoF = 0.96

Single crystals for structure determination were obtained by recrystallization from acetone at room temperature. Interestingly, the molecule crystallizes in two different conformations, leading to an opposed orientation in the packing.

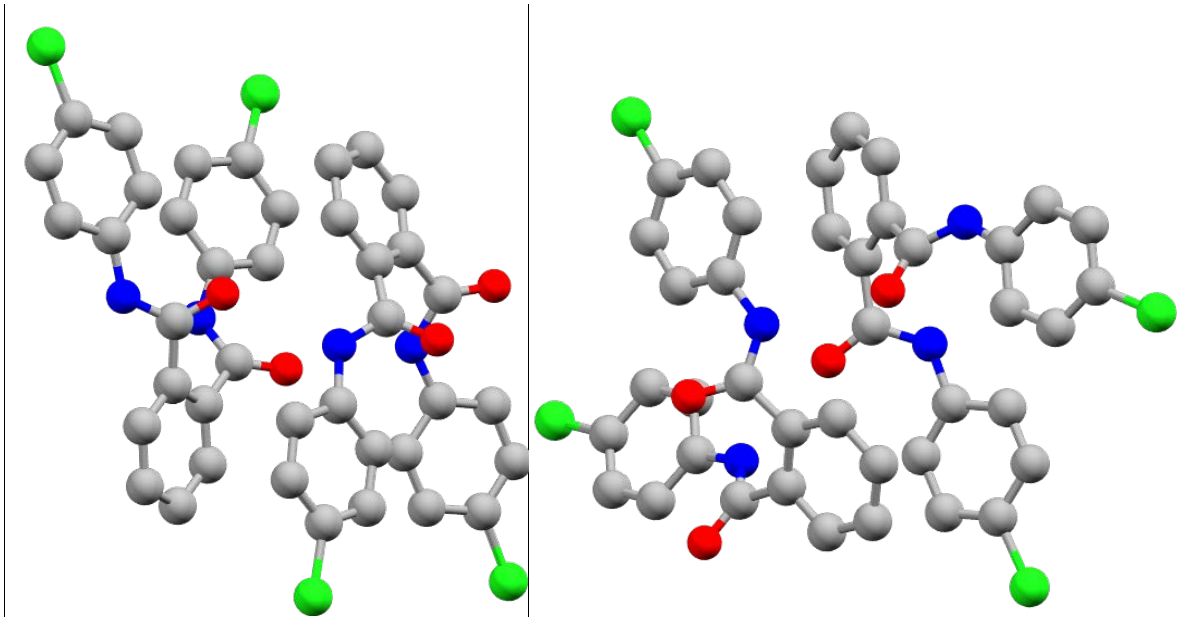

Figure 2: Molecular structure of derivative 1d by X-ray analysis (left: side view; right: top view).

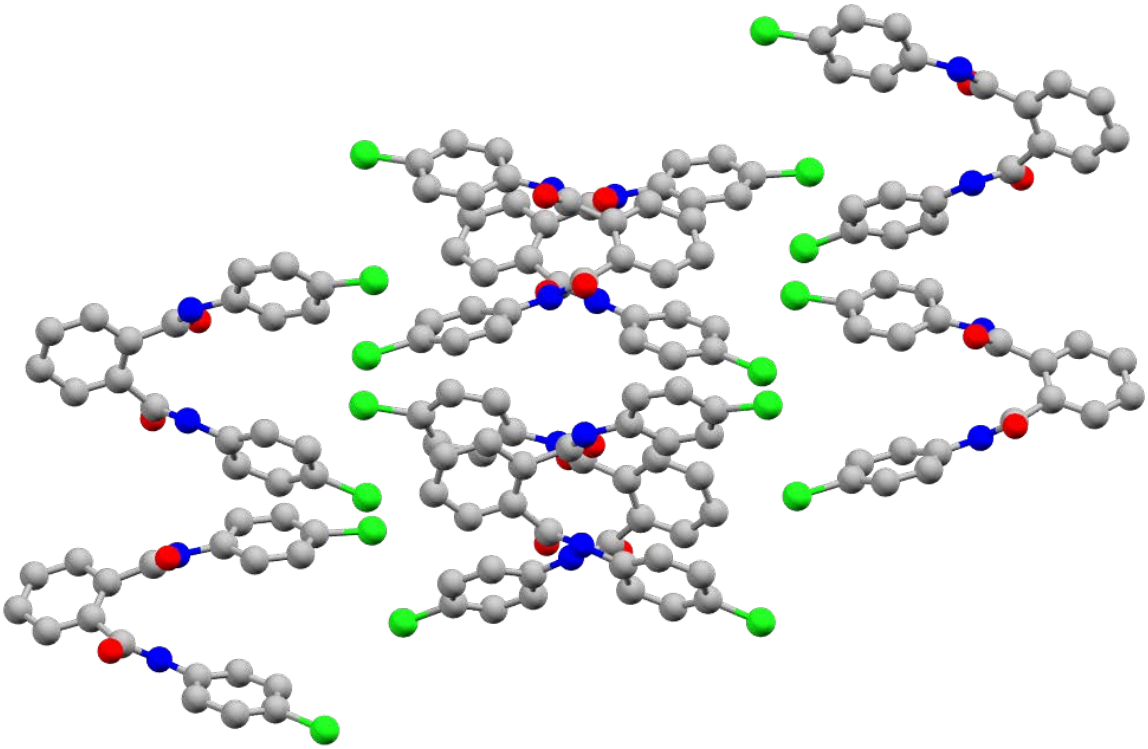

Figure 3: Packing of 1d in the solid state.

Crystal structure determination of **2d** (CCDC 1568133): $C_{20}H_{12}Cl_2N_2O_2$, M_r = 383.23 g/mol, colorless block (0.080 x 0.36 x 0.36 mm^3), C 2/c (monoklin), a = 12.6950 Å, b = 23.104 Å, c = 13.6145 Å, V = 3538.3 $Å^3$, Z = 8, F(000) = 1568, ρ = 1.439 g/cm^3, μ = 0.38 mm^{-1}, Mo-Kα graphite monochromator, -80 °C, 10403 reflections, 4309 independent reflections, wR_2 = 0.1888, R_1 = 0.0715, 0.24 e/$Å^3$, –0.45 e/$Å^3$, GoF = 1.035

Single crystals for structure determination were obtained by recrystallization from ethanol at room temperature. The molecule crystallizes in two different conformations similar to the starting material.

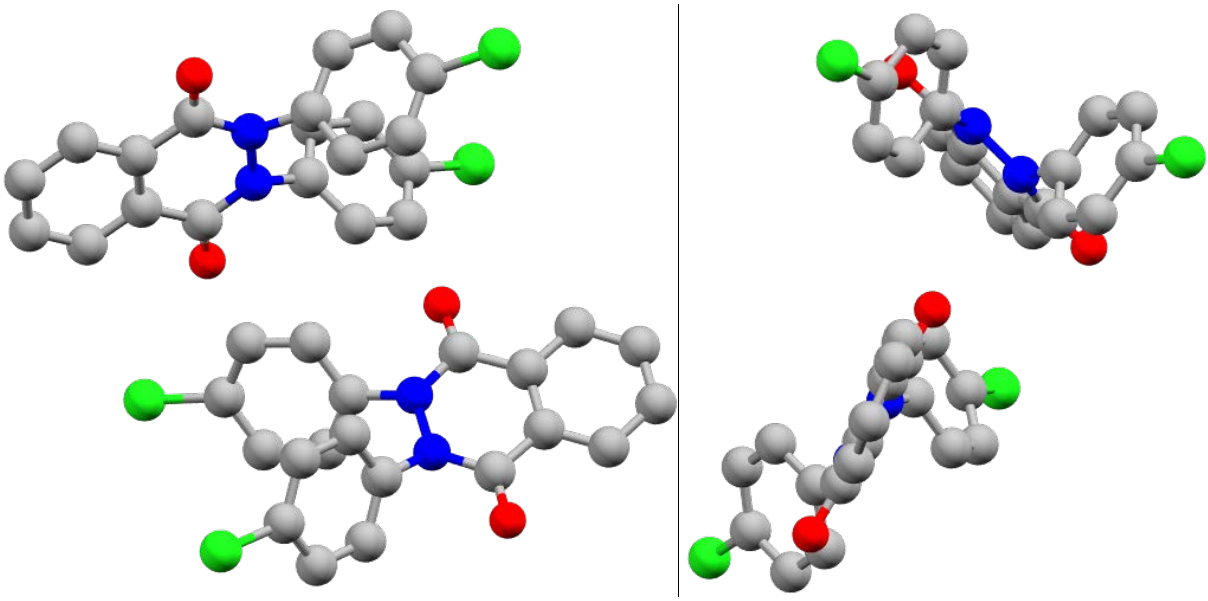

Figure 4: Molecular structure of derivative 2d by X-ray analysis (left: side view of the main conformation; right: side view with both conformations indicated).

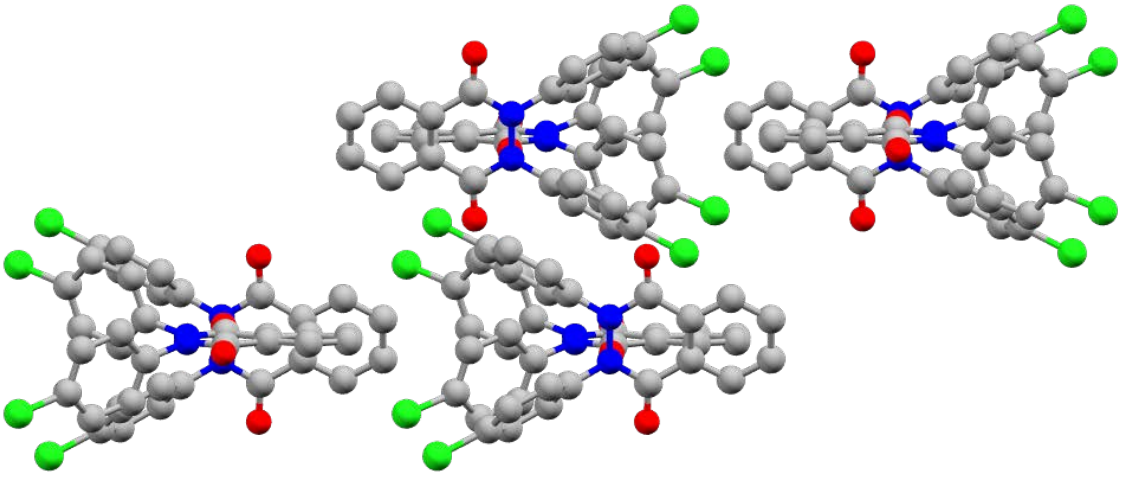

Figure 5: Packing of 2d in the solid state.

Cyclovoltammetric data

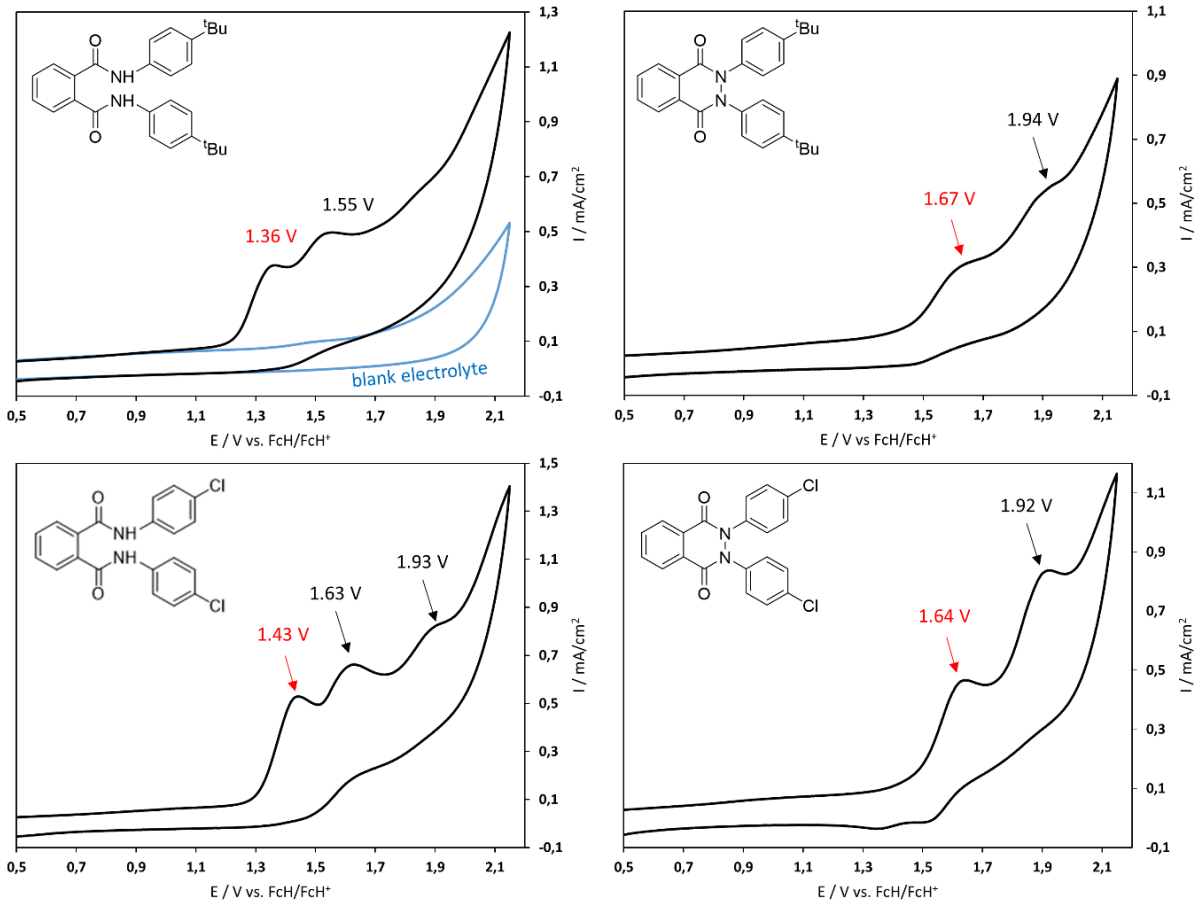

Figure 6: Cyclic voltammogramms of four selected examples. 1 mM substrate in 0.1 M NBu_4PF_6 in HFIP; Working electrode: glassy carbon; reference electrode: Ag/AgCl in sat. LiCl/EtOH; counter electrode: glassy carbon; scan rate: 200 mV/s

NMR spectra

N,N'-Di(4-methylphenyl)phthaldiamide (1a)

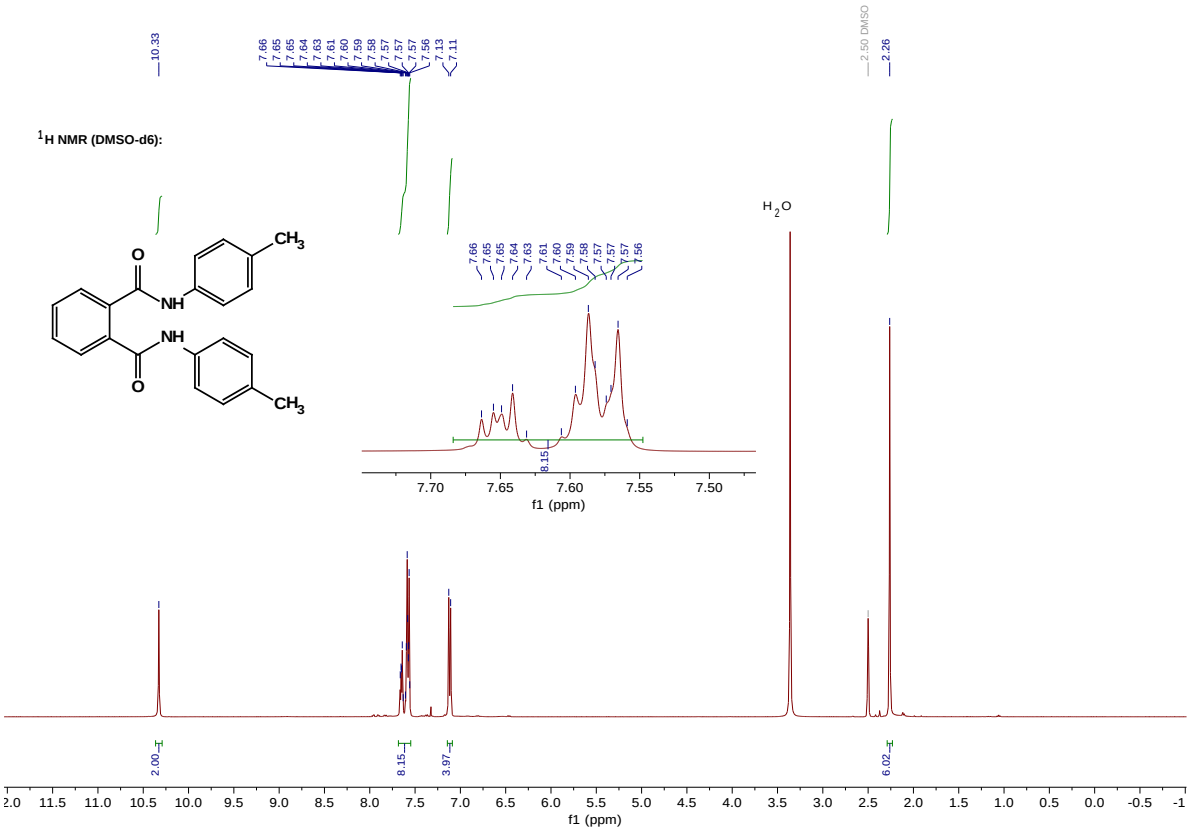

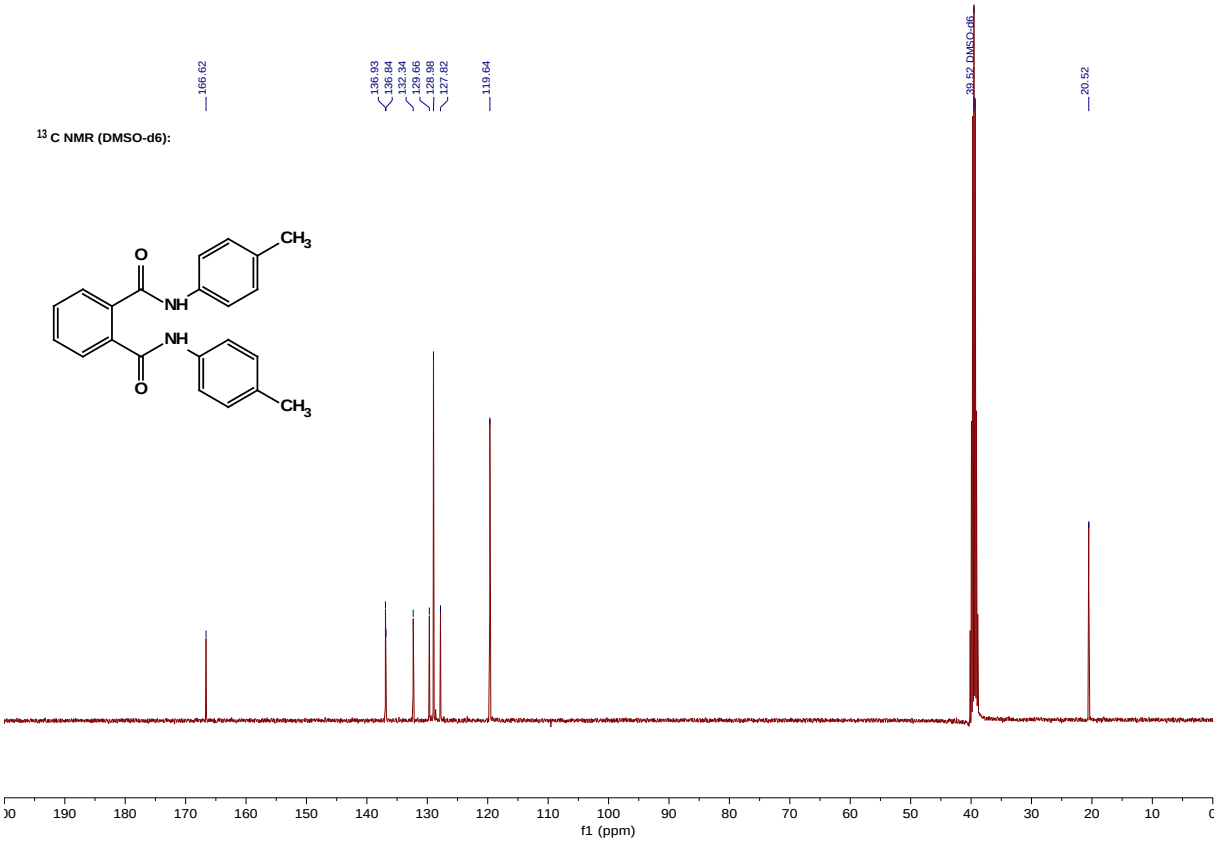

N,N'-Bis(4-(1,1-dimethylethyl)phenyl)phthaldiamide (1b)

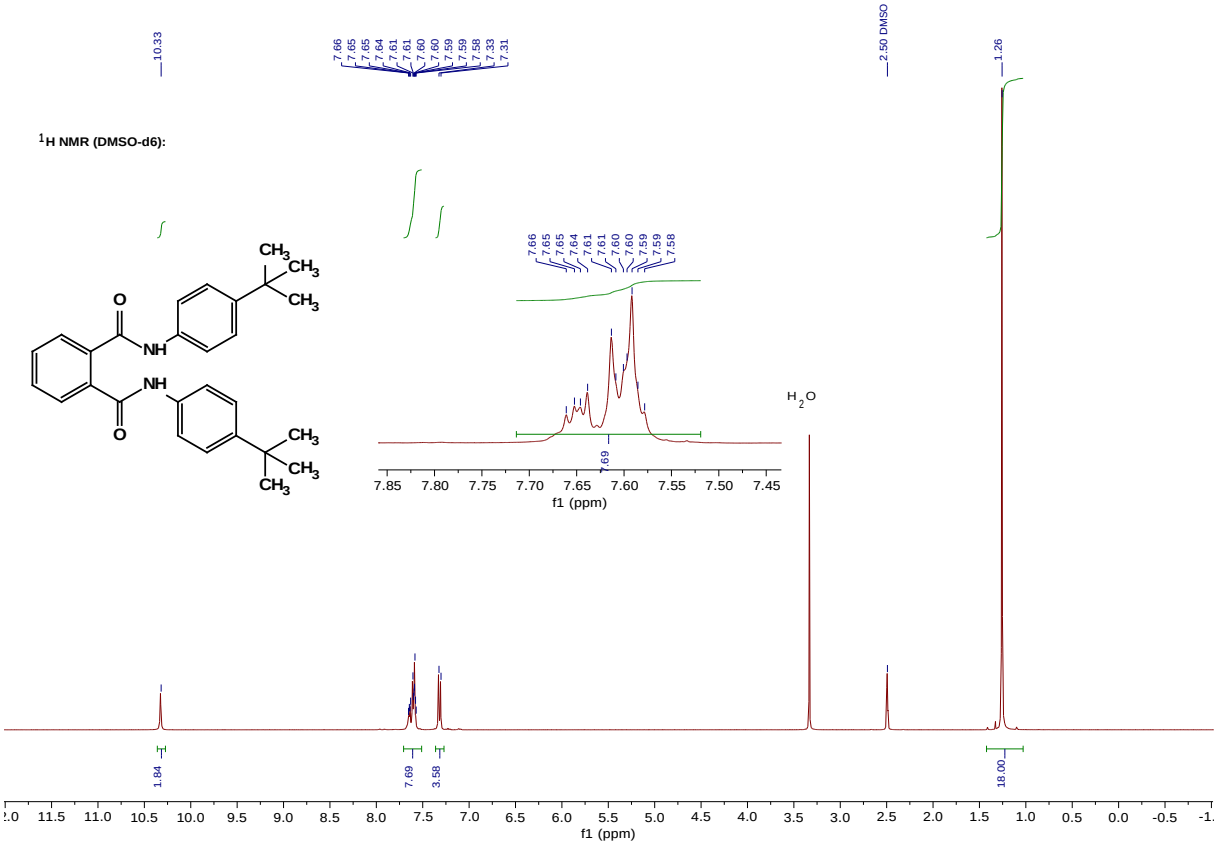

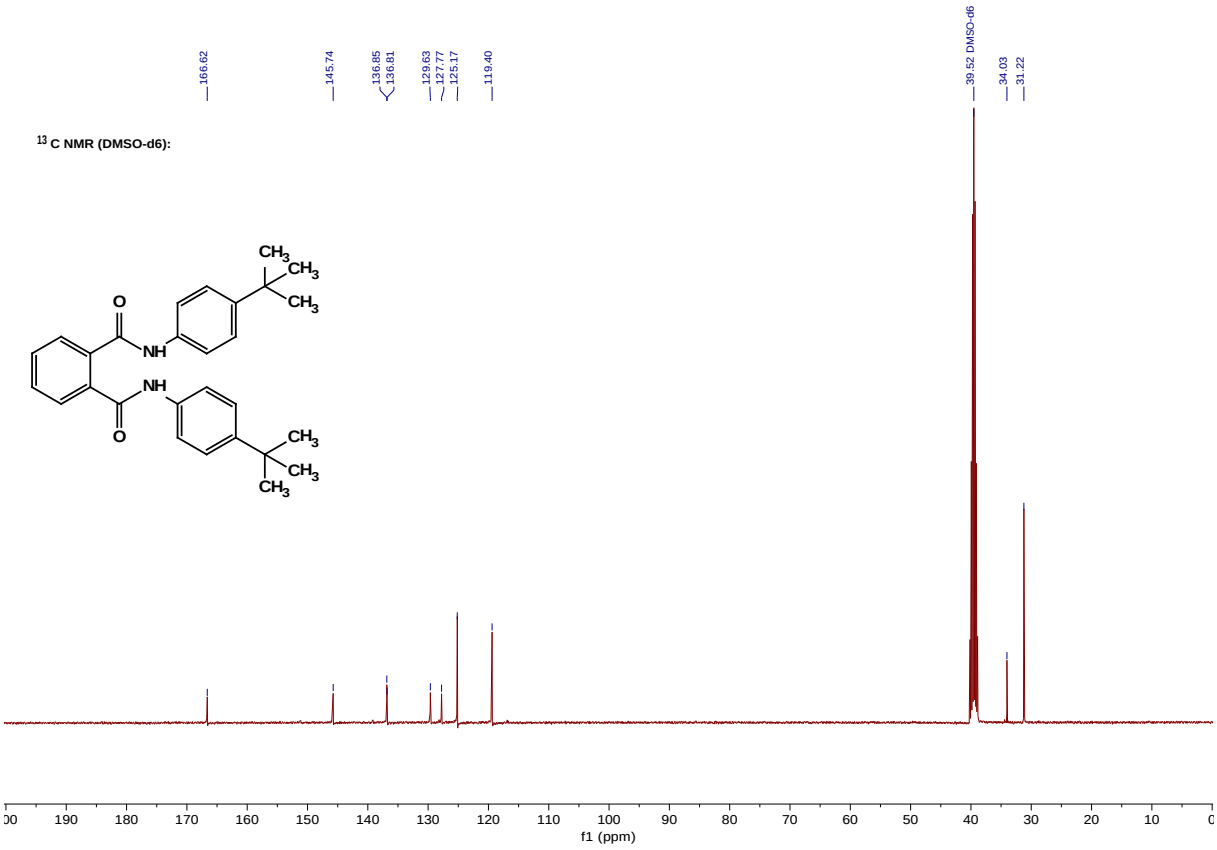

N,N'-Bis(3-(1,1-dimethylethyl)phenyl)phthaldiamide (1c)

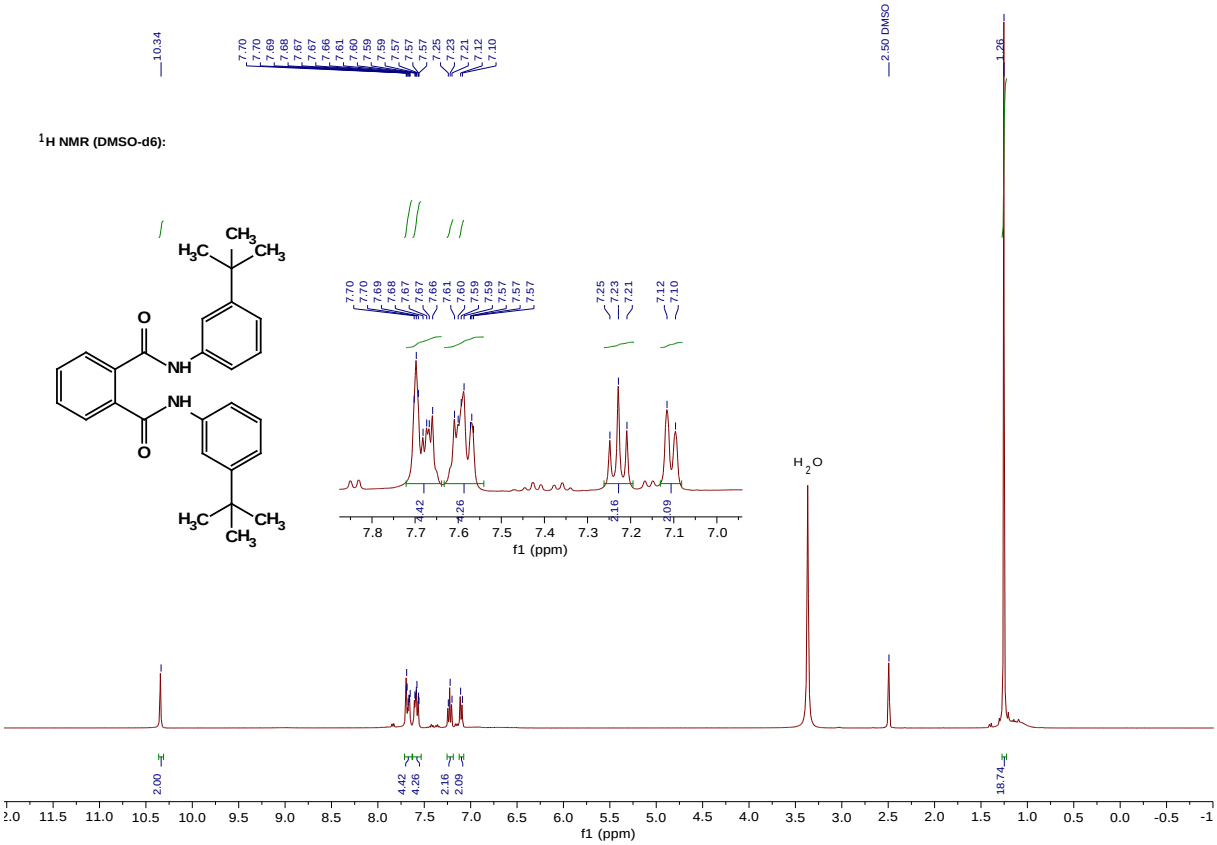

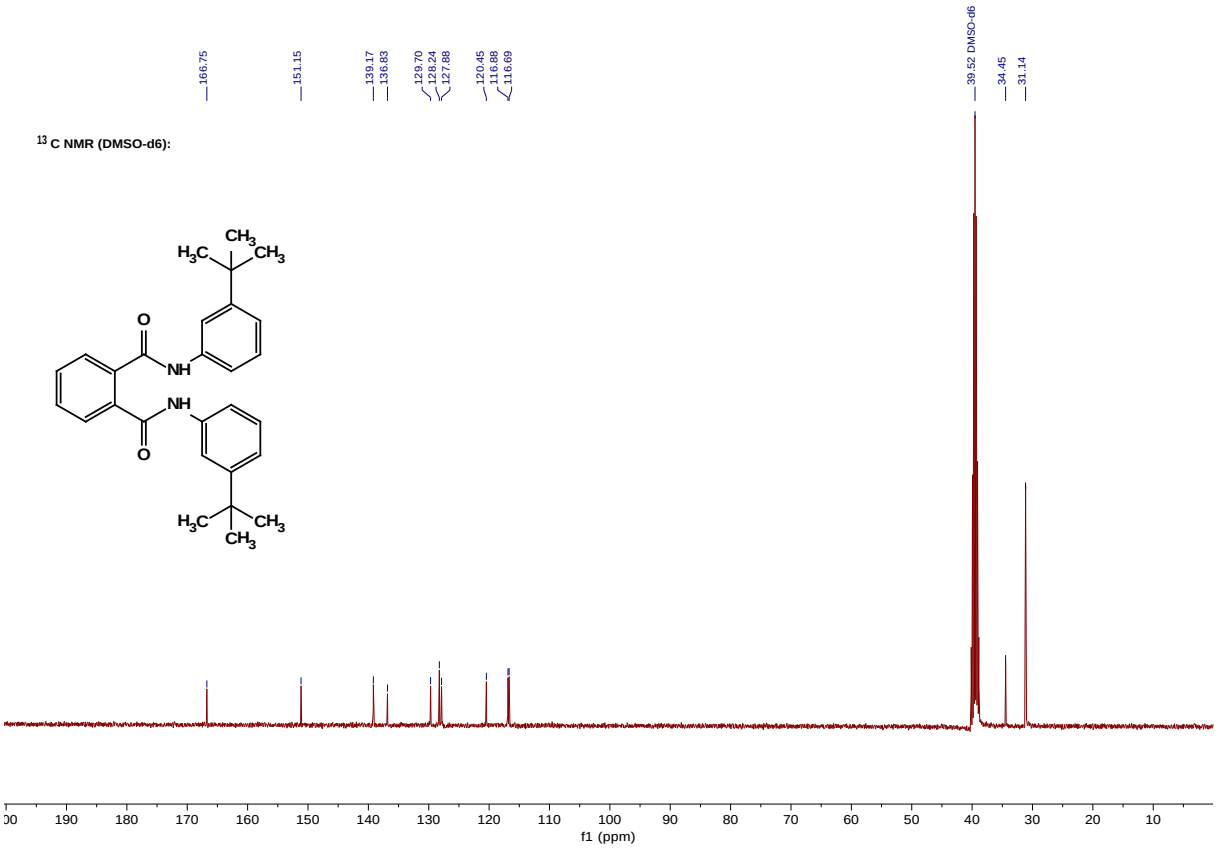

N,N'-Di(4-chlorophenyl)phthaldiamide (1d)

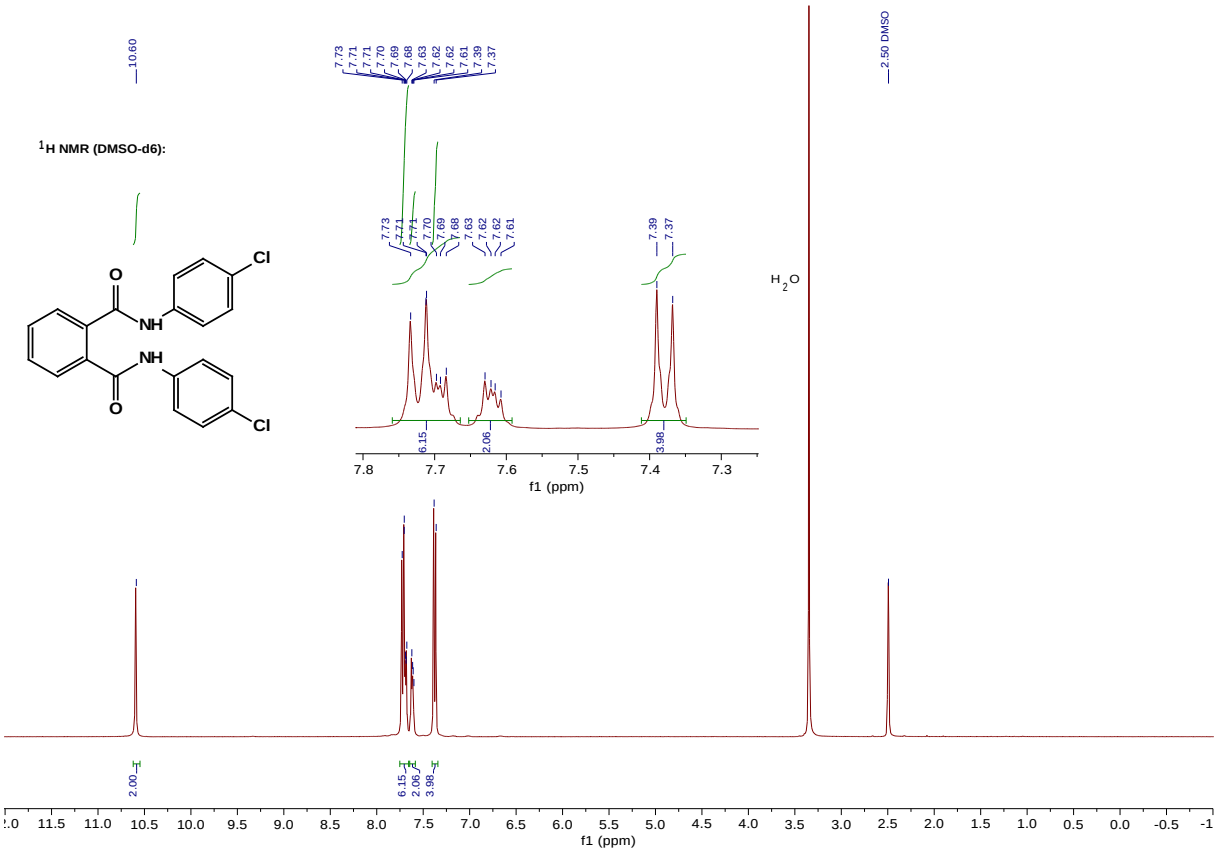

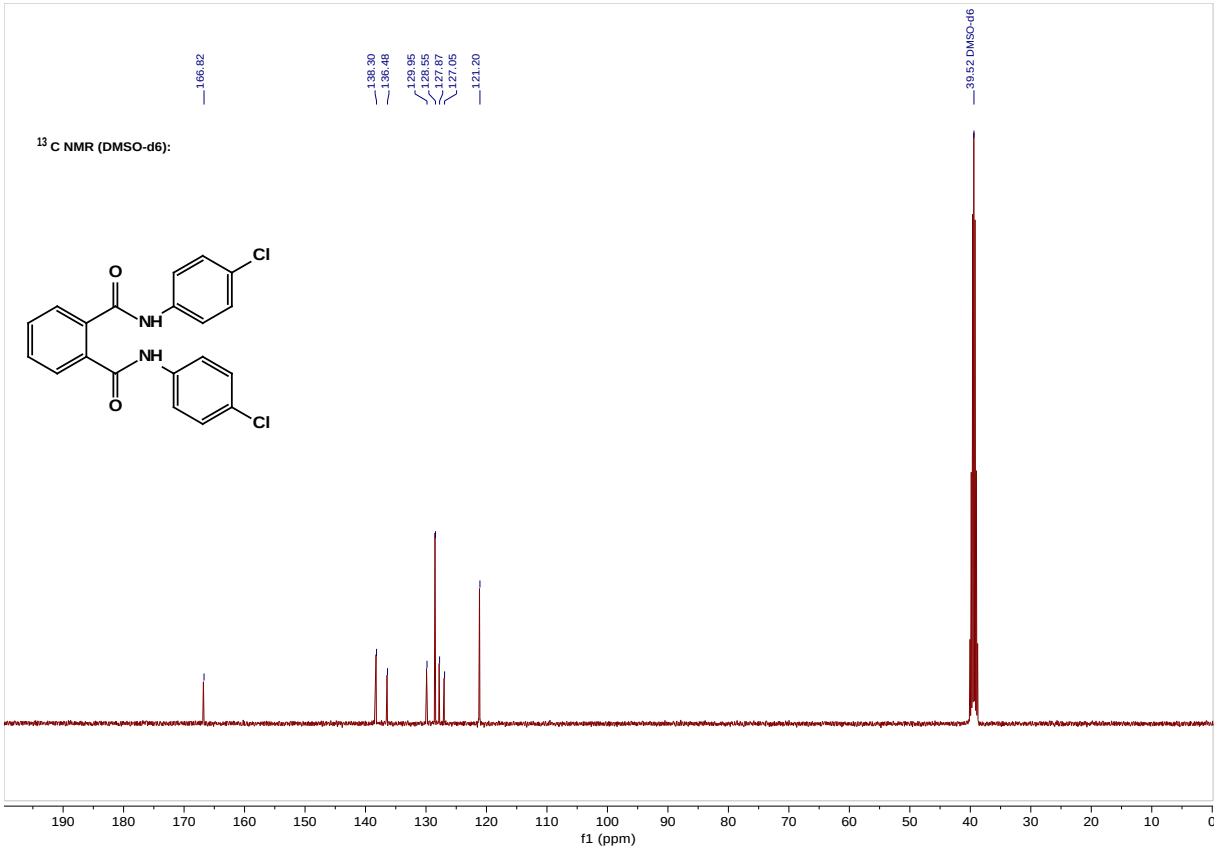

N,N'-Di(4-fluorophenyl)phthaldiamide (1e)

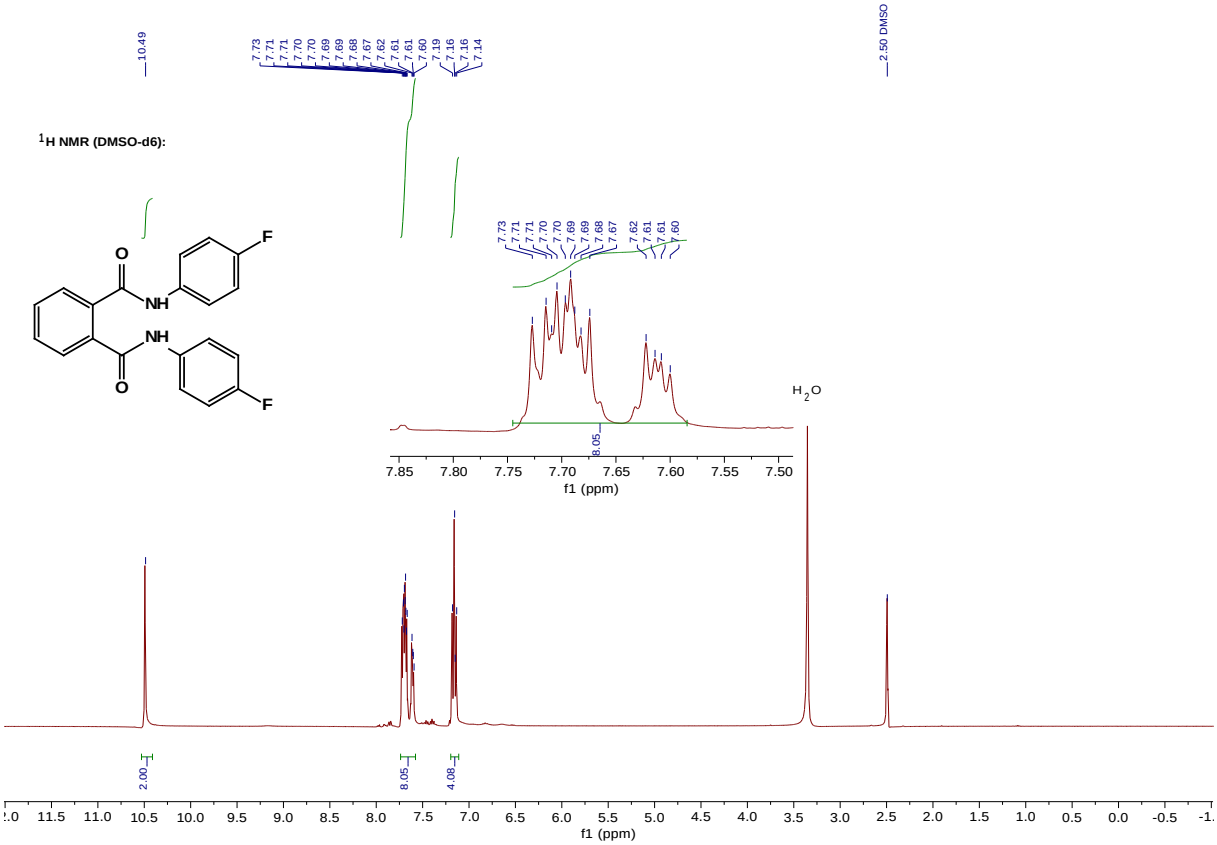

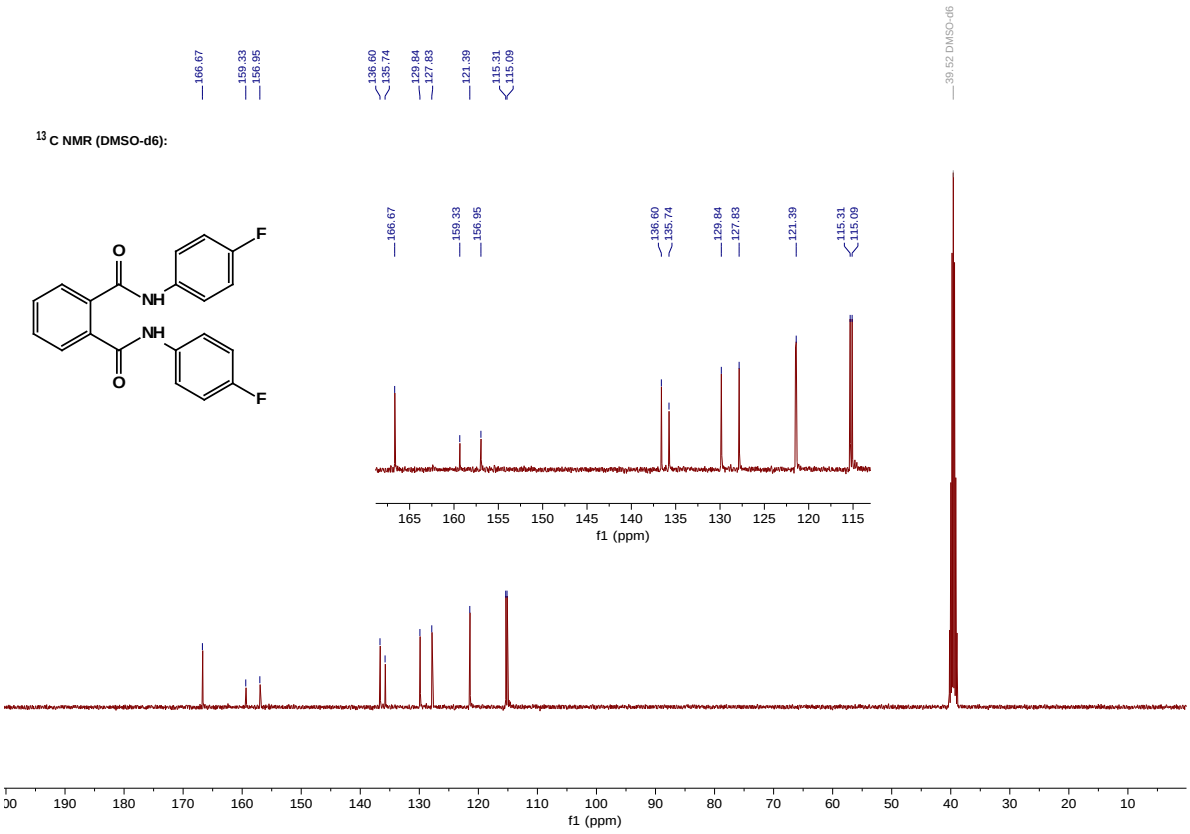

^{19}F NMR (DMSO-d6):

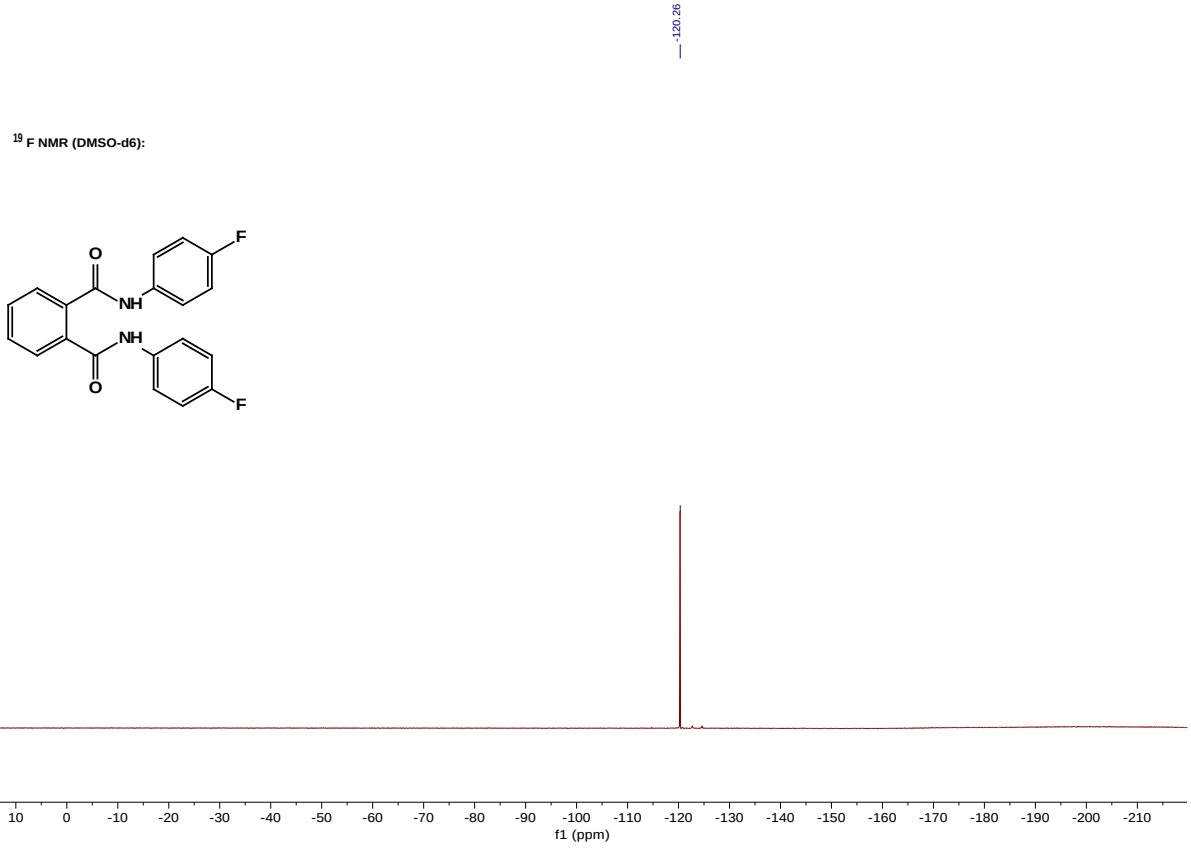

N,N'-Bis(2,4-difluorophenyl)phthaldiamide (1f)

^{1}H NMR (DMSO-d6):

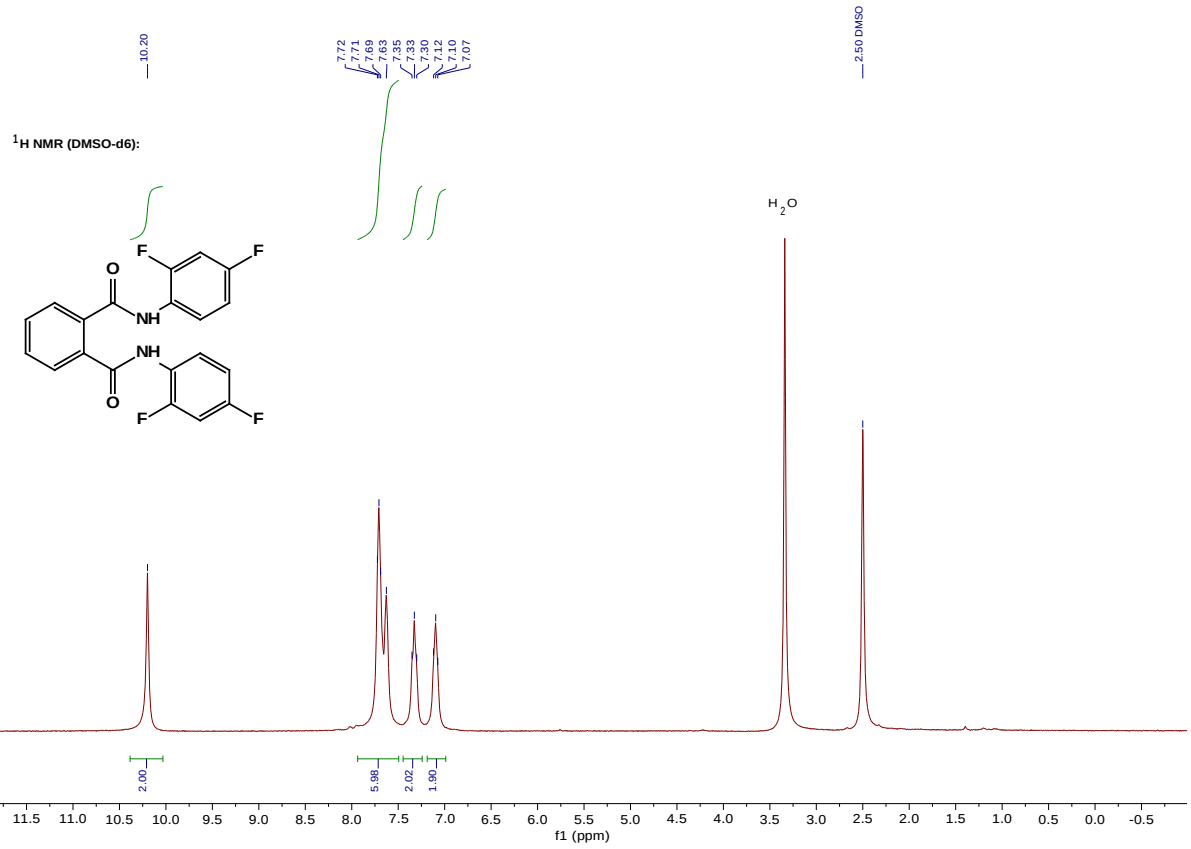

^{13}C NMR (DMSO-d6):

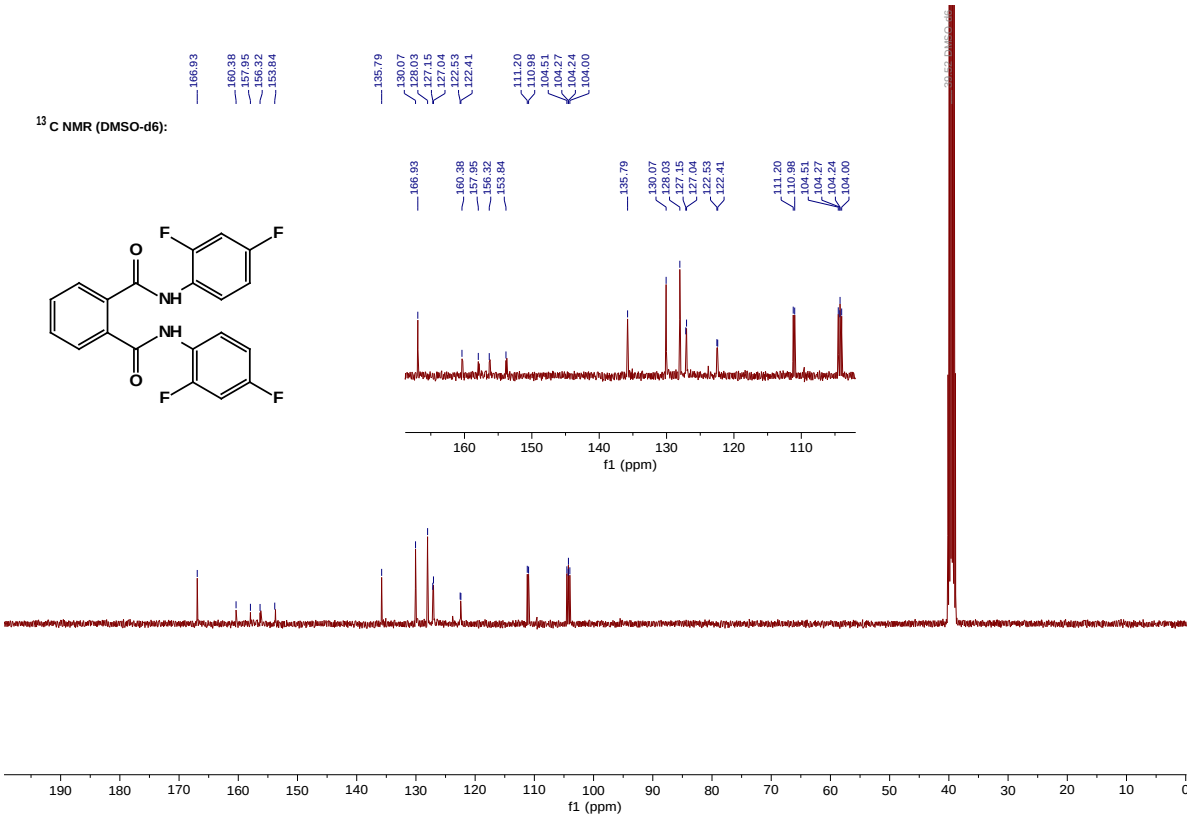

^{19}F NMR (DMSO-d6):

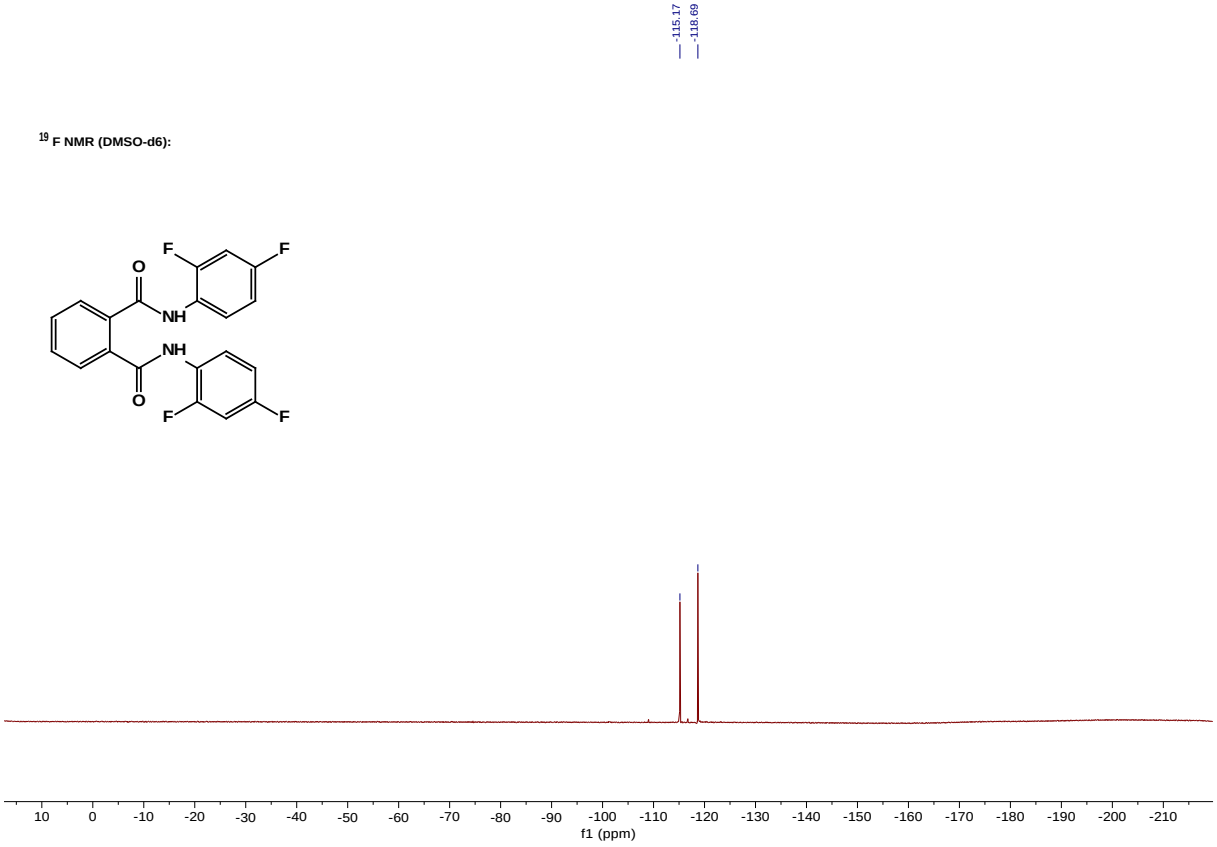

N,N'-Di(4-methoxyphenyl)phthaldiamide (1g)

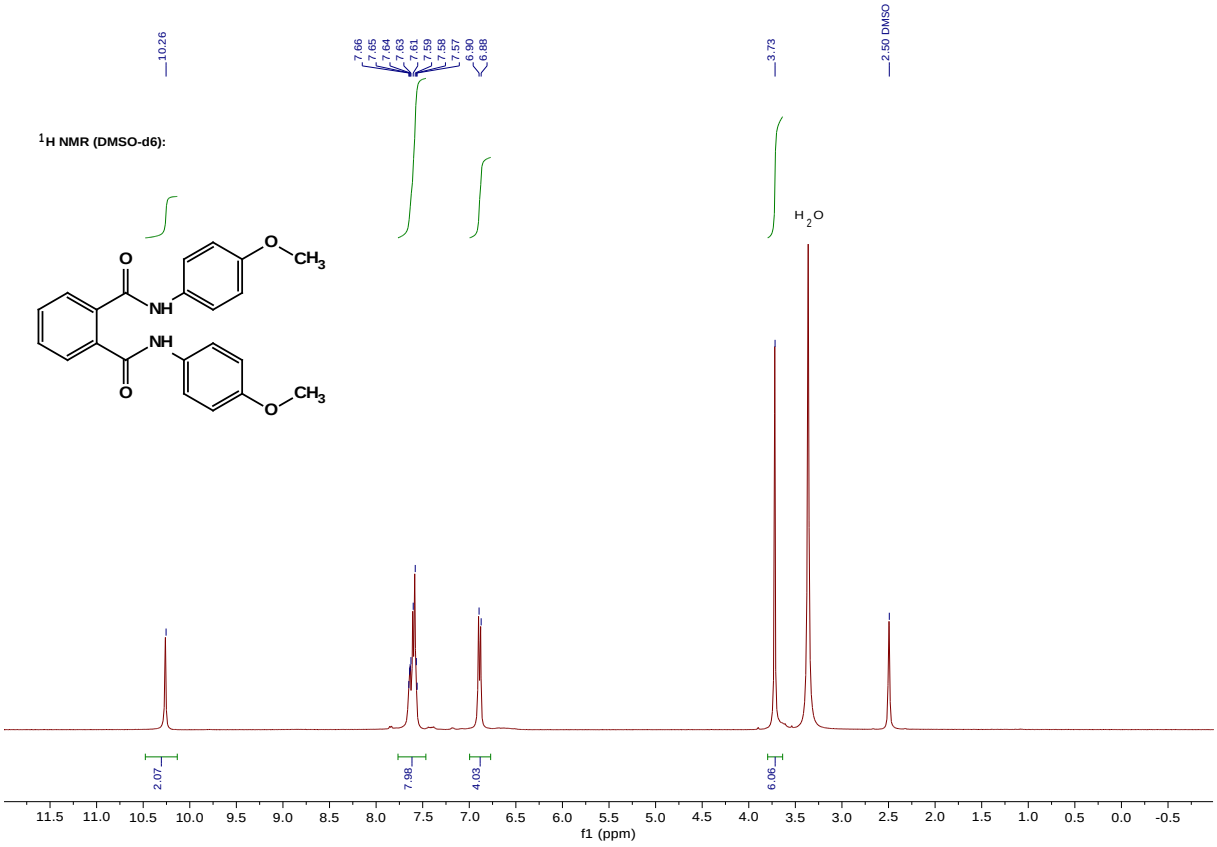

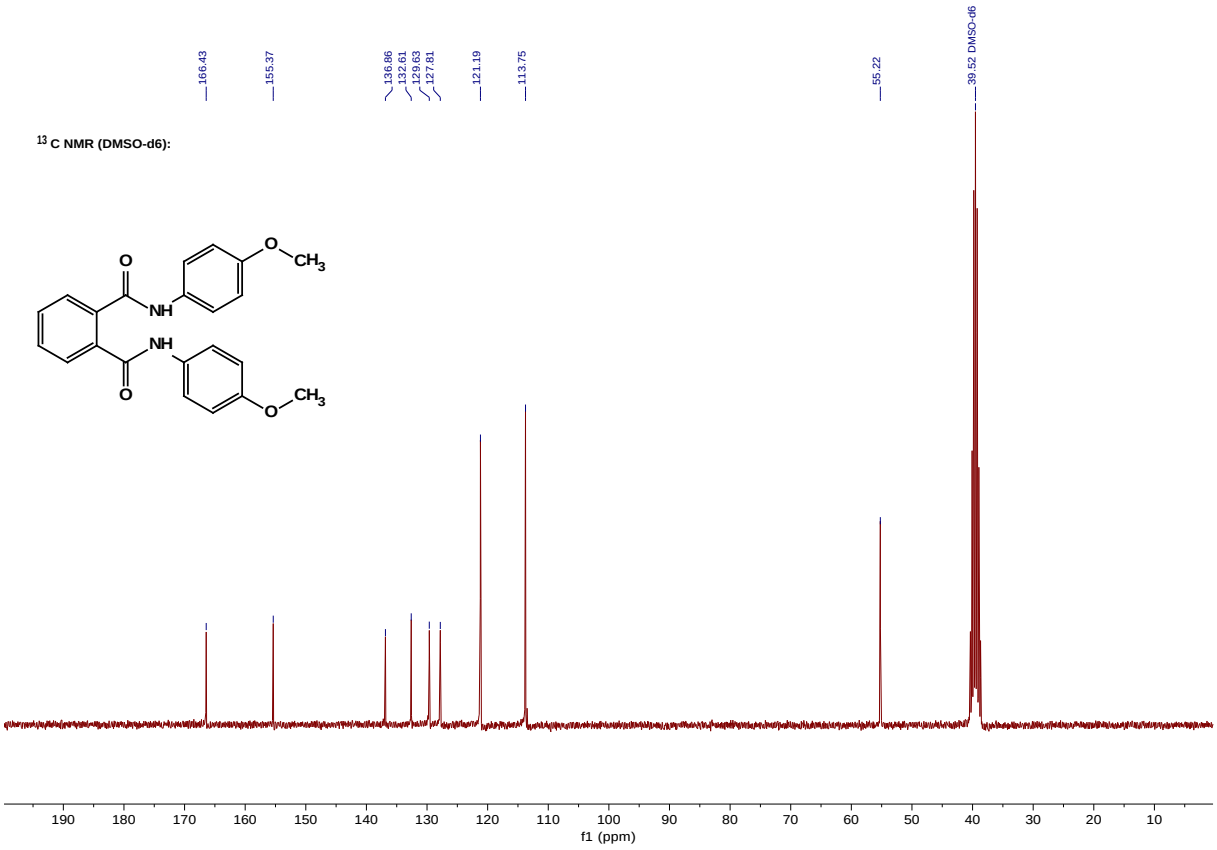

N-(4-Chlorophenyl)-*N*‘-(4-methylphenyl)phthaldiamide (1h)

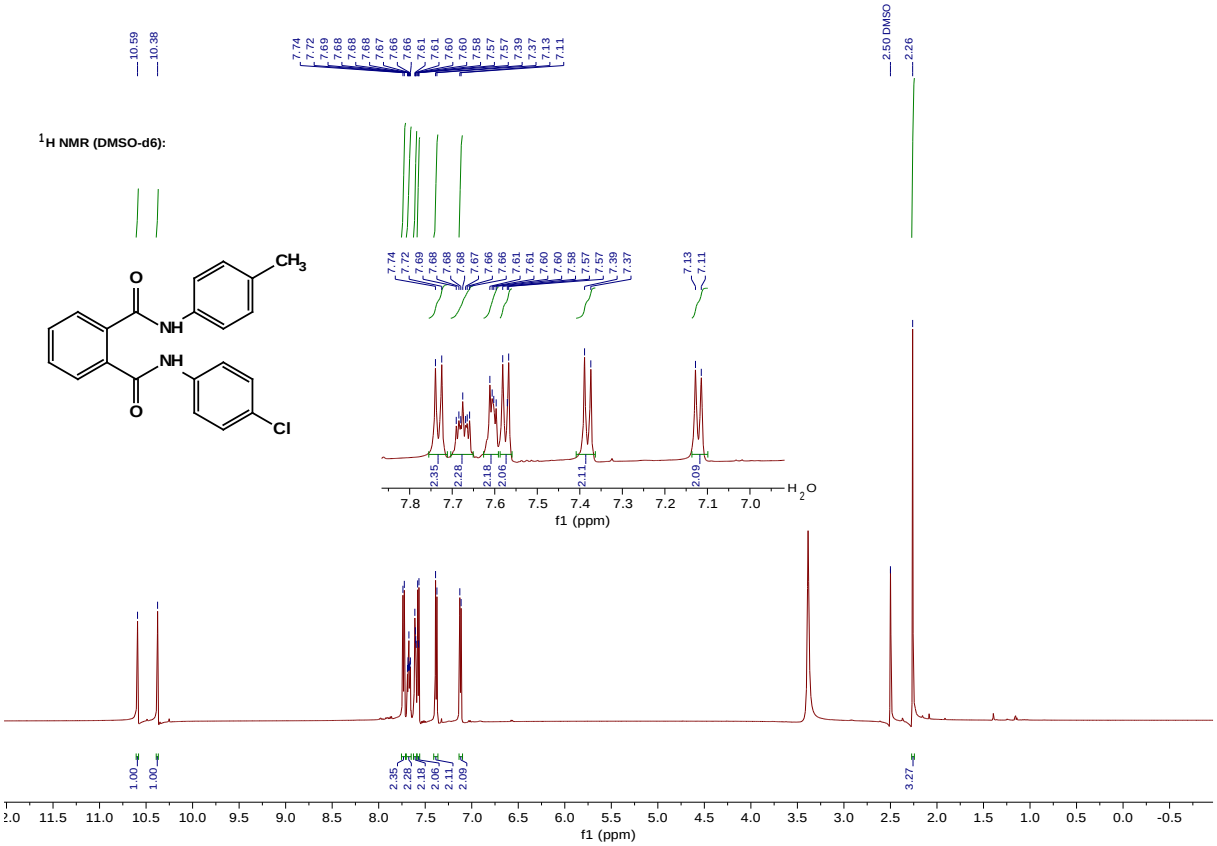

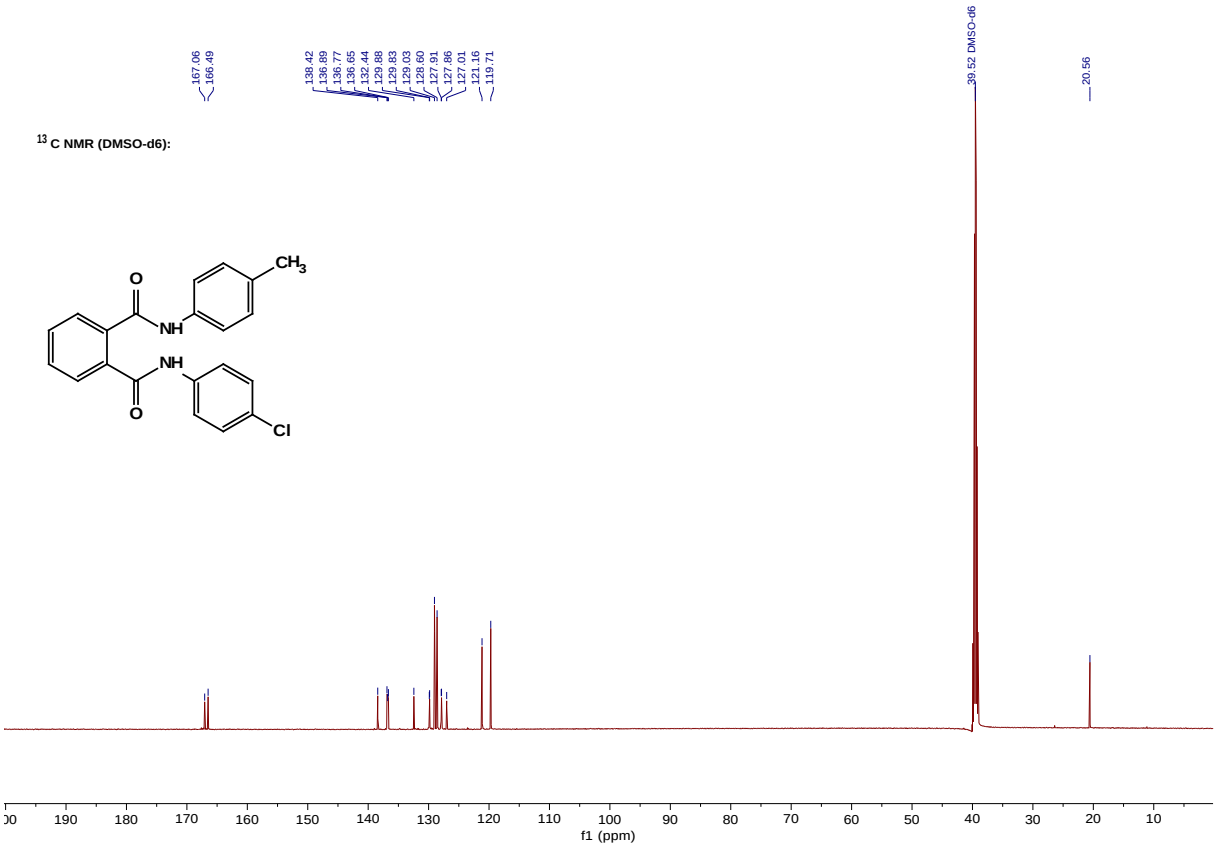

N-(4-Chlorophenyl)-*N'*-(4-trifluoromethylsulfonyloxyphenyl)phthaldiamide (1i)

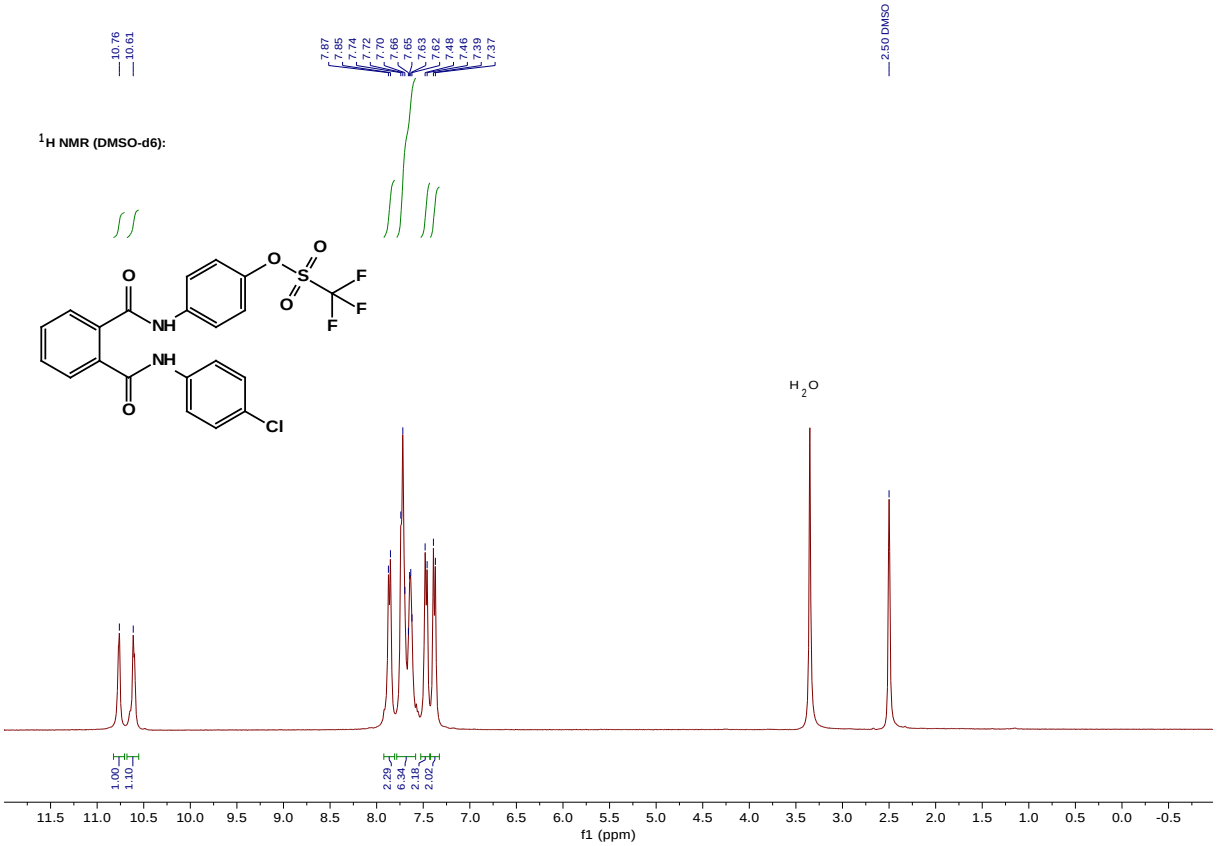

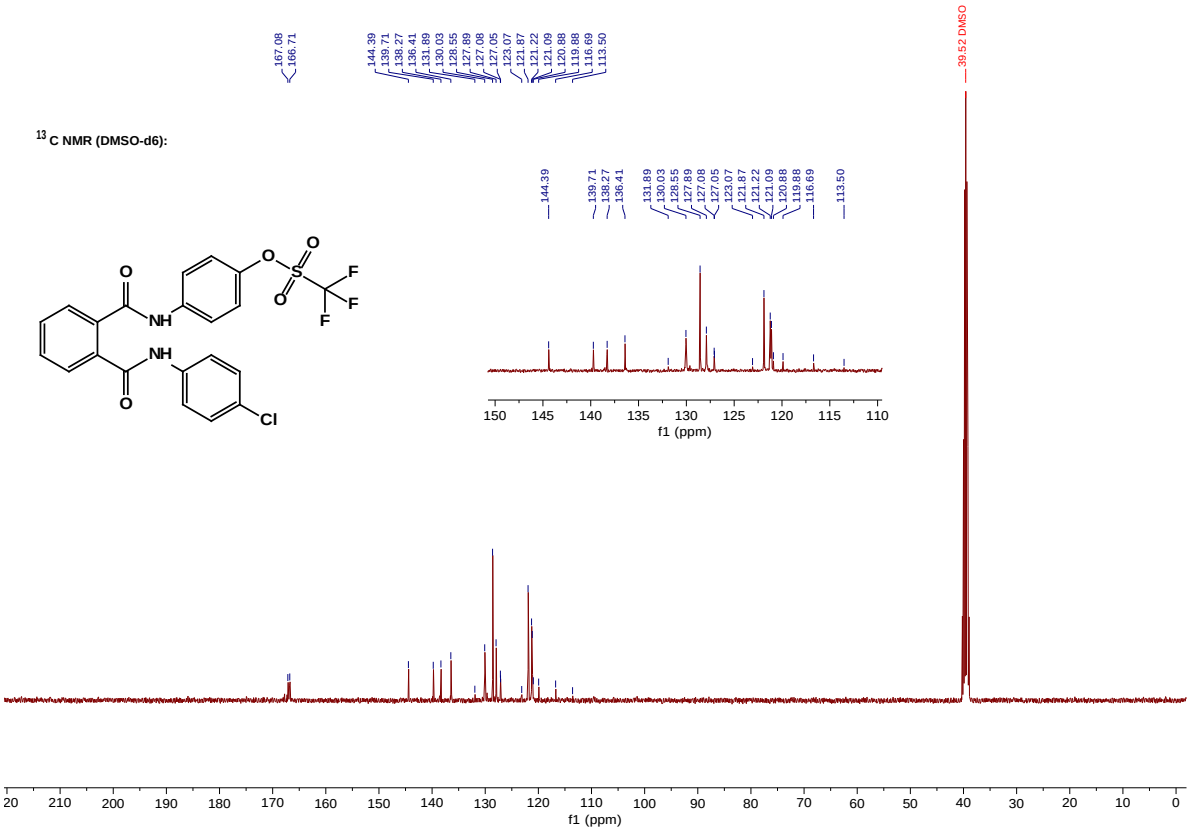

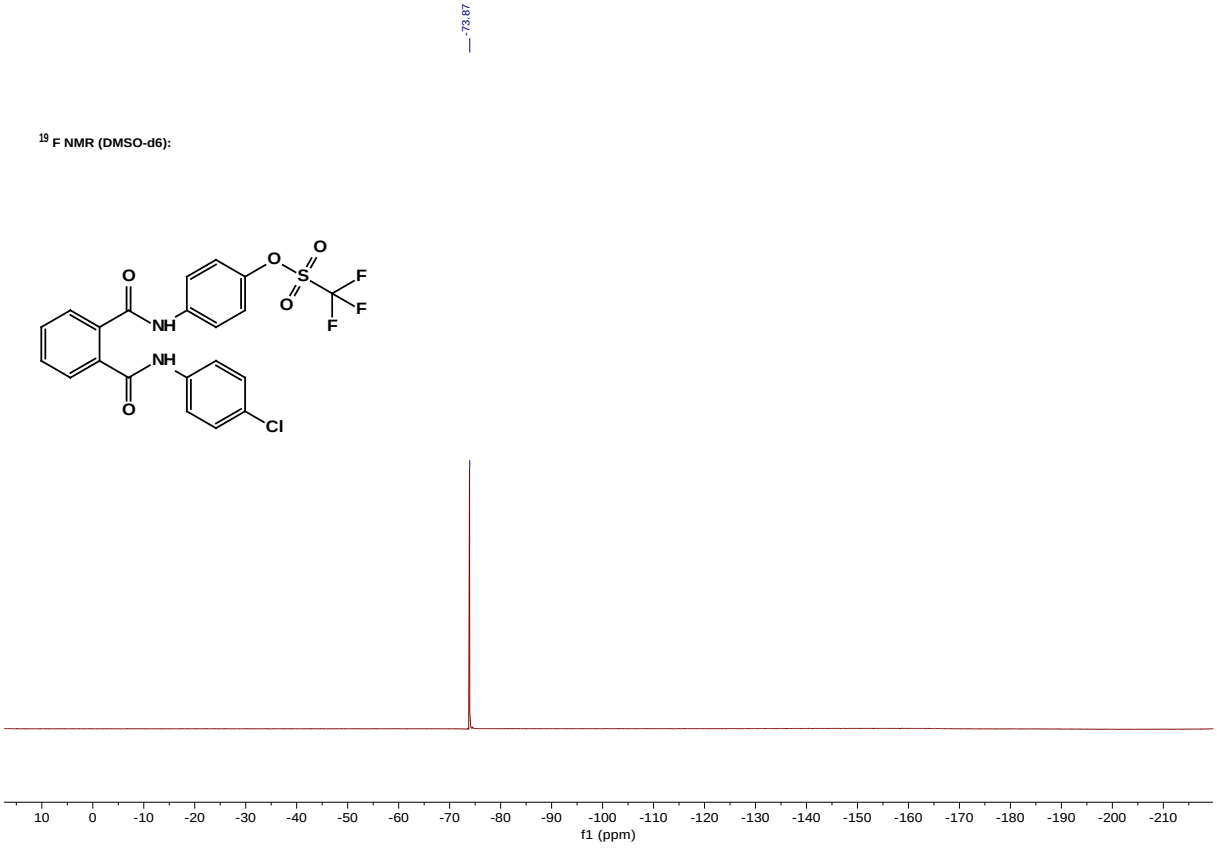

N-(3-Bromo-4-methylphenyl)-*N'*-(4-chlorophenyl)phthaldiamide (1j)

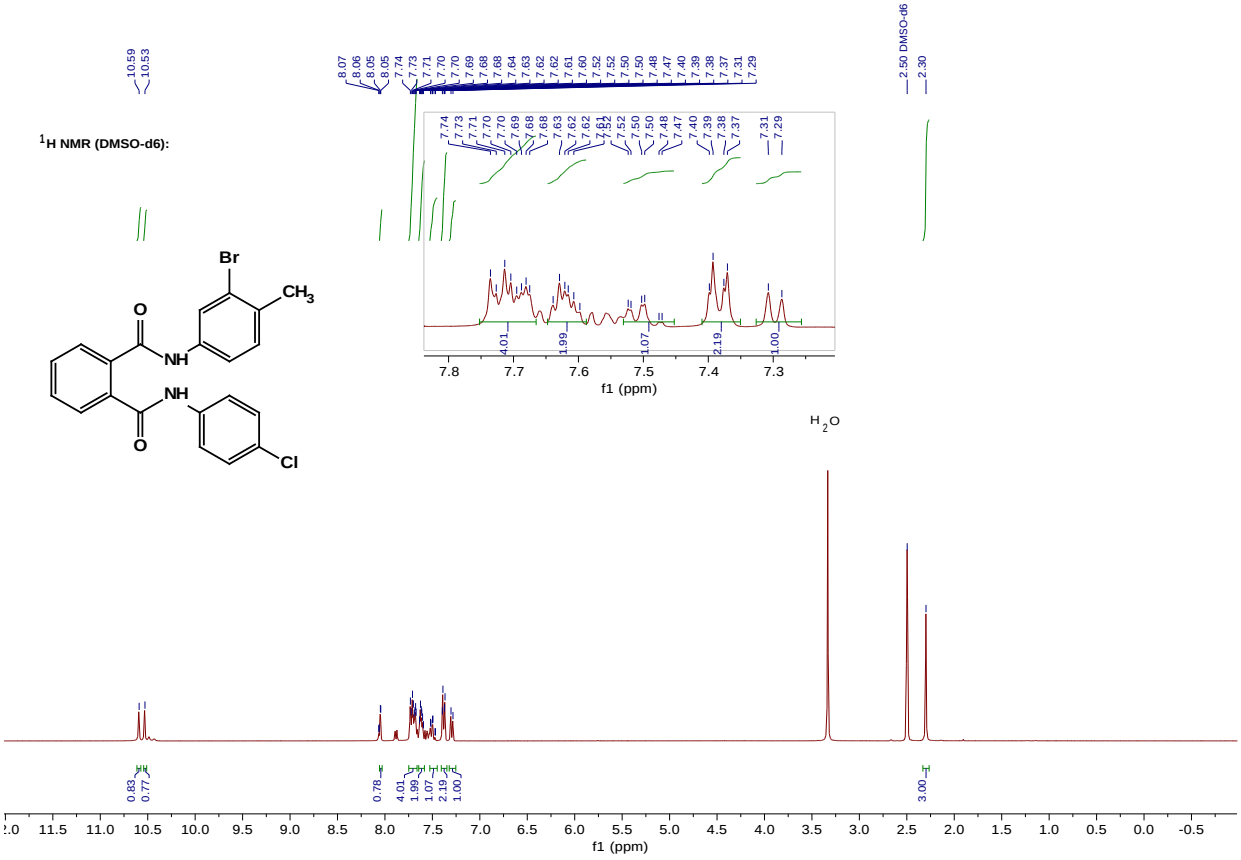

^{13}C NMR (DMSO-d6):

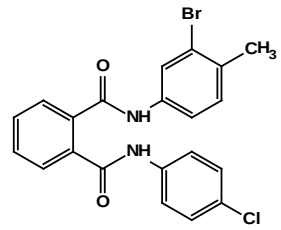

N-(3-Bromo-4-methylphenyl)-*N'*-(4-methylphenyl)phthaldiamide (1k)

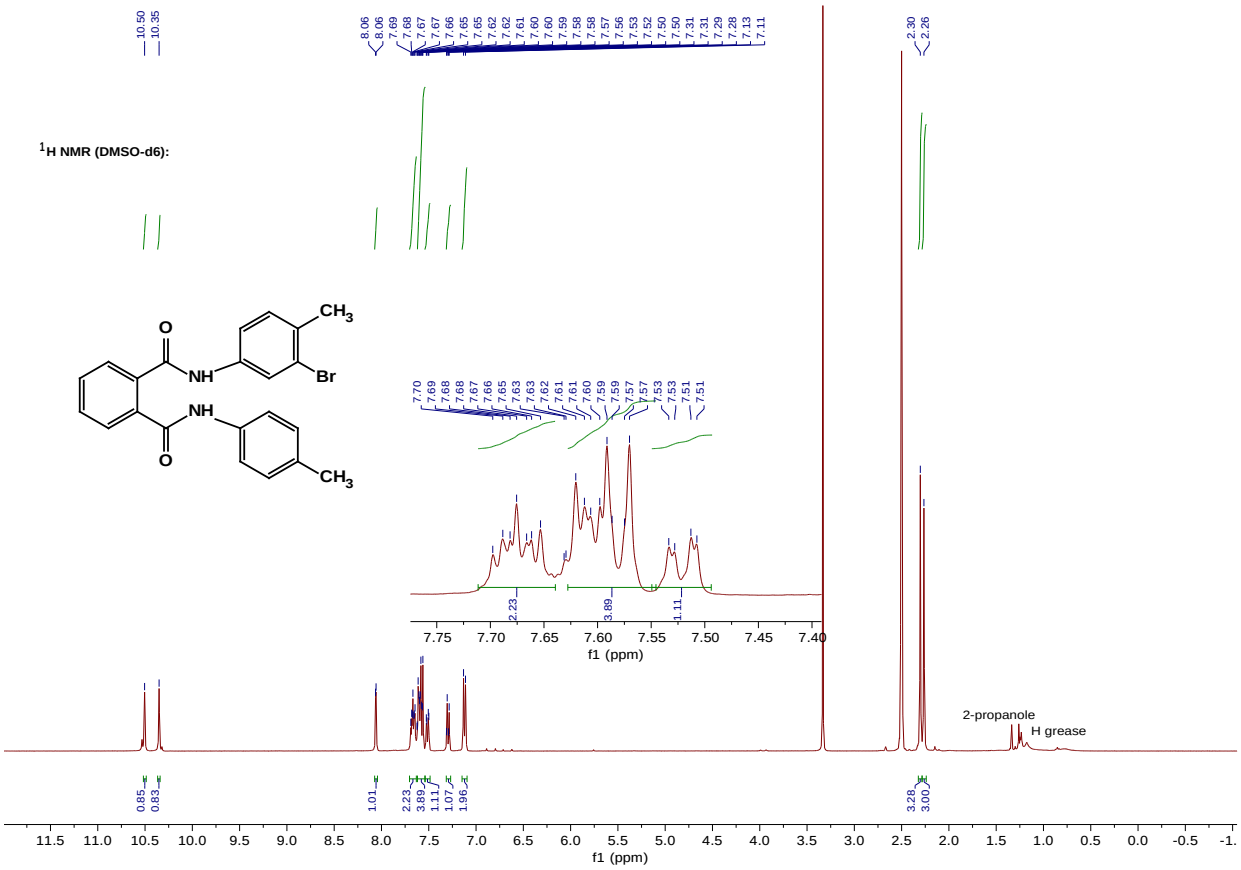

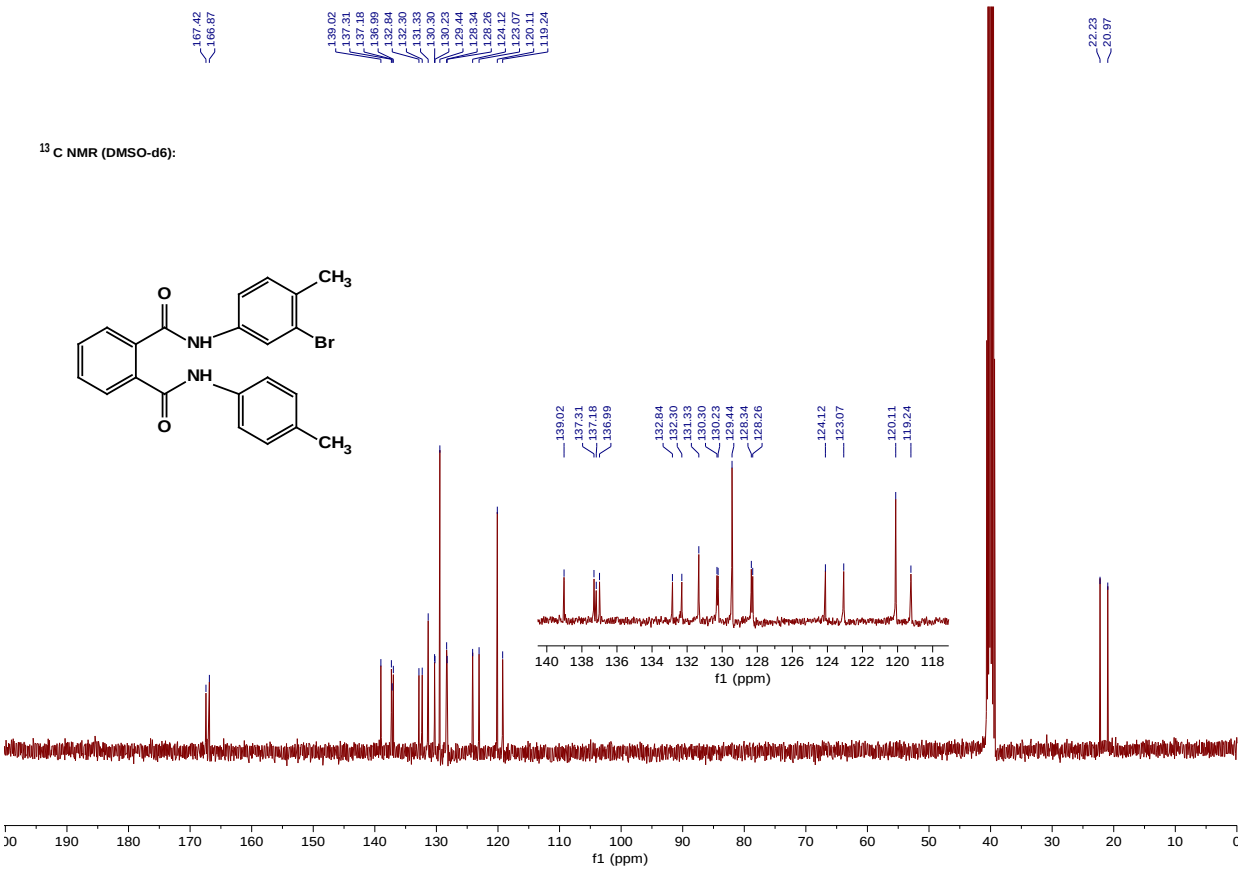

N-(4-Chlorophenyl)-*N'*-(3-cyano-4-methylphenyl)phthaldiamide (1l)

^{1}H NMR (DMSO-d6):

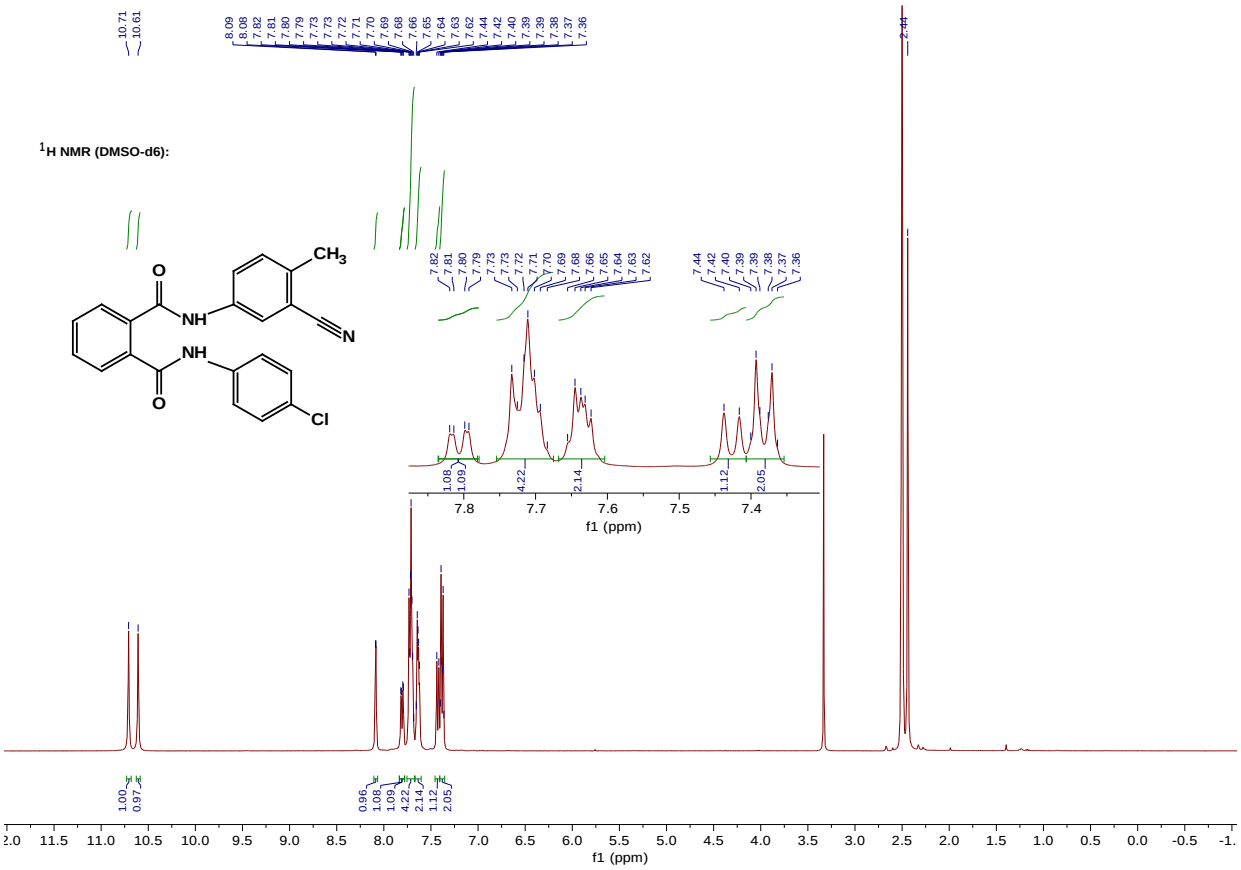

^{13}C NMR (DMSO-d6):

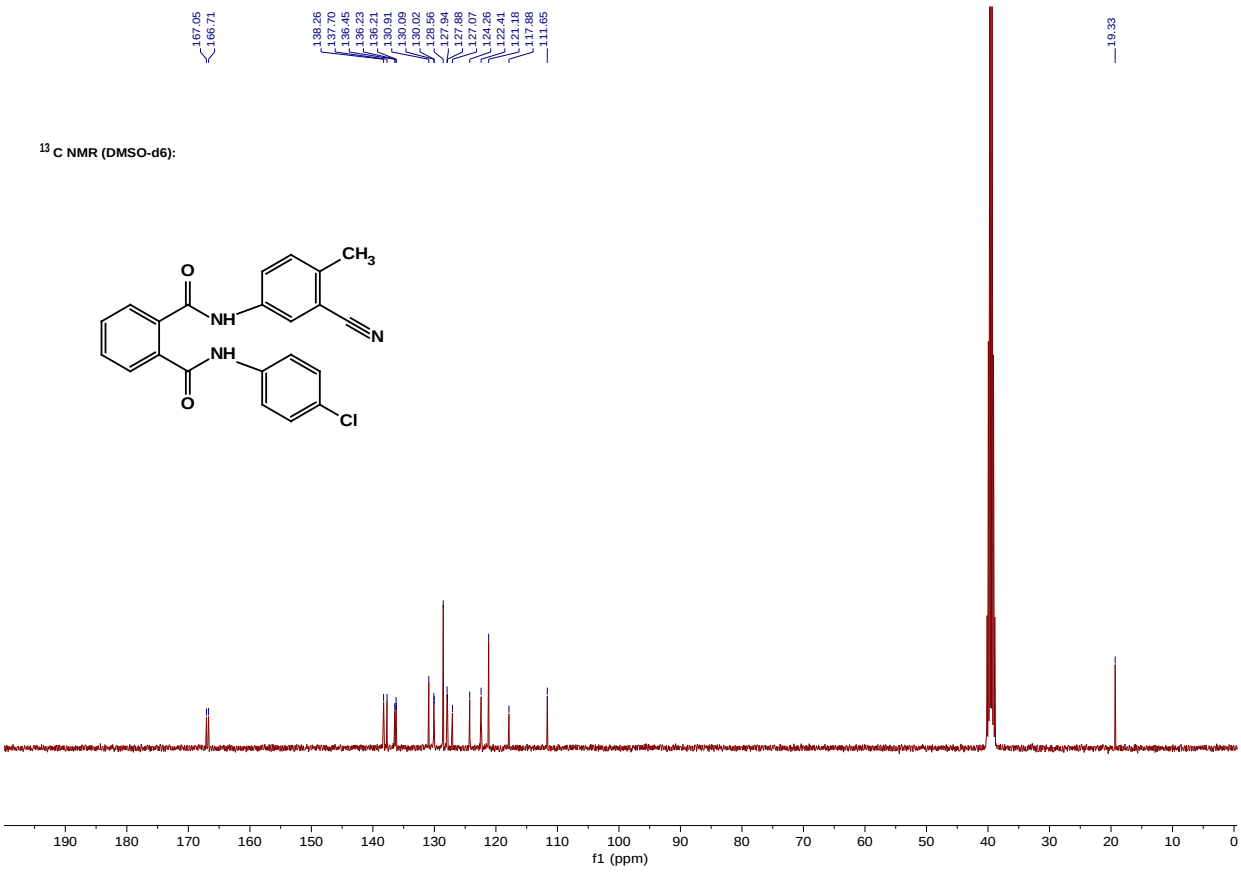

N,*N'*-Di(4-chlorophenyl)-pyridine-3,4-diamide (1m)

^{1}H NMR (DMSO-d6):

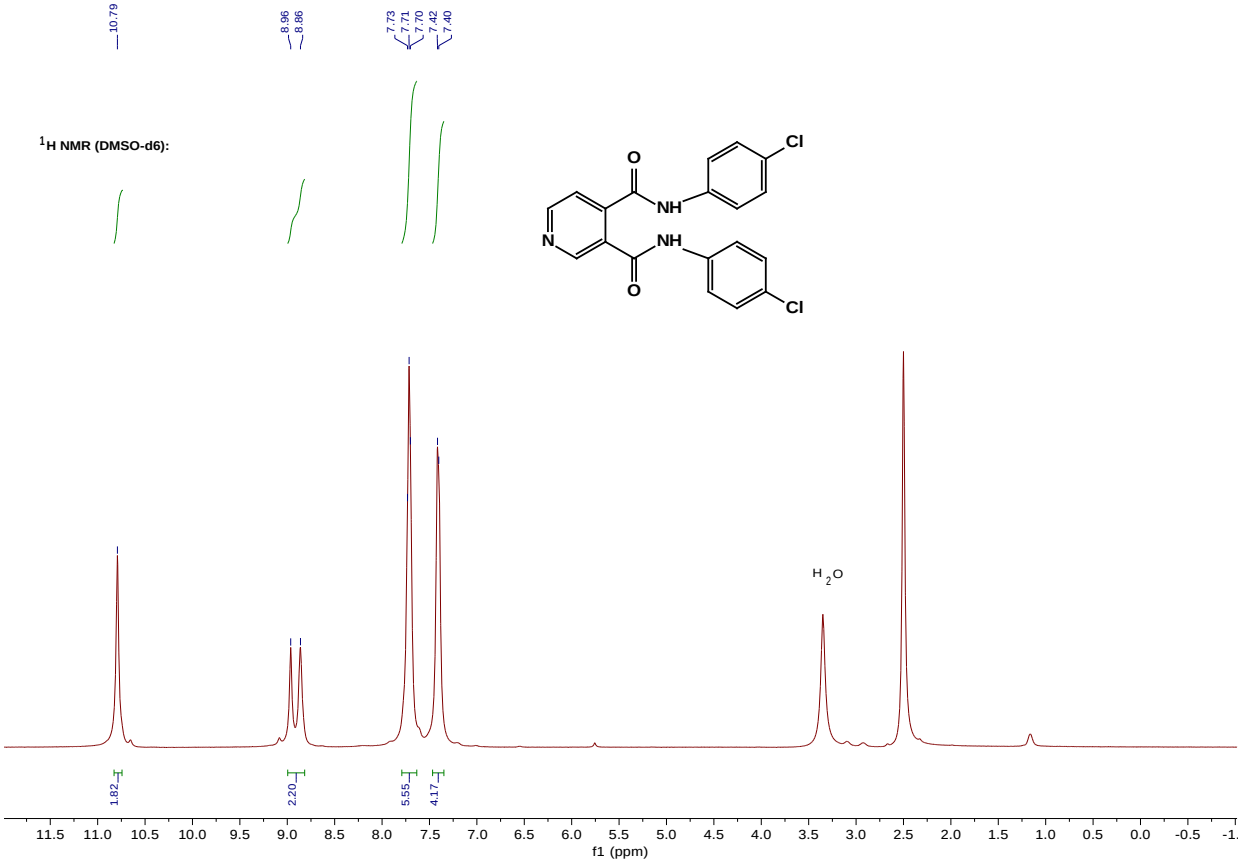

^{13}C NMR (DMSO-d6):

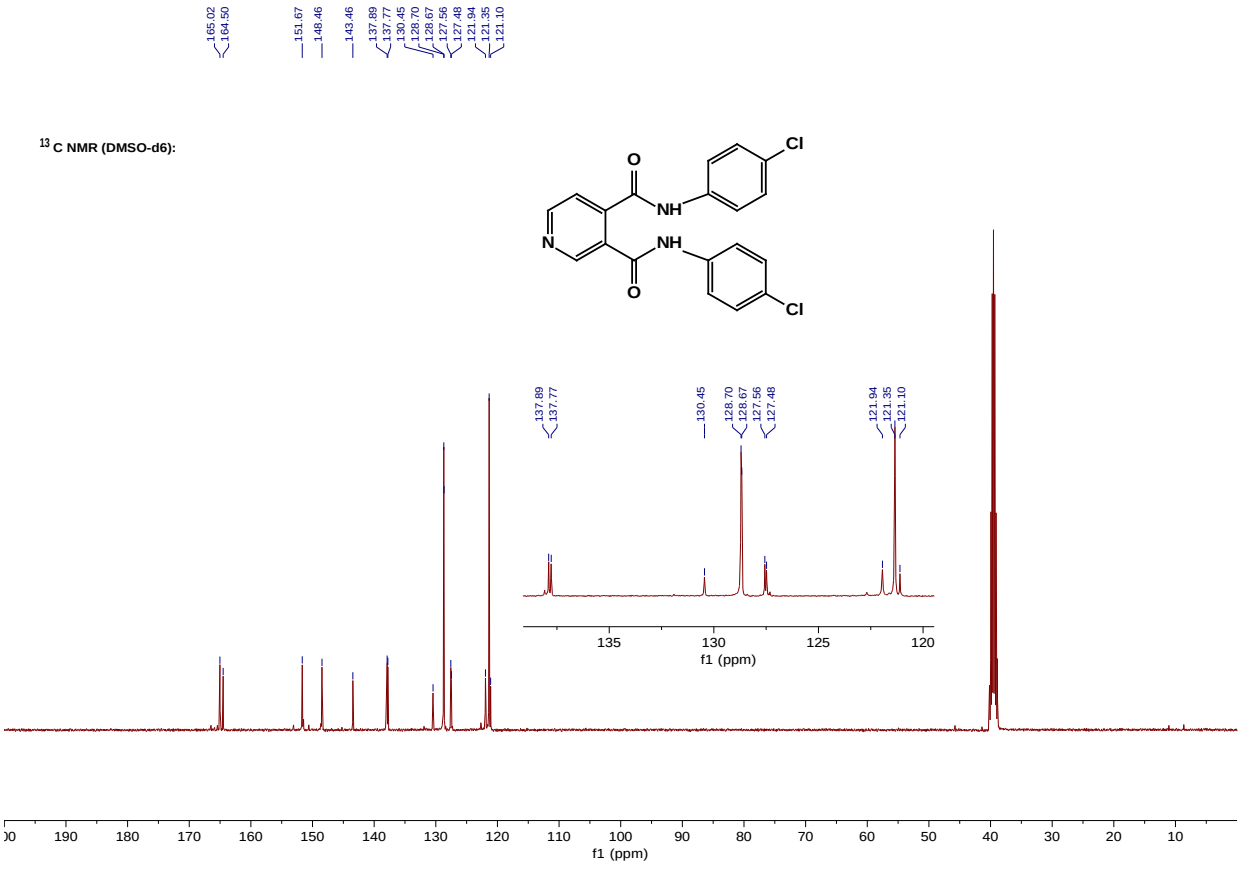

4-Bromo-*N*,*N'*-di(4-chlorophenyl)phthaldiamide (1n)

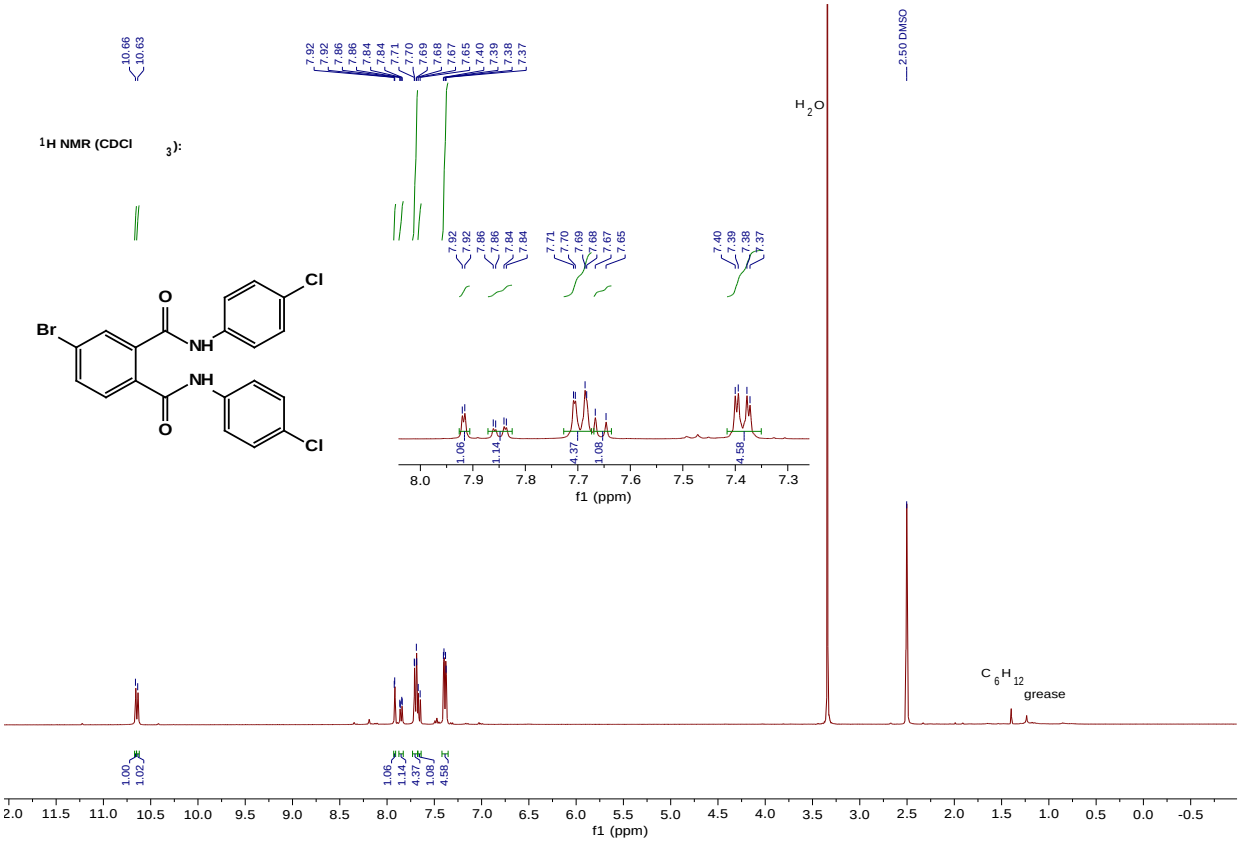

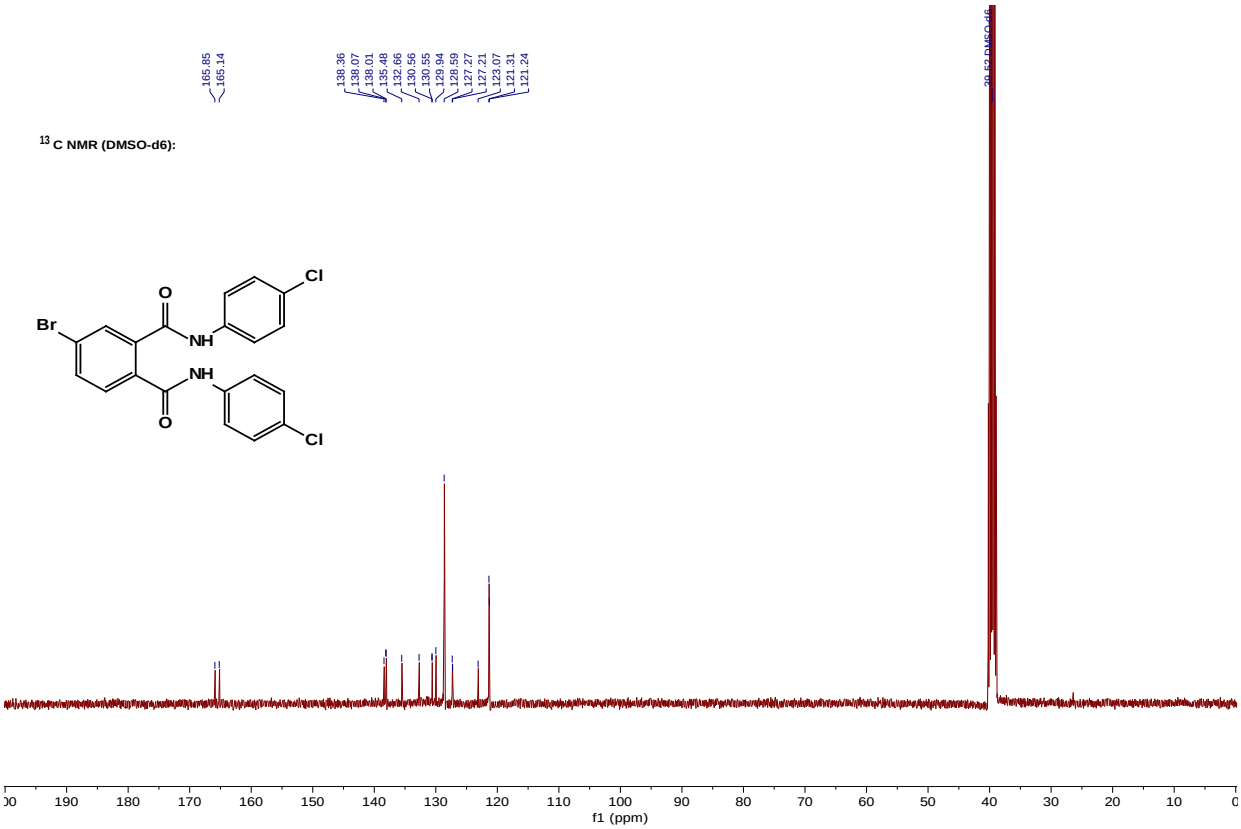

N,*N'*-Di(4-chlorophenyl)-4-methyl-phthaldiamide (1o)

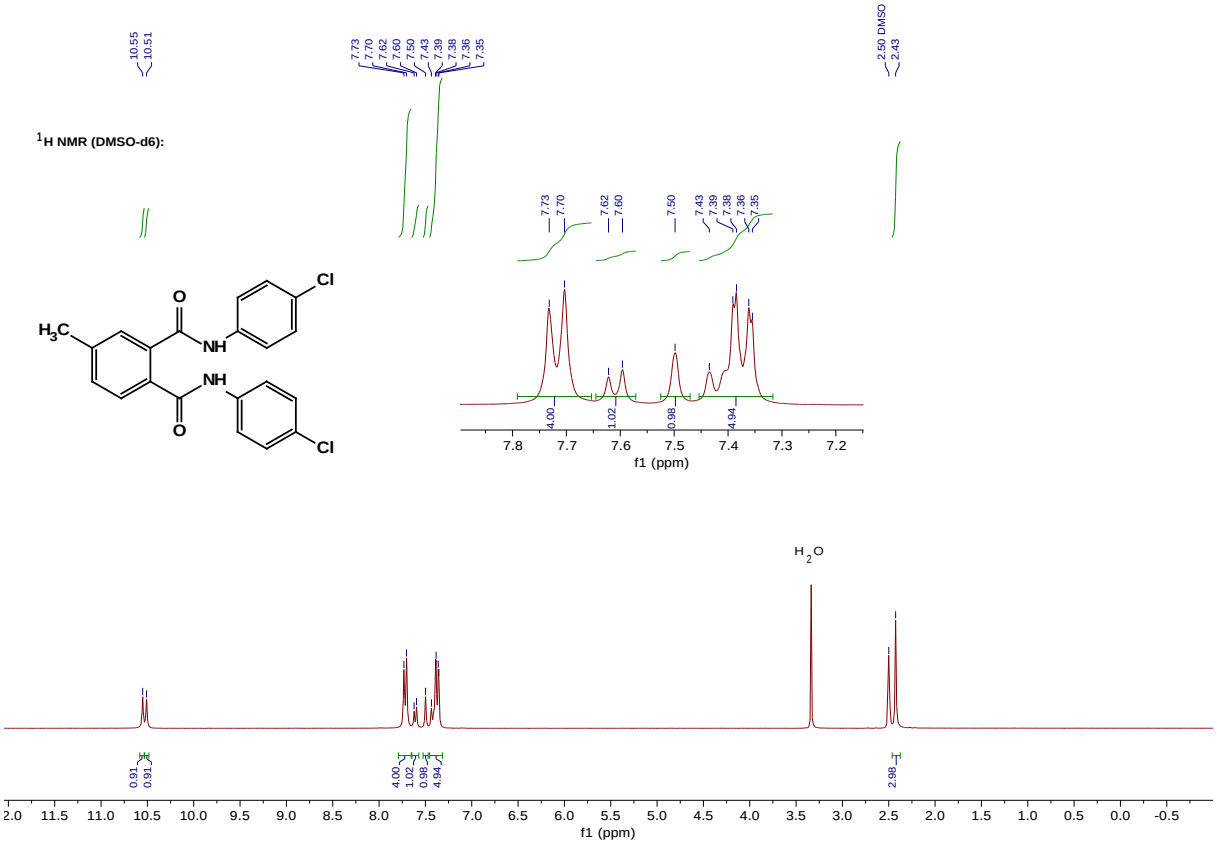

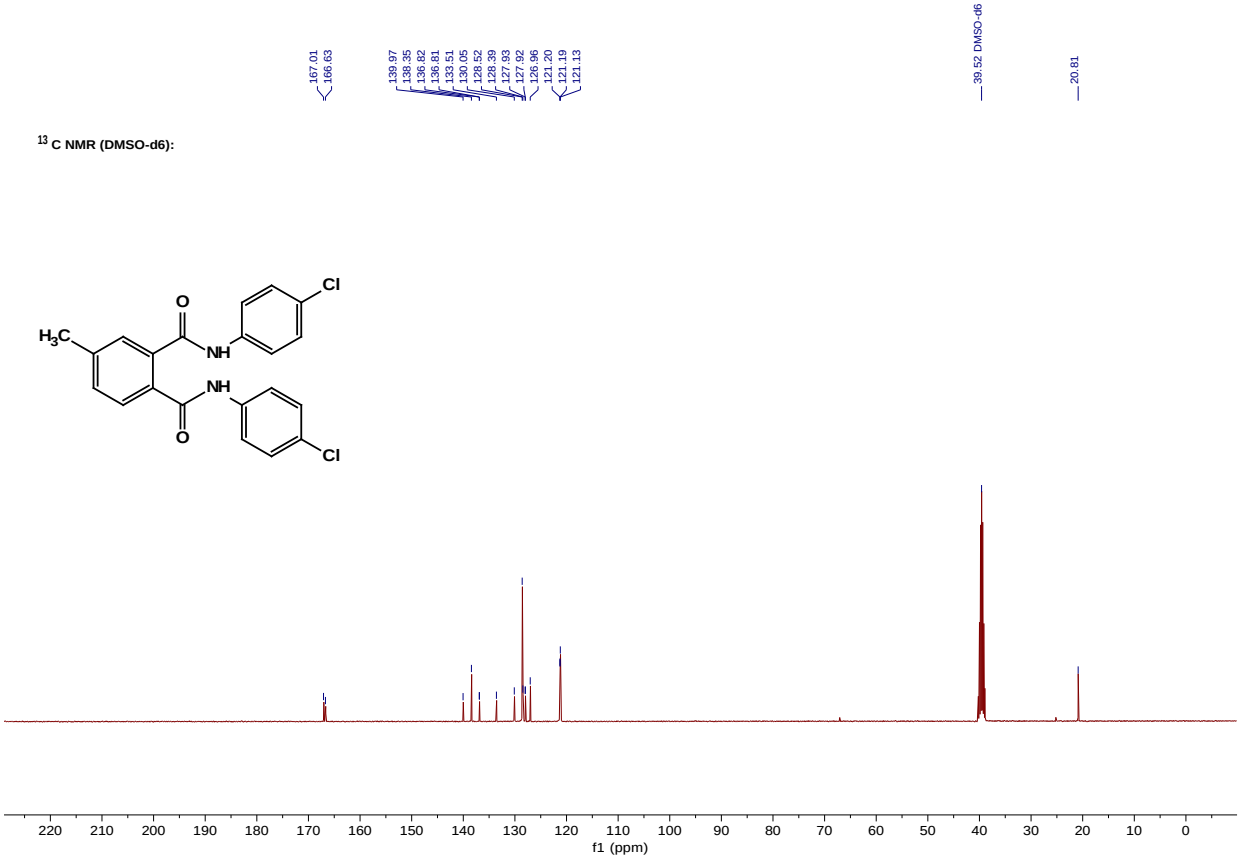

N,N'-Diphenylphthaldiamide (1p)

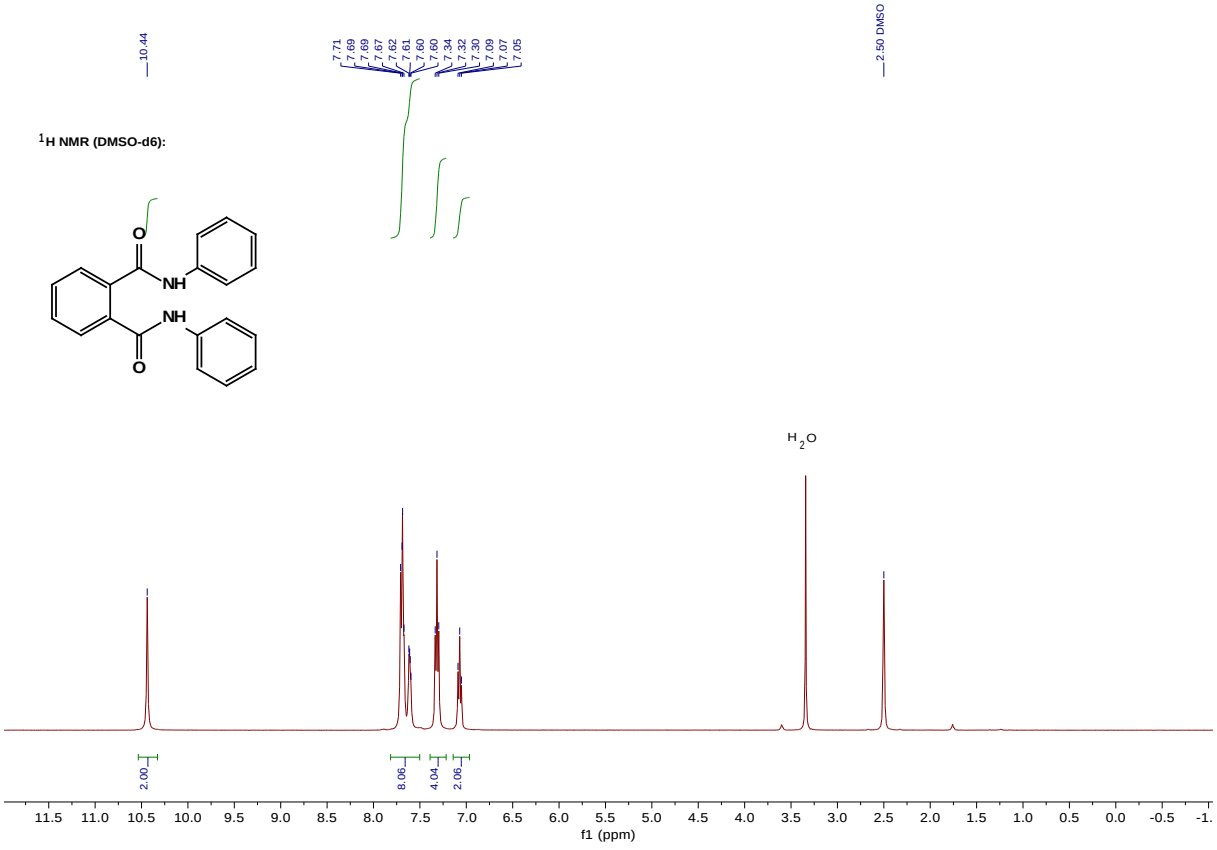

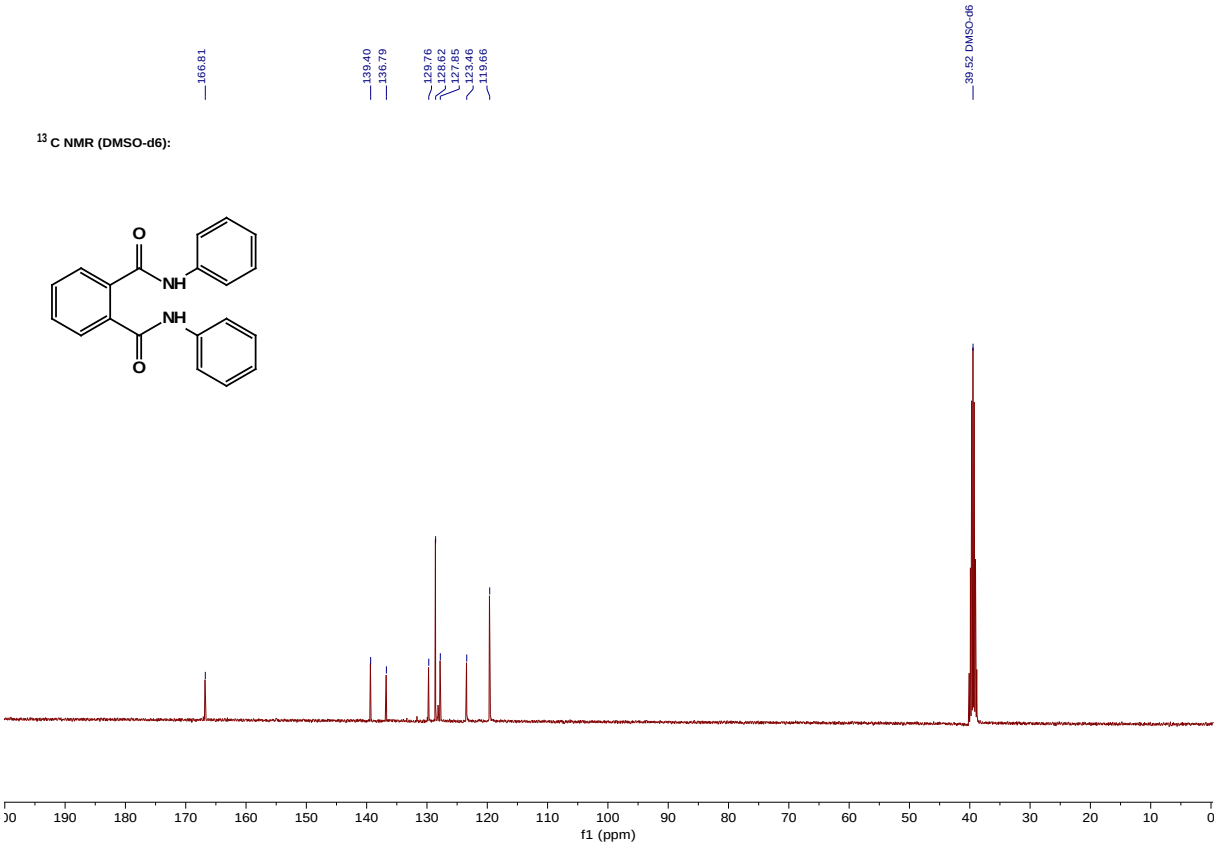

2,3-Di(4-methylphenyl)-2,3-dihydrophthalazin-1,4-dione (2a)

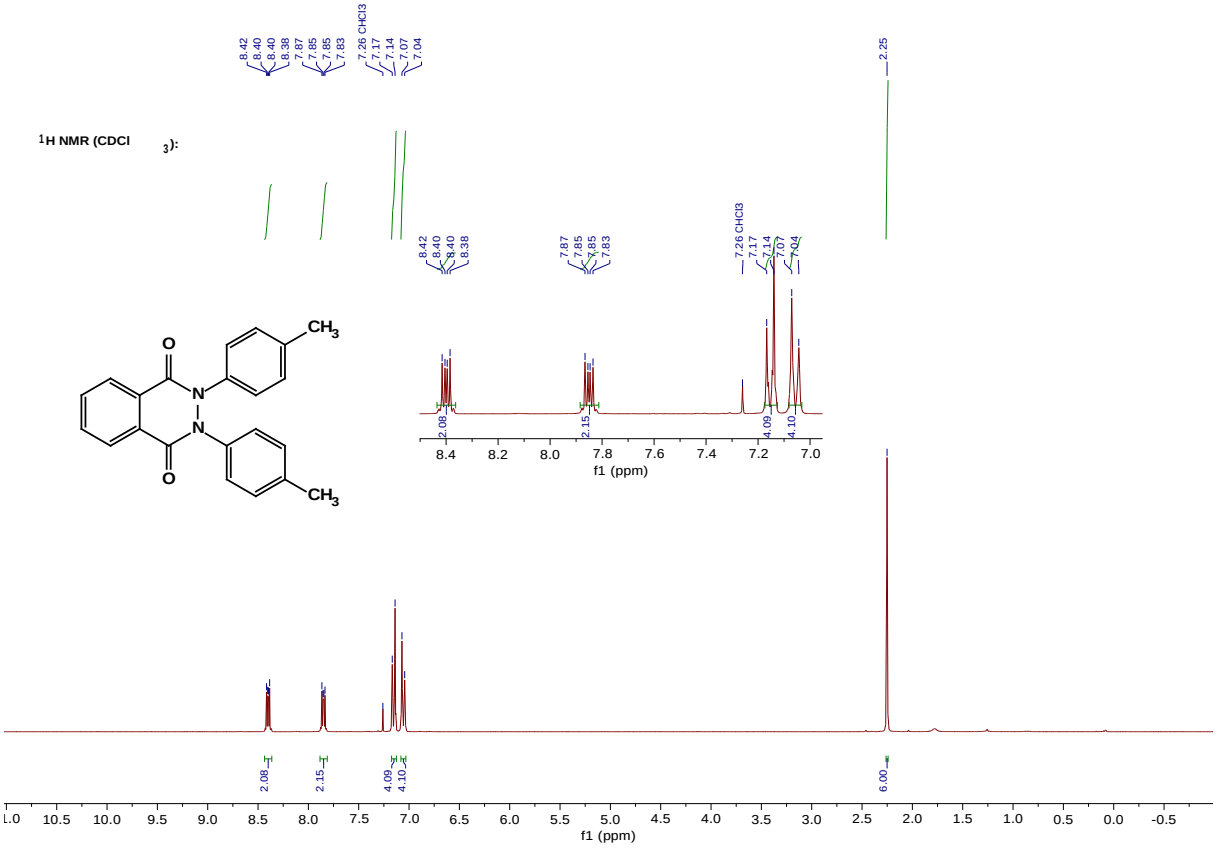

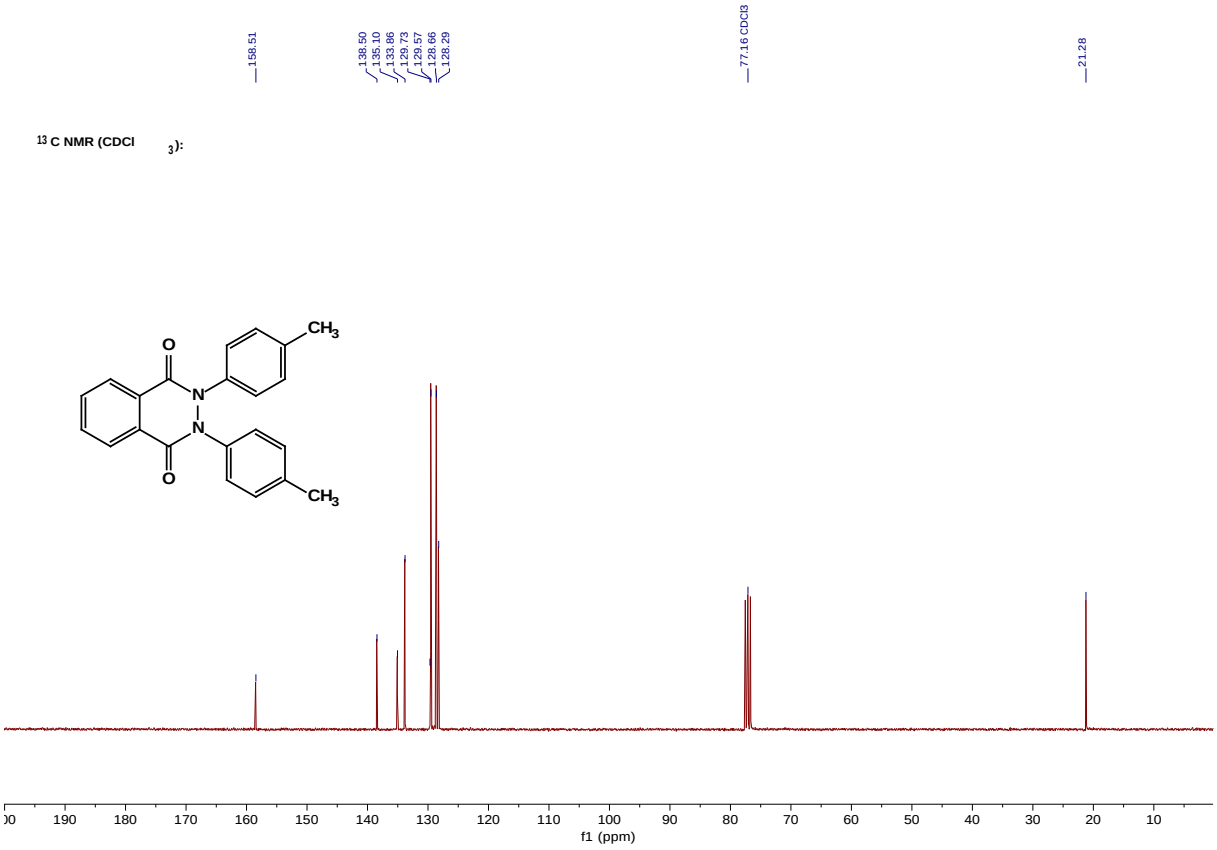

2,3-Bis(4-(1,1-dimethylethyl)phenyl)-2,3-dihydrophthalazin-1,4-dione (2b)

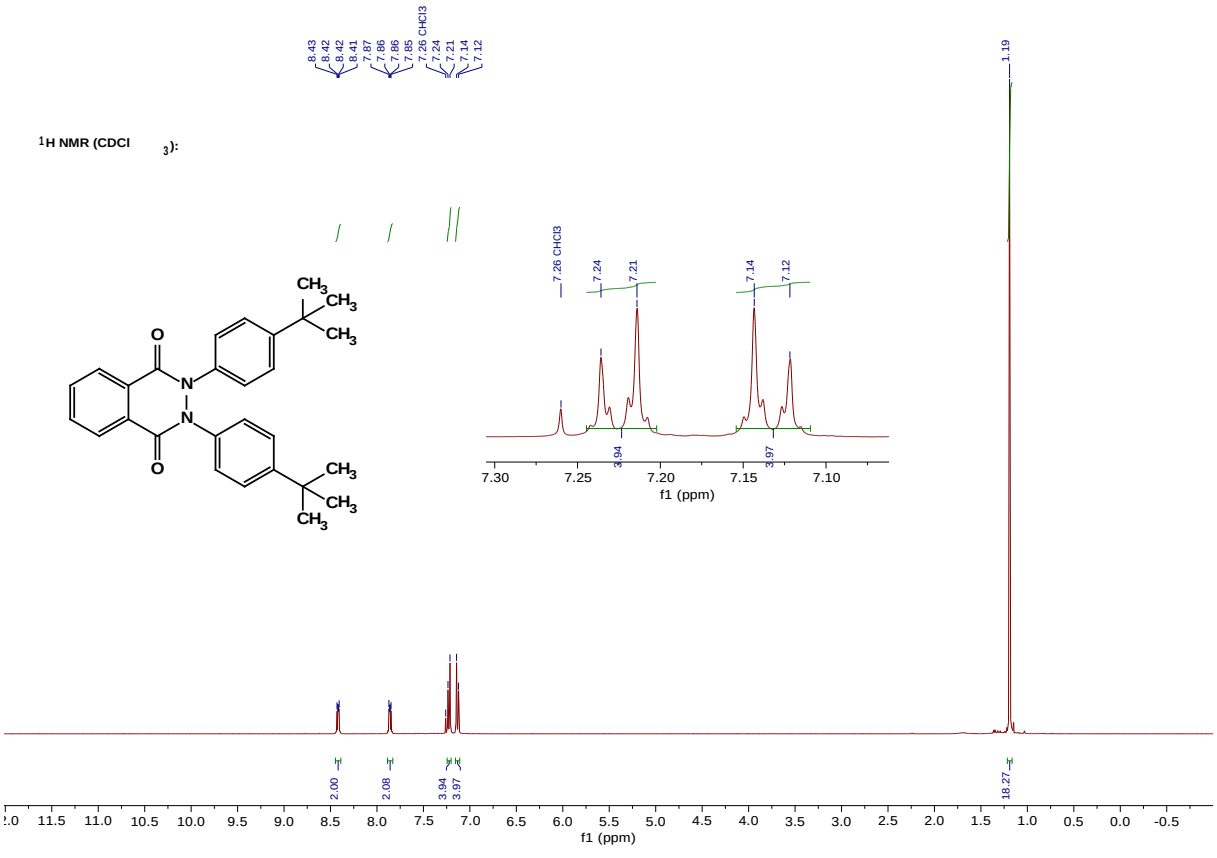

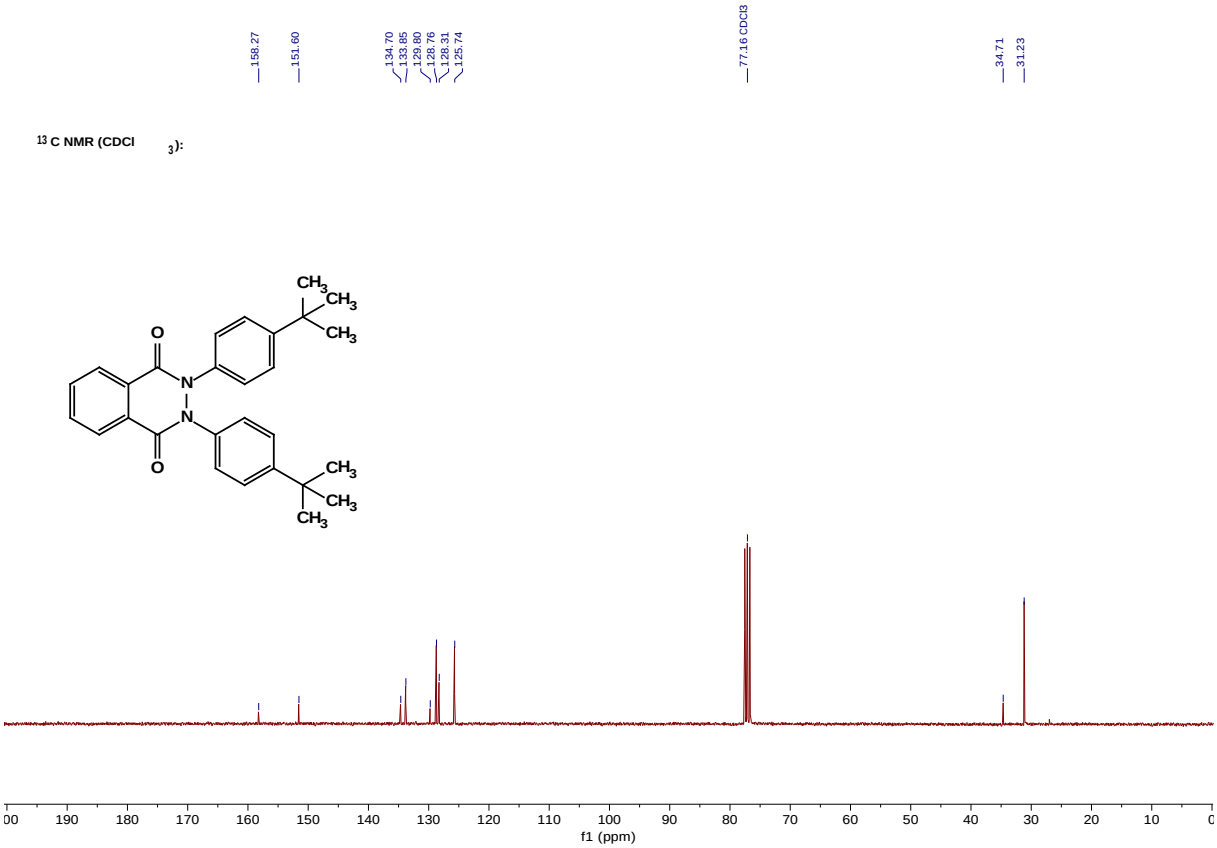

2,3-Bis(3-(1,1-dimethylethyl)phenyl)-2,3-dihydrophthalazin-1,4-dione (2c)

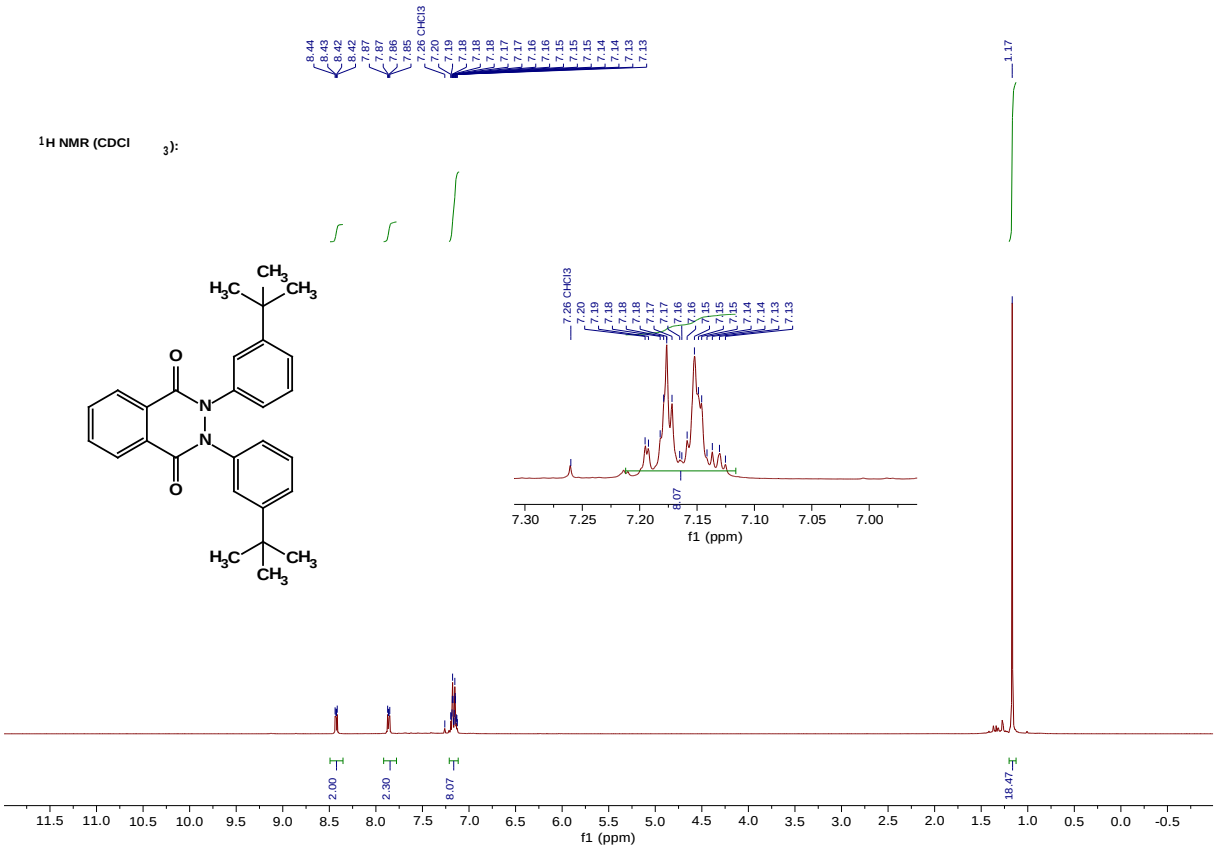

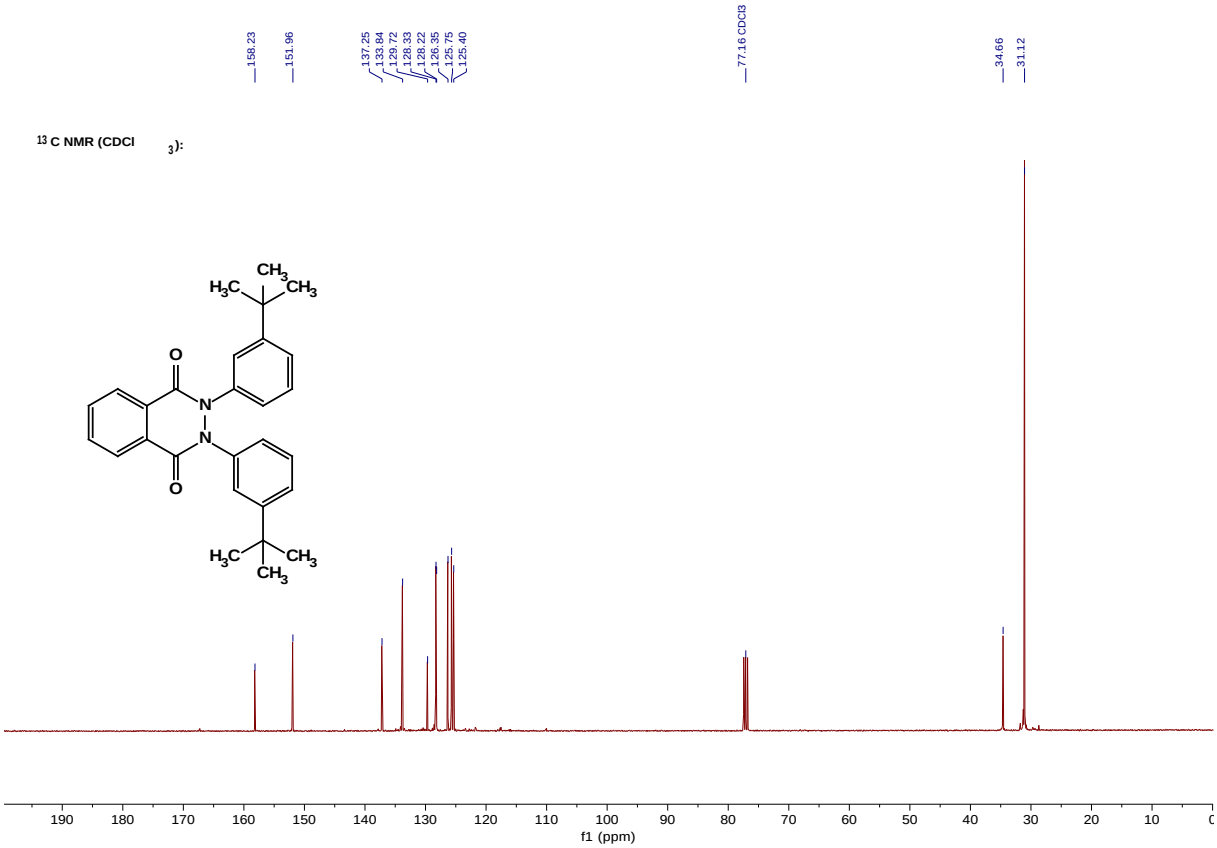

2,3-Di(4-chlorophenyl)-2,3-dihydrophthalazin-1,4-dione (2d)

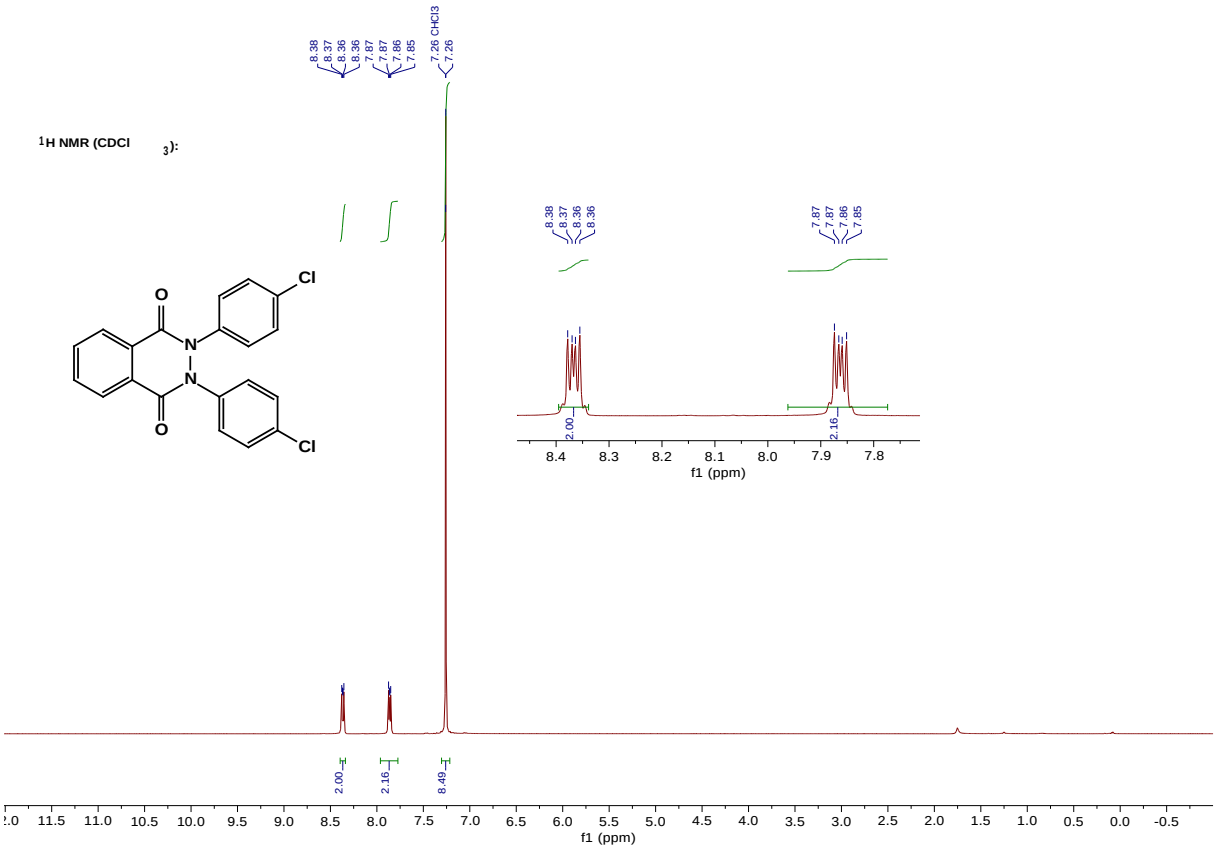

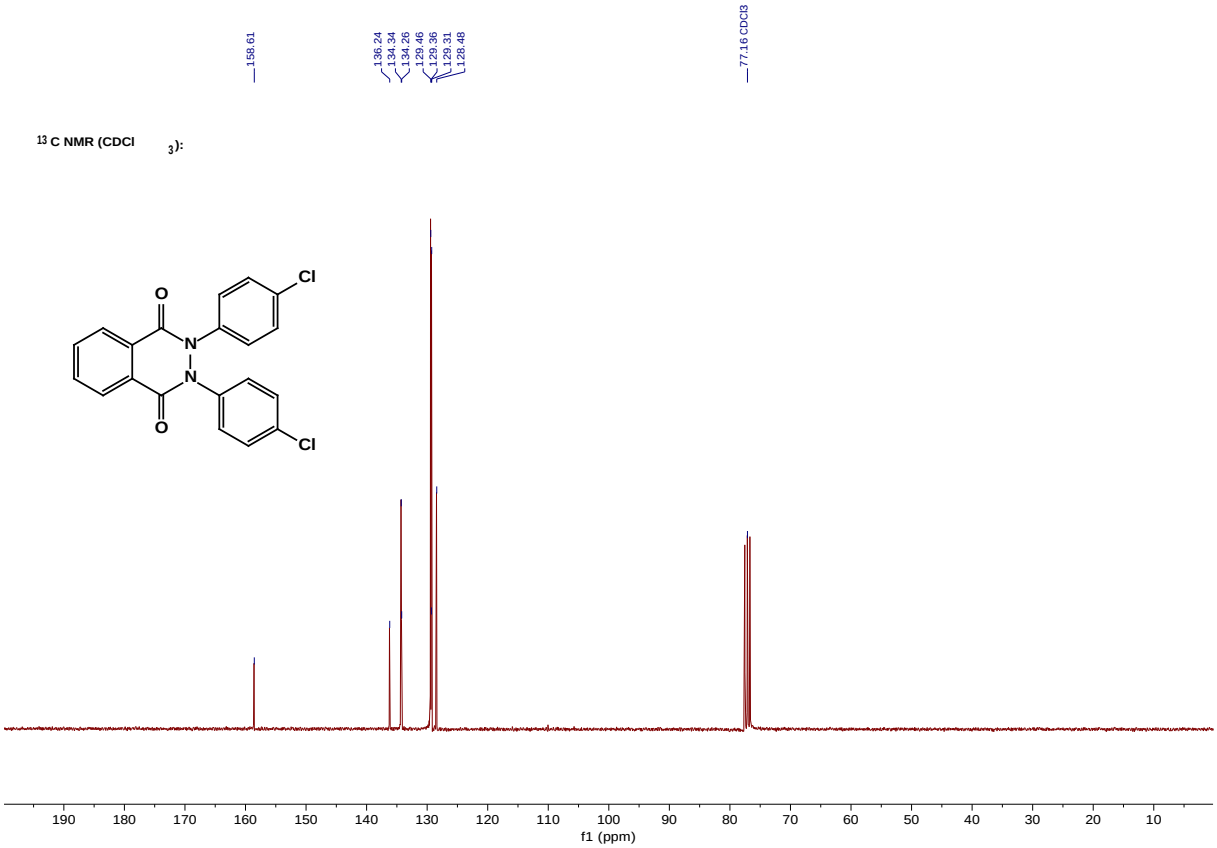

2,3-Di(4-fluorophenyl)-2,3-dihydrophthalazin-1,4-dione (2e)

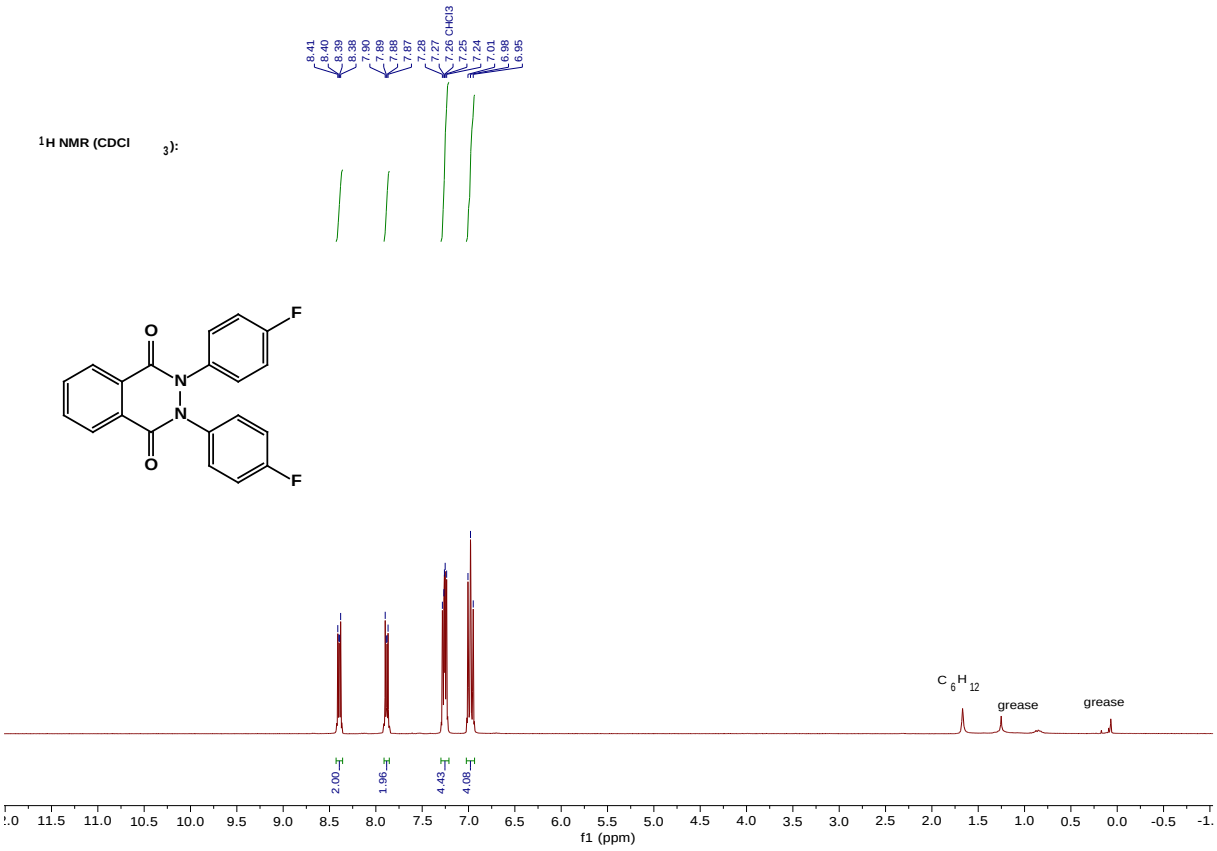

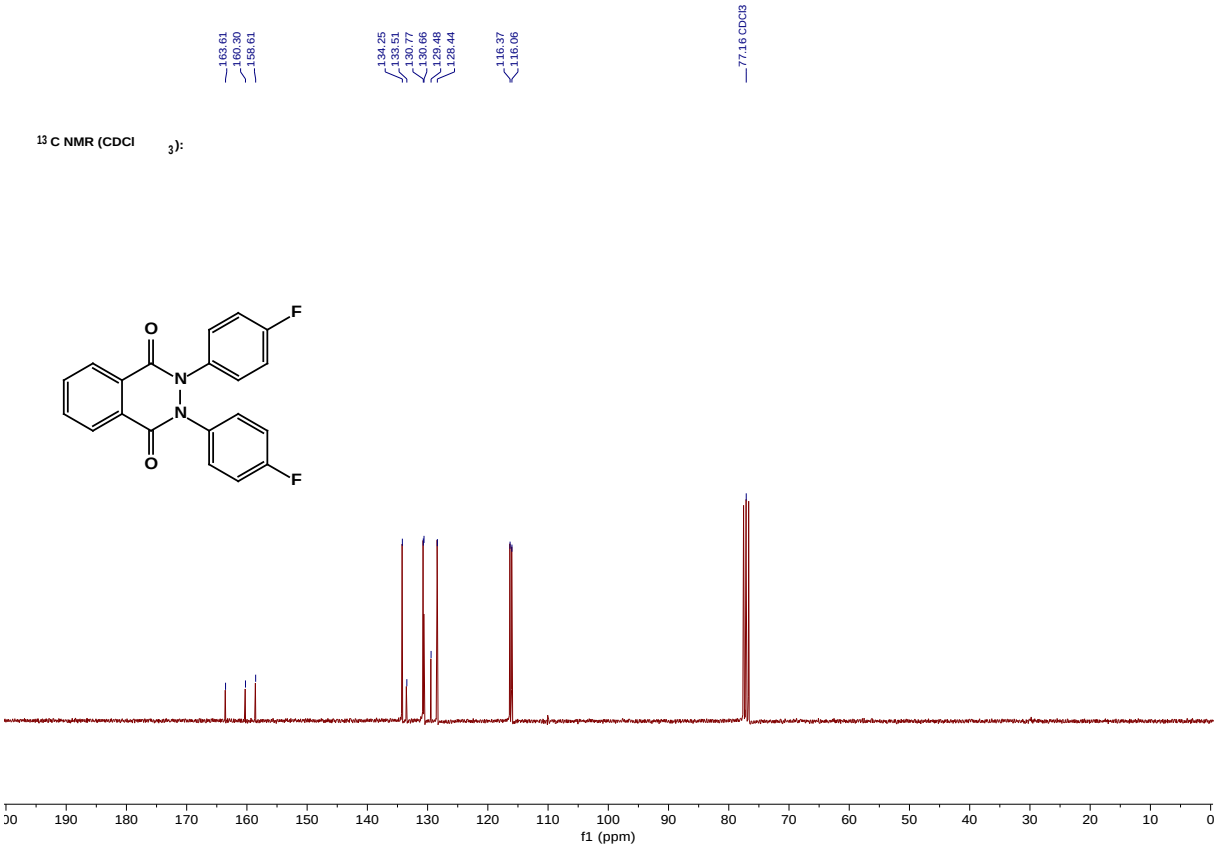

^{13}C NMR (CDCl$_3$):

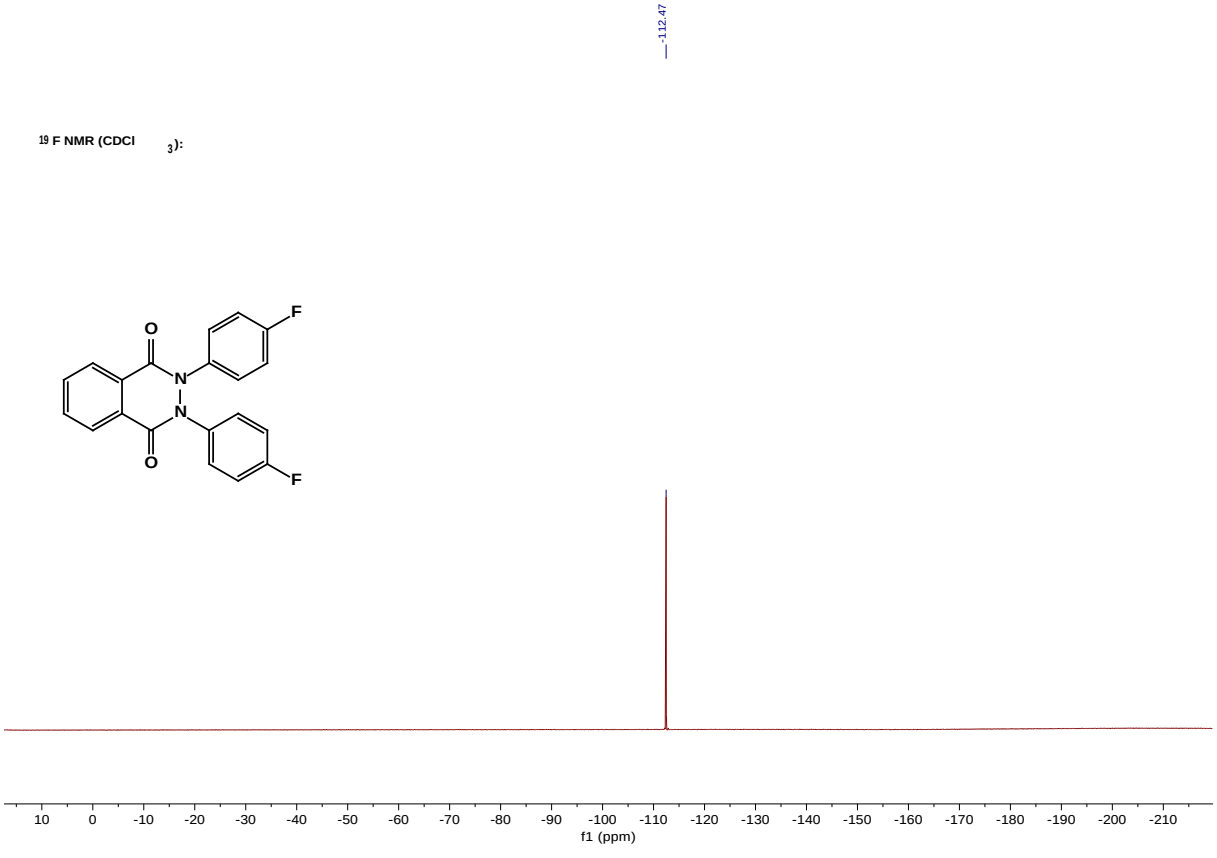

^{19}F NMR (CDCl$_3$):

2,3-Bis(2,4-difluorophenyl)-2,3-dihydrophthalazin-1,4-dion (2f)

^{1}H NMR ($CDCl_3$):

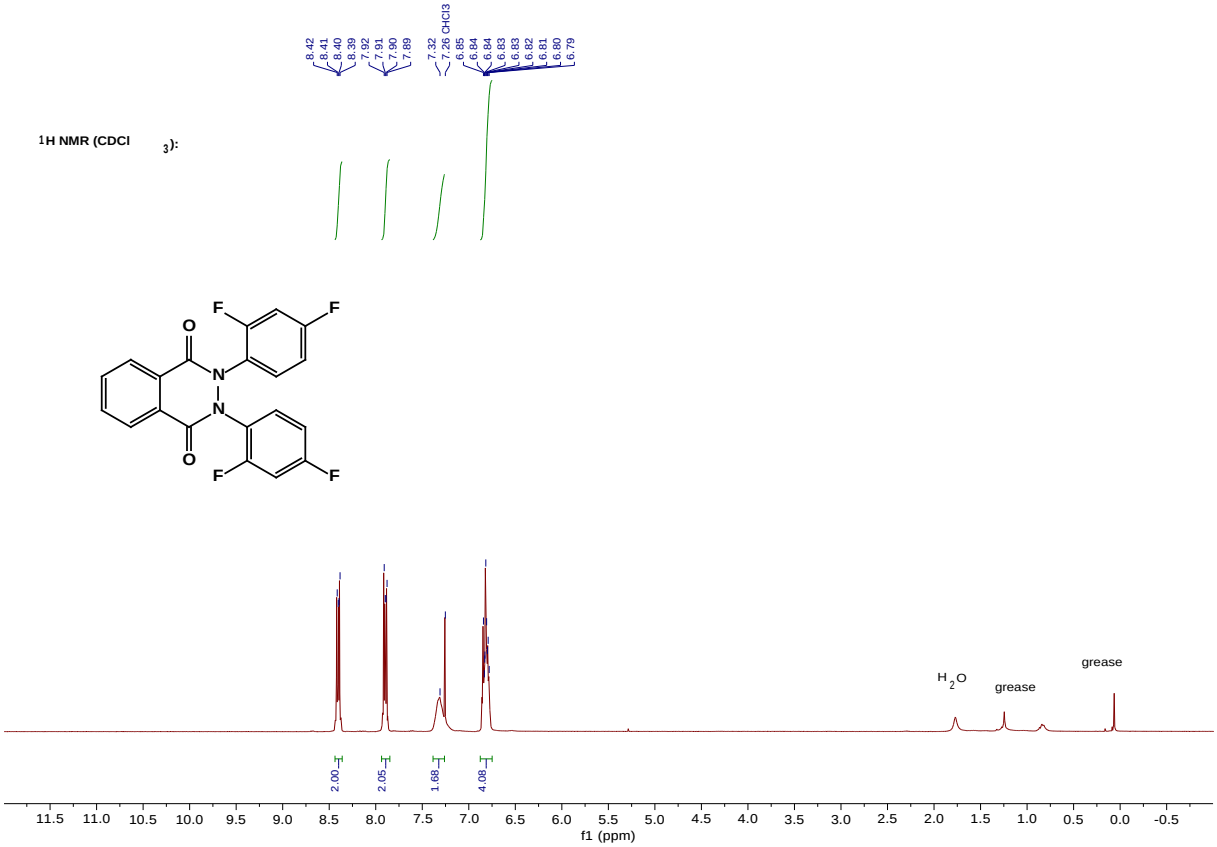

^{13}C NMR ($CDCl_3$):

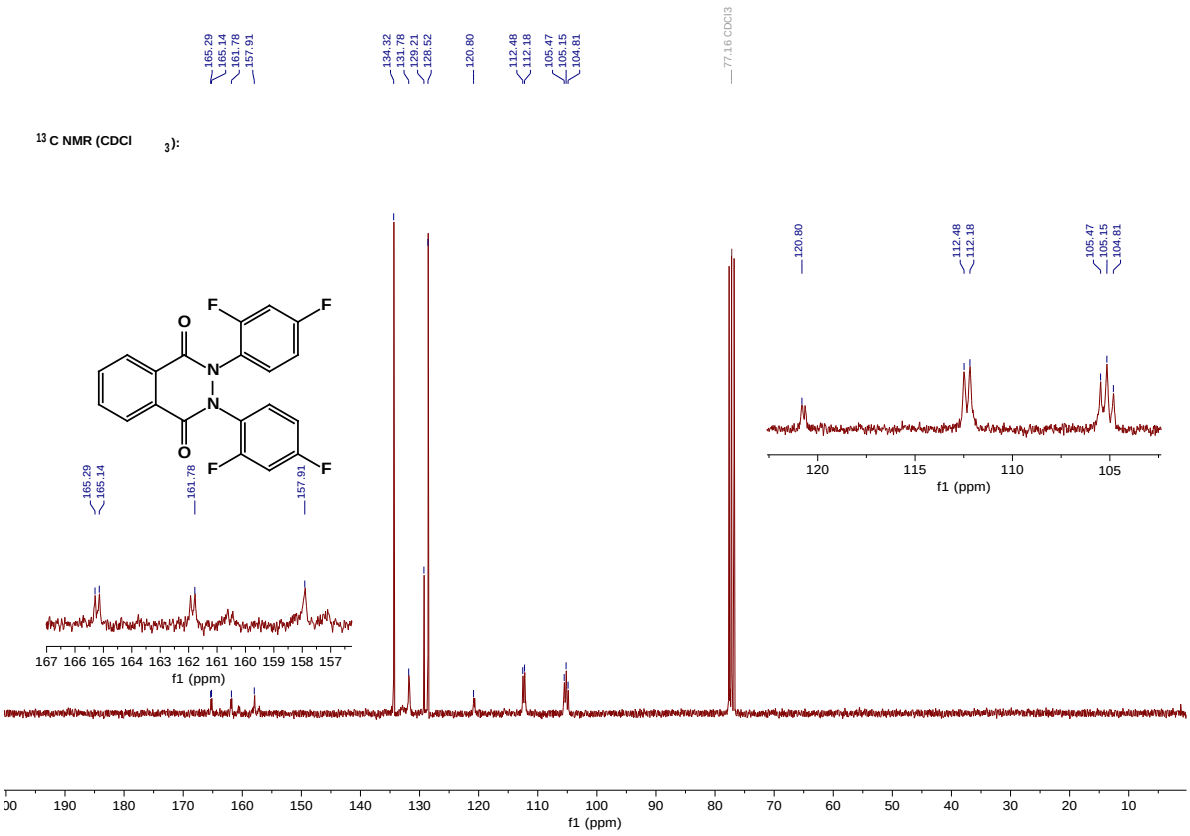

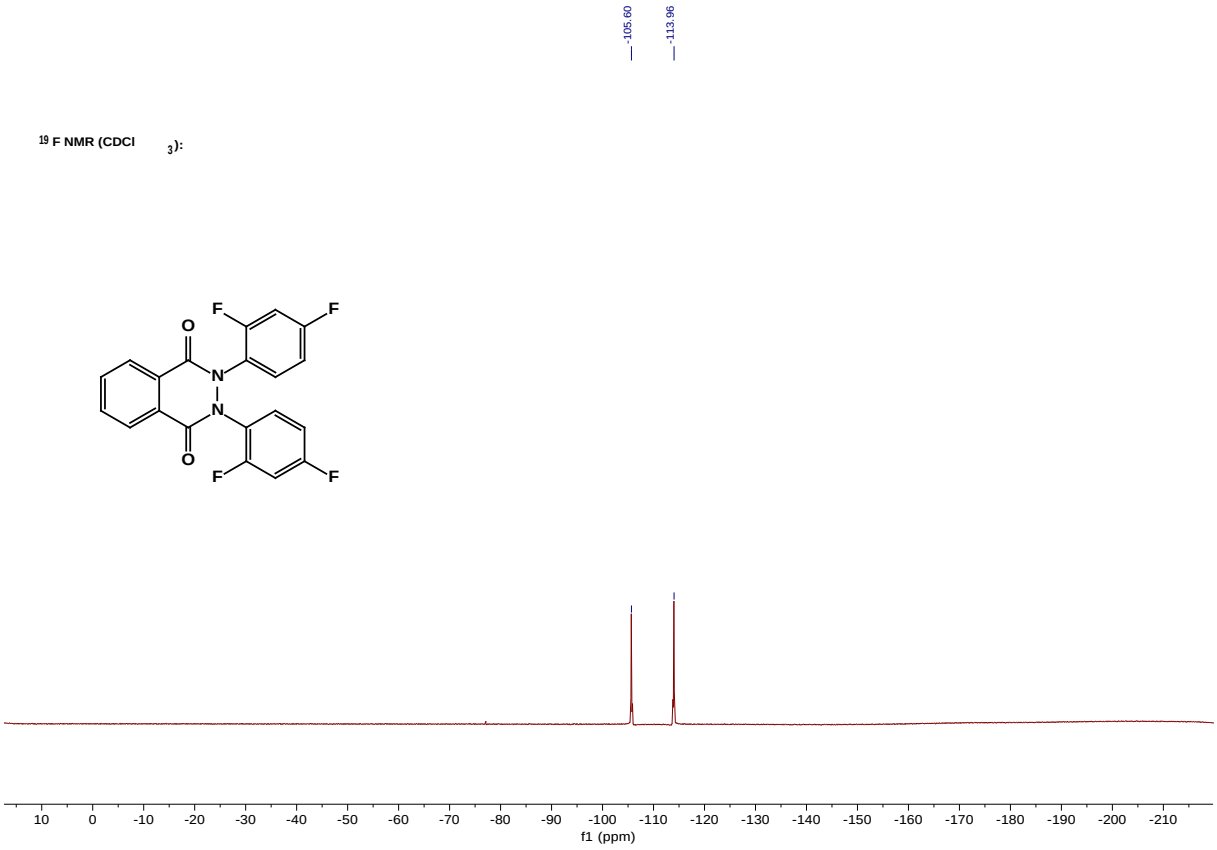

2,3-Di(4-methoxyphenyl)-2,3-dihydrophthalazin-1,4-dione (2g)

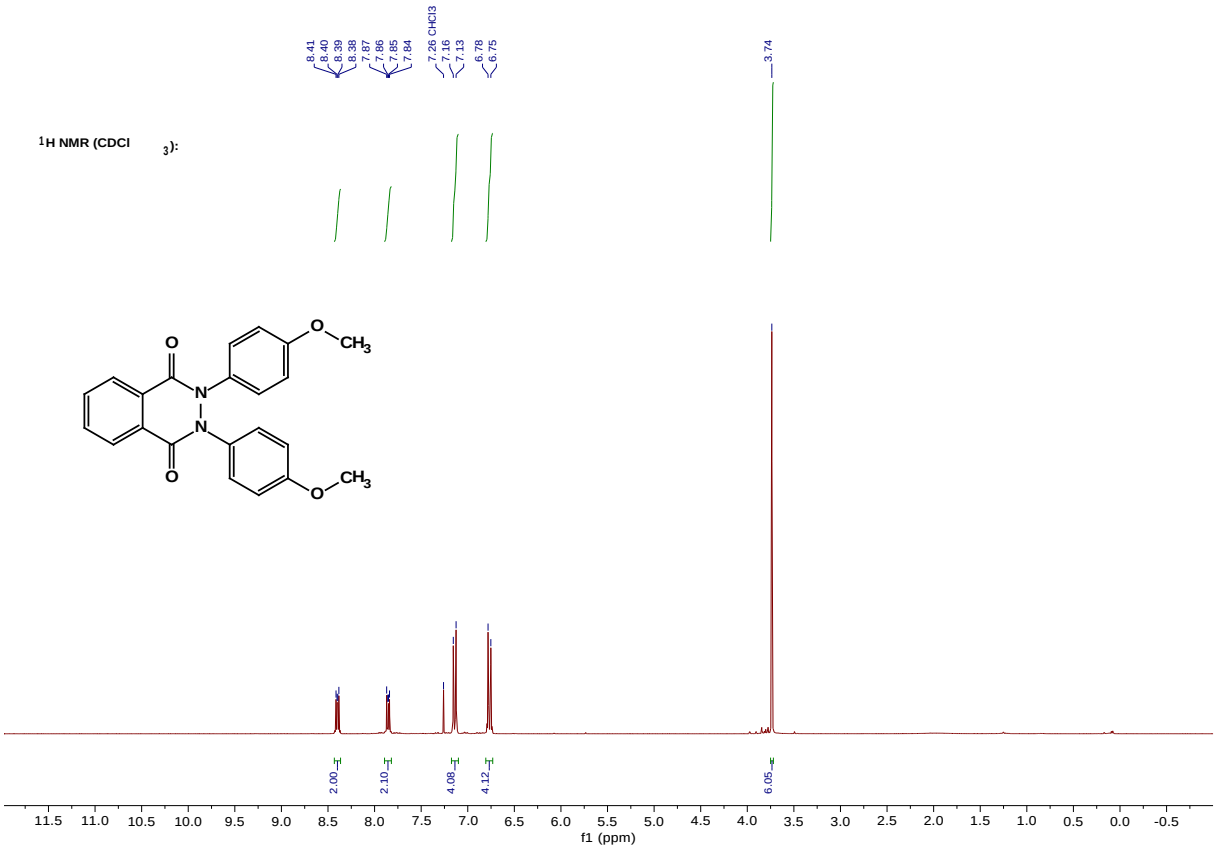

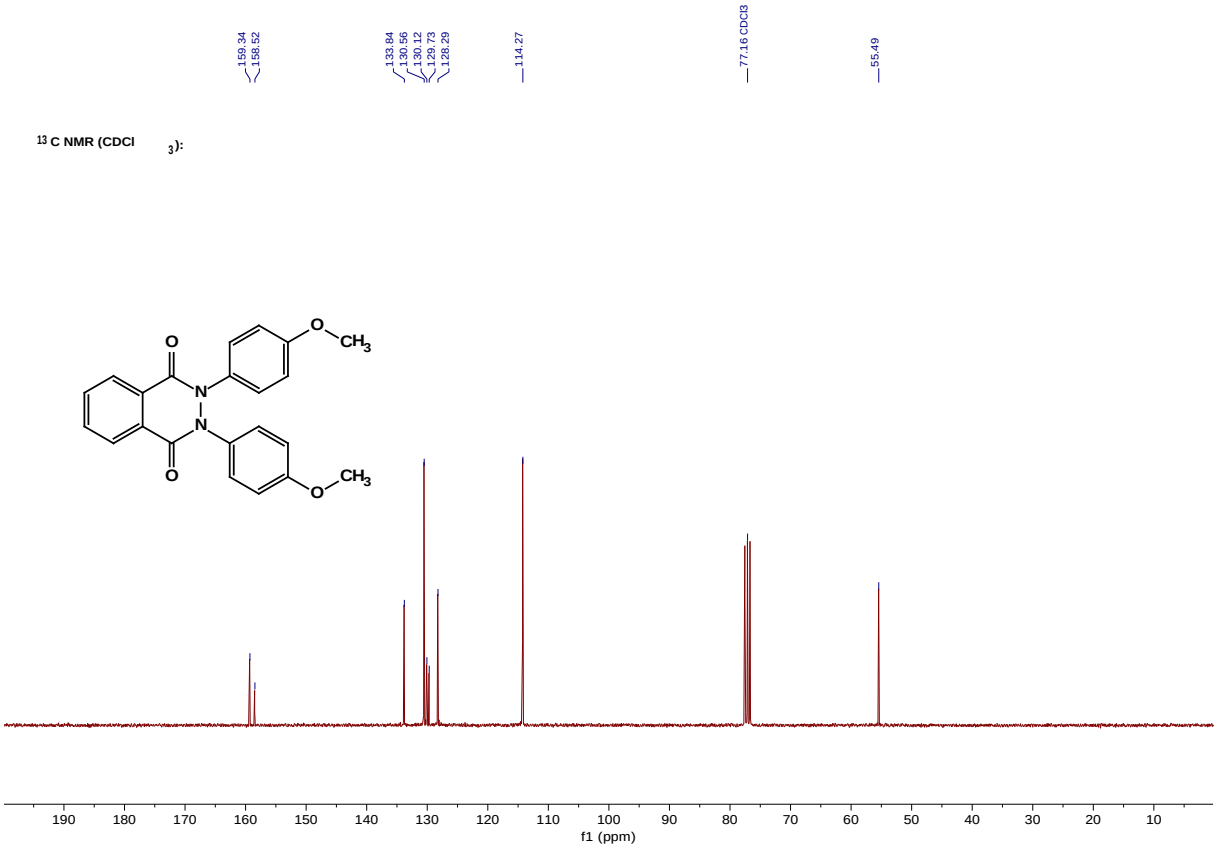

2-(4-Chlorophenyl)-3-(4-methylphenyl)-2,3-dihydrophthalazin-1,4-dione (2h)

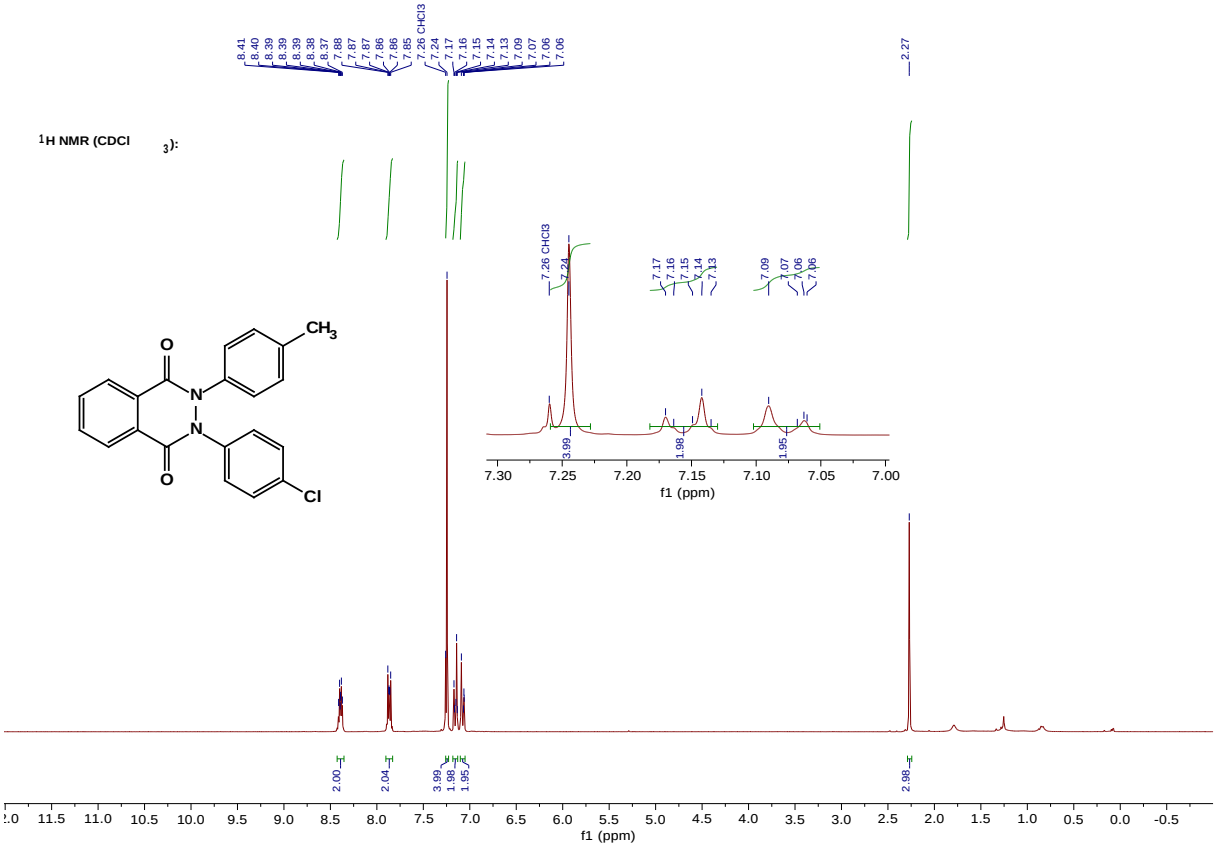

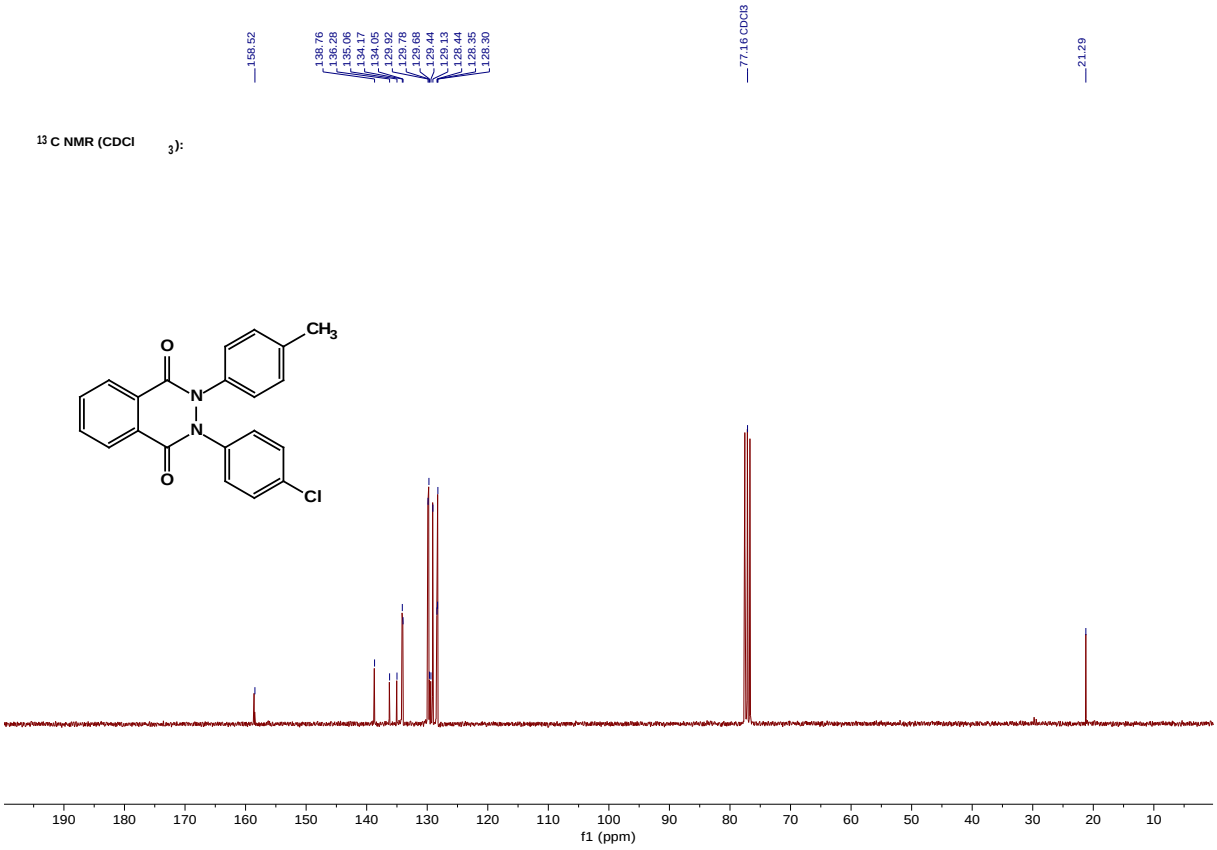

2-(4-Chlorophenyl)-3-(4-trifluoromethylsulfonyloxyphenyl)-2,3-dihydrophthalazin-1,4-dione (2i)

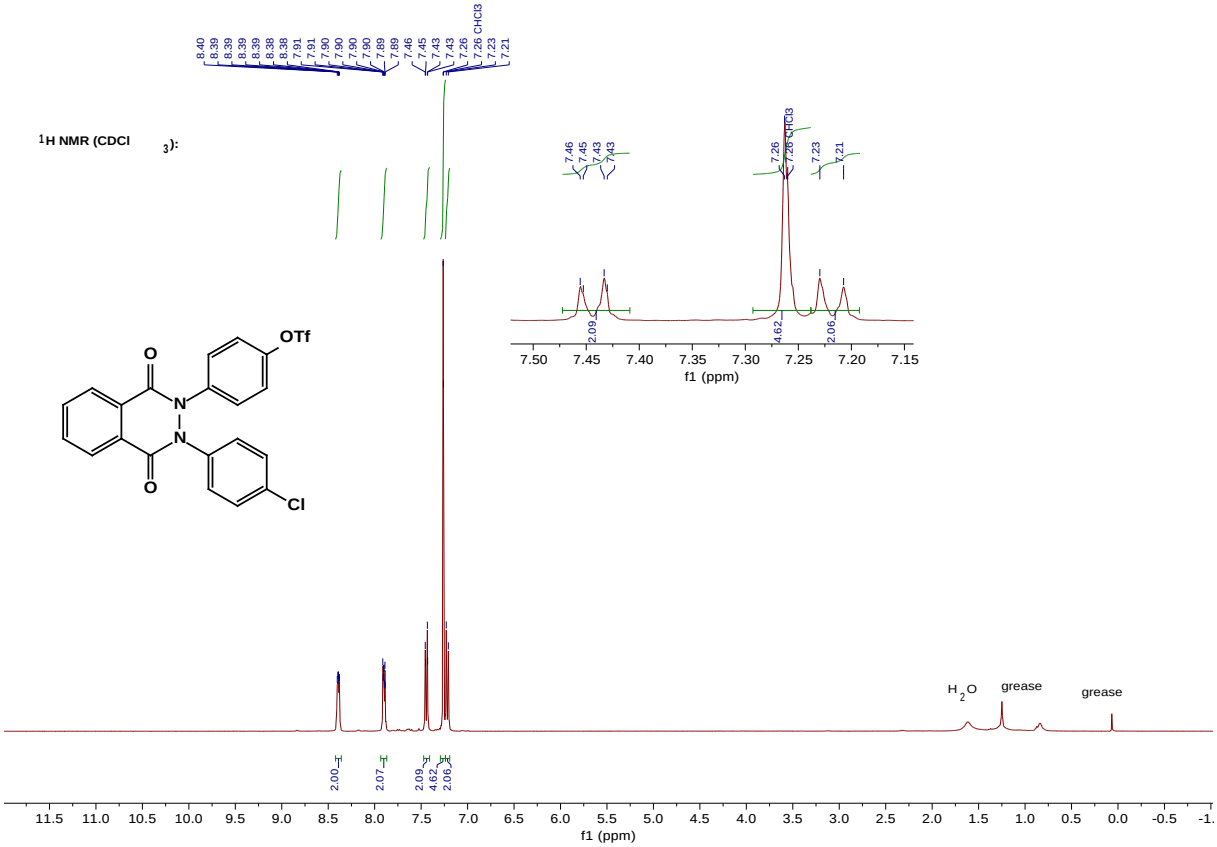

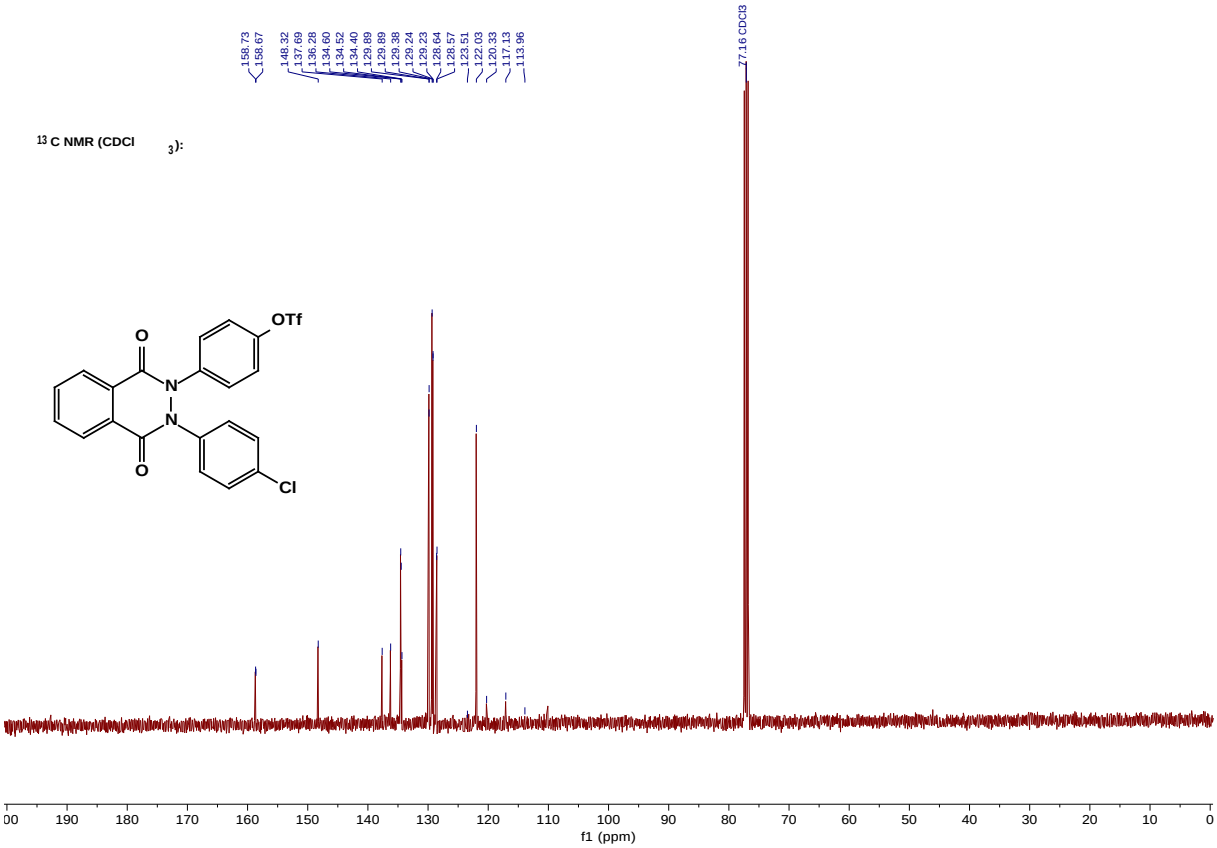
158.73
158.67
148.32
137.69
136.28
134.60
134.52
134.40
129.89
129.89
129.38
129.24
129.23
128.64
128.57
123.51
122.03
120.33
117.13
113.96
77.16 CDCl3
13 C NMR (CDCl 3):
OTf
O
N
N
O
Cl
f1 (ppm)

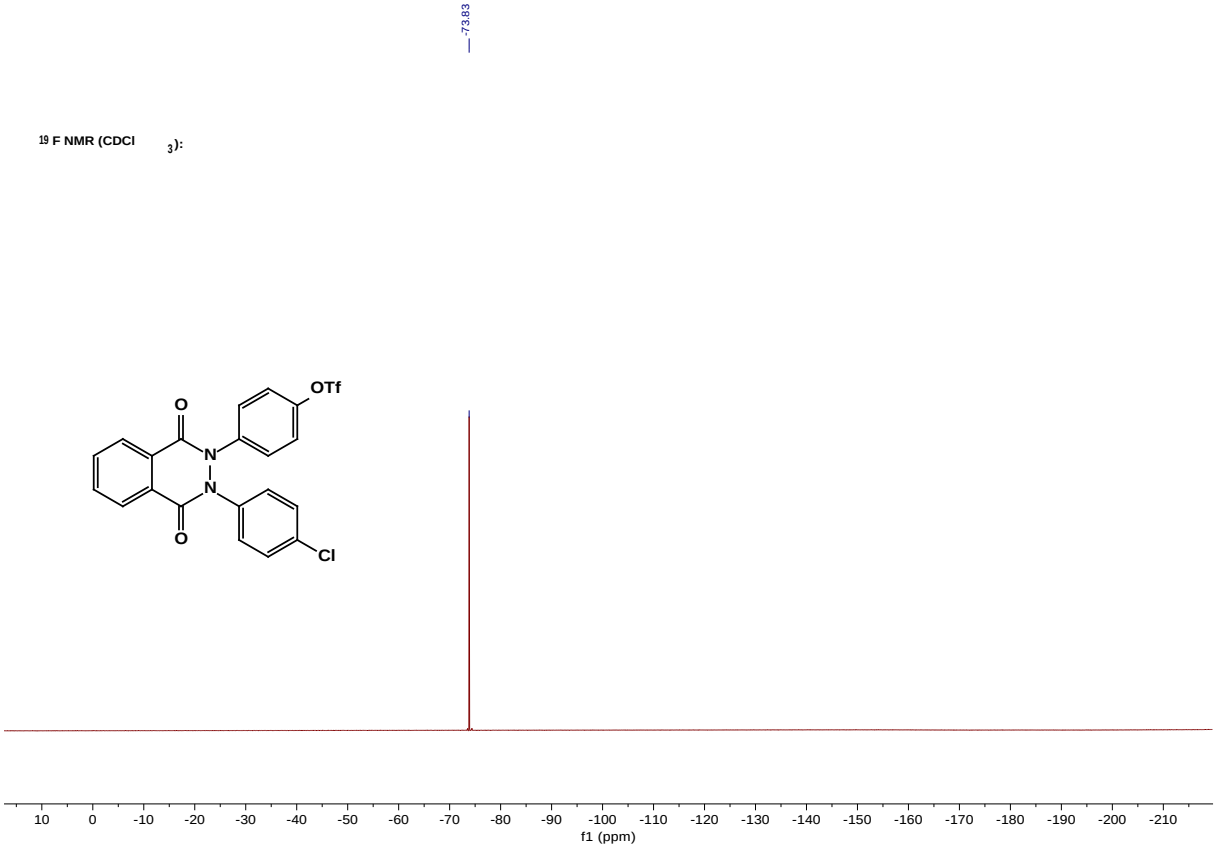
-73.83
19 F NMR (CDCl 3):
OTf
O
N
N
O
Cl
f1 (ppm)

2-(3-Bromo-4-methylphenyl)-3-(4-chlorophenyl)-2,3-dihydrophthalazin-1,4-dione (2j)

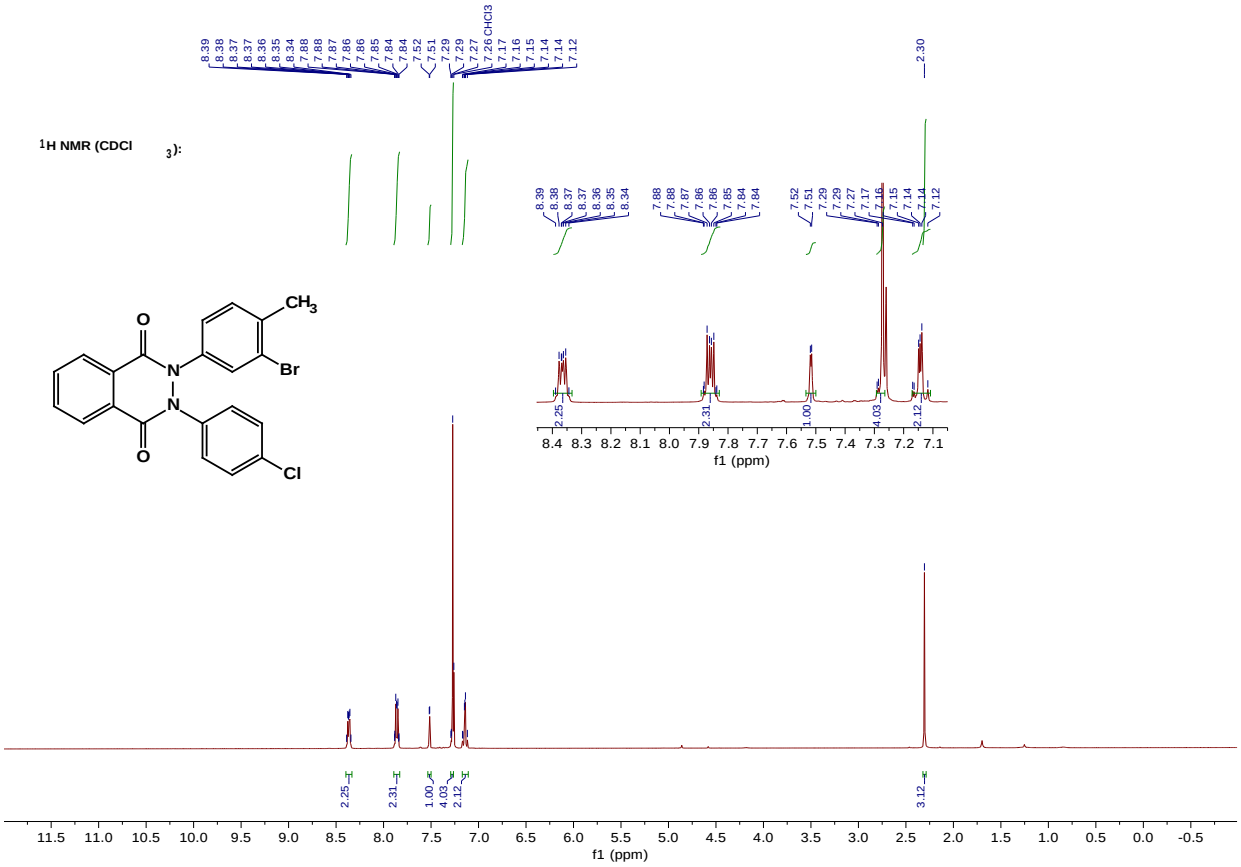

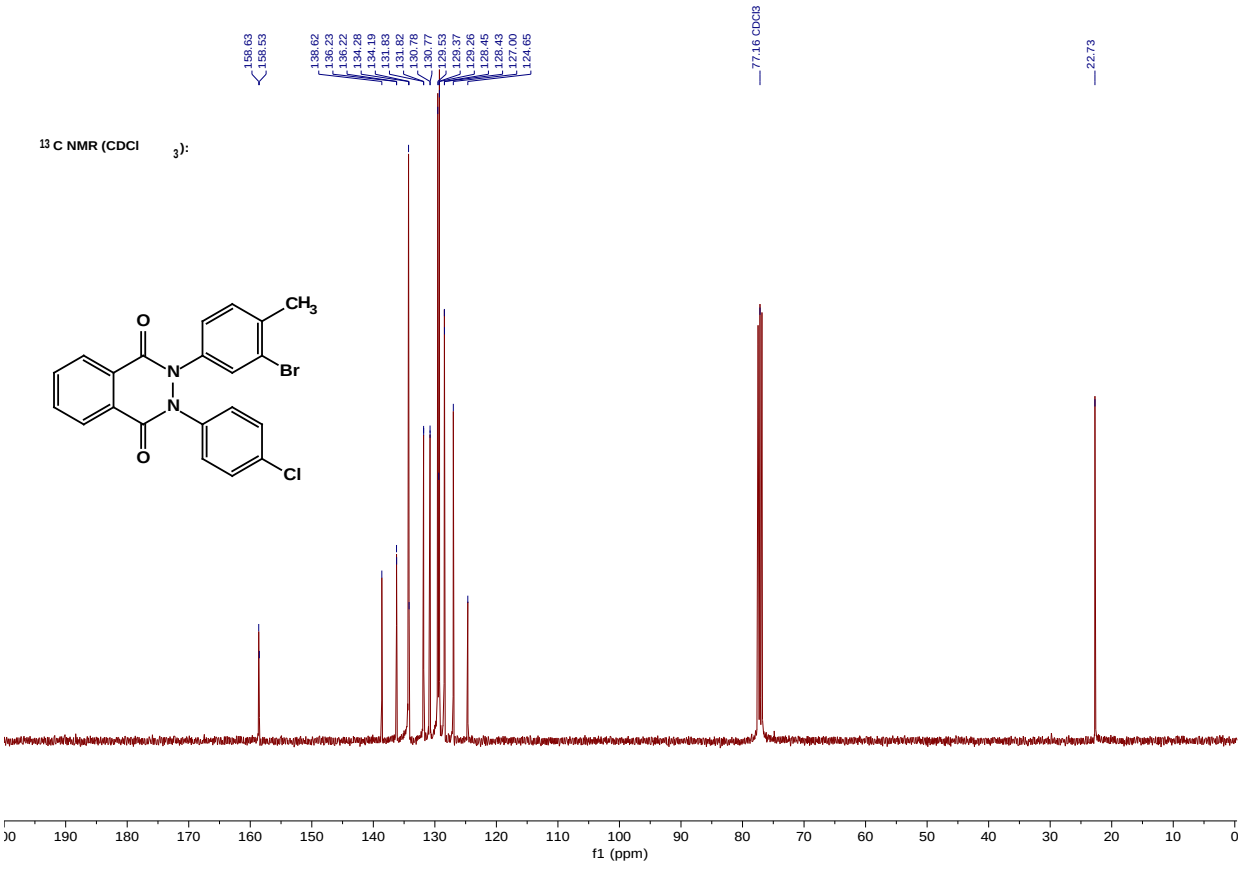

N-(3-Bromo-4-methylphenyl)-*N'*-(4-methylphenyl)phthaldiamide (2k)

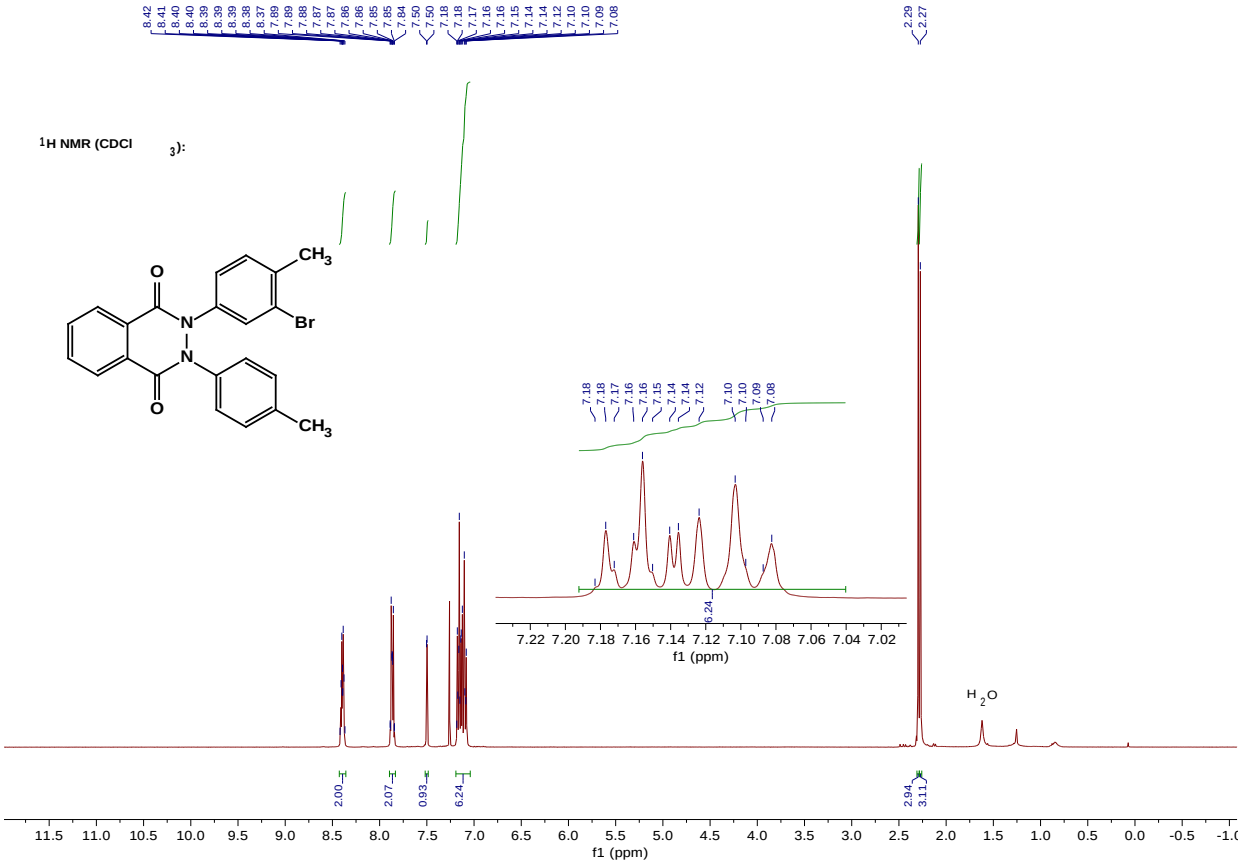

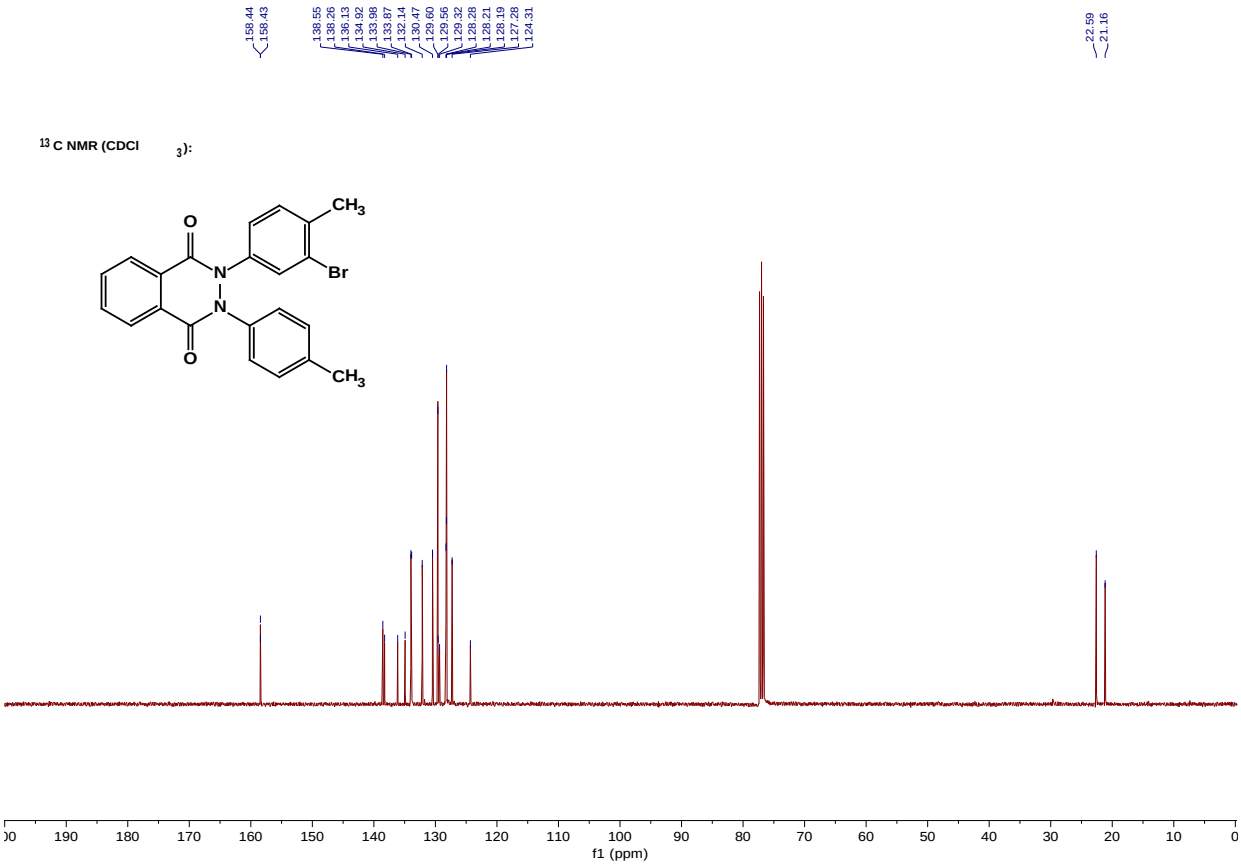

2-(4-Chlorophenyl)-3-(3-cyano-4-methylphenyl)-2,3-dihydrophthalazin-1,4-dione (2l)

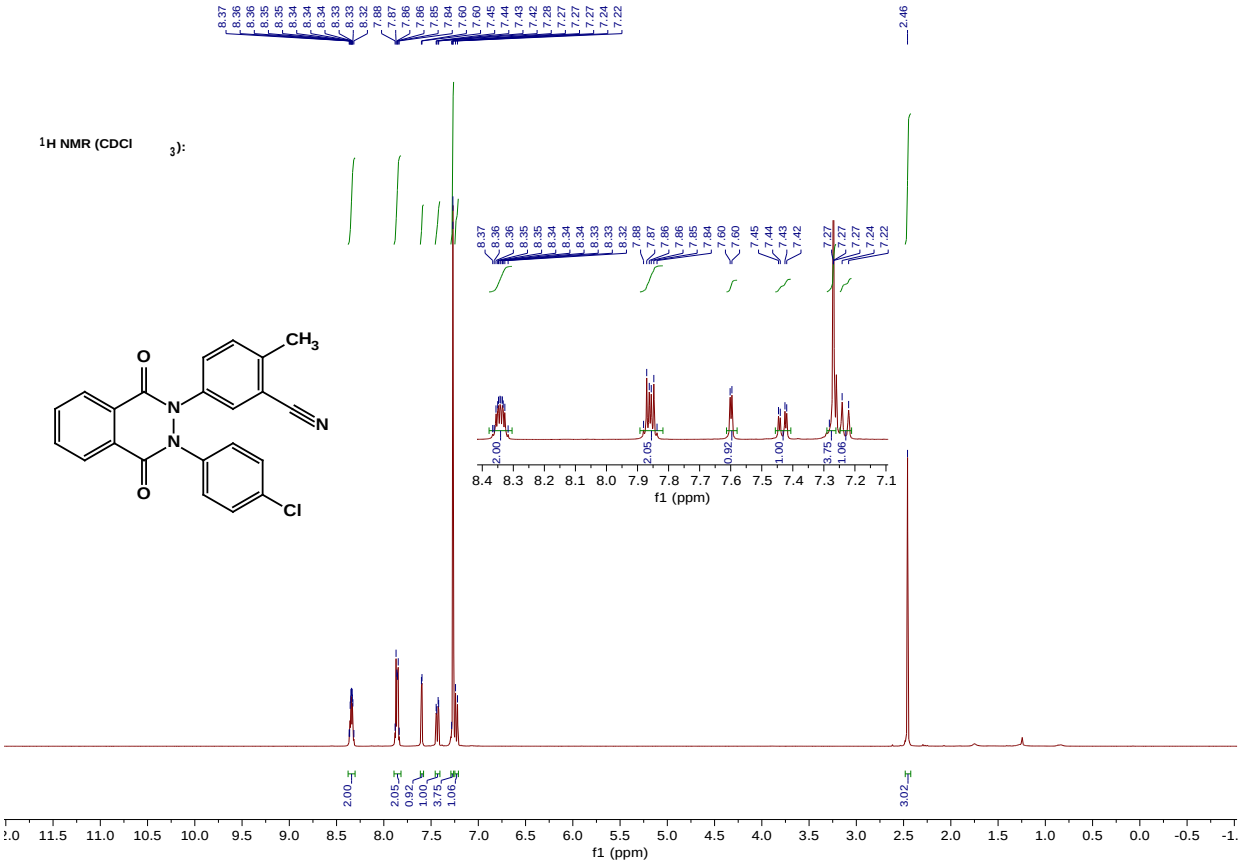

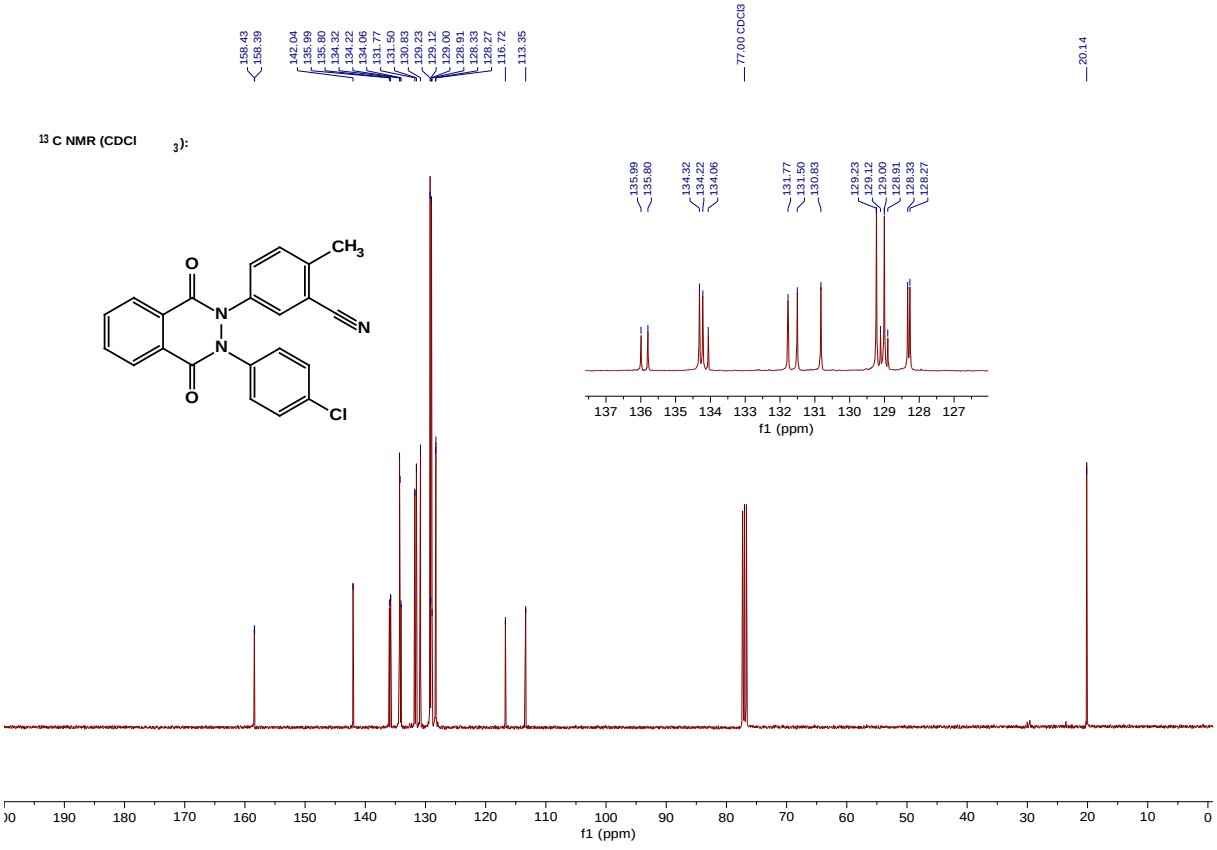

2,3-Di(4-chlorophenyl)-pyrido-[3,4-d]-pyridazin-1,4-dion (2m)

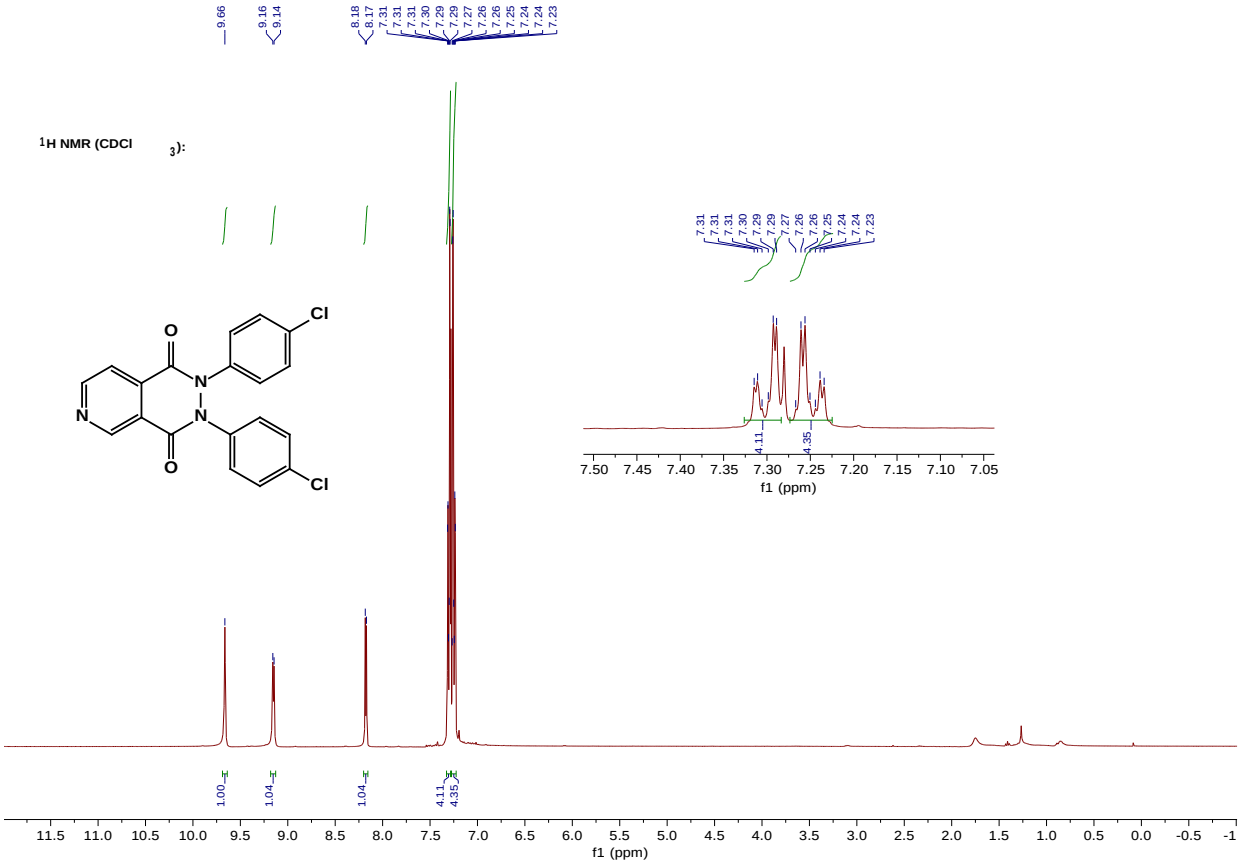

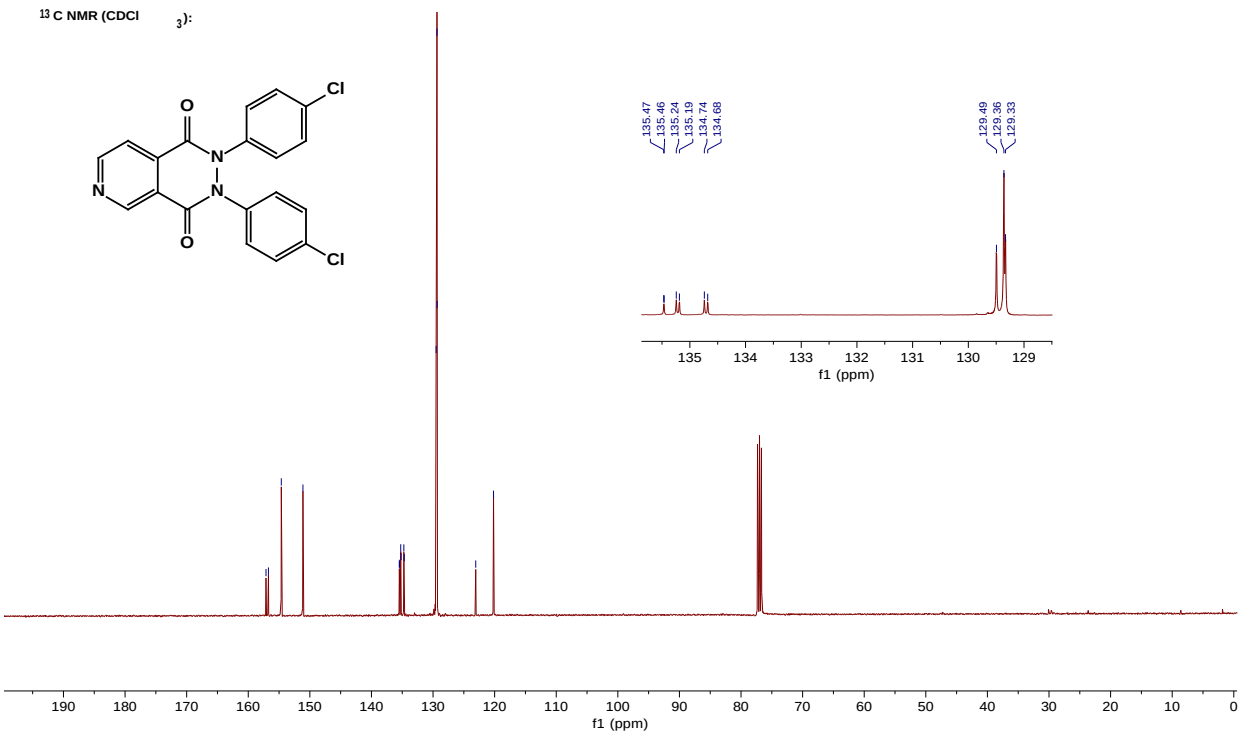

6-Bromo-2,3-di(4-chlorophenyl)-2,3-dihydrophthalazin-1,4-dione (2n)

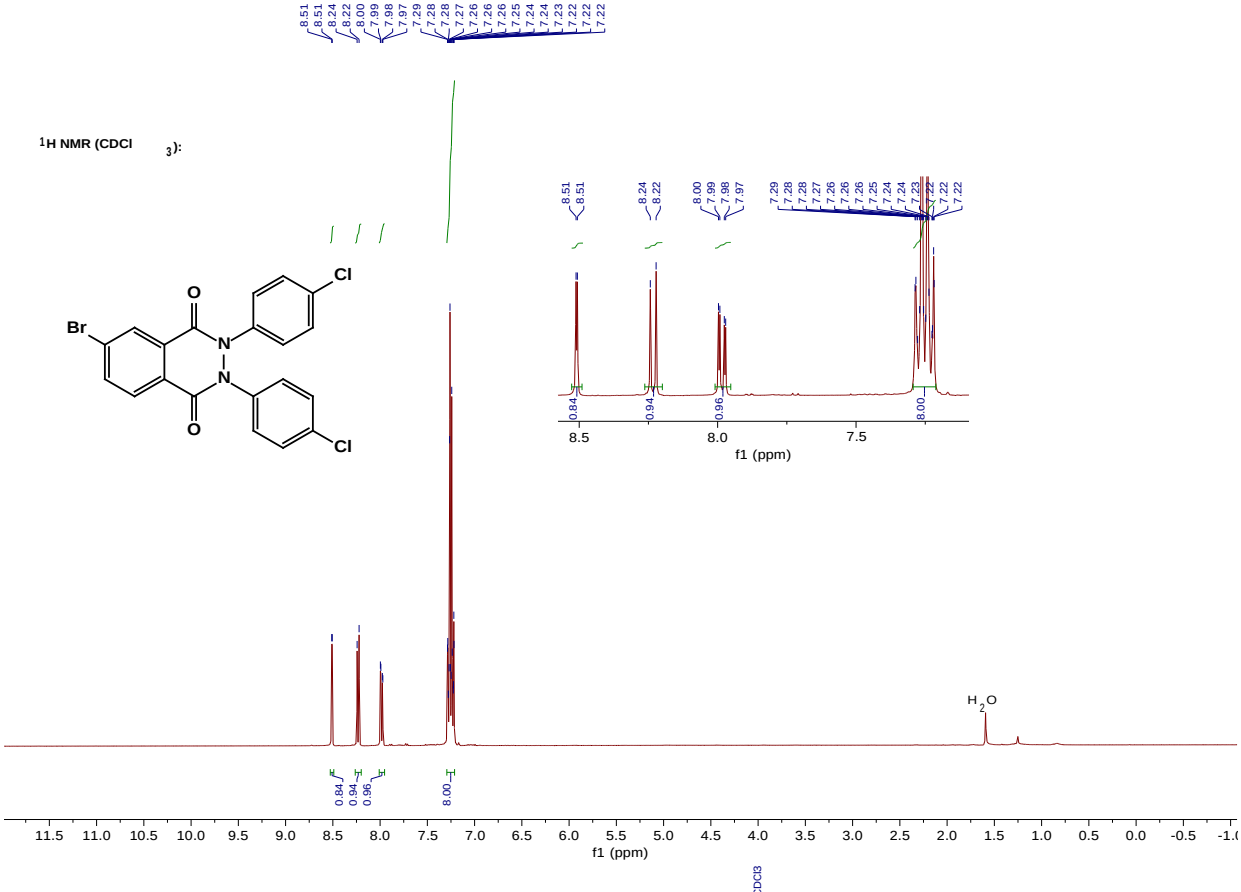

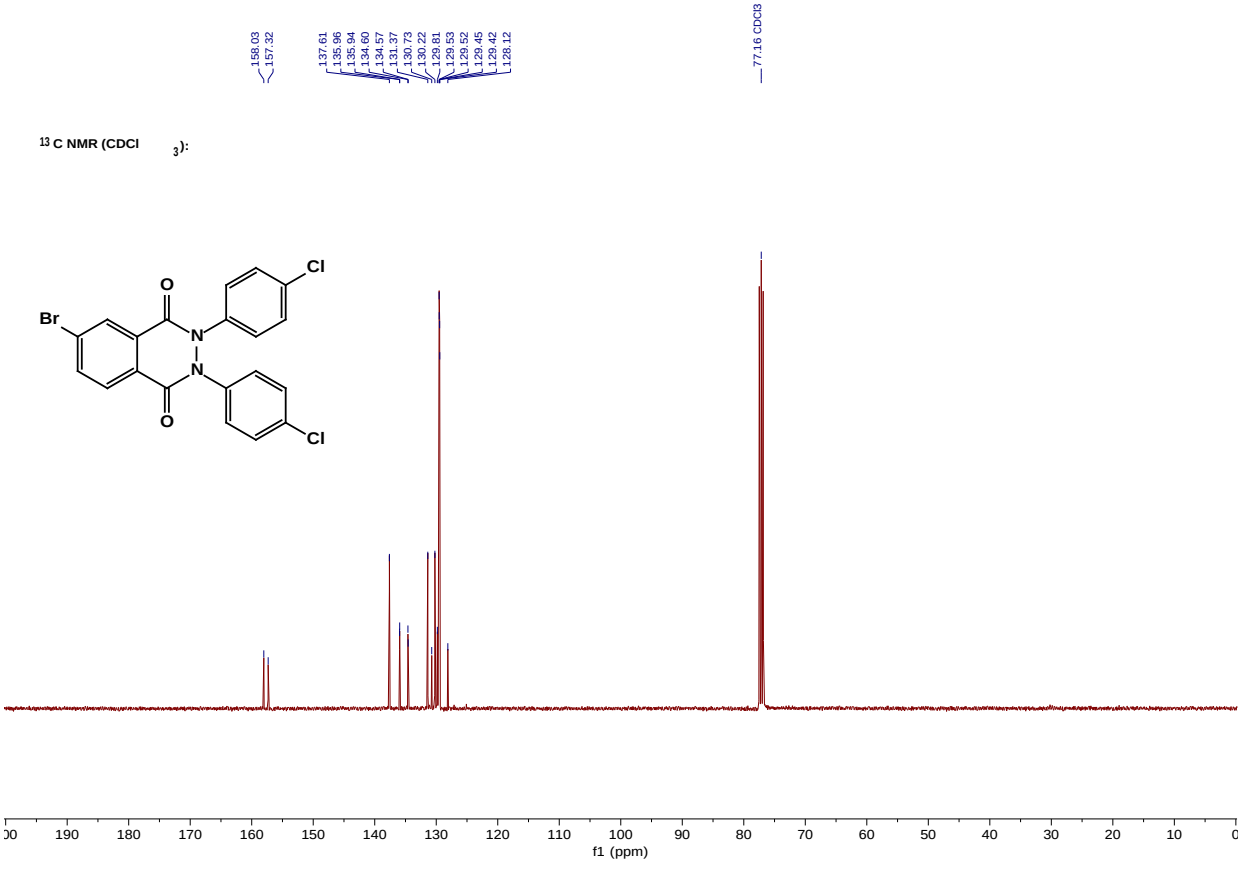

2,3-Di(4-chlorophenyl)-6-methyl-2,3-dihydrophthalazin-1,4-dione (2o)

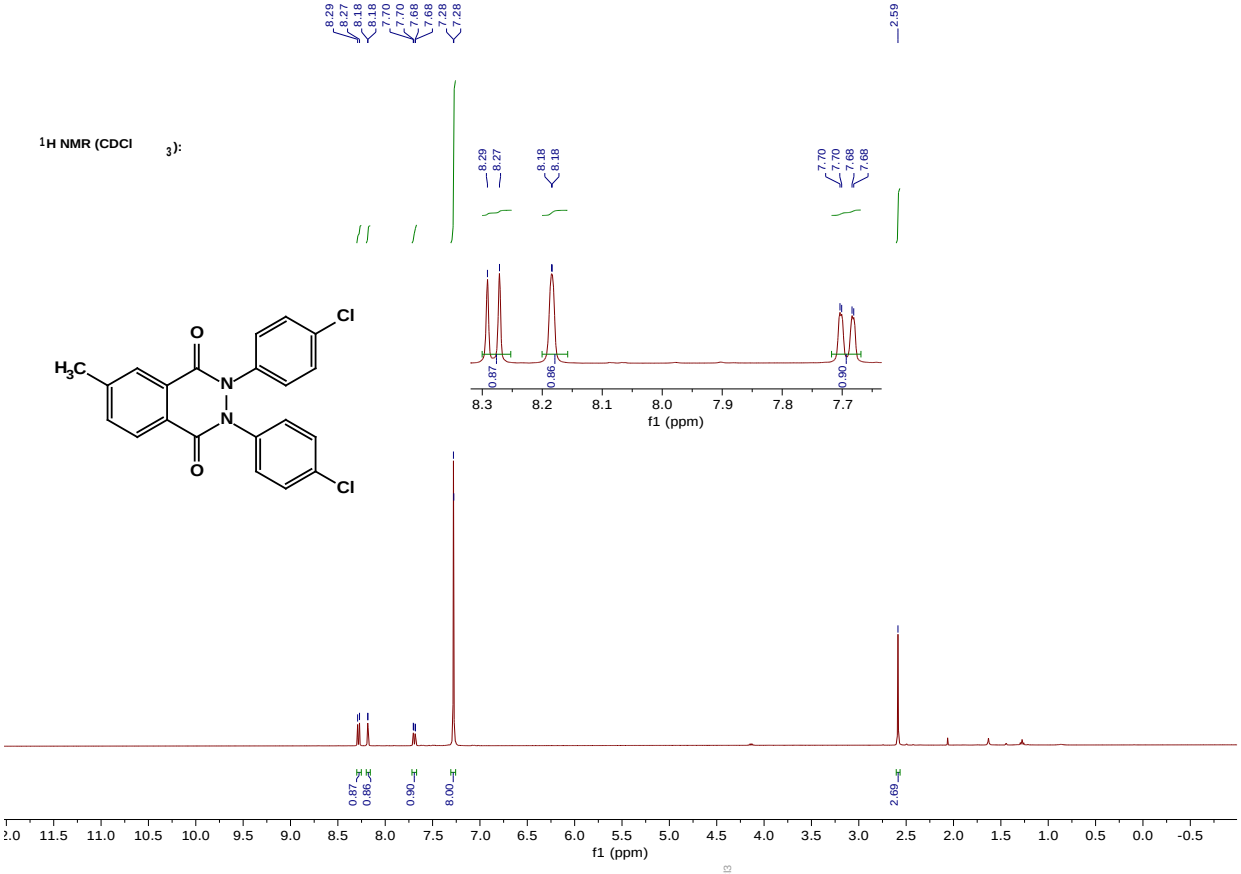

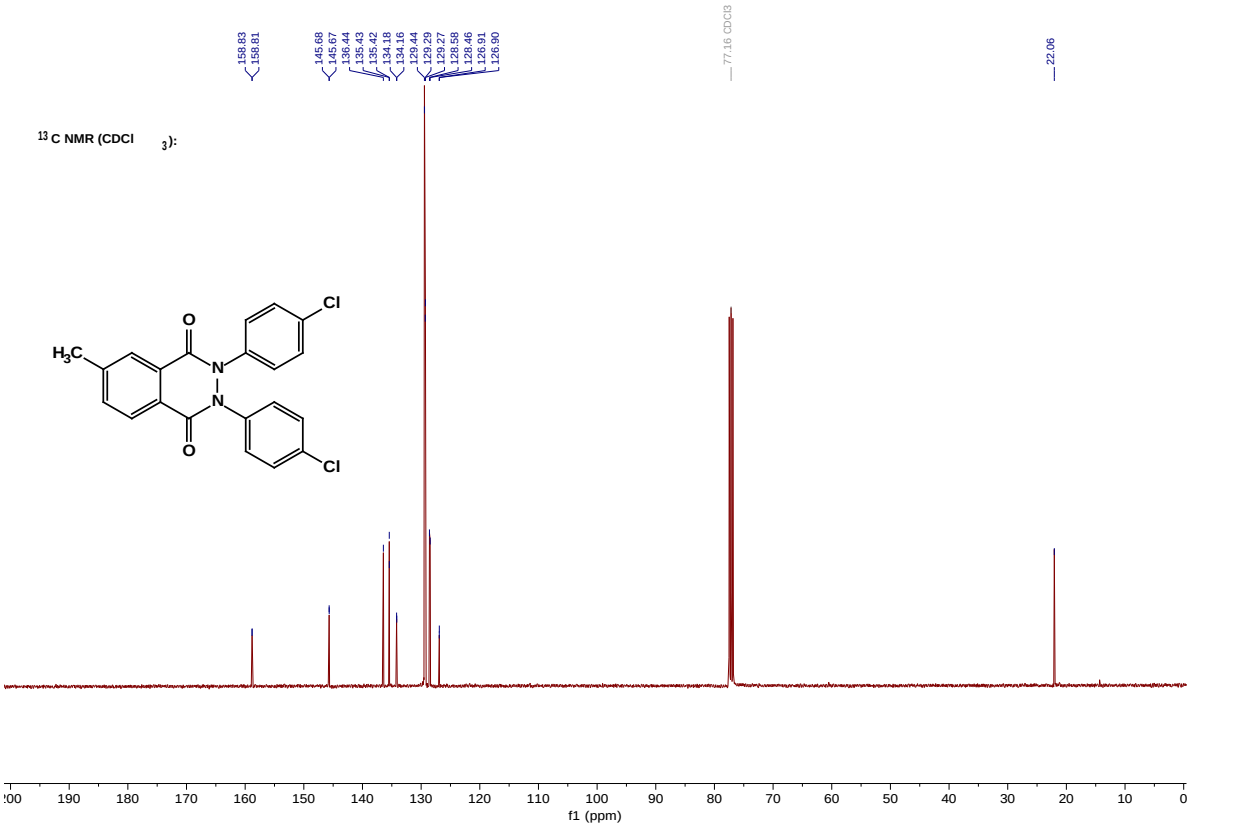

2,3-Diphenyl-2,3-dihydrophthalazin-1,4-dione (2p)

^{1}H NMR (CDCl$_3$):

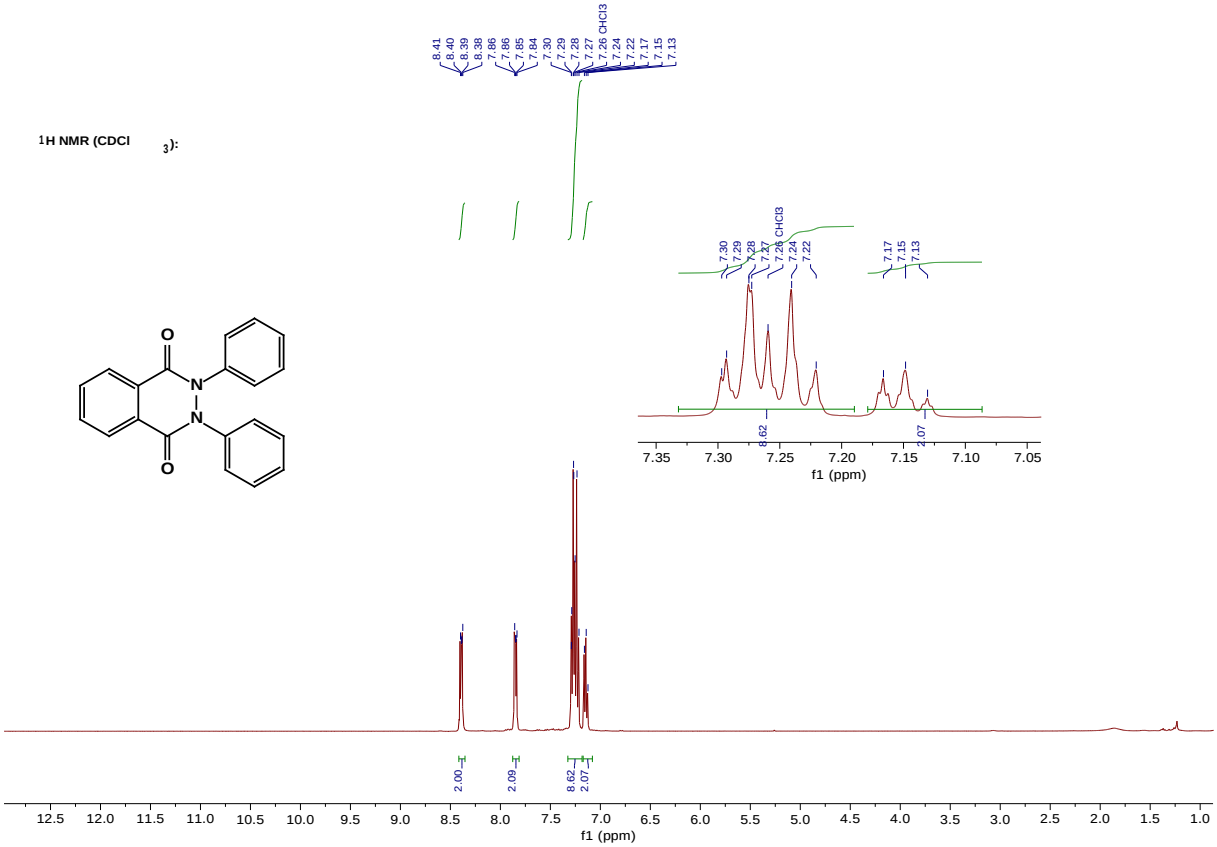

^{13}C NMR (CDCl$_3$):

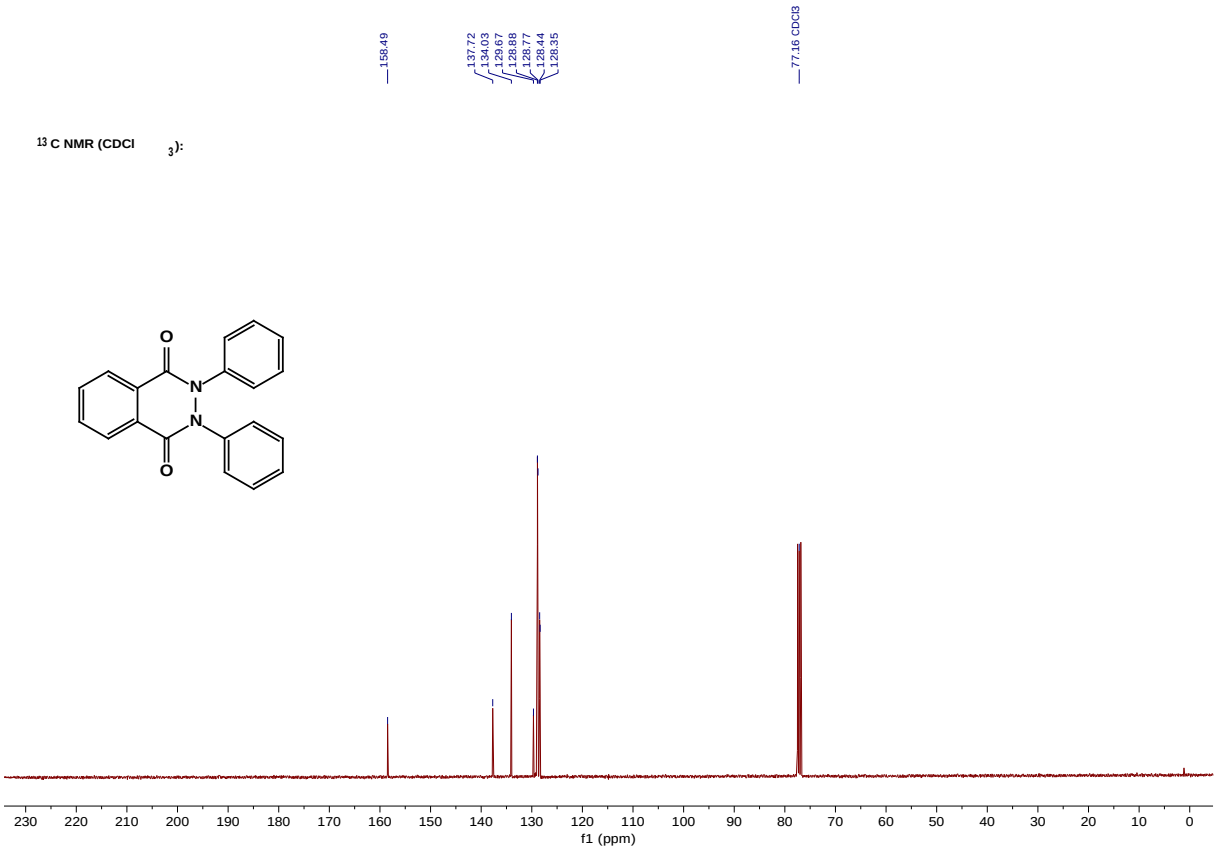

4,4‘-Dichloroazobenzene (5)

^{1}H NMR ($CDCl_3$):

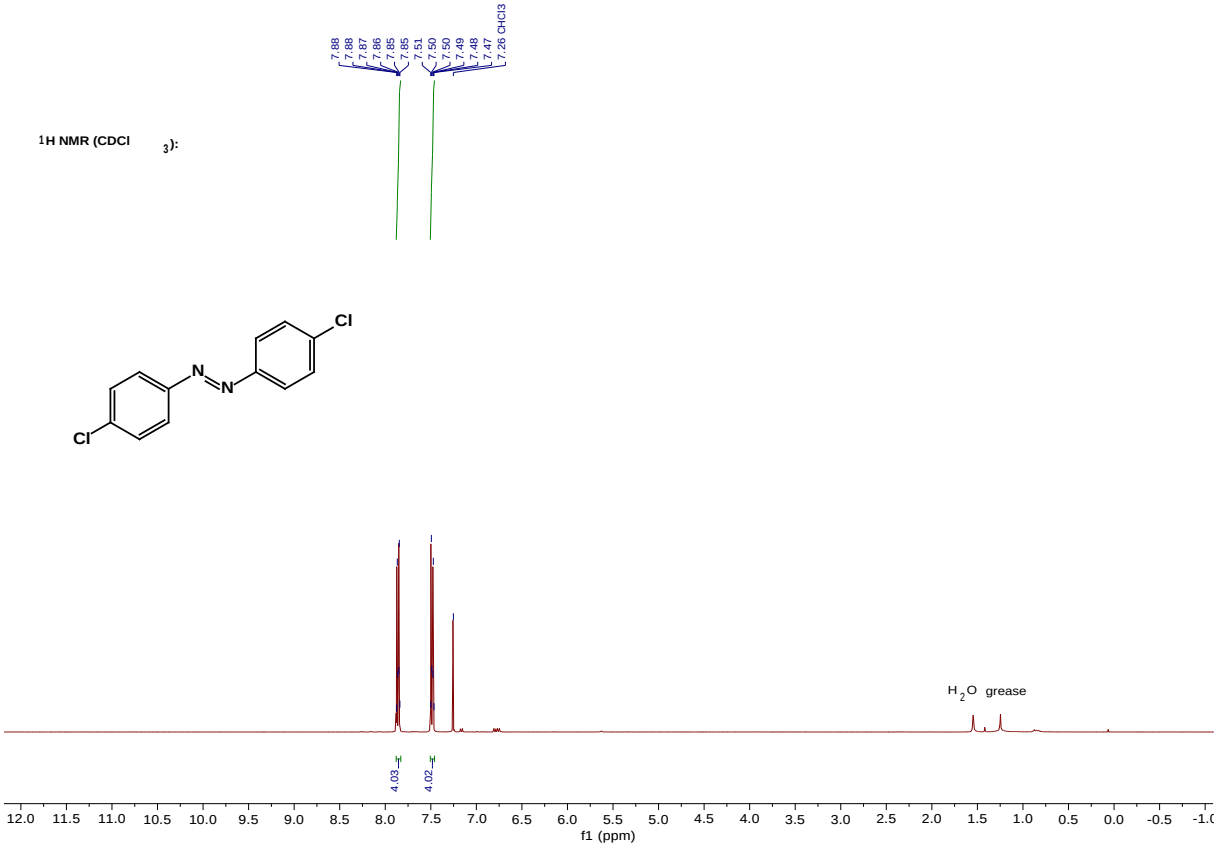

References

[1] W. L. F. Armarego, C. Chai Li Lin, *Purification of laboratory chemicals*, BH Butterworth-Heinemann/Elsevier, Amsterdam, **2013**.

[2] S. Berger, S. Braun, H.-O. Kalinowski, *NMR-Spektroskopie von Nichtmetallen*, Thieme, Stuttgart, **1994**.

[3] G. M. Sheldrick, *SHELXS97* and *SHELXL97: Programm for the Refinement of Crystal Structures;* Dept. of Structural Chemistry, University of Göttingen: Germany, **1997**

[4] F. L. Dunlap, F. W. Cummer, *J. Am. Chem. Soc.* **1903**, *25*, 612–621.

[5] C. J. Perry, Z. Parveen,. *J. Chem. Soc., Perkin Trans. 2* **2001**, 512–521.

[6] G. D. de Toranzo, J. A. Brieux, *J. Am. Chem. Soc.***1967**, *10*, 982–983.

[7] W. R. Roderick, P. L. Bathia, *J. Org. Chem.* **1963**, *28*, 2018–2024.

[8] C. Gütz, B. Klöckner, S. R. Waldvogel, *Org. Process Res. Dev.* **2016**, *20*, 26–32.

[9] A. Wiebe, D. Schollmeyer, K. M. Dyballa, R. Franke, S. R. Waldvogel, *Angew. Chem. Int. Ed.* **2016**, *55*, 11801–11805; *Angew. Chem.* **2016**, *128*, 11979–11983.

[10] L. Hoesch, M. Karpf, E. Dunkelblum, A. S. Dreiding, *Helv. Chim. Acta* **1977**, *60*, 816–830.

[11] Y. K. Yee, A. L. Tebbe, J. H. Linebarger, D. W. Beight, T. J. Craft, D. Gifford-Moore, T. Goodson Jr., D. K. Herron, V. J. Klimkowski, J. A. Kyle, J. S. Sawyer, G. F. Smith, J. M. Tinsley, R. D. Towner, L. Weir, M. R. Wiley, *J. Med. Chem.* **2000**, *43*, 873–882.

[12] N. Sakai, K. Fujii, S. Nabeshima, R. Ikeda, T. Konakahara, *Chem. Commun.* **2010***, 46*, 3173–3175.

JACS
JOURNAL OF THE AMERICAN CHEMICAL SOCIETY
Article
pubs.acs.org/JACS

Insights into the Mechanism of Anodic N–N Bond Formation by Dehydrogenative Coupling

Tile Gieshoff,[†,‡,⊥] Anton Kehl,[†] Dieter Schollmeyer,[†] Kevin D. Moeller,[⊥] and Siegfried R. Waldvogel*[,†,‡]

[†]Institute of Organic Chemistry, Johannes Gutenberg University Mainz, 55128 Mainz, Germany
[‡]Graduate School Materials Science in Mainz, Johannes Gutenberg University Mainz, 55128 Mainz, Germany
[⊥]Department of Chemistry, Washington University, St. Louis, Missouri 63130, United States

Supporting Information

ABSTRACT: The electrochemical synthesis of pyrazolidine-3,5-diones and benzoxazoles by N–N bond formation and C,O linkage, respectively, represents an easy access to medicinally relevant structures. Electrochemistry as a key technology ensures a safe and sustainable approach. We gained insights in the mechanism of these reactions by combining cyclovoltammetric and synthetic studies. The electron-transfer behavior of anilides and dianilides was studied and led to the following conclusion: The N–N bond formation involves a diradical as intermediate, whereas the benzoxazole formation is based on a cationic mechanism. Besides these studies, we developed a synthetic route to mixed dianilides as starting materials for the N–N coupling. The compatibility with valuable functionalities like triflates and mesylates for follow-up reactions as well as the comparison of different electrochemical set-ups also enhanced the applicability of this method.

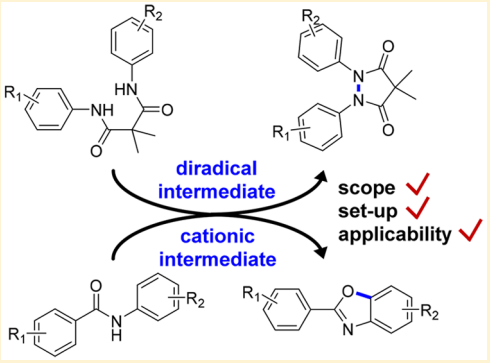

INTRODUCTION

Pyrazolidine-3,5-diones and benzoxazoles are important heterocyclic motifs appearing in natural products and drugs.[1] Phenylbutazon,[2] pseudopteroxazole,[3] UK-1,[4] and ERB-041[5] represent just a few examples of the medicinally relevant compounds that possess these key ring skeletons. Because of this relevance, several methods to access such heterocyclic motifs have been reported.[6] Nevertheless, limitations regarding the sustainability and generality of these reactions are consistent with the need for the development of alternative methods. For example, the conventional synthesis of pyrazolidine-3,5-diones requires the use of highly carcinogenic *N,N′*-diarylhydrazines. This leads to the need for additional safety precautions and challenges in connection with reaction scale-up.[7] Moreover, complex substitution patterns require additional synthetic steps following construction of the central ring skeleton.[8] For the synthesis of benzoxazoles, the principal synthetic strategies are based on condensation reactions involving 2-aminophenols or coupling reactions of anilide substrates. These approaches usually require elevated temperatures and catalysts and result in significant reagent waste.[9]

As an alternative, we recently reported a simple route to pyrazolidine-3,5-diones via the electrochemical formation of a N–N bond. The reactions can be conducted in a simple undivided cell at constant current conditions.[10] This approach dispenses with the need for toxic *N,N′*-diarylhydrazines and gives a straightforward access to more complex substitution patterns. When the approach was applied to the formation of six-membered rings, we learned that a slower N–N bond formation led to competitive formation of a benzoxazole ring by the generation of a C,O linkage (Scheme 1).[11] While the yield of the reaction was low, the finding suggested that it might be possible to convert easily accessible anilides into either a pyrazolidine-3,5-dione or benzoxazoles by the control of reactions conditions and selection of substrates. However, developing such a strategy requires an understanding of the reaction mechanisms that govern product formation in two

Scheme 1. Competing Formation of the N–N and C–O Bonds

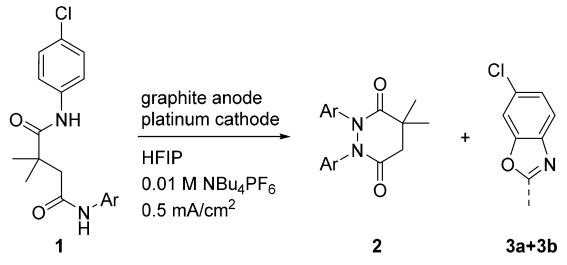

Ar = 4-chlorophenyl
HFIP = 1,1,1,3,3,3-hexafluoroisopropanol

Received: July 18, 2017
Published: August 9, 2017

DOI: 10.1021/jacs.7b07488
J. Am. Chem. Soc. 2017, 139, 12317–12324

competing pathways (Scheme 2). We report here those mechanistic details along with a general strategy for elucidating

Scheme 2. Electrochemical Formation of Pyrazolidine-3,5-diones and Benzoxazoles

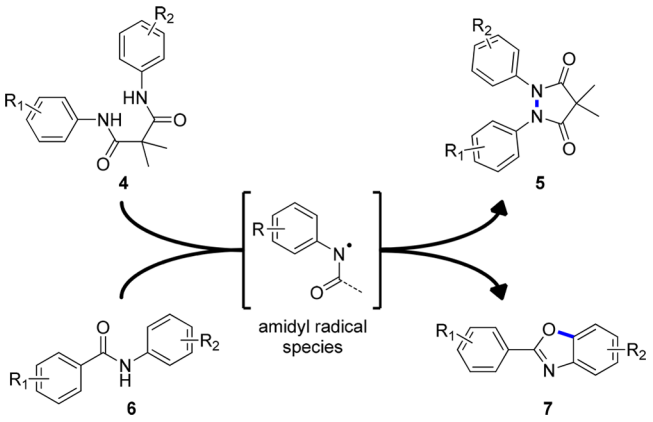

the pathways that originate from the generation of an amidyl radical intermediate under oxidative conditions.

As suggested in the preceding statement, the key reactive species central to both reaction pathways is an amidyl radical. The structure, generation, and reactivity of such amidyl radicals are important topics in contemporary research because the intermediates play a role in rearrangement reactions, cyclizations, and hydroamination reactions. The generation of amidyl radicals typically relies on the cleavage of halogenated amides.[12] In contrast, the electrochemical approach used here allows for the direct formation of the intermediates from an amide, and hence the generation of amidyl radicals from non-activated starting materials. The use of electrochemistry for the oxidation reactions was selected because of the opportunities it provides for sustainability and extraordinary reaction pathways.[13] In the current reactions, only a minimal amount of waste is generated, and electric current serves as an inexpensive and renewable redox reagent. The use of a low supporting electrolyte concentration (0.01 M) and 1,1,1,3,3,3-hexafluoroisopropanol (HFIP) as a recyclable solvent minimized both reagent use and the fluorine footprint of the reaction. HFIP has a key role in these transformations, since it exclusively enables efficient conversions due to its radical stabilizing properties.[14]

Work to understand the mechanism of the current reactions initially focused on the formation of N–N bonds. This effort was motivated by the synthetic potential of the reactions and the opportunity to further enhance that potential by expanding the scope of the reactions to include substituents (like triflates[15] or mesylates[16]) that are compatible with further elaboration of the products. The key, of course, is understanding how such substituents alter the reactivity of the intermediates involved, an understanding that impacts not only the current reactions but potentially a wide variety of oxidative processes.

RESULTS AND DISCUSSION

Elucidation of Mechanistic Assumptions. The electrochemical N–N bond formation reaction is initiated by the direct oxidation of the anilide at the anode. After a single electron transfer (SET; see Scheme 3), the radical cation formed is more acidic than the corresponding anilide by several orders of magnitude.[17] Deprotonation of the radical cation is fast and, in this case, can be supported by cathodically

Scheme 3. General Steps of the Anilide Oxidation and Possible Mechanisms of the N–N Bond Formation To Give Pyrazolidine-3,5-diones

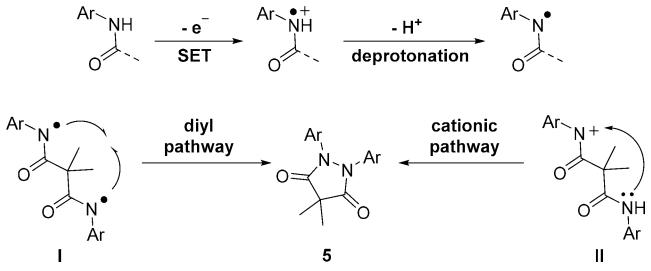

generated alcoholate anions derived from HFIP. After generation of the amidyl radical, there are two possible mechanistic pathways that can be followed. One possibility is that the amidyl radical will be oxidized again at the anode to form a cation (**II**). This cation is then trapped by the second anilide to form the N–N bond. The second involves an oxidation not of the amidyl radical but of the second anilide present in the substrate. In this case, the N–N bond would be formed by an intramolecular recombination of diradical **I**.

In order to differentiate these possibilities, it is important to understand the oxidation potentials involved. If the oxidation potential (E_{ox}) of the amidyl radical (see Scheme 2) is lower than the oxidation potential of the other anilide site, the formation of cation **II** would be favored. If the oxidation potential of the second anilide is lower than the amidyl radical, then the formation of diradical **I** would be promoted. To gain insight into these relative oxidation potentials, we undertook an electroanalytical study to complement the synthetic investigations. It was our hope that a combination of oxidation potential measurements and synthetic verification of the insights provided would allow us to distinguish between the two possible mechanistic pathways.

Cyclovoltammetric Measurements of Test Substrates. Since it is not possible to measure the oxidation potential of an isolated anilide moiety in a dianilide, the oxidation potentials were measured for a monoanilide test substrate. Pivaloyl anilides with different substitution patterns were used to test the electronic parameters required for a successful reaction. The substrates were easily accessible by treatment of the corresponding anilines with pivaloyl chloride. Each substrate was then investigated by cyclic voltammetry in order to determine the oxidation potential for both the initial anilide ($E_{ox,1}$) and the resulting amidyl radical ($E_{ox,2}$) (Scheme 4).

Scheme 4. Oxidation Steps of Anilides

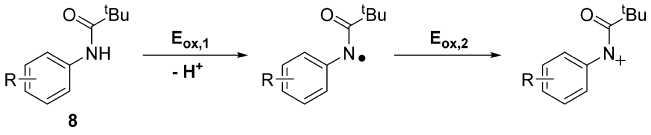

Figure 1 displays the cyclic voltammograms of the pivaloyl-derivatized anilines. The blank measurement reveals a potential limit of the electrolyte around 1.8 and −0.5 V vs (FcH/FcH^+). In the voltammograms of compounds **8a** and **8c–8g**, two distinct oxidation peaks are visible. Depending on the substitution pattern, the $E_{ox,1}$ peak can overlap with the current at the potential limit, leading to "shoulder-shaped" peaks. This becomes most visible at substrate **8f**. Since it demands a higher

DOI: 10.1021/jacs.7b07488
J. Am. Chem. Soc. 2017, 139, 12317–12324

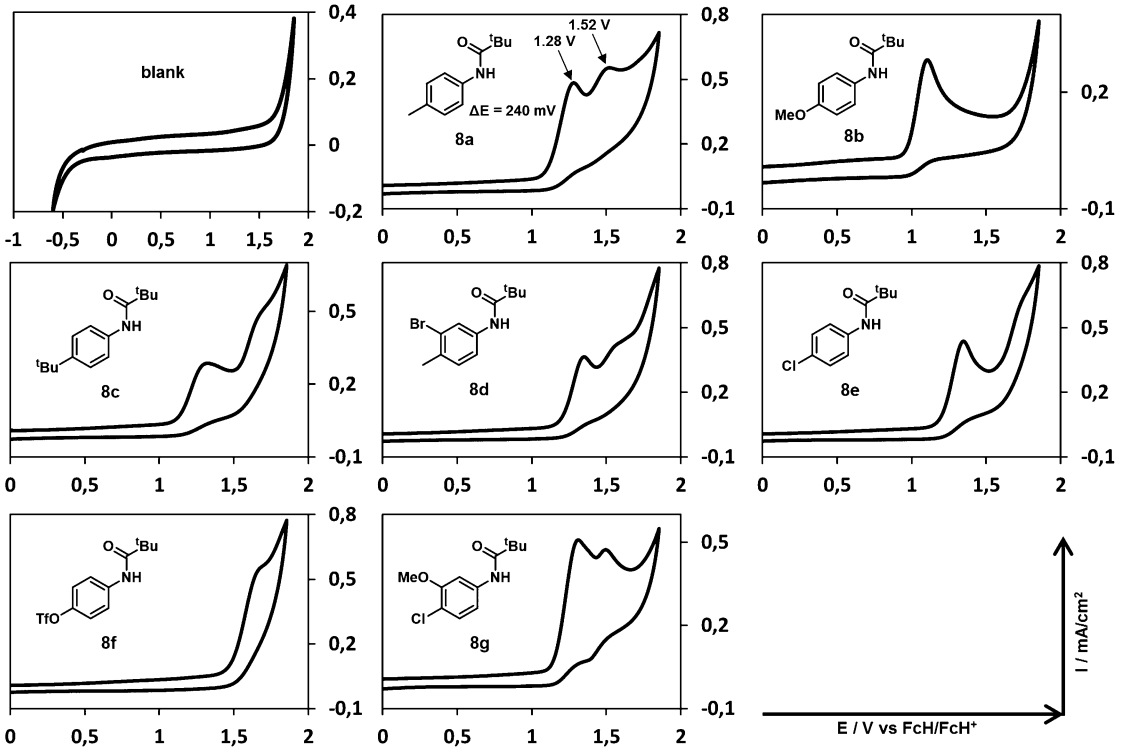

Figure 1. Cyclic voltammograms of pivaloyl anilides as test compounds. Conditions: 1 mM substrate in 0.1 M NBu_4PF_6 (5 mL); WE, glassy carbon; CE, glassy carbon; RE, Ag/AgCl in saturated LiCl in EtOH; scan ratec 200 mV/s); final reference vs ferrocene (FcH/FcH^+).

voltage to oxidize the corresponding amidyl radical, the peak for the $E_{ox,2}$ step frequently shows this behavior. In the case of the triflate-substituted derivative (**8f**), $E_{ox,2}$ is completely buried under the potential limit wave. The results of the cyclovoltmmetric measurements are in accordance with the electron density of the aromatic ring. The voltage difference of $E_{ox,1}$ and $E_{ox,2}$ depends on the substituents on the rings and their ability to stabilize cation formation. For example, *para*-methyl groups lead to a smaller voltage difference (**8a**, 240 mV, and **8d**, 230 mV) than other substrates (**8c**, 380 mV, and **8e**, 410 mV). For substrate **8b** with the even more electron-releasing *para*-methoxy group, no difference between the two oxidation potentials was observed. The second oxidation step is favored, since the cation formed is stabilized by resonance by the methoxy group as a quinone imine-like structure. Substrate **8g** results in a differently shaped voltammogram with a low peak current of the $E_{ox,2}$ step. The small current seen for the amidyl oxidation is consistent with decomposition of the amidyl radical, a suggestion that manifests at the low yield of product obtained from reactions with this substrate (see below). A rationale might be the interplay of the electron-withdrawing chloro substituent and the strong electron-releasing methoxy group, potentially leading to polymerization and decomposition. Table 1 displays the data for both oxidation steps.

This study was conducted to achieve an insight into the electron-transfer steps of the electrochemical oxidation of anilides. In general, the measurement of two distinct peaks for oxidations steps immediately suggested a diyl mechanism, since symmetric dianilides always lead to N–N bond formation.[10] With the success of these studies, attention was turned toward understanding the more complex dianilide systems.

Synthesis and Electrolysis of Mixed Dianilides. Based on oxidation potentials of the individual anilide moieties, we synthesized several mixed dianilides. We focused on the

Table 1. Oxidation Potentials $E_{ox,1}$ and $E_{ox,2}$ of Test Substrates vs FcH/FcH^+

entry	substrate	$E_{ox,1}$/V	$E_{ox,2}$/V
1	**8a**	1.28	1.52
2	**8b**	1.10	1.10
3	**8c**	1.31	1.69
4	**8d**	1.34	1.57
5	**8e**	1.35	1.76
6	**8f**	1.69	–
7	**8g**	1.31	1.49

combination of anilides with E_{ox} values, which based on the data presented would lead either to the formation of a diradical or to the formation of a cation. The goal was to probe what products would form from each of the proposed mechanistic pathways. In addition, the selective access to mixed dianilides enables both the synthesis of a variety of products and the ability to design a product that is ideally functionalized for further development in subsequent synthetic transformations. In order to gain access to a variety of dianilides, the synthetic route shown in Scheme 5 was developed. In this chemistry, a coupling reaction was performed using substrate **9** and a variety of anilines, the alcohol converted to an acid, and then a second coupling performed. The oxidation step in the sequence could be conducted with a catalytic amount of the chromate reagent in a number of cases.[18]

The detailed syntheses of the substrates can be found in the Supporting Information. One variation of note here is that the synthesis of the triflate derivatives **4c** and **4e** could not be obtained directly from the chemistry shown. In these cases, the phenol derivative was initially synthesized and the triflate group added with triflic anhydride in a subsequent step.[19]

DOI: 10.1021/jacs.7b07488
J. Am. Chem. Soc. 2017, 139, 12317–12324

Scheme 5. Synthetic Route to Mixed Dianilides

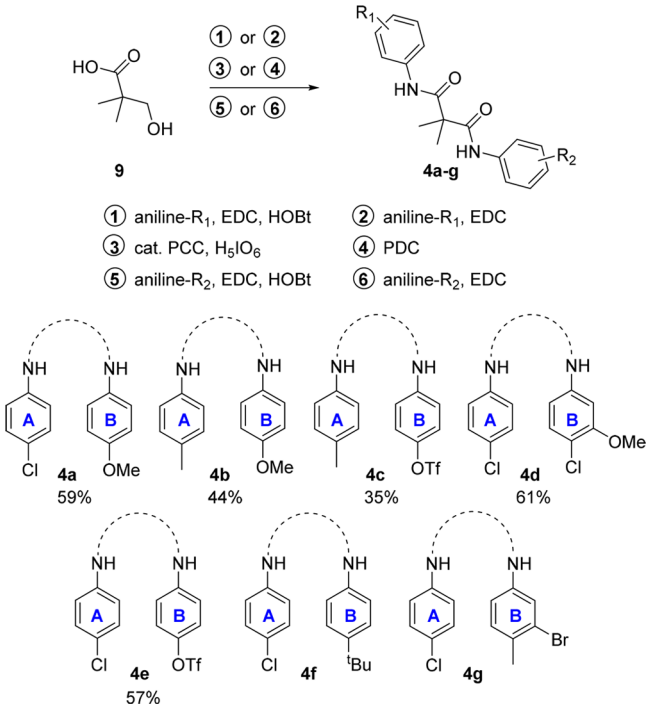

An overview of the oxidation potentials of the combined anilide sites and the corresponding products is displayed in Table 2. The electrolysis products of the conversion are shown in Chart 1. If we take the determined E_{ox} data of the test substrates into account for the prediction of the electron-transfer behavior, mixed dianilides **4a**, **4b**, and **4c** are expected to form a cationic intermediate, and substrates **4d**, **4e**, **4f**, and **4g** a diradical intermediate. For example, consider the data shown for substrate **4a**. In this case, both the oxidation potentials for anilide site B (1.10 V) are below the initial potential for site A (1.35 V). Hence, the second oxidation at site B should occur prior to the initial oxidation at site A; the conditions required for cation formation. Compare that data with those for substrate **4d**. Here, the second oxidation at site B occurs at a higher potential than the initial oxidation at site A, the conditions required for diradical behavior.

Table 2. Overview of the Electrolysis of Mixed Dianilides[a]

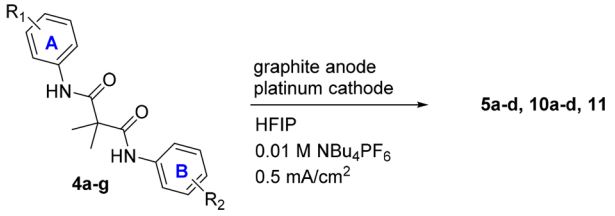

Entry	Substrate	Anilide site	$E_{ox,1}$ / V*	$E_{ox,2}$ / V*	Product
1	**4a**	A	1.35	1.76	**10a** (56%)
		B	1.10	1.10	
2	**4b**	A	1.28	1.52	**10b** (60%)
		B	1.10	1.10	
3	**4c**	A	1.28	1.52	**10c** (37%)
		B	1.69	-	
4	**4d**	A	1.35	1.76	**11** (10%) **5a** (11%)
		B	1.31	1.49	
5	**4e**	A	1.35	1.76	**5b** (34%)
		B	1.69	-	
6	**4f**	A	1.35	1.76	**5c** (49%)
		B	1.31	1.69	
7	**4g**	A	1.35	1.76	**5d** (55%)
		B	1.34	1.57	

[a]Red color indicates that these are the first two proceeding oxidation steps.

Chart 1. Electrolysis Products Derived from the Conversion of Mixed Dianilides[a]

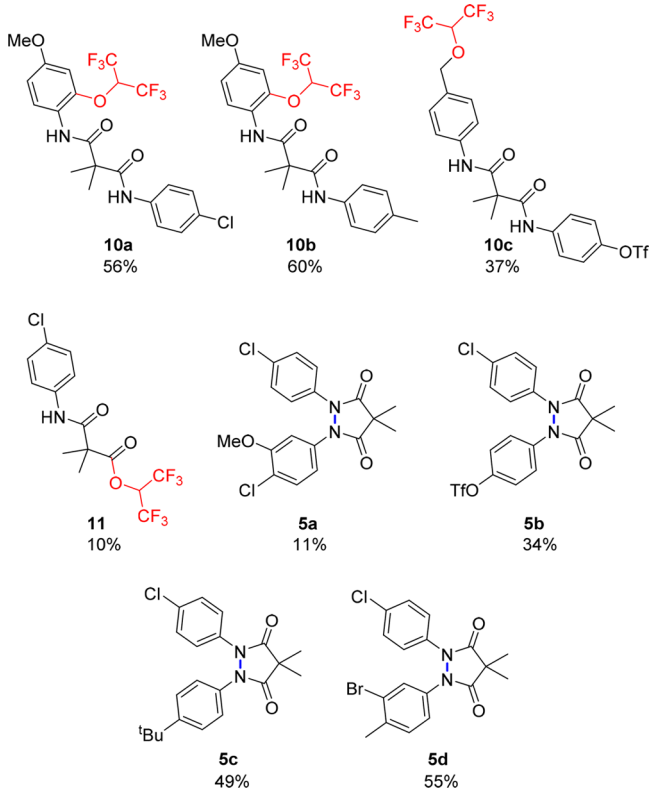

[a]Yields for substrate **5c** and **5d** were already reported in a former publication.

The electrolysis of the mixed dianilides revealed the formation of interesting products. Instead of forming the N–N bond, dianilides **4a**, **4b**, and **4c** formed HFIP incorporated products **10a**, **10b**, and **10c** and only small traces of N–N bond-formed products were detectable. When *para*-methoxy-substituted anilides were used, the addition of HFIP occurred at the aromatic *ortho*-position. In case of a *para*-methyl substitution, addition occurred at the benzylic position. This substitution is most consistent with the loss of a proton from the cationic intermediate (**IV**) to form an azoquinone methide derivative. This result would appear to confirm the accuracy of the prediction made on the basis of the oxidation potentials shown in Table 2. Compounds **4e**, **4f**, and **4g** formed pyrazolidine-3,5-diones **5b**, **5c**, and **5d** as products by an N–N bond formation. The E_{ox} values for these compounds were all consistent with the formation of a diradical intermediate. Substrate **4d** formed a product (**10d**) consistent with alcoholysis of the amidyl group along with the desired pyrazolidine-3,5-dione product (**5a**). This decomposition product is consistent with the different CV behavior for the

DOI: 10.1021/jacs.7b07488
J. Am. Chem. Soc. 2017, 139, 12317–12324

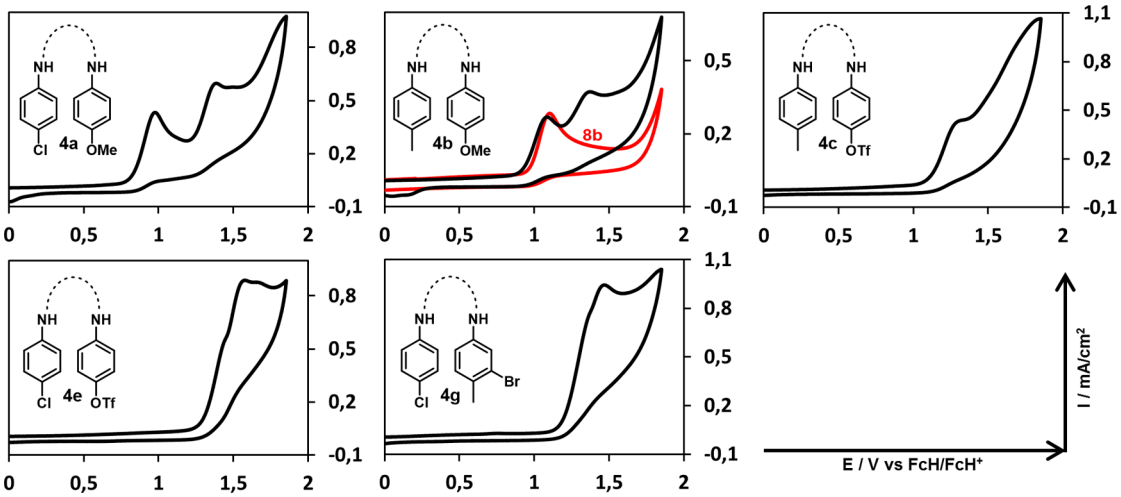

Figure 2. Cyclic voltammogram of mixed dianilides. Conditions: 1 mM substrate in 0.1 M NBu_4PF_6 (5 mL); WE, glassy carbon; CE, glassy carbon; RE, Ag/AgCl in saturated LiCl in EtOH; scan rate, 200 mV/s; final reference vs FcH/FcH^+.

group noted above in connection with Figure 1. Based solely on the oxidation potentials, N−N bond formation is more likely than cation formation, so at this time the mechanistic origin of the decomposition pathway remains unsolved. Competing diradical and cationic pathways are possible.

Cyclovoltammetric Measurements of Mixed Dianilides. Beside the cyclovoltmmetric study of the test substrates and the synthetic study, we were also interested in the electron-transfer behavior of the dianilides within a cyclic voltammetry study (Figure 2).

As expected, the voltammograms of the mixed dianilides demonstrate a different electron-transfer behavior for cation-forming and diradical-forming dianilides. The voltammograms of substrates **4a**, **4b**, and **4c** show a significant difference between the oxidation potentials of the two groups, whereas those of compounds **4e** and **4g** reveal two oxidation peaks very close to each other. These data once again suggest cation formation in **4a**−**4c** and diradical formation for substrates **4e** and **4g**. In this way, the data are again fully consistent with the observations made above. It appears that N−N bond formation is the result of a diradical intermediate (see Scheme 3, intermediate **I**).

Theoretical considerations also support this argument. The unpaired electron can populate both σ- and π-orbitals, while the exact structure depends on many factors, e.g., substitution pattern.[20] Moreover, there is an attractive interaction among σ-radical and σ^*-orbital. The corresponding cation is located in the π-orbital and stabilized by the aromatic ring. It is likely that a σ-radical facilitates the subsequent recombination, whereas a π-cation would exacerbates a selective cyclization reaction and rather leads to side reactions.

Adaption to the Benzoxazole Mechanism. As mentioned in the Introduction, much of this work was motivated by the opportunity to generate both the N−N bond-forming products and benzoxazole products from closely related substrates. The benzoxazole was initially an unexpected side product found in a reaction planned for N−N bond formation. With an understanding of how the N−N bond-forming reactions can be designed, we were a in position to tackle the challenge of selectively generating the benzoxazole ring system. One observation made during the synthesis of benzoxazoles[11] provided significant guidance for this endeavor. That observation is that a *para*-methyl substitution on the anilide significantly inhibits benzoxazole formation. Instead, the reactions tend to lead to HFIP ether derivatives (**6a**) in a fashion directly analogous to the earlier formation of product **10c**. This finding was initially unexpected, since *para*-methyl groups are beneficial for the generation of N−N bonds. This suggested that benzoxazole formation might be derived from the generation of a cationic intermediates. In such a case, the formation of amidyl cation (**III**) can lead to deprotonation at the benzylic carbon, the formation of an azoquinone methide (**IV**), and solvent trapping (Scheme 6). The combination of

Scheme 6. Solvent Trapping Product and the Cationic Intermediate in the Benzoxazole Formation

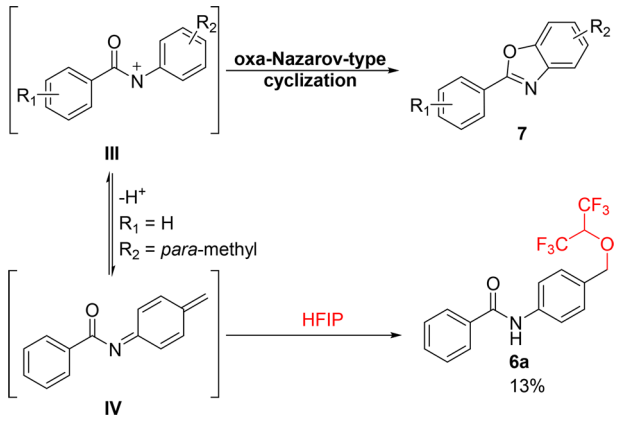

this finding with the mechanistic study above led us to conclude that the mechanism for the benzoxazole formation most likely proceeds through a cationic intermediate (**III**), which can undergo an oxa-Nazarov-type cyclization.[21]

With this knowledge, the design of new substrates for benzoxazole products becomes viable. In this context, it is interesting to note that, in the benzoxazole syntheses, the solvent trapping products that appear to interfere with the N−N bond-forming reactions above are not a problem, even when *para*-methoxy groups are present (Chart 1). This divergent behavior originates from a competition between carbonyl oxygen addition to the aryl ring (benzoxazole formation) and solvent (HFIP) trapping of the ring. This competition is shifted

DOI: 10.1021/jacs.7b07488
J. Am. Chem. Soc. 2017, 139, 12317−12324

toward solvent trapping when a dianilide is used as the substrate. It appears that hydrogen bonding between the carbonyl and the second anilide in the molecule lowers the nucleophilicity of the carbonyl oxygen and favors HFIP addition. The hydrogen bonding is detectable in crystallographic studies of substrate **10c** (see Supporting Information).

Optimization of Scope and Reaction Set-Up. With the mechanism for the reaction determined, we turned our attention toward evaluating the synthetic scope and utility of the reactions. In our previous work, *para*-chloro and *meta*-bromo substitutions were most valuable from a synthetic point of view. However, the latter only afforded the desired N–N product in a 33% yield. Moreover, the reactions were restricted to products that contained a para-substituent.[10] With the selective synthesis for mixed dianilides and the mechanistic insights in hand, these limitations could be addressed. To this end, the chemistry was explored for its compatibility with synthetically versatile triflate and mesylate groups. In addition, we investigated the influence of bulky *meta*-substitutions in order to determine if they would prevent side reactions at substituent-free *para*-positions. As shown in Chart 2, the

Chart 2. Extension of the Scope to Triflates, Mesylates, and *para*-Unblocked Derivatives

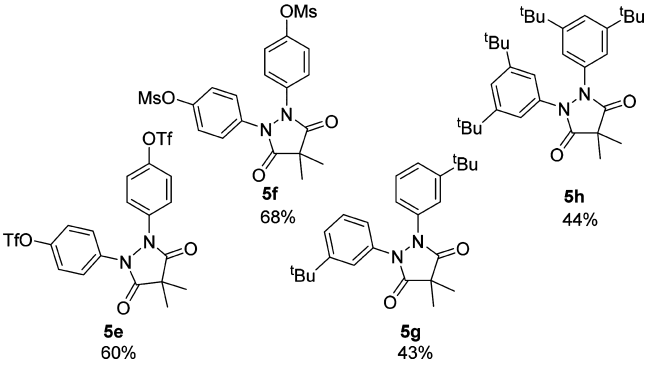

conversion of symmetric triflates and mesylates substrates into the desired products showed that the groups were tolerated by the reactions, and the use of a bulky *meta*-substituent did have a positive effect on the reactions.

The formation of **5b** was particularly interesting because it involved the generation of an unsymmetrical product wherein the two aromatic rings were synthetically differentiated, but the initial yield for this reaction was low (34%). When we worked on the benzoxazoles formation, we demonstrated the utility of varying the reaction set-up as a means of optimizing the yield for a particular product.[11] With several substrates, we tested the two main electrochemical set-ups used for constant current electrolysis with regard to their influence on the N–N bond formation (see Figure 3). Set-up **A** includes a beaker-type cell

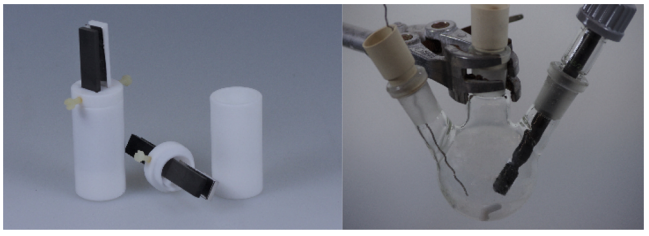

Figure 3. Set-ups **A** (left) and **B** (right).

with a flat isostatic graphite anode and a platinum plate cathode in a parallel orientation to each other.[22] Set-up **B** is based on a 25 mL three-necked flask with a reticulated vitreous carbon (RVC) anode and a platinum wire cathode placed angularly to each other. Chart 3 demonstrates that the performance of the

Chart 3. Comparison of Electrolysis Set-Up[a]

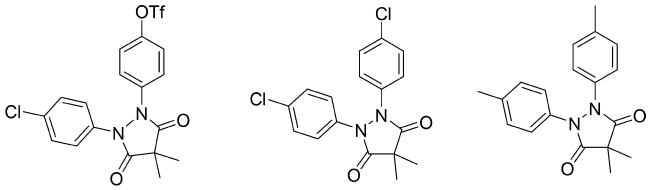

5b	**5i**	**5j**
34%[A]	89%[A]	52%[A]
84%[B]	91%[B]	43%[B]

[a]Yields for substrates **11e** and **11f** using set-up **A** were already reported in a previous publication, isolated from a 25 mL cell.[10]

cells was dependent on the substrate used. On one hand, compound **5b** was isolated in 84%, when set-up **B** was used. On the other hand, set-up **A** worked better with compound **5j**. Compound **5i** gives similar yields in both set-ups, but RVC as anode material enables higher currents and therefore a more time-efficient conversion. It is important to note that, for an initial pass, either set-up can be used to test the viability of a reaction. One can then adjust the nature of the reaction set-up after it is clear that the electrolysis works.

■ CONCLUSION

The advancement of electro-organic synthesis is dependent on both the development of new reactions of synthetic value and the development of the mechanistic insights necessary to make conclusions about and extend the scope of those reactions. In the example presented here, we outlined both the synthetic potential of anodic oxidations leading to amidyl radicals and subsequent N–N bond formation reaction and benzoxazole synthesis and the data supporting the mechanistic parameters that govern product formation. In addition, we highlighted how a combination of cyclovoltammetric and synthetic studies can be used to gain those insights. N–N bond formation in the systems studied is the result of a diradical coupling mechansim, whereas benzoxazole formation is the result of a cationic oxa-Nazarov-type cyclization. These insights led to the formation of products from mixed dianilide substrates, the use of synthetically valuable triflate and mesylate substrates in the reactions, and an important illustration of how different reaction set-ups can be used to optimize an electro-organic conversion.

■ EXPERIMENTAL SECTION

Electrolysis Protocol, Set-up A. A solution of 0.2 mmol of electrolysis substrate and 19 mg of tetrabutylammonium hexafluorophosphate (0.01 M) in 5 mL of hexafluoroisopropanol (HFIP) is placed in a 5 mL Teflon cell.[22] The solution is electrolyzed with a current of 0.5 mA/cm^2 (active electrode area 1.6 cm^2) using an isostatic graphite plate anode and a platinum plate cathode, until 2–3 F is applied. The conversion is controlled via gas chromatography. After electrolysis, the solvent is recovered by distillation and the product isolated via column chromatography on silica with mixtures of cyclohexane and ethyl acetate.

Electrolysis Protocol, Set-up B. A solution of 0.4 mmol of anilide derivative and 38 mg of tetrabutylammonium hexafluorophosphate (0.01 M) in 10 mL of HFIP is placed in a 25 mL three-necked round-

DOI: 10.1021/jacs.7b07488
J. Am. Chem. Soc. 2017, 139, 12317–12324

bottom flask. A reticulated vitreous carbon (100 PPI) anode and a platinum wire cathode is placed in the solution and sonicated for 30 s. The solution is electrolyzed with a constant current of 8.4 mA until 2–2.2 F is applied. Full conversion is checked by thin-layer chromatography. After electrolysis, the solvent is removed via distillation and product isolated via column chromatography on silica with mixtures of hexanes and ethyl acetate.

Cyclic Voltammetry Protocol. A 1 mM solution of substrate in 5 mL of HFIP (0.1 M $TABPF_6$) is placed in a 10 mL cell. Cyclic voltammetry is performed with a 200 mV/s scan rate using a glassy carbon working electrode (WE), glassy carbon counter electrode (CE), and Ag/AgCl reference electrode (RE) in saturated LiCl in EtOH. The peak potentials are referenced versus FcH/FcH^+, and in case of an overlap, the exact value is determined by calculating the minimum of the slope.

Synthesis and Characterization of Electrolysis Products. *N-(4-Chlorophenyl)-N′-(2-(1,1,1,3,3,3-hexafluoropropan-2-yloxy)-4-methoxy)-2,2-dimethylmalondiamide (**10a**).* Electrolysis in set-up **A** yielded 57 mg of colorless oil (0.11 mmol, 56%): ^{1}H NMR (400 MHz, $CDCl_3$) δ = 9.20 (s, 1H), 8.36 (s, 1H), 8.21 (d, J = 9.0 Hz, 1H), 7.63–7.48 (m, 2H), 7.38–7.24 (m, 2H), 6.72 (dd, J = 9.0, 2.6 Hz, 1H), 6.61 (d, J = 2.6 Hz, 1H), 4.91 (hept, J = 5.6 Hz, 1H), 3.83 (s, 3H), 1.68 (s, 6H); ^{13}C NMR (101 MHz, $CDCl_3$) δ = 172.58, 170.26, 157.26, 147.89, 136.43, 129.22, 128.91, 123.30, 121.35, 121.16, 120.78 (q, J = 280.9 Hz), 108.57, 101.97, 76.53 (hept, J = 33.7 Hz), 55.75, 50.89, 24.03; ^{19}F NMR (377 MHz, $CDCl_3$) δ = −74.64; HRMS for $C_{21}H_{19}{}^{35}ClF_6N_2O_4$ (ESI+) $[M+Na]^+$: calcd 535.0835, found 535.0845.

*N-(2-(1,1,1,3,3,3-Hexafluoropropan-2-yloxy)-4-methoxy)-N′-(4-methylphenyl)-2,2-dimethylmalondiamide (**10b**).* Electrolysis in set-up **A** yielded 58 mg of colorless oil (0.12 mmol, 58%): ^{1}H NMR (400 MHz, $CDCl_3$) δ = 8.88 (s, 1H), 8.22 (s, 1H), 8.22 (d, J = 9.0 Hz, 1H), 7.54–7.39 (m, 2H), 7.21–7.08 (m, 2H), 6.71 (dd, J = 9.0, 2.5 Hz, 1H), 6.61 (d, J = 2.3 Hz, 1H), 4.94 (hept, J = 5.5 Hz, 1H), 3.81 (s, 3H), 2.32 (s, 3H), 1.68 (s, 6H); ^{13}C NMR (101 MHz, $CDCl_3$) δ = 172.45, 170.29, 157.10, 147.90, 135.21, 133.99, 129.39, 123.29, 121.65 (q, J = 280.9 Hz), 121.56, 120.01, 108.49, 101.96, 76.22 (hept, J = 33.8 Hz), 55.70, 50.87, 23.99, 20.83; ^{19}F NMR (377 MHz, $CDCl_3$) δ = −74.63; HRMS for $C_{22}H_{22}F_6N_2O_4$ (ESI+) $[M + Na]^+$: calcd 515.1381, found 515.1390.

*N-(4-(1-(1,1,1,3,3,3-Hexafluoropropan-2-yloxy)methyl)phenyl)-N′-(4-trifluoromethylsulfonyloxyphenyl)-2,2-dimethylmalondiamide (**10c**).* Electrolysis in set-up **A** yielded 45 mg of colorless solid (0.07 mmol, 37%): mp 102.0–103.0 °C (cyclohexane); ^{1}H NMR (400 MHz, $CDCl_3$) δ = 8.90 (s, 1H), 8.33 (s, 1H), 7.67–7.61 (m, 2H), 7.59–7.52 (m, 2H), 7.36–7.30 (m, 2H), 7.25–7.19 (m, 2H), 4.82 (s, 2H), 4.10 (hept, J = 5.9 Hz, 1H), 1.68 (s, 6H ^{13}C NMR (101 MHz, $CDCl_3$) δ = 171.90, 171.29, 145.57, 137.69, 137.53, 131.35, 129.60, 121.97, 121.54, 121.51 (q, J = 284.5 Hz), 120.65, 118.71 (q, J = 320.5), 75.37, 74.26 (hept, J = 33.3 Hz), 50.91, 24.12; ^{19}F NMR (377 MHz, $CDCl_3$) δ = −73.95, −74.74; HRMS for $C_{22}H_{19}F_9N_2O_6$ (ESI+) $[M+H]^+$: calcd 611.0898, found 611.0916.

*N-(4-Chlorophenyl)-O-(1,1,1,3,3,3-hexafluoropropan-2-yl)-2,2-dimethylmalonmonoamide (**11**).* Electrolysis in set-up **A** yielded 8 mg of colorless oil (0.020 mmol, 10%): ^{1}H NMR (400 MHz, $CDCl_3$) δ = 7.86 (s, 1H), 7.49–7.42 (m, 2H), 7.38–7.31 (m, 2H), 5.83 (hept, J = 6.0 Hz, 1H), 1.68 (s, 6H ^{13}C NMR (101 MHz, $CDCl_3$) δ = 171.75, 167.77, 135.62, 130.12, 129.13, 121.60, 120.16 (q, J = 282.6 Hz), 67.25 (hept, J = 35.2 Hz), 50.84, 23.30; ^{19}F NMR (377 MHz, $CDCl_3$) δ = −74.32; HRMS for $C_{14}H_{12}{}^{35}ClF_6NO_3$ (ESI+) $[M+H]^+$: calcd 392.0483, found 392.0484.

*1-(4-Chlorophenyl)-2-(3-methoxy-4-chlorophenyl)-4,4-dimethylpyrazolidine-3,5-dione (**5a**).* Electrolysis in set-up **A** yielded 8 mg of colorless oil (0.021 mmol, 11%): ^{1}H NMR (400 MHz, $CDCl_3$) δ = 7.37–7.32 (m, 2H), 7.32–7.27 (m, 3H), 7.00 (d, J = 2.4 Hz, 1H), 6.79 (dd, J = 8.5, 2.4 Hz, 1H), 3.86 (s, 3H), 1.53 (s, 6H); ^{13}C NMR (101 MHz, $CDCl_3$) δ = 174.12,174.09, 155.31, 135.29, 134.54, 132.49, 130.28, 129.35, 123.20, 120.71, 114.18, 106.63, 56.27, 44.39, 21.81; HRMS for $C_{18}H_{16}{}^{35}Cl_2N_2O_3$ (ESI+) $[M+H]^+$: calcd 379.0611, found 379.0612.

*1-(4-Chlorophenyl)-2-(4-trifluoromethylsulfonyloxyphenyl)-4,4-dimethylpyrazolidine-3,5-dione (**5b**).* Electrolysis in set-up **B** yielded 146 mg of colorless solid (0.34 mmol, 84%): mp 89.0–89.5 °C (EtOAc); ^{1}H NMR (400 MHz, $CDCl_3$) δ = 7.47–7.41 (m, 2H), 7.38–7.32 (m, 2H), 7.31–7.25 (m, 4H), 1.52 (s, 6H); ^{13}C NMR (101 MHz, $CDCl_3$) δ = 174.24,174.04, 147.05, 135.68, 134.46, 132.65, 129.47, 123.12, 123.07, 122.19, 44.30, 21.82; ^{19}F NMR (377 MHz, $CDCl_3$) δ = −73.95; HRMS for $C_{18}H_{14}{}^{35}ClF_3N_2O_5S$ (ESI+) $[M + Na]^+$: calcd 485.0162, found 485.0158.

*1,2-Bis(4-trifluoromethylsulfonyloxyphenyl)-4,4-dimethylpyrazolidine-3,5-dione (**5e**).* Electrolysis in set-up **B** yielded 137 mg of colorless solid (0.24 mmol, 60%): mp 90.4–91.4 °C (EtOAc); ^{1}H NMR (400 MHz, $CDCl_3$) δ = 7.48–7.41 (m, 4H), 7.33–7.27 (m, 4H),), 1.54 (s, 6H); ^{13}C NMR (101 MHz, $CDCl_3$) δ = 174.11, 147.18, 135.74, 122.99, 122.36, 118.63 (q, J = 320.8 Hz), 44.30, 21.85; ^{19}F NMR (377 MHz, $CDCl_3$) δ = −73.94. Anal. Calcd for $C_{19}H_{14}F_6N_2O_8$: C, 39.59; H, 2.45; N, 4.86; S, 11.12. Found: C, 39.74; H, 2.69; N, 4.83; S, 11.14.

*1,2-Bis(4-mesylphenyl)-4,4-dimethylpyrazolidine-3,5-dione (**5f**).* Electrolysis in set-up **B** with 0.31 mmol of dianilide in 8 mL of HFIP (30 mg of NBu_4PF_6) yielded 99 mg of colorless solid (0.21 mmol, 68%): mp 140.0–141.0 °C (EtOAc); ^{1}H NMR (400 MHz, $CDCl_3$) δ = 7.44–7.38 (m, 4H), 7.33–7.27 (m, 4H), 1.52 (s, 6H); ^{13}C NMR (101 MHz, $CDCl_3$) δ = 174.28, 147.08, 134.92, 123.26, 122.91, 44.27, 37.57, 21.82; HRMS for $C_{19}H_{20}N_2O_5S_2$ (ESI+) $[M + Na]^+$: calcd 491.0559, found 491.0566.

*1,2-Bis(3-(1,1-dimethylethyl)phenyl)-4,4-dimethylpyrazolidine-3,5-dione (**5g**).* Electrolysis in set-up **A** yielded 34 mg of colorless oil (0.087 mmol, 43%): ^{1}H NMR (400 MHz, $CDCl_3$) δ = 7.30–7.24 (m, 2H), 7.23–7.17 (m, 6H), 1.56 (s, 6H), 1.19 (s, 18H); ^{13}C NMR (101 MHz, $CDCl_3$) δ = 173.12, 152.09, 135.25, 128.57, 123.56, 120.06, 44.54, 34.70, 31.06, 21.81; HRMS for $C_{25}H_{32}N_2O_2$ (ESI+) $[M + Na]^+$: calcd 415.2361, found 415.2366.

*1,2-Bis(3,5-di(1,1-dimethylethyl)phenyl)-4,4-dimethylpyrazolidine-3,5-dione (**5h**).* Electrolysis in set-up **A** yielded 44 mg of colorless oil (0.088 mmol, 44%): ^{1}H NMR (400 MHz, $CDCl_3$) δ = 7.15 (t, J = 1.7 Hz, 2H), 7.03 (d, J = 1.7 Hz, 4H), 1.55 (s, 6H), 1.16 (s, 36H); ^{13}C NMR (101 MHz, $CDCl_3$) δ = 173.00, 151.47, 134.30, 120.23, 117.69, 44.72, 34.84, 31.18, 21.79; HRMS for $C_{33}H_{48}N_2O_2$ (ESI+) $[M+H]^+$: calcd 505.3794, found 505.3787.

*1,2-Bis(4-chlorophenyl)-4,4-dimethyltetrahydropyridazine-3,6-dione (**2**).* Electrolysis in set-up **A** using 1 mmol of dianilide in a 25 mL cell (25 mL of HFIP, 100 mg of NBu_4PF_6) yielded 63 mg of yellow solid (0.17 mmol, 17%): mp 211.0–211.8 °C; ^{1}H NMR (400 MHz, DMSO-d_6) δ = 7.52–7.46 (m, 2H), 7.44–7.40 (m, 2H), 7.39–7.34 (m, 4H) 2.93 (s, 2H), 1.24 (s, 6H); ^{13}C NMR (101 MHz, $CDCl_3$) δ = 173.22, 167.58, 136.33, 135.79, 132.49, 132.41, 129.10, 128.98, 125.58, 125.07, 43.38, 38.12, 23.49; HRMS for $C_{18}H_{16}{}^{35}Cl_2N_2O_2$ (ESI+) $[M+H]^+$: calcd 363.0667, found 363.0666.

*6-Chloro-2-(N-(4-chlorophenyl)-1,1-dimethyl)propanamide-1,3-benzoxazole (**3a**) and 6-Chloro-2-(N-(4-chlorophenyl)-2,2-dimethyl)propanamide-1,3-benzoxazole (**3b**).* Electrolysis in set-up **A** using 1 mmol of dianilide in a 25 mL cell (25 mL of HFIP, 100 mg of NBu_4PF_6) yielded 55 mg of a red solid as a 3:1 mixture of both isomers, whereby **3a** is the main compound (0.15 mmol, 15%): ^{1}H NMR (400 MHz, $CDCl_3$) δ = 9.14 (s, 1H), 8.81 (s, 0.2H), 7.80 (s, 0.2H), 7.65–7.63 (m, 1H), 7.54 (d, J = 1.9 Hz, 0.7H), 7.40–7.37 (m, 2H), 7.35 (dd, J = 8.5, 1.9 Hz, 0.8H), 7.23–7.19 (m, 2H), 2.94 (s, 1.5H), 2.93 (s, 0.5H), 1.57 (s, 6H); ^{13}C NMR (101 MHz, $CDCl_3$) δ = 174.10, 172.91, 168.38, 168.15, 150.89, 149.31, 139.98, 138.90, 136.56, 136.40, 130.86, 128.88, 125.29, 120.68, 120.62, 120.49, 119.87, 112.54, 111.45, 48.33, 48.15, 37.15, 27.09, 27.00; HRMS for $C_{18}H_{16}{}^{35}Cl_2N_2O_2$ (ESI+) $[M+H]^+$: calcd 363.0667, found 363.0652.

*N-(4-(1-(1,1,1,3,3,3-Hexafluoropropan-2-yloxy)-methyl)phenyl)-benzamide (**6a**).* Electrolysis in set-up **A** yielded 10 mg of white solid (0.026 mmol, 13%): mp 150.0–150.3 °C; ^{1}H NMR (400 MHz, $CDCl_3$) δ = 7.90 (s, 1H), 7.89–7.85 (m, 2H), 7.72–7.67 (m, 2H), 7.60–7.54 (m, 1H), 7.52–7.47 (m, 2H), 7.40–7.35 (m, 2H) 4.85 (s, 2H), 4.12 (hept, J = 6.0 Hz, 1H); ^{13}C NMR (101 MHz, $CDCl_3$) δ = 165.75, 138.63, 134.70, 132.04, 130.55, 129.76, 128.85, 127.00, 121.57 (q, J = 284.5 Hz), 120.22, 75.43, 74.05 (hept, J = 32.7 Hz); HRMS for $C_{17}H_{13}F_6NO_2$ (ESI+) $[M+H]^+$: calcd 378.0923, found 378.0914.

DOI: 10.1021/jacs.7b07488
J. Am. Chem. Soc. 2017, 139, 12317–12324

■ ASSOCIATED CONTENT

Supporting Information

The Supporting Information is available free of charge on the ACS Publications website at DOI: 10.1021/jacs.7b07488.

Experimental and analytical details for the synthesis of test substrates, symmetric dianilides, and mixed dianilides, NMR spectra, and crystallographic details (PDF)
Crystallographic data for **2** (CIF)
Crystallographic data for **3a** (CIF)
Crystallographic data for **10c** (CIF)

■ AUTHOR INFORMATION

Corresponding Author

*waldvogel@uni-mainz.de

ORCID

Kevin D. Moeller: 0000-0002-3893-5923
Siegfried R. Waldvogel: 0000-0002-7949-9638

Notes

The authors declare no competing financial interest.

■ ACKNOWLEDGMENTS

T.G. is a recipient of a DFG fellowship by the Excellence Initiative by the Graduate School Materials Science in Mainz (GSC 266). The work done in the laboratories of K.D.M. was supported by the U.S. National Science Foundation (CHE-1463913). The support by The Advanced Lab for Electrochemistry and Electrosynthesis – ELYSION (Carl Zeiss Stiftung) and the DFG (WA 1276/17-1) is highly appreciated.

■ REFERENCES

(1) (a) Aiba née Kaneko, M.; Hirota, M.; Kouzuki, H.; Mori, M. *J. Toxicol. Sci.* **2015**, *40*, 77–98. (b) Zhang, X.-Y.; Gu, Y.-F.; Chen, T.; Yang, D.-X.; Wang, X.-X.; Jiang, B.-L.; Shao, K.-P.; Zhao, W.; Wang, C.; Wang, J.-W.; Zhang, Q.-R.; Liu, H.-M. *MedChemComm* **2015**, *6*, 1781–1786. (c) Nishiu, J.; Ito, M.; Ishida, Y.; Kakutani, M.; Shibata, T.; Matsushita, M.; Shindo, M. *Diabetes, Obes. Metab.* **2006**, *8*, 508–516. (d) Deng, G.; Li, W.; Shen, J.; Jiang, H.; Chen, K.; Liu, H. *Bioorg. Med. Chem. Lett.* **2008**, *18*, 5497–5502. (e) Gilbert, A. M.; Failli, A.; Shumsky, J.; Yang, Y.; Severin, A.; Singh, G.; Hu, W.; Keeney, D.; Petersen, P. J.; Katz, A. H. *J. Med. Chem.* **2006**, *49*, 6027–6036. (f) Kutterer, K. M.; Davis, J. M.; Singh, G.; Yang, Y.; Hu, W.; Severin, A.; Rasmussen, B. A.; Krishnamurthy, G.; Failli, A.; Katz, A. H. *Bioorg. Med. Chem. Lett.* **2005**, *15*, 2527–2531.

(2) Steinhilber, D.; Schubert-Zsilavecz, M.; Roth, H. J. *Medizinische Chemie: Targets, Arzneistoffe, Chemische Biologie*; Dt. Apotheker-Verlag: Stuttgart, 2010.

(3) Davidson, J. P.; Corey, E. J. *J. Am. Chem. Soc.* **2003**, *125*, 13486–13489.

(4) Ueki, M.; Ueno, K.; Miyadoh, S.; Abe, K.; Shibata, K.; Taniguchi, M.; Oi, S. *J. Antibiot.* **1993**, *46*, 1095–1100.

(5) Leventhal, L.; Brandt, M. R.; Cummons, T. A.; Piesla, M. J.; Rogers, K. E.; Harris, H. A. *Eur. J. Pharmacol.* **2006**, *553*, 146–148.

(6) (a) Alvarez-Builla, J.; Vaquero, J. J.; Barluenga, J. *Modern Heterocyclic Chemistry*; Wiley-VCH Verlag GmbH & Co. KGaA: Weinheim, Germany, 2011. (b) Joule, J. A.; Mills, K. *Heterocyclic Chemistry*, 5th ed.; Wiley-Blackwell: Hoboken, NJ, 2013. (c) Francke, R. *Beilstein J. Org. Chem.* **2014**, *10*, 2858–2873.

(7) (a) *Carcinog. Technol. Rep. Ser. - U. S., Natl. Cancer Inst.* **1978**, *92*, 1–123. (b) Dodd, D. E.; Pluta, L. J.; Sochaski, M. A.; Wall, H. G.; Thomas, R. S. *Int. J. Toxicol.* **2012**, *31*, 564–571.

(8) Li, G.-Q.; Gao, H.; Keene, C.; Devonas, M.; Ess, D. H.; Kürti, L. *J. Am. Chem. Soc.* **2013**, *135*, 7414–7417.

(9) (a) Mayo, M. S.; Yu, X.; Zhou, X.; Feng, X.; Yamamoto, Y.; Bao, M. *J. Org. Chem.* **2014**, *79*, 6310–6314. (b) Ueda, S.; Nagasawa, H. *J. Org. Chem.* **2009**, *74*, 4272–4277. (c) Khatun, N.; Guin, S.; Rout, S. K.; Patel, B. K. *RSC Adv.* **2014**, *4*, 10770. (d) Alla, S. K.; Sadhu, P.; Punniyamurthy, T. *J. Org. Chem.* **2014**, *79*, 7502–7511.

(10) Gieshoff, T.; Schollmeyer, D.; Waldvogel, S. R. *Angew. Chem., Int. Ed.* **2016**, *55*, 9437–9440.

(11) Gieshoff, T.; Kehl, A.; Schollmeyer, D.; Moeller, K. D.; Waldvogel, S. R. *Chem. Commun.* **2017**, *53*, 2974–2977.

(12) Zard, S. Z. *Chem. Soc. Rev.* **2008**, *37*, 1603.

(13) (a) Horn, E. J.; Rosen, B. R.; Baran, P. S. *ACS Cent. Sci.* **2016**, *2*, 302–308. (b) Frontana-Uribe, B. A.; Little, R. D.; Ibanez, J. G.; Palma, A.; Vasquez-Medrano, R. *Green Chem.* **2010**, *12*, 2099–2119. (c) Yoshida, J.-i.; Kataoka, K.; Horcajada, R.; Nagaki, A. *Chem. Rev.* **2008**, *108*, 2265–2299. (d) Waldvogel, S. R.; Möhle, S. *Angew. Chem., Int. Ed.* **2015**, *54*, 6398–6399. (e) Waldvogel, S. R.; Janza, B. *Angew. Chem., Int. Ed.* **2014**, *53*, 7122–7123. (f) Horn, E. J.; Rosen, B. R.; Chen, Y.; Tang, J.; Chen, K.; Eastgate, M. D.; Baran, P. S. *Nature* **2016**, *533*, 77–81. (g) Kawamata, Y.; Yan, M.; Liu, Z.; Bao, D.-H.; Chen, J.; Starr, J. T.; Baran, P. S. *J. Am. Chem. Soc.* **2017**, *139*, 7448–7451. (h) Waldvogel, S. R.; Selt, M. *Angew. Chem., Int. Ed.* **2016**, *55*, 12578–12580. (i) Hammerich, O., Speiser, B., Eds. *Organic electrochemistry*, 5th ed., revised and expanded; CRC Press: Boca Raton, FL, 2016. (j) Zhao, H.-B.; Hou, Z.-W.; Liu, Z.-J.; Zhou, Z.-F.; Song, J.; Xu, H.-C. *Angew. Chem., Int. Ed.* **2017**, *56*, 587–590. (k) Lips, S.; Wiebe, A.; Elsler, B.; Schollmeyer, D.; Dyballa, K. M.; Franke, R.; Waldvogel, S. R. *Angew. Chem., Int. Ed.* **2016**, *55*, 10872–10876. (l) Wiebe, A.; Schollmeyer, D.; Dyballa, K. M.; Franke, R.; Waldvogel, S. R. *Angew. Chem., Int. Ed.* **2016**, *55*, 11801–11805. (m) Schulz, L.; Enders, M.; Elsler, B.; Schollmeyer, D.; Dyballa, K. M.; Franke, R.; Waldvogel, S. R. *Angew. Chem., Int. Ed.* **2017**, *56*, 4877–4881. (n) Gütz, C.; Selt, M.; Bänziger, M.; Bucher, C.; Römelt, C.; Hecken, N.; Gallou, F.; Galvão, T. R.; Waldvogel, S. R. *Chem. - Eur. J.* **2015**, *21*, 13878–13882.

(14) (a) Francke, R.; Cericola, D.; Kötz, R.; Weingarth, D.; Waldvogel, S. R. *Electrochim. Acta* **2012**, *62*, 372–380. (b) Eberson, L.; Hartshorn, M. P.; Persson, O. *J. Chem. Soc., Perkin Trans. 2* **1995**, 1735–1744. (c) Eberson, L.; Hartshorn, M. P.; Persson, O.; Radner, F. *Chem. Commun.* **1996**, 2105–2112. (d) Elsler, B.; Wiebe, A.; Schollmeyer, D.; Dyballa, K. M.; Franke, R.; Waldvogel, S. R. *Chem. - Eur. J.* **2015**, *21*, 12321–12325. (e) Hollóczki, O.; Berkessel, A.; Mars, J.; Mezger, M.; Wiebe, A.; Waldvogel, S. R.; Kirchner, B. *ACS Catal.* **2017**, *7*, 1846–1852.

(15) (a) Tasker, S. Z.; Standley, E. A.; Jamison, T. F. *Nature* **2014**, *509*, 299–309. (b) Ackerman, L. K. G.; Lovell, M. M.; Weix, D. J. *Nature* **2015**, *524*, 454–457.

(16) So, C. M.; Kwong, F. Y. *Chem. Soc. Rev.* **2011**, *40*, 4963–4972.

(17) Baciocchi, E.; Møllendal, H.; Aksnes, D. W.; Brekke, T.; Maartmann-Moe, K.; Tønnesen, H. H.; Tokii, T. *Acta Chem. Scand.* **1990**, *44*, 645–652.

(18) Hunsen, M. *Synthesis* **2005**, *2005*, 2487–2490.

(19) Seganish, W. M.; DeShong, P. *J. Org. Chem.* **2004**, *69*, 1137–1143.

(20) (a) Naumov, P.; Topcu, Y.; Eckert-Maksic, M.; Glasovac, Z.; Pavosevic, F.; Kochunnoonny, M.; Hara, H. *J. Phys. Chem. A* **2011**, *115*, 7834–7848. (b) Muchall, H. M.; Werstiuk, N. H.; Lessard, J. *J. Mol. Struct.: THEOCHEM* **1999**, *469*, 135–142.

(21) Di Grandi, M. J. *Org. Biomol. Chem.* **2014**, *12*, 5331–5345.

(22) Gütz, C.; Klöckner, B.; Waldvogel, S. R. *Org. Process Res. Dev.* **2016**, *20*, 26–32.

DOI: 10.1021/jacs.7b07488
J. Am. Chem. Soc. 2017, 139, 12317–12324

Insights into the Mechanism of the Anodic N-N Bond Formation by Dehydrogenative Coupling

Tile Gieshoff, Anton Kehl, Dieter Schollmeyer, Kevin D. Moeller, Siegfried R. Waldvogel*

TABLE OF CONTENTS

General information

All reagents were used in analytical grades and were obtained from commercial sources. Solvents were purified by standard methods.[1] For electrochemical reactions, different electrode materials were used: isostatic graphite electrodes were obtained from SGL Carbon, Bonn, Germany.

Column chromatography was performed on silica gel 60 M (0.040-0.063 mm, Macherey-Nagel GmbH & Co, Düren, Germany) with a maximum pressure of 2.0 bar. Either a glass column or a preparative chromatography system (Büchi-Labortechnik GmbH, Essen, Germany) were used with a Büchi Control Unit C-620, an UV detector Büchi UV photometer C-635, Büchi fraction collector C-660 and two Pump Modules C-605 for adjusting the solvent mixtures. Mixtures of hexane and ethyl acetate (7:1) or cyclohexane and ethyl acetate (10:1) were used as eluents. Silica gel 60 sheets on aluminum (F254, Merck, Darmstadt, Germany) were employed for thin layer chromatography.

Gas chromatography was performed on a Shimadzu GC-2025 (Shimadzu, Japan) using a Zebron ZB-5MSi column (Phenomenex, USA; length: 30 m, inner diameter: 0.25 mm, film: 0.25 µm, pre-column: 5 m, carrier gas: hydrogen). GC-MS measurements were carried out on a Shimadzu GC-2010 (Shimadzu, Japan) using a Zebron ZB-5MSi column (Phenomenex, USA; length: 30 m, inner diameter: 0.25 mm, film: 0.25 µm, pre-column: 5 m, carrier gas: helium) combined with a GCMS-QP2010.

Microanalysis was performed by a VarioMICRO cube (Elementar Analysesysteme, Hanau, Germany).

Melting points were determined by a Melting Point Apparatus SMP3 (Stuart Scientific, Staffordshire, U.K.) and are uncorrected.

Spectroscopy and spectrometry: ^{1}H NMR, ^{13}C NMR and ^{19}F spectra were recorded at 25 °C by using a Bruker Avance II 400 or a Bruker Avance III HD 400 (Analytische Messtechnik, Karlsruhe, Germany). Chemical shifts (δ) are reported in parts per million (ppm) relative to TMS as internal standard or traces of $CHCl_3$ (^{1}H 7.26 ppm, ^{13}C 77.16 ppm), DMSO (1H 2.50 ppm, ^{13}C 39.52 ppm), or CH_2Cl_2 (^{1}H 5.32 ppm, ^{13}C 53.84 ppm) in the corresponding deuterated solvent. For the ^{19}F spectra, α-trifluorotoluene served as external standard (δ = –63.9 ppm).[2] Mass spectra and high resolution mass spectra were obtained by using a Agilent 6545 Q-ToF MS apparatus employing ESI+.

X-ray analysis: All data were collected on a STOE IPDS2T diffractometer (Oxford Cryostream 700er series, Oxford Cryosystems) using graphite monochromated Mo K_α radiation (λ= 0.71073 Å). Intensities were measured using fine-slicing ω and φ-scans and corrected for background, polarization and Lorentz effects. The structures were solved by direct methods and refined anisotropically by the least-squares procedure implemented in the SHELX program system.[3]

The supplementary crystallographic data for this paper can be obtained free of charge from The Cambridge Crystallographic Data Center via www.ccdc.cam.ac.uk/data_request/cif. Deposition numbers and further details are given with the individual characterization data.

Synthesis of test substrates

Substituted pivalanilides were prepared from acid chlorides and corresponding anilines according to the literature.[4] The corresponding anilide for the synthesis of benzoxazole **10** was synthesized according to the literature.[4b] Dianilide **1** was synthesized analogous to the protocols reported.[4d]

Synthesis of symmetric dianilides

***N*,*N*'-Di(4-hydroxyphenyl)-2,2-dimethylmalondiamide**

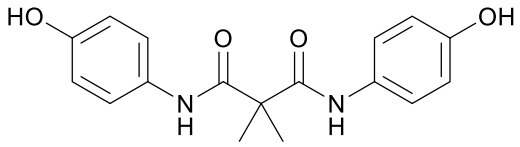

To a solution of 437 mg 4-aminophenol (4 mmol) and 0.56 mL NEt_3 (4 mmol) in 40 mL ethyl acetate, a solution of 338 mg dimethylmalonyl chloride (2 mmol) in 10 mL ethyl acetate was added at 0 °C within 15 min. A precipitate forms and the mixture was allowed to warm to room temperature and was then stirred for 4 h. The mixture was washed with 30 mL H_2O and the aqueous layer was extracted with 30 mL EtOAc. The combined organic fractions were washed with 1 M HCl (30 mL), sat. $NaHCO_3$ (30 mL), brine (30 mL), and dried with $MgSO_4$. After removal of the solvent at reduced pressure, 598 mg product were obtained as colorless crystalline solid (1.9 mmol, 95%).

^{1}H NMR (400 MHz, DMSO-d_6) δ = 9.17 (s, 2H), 9.15 (s, 2H), 7.41 – 7.36 (m, 4H), 6.70 – 6.65 (m, 4H), 1.49 (s, 6H).

^{13}C NMR (101 MHz, DMSO-d_6) δ = 171.81, 153.95, 131.02, 122.78, 115.22, 51.66, 24.06.

HRMS for $C_{17}H_{18}N_2O_4$ (ESI+) [M+Na^+]: calc.: 337.1164, found: 337.1157.

MP: 218.0–219.0 °C (EtOAc)

2,2-Dimethyl-*N*,*N*'-di(4-trifluoromethylsulfonyloxyphenyl)malondiamide

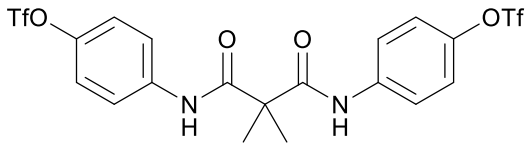

To a solution of 157 mg *N*,*N*'-Di(4-hydroxyphenyl)-2,2-dimethylmalondiamide (0.5 mmol) in 2.5 mL pyridine, 202 µL Tf_2O (1.2 mmol) was added dropwise at 0 °C. The dark solution was stirred 10 min at 0 °C and 12 h at room temperature. 20 mL Et_2O were added and the organic layer was washed with 1 M aqueous $CuSO_4$ (3x 10 mL), H_2O (20 mL), and dried with $MgSO_4$.[4a] After removal of the solvent at reduced pressure, 261 mg product were obtained as yellow crystalline solid (0.45 mmol, 91%).

^{1}H NMR (400 MHz, $CDCl_3$) δ = 8.58 (s, 2H), 7.66 – 7.61 (m, 4H), 7.27 – 7.22 (m, 4H), 1.69 (s, 6H).

^{13}C NMR (101 MHz, DMSO-d_6) δ = 171.97, 144.39, 139.53, 123.05 – 113.48 (q, *J* = 320.8 Hz) 121.75, 52.27, 23.29.

^{19}F NMR (377 MHz, $CDCl_3$) δ = -73.89.

HRMS for $C_{19}H_{16}F_6N_2O_8S_2$ (ESI+) [M+H$^+$]: calc.: 579.0331, found: 579.0308.

MP: 153.3–153.9 °C (Et_2O)

2,2-Dimethyl-*N*,*N*'-di(4-mesylphenyl)malondiamide

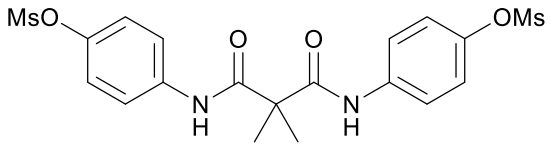

To a solution of 157 mg *N*,*N*'-Di(4-hydroxyphenyl)-2,2-dimethylmalondiamide (0.5 mmol) and 0.28 mL NEt_3 (2 mmol) in 5 mL EtOAc, 100 µL MsCl (1.3 mmol) was added dropwise at 0 °C. After addition, the mixture was allowed to warm to room temperature and stirred for 10 min. 20 mL H_2O were added and the organic layer was washed with 20 mL H_2O, and dried with $MgSO_4$.[4c] After removal of the solvent at reduced pressure, 181 mg product were obtained as yellow crystalline solid (0.40 mmol, 80%).

^{1}H NMR (400 MHz, $CDCl_3$) δ = 8.54 (s, 2H), 7.62 – 7.57 (m, 4H), 7.29 – 7.25 (m, 4H), 3.13 (s, 6H), 1.69 (s, 6H).

^{13}C NMR (101 MHz, DMSO-d_6) δ = 172.27, 144.94, 138.65, 122.77, 121.94, 52.54, 37.62, 23.81.

HRMS for $C_{19}H_{22}N_2O_8S_2$ (ESI+) [M+Na$^+$]: calc.: 493.0715, found: 493.0718.

MP: 153.0–153.4 °C (EtOAc)

2,2-Dimethyl-*N*,*N*'-di(3-(1,1-dimethylethyl)phenyl)malondiamide

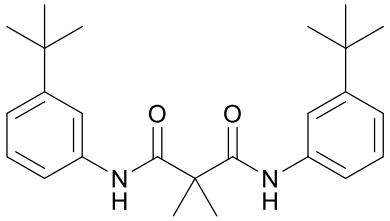

To a 0 °C cooled solution of 895 mg 3-(1,1-dimethylethyl)aniline (6 mmol) and 0.83 mL NEt_3 (6 mmol) in 60 mL dichloromethane was added dropwise a solution of 517 mg dimethylmalonyl chloride (3 mmol) in 40 mL dichloromethane. After addition, the solution was allowed to warm to room temperature and stirred for 4 hours. The combined organic fractions were washed with 1 M HCl (100 mL), sat. $NaHCO_3$ (100 mL), H_2O (100 mL), and dried with $MgSO_4$. After removal of the solvent at reduced pressure, 977 mg product were obtained as colorless crystalline solid (2.48 mmol, 87%).

^{1}H NMR (400 MHz, $CDCl_3$) δ = 8.41 (s, 2H), 7.51 – 7.48 (m, 2H), 7.43 – 7.39 (m, 2H), 7.32 – 7.23 (m, 2H), 1.70 (s, 6H), 1.32 (s, 18H).

^{13}C NMR (101 MHz, $CDCl_3$) δ = 171.46, 152.31, 137.06, 128.66, 121.94, 117.63, 117.49, 50.85, 34.77, 31.27, 24.21.

HRMS for $C_{25}H_{34}N_2O_2$ (ESI+) [M+Na$^+$]: calc.: 417.2518, found: 417.2520.

MP: 215.0–216.0 °C (CH_2Cl_2)

2,2-Dimethyl-*N*,*N*'-di(3,5-di-(1,1-dimethylethyl)phenyl)malondiamide

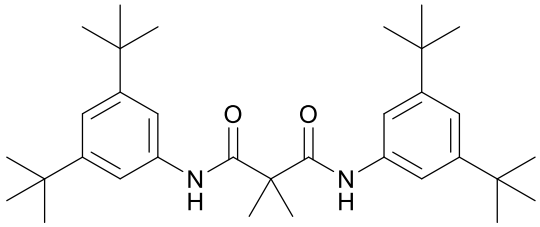

To a 0 °C cooled solution of 616 mg 3,5-di(1,1-dimethylethyl)aniline (3 mmol) and 0.42 mL NEt_3 (3 mmol) in 40 mL dichloromethane was added dropwise a solution of 254 mg dimethylmalonyl chloride (1.5 mmol) in 30 mL dichloromethane. After addition, the solution was allowed to warm to room temperature and stirred for 4 hours. The combined organic fractions were washed with 1 M HCl (100 mL), sat. $NaHCO_3$ (100 mL), H_2O (100 mL), and dried with $MgSO_4$. After removal of the solvent at reduced pressure, 758 mg product were obtained as colorless crystalline solid (1.50 mmol, 100%).

^{1}H NMR (400 MHz, CD_2Cl_2) δ = 8.38 (s, 2H), 7.42 – 7.39 (m, 4H), 7.24 (t, *J* = 1.8 Hz, 2H), 1.70 (s, 6H), 1.34 (s, 36H).

^{13}C NMR (101 MHz, CD_2Cl_2) δ = 171.45, 151.62, 136.98, 118.80, 115.16, 50.80, 34.82, 31.10, 23.96.

HRMS for $C_{33}H_{50}N_2O_2$ (ESI+) [M+H$^+$]: calc.: 507.3951, found: 507.3957.

MP: 335.5–336.0 °C (CH_2Cl_2)

Synthesis of mixed dianilides

_N_-(4-Chlorophenyl)-3-hydroxy-2,2-dimethylpropionamide

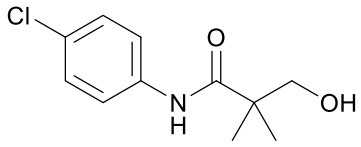

To a solution of 354 mg 3-hydroxy-2,2-dimethylpropionic acid (3 mmol), 383 mg 4-chloroaniline (3 mmol), 405 mg 1-hydrobenzotriazole (3 mmol) in 20 mL dichloromethane, 575 mg 1-ethyl-3-(3-dimethylaminopropyl)carbodiimide (3 mmol) was added. After stirring overnight, the mixture was quenched with brine (30 mL) and the aqueous layer was extracted with ethyl acetate (2x 20 mL). The combined organic fractions are washed with sat. aqueous $NaHCO_3$ (30 mL), 1 M HCl (30 mL), brine (30 mL), and dried with $MgSO_4$. After removal of the solvent at reduced pressure, 592 mg raw product were obtained as colorless crystalline solid (2.60 mmol, 87%) and used without further purification.

3-Hydroxy-*N*-(4-methylphenyl)-2,2-dimethylpropionamide

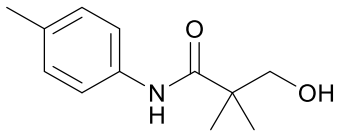

To a solution of 354 mg 3-hydroxy-2,2-dimethylpropionic acid (3 mmol), 322 mg 4-chloroaniline (3 mmol), 405 mg 1-hydrobenzotriazole (3 mmol) in 20 mL dichloromethane, 575 mg 1-ethyl-

3-(3-dimethylaminopropyl)carbodiimide (3 mmol) was added. After stirring overnight, the mixture was quenched with brine (30 mL) and the aqueous layer was extracted with ethyl acetate (2x 20 mL). The combined organic fractions are washed with sat. aqueous $NaHCO_3$ (30 mL), 1 M HCl (30 mL), brine (30 mL), and dried with $MgSO_4$. After removal of the solvent at reduced pressure, 491 mg raw product were obtained as colorless crystalline solid (2.36 mmol, 87%) and used without further purification.

***N*-(4-Chlorophenyl)-2,2-dimethylmalonic acid monoamide**

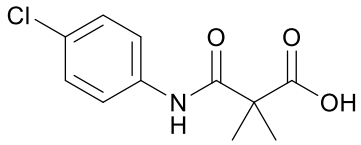

To a suspension of 683 mg *N*-(4-Chlorophenyl)-3-hydroxy-2,2-dimethylpropionamide (3 mmol) in 20 mL MeCN, 1.709 g H_5IO_6 was added at 0 °C. After 15 min stirring, 48 mg PCC (pyridinium chlorochromate, 0.22 mmol) in 10 mL MeCN were added. After overnight stirring, the mixture was diluted with 50 mL EtOAc, washed with brine-water (1:1, 40 mL), saturated $NaHSO_3$ (40 mL), brine (40 mL) and dried with $MgSO_4$.After removal of the solvent, 629 mg After removal of the solvent at reduced pressure, 629 mg raw product were obtained as colorless crystalline solid (2.60 mmol, 87%) and used without further purification.

***N*-(4-Methylphenyl)-2,2-dimethylmalonic acid monoamide**

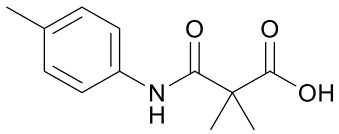

To a solution of 421 mg 3-Hydroxy-*N*-(4-methylphenyl)-2,2-dimethylpropionamide (2.03 mmol) in 60 mL dimethylformamide, 3.760 g PDC (pyridinium dichromate, 10 mmol) were added. The mixture was stirred for 3 days. After addition of 50 mL brine, the mixture was extracted with EtOAc (3x 30 mL). The combined organic layers were dried with $MgSO_4$. After removal of the solvent at reduced pressure, 377 mg raw product were obtained as colorless crystalline solid (1.55 mmol, 77%) and used without further purification.

***N*-(4-Chlorophenyl)-*N'*-(4-hydroxyphenyl)-2,2-dimethylmalondiamide**

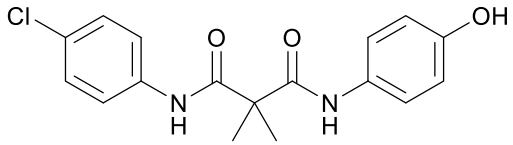

To a solution of 266 mg *N*-(4-Chlorophenyl)-2,2-dimethylmalonic acid monoamide (1.1 mmol) and 144 mg 4-aminophenol (1.32 mmol) in 11 mL dichloromethane, 316 mg 3-(3-dimethylaminopropyl)carbodiimide (1.65 mmol) were added. After stirring overnight, the mixture was quenched with brine (30 mL) and the aqueous layer was extracted with ethyl acetate (2x 40 mL). The combined organic fractions are washed with 1 M HCl (30 mL), sat. aqueous $NaHCO_3$ (30 mL), brine (30 mL), and dried with $MgSO_4$. After removal of the solvent at reduced pressure, 289 mg raw product were obtained as colorless crystalline solid (0.87 mmol, 79%) and used without further purification.

***N*-(4-Methylphenyl)-*N'*-(4-hydroxyphenyl)-2,2-dimethylmalondiamide**

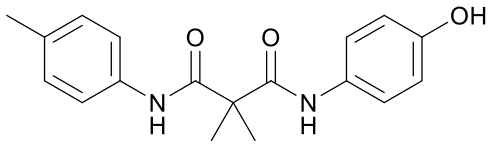

To a solution of 329 mg *N*-(4-Methylphenyl)-2,2-dimethylmalonic acid monoamide (1.5 mmol) and 195 mg 4-aminophenol (1.79 mmol) in 15 mL dichloromethane, 428 mg 3-(3-dimethylaminopropyl)carbodiimide (2.23 mmol) were added. After stirring overnight, the mixture was quenched with brine (30 mL) and the aqueous layer was extracted with ethyl acetate (2x 40 mL). The combined organic fractions are washed with 1 M HCl (30 mL), sat. aqueous $NaHCO_3$ (30 mL), brine (30 mL), and dried with $MgSO_4$. After removal of the solvent at reduced pressure, 305 mg raw product were obtained as colorless crystalline crystalline solid (0.98 mmol, 66%) and used without further purification.

***N*-(4-Chlorophenyl)-*N'*-(4-methoxyphenyl)-2,2-dimethylmalondiamide (4a)**

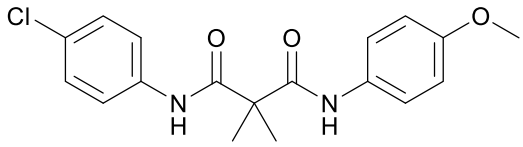

To a solution of 306 mg *N*-(4-Chlorophenyl)-2,2-dimethylmalonic acid monoamide (1.27 mmol), 156 mg 4-methoxyaniline (1.27 mmol), 172 mg 1-hydrobenzotriazole (1.27 mmol) in 10 mL dichloromethane, 244 mg 1-ethyl-3-(3-dimethylaminopropyl)-carbodiimide (1.27 mmol) were added. After stirring overnight, the mixture was quenched with brine (20 mL) and the aqueous layer was extracted with ethyl acetate (2x 20 mL). The combined organic fractions are washed with sat. aqueous $NaHCO_3$ (20 mL), 1 M HCl (20 mL), brine (20 mL), and dried with $MgSO_4$. After removal of the solvent at reduced pressure, 315 mg product were obtained as colorless crystalline solid (0.91 mmol, 75%).

^{1}H NMR (400 MHz, $CDCl_3$) δ = 8.94 (s, 1H), 8.10 (s, 1H), 7.55 – 7.49 (m, 2H), 7.46 – 7.38 (m, 2H), 7.34 – 7.27 (m, 2H), 6.93 – 6.87 (m, 2H), 3,82 (s, 3H), 1.69 (s, 6H).

^{13}C NMR (101 MHz, $CDCl_3$) δ = 171.99, 171.11, 157.03, 136.17, 129.96, 129.54, 128.99, 122.52, 121.41, 114.22, 55.50, 50.54, 24.26.

HRMS for $C_{18}H_{19}{}^{35}ClN_2O_3$ (ESI+) [$M+H^+$]: calc.: 347.1162, found: 347.1168.

MP: 182.5–183.0 °C (EtOAc)

***N*-(4-Methoxyphenyl)-*N'*-(4-methylphenyl)-2,2-dimethylmalondiamide (4b)**

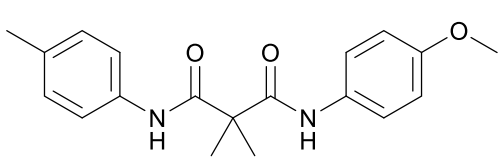

To a solution of 213 mg *N*-(4-Methylphenyl)-2,2-dimethylmalonic acid monoamide (0.96 mmol), 118 mg 4-methoxyaniline (0.96 mmol), 130 mg 1-hydrobenzotriazole (0.96 mmol) in 10 mL dichloromethane, 184 mg 1-ethyl-3-(3-dimethylaminopropyl)-carbodiimide (0.96 mmol) were added. After stirring overnight, the mixture was quenched with brine (20 mL) and the aqueous layer was extracted with ethyl acetate (2x 20 mL). The combined organic fractions are washed with sat. aqueous $NaHCO_3$ (20 mL), 1 M HCl (20 mL),

brine (20 mL), and dried with $MgSO_4$. After removal of the solvent at reduced pressure, 225 mg product were obtained as colorless crystalline solid (0.69 mmol, 72%).

^{1}H NMR (400 MHz, $CDCl_3$) δ = 8.50 (s, 1H), 8.38 (s, 1H), 7.49 – 7.39 (m, 4H), 7.19 – 7.11 (m, 2H), 6.93 – 6.85 (m, 2H), 3,82 (s, 3H), 2.34 (s, 3H), 1.69 (s, 6H).

^{13}C NMR (101 MHz, $CDCl_3$) δ = 171.53, 171.44, 156.77, 134.81, 134.47, 130.38, 129.50, 122.23, 120.38, 114.16, 55.49, 50.50, 24.26, 20.89.

HRMS for $C_{19}H_{22}N_2O_3$ (ESI+) [M+Na$^+$]: calc.: 349.1528, found: 349.1533.

MP: 185.0–186.0 °C (EtOAc)

***N*-(4-Methylphenyl)-*N'*-(4-trifluoromethylsulfonyloxyphenyl)-2,2-dimethylmalondiamide (4c)**

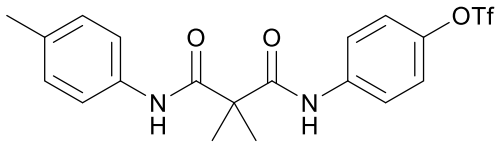

To a solution of 304 mg *N*-(4-Methylphenyl)-*N'*-(4-hydroxyphenyl)-2,2-dimethylmalondiamide (0.97 mmol) in 10 mL pyridine, 197 µL Tf_2O (1.17 mmol) were added dropwise at 0 °C. The dark solution was stirred 10 min at 0 °C and 12 h at room temperature. 20 mL Et_2O were added and the organic layer was washed with 1 M aqueous $CuSO_4$ (3x 10 mL), H_2O (20 mL), and dried with $MgSO_4$.[4a] After removal of the solvent at reduced pressure, 380 mg product were obtained as yellow crystalline solid (0.86 mmol, 88%).

^{1}H NMR (400 MHz, $CDCl_3$) δ = 9.25 (s, 1H), 7.99 (s, 1H), 7.70 – 7.63 (m, 2H), 7.42 – 7.37 (m, 2H), 7.27 – 7.22 (m, 2H), 7.22 – 7.13 (m, 2H), 2.35 (s, 3H), 1.70 (s, 6H).

^{13}C NMR (101 MHz, DMSO-d_6) δ = 172.20, 170.99, 145.40, 137.78, 135.20, 134.18, 129.64, 123.51 – 113.94 (q, *J* = 319.6 Hz), 121.93, 121.33, 120.81, 50.67, 24.26, 20.92.

^{19}F NMR (377 MHz, $CDCl_3$) δ = -73.88.

HRMS for $C_{19}H_{19}F_3N_2O_5S$ (ESI+) [M+H$^+$]: calc.: 445.1045, found: 445.1044.

MP: 146.0–146.5 °C (Et_2O)

***N*-(4-Chlorophenyl)-*N*-(4-chloro-3-methoxyphenyl)-2,2-dimethylmalondiamide (4d)**

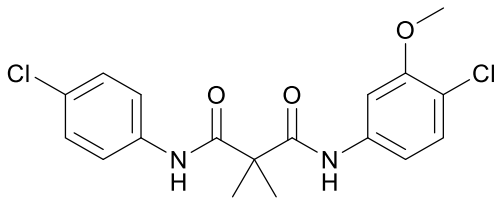

To a solution of 183 mg *N*-(4-Chlorophenyl)-2,2-dimethylmalonic acid monoamide (0.76 mmol), 119 mg 3-chloro-4-methoxyaniline (0.76 mmol), 102 mg 1-hydrobenzotriazole (0.76 mmol) in 10 mL dichloromethane, 145 mg 1-ethyl-3-(3-dimethylaminopropyl)-carbodiimide (0.76 mmol) were added. After stirring overnight, the mixture was quenched with brine (20 mL) and the aqueous layer was extracted with ethyl acetate (2x 20 mL). The combined organic fractions are washed with sat. aqueous $NaHCO_3$ (20 mL), 1 M HCl (20 mL),

brine (20 mL), and dried with $MgSO_4$. After removal of the solvent at reduced pressure, column chromatography (cyclohexane:ethyl acetate 9:1) afforded 226 mg product as colorless crystalline solid (0.59 mmol, 78%).

^{1}H NMR (400 MHz, $CDCl_3$) δ = 8.62 (s, 1H), 8.40 (s, 1H), 7.53 – 7.48 (m, 2H), 7.48 (d, *J* = 2.4 Hz, 1H), 7.35 – 7.31 (m, 2H), 7.29 (d, *J* = 5.7 Hz, 1H), 6.92 (dd, *J* = 8.5, 2.4 Hz, 1H), 3,93 (s, 3H), 1.71 (s, 6H).

^{13}C NMR (101 MHz, $CDCl_3$) δ = 171.63, 171.26, 155.23, 137.13, 135.69, 130.11, 130.08, 129.11, 121.71, 118.05, 112.57, 104.56, 56.21, 50.85, 24.23.

HRMS for $C_{18}H_{18}{}^{35}Cl_2N_2O_3$ (ESI+) [M+H$^+$]: calc.: 381.0767, found: 381.076.

MP: 185.0–186.0 °C (EtOAc)

***N*-(4-Chlorophenyl)-*N'*-(4-trifluoromethylsulfonyloxyphenyl)-2,2-dimethylmalondiamide (4e)**

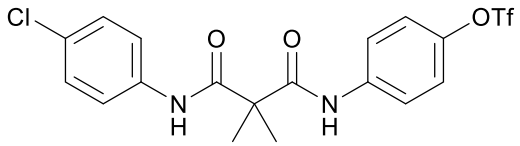

To a solution of 156 mg *N*-(4-Chlorophenyl)-*N'*-(4-hydroxyphenyl)-2,2-dimethylmalondiamide (0.47 mmol) in 5 mL pyridine, 94 µL Tf_2O (0.56 mmol) were added dropwise at 0 °C. The dark solution was stirred 10 min at 0 °C and 12 h at room temperature. 20 mL Et_2O were added and the organic layer was washed with 1 M aqueous $CuSO_4$ (3x 10 mL), H_2O (20 mL), and dried with $MgSO_4$.[4a] After removal of the solvent at reduced pressure, 188 mg product were obtained as yellow crystalline solid (0.43 mmol, 92%).

^{1}H NMR (400 MHz, $CDCl_3$) δ = 8.87 (s, 1H), 8.27 (s, 1H), 7.72 – 7.63 (m, 2H), 7.53 – 7.45 (m, 2H), 7.37 – 7.31 (m, 2H), 7.32 – 7.23 (m, 2H), 1.71 (s, 6H).

^{13}C NMR (101 MHz, $CDCl_3$) δ = 171.77, 171.19, 145.60, 137.47, 136.54, 130.28, 129.15, 123.54 – 113.95 (q, *J* = 319.8 Hz) 122.03, 121.76, 121.49, 50.81, 24.22.

^{19}F NMR (377 MHz, $CDCl_3$) δ = -73.87.

HRMS for $C_{18}H_{16}{}^{35}ClF_3N_2O_5S$ (ESI+) [M+H$^+$]: calc.: 465.0499, found: 465.0513.

MP: 173.5–174.0 °C (Et_2O)

Crystallographic Data

Crystal structure determination of **2** (CCDC 1561792): $C_{18}H_{16}Cl_2N_2O_2$, M_r = 362.06 g/mol, colorless plate (0.12 x 0.42 x 0.43 mm^3), P $2_1/n$ (monoklin), a = 12.6885 Å, b = 8.7452 Å, c = 15.7923 Å, V = 1722.2 $Å^3$, Z = 4, F(000) = 752, ρ = 1.401 g/cm^3, μ = 0.39 mm^{-1}, Mo-Kα graphite monochromator, -100 °C, 10217 reflections, 4079 independent reflections, wR_2 = 0.1097, R_1 = 0.0437, 0.31 e/$Å^3$, –0.22 e/$Å^3$, GoF = 1.035

Single crystals for structure determination were obtained by recrystallization from ethanol at room temperature.

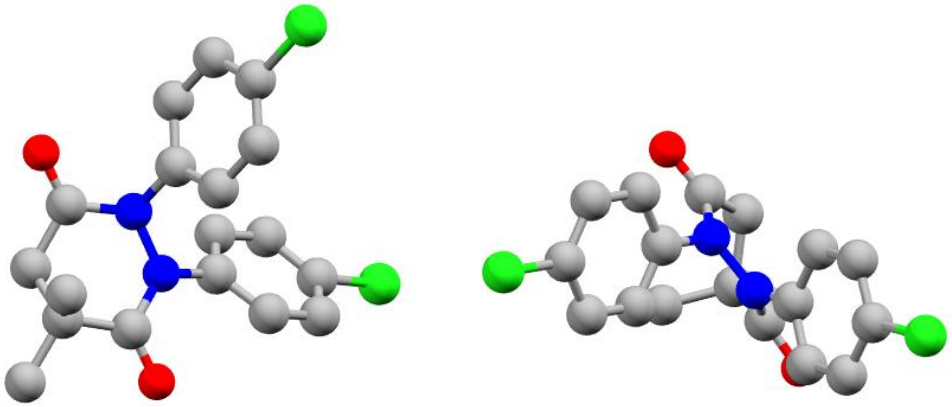

Figure 1: Molecular structure of derivative 2 by X-ray analysis (left: side view; right: top view).

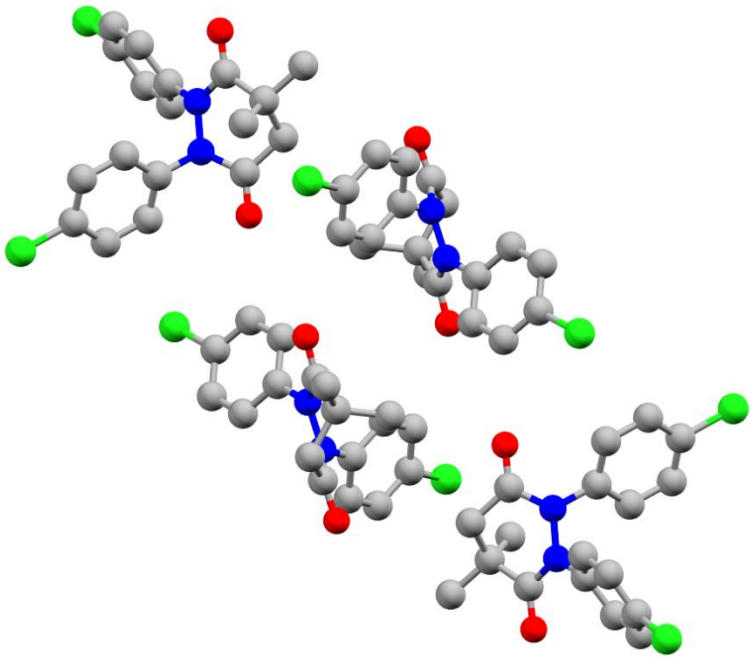

Figure 2: Packing of 2 in the solid state.

Crystal structure determination of **3a** (CCDC 1561793): $C_{18}H_{16}Cl_2N_2O_2$, M_r = 362.1 g/mol, colorless block (0.20 x 0.31 x 0.34 mm^3), P $2_1/c$ (monoklin), a = 9.6978 Å, b = 19.0063 Å, c = 9.8181 Å, V = 1721.6 $Å^3$, Z = 4, F(000) = 752, ρ = 1.401 g/cm^3, μ = 0.39 mm^{-1}, Mo-Kα graphite monochromator, -100 °C, 11963 reflections, 4078 independent reflections, wR_2 = 0.1617, R_1 = 0.065, 1.26 e/$Å^3$, –0.47 e/$Å^3$, GoF = 1.107

Single crystals for structure determination were obtained by recrystallization from ethanol at room temperature. In the packing, a disorder with two possible conformations arises from the rotatability of the aromatic ring along the C_{10}-C_2 axis.

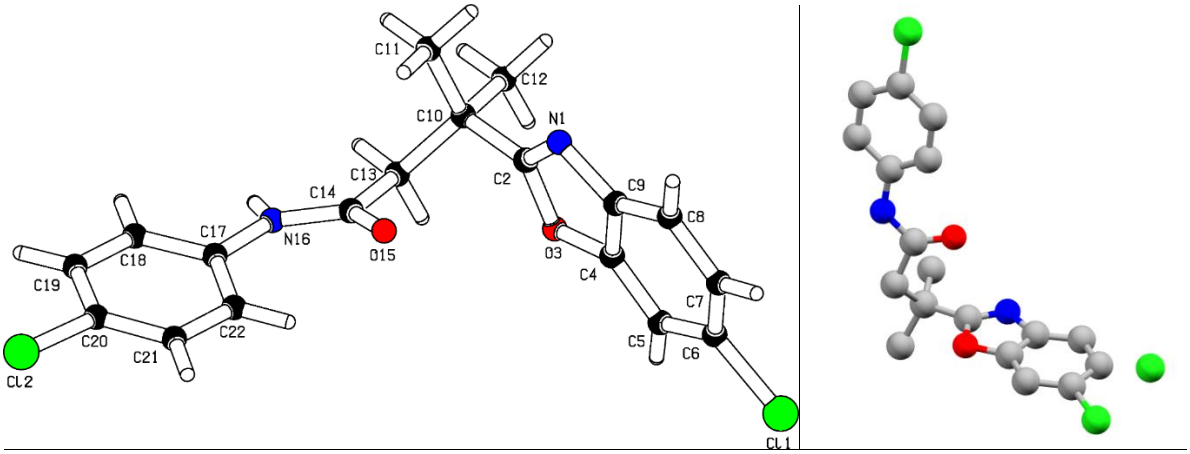

Figure 3: Molecular structure of derivative 3 by X-ray analysis (left: side view of the main conformation; right: side view with both conformations indicated).

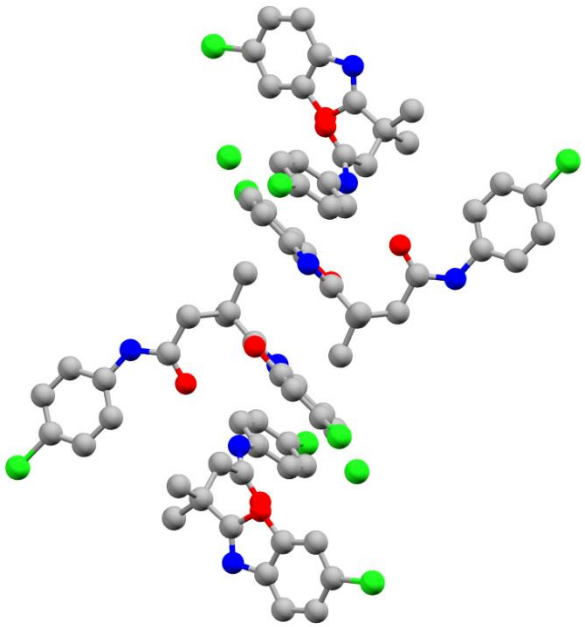

Figure 4: Packing of 3 ain the solid state.

Crystal structure determination of **10c** (CCDC 1561794): $C_{22}H_{19}F_9N_2O_6S$, M_r = 641.45 g/mol, colorless needle (0.02 x 0.02 x 0.21 mm^3), P -1 (triklin), a = 10.0415 Å, b = 10.4848 Å, c = 14.8890 Å, V = 1306.8 $Å^3$, Z = 2, F(000) = 620, ρ = 1.551 g/cm^3, μ = 2.083 mm^{-1}, Cu-Kα IμS mirror system, -80 °C, 13257 reflections, 4522 independent reflections, wR_2 = 0.5386, R_1 = 0.1821, 0.63 e/$Å^3$, –0.44 e/$Å^3$, GoF = 1.33

Single crystals for structure determination were obtained by recrystallization from cyclohexane at room temperature. In the crystal structure, a significant intramolecular hydrogen bonding between both amides is present. Weak diffraction arises from small crystals growth.

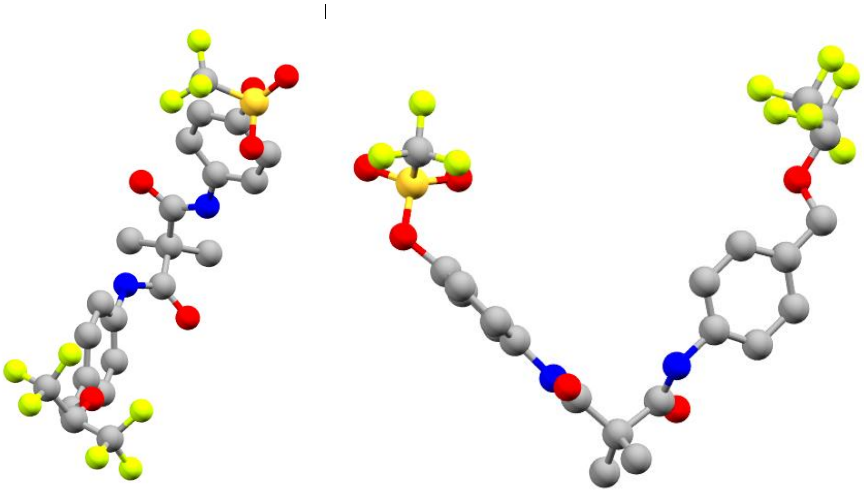

Figure 5: Molecular structure of derivative 9c by X-ray analysis (left: top view; right: side view).

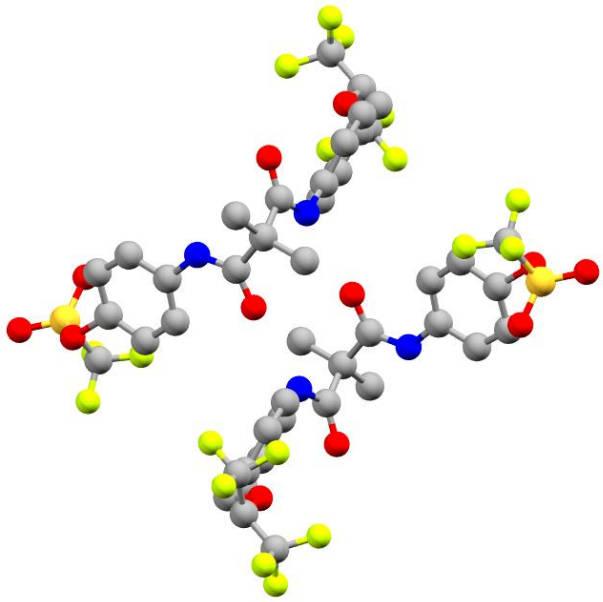

Figure 6: Packing of 9c in the solid state.

NMR spectra

***N,N'*-Di(4-hydroxyphenyl)-2,2-dimethylmalondiamide**

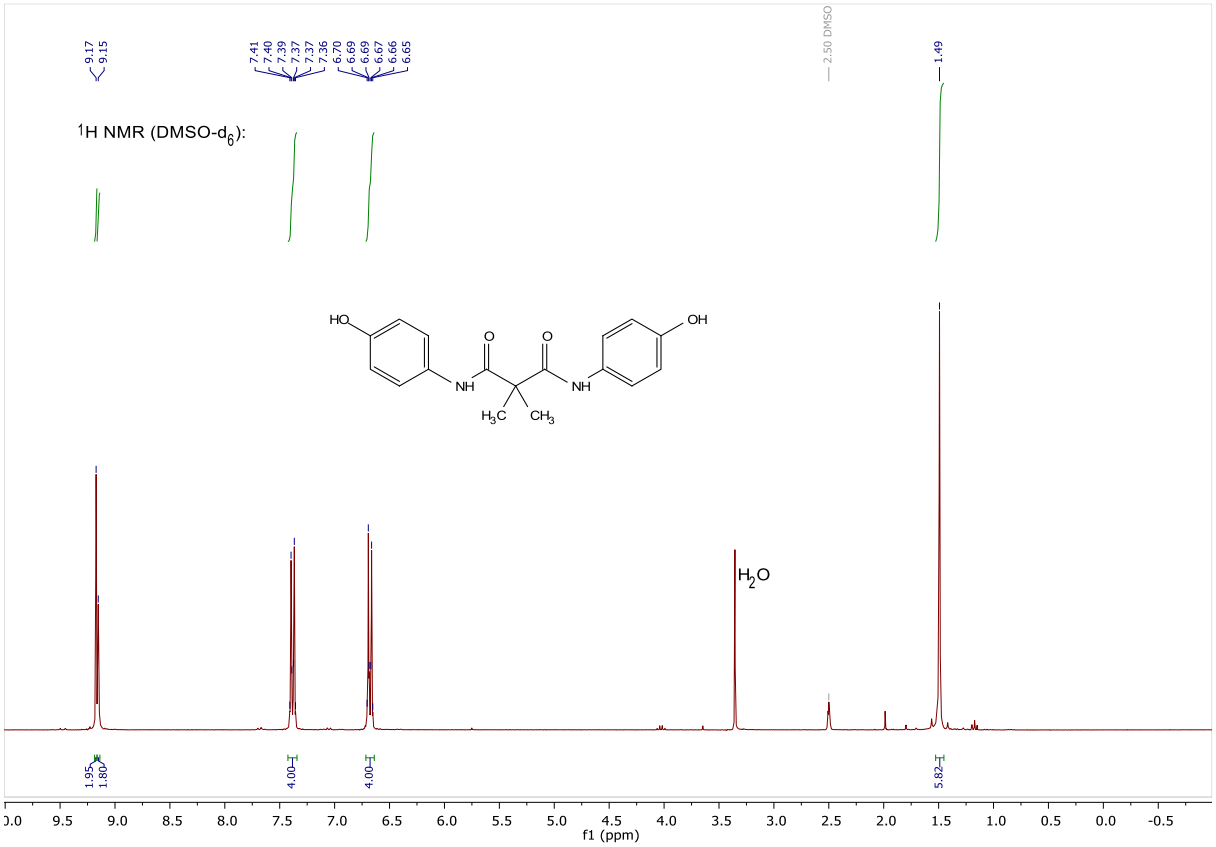

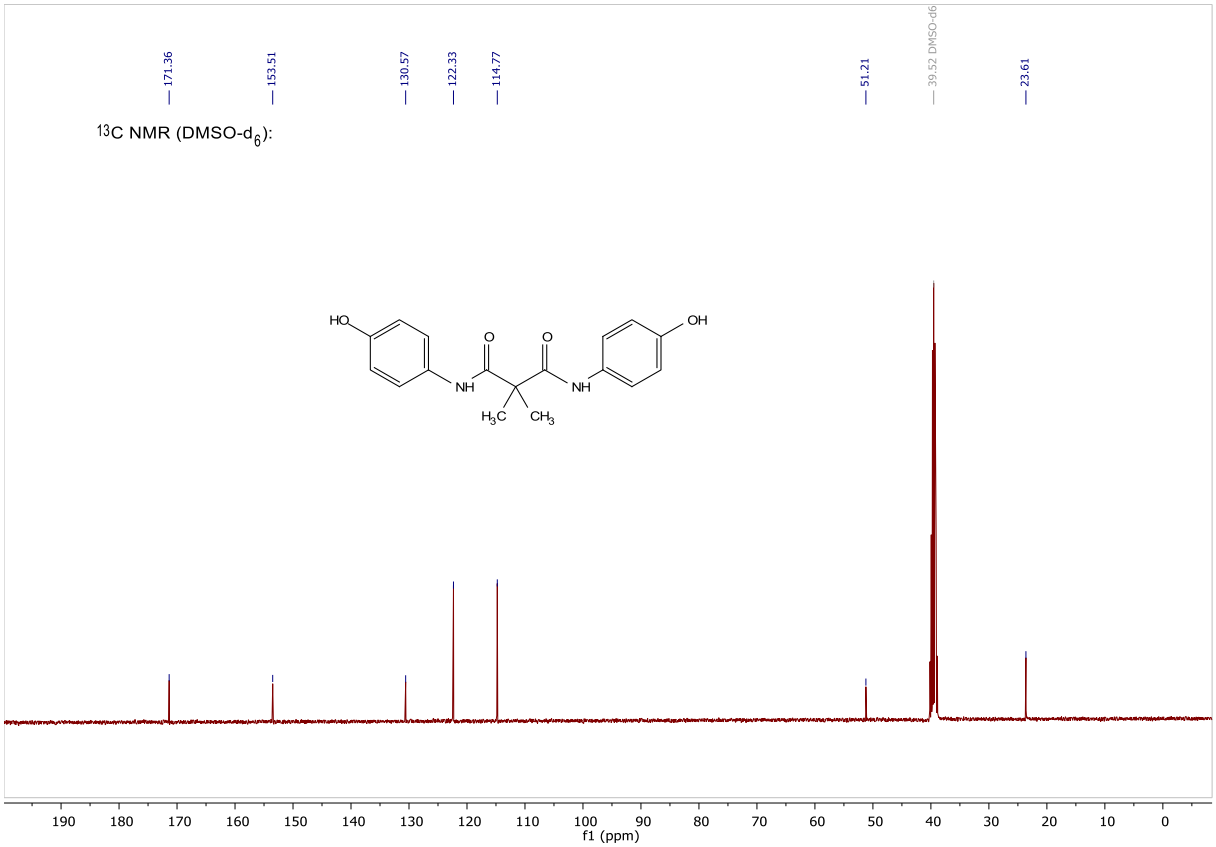

2,2-Dimethyl-*N*,*N*'-di(4-trifluoromethylsulfonyloxyphenyl)malondiamide

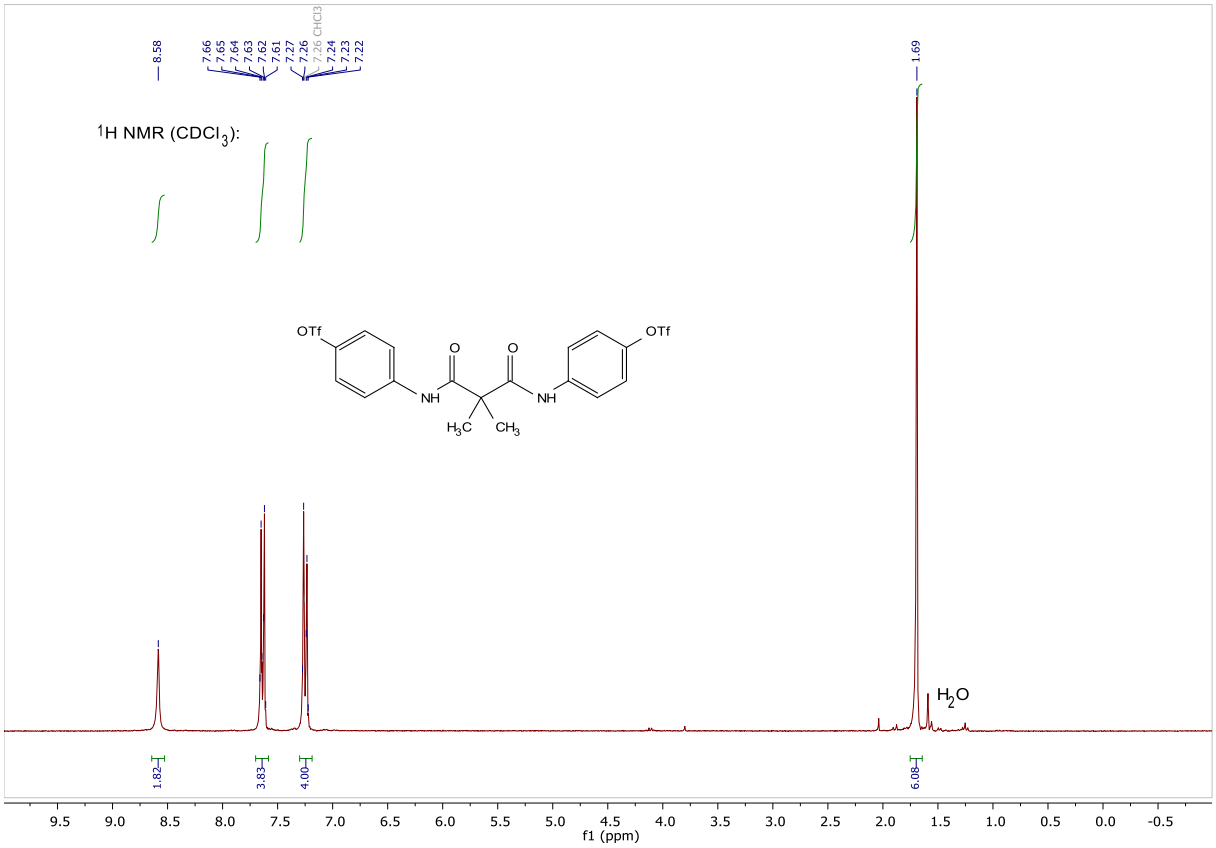

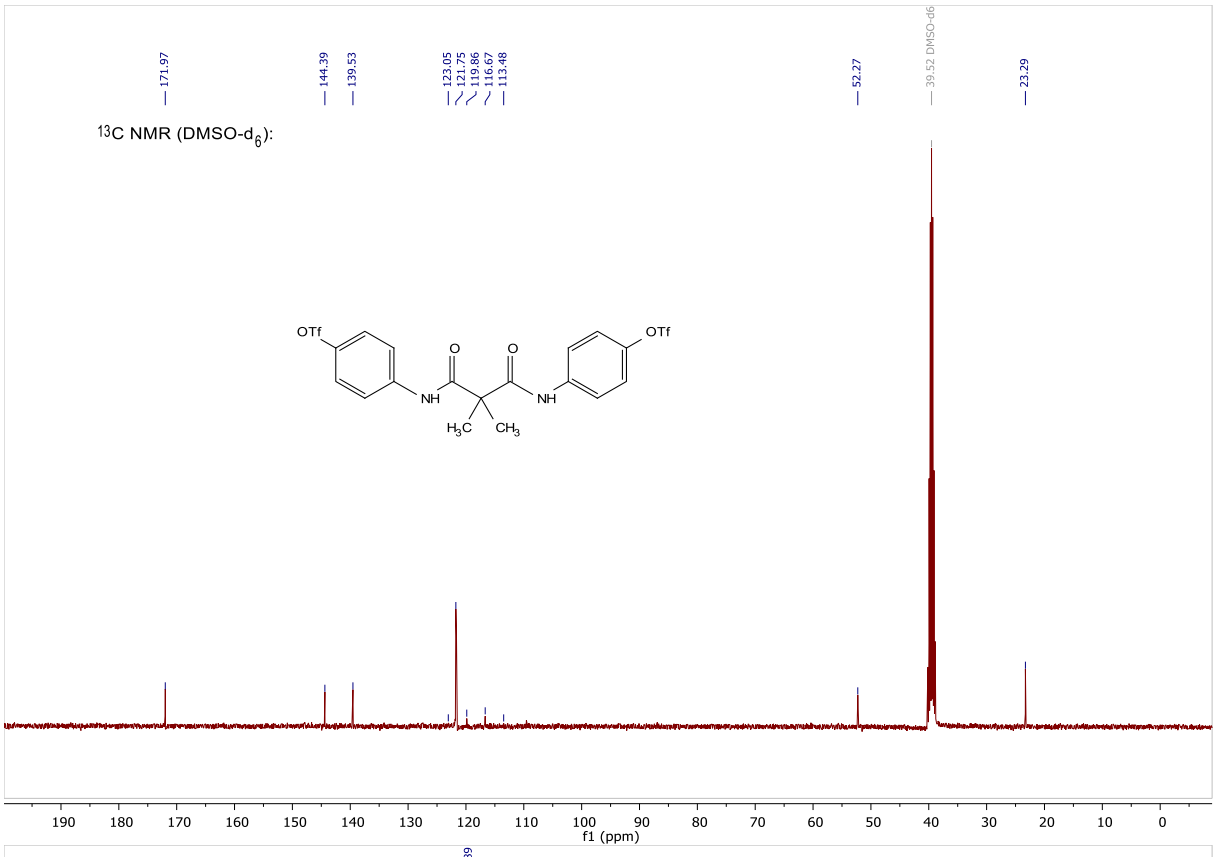
171.97
144.39
139.53
123.05
121.75
119.86
116.67
113.48
52.27
39.52 DMSO-d6
23.29
^{13}C NMR (DMSO-d$_6$):
OTf
OTf
O
O
NH
NH
H$_3$C
CH$_3$
190 180 170 160 150 140 130 120 110 100 90 80 70 60 50 40 30 20 10 0
f1 (ppm)

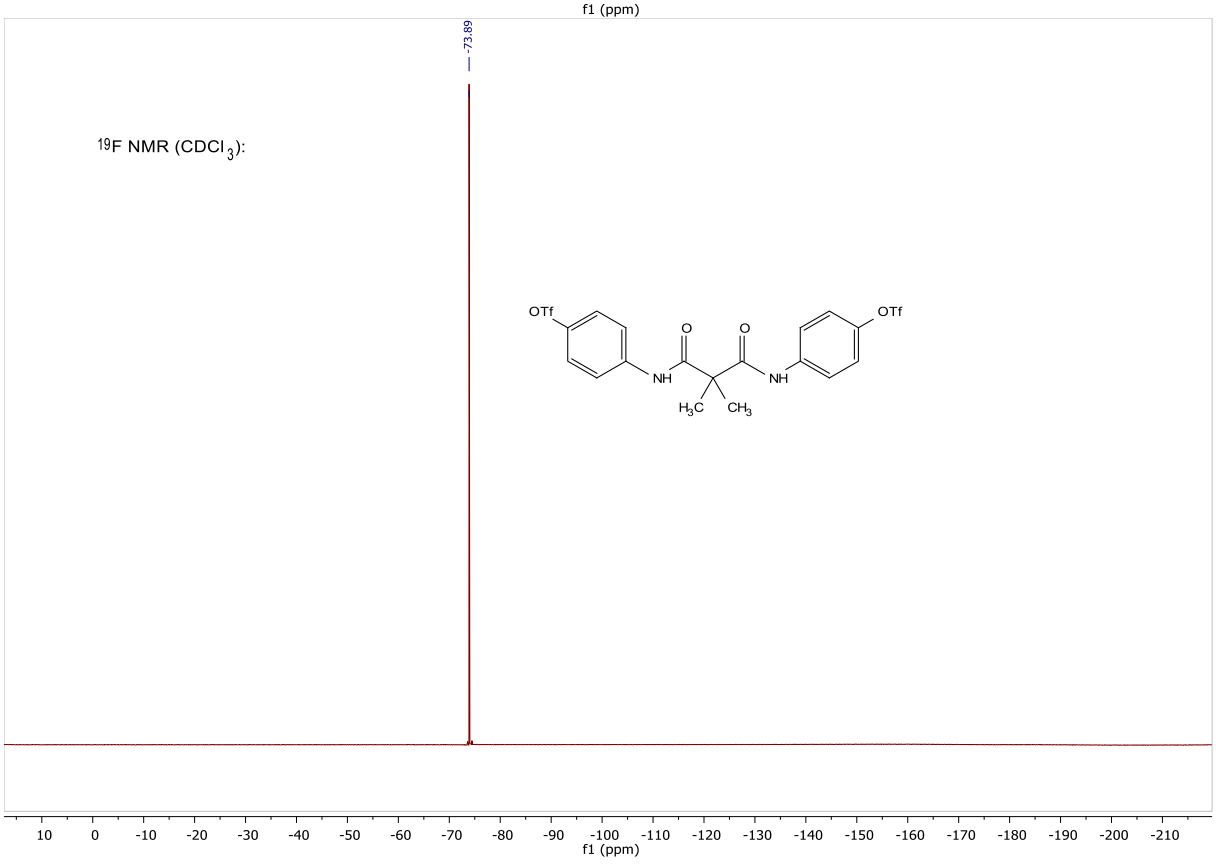
-73.89
^{19}F NMR (CDCl$_3$):
OTf
OTf
O
O
NH
NH
H$_3$C
CH$_3$
10 0 -10 -20 -30 -40 -50 -60 -70 -80 -90 -100 -110 -120 -130 -140 -150 -160 -170 -180 -190 -200 -210
f1 (ppm)

2,2-Dimethyl-*N*,*N*'-di(4-mesylphenyl)malondiamide

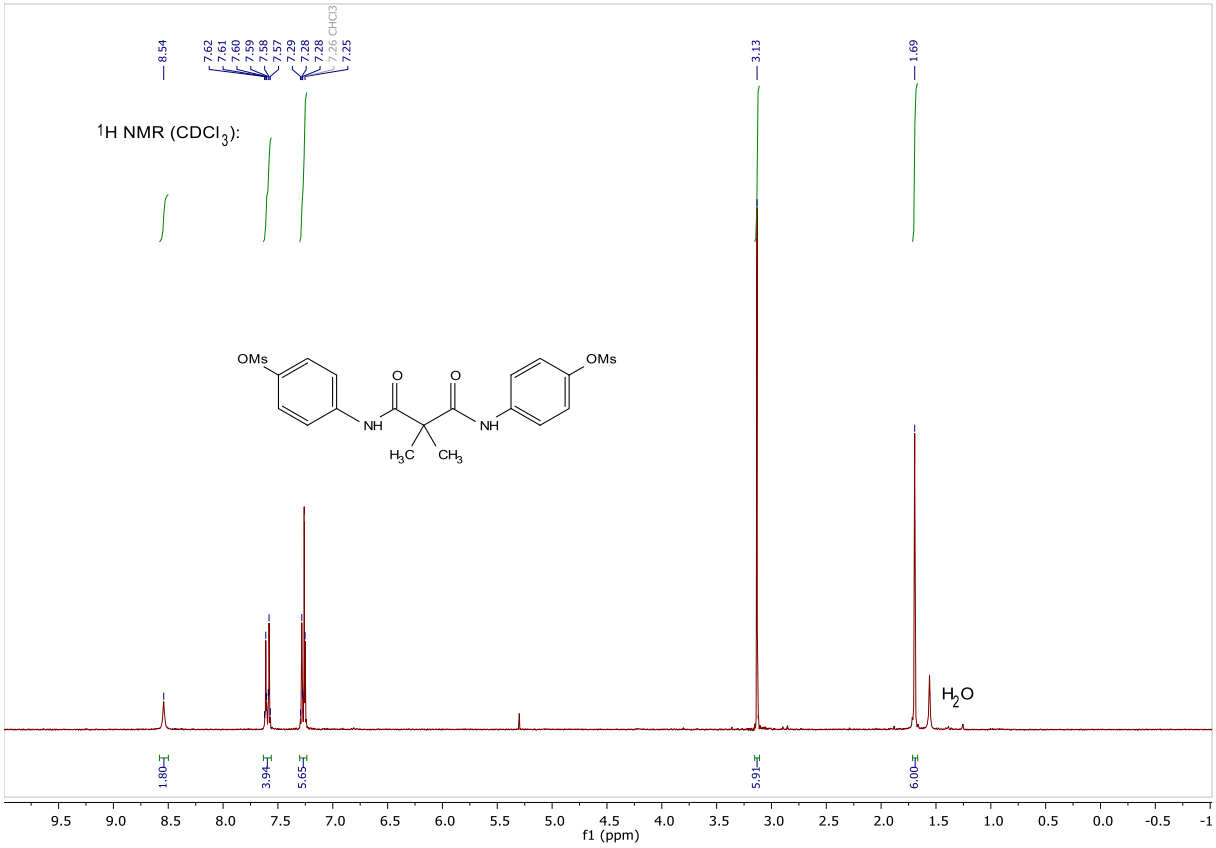

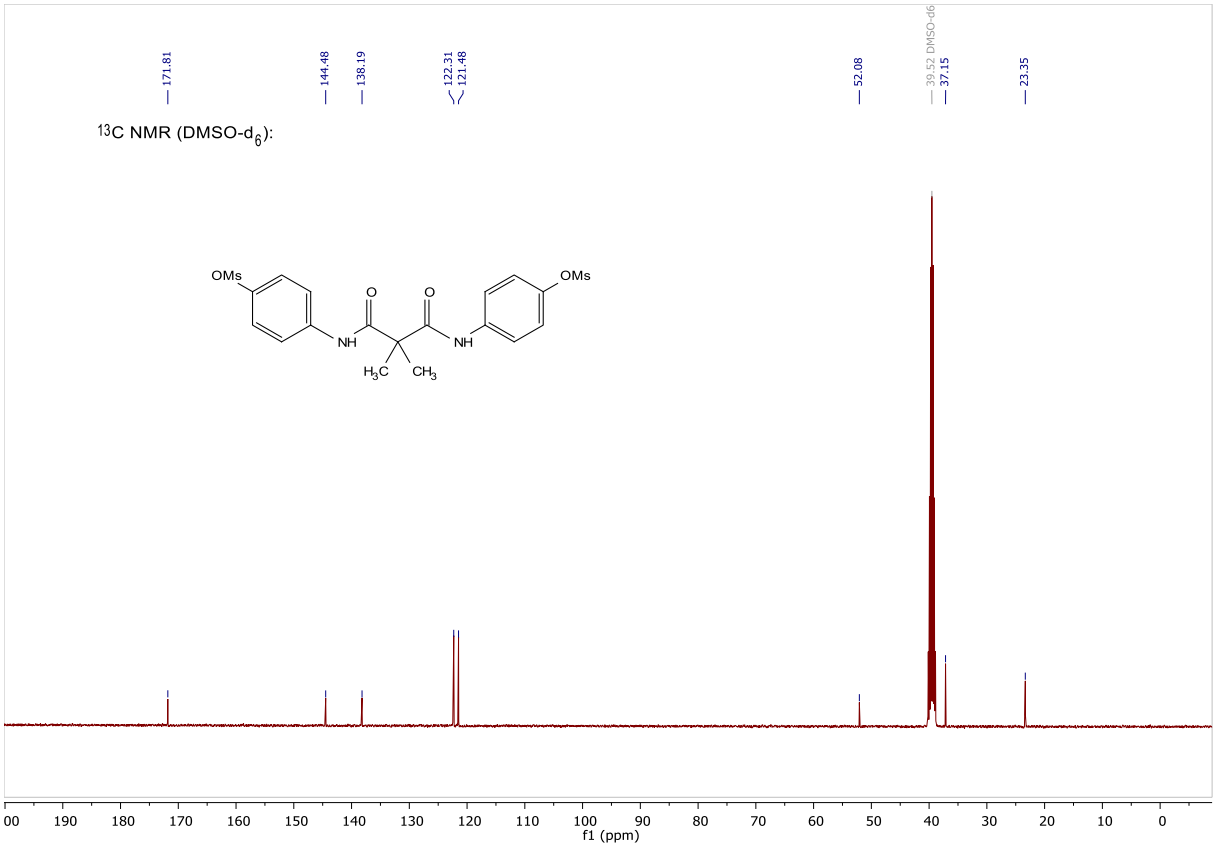

2,2-Dimethyl-*N*,*N*'-di(3-(1,1-dimethylethyl)phenyl)malondiamide

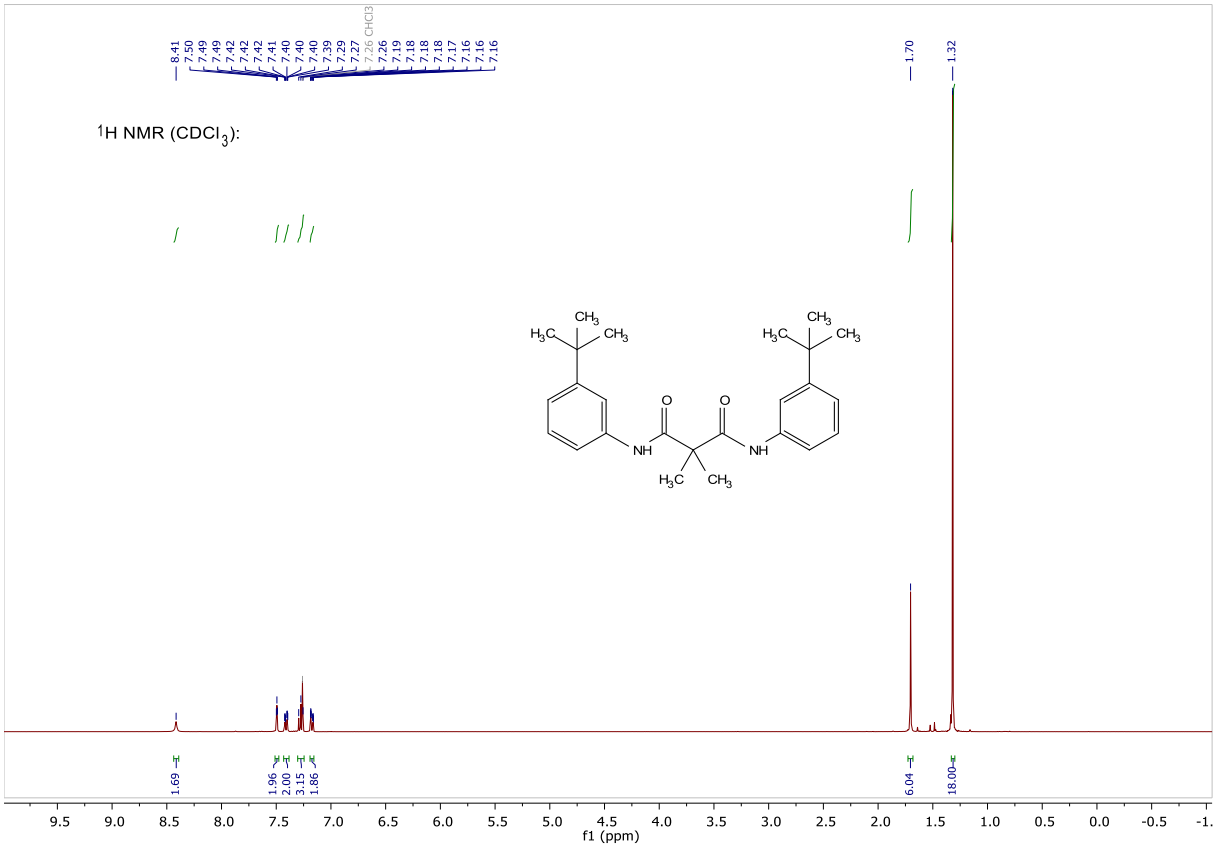

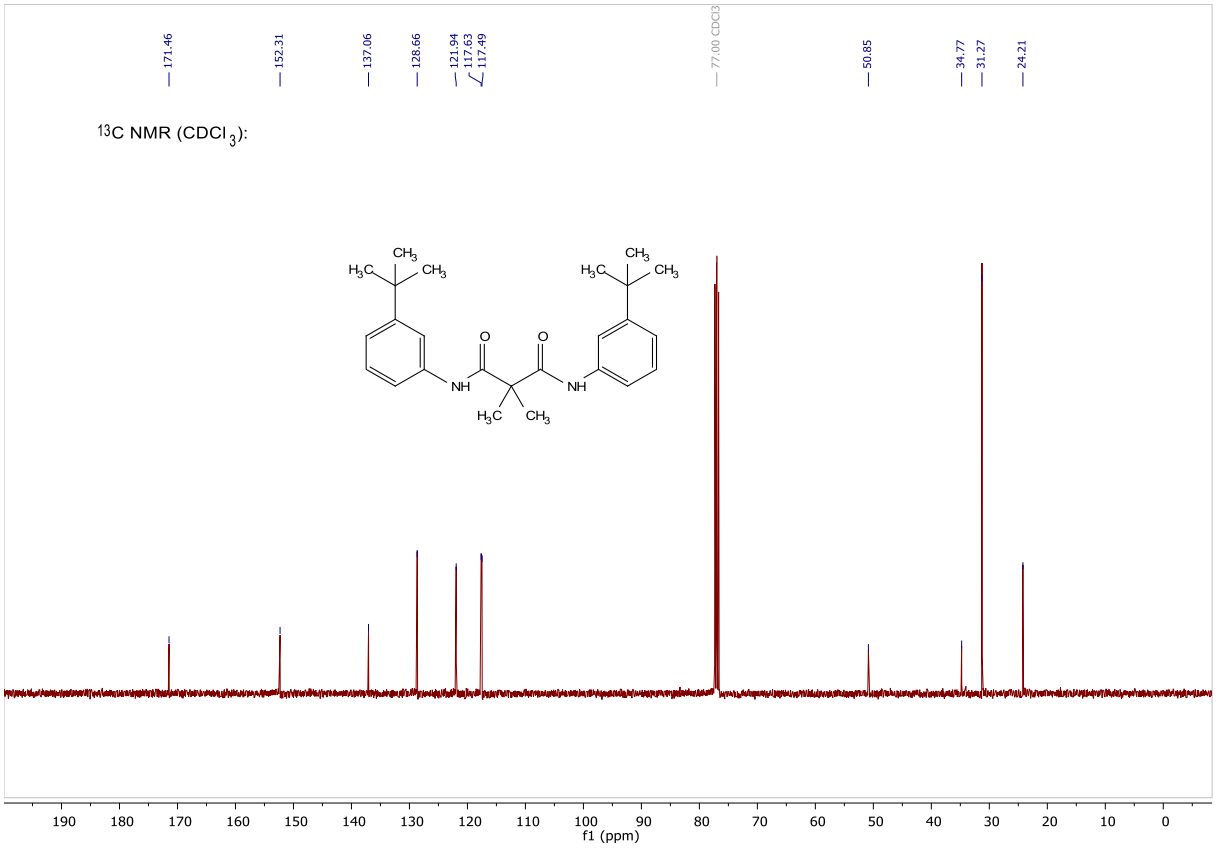

2,2-Dimethyl-*N*,*N*'-di(3,5-di-(1,1-dimethylethyl)phenyl)malondiamide

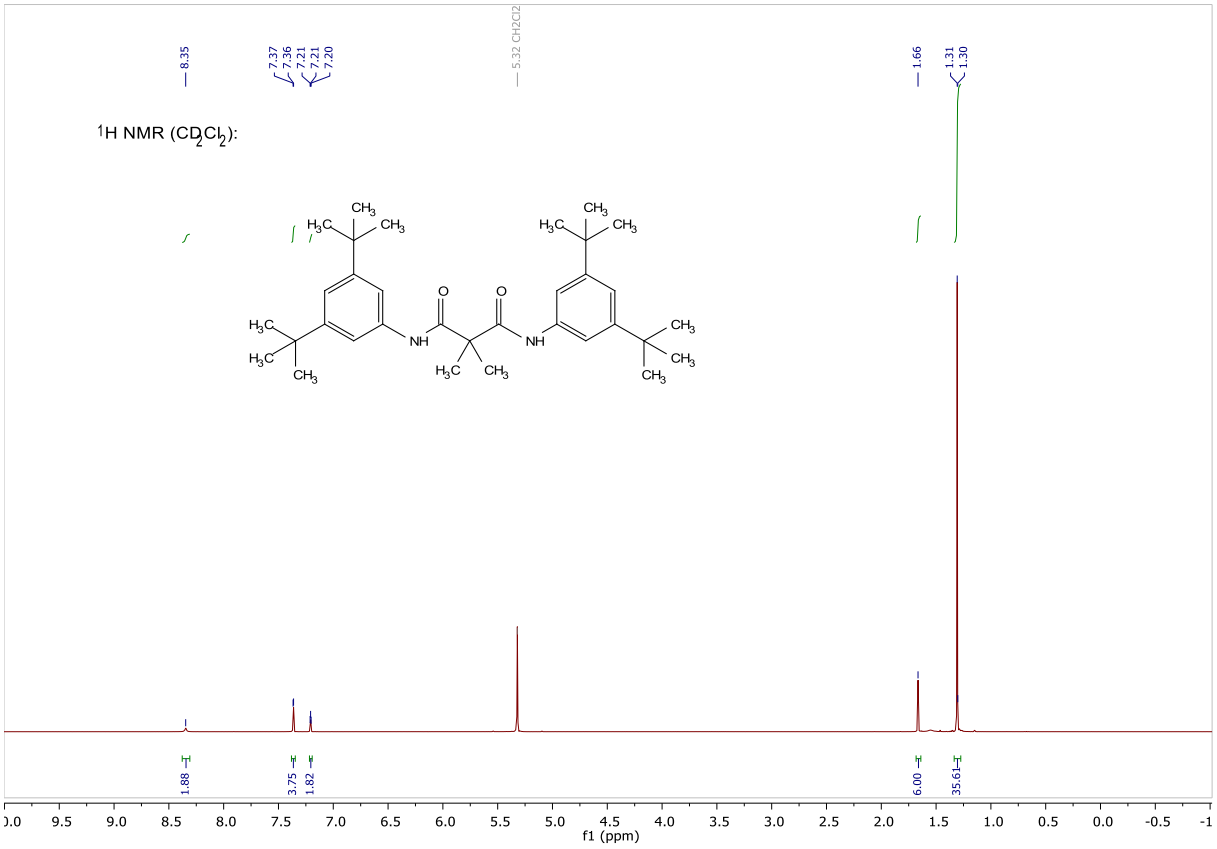

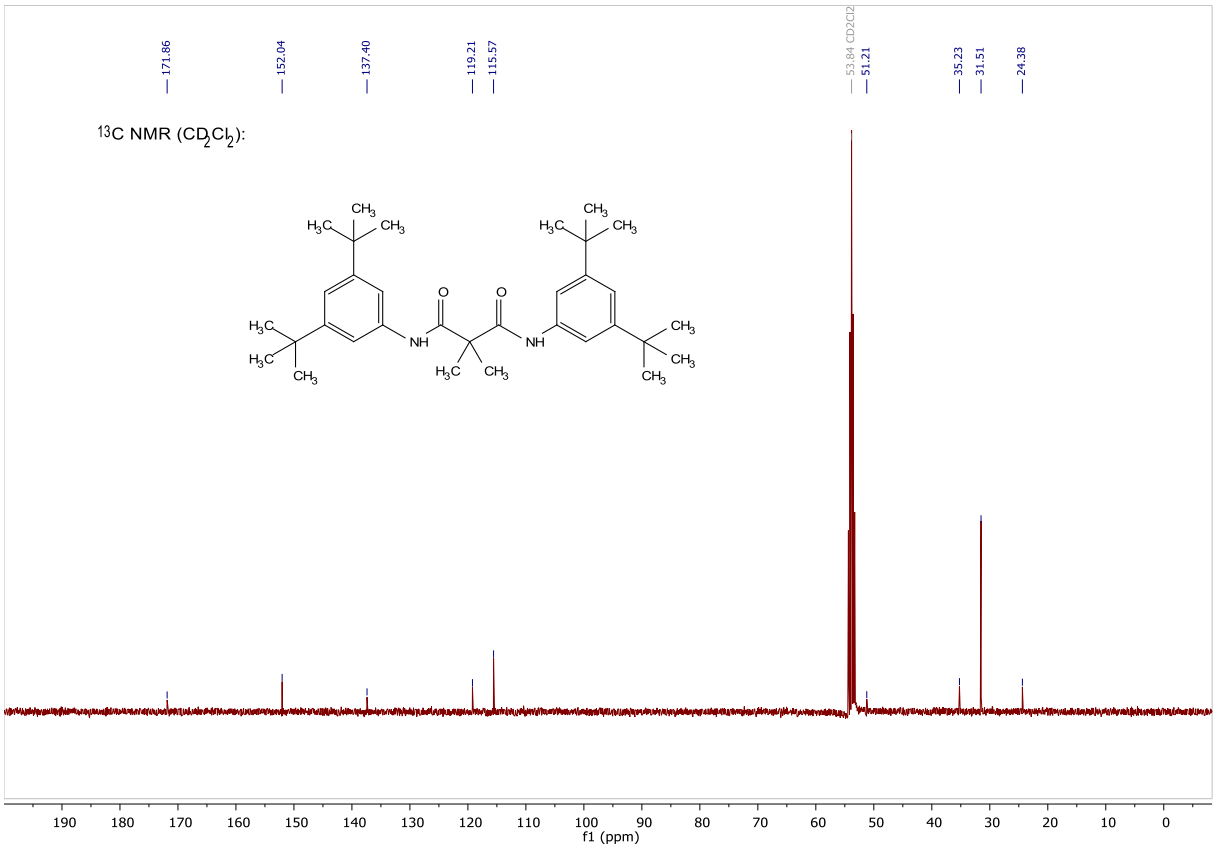

***N*-(4-Chlorophenyl)-*N*-(4-trifluoromethylsulfonyloxyphenyl)-2,2-dimethylmalondiamide (4e)**

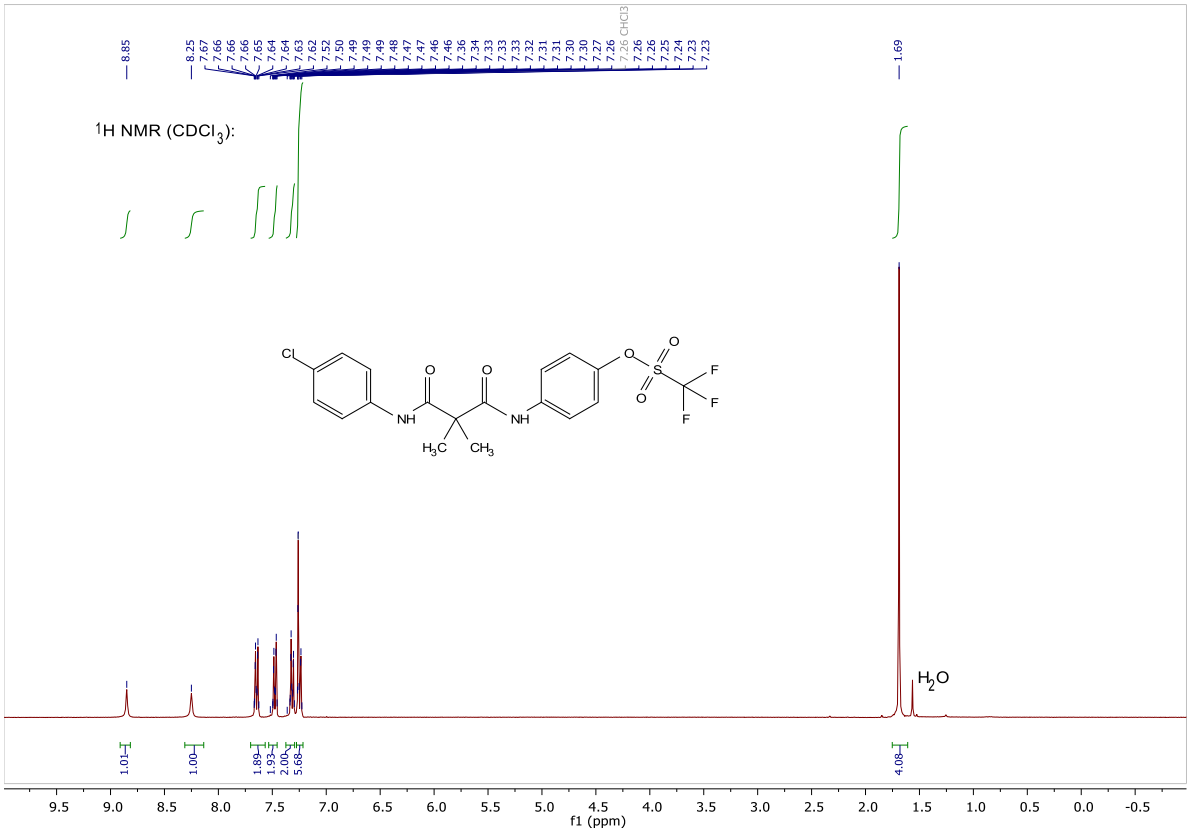

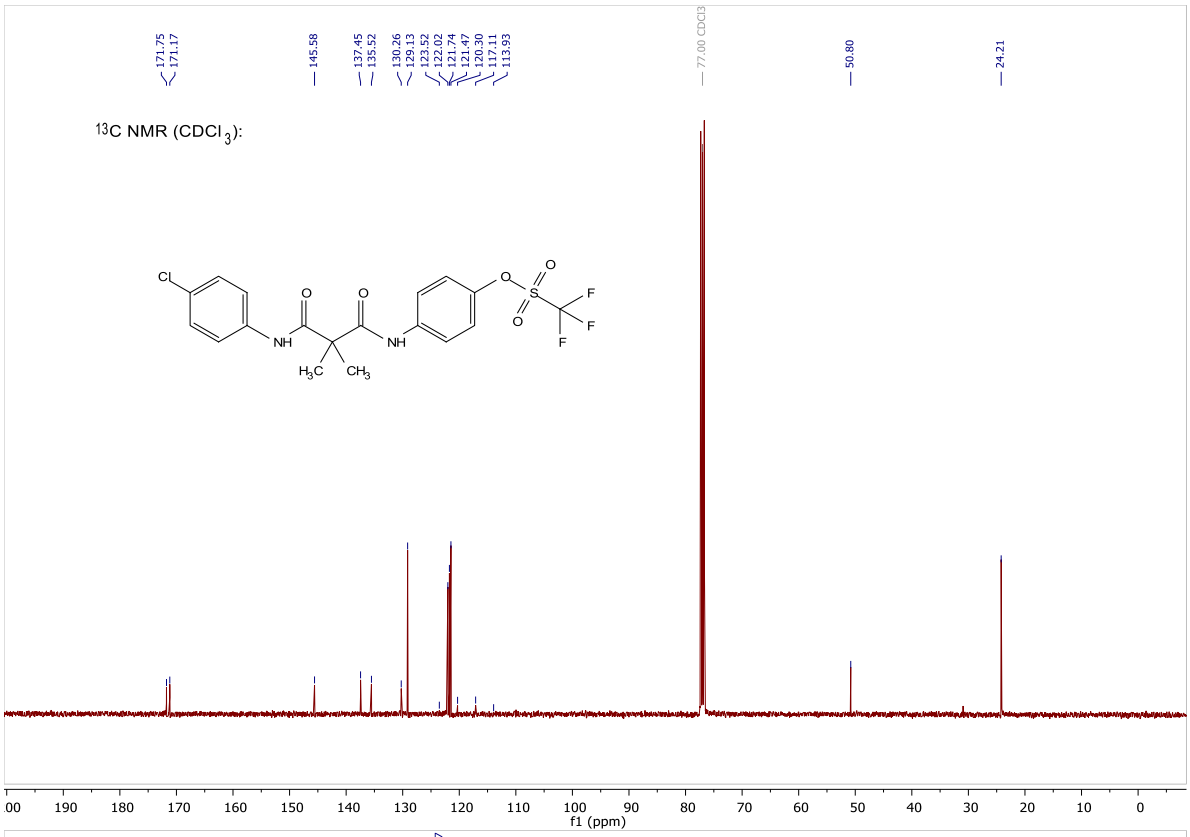
171.75
171.17
145.58
137.45
135.52
130.26
129.13
123.52
122.02
121.74
121.47
120.30
117.11
113.93
77.00 CDCl3
50.80
24.21
13C NMR (CDCl3):
Cl
NH
O
O
NH
H3C
CH3
O
S
O
O
F
F
F
f1 (ppm)

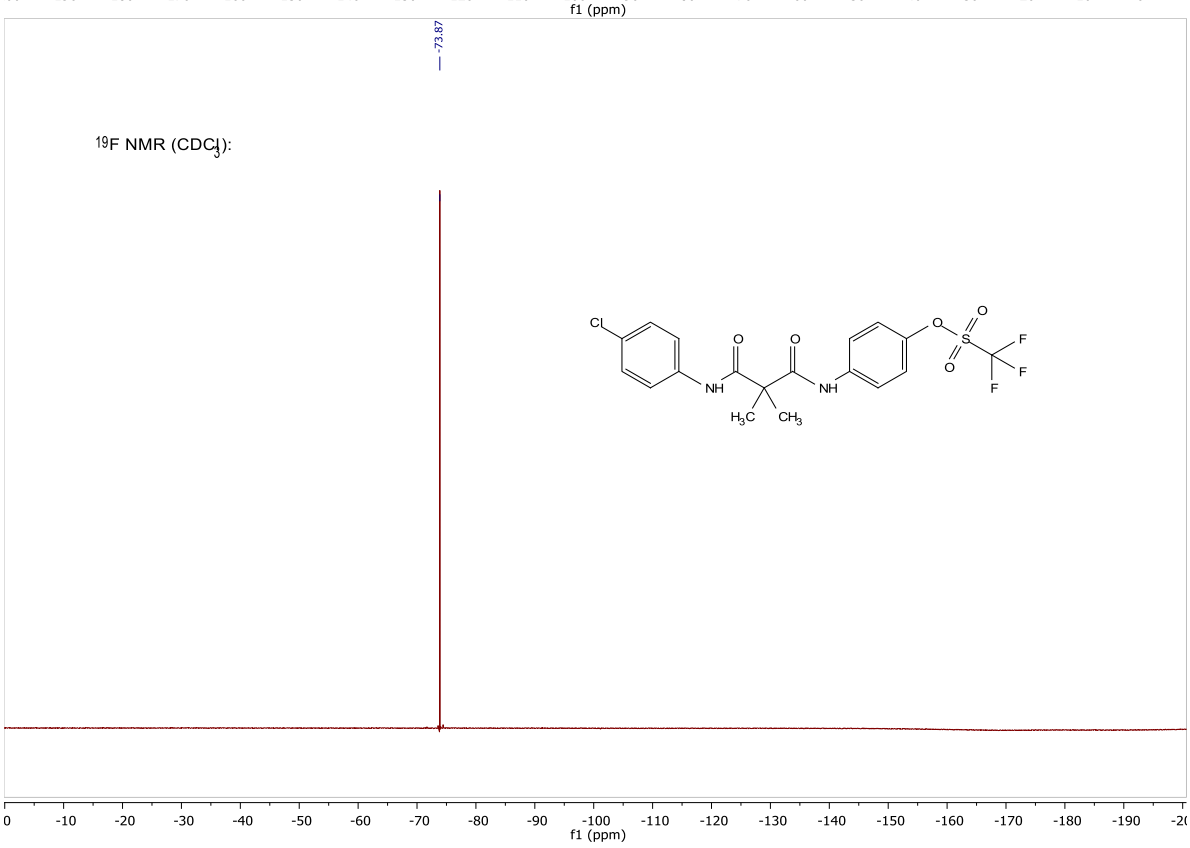
-73.87
19F NMR (CDCl3):
Cl
NH
O
O
NH
H3C
CH3
O
S
O
O
F
F
F
f1 (ppm)

***N*-(4-Methylphenyl)-*N*-(4-trifluoromethylsulfonyloxyphenyl)-2,2-dimethylmalondiamide (4c)**

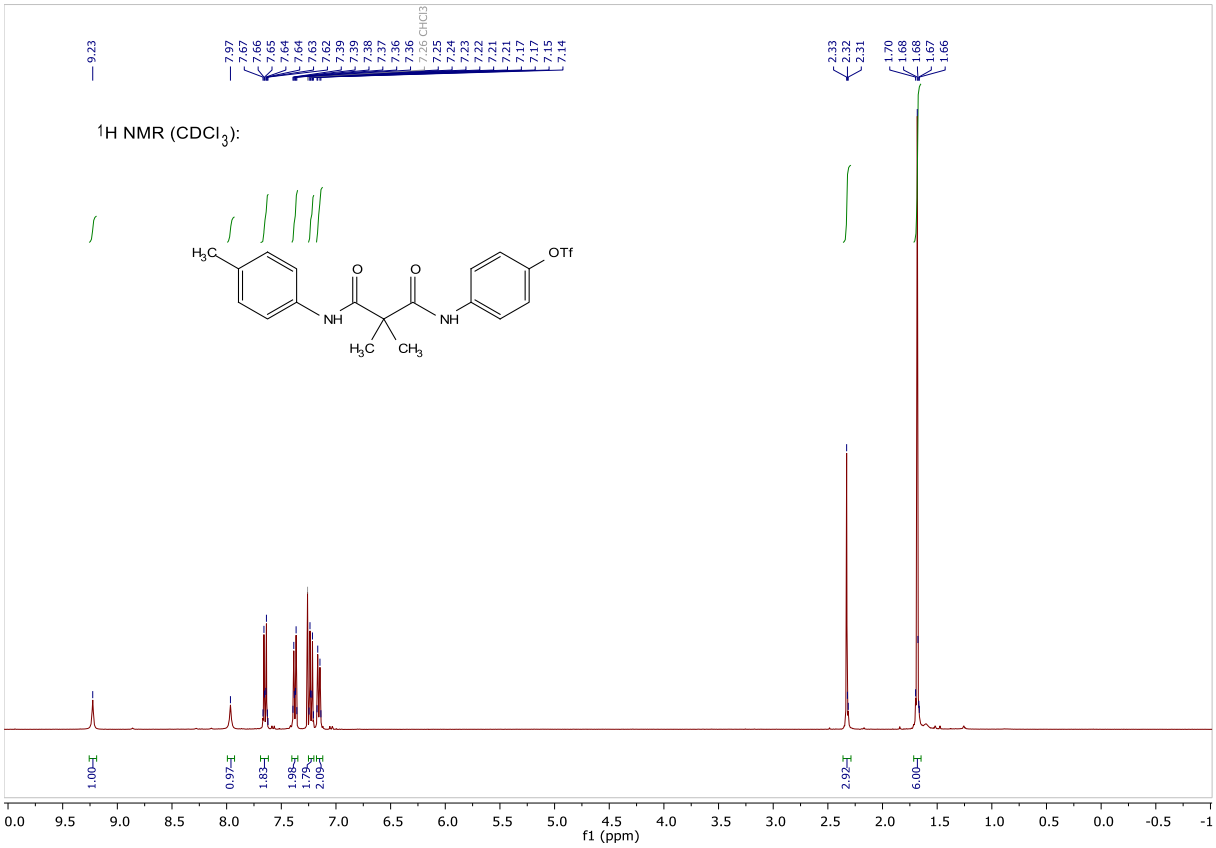

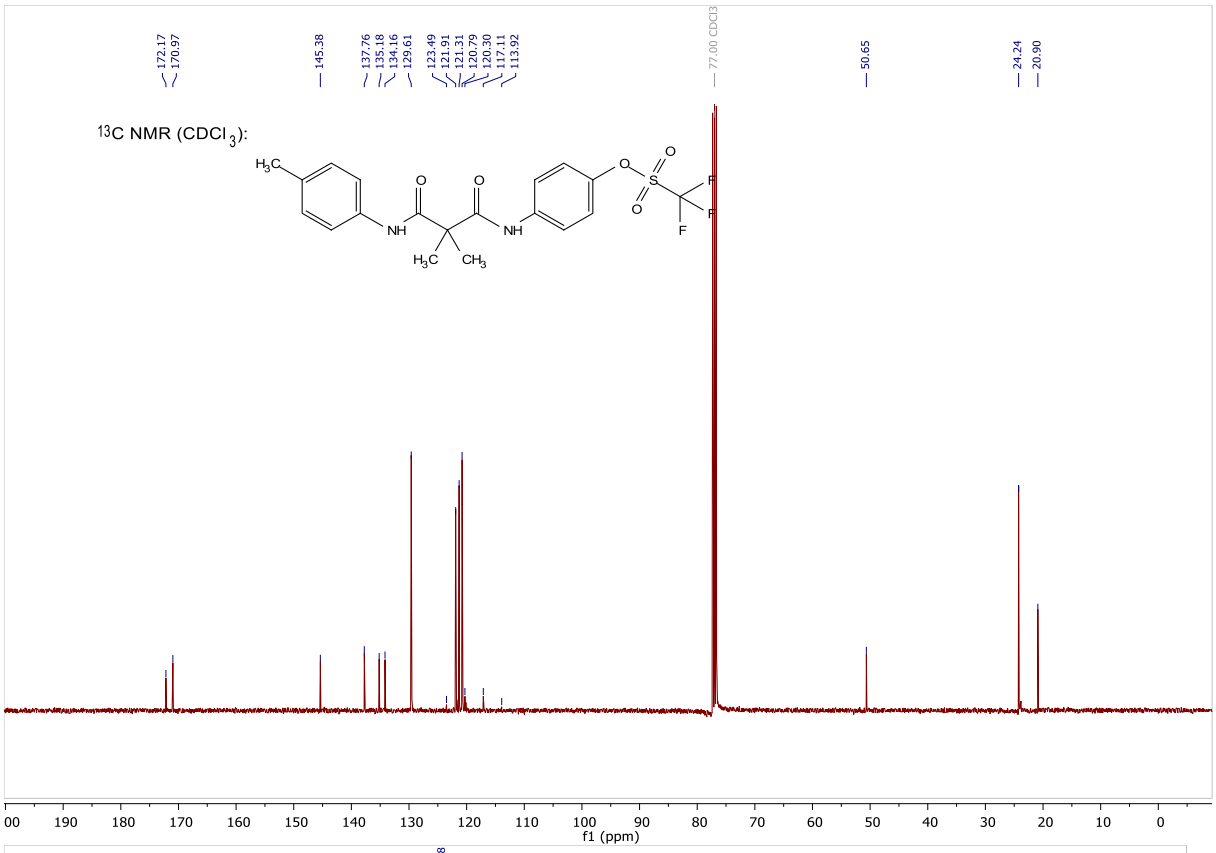
172.17
170.97
145.38
137.76
135.18
134.16
129.61
123.49
121.91
121.31
120.79
120.30
117.11
113.92
77.00 CDCl3
50.65
24.24
20.90
13C NMR (CDCl3):
f1 (ppm)

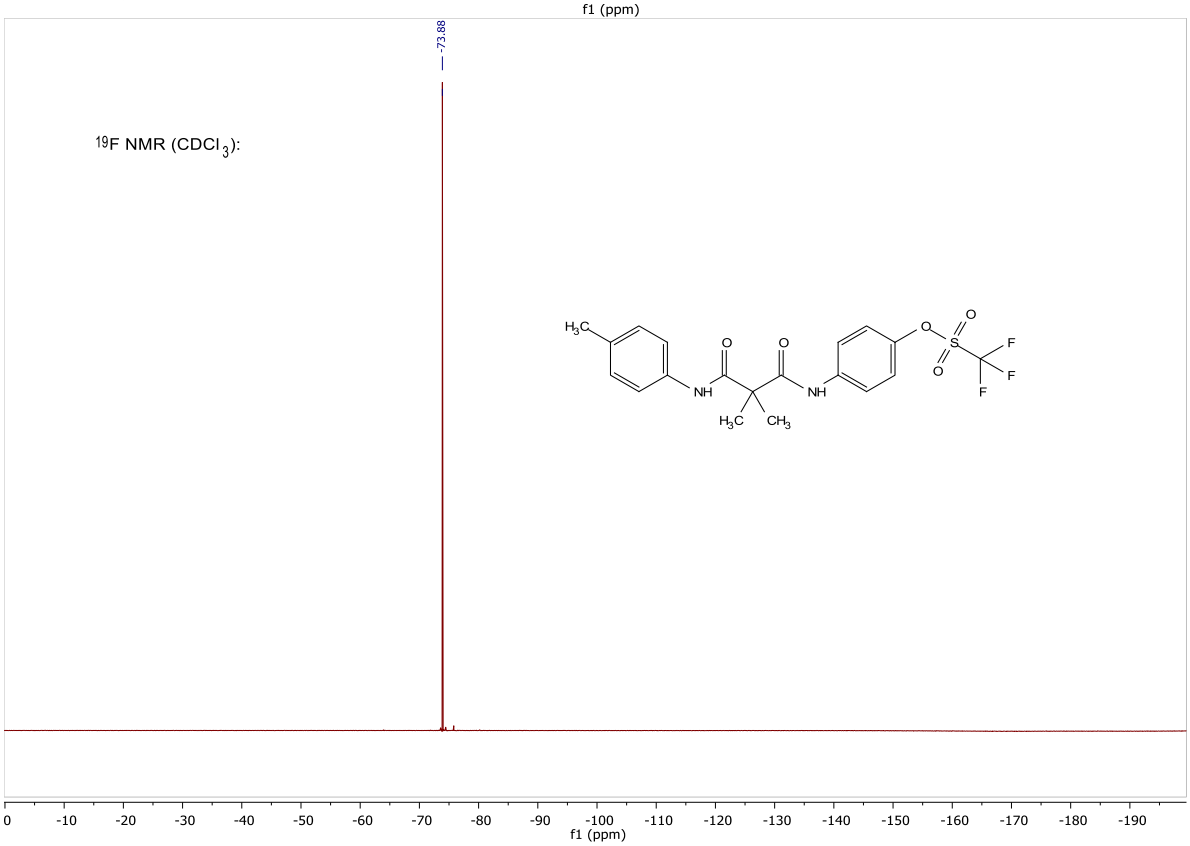
-73.88
19F NMR (CDCl3):
f1 (ppm)

***N*-(4-Chlorophenyl)-*N*-(4-methoxyphenyl)-2,2-dimethylmalondiamide (4a)**

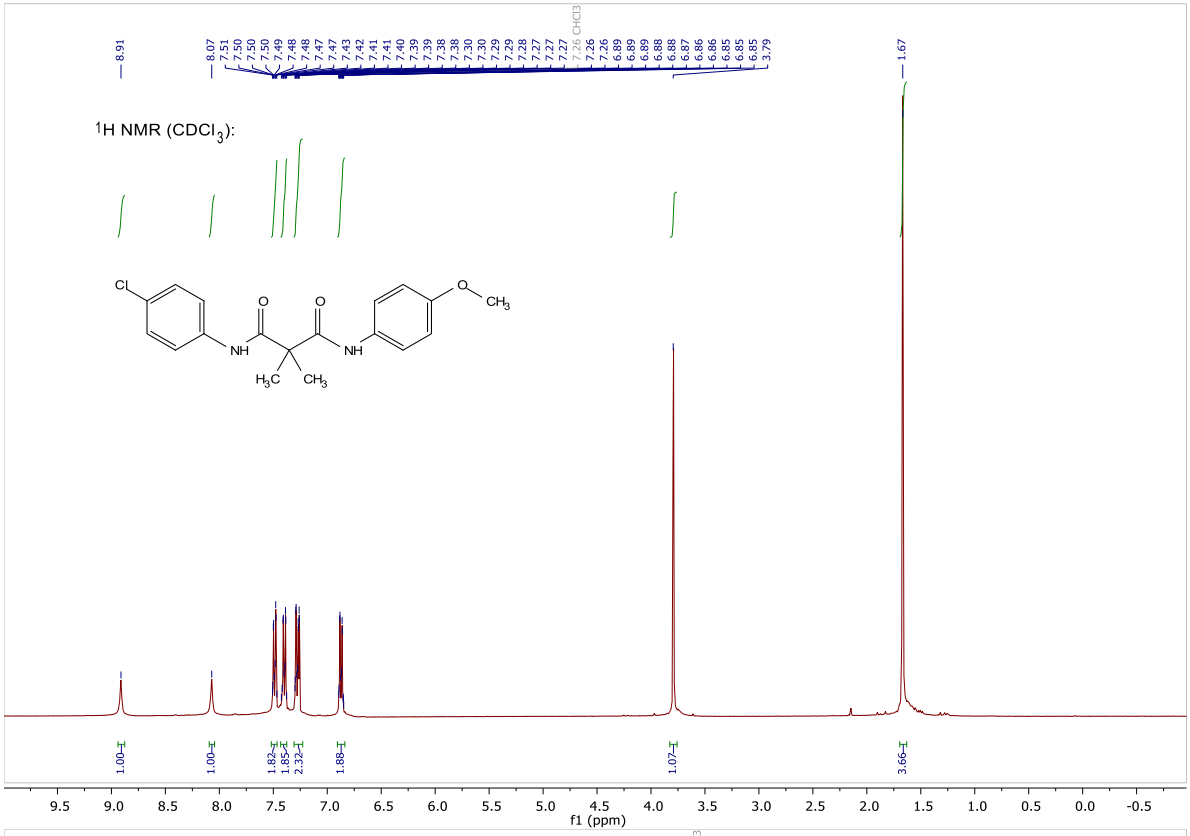

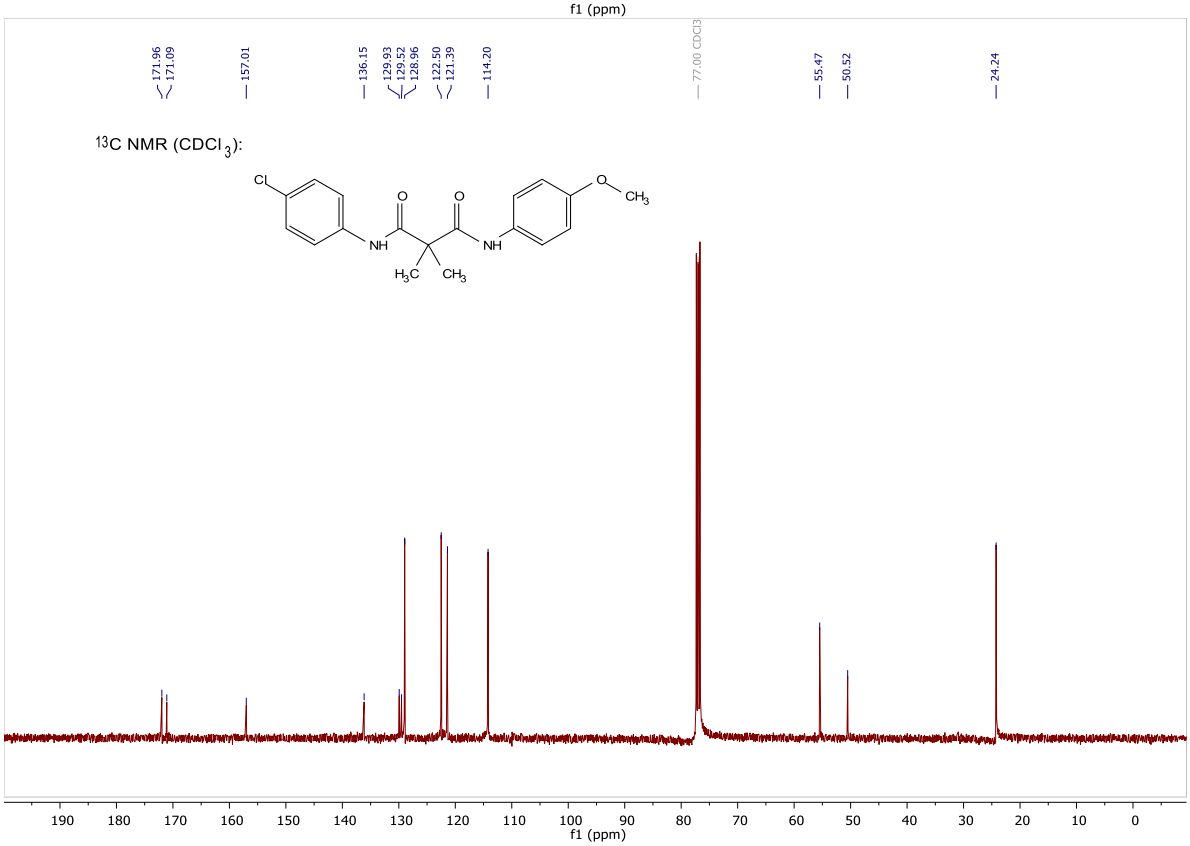

***N*-(4-Methoxyphenyl)-*N*-(4-methylphenyl)-2,2-dimethylmalondiamide (4b)**

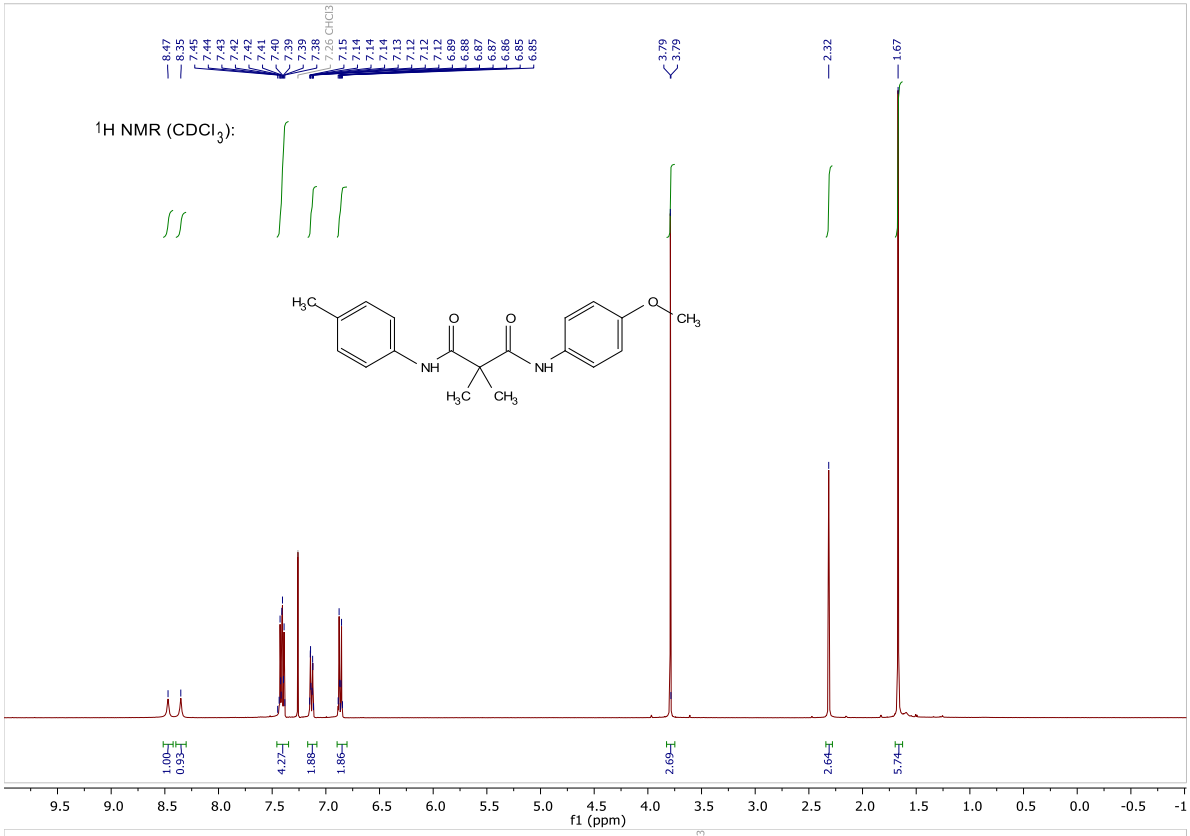

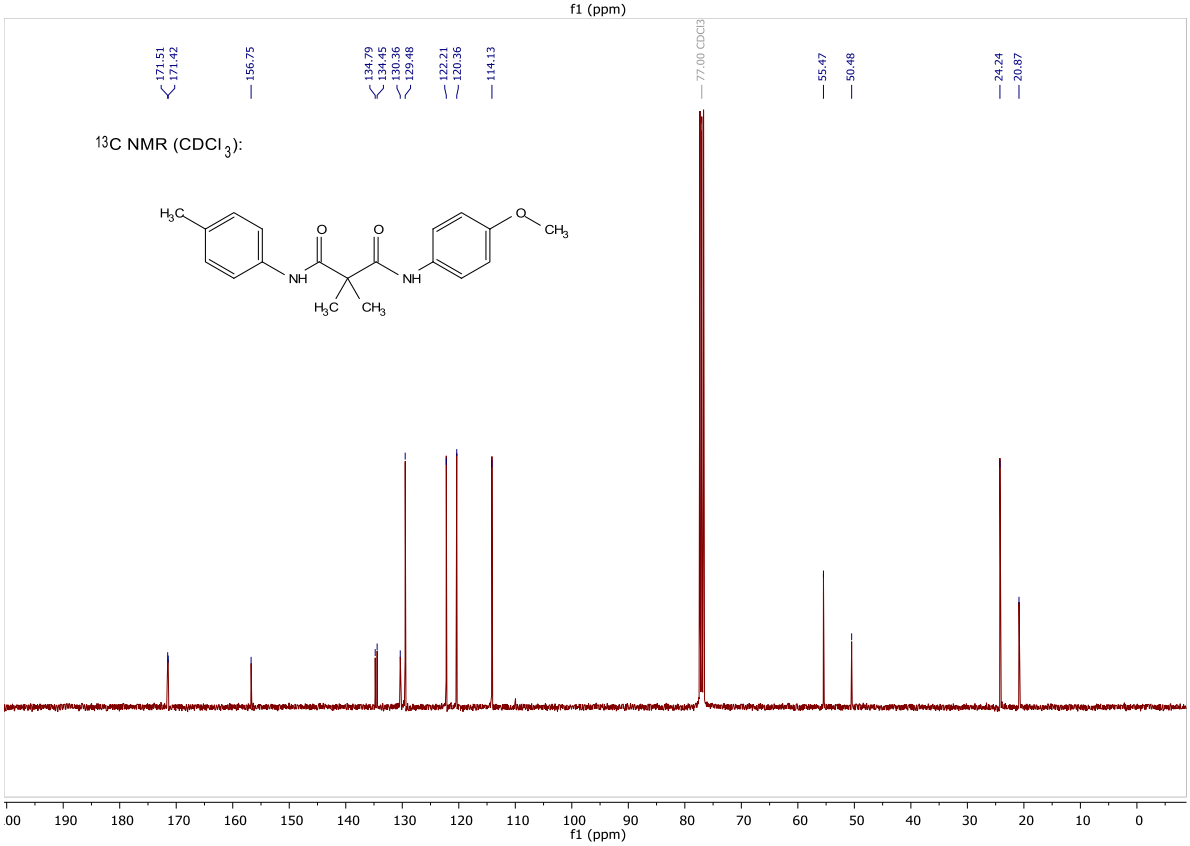

***N*-(4-Chlorophenyl)-*N*-(4-chloro-3-methoxyphenyl)-2,2-dimethylmalondiamide (4d)**

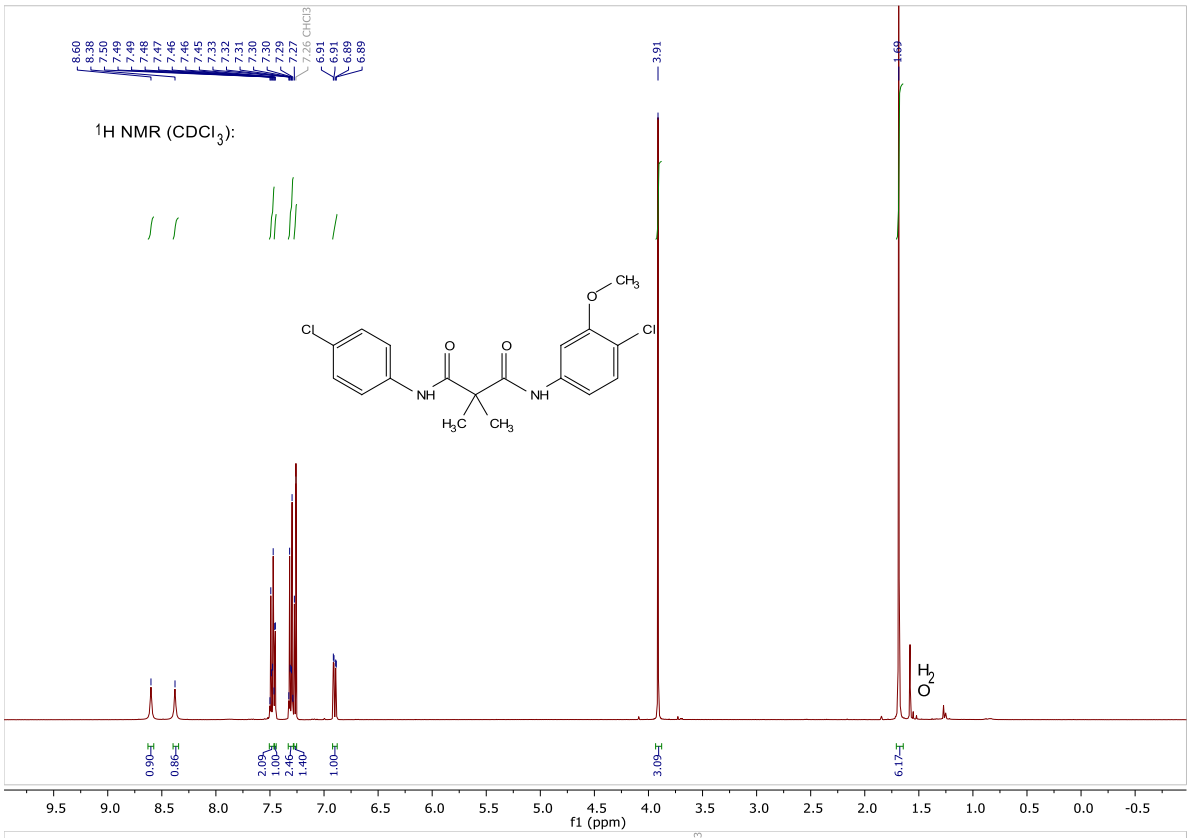

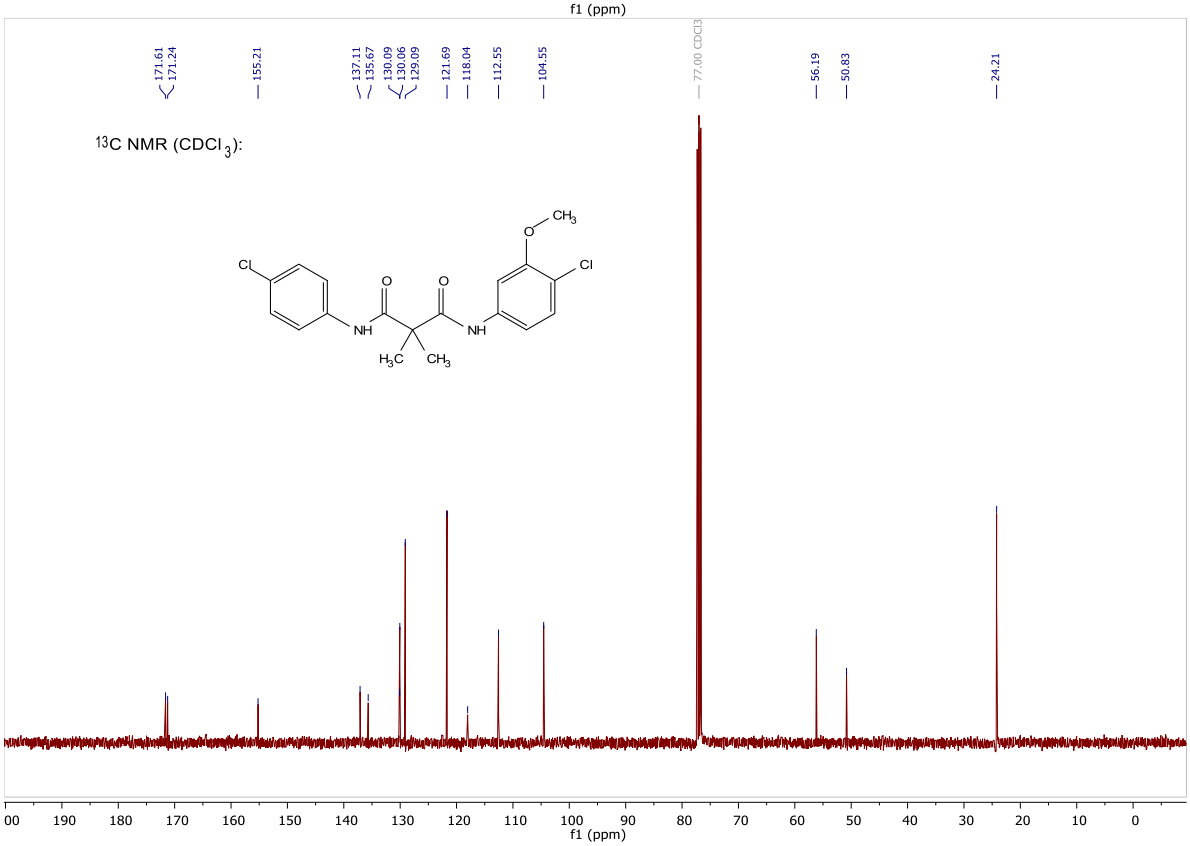

***N*-(4-Chlorophenyl)-*N'*-(2-(1,1,1,3,3,3-hexafluoropropan-2-yloxy)-4-methoxy)-2,2-dimethylmalondiamide (10a)**

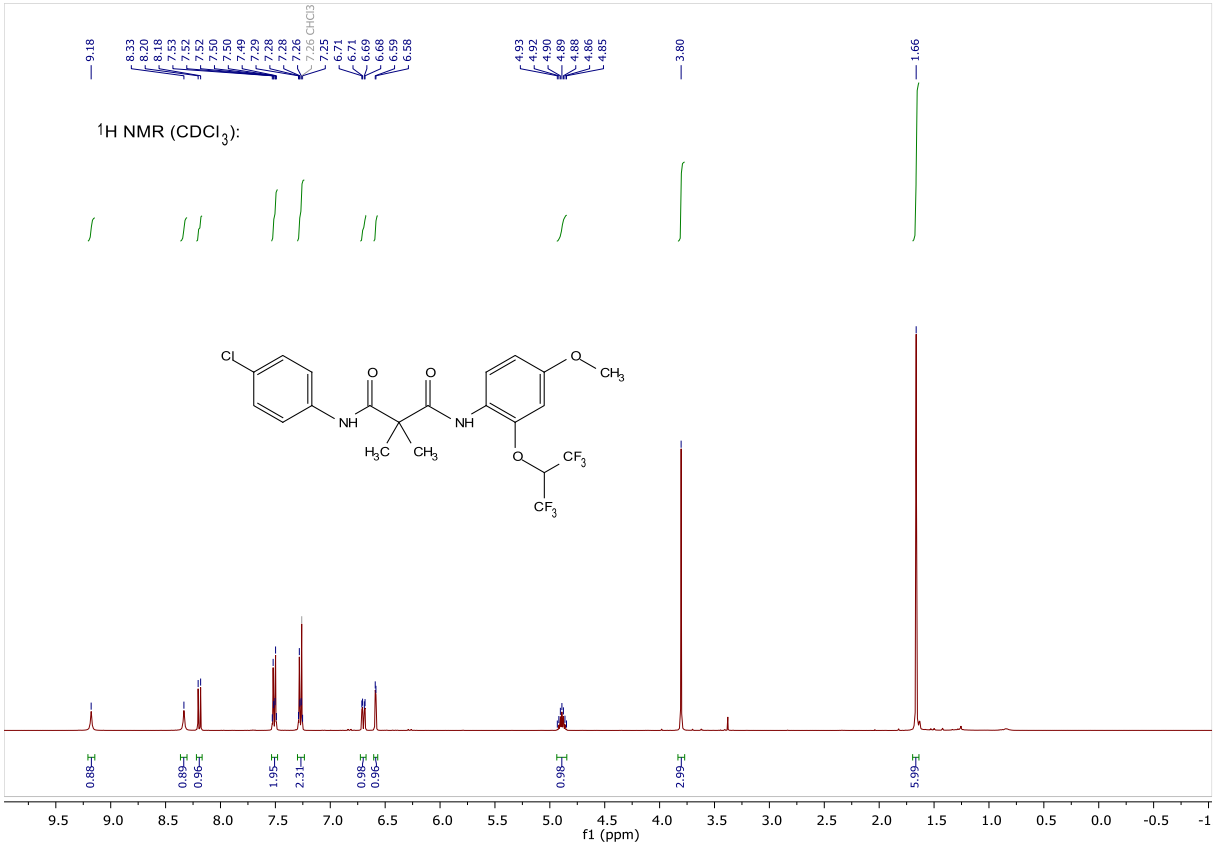

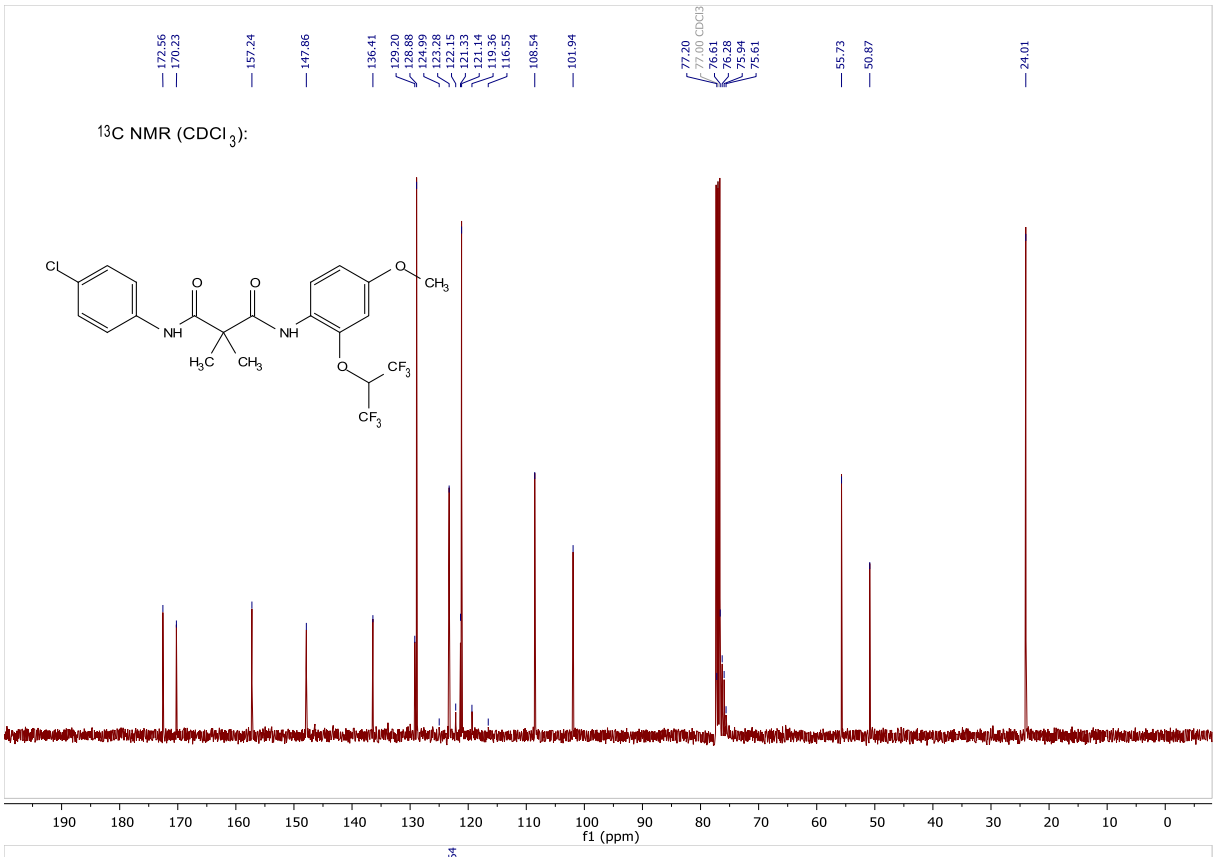
172.56
170.23
157.24
147.86
136.41
129.20
128.88
124.99
123.28
122.15
121.33
121.14
119.36
116.55
108.54
101.94
77.20
77.00 CDCl3
76.61
76.28
75.94
75.61
55.73
50.87
24.01
13C NMR (CDCl3):
Cl
O
O
NH
NH
H3C
CH3
O
CH3
O
CF3
CF3
190 180 170 160 150 140 130 120 110 100 90 80 70 60 50 40 30 20 10 0
f1 (ppm)

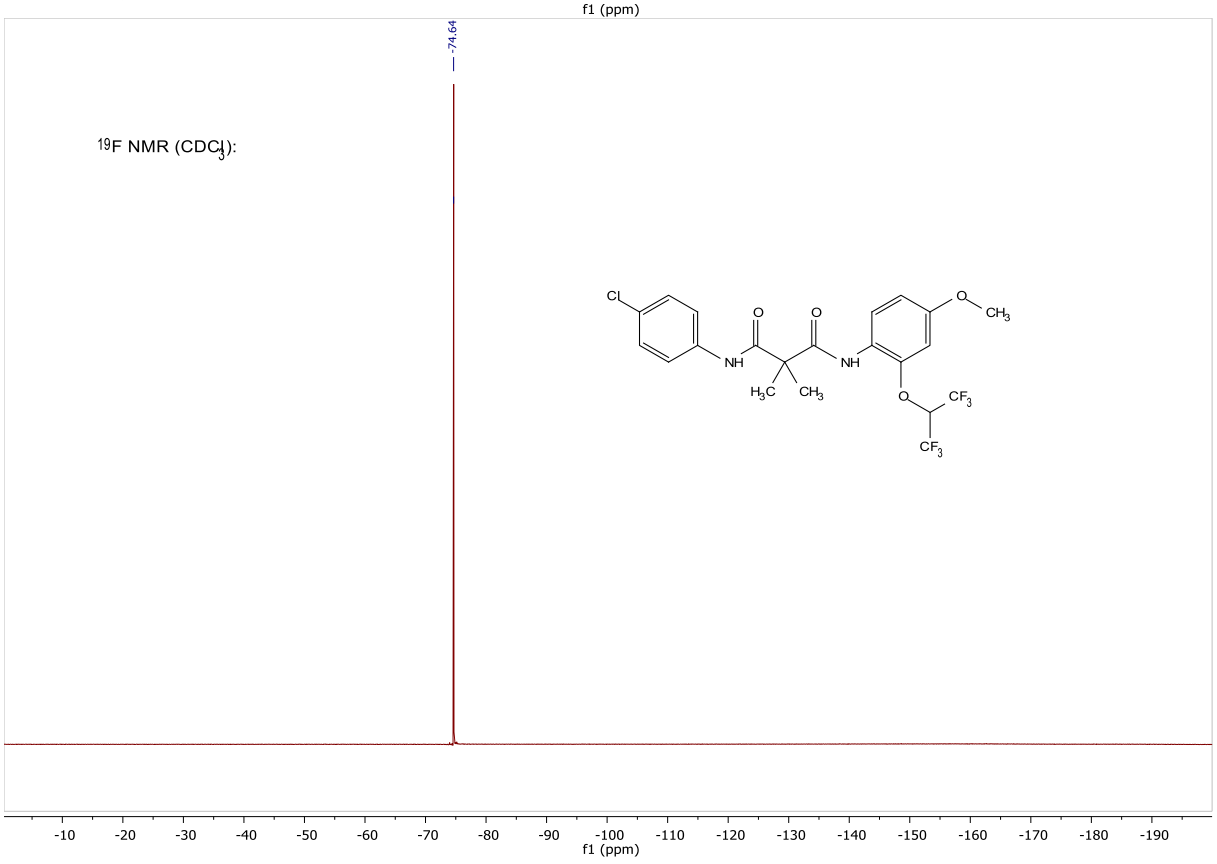
-74.64
19F NMR (CDCl3):
Cl
O
O
NH
NH
H3C
CH3
O
CH3
O
CF3
CF3
-10 -20 -30 -40 -50 -60 -70 -80 -90 -100 -110 -120 -130 -140 -150 -160 -170 -180 -190
f1 (ppm)

***N*-(2-(1,1,1,3,3,3-Hexafluoropropan-2-yloxy)-4-methoxy)-*N*-(4-methylphenyl)-2,2-dimethylmalondiamide (10b)**

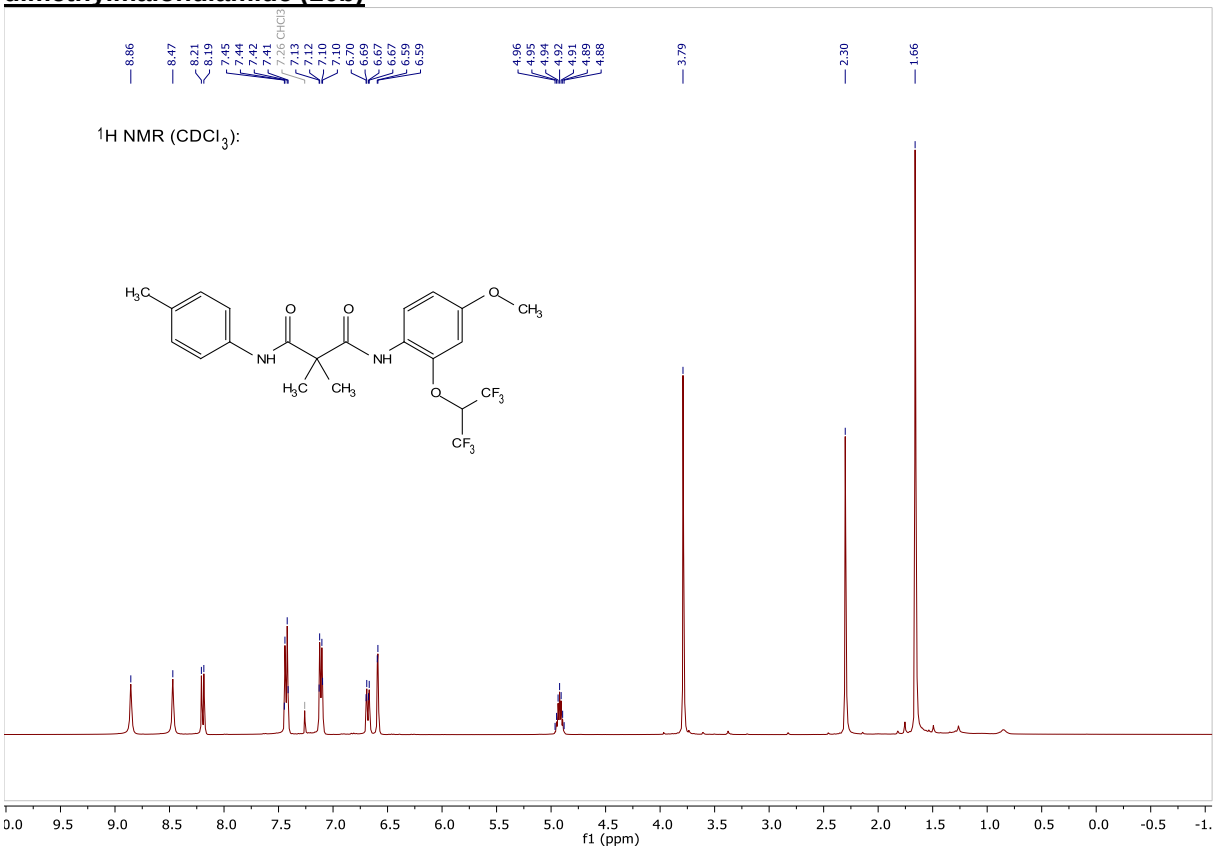

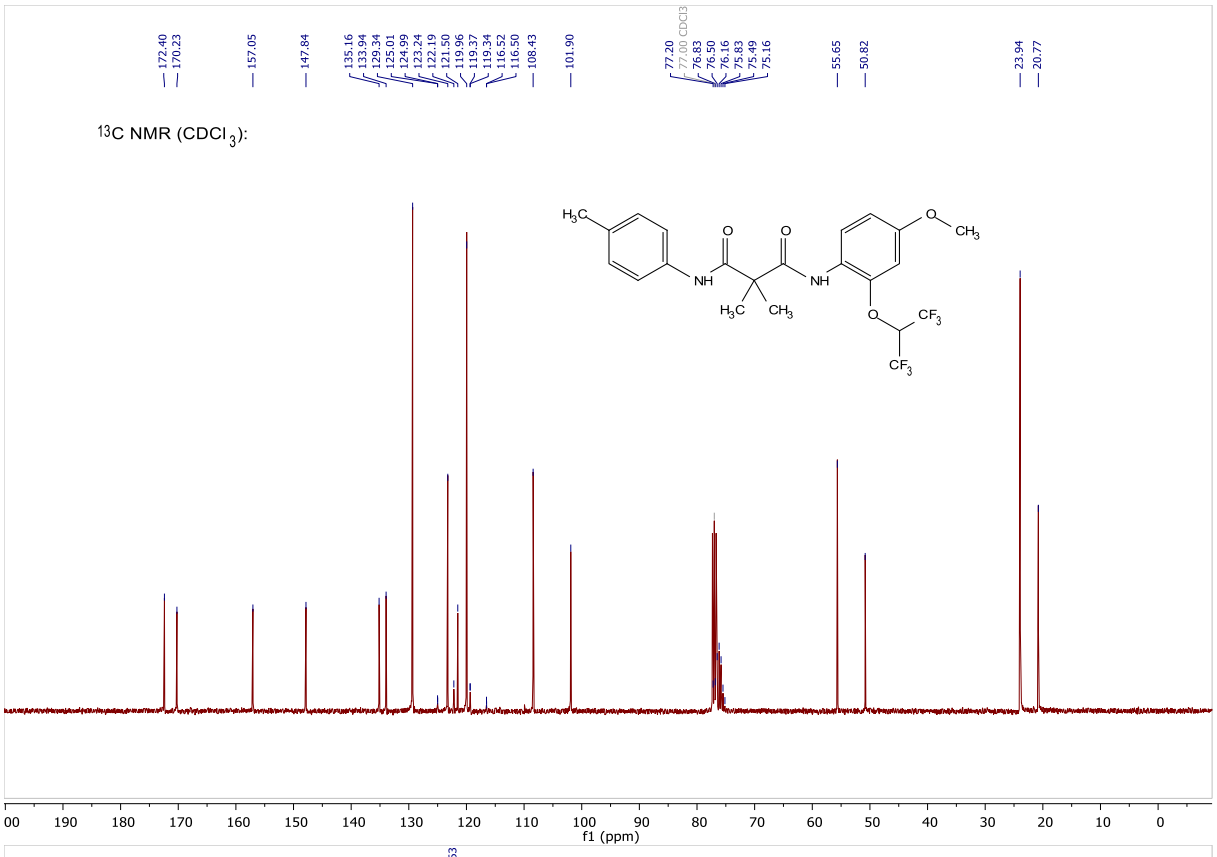
172.40
170.23
157.05
147.84
135.16
133.94
129.34
125.01
124.99
123.24
122.19
121.50
119.96
119.37
119.34
116.52
116.50
108.43
101.90
77.20
77.00 CDCl3
76.83
76.50
76.16
75.83
75.49
75.16
55.65
50.82
23.94
20.77
13C NMR (CDCl3):
f1 (ppm)

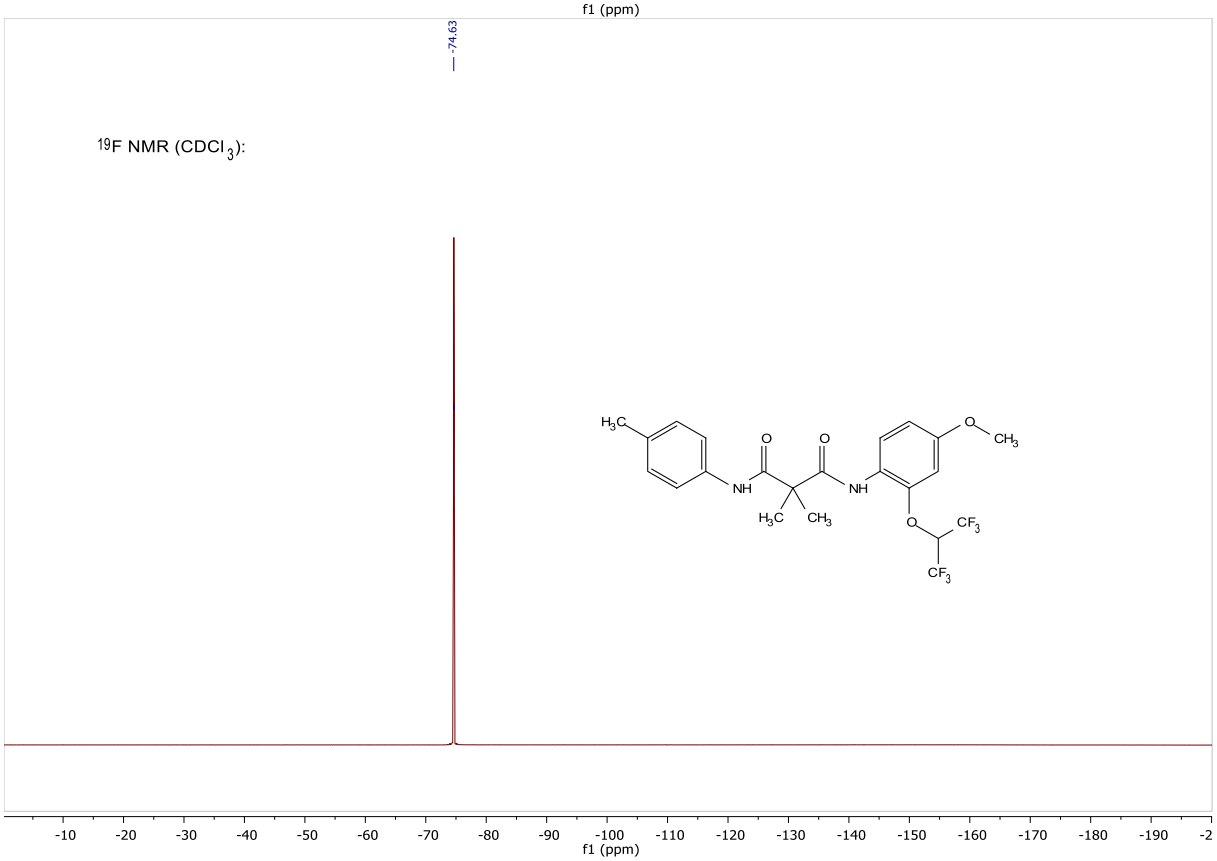
-74.63
19F NMR (CDCl3):
f1 (ppm)

***N*-(4-(1-(1,1,1,3,3,3-Hexafluoropropan-2-yloxy)-methyl)phenyl)-*N*-(4-trifluoromethylsulfonyloxyphenyl)-2,2-dimethylmalondiamide (10c)**

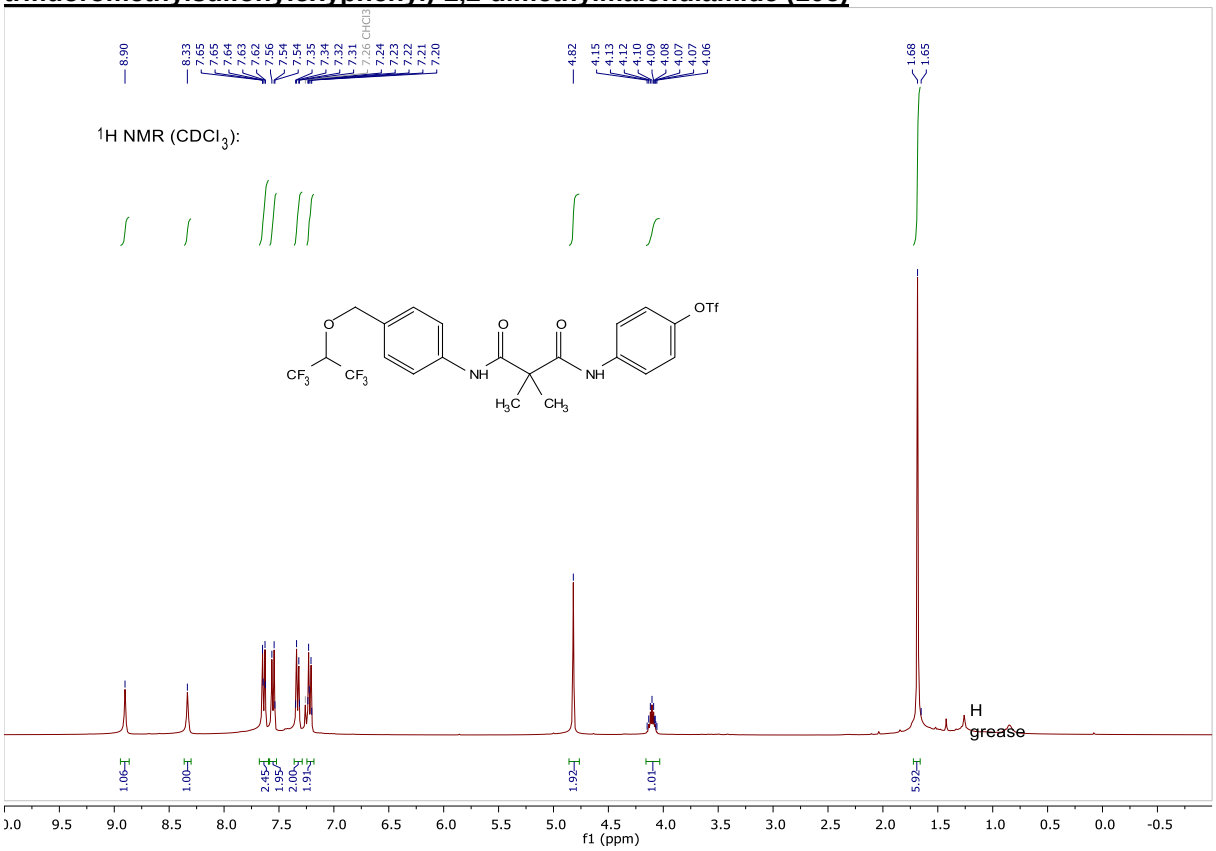

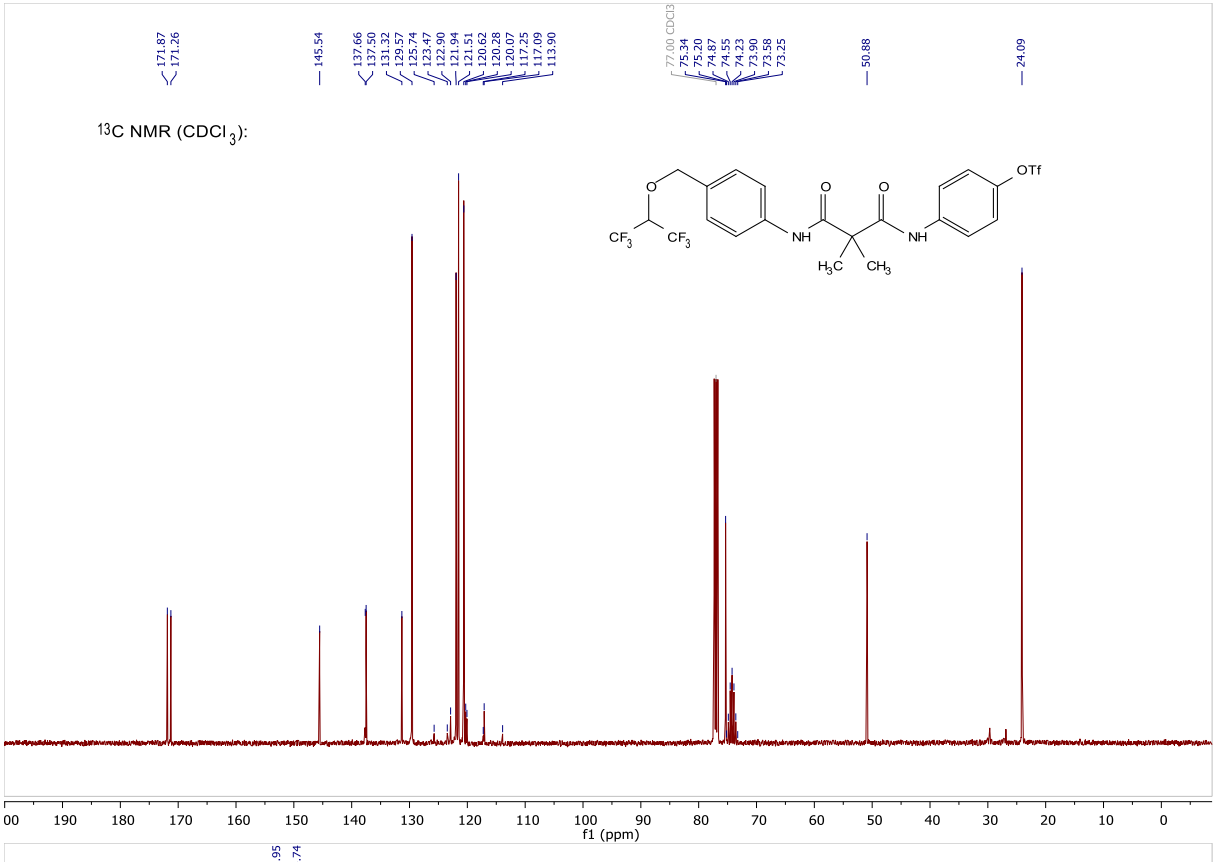
171.87
171.26
145.54
137.66
137.50
131.32
129.57
125.74
123.47
122.90
121.94
121.51
120.62
120.28
120.07
117.25
117.09
113.90
77.00 CDCl3
75.34
75.20
74.87
74.55
74.23
73.90
73.58
73.25
50.88
24.09
13C NMR (CDCl3):
OTf
O
CF3
CF3
NH
O
O
NH
H3C
CH3
f1 (ppm)

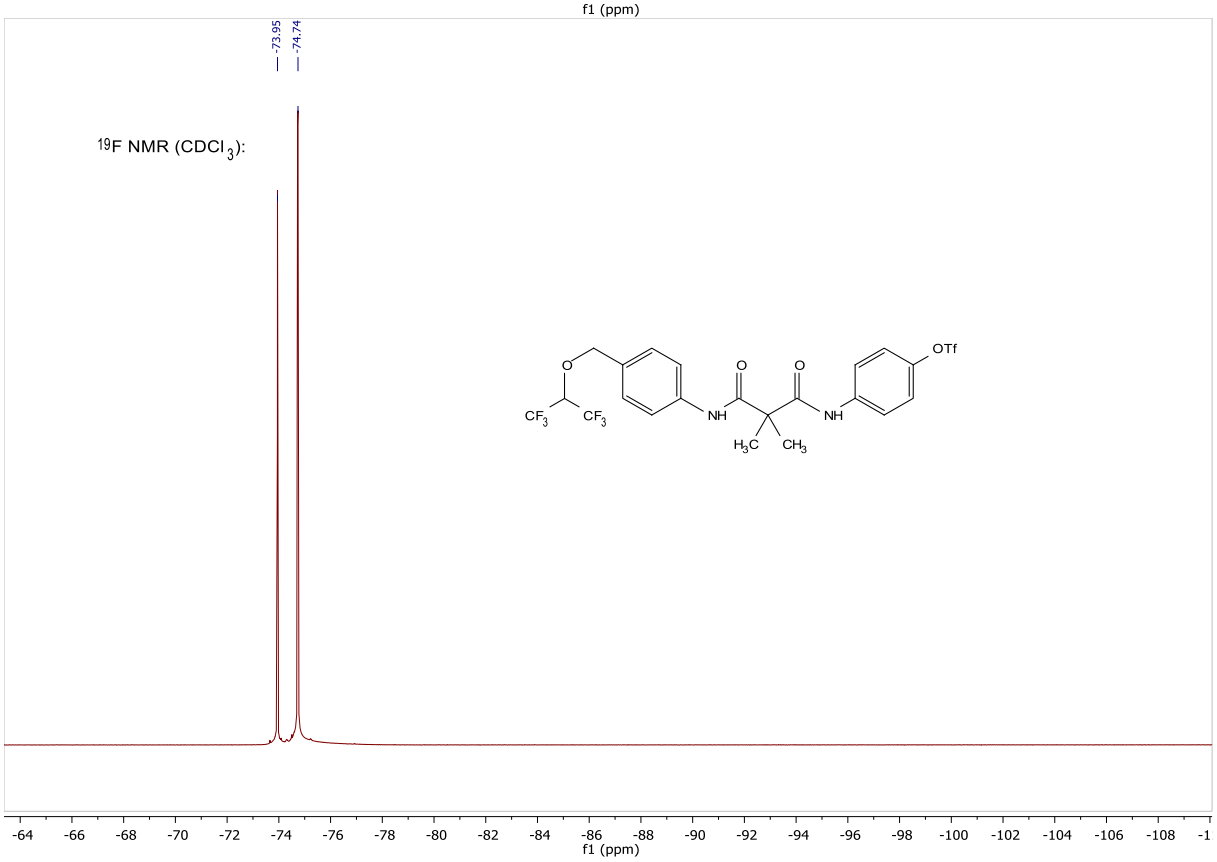
-73.95
-74.74
19F NMR (CDCl3):
OTf
O
CF3
CF3
NH
O
O
NH
H3C
CH3
f1 (ppm)

***N*-(4-Chlorophenyl)-*O*-(1,1,1,3,3,3-hexafluoropropan-2-yl)-2,2-dimethylmalonmonoamide (11)**

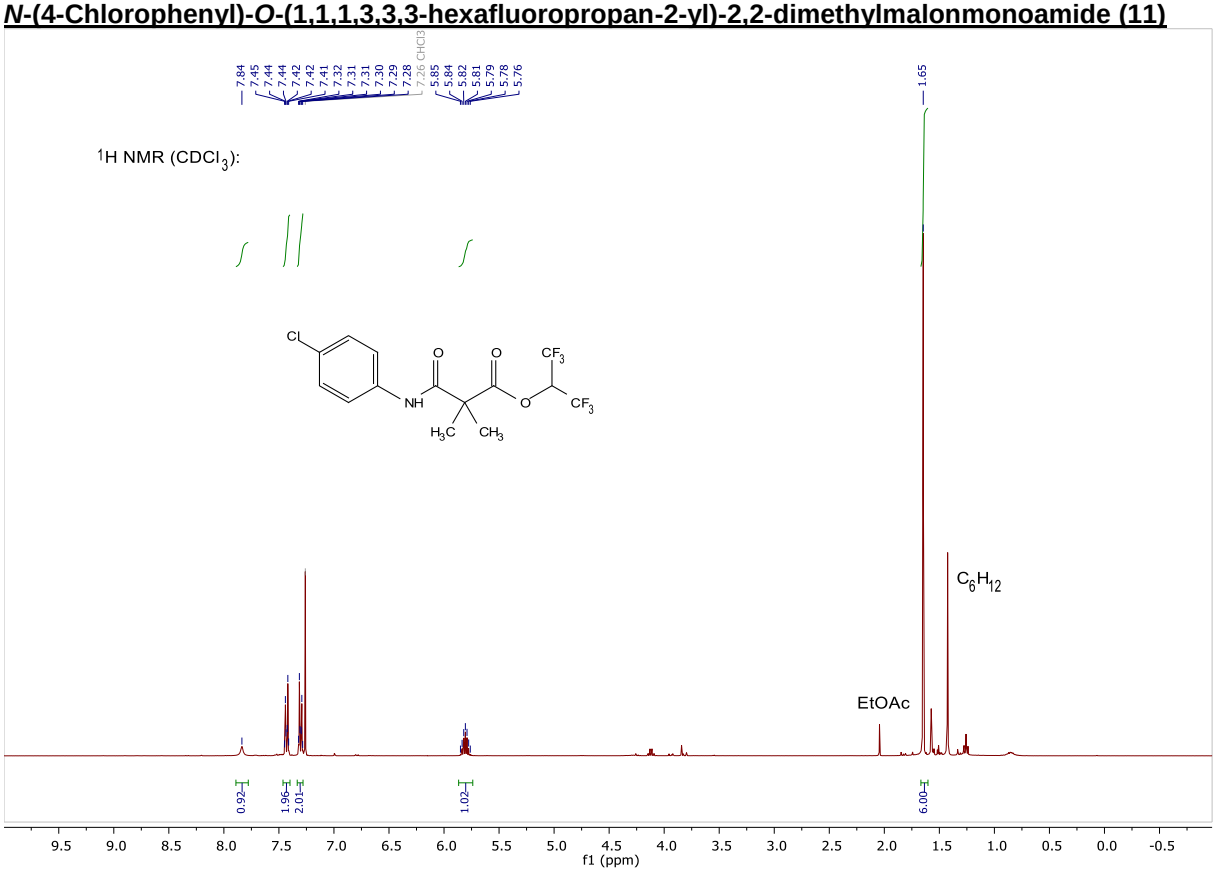

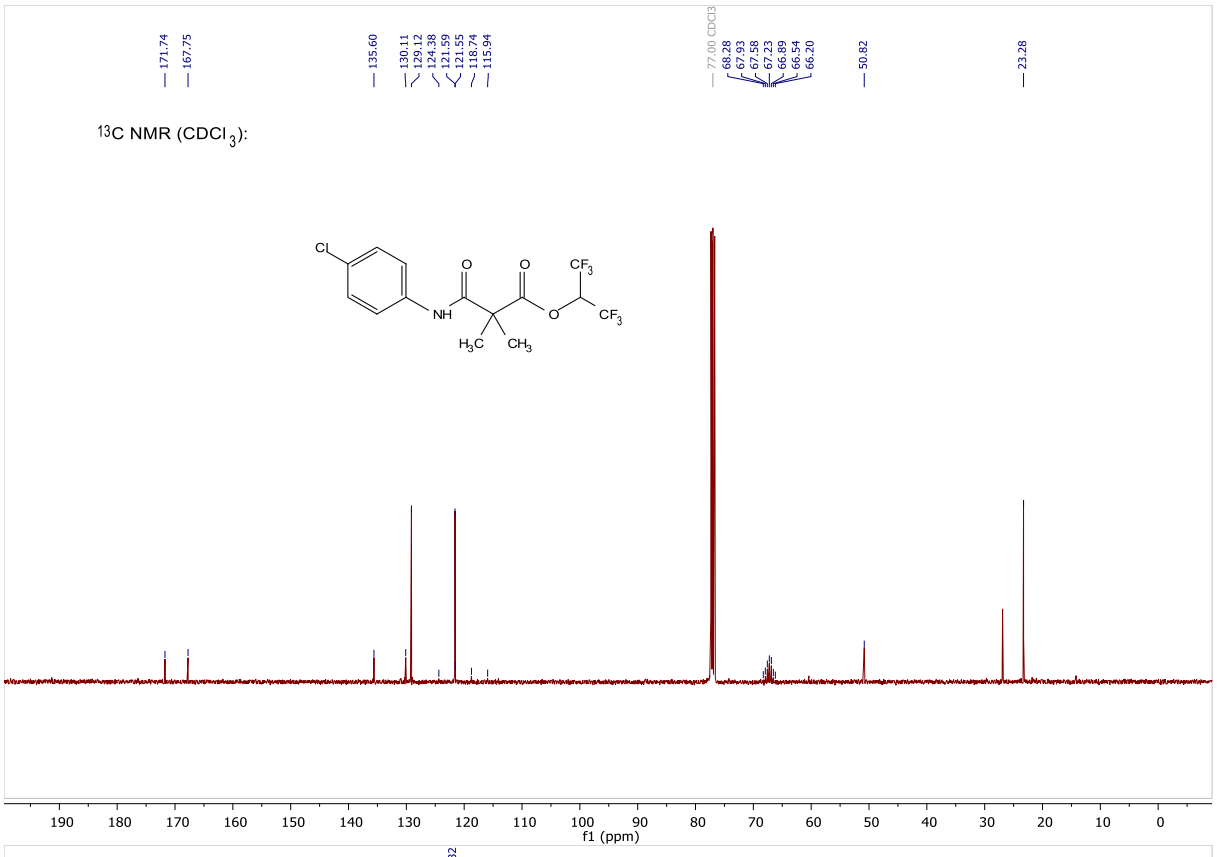
171.74
167.75
135.60
130.11
129.12
124.38
121.59
121.55
118.74
115.94
77.00 CDCl3
68.28
67.93
67.58
67.23
66.89
66.54
66.20
50.82
23.28
13C NMR (CDCl3):
Cl
NH
O
O
O
CF3
CF3
H3C
CH3
190 180 170 160 150 140 130 120 110 100 90 80 70 60 50 40 30 20 10 0
f1 (ppm)

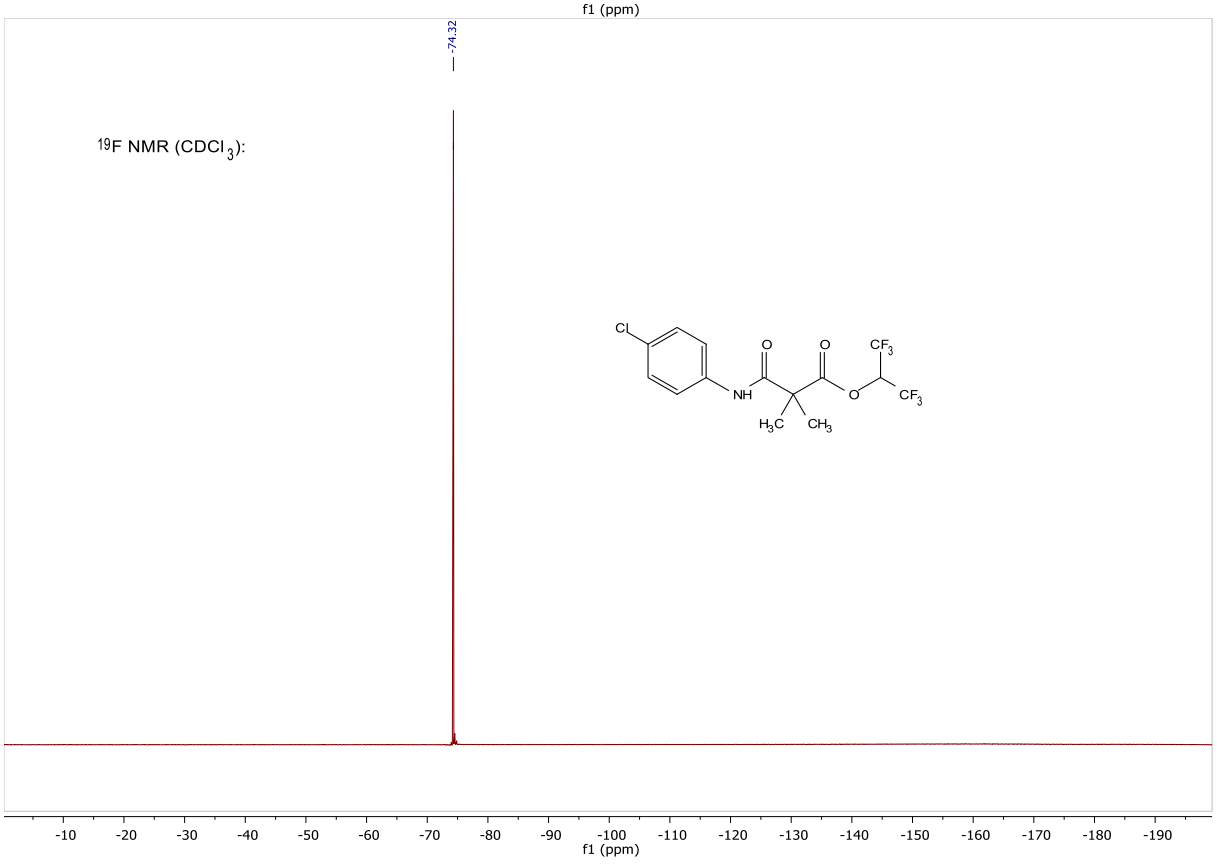
-74.32
19F NMR (CDCl3):
Cl
NH
O
O
O
CF3
CF3
H3C
CH3
-10 -20 -30 -40 -50 -60 -70 -80 -90 -100 -110 -120 -130 -140 -150 -160 -170 -180 -190
f1 (ppm)

1-(4-Chlorophenyl)-2-(3-methoxy-4-chlorophenyl)-4,4-dimethylpyrazolidin-3,5-dione (5a)

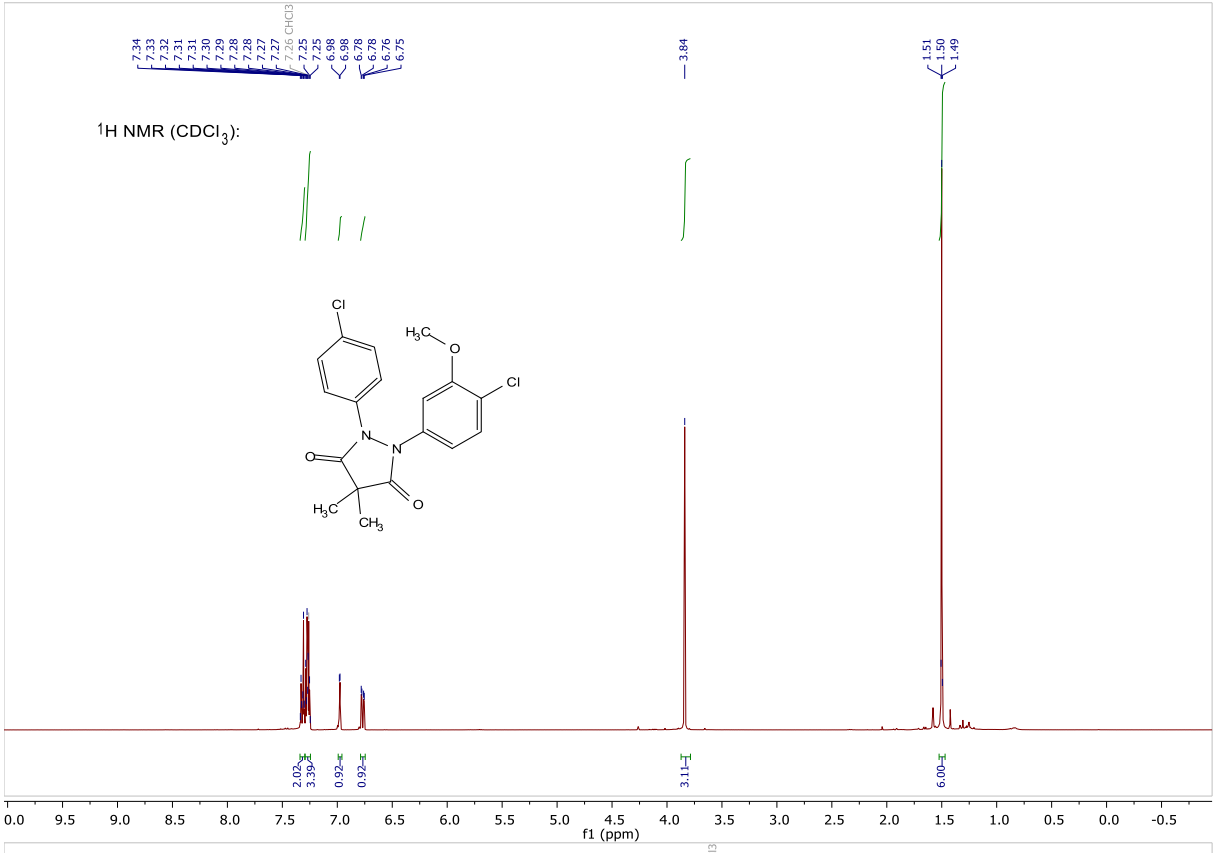

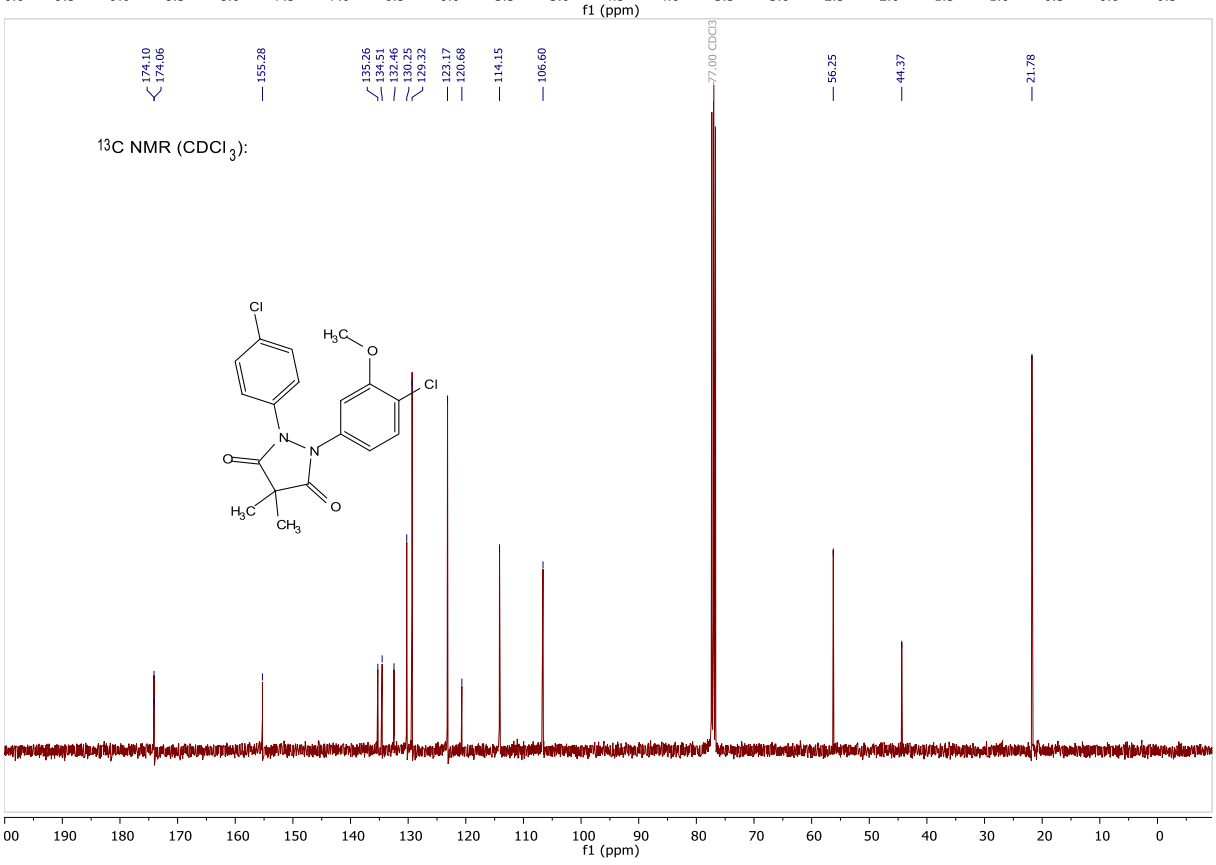

1-(4-Chlorophenyl)-2-(4-trifluoromethylsulfonyloxyphenyl)-4,4-dimethylpyrazolidin-3,5-dione (5b)

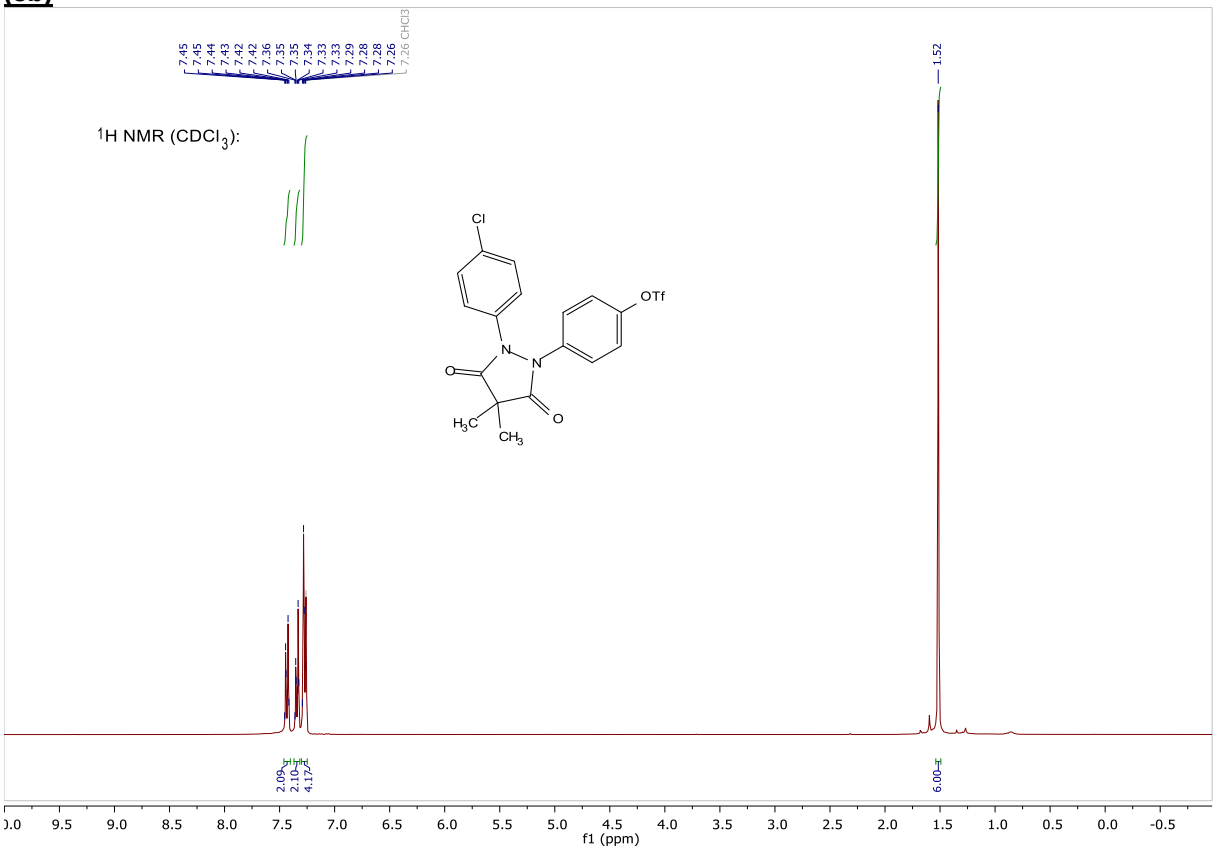

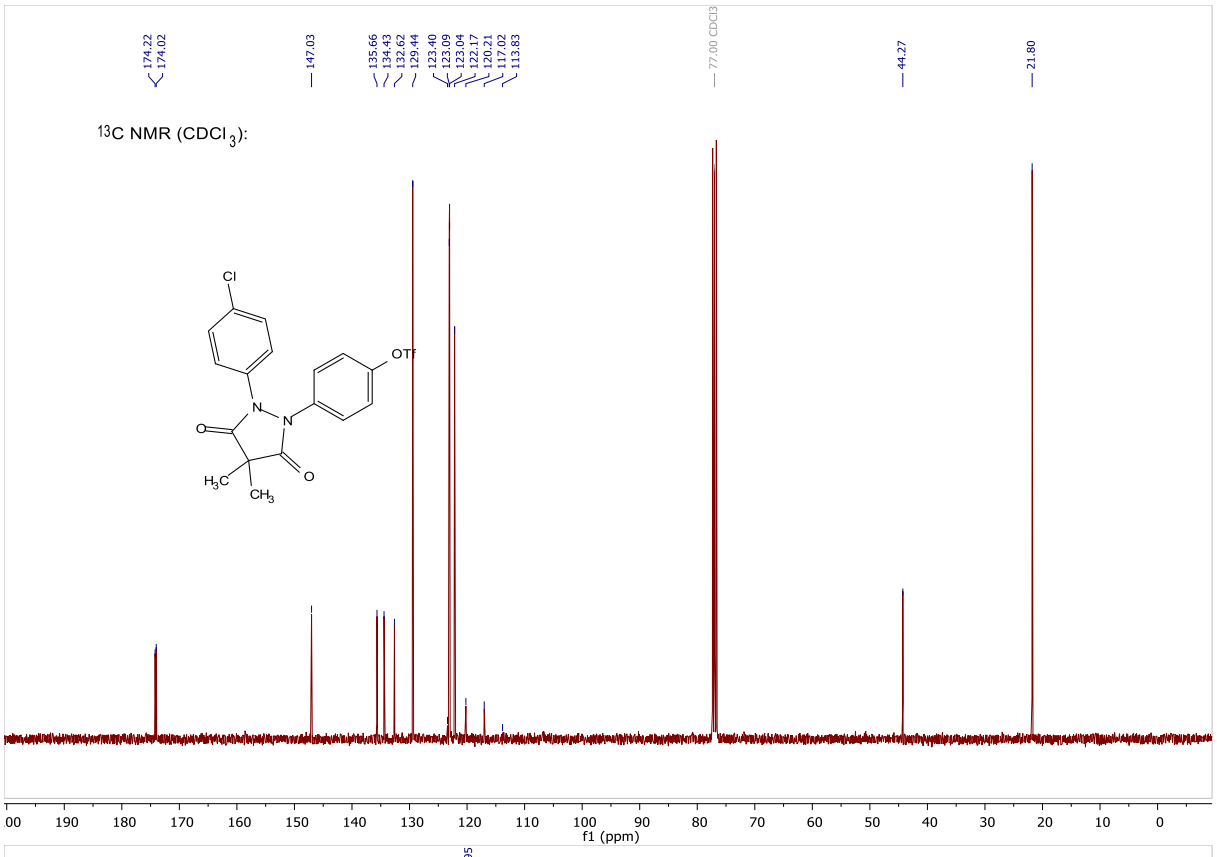
174.22
174.02
147.03
135.66
134.43
132.62
129.44
123.40
123.09
123.04
122.17
120.21
117.02
113.83
77.00 CDCl3
44.27
21.80
13C NMR (CDCl3):
Cl
OTf
N
N
O
O
H3C
CH3
f1 (ppm)

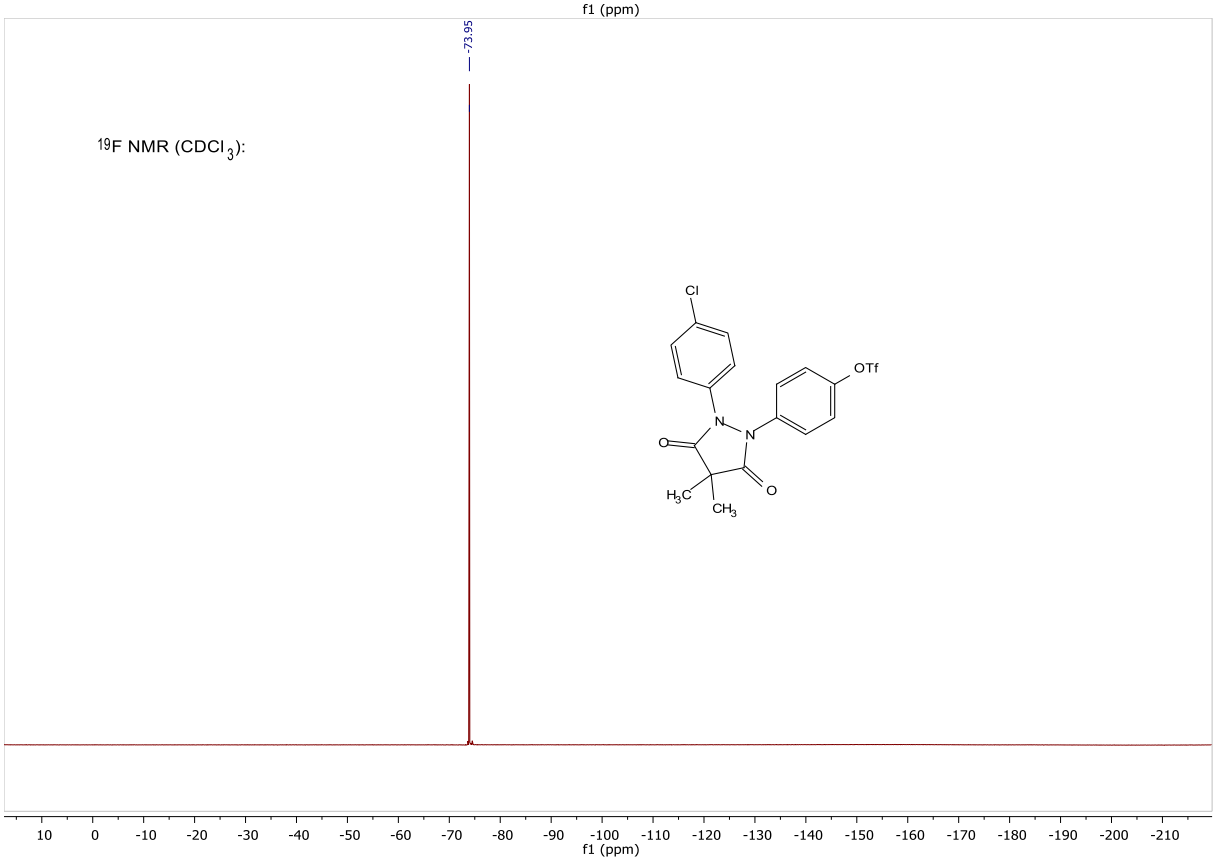
-73.95
19F NMR (CDCl3):
Cl
OTf
N
N
O
O
H3C
CH3
f1 (ppm)

1,2-Bis-(4-trifluoromethylsulfonyloxyphenyl)-4,4-dimethylpyrazolidin-3,5-dione (5e)

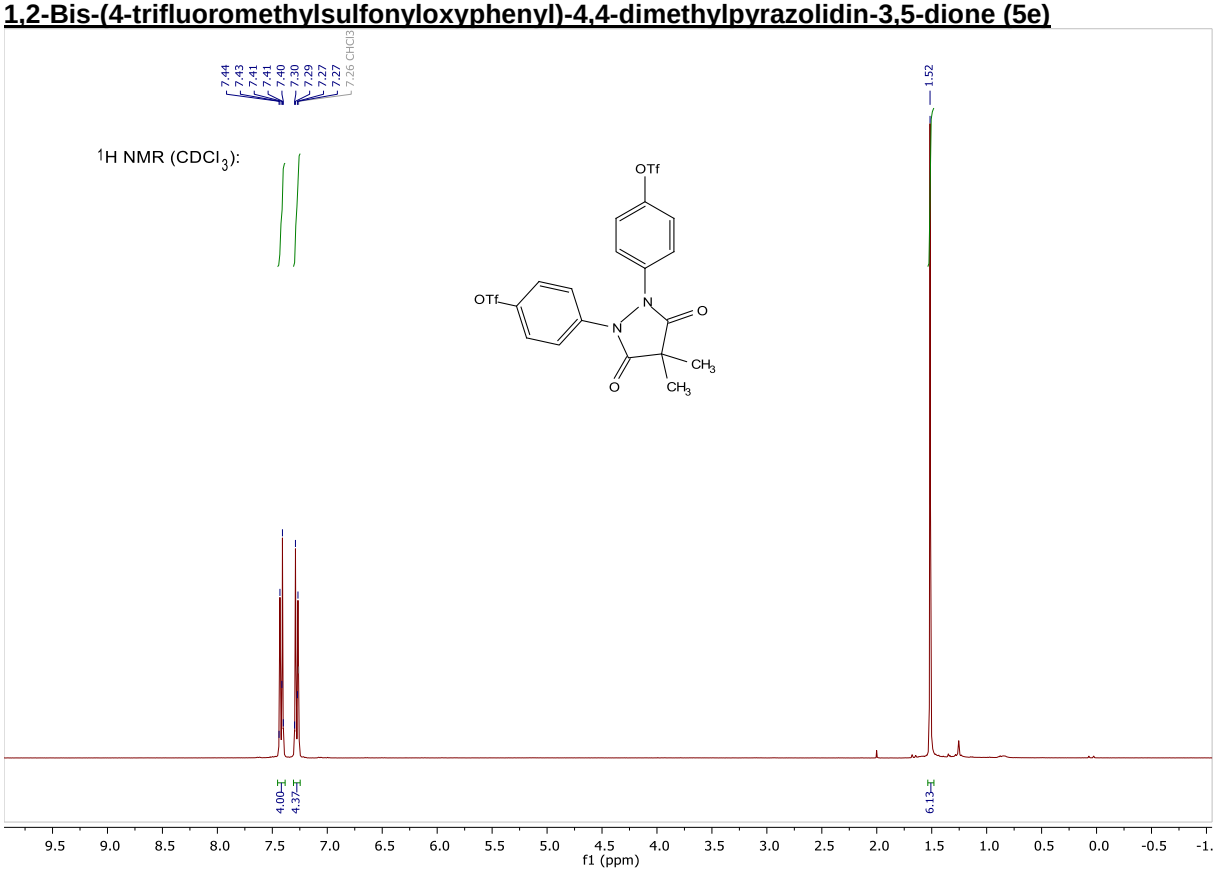

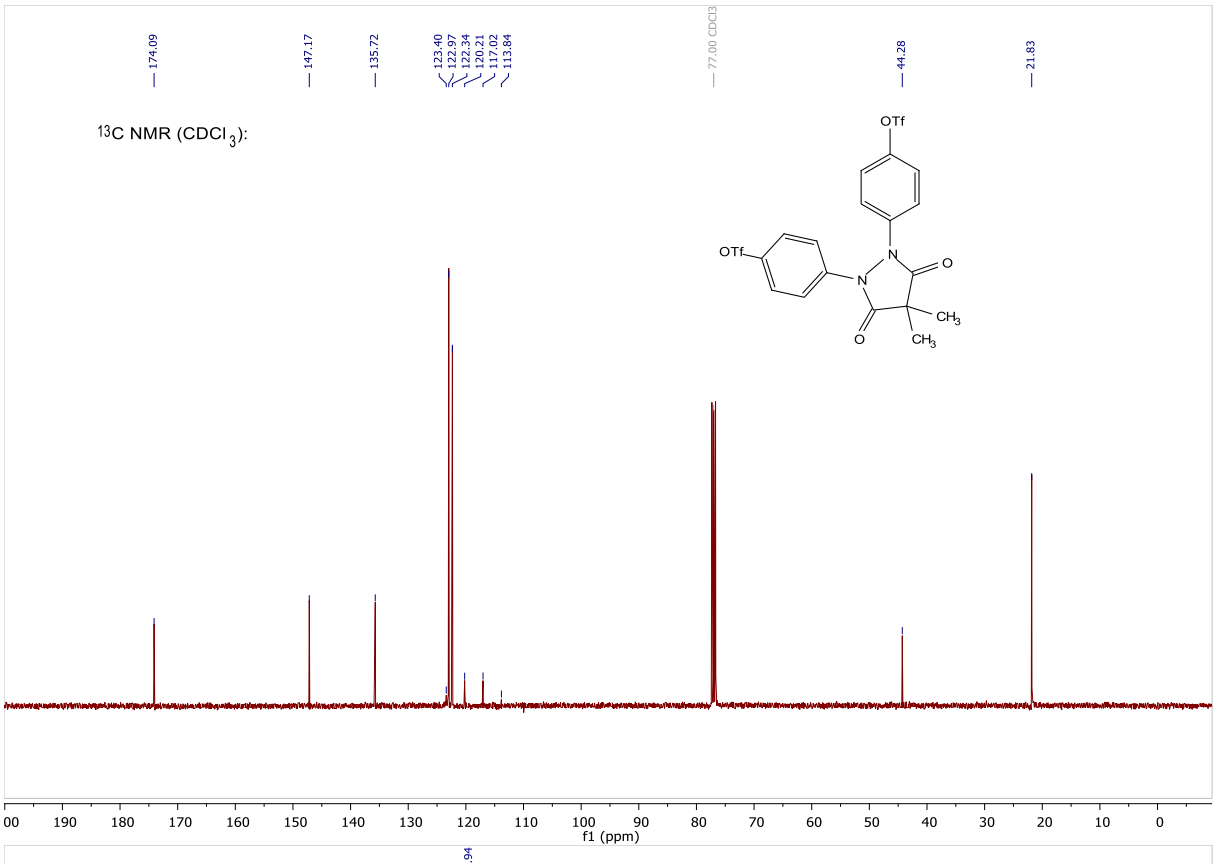
174.09
147.17
135.72
123.40
122.97
122.34
120.21
117.02
113.84
77.00 CDCl3
44.28
21.83
13C NMR (CDCl3):
OTf
OTf
N
N
O
O
CH3
CH3
f1 (ppm)

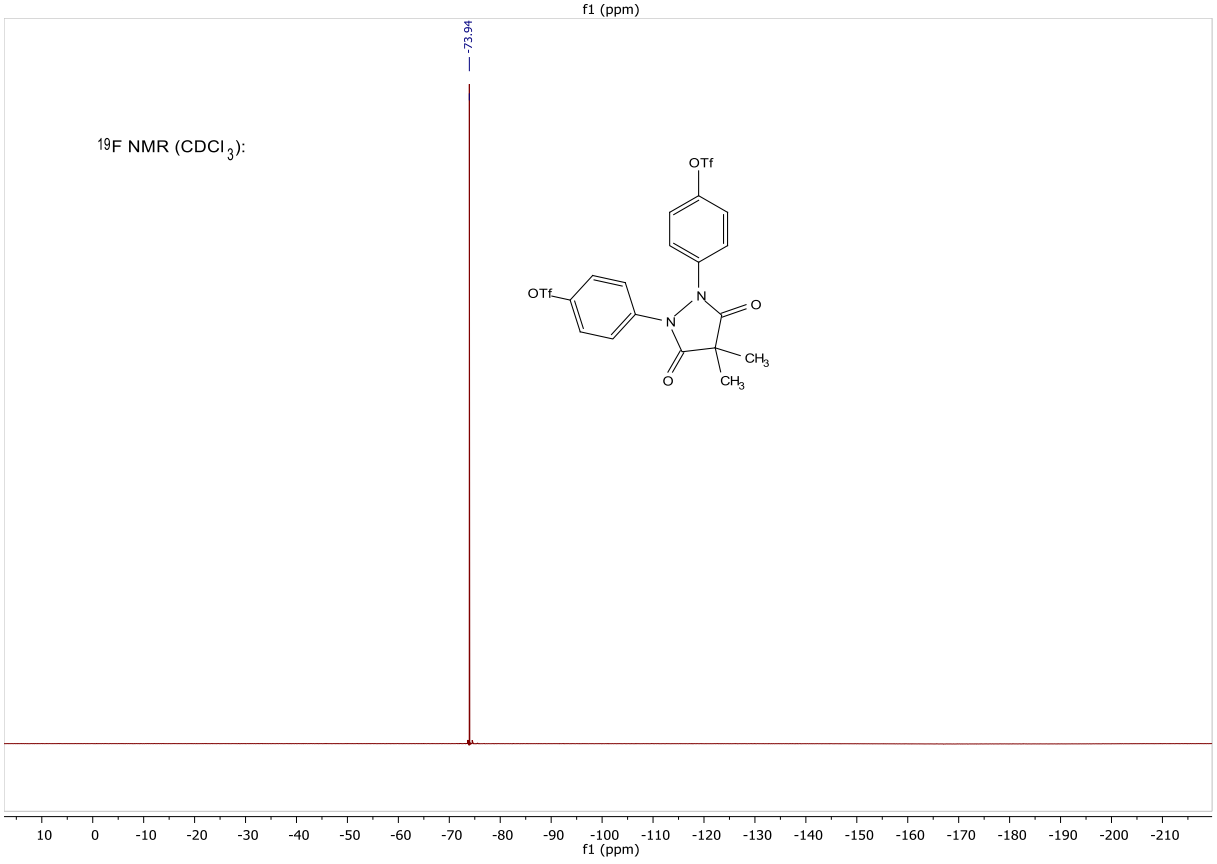
-73.94
19F NMR (CDCl3):
OTf
OTf
N
N
O
O
CH3
CH3
f1 (ppm)

1,2-Bis-(4-mesylphenyl)-4,4-dimethylpyrazolidin-3,5-dione (5f)

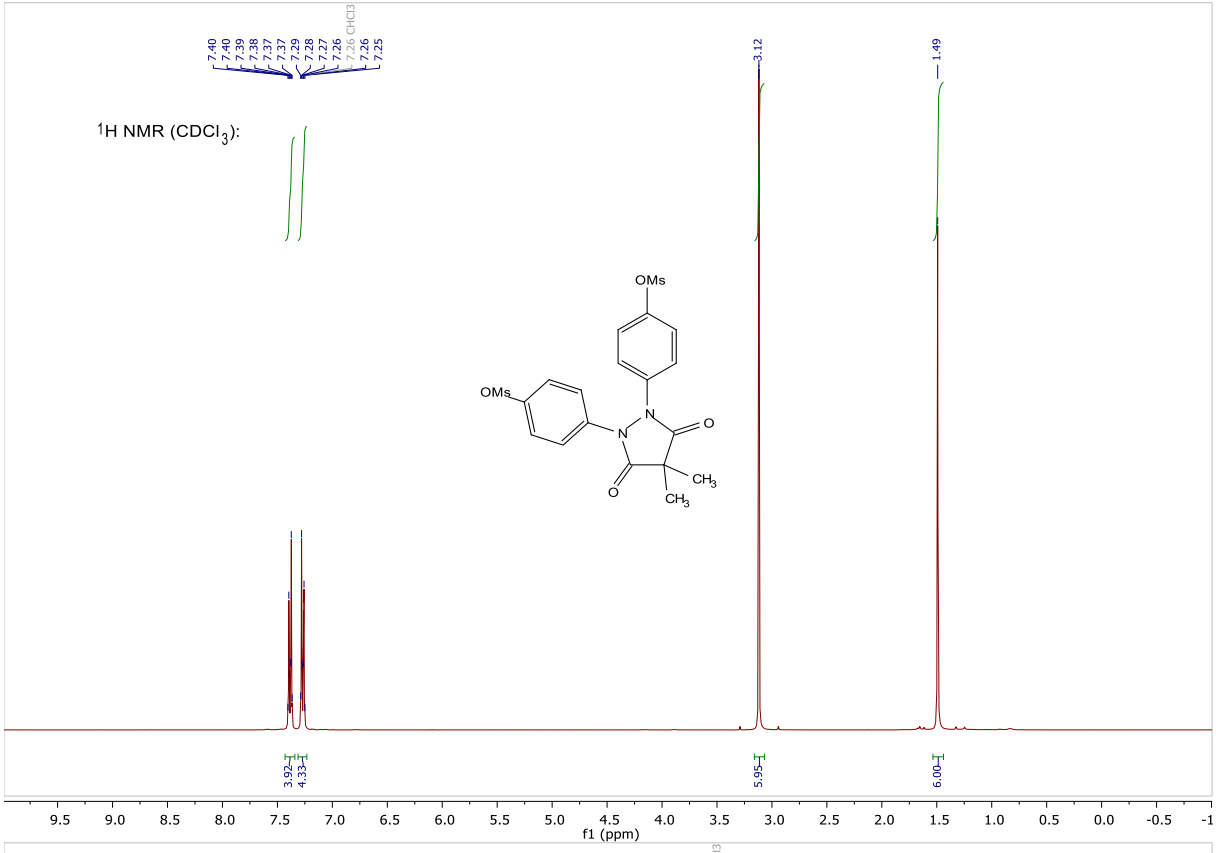

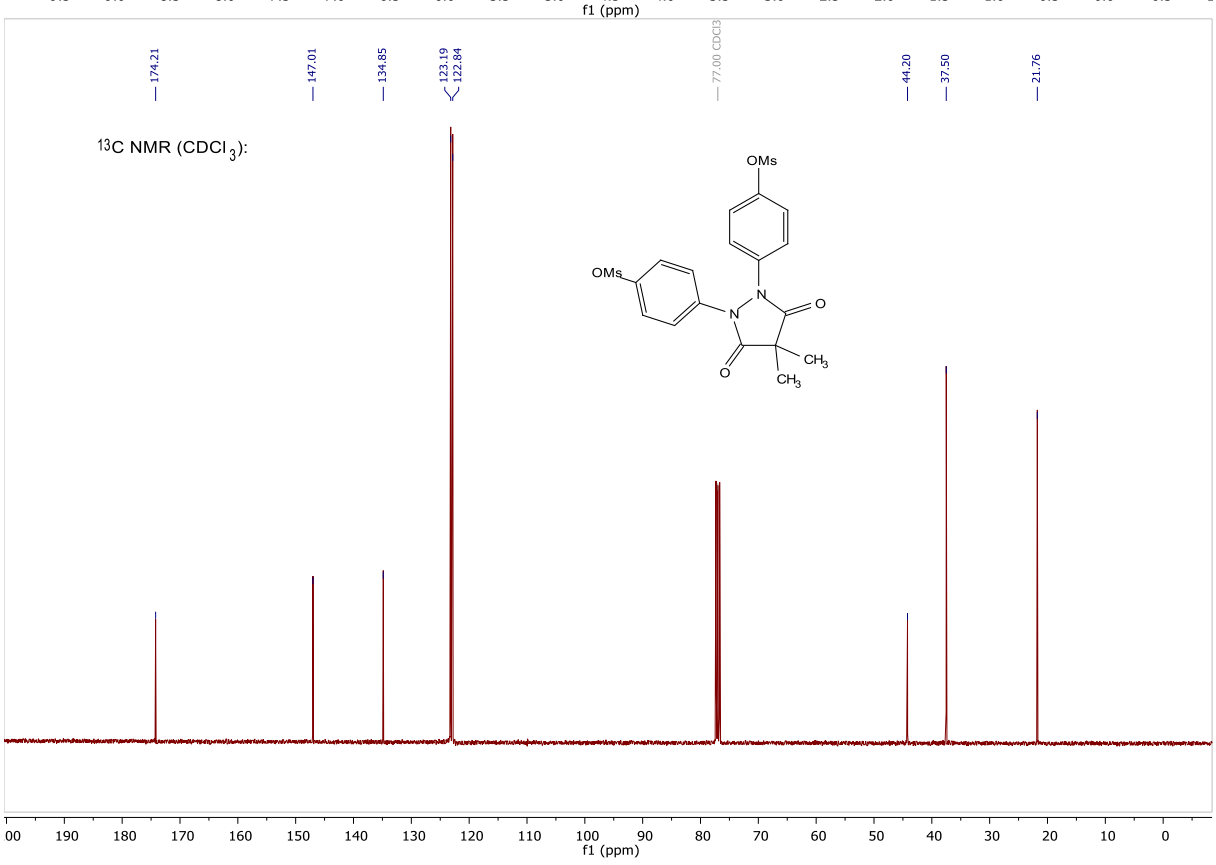

1,2-Bis-(3-(1,1-dimethylethyl)phenyl)-4,4-dimethylpyrazolidin-3,5-dione (5g)

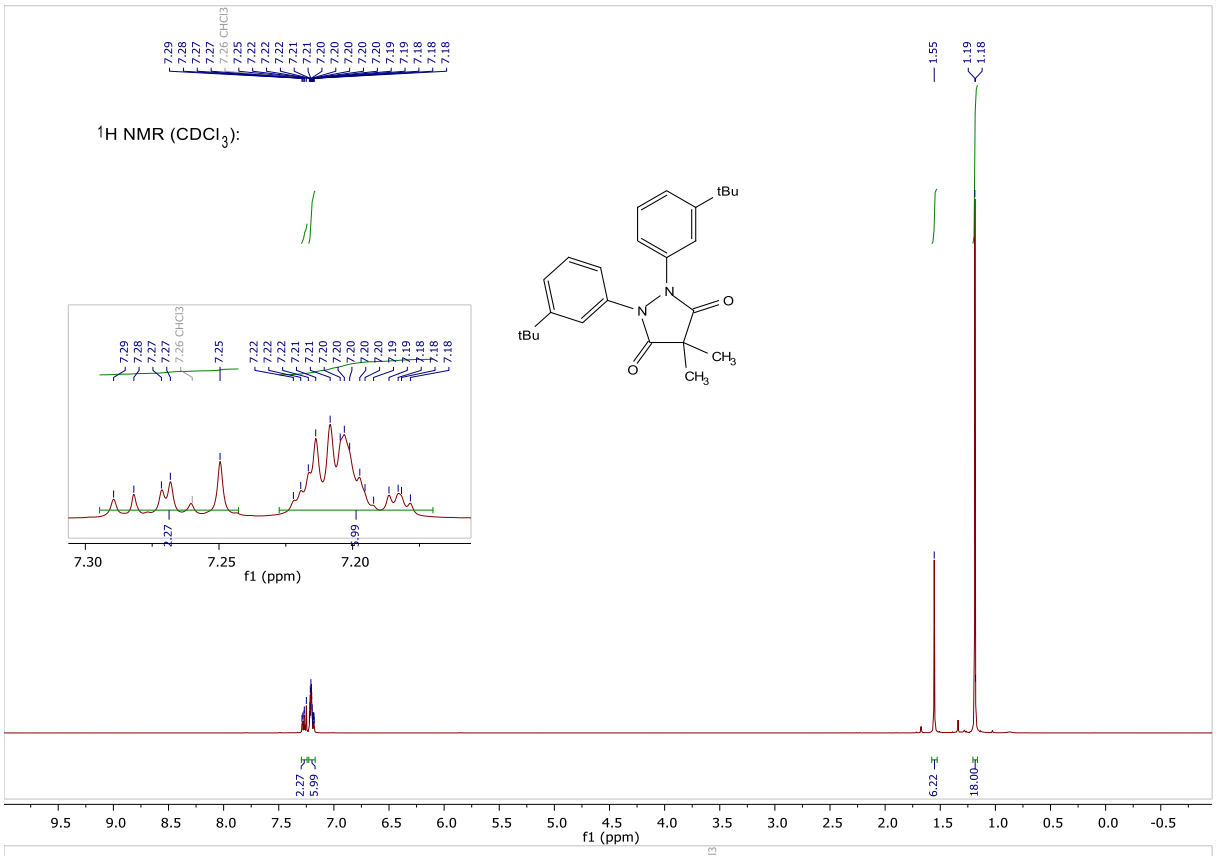

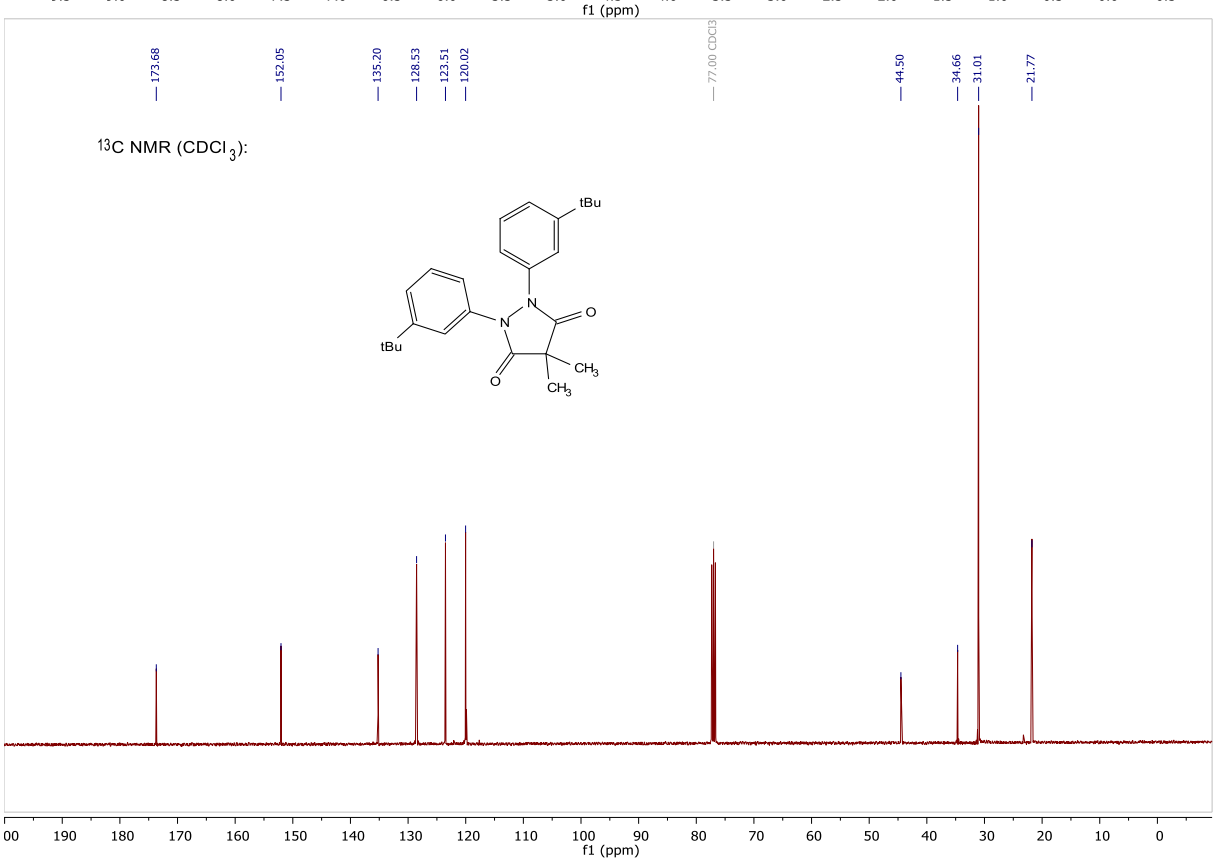

1,2-Bis-(3,5-di(1,1-dimethylethyl)phenyl)-4,4-dimethylpyrazolidin-3,5-dione (5h)

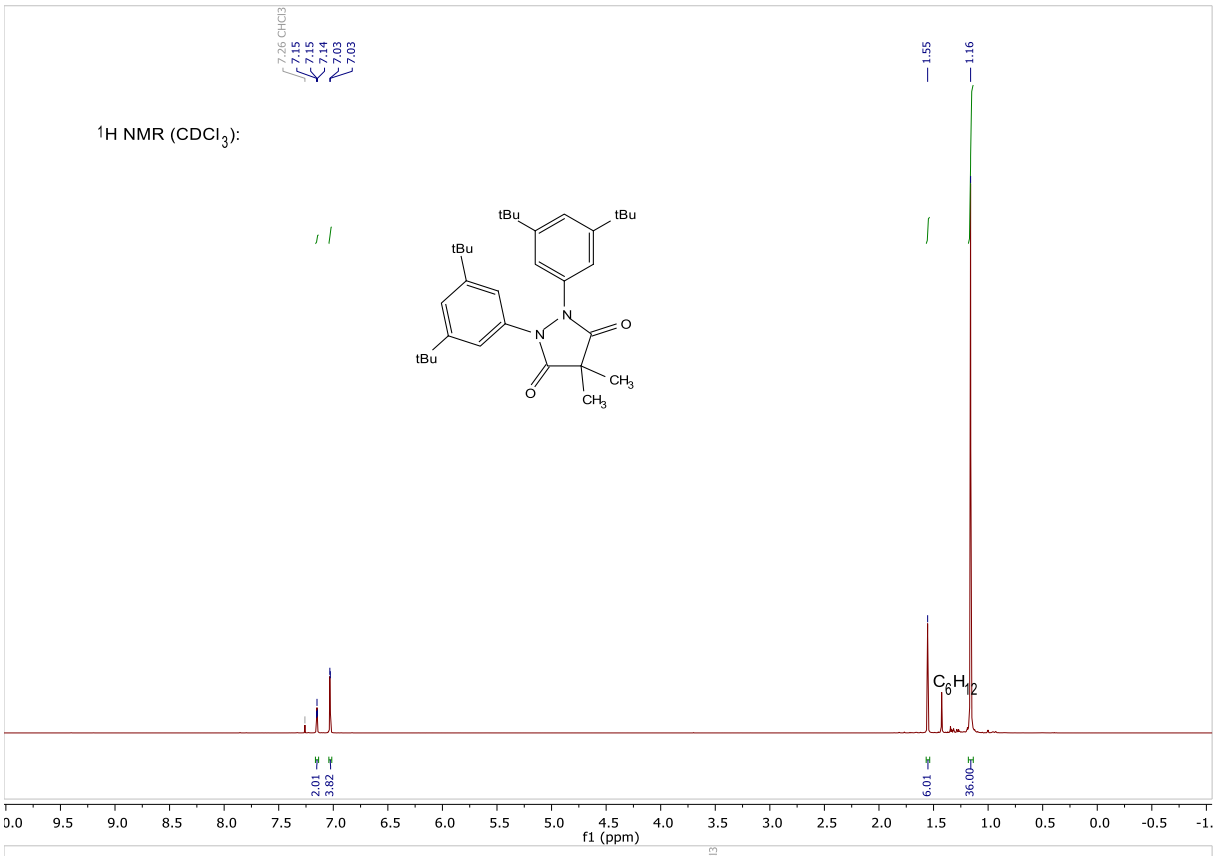

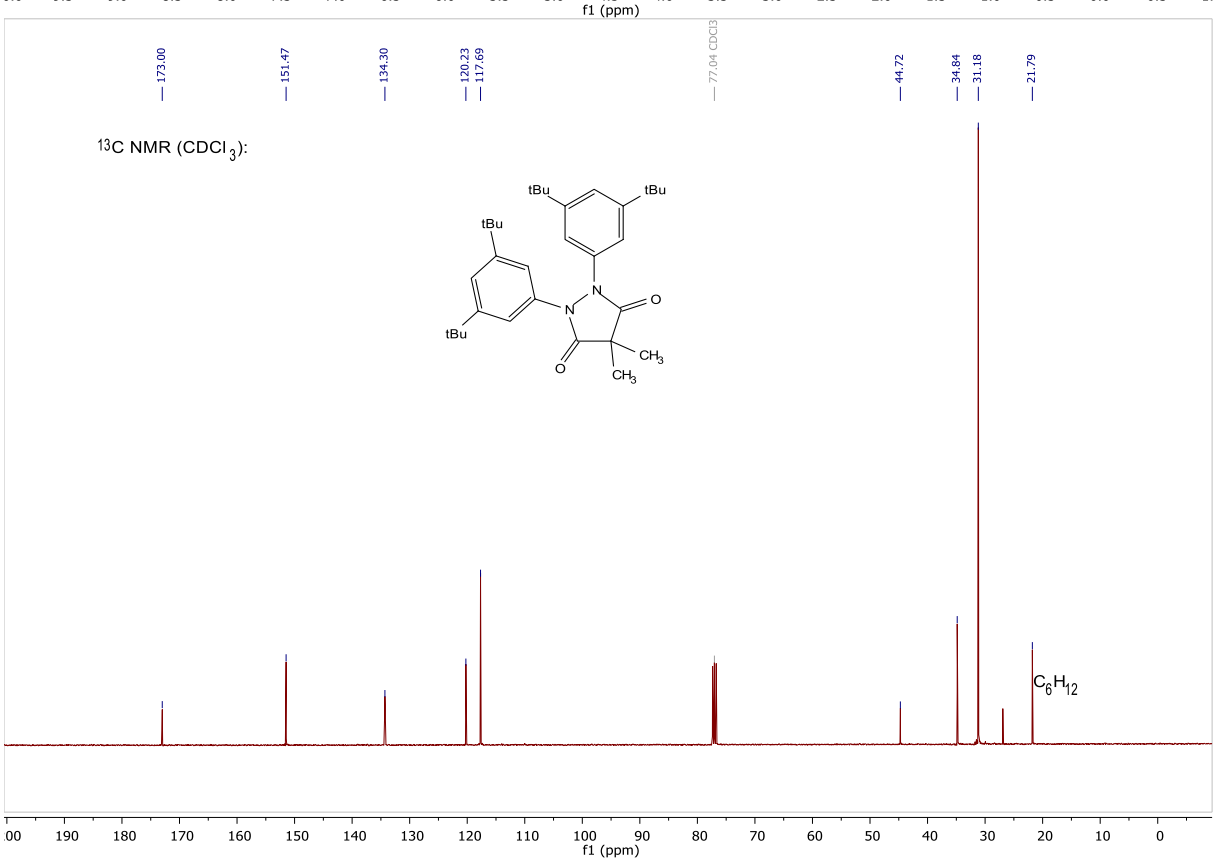

1,2-Bis-(4-chlorophenyl)-4,4-dimethyl-tetrahydropyridazine-3,6-dione (2)

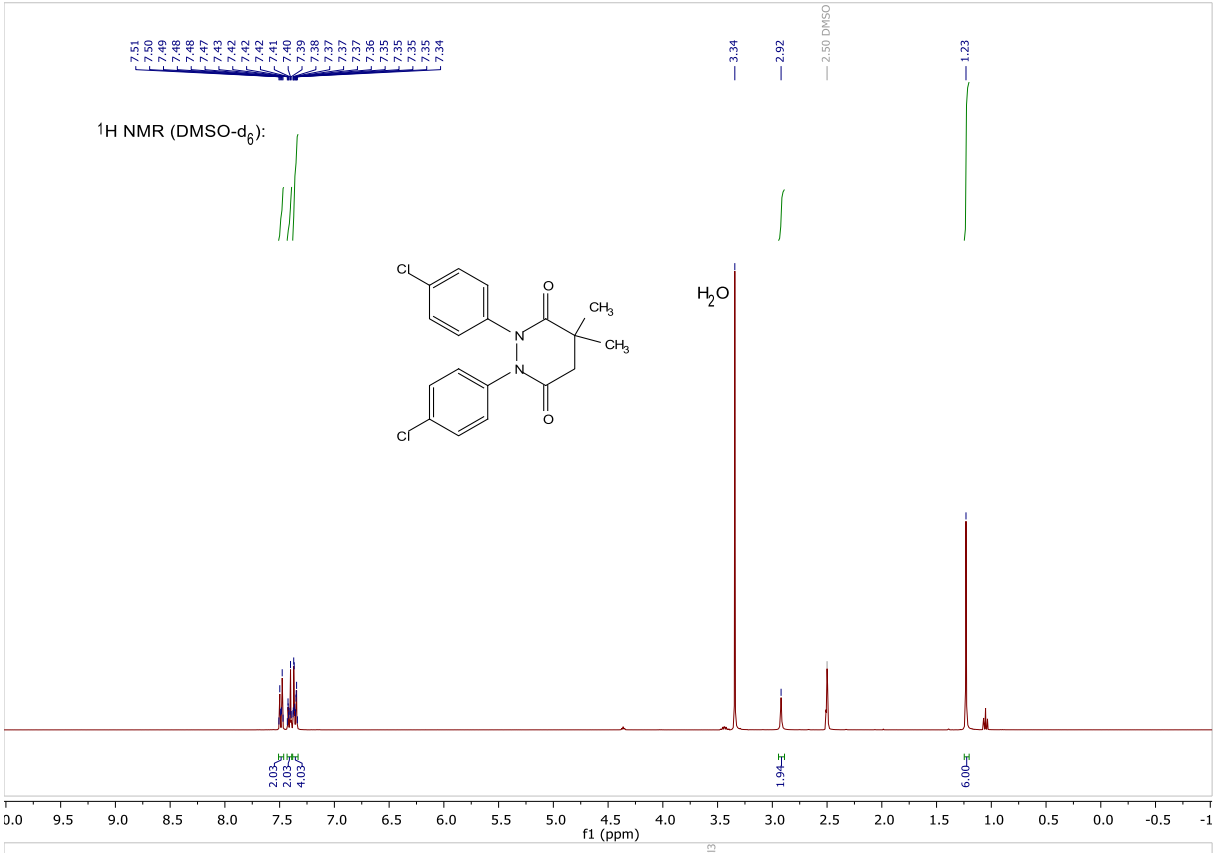

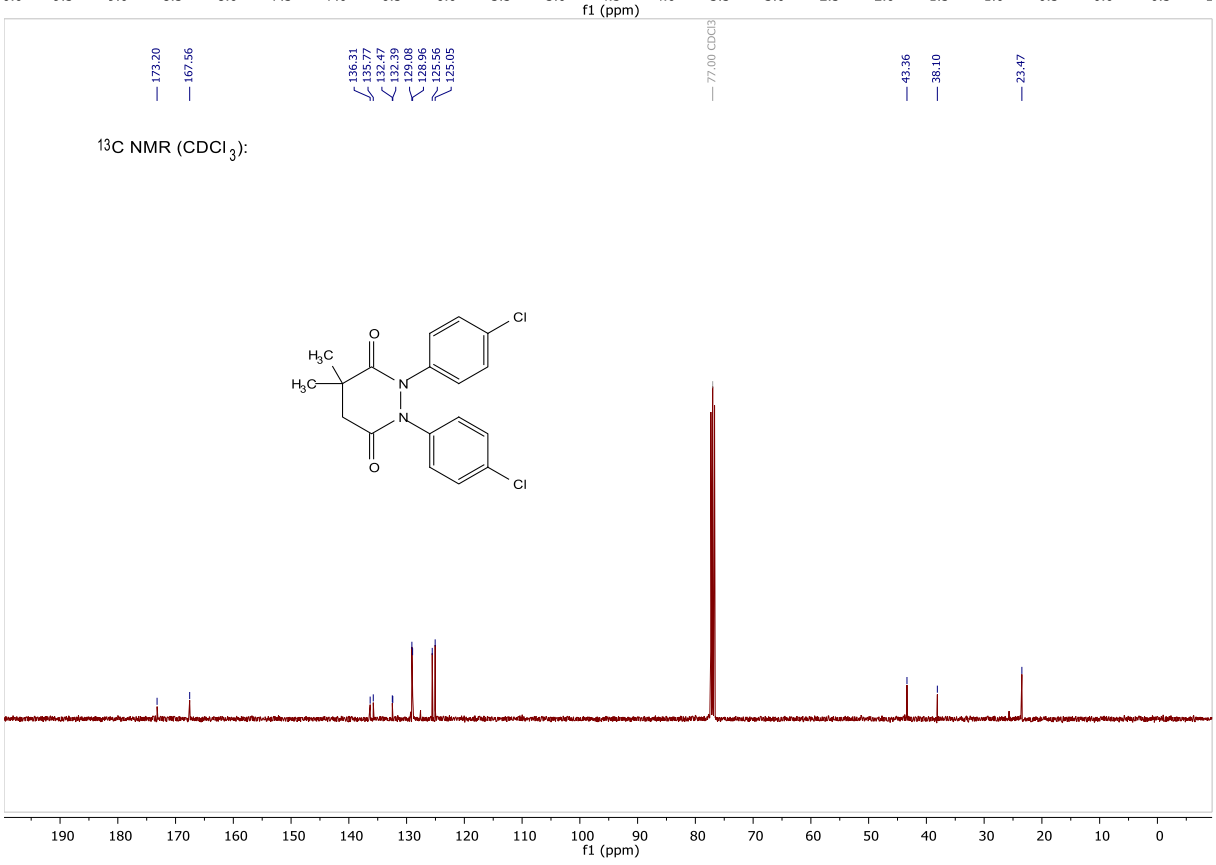

6-Chloro-2-(*N*-(4-chlorophenyl)-1,1-dimethyl)propanamide-1,3-benzoxazole (3a) and 6-Chloro-2-(*N*-(4-chlorophenyl)-2,2-dimethyl)propanamide-1,3-benzoxazole (3b)

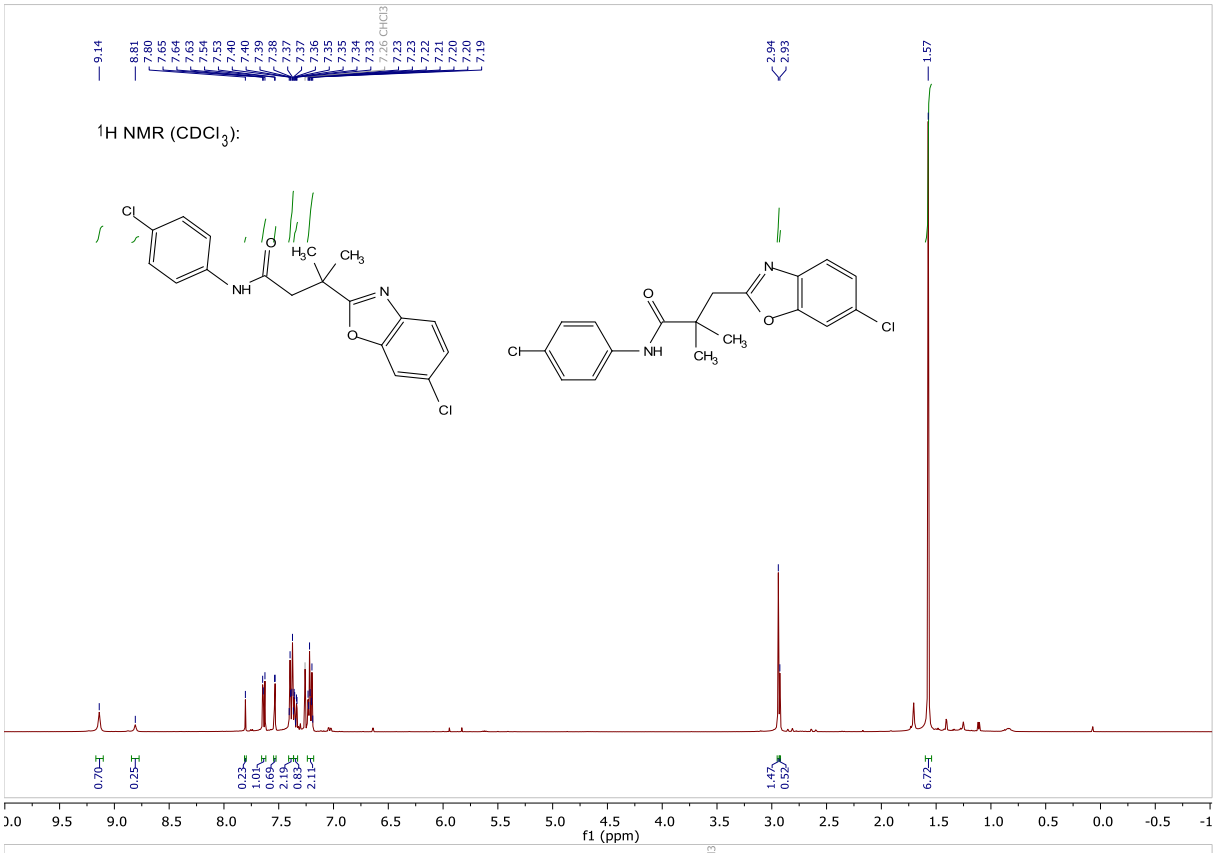

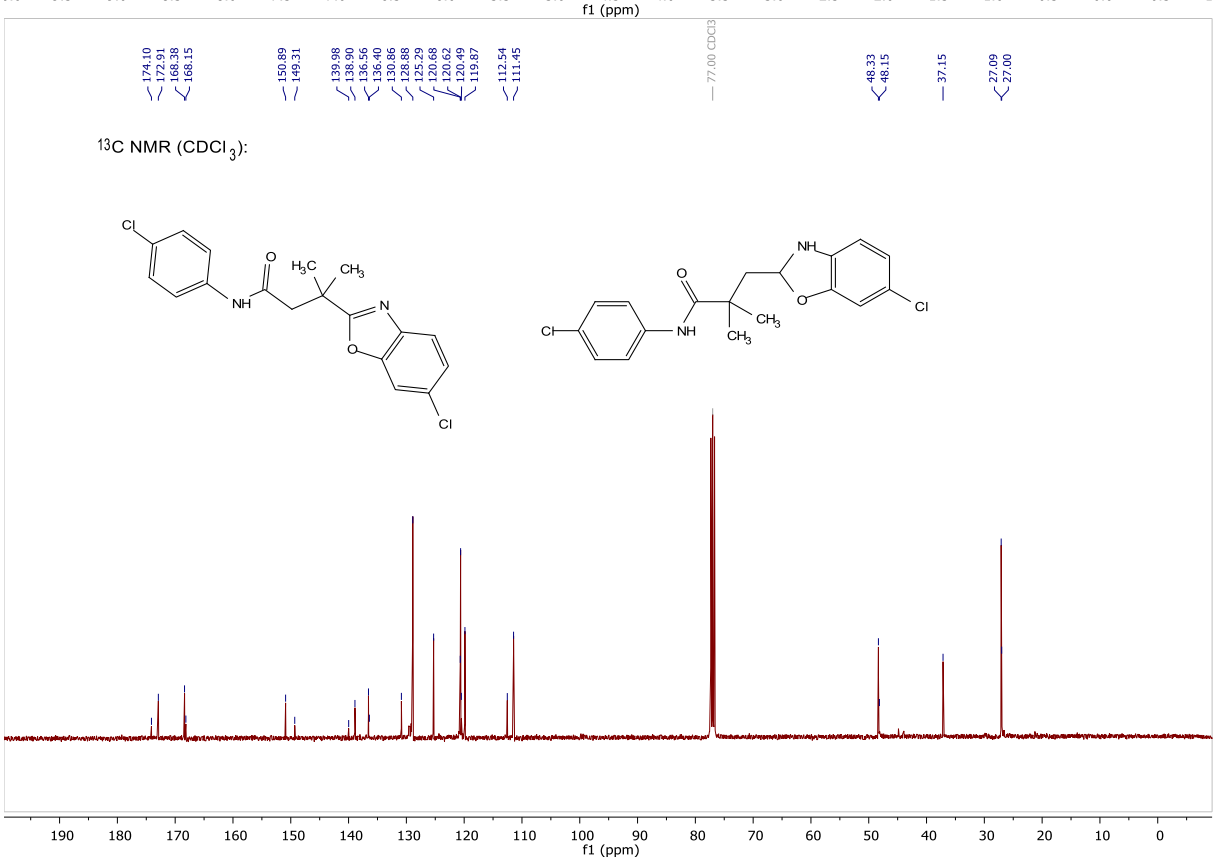

***N*-(4-(1-(1,1,1,3,3,3-Hexafluoropropan-2-yloxy)-methyl)phenyl)benzamide (6a)**

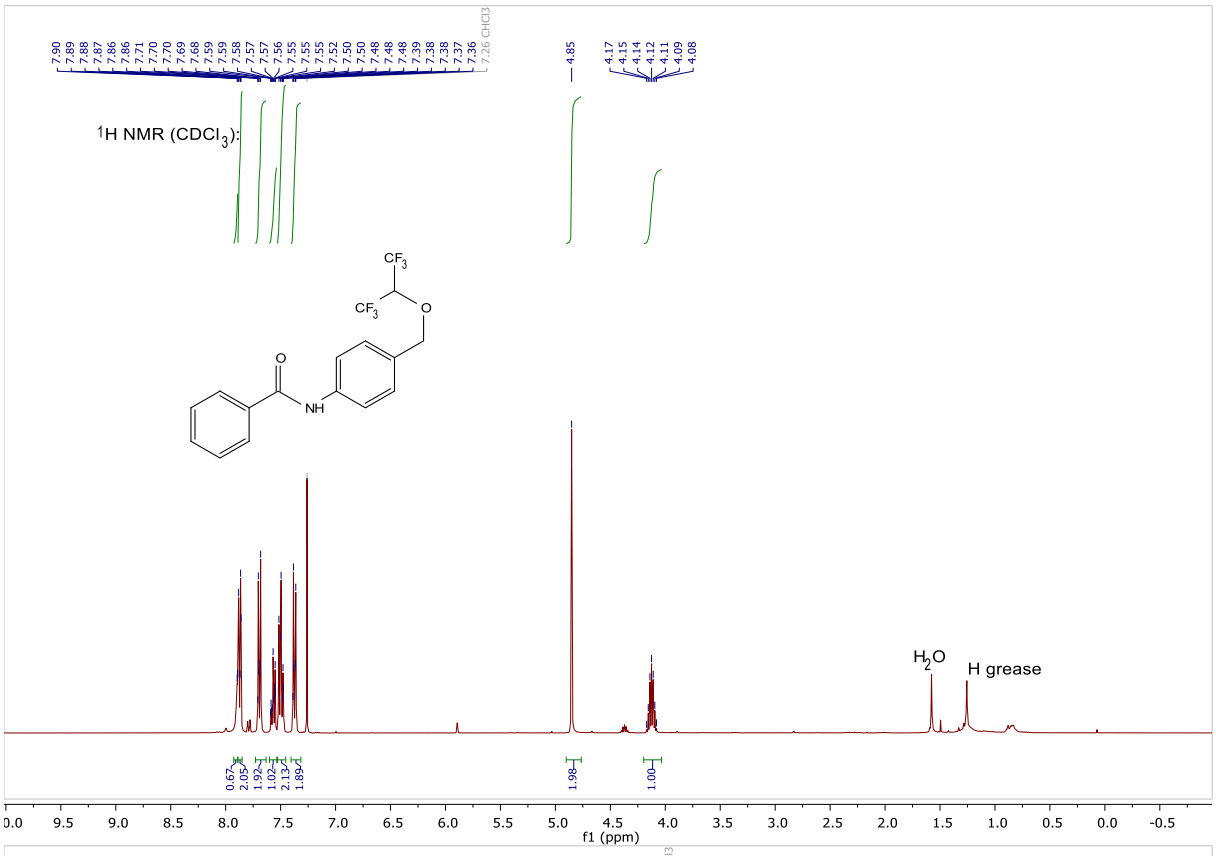

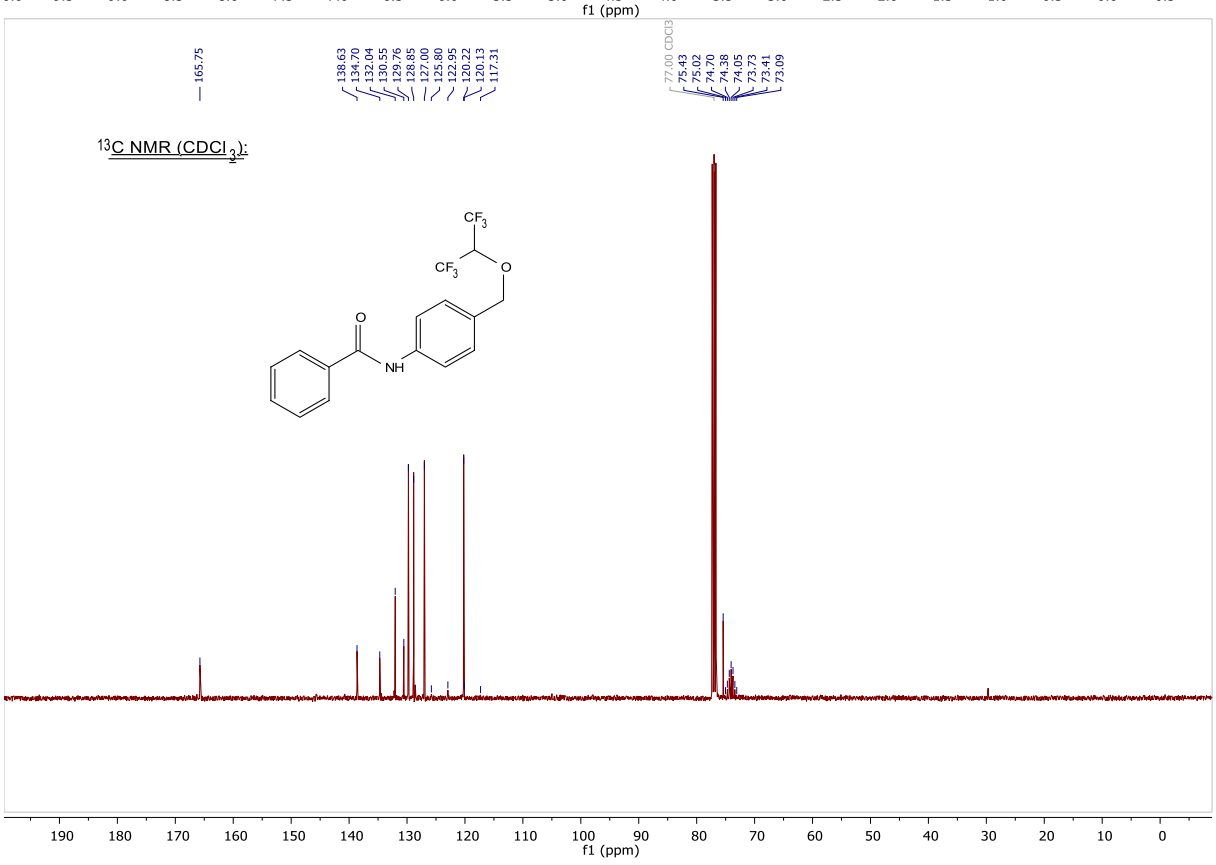

References

[1] Armarego, W. L. F.; Chai, C. L. L. *Purification of laboratory chemicals*, Butterworth-Heinemann, Amsterdam, 5th ed., **2003**.

[2] Berger, S.; Braun, S.; Kalinowski, H.-O. *NMR-Spektroskopie von Nichtmetallen*, Thieme, Stuttgart, **1994**.

[3] Sheldrick, G. M.; *SHELXS97* and *SHELXL97: Programm for the Refinement of Crystal Structures;* Dept. of Structural Chemistry, University of Göttingen: Germany, **1997**.

[4] a) Seganish, W. M.; DeShong, P. *J. Org. Chem.*, 2004, **69**, 1137–1143; b) Buckingham, F.; Calderwood, S.; Checa, B.; Keller, T.; Tredwell, M.; Collier, T. L.; Newington, I. M.; Bhalla, R.; Glaser, M.; Gouverneur, V. *J. Fluorine Chem.* 2015, **180**, 33–39; c) Lei, X.; Jalla, A.; Abou Shama, M.; Stafford, J.; Cao, B. *Synthesis* **2015**, *47*, 2578–2585. d) Kubicova, L.; Waisser, K.; Kunes, J.; Kralova, K.; Odlerova, Z.; Slosarek, M.; Janota, J.; Svoboda, Z. *Molecules* **2000**, *5*, 714–726.

ChemPubSoc Europe

DOI: 10.1002/chem.201804638

CHEMISTRY A European Journal Communicatio

Check for updates

Heterocycles

Electrochemical Synthesis of 5-Aryl-phenanthridin-6-one by Dehydrogenative N,C Bond Formation

Anton Kehl, Valentina M. Breising, Dieter Schollmeyer, and Siegfried R. Waldvogel*[a]

Abstract: Currently, the general synthesis of 5-aryl-phenanthridin-6-ones relies on the involvement of metal catalysis. Despite the urgent demand for green alternatives, avoiding synthetic routes that require transition metals for key roles is still challenging. Electrochemical efforts employing a constant potential protocol in divided cells revealed a possible alternative to the catalytic approach. A constant current protocol, undivided cells, and a remarkably low supporting electrolyte concentration enable a novel access to *N*-aryl-phenanthridin-6-ones by anodic N,C bond formation using directly generated amidyl radicals. Easy accessible starting materials, a broad scope of applicable functional groups, good yields, and a very simple set-up are the benefits of this sustainable method.

6(5H)-Phenanthridinone was first mentioned by Pictet and Ankersmit in 1891, who employed nitrophenylbenzoic acid and zinc dust in ammonia, although the structure could not be sufficiently confirmed.[1] In 1893, Graebe and Wander synthesized phenanthridinone derivatives by treating diphenamic acid with sodium hypobromite as oxidizer. The structural assumption was confirmed by control experiments, and reported matching analytical data provided by Pictet and Ankersmit.[2] As far as application of this compound class is concerned, some derivatives were allegedly used as vat dye or dye precursors.[3] Currently, phenanthridinone represents a structural motif occurring in various compounds with medicinal relevance or natural products.[4] *N*-Aryl-phenanthridin-6-one derivatives in particular are applicable in electronic devices (e.g., OLEDs) or pharmaceutically active ingredients.[5]

General synthetic approaches rely on metal-assisted catalysis,[6] such as Pd,[6a–e,g,h] Ni,[6f] or Cu catalysts,[6i] organic mediators,[7] radical initiators,[8] or photocatalysis-employing Ir-complexes.[9] These routes are accompanied by severe disadvantages such as harsh conditions, the necessity for additives or complex ligands, leastwise stoichiometric mediators, bases or oxidizers, leaving groups or elaborated precursors. Furthermore, larger amounts of reagent waste, sophisticated synthetic conditions such as inert atmosphere as well as elevated pressure, and a necessity of partially expensive reagents emerge as unfavorable aspects from the aforementioned approaches. Hence, these methods exhibit a negative footprint onto atom economy and ecology. Therefore, methodologies that are able to circumvent these drawbacks are highly desired and a hot topic of current research.[10e,f,g] Recently, electro-organic chemistry has had a renaissance due to its inherently safe nature and access to extraordinary reaction pathways.[10] Electrochemistry can be seen as a green alternative to classical organic chemistry owing to the fact that it reverts solely to the electric current as an inexpensive and sustainable oxidizing or reducing agent, which minimizes the amount of waste dramatically.[11] Initial efforts to electrochemically generate *N*-aryl-phenanthridin-6-one derivatives were made in the 1970s by establishing a constant potential setup in divided cells (Scheme 1, upper part).[12] Reductive means were used to cleave a carbon–halogen bond in order to generate radicals for the cyclization reaction. Unfortunately, this method is afflicted by a narrow scope, a sophisticated setup and problematic Hg as cathode material. Recently, Zeng et al. reported a protocol to construct phenanthredin-6-one by employing a constant current setup in undivided cells

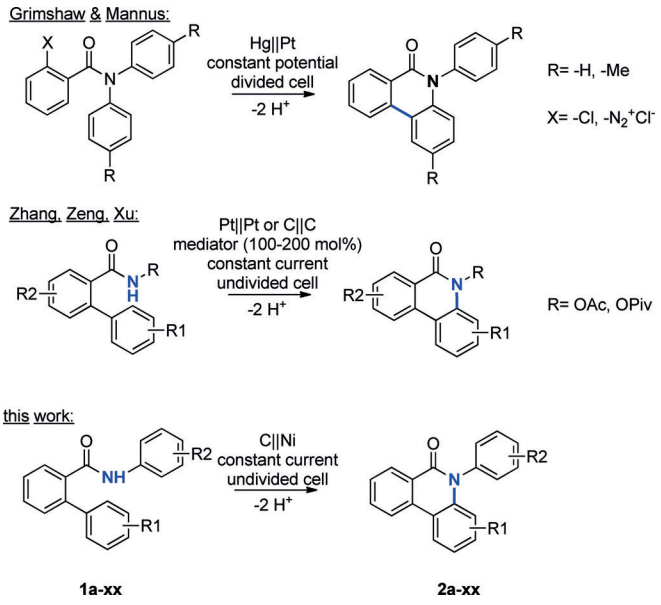

Scheme 1. Electrochemical approaches to phenanthridin-6-one derivatives and the key step for the synthesis of *N*-aryl-phenanthridin-6-ones.

[a] *A. Kehl, V. M. Breising, Dr. D. Schollmeyer, Prof. Dr. S. R. Waldvogel*
Johannes Gutenberg-Universität Mainz
Institut für Organische Chemie
Duesbergweg 10–14, 55128 Mainz (Germany)
E-mail: waldvogel@uni-mainz.de
Homepage: https://www.blogs.uni-mainz.de/fb09akwaldvogel

Supporting information and the ORCID identification number(s) for the author(s) of this article can be found under: https://doi.org/10.1002/chem.201804638.

with the aid of an anodically generated reagent (mediator) in order to facilitate the cyclization reaction, limited only to *N*-acetyl or *N*-pivaloyl functionalities (Scheme 1, middle part).[13] A leastwise stoichiometric amount of the mediator (NaBr), depending on the setup, and in special cases also Na_2CO_3 as additive are required. With a current efficiency of 0.4 (platinum electrodes) this process consumes unusual large amounts of applied charge. The authors propose that amidyl radicals are generated by a homolytically cleaved nitrogen–halide bond followed by a cyclization and a final oxidation step.

The application of amidyl radicals as reactive intermediates are well-known and associated with hydroaminations,[14a] rearrangements,[14b] and cyclization reactions.[14b,15] The generation of amidyl radicals by oxidative cleavage of the nitrogen–hydrogen bond is highly desirable due to the lack of pre-functionalization. Electro-organic chemistry is able to engage this issue by mediated[15h] or direct oxidation[15i] at the anode. Recently, we reported a methodology to afford amidyl radicals by direct oxidation in order to construct five- and six-membered heterocycles by dehydrogenative N,N coupling reactions.[16] In order to expand the scope of heterocycles and to demonstrate the capability of the electrolyte system, we report a new synthetic approach for *N*-aryl-phenanthredin-6-ones (Scheme 1, lower part). Easily accessible biphenyl anilides as starting material, inexpensive electrode materials, and a simple and reproducible method characterize this synthetic route as a general applicable and straightforward access to this particular class of compounds.

The synthesis of the precursors can be easily conducted in good yields by treatment of biphenyl-2-carboxylic acid with oxalyl chloride,[17] removing excess of oxalyl chloride and subsequent addition of the corresponding aniline derivative.

The electrolytic conditions for the direct N,C coupling were elucidated within screening studies. This optimization of parameters was conducted in Teflon cells (volume: 5 mL), which provide—in combination with an undivided cell setup—a time-efficient and straightforward screening approach.[18] The conditions for the synthesis of pyrazolidin-3,5-diones were chosen as the starting point due to their suitability to generate amidyl radicals in the course of N,N bond formation. *N*-(4-Chlorophenyl) biphenyl-2-carboxamide (**2a**) was chosen as test substrate, because this particular anilide moiety had demonstrated an excellent compatibility with the electrochemical conditions at hand.[16a,c] Commencing with the aforementioned conditions gave a ^{1}H NMR yield of 50% of the desired product (Table 1, entry 1). We also tested acetonitrile and methanol as solvent. On the one hand, the reaction in acetonitrile indicated no conversion of the starting material, on the other hand, the electrolysis in methanol revealed a complicated mixture containing starting material, product, methoxylated starting material, and other non-identified compounds according to the gas-chromatographic measurements. 1,1,1,3,3,3-Hexafluoroisopropanol (HFIP) exclusively provides an effective and selective conversion, which is based on its radical stabilizing properties.[19] The fact that HFIP is recovered almost entirely by distillation ensures a low fluorine footprint.[20] Furthermore, boron-doped diamond (55% ^{1}H NMR yield) and glassy carbon (58% ^{1}H NMR yield) were evaluated as anode materials to give similar results regarding the conversion and yield. Hence, we decided to stay with isostatic graphite to provide a readily available and inexpensive anode material. A vital and powerful parameter in electro-organic synthesis is current density. The optimization revealed, that best results are obtained with a current density of 1 mA cm^{-2} (Table 1). Higher current density such as 4 and 5 mA cm^{-2} result in lower yields due to degradation reactions. In addition, the supporting electrolyte concentration of 0.01 M (50% ^{1}H NMR yield) can be decreased to 0.0025 M (51% ^{1}H NMR yield) without affecting the yield and providing sufficient conductivity. In most cases, the conversion of the starting material was incomplete. This issue was addressed by changing the cathode material in order to provide a more efficient cathodic reaction by using electrode materials with a lower over-potential for hydrogen evolution (Table 2). Graphite and steel as cathode materials achieved slightly lower yields than platinum or nickel, but hold the advantage of being suitable for pharmaceutical applications. Except for graphite, all other evaluated cathode materials indicated full conversion of the starting material with an applied charge amount of 2.2 F. However, nickel was chosen to proceed with further electrolytic conversions. The optimized parameters were tested with glassy carbon as anode once more to check the impact onto the yield; however, no amelioration in the yield was observed.

Table 1. Influence of the current density onto the yield of **2a**.

Entry	Current density [mA cm^{-2}]	Yield [%][a]
1	0.5	50
2	1	70
3	1.5	63
4	2	56
5	2.5	46
6	3	52
7	4	49
8	5	36

Conditions: 0.2 mmol substrate, 0.01 M NBu_4PF_6, graphite electrodes (highly isostatic graphite Sigrafine™ V2100), HFIP, charge 2.2 F, undivided Teflon cell (5 mL); [a] ^{1}H NMR yields.

The optimized parameters were applied on a collection of biphenyl anilide substrates and resulted in a scope of *N*-aryl-phenanthridin-6-one derivatives with various functional groups

Table 2. Influence of the cathode material onto the yield of **2a**.

Entry	Cathode	Yield [%][a]
1	Graphite[b]	75
2	Platinum	80
3	Nickel	85
4	Nickel[c]	85
5	Steel[d]	72

Conditions: 0.2 mmol substrate, 0.0025 M NBu_4PF_6, anode: graphite, current density: 1 mA cm^{-2}, HFIP, charge 2.2 F, undivided Teflon cell (5 mL); [a] isolated yield; [b] 3.2 F applied for full conversion; [c] anode: glassy carbon; [d] A5-stainless-steel (VA 1.4571).

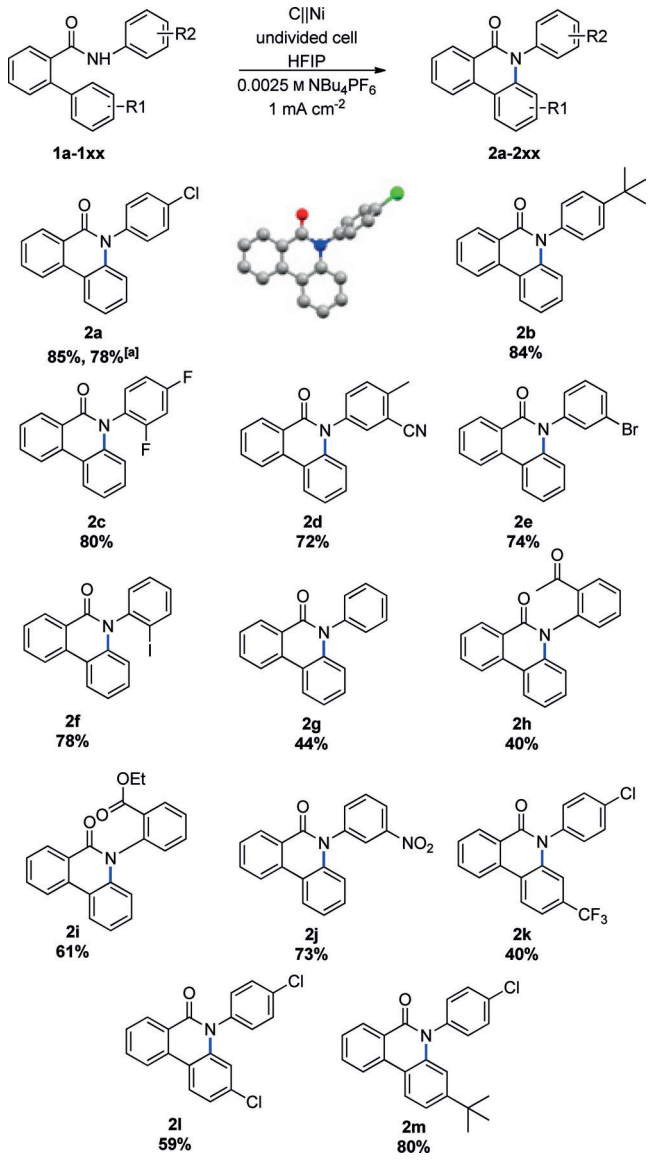

Scheme 2. Optimized parameters for the electrochemical N,C cyclization and scope. 5 mL Teflon cell, 0.2 mmol scale, [a] 80 mL beaker-type cell, 6.3 mmol substrate.

and substitution patterns at the aniline moiety and the biphenyl entity (Scheme 2).

The majority of compounds were synthesized in good to excellent yields, tolerating chloro- (**2a**, **2k**, **2l**, **2m**), fluoro- (**2c**, **2k**), bromo- (**2e**), iodo- (**2f**), nitro- (**2j**), keto- (**2h**), ester- (**2l**), or nitrile (**2d**) substituents, which allow subsequent reactions. The highest yield of 85% was achieved with compound **2a**, which was the designated compound for our optimization procedures. **2a** was also employed to demonstrate the up-scaling ability of this method by giving 78% yield (gram scale). The formation of the N,C coupled product was confirmed via X-ray structure analysis of a suitable single crystal of **2a** (Scheme 2). As anticipated, the X-ray structure analysis revealed that the aryl moiety of the aniline is oriented orthogonally with regards to the lactam moiety. Unsurprisingly, derivatives with a blocked *para*-positon (**2a**, **2b**, **2c**, **2d**, **2m**) provide excellent yields. Whereas **2g** exhibits a lower yield due to possible side reactions.[15] Interestingly, derivative **2e**, **2f**, **2i**, and **2j** which also exhibit a free *para*-position result in much better yields compared with **2g**.

Derivative **2k** yields moderately even though the 4-chlorophenyl moiety was employed. This reaction revealed an incomplete conversion of the substrate regardless the amount of charge applied. However, electron-withdrawing (**2c**, **2j**) as well as bulky moieties (**2b**) incorporated by the aniline component work well. In terms of the mechanism (Scheme 3), it is likely

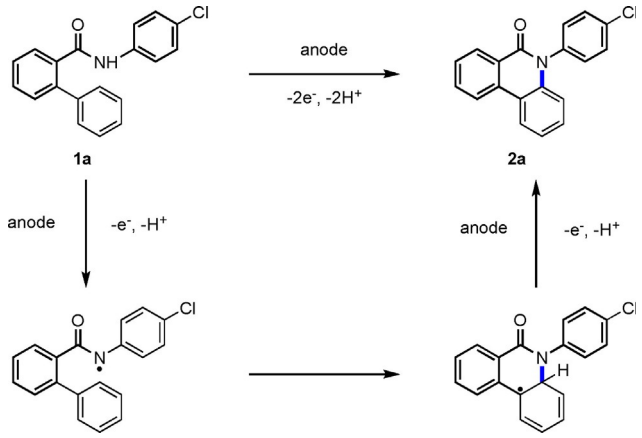

Scheme 3. Proposed mechanism.

that the cyclization is initiated by the generation of an amidyl radical through a direct oxidation of the substrate at the anode. The deprotonation of the anilide could be executed by an in situ generated HFIP anion. The amidyl radical can be stabilized by the *N*-aryl system. The N,C bond formation proceeds between the amidyl radical and the second, in this case unsubstituted phenyl moiety of the biphenyl scaffold resulting in a radical within the lactam system. After a second oxidation step combined with a follow-up extrusion of a proton, the product is accomplished.

We established a new and sustainable access to *N*-aryl-phenanthredin-6-ones by employing direct anodic oxidation. This protocol features a high current efficiency and operates without the necessity for a mediator. Easily accessible and inexpensive starting materials, a simple set-up, remarkably low supporting electrolyte concentrations, metal catalyst- and organic oxidizer-free conditions as well as inexpensive electrode materials provide a straightforward and sustainable route to this class of compounds. A variety of derivatives is possible, valuable functionalities, which enable subsequent reactions, are tolerated. Up-scaling of this method is easily possible.

Acknowledgements

The support by The Advanced Lab for Electrochemistry and Electrosynthesis–ELYSION (Carl Zeiss Stiftung) and the DFG (WA 1276/17-1) is highly appreciated.

Conflict of interest

The authors declare no conflict of interest.

Keywords: electrochemistry · green chemistry · heterocycles · N,C coupling · *N*-aryl-phenanthrendin-6-ones

[1] A. Pictet, H. J. Ankersmit, *Liebigs Ann. Chem.* **1891**, *266*, 138 – 153.
[2] C. Graebe, A. Wander, *Liebigs Ann. Chem.* **1893**, *276*, 245 – 253.
[3] Authors unknown (BASF), DE236857C, **1910**.
[4] a) D. Weltin, V. Picard, K. Aupeix, M. Varin, D. Oth, J. Marchal, P. Dufour, P. Bischoff, *Int. J. Immunopharmacol* **1995**, *17*, 265 – 271; b) Z. Tu, W. Chu, J. Zhang, C. S. Dence, M. J. Welch, R. H. Mach, *Nucl. Med. Biol.* **2005**, *32*, 437 – 443; c) S. D. Shnyder, P. A. Cooper, N. J. Millington, J. H. Gill, M. C. Bibby, *J. Nat. Prod.* **2008**, *71*, 321 – 324; d) S. Patil, S. Kamath, T. Sanchez, N. Neamati, R. F. Schinazi, J. K. Buolamwini, *Bioorg. Med. Chem.* **2007**, *15*, 1212 – 1228; e) J. Ishida, K. Hattori, H. Yamamoto, A. Iwashita, K. Mihara, N. Matsuoka, *Bioorg. Med. Chem. Lett.* **2005**, *15*, 4221 – 4225; f) T. A. Grese, M. D. Adrian, D. L. Phillips, P. K. Shetler, L. L. Short, A. L. Glasebrook, H. U. Bryant, *J. Med. Chem.* **2001**, *44*, 2857 – 2860; g) D. Bellocchi, A. Macchiarulo, G. Costantino, R. Pellicciari, *Bioorg. Med. Chem.* **2005**, *13*, 1151 – 1157; h) Z. Jin, *Nat. Prod. Rep.* **2011**, *28*, 1126 – 1142; i) M. He, C. Qu, O. Gao, X. Hu, X. Hong, *RSC Adv.* **2015**, *5*, 16562 – 16574.
[5] a) P. Stoessel, A. H. Parham, C. Pflumm, A. Jatsch, J. Kaiser, WO2014194971A1, **2014**; b) A. Jatsch, A. Parham, R. Linge, T. Grossmann, WO2018099846A1, **2018**; c) J. T. Dalton, C. Barrett, Y. He, S.-S. Hong, D. D. Miller, M. L. Mohler, R. Narayanan, Z. Wu, WO2007062230A2, **2007**.
[6] a) T.-Y. Zhang, J.-B. Lin, Q.-Z. Li, J.-C. Kang, J.-L. Pan, S.-H. Hou, C. Chen, S.-Y. Zhang, *Org. Lett.* **2017**, *19*, 1764 – 1767; b) Y. Yang, H. Huang, L. Wu, Y. liang, *Org. Biomol. Chem.* **2014**, *12*, 5351 – 5355; c) G.-W. Wang, T.-T. Yuan, D.-D. Li, *Angew. Chem. Int. Ed.* **2011**, *50*, 1380 – 1383; *Angew. Chem.* **2011**, *123*, 1416 – 1419; d) V. H. Thorat, N. S. Upadhyay, M. Murakami, C.-H. Cheng, *Adv. Synth. Catal.* **2018**, *360*, 284 – 289; e) V. Rajeshkumar, T.-H. Lee, S.-C. Chuang, *Org. Lett.* **2013**, *15*, 1468 – 1471; f) X. Li, J. Pan, S. Song, N. Jiao, *Chem. Sci.* **2016**, *7*, 5384 – 5389; g) J. Karthikeyan, C.-H. Cheng, *Angew. Chem. Int. Ed.* **2011**, *50*, 9880 – 9883; *Angew. Chem.* **2011**, *123*, 10054 – 10057; h) T. Furuta, Y. Kitamura, A. Hashimoto, S. Fujii, K. Tanaka, T. Kan, *Org. Lett.* **2007**, *9*, 183 – 186; i) B. Banerji, S. Chatterjee, K. Chandrasekhar, C. Nayan, S. K. Killi, *Eur. J. Org. Chem.* **2017**, 5214 – 5218.
[7] S. Wang, P. Shao, G. Du, C. Xi, *J. Org. Chem.* **2016**, *81*, 6672 – 6676.
[8] M. Yuan, L. Chen, J. Wang, S. Chen, K. Wang, Y. Xue, G. Yao, Z. Luo, Y. Zhang, *Org. Lett.* **2015**, *17*, 346 – 349.
[9] Y. Moon, E. Jang, S. Choi, S. Hong, *Org. Lett.* **2018**, *20*, 240 – 243.
[10] a) S. R. Waldvogel, S. Lips, M. Selt, B. Riehl, C. J. Kampf, *Chem. Rev.* **2018**, *118*, 6706 – 6765; b) M. Yan, Y. Kawamata, P. S. Baran, *Chem. Rev.* **2017**, *117*, 13230 – 13319; c) A. Wiebe, T. Gieshoff, S. Möhle, E. Rodrigo, M. Zirbes, S. R. Waldvogel, *Angew. Chem. Int. Ed.* **2018**, *57*, 5594 – 5619; *Angew. Chem.* **2018**, *130*, 5694 – 5721; d) S. Möhle, M. Zirbes, E. Rodrigo, T. Gieshoff, A. Wiebe, S. R. Waldvogel, *Angew. Chem. Int. Ed.* **2018**, *57*, 6018 – 6041; *Angew. Chem.* **2018**, *130*, 6124 – 6149; e) S. R. Waldvogel, B. Janza, *Angew. Chem. Int. Ed.* **2014**, *53*, 7122 – 7123; *Angew. Chem.* **2014**, *126*, 7248 – 7249; f) S. R. Waldvogel, S. Möhle, *Angew. Chem. Int. Ed.* **2015**, *54*, 6398 – 6399; *Angew. Chem.* **2015**, *127*, 6496 – 6497; g) S. R. Waldvogel, M. Selt, *Angew. Chem. Int. Ed.* **2016**, *55*, 12578 – 12580; *Angew. Chem.* **2016**, *128*, 12766 – 12768; h) C. Gütz, M. Selt, M. Bänziger, C. Bucher, C. Römelt, N. Hecken, F. Gallou, T. R. Galvão, S. R. Waldvogel, *Chem. Eur. J.* **2015**, *21*, 13878 – 13882; i) J. Chen, W.-Q. Yan, C. M. Lam, C.-C. Zeng, L.-M. Hu, R. D. Little, *Org. Lett.* **2015**, *17*, 986 – 989; j) S. Herold, S. Moehle, M. Zirbes, F. Richter, H. Nefzger, S. R. Waldvogel, *Eur. J. Org. Chem.* **2016**, 1274 – 1278; k) T. Morofuji, A. Shimizu, J.-i. Yoshida, *J. Am. Chem. Soc.* **2013**, *135*, 5000 – 5003; l) R. Francke, R. D. Little, *J. Am. Chem. Soc.* **2014**, *136*, 427 – 435; m) A. Wiebe, D. Schollmeyer, K. M. Dyballa, R. Franke, S. R. Waldvogel, *Angew. Chem. Int. Ed.* **2016**, *55*, 11801 – 11805; *Angew. Chem.* **2016**, *128*, 11979 – 11983; n) S. Lips, A. Wiebe, B. Elsler, D. Schollmeyer, K. M. Dyballa, R. Franke, S. R. Waldvogel, *Angew. Chem. Int. Ed.* **2016**, *55*, 10872 – 10876; *Angew. Chem.* **2016**, *128*, 11031 – 11035.
[11] a) H. J. Schäfer, *C. R. Chim.* **2011**, *14*, 745 – 765; b) B. A. Frontana-Uribe, R. D. Little, J. G. Ibanez, A. Palma, R. Vasquez-Medrano, *Green Chem.* **2010**, *12*, 2099 – 2119.
[12] J. Grimshaw, D. Mannus, *J. Chem. Soc. Perkin Trans. 1* **1977**, 2456.
[13] S. Zhang, L. Li, M. Xue, R. Zhang, K. Xu, C. Zeng, *Org. Lett.* **2018**, *20*, 3443 – 3446.
[14] a) S. Z. Zard, *Chem. Soc. Rev.* **2008**, *37*, 1603 – 1618; b) N. Fuentes, W. Kong, L. Fernández-Sánchez, E. Merino, C. Nevado, *J. Am. Chem. Soc.* **2015**, *137*, 964 – 973.
[15] a) K. C. Nicolaou, P. S. Baran, Y.-L. Zhong, S. Barluenga, K. Hunt, R. Kranich, J. A. Vega, *J. Am. Chem. Soc.* **2002**, *124*, 2233 – 2244; b) Y.-F. Wang, H. Chen, X. Zhu, S. Chiba, *J. Am. Chem. Soc.* **2012**, *134*, 11980 – 11983; c) B. Janza, A. Studer, *J. Org. Chem.* **2005**, *70*, 6991 – 6994; d) S. Maity, N. Zheng, *Angew. Chem. Int. Ed.* **2012**, *51*, 9562 – 9566; *Angew. Chem.* **2012**, *124*, 9700 – 9704; e) X.-Q. Hu, J.-R. Chen, Q. Wei, F.-L. Liu, Q.-H. Deng, A. M. Beauchemin, W.-J. Xiao, *Angew. Chem. Int. Ed.* **2014**, *53*, 12163 – 12167; *Angew. Chem.* **2014**, *126*, 12359 – 12363; f) G. J. Choi, R. R. Knowles, *J. Am. Chem. Soc.* **2015**, *137*, 9226 – 9229; g) C. Moutrille, S. Z. Zard, *Chem. Commun.* **2004**, 1848 – 1849; h) L. Zhu, P. Xiong, Z.-Y. Mao, Y.-H. Wang, X. Yan, X. Lu, H.-C. Xu, *Angew. Chem. Int. Ed.* **2016**, *55*, 2226 – 2229; *Angew. Chem.* **2016**, *128*, 2266 – 2269; i) H.-C. Xu, J. M. Campbell, K. D. Moeller, *J. Org. Chem.* **2014**, *79*, 379 – 391.
[16] a) T. Gieshoff, D. Schollmeyer, S. R. Waldvogel, *Angew. Chem. Int. Ed.* **2016**, *55*, 9437 – 9440; *Angew. Chem.* **2016**, *128*, 9587 – 9590; b) T. Gieshoff, A. Kehl, D. Schollmeyer, K. D. Moeller, S. R. Waldvogel, *J. Am. Chem. Soc.* **2017**, *139*, 12317 – 12324; c) A. Kehl, T. Gieshoff, D. Schollmeyer, S. R. Waldvogel, *Chem. Eur. J.* **2018**, *24*, 590 – 593.
[17] A. R. Blaazer, J. H. M. Lange, M. A. W. van der Neut, A. Mulder, F. S. den Boon, T. R. Werkman, C. G. Kruse, W. J. Wadman, *Eur. J. Med. Chem.* **2011**, *46*, 5086 – 5098.
[18] C. Gütz, B. Klöckner, S. R. Waldvogel, *Org. Process Res. Dev.* **2016**, *20*, 26 – 32.
[19] a) A. Kirste, M. Nieger, I. M. Malkowsky, F. Stecker, A. Fischer, S. R. Waldvogel, *Chem. Eur. J.* **2009**, *15*, 2273 – 2277; b) A. Kirste, G. Schnakenburg, F. Stecker, A. Fischer, S. R. Waldvogel, *Angew. Chem. Int. Ed.* **2010**, *49*, 971 – 975; *Angew. Chem.* **2010**, *122*, 983 – 987; c) R. Francke, D. Cericola, R. Kötz, D. Weingarth, S. R. Waldvogel, *Electrochim. Acta* **2012**, *62*, 372 – 380; d) O. Holloczki, A. Berkessel, J. Mars, M. Mezger, A. Wiebe, S. R. Waldvogel, B. Kirchner, *ACS Catal.* **2017**, *7*, 1846 – 1852; e) B. Elsler, D. Schollmeyer, K. M. Dyballa, R. Franke, S. R. Waldvogel, *Angew. Chem. Int. Ed.* **2014**, *53*, 5210 – 5213; *Angew. Chem.* **2014**, *126*, 5311 – 5314; f) B. Elsler, A. Wiebe, D. Schollmeyer, K. M. Dyballa, R. Franke, S. R. Waldvogel, *Chem. Eur. J.* **2015**, *21*, 12321 – 12325.
[20] I. Colomer, A. E. R. Chamberlain, M. B. Haughey, T. J. Donohoe, *Nat. Rev. Chem.* **2017**, *1*, 88.

Manuscript received: September 11, 2018
Accepted manuscript online: October 8, 2018
Version of record online: October 30, 2018

CHEMISTRY
A European Journal

Supporting Information

Electrochemical Synthesis of 5-Aryl-phenanthridin-6-one by Dehydrogenative N,C Bond Formation

Anton Kehl, Valentina M. Breising, Dieter Schollmeyer, and Siegfried R. Waldvogel*[a]

chem_201804638_sm_miscellaneous_information.pdf

TABLE OF CONTENTS

General information

All reagents were used in analytical grades and were obtained from commercial sources. Solvents were purified by standard methods.[1] For electrochemical reactions, different electrode materials (see below) were used.

Column chromatography was performed on silica gel 60 M (0.040-0.063 mm, Macherey-Nagel GmbH & Co, Düren, Germany) with a maximum pressure of 2.0 bar. A preparative chromatography system (Büchi-Labortechnik GmbH, Essen, Germany) was used with a Büchi Control Unit C-620, an UV detector Büchi UV photometer C-635, Büchi fraction collector C-660 and two Pump Modules C-605 for adjusting the solvent mixtures. Mixtures of cyclohexane and ethyl acetate were used as eluents. Silica gel 60 sheets on aluminum (F254, Merck, Darmstadt, Germany) were employed for thin layer chromatography.

Gas chromatography was performed on a Shimadzu GC-2025 (Shimadzu, Japan) using a Zebron ZB-5MSi column (Phenomenex, USA; length: 30 m, inner diameter: 0.25 mm, film: 0.25 µm, pre-column: 5 m, carrier gas: hydrogen). GC-MS measurements were carried out on a Shimadzu GC-2010 (Shimadzu, Japan) using a Zebron ZB-5MSi column (Phenomenex, USA; length: 30 m, inner diameter: 0.25 mm, film: 0.25 µm, pre-column: 5 m, carrier gas: helium) combined with a GCMS-QP2010.

Melting points were determined by a Melting Point Apparatus SMP3 (Stuart Scientific, Staffordshire, U.K.) or M-565 (Büchi, Flawil, Switzerland) and are uncorrected.

Spectroscopy and spectrometry: ^{1}H NMR, ^{13}C NMR and ^{19}F spectra were recorded at 25 °C by using a Bruker Avance II 400 or a Bruker Avance III HD 400 (Analytische Messtechnik, Karlsruhe, Germany). Chemical shifts (δ) are reported in parts per million (ppm) relative to TMS as internal standard or traces of $CHCl_3$ or DMSO-d_5 in the corresponding deuterated solvent. For the ^{19}F spectra, α-trifluortoluene served as external standard (δ = –63.9 ppm).[2] Mass spectra and high resolution mass spectra were obtained by using a QTof Ultima 3 (Waters, Milford, Massachusetts) apparatus employing ESI+.

Electrode materials: Highly isostatic graphite Sigrafine™ V2100 was obtained from SGL Carbon, Bonn, Germany. The geometries were machined from a big block. BDD electrode with a DIACHEM® 15 µM boron-doped diamond layer on silicon were obtained from *CONDIAS GmbH*, Itzehoe, Germany.

X-ray analysis: All data were collected on a STOE IPDS2T diffractometer (Oxford Cryostream 700er series, Oxford Cryosystems) using graphite monochromated Mo K_α radiation (λ= 0.71073 Å). Intensities were measured using fine-slicing ω and φ-scans and corrected for background, polarization and Lorentz effects. The structures were solved by direct methods and refined anisotropically by the least-squares procedure implemented in the SHELX program system.[3]

The supplementary crystallographic data for this paper can be obtained free of charge from The Cambridge Crystallographic Data Center via www.ccdc.cam.ac.uk/data_request/cif. Deposition numbers and further details are given with the individual characterization data.

General procedures

Synthesis of starting materials

The required substituted benzanilides and biphenyl anilides were prepared according to the literature.[4,5]

General protocol for the synthesis of biphenyl anilide derivatives A[4]

To a cooled solution (0 °C) of 1.00 g (5.0 mmol, 1.0 eqiuv.) of 2-biphenylcarboxlic acid in 20 mL dichloromethane 0.01 mL DMF followed by a solution consisting of 0.76 g (0.51 mL, 6.0 mmol, 1.2 equiv.) oxalyl chloride in 5 mL dichloromethane were added. Cooling was stopped after the addition of the oxalyl chloride solution. The mixture was stirred overnight (ca. 18 h) at room temperature. Dichloromethane was removed at reduced pressure and the residue was dissolved in 60 mL ethyl acetate. After the addition of 0.61 g (0.83 mL, 6.0 mmol, 1.2 equiv.) of triethylamine and a solution of 5.0 mmol (1.0 equiv.) of aniline derivative in 10 mL ethyl acetate the reaction mixture was stirred for 2 h at room temperature, filtered and the solvent was evaporated under reduced pressure. If further purification was required, the solid was recrystallized from a suitable solvent in the boiling heat and were allowed to cool to ambient temperature.

General protocol for the synthesis of biphenyl anilide derivatives B[5]

To a solution of 5 mmol (1 equiv.) of 2-bromo-*N*-(4-chlorophenyl)benzamide in 50 mL anhydrous toluene 5 mol% of tetrakis(triphenylphosphine)palladium(0) was added and stirred for 15 minutes at room temperature. After adding 6 eq. of a 2 M potassium carbonate solution and 6 mmol (1.2 equiv.) of an arylboronic acid the solution was heated at 90 °C overnight (ca. 16 h). The solution was cooled to room temperature, diluted with water, and extracted with dichloromethane. The combined organic layer was washed with brine, dried with magnesium sulfate, and the solvent was removed under reduced pressure. The residue was recrystallized from a suitable solvent in the boiling heat and were allowed to cool to ambient temperature.

General protocol for the electrochemical synthesis of *N*-aryl-phenanthredin-6-one derivatives D

D1: Application of undivided screening cells (5mL)

A solution of 0.2 mmol biphenyl anilide and 5 mg (0.0025 M) tetrabutylammonium hexafluorophosphate (NBu_4PF_6) in 5 mL 1,1,1,3,3,3-hexafluoroisopropanol (HFIP) employing a graphite anode and a nickel cathode was electrolyzed. The electrolysis was performed under constant current conditions (current density j = 1 mA/cm^2, active surface 1.5 cm^2). After completion of the reaction according to TLC analysis, HFIP was recycled by distillation at reduced pressure (200-90 mbar, 50 °C). The purification of the product was conducted by column chromatography with the following gradient sequence: 2 minutes 100% cyclohexane; elevation of the ethyl acetate amount 0-10% within 30 minutes; if not stated otherwise.

D2: Application of beaker-type glass cells (80 mL)

Protocol D2 is similar to protocol D1 with the following modifications: 6.3 mmol of substrate and 77 mg (0.0025 M) NBu_4PF_6 are dissolved in 80 mL HFIP (current density j = 1 mA/cm^2, active surface 8.8 cm^2)

Electrolysis set-ups and electrode materials screening

Set-ups with electrodes in a parallel orientation were either conducted in a 5 mL Teflon cell[6] (Figure 1, left) with 7 cm x 1 cm electrodes or in a 80 mL beaker-type cell[7] (Figure 1, right) with 2 cm x 6 cm x 3 mm electrodes. Terminal voltage in 80 mL in glass cells typically is around 11 V. The screening set-up is also commercially available as IKA Screenings System, IKA-Werke GmbH & Co. KG, Staufen, Germany.

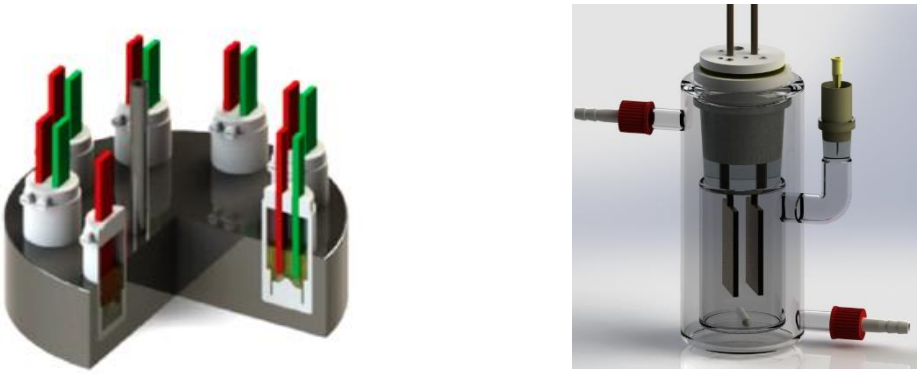

Figure 1: left: 5 mL Teflon cells;[8] right: 80 mL beaker-type cell.

Synthesis of *N*-aryl-biphenyl-2-carboxamides

N-(4-Chlorophenyl)-biphenyl-2-carboxamide (1a)

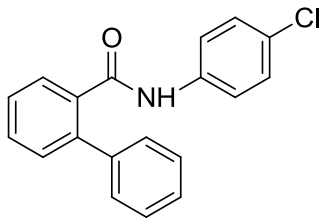

According to protocol A, 1.28 g (10.0 mmol, 1 equiv.) of 4-chloroaniline and 2.00 g (10.0 mmol, 1 equiv.) of 2-biphenylcarboxylic acid yielded 2.50 g (yield: 80%; 8.0 mmol) product as colorless crystalline solid after recrystallization from ethyl acetate (20 mL).

^{1}H NMR (400 MHz, DMSO-d_6) δ [ppm] = 10.37 (s, 1H), 7.62–7.53 (m, 4H), 7.52–7.46 (m, 2H), 7.46–7.40 (m, 2H), 7.39–7.27 (m, 5H).

^{13}C NMR (100 MHz, DMSO-d_6) δ [ppm] = 167.9, 139.9, 139.3, 138.0, 136.8, 130.0, 129.9, 128.5, 128.3, 128.3, 127.8, 127.3, 127.3, 127.1, 121.1.

HRMS for $C_{19}H_{14}{}^{35}ClNO$ (ESI+) $[M+H]^+$: calc.: 308.0837, found: 308.0842.

MP: 168.2–168.9 °C.

N-(4-*tert*-Butylphenyl)-biphenyl-2-carboxamide (1b)

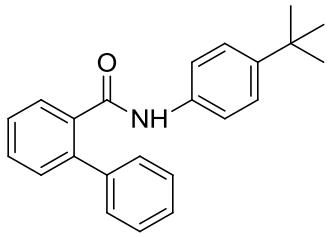

According to the protocol A, 0.37 g (2.5 mmol, 1 equiv.) of 4-*tert*-butylaniline, 0.50 g (2.5 mmol, 1 equiv.) 2-biphenylcarboxylic acid yielded 0.65 g (yield: 80%; 2.0 mmol) of product as colorless crystalline solid after recrystallization from cyclohexane (60 mL).

^{1}H NMR (400 MHz, DMSO-d_6) δ [ppm] = 10.16 (s, 1H), 7.59–7.52 (m, 2H), 7.51–7.41 (m, 6H), 7.40–7.35 (m, 2H), 7.33–7.22 (m, 3H), 1.25 (s, 9H).

^{13}C NMR (100 MHz, DMSO-d_6) δ [ppm] = 167.6, 145.8, 140.1, 139.2, 137.2, 136.5, 130.0, 129.7, 128.3, 128.3, 127.8, 127.2, 127.2, 125.2, 119.4, 34.0, 31.2.

HRMS for $C_{23}H_{23}NO$ (ESI+) $[M+H]^+$: calc.: 330.1852, found: 330.1851.

MP: 157.9–159.6 °C.

***N*-(2,4-Difluorophenyl)-biphenyl-2-carboxamide (1c)**

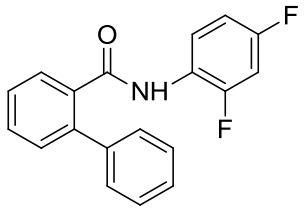

According to protocol A, 0.65 g (5.0 mmol, 1 equiv.) of 2,4-difluoroaniline and 1.00 g (5.0 mmol, 1 equiv.) of 2-biphenylcarboxylic acid yielded 1.33 g (yield: 85%; 4.3 mmol) product as colorless crystalline solid after recrystallization from cyclohexane (30 mL).

^{1}H NMR (400 MHz, DMSO-d_6) δ [ppm] = 10.02 (s, 1H), 7.64–7.55 (m, 2H), 7.54–7.45 (m, 5H), 7.44–7.38 (m, 2H), 7.35 (m, 1H), 7.28 (m, 1H), 7.05 (m, 1H).

^{13}C NMR (100 MHz, DMSO-d_6) δ [ppm] = 168.2, 159.3 (d, *J* = 240.0 Hz), 155.3 (d, *J* = 240.0 Hz), 140.0, 139.4, 136.4, 130.0, 129.9, 128.4, 128.2, 127.9, 127.3, 127.2, 127.1 (dd, *J* = 10.0, 3.0 Hz), 122.1 (dd, *J* = 20.0, 3.0 Hz), 111.1 (dd, *J* = 20.0, 3.0 Hz), 104.3 (t, *J* = 24.0 Hz).

^{19}F NMR (377 MHz, DMSO-d_6) δ [ppm] = -114.86, -118.37.

HRMS for $C_{19}H_{13}F_2NO$ (ESI+) $[M+H]^+$: calc.: 310.1038, found: 310.1039.

MP: 103.4–104.5 °C.

***N*-(3-Cyano-4-methylphenyl)-biphenyl-2-carboxamide (1d)**

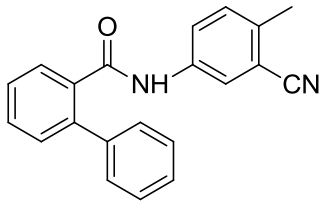

According to the protocol A, 0.33 g (2.5 mmol, 1 equiv.) of 5-amino-2-methylbenzonitrile and 0.50 g (2.5 mmol, 1 equiv.) 2-biphenylcarboxylic acid yielded 0.53 g (yield: 64%; 1.6 mmol) of product as colorless crystalline solid after recrystallization from ethyl acetate (10 mL).

^{1}H NMR (400 MHz, DMSO-d_6) δ [ppm] = 10.47 (s, 1H), 7.92 (d, *J* = 2.3 Hz, 1H), 7.64–7.56 (m, 3H), 7.55–7.46 (m, 2H), 7.45–7.35 (m, 5H), 7.33–7.27 (m, 1H), 2.40 (s, 3H).

^{13}C NMR (100 MHz, DMSO-d_6) δ [ppm] = 168.1, 139.9, 139.4, 137.4, 136.5, 136.3, 130.9, 130.1, 130.1, 128.3, 128.3, 127.8, 127.4, 127.3, 124.2, 122.3, 117.8, 111.6, 19.3.

HRMS for $C_{21}H_{16}N_2O$ (ESI+) $[M+H]^+$: calc.: 313.1335, found: 313.1345.

MP: 160.3–161.9 °C.

***N*-(3-Bromophenyl)-biphenyl-2-carboxamide (1e)**

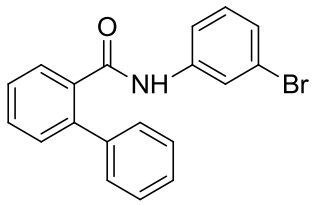

According to protocol A, 0.86 g (5.0 mmol, 1 equiv.) of 3-bromoaniline and 1.00 g (5.0 mmol, 1 equiv.) of 2-biphenylcarboxylic acid yielded 1.53 g (yield: 85%; 4.3 mmol) product as colorless crystalline solid after recrystallization from cyclohexane (50 mL).

^{1}H NMR (400 MHz, DMSO-d_6) δ [ppm] = 10.43 (s, 1H), 7.87 (s, 1H), 7.59 (m, 2H), 7.53–7.35 (m, 7H), 7.31 (m, 1H), 7.27–7.20 (m, 2H).

^{13}C NMR (100 MHz, DMSO-d_6) δ [ppm] = 168.1, 140.7, 139.9, 139.4, 136.7, 130.7, 130.1, 130.0, 128.4, 128.3, 127.9, 127.4, 127.3, 126.2, 121.8, 121.5, 118.3.

HRMS for $C_{19}H_{14}{}^{78}BrNO$ (ESI+) $[M+H]^+$: calc.: 352.0332, found: 352.0345.

MP: 138.8–139.9 °C.

***N*-(2-Iodophenyl)-biphenyl-2-carboxamide (1f)**

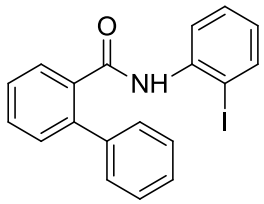

According to the protocol A, 0.55 g (2.5 mmol, 1 equiv.) of 2-iodoaniline and 0.50 g (2.5 mmol, 1 equiv.) 2-biphenylcarboxylic acid yielded 0.53 g (yield: 64%; 1.6 mmol) of product as colorless crystalline solid after recrystallization from cyclohexane (15 mL).

^{1}H NMR (400 MHz, DMSO-d_6) δ [ppm] = 9.92 (s, 1H), 7.88 (dd, *J* = 7.9, 1.4 Hz, 1H), 7.70 (dd, *J* = 7.9, 1.4 Hz, 1H), 7.62–7.42 (m, 7H), 7.41–7.33 (m, 2H), 7.28–7.22 (m, 1H), 7.00 (m, 1H).

^{13}C NMR (100 MHz, DMSO-d_6) δ [ppm] = 167.9, 140.1, 139.5, 139.4, 138.9, 136.7, 130.0, 129.9, 128.7, 128.6, 128.3, 128.0, 127.7, 127.5, 127.4, 127.1, 97.4.

HRMS for $C_{19}H_{14}INO$ (ESI+) $[M+H]^+$: calc.: 400.0193, found: 400.0188.

MP: 97.0–98.3 °C.

***N*-Phenyl-biphenyl-2-carboxamide (1g)**

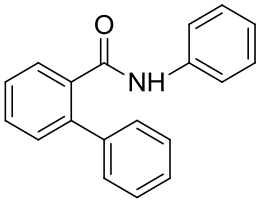

According to the protocol A, 0.23 g (2.5 mmol, 1 equiv.) of aniline and 0.50 g (2.5 mmol, 1 equiv.) 2-biphenylcarboxylic acid yielded 0.53 g (yield: 60%; 1.5 mmol) of product as colorless crystalline solid after recrystallization from cyclohexane (30 mL).

^{1}H NMR (400 MHz, DMSO-d_6) δ [ppm] = 10.23 (s, 1H), 7.59–7.44 (m, 8H), 7.41–7.34 (m, 2H), 7.33–7.23 (m, 3H), 7.07–7.01 (m, 1H).

^{13}C NMR (100 MHz, DMSO-d_6) δ [ppm] = 167.9, 140.1, 139.2, 139.1, 137.1, 130.0, 129.8, 128.6, 128.4, 128.3, 127.8, 127.3, 127.2, 123.5, 119.7.

HRMS for $C_{19}H_{15}NO$ (ESI+) $[M+H]^+$: calc.: 274.1226, found: 274.1229.

MP: 110.3–110.9 °C.

The analytical data match the reported data.[8]

***N*-(2-Acetylphenyl)-biphenyl-2-carboxamide (1h)**

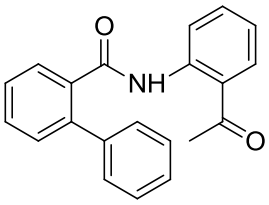

According to protocol A, 0.34 g (2.5 mmol, 1 equiv.) of 2-acetylaniline and 0.50 g (2.5 mmol, 1 equiv.) of 2-biphenylcarboxylic acid yielded 0.32 g (yield: 40%; 1.0 mmol) product as colorless crystalline solid after recrystallization from cyclohexane (50 mL).

^{1}H NMR (400 MHz, DMSO-d_6) δ [ppm] = 11.40 (s, 1H), 8.34 (d, *J* = 8.8 Hz, 1), 7.94 (dd, *J* = 8.0, 1.4 Hz, 1H), 7.68–7.49 (m, 5H), 7.41–7.26 (m, 5H), 7.20 (dt, *J* = 8.0, 1.4 Hz, 1H), 2.51 (s, 3H).

^{13}C NMR (100 MHz, DMSO-d_6) δ [ppm] = 202.4, 167.9, 139.6, 139.4, 138.9, 136.4, 134.2, 131.6, 130.6, 130.4, 128.5, 128.3, 128.0, 127.7, 127.4, 124.0, 123.3, 120.3, 28.6.

HRMS for $C_{21}H_{17}NO_2$ (ESI+) $[M+H]^+$: calc.: 316.1332, found: 316.1334.

MP: 127.9–129.1 °C.

Ethyl 2-((1,1'-biphenyl)-2-ylcarboxamido)benzoate (1i)

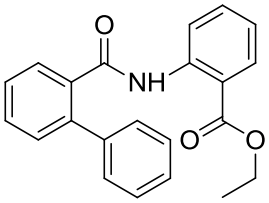

According to protocol A, 0.42 g (2.5 mmol, 1 equiv.) of ethyl anthranilate and 0.50 g (2.5 mmol, 1 equiv.) of 2-biphenylcarboxylic acid yielded 0.57 g (yield: 65%; 1.7 mmol) product as colorless crystalline solid after recrystallization from cyclohexane (75 mL).

^{1}H NMR (400 MHz, DMSO-d_6) δ [ppm] = 10.83 (s, 1H), 8.31 (d, *J* = 8.4 Hz, 1H), 7.87 (dd, *J* = 7.9, 1.7 Hz, 1H), 7.69 (dd, *J* = 7.9, 1.7 Hz, 1H), 7.64–7.49 (m, 4H), 7.42–7.26 (m, 5H), 7.20–7.16 (m, 1H), 4.21 (q, *J* = 7.1 Hz, 2H), 1.26 (t, J = 7.1 Hz, 3H).

^{13}C NMR (100 MHz, DMSO-d_6) δ [ppm] = 167.7, 166.9, 139.7, 139.6, 139.4, 136.4, 134.1, 130.7, 130.6, 130.4, 128.5, 128.4, 128.1, 127.7, 127.5, 123.4, 120.6, 117.4, 61.3, 14.0.

HRMS for $C_{22}H_{19}NO_3$ (ESI+) $[M+H]^+$: calc.: 346.1438, found: 346.1435.

MP: 109.0–109.8 °C.

***N*-(3-Nitrophenyl)-biphenyl-2-carboxamide (1j)**

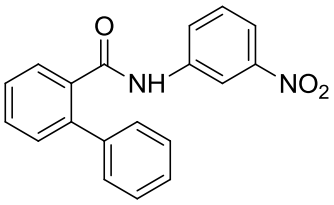

According to protocol A, 0.35 g (2.5 mmol, 1 equiv.) of 3-nitroaniline and 0.50 g (2.5 mmol, 1 equiv.) of 2-biphenylcarboxylic acid yielded 0.56 g (yield: 69%; 1.8 mmol) product as yellow crystalline solid after recrystallization from cyclohexane (80 mL).

^{1}H NMR (400 MHz, DMSO-d_6) δ [ppm] = 10.76 (s, 1H), 8.59 (m, 1H), 7.92–7.83 (m, 2H), 7.65–7.49 (m, 5H), 7.45–7.28 (m, 5H).

^{13}C NMR (100 MHz, DMSO-d_6) δ [ppm] = 168.4, 147.9, 142.0, 139.9, 139.5, 136.4, 130.3, 130.1, 128.4, 128.3, 127.9, 127.4, 127.3, 125.5, 118.1, 113.5.

HRMS for $C_{19}H_{14}N_2O_3$ (ESI+) $[M+H]^+$: calc.: 319.1077, found: 319.1079.

MP: 155.2–156.1 °C.

***N*-(4-Chlorophenyl)-4'-trifluoromethylbiphenyl-2-carboxamide (1k)**

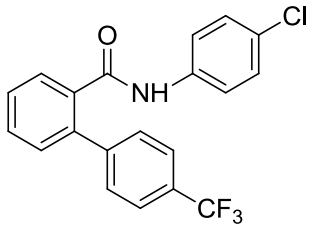

According to protocol A, 0.64 g (5.0 mmol, 1 equiv.) of 4-chloroaniline and 1.33 g (5.0 mmol, 1 equiv.) of 4'-trifluoromethyl-2-biphenylcarboxylic acid yielded 1.42 g (yield: 76%; 3.8 mmol) product as colorless crystalline solid after recrystallization from cyclohexane (50 mL).

^{1}H NMR (400 MHz, DMSO-d_6) δ [ppm] = 10.50 (s, 1H), 7.75 (d, *J* = 8.1 Hz, 2H), 7.63 (m, 4H), 7.59–7.50 (m, 4H), 7.34 (m, 2H).

^{13}C NMR (100 MHz, DMSO-d_6) δ [ppm] = 167.4, 144.2, 138.0, 137.9, 136.7, 130.2, 130.1, 129.1, 128.6, 128.1 (m), 127.8 (q, *J* = 32 Hz), 127.3, 125.2, 125.1, 124.2 (q, *J* = 270 Hz), 121.1.

^{19}F NMR (377 MHz, DMSO-d_6) δ [ppm] = -62.07.

HRMS for $C_{20}H_{13}{}^{35}ClF_3NO$ (ESI+) $[M+H]^+$: calc.: 376.0711, found: 376.0713.

MP: 199.7–201.9 °C.

***N*-(4-Chlorophenyl)-4'-chlorobiphenyl-2-carboxamide (1l)**

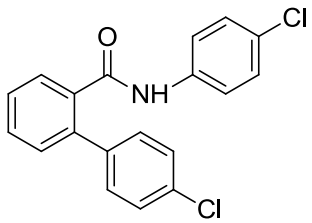

According to protocol B, 0.94 g (6.0 mmol, 1.2 equiv.) of 4-chlorophenylboronic acid and 1.55 g (5.0 mmol, 1 equiv.) of 2-bromo-*N*-(4-chlorophenyl)benzamide yielded 1.47 g (yield: 86%; 4.3 mmol) product as colorless crystalline solid after recrystallization from methanol (30 mL).

^{1}H NMR (400 MHz, DMSO-d_6) δ [ppm] = 10.45 (s, 1H), 7.63–7.55 (m, 4H), 7.55–7.40 (m, 6H), 7.38–7.30 (m, 2H).

^{13}C NMR (100 MHz, DMSO-d_6) δ [ppm] = 167.7, 138.8, 138.1, 138.0, 136.7, 132.3, 130.2, 130.1, 130.0, 128.6, 128.3, 128.0, 127.7, 127.2, 121.1.

HRMS for $C_{19}H_{13}{}^{35}Cl_2NO$ (ESI+) $[M+H]^+$: calc.: 342.0452, found: 342.0454.

MP: 171.8–173.7 °C.

4'-*tert*-Butyl-*N*-(4-chlorophenyl)-biphenyl-2-carboxamide (1m)

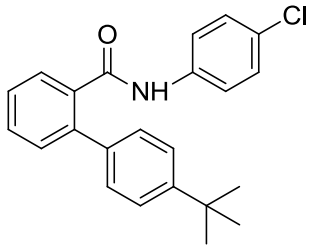

According to protocol B, 1.07 g (6.0 mmol, 1.2 equiv.) of 4-*tert*-butylphenylboronic acid and 1.55 g (5.0 mmol, 1 equiv.) of 2-bromo-*N*-(4-chlorophenyl)benzamide yielded 1.32 g (yield: 72%; 3.6 mmol) product as colorless crystalline solid after recrystallization from cyclohexane (20 mL).

^{1}H NMR (400 MHz, DMSO-d_6) δ [ppm] = 10.39 (s, 1H), 7.58–7.54 (m, 4H), 7.49–7.45 (m, 2H), 7.40–7.32 (m, 6H), 1.26 (s, 9H).

^{13}C NMR (100 MHz, DMSO-d_6) δ [ppm] = 168.0, 149.6, 139.1, 138.0, 137.0, 136.7, 130.1, 130.0, 128.5, 128.0, 127.9, 127.1, 127.0, 125.1, 121.1, 34.3, 31.1.

HRMS for $C_{23}H_{22}{}^{35}ClNO$ (ESI+) $[M+H]^+$: calc.: 364.1463, found: 364.1457.

MP: 182.5–184.6 °C.

Synthesis of *N*-Arylphenanthredinones

N-(4-Chlorophenyl)-phenanthredin-6-one (2a)

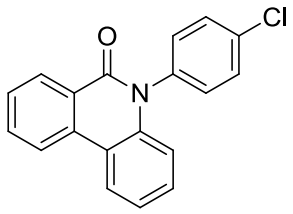

Small scale: According to protocol D1, 62 mg (0.20 mmol, 1 equiv.) of **1a** and 5 mg NBu_4PF_6 in 5 mL HFIP were electrolyzed in a 5 mL screening cell. An amount of 2.2 F of electric charge was applied to afford 52 mg (yield: 85%; 0.17 mmol) of colorless crystalline solid.

Large scale: According to protocol D2, 1.95 g (6.3 mmol, 1 equiv.) of **1a** and 77 mg NBu_4PF_6 in 80 mL HFIP were electrolyzed in a 80 mL beaker-type cell. An amount of 2.2 F of electric charge was applied to afford 1.49 g (yield: 78%; 4.9 mmol) of colorless crystalline solid.

^{1}H NMR (300 MHz, $CDCl_3$) δ [ppm] = 8.59–8.51 (m, 1H), 8.37–8.27 (m, 2H), 7.83 (ddd, *J* = 8.3, 7.2, 1.5 Hz, 1H), 7.67–7.55 (m, 3H), 7.37–7.26 (m, 4H), 6.74–6.66 (m, 1H).

^{13}C NMR (75 MHz, $CDCl_3$) δ [ppm] = 161.8, 139.0, 136.9, 134.9, 134.1, 133.2, 130.7, 130.6, 129.4, 129.2, 128.4, 125.8, 123.3, 123.0, 122.0, 119.2, 116.9.

HRMS for $C_{19}H_{12}{}^{35}ClNO$ (ESI+) $[M+H]^+$: calc.: 306.0680, found: 306.0682.

MP: 254.2–256.8 °C (cyclohexane/ethylacetate).

N-(4-*tert*-Butylphenyl)-phenanthredin-6-one (2b)

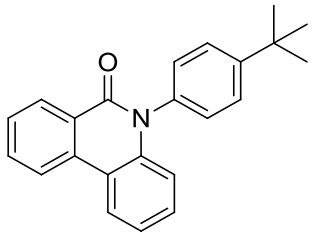

According to protocol D1, 66 mg (0.20 mmol, 1 equiv.) of **1b** and 5 mg NBu_4PF_6 in 5 mL HFIP were electrolyzed in a 5 mL screening cell. An amount of 2.2 F of electric charge was applied to afford 55 mg (yield: 84%; 0.17 mmol) of colorless crystalline solid.

^{1}H NMR (400 MHz, $CDCl_3$) δ [ppm] = 8.57 (dd, *J* = 8.0, 1.5, 1H), 8.37–8.28 (m, 2H), 7.81 (ddd, *J* = 8.0, 7.2, 1.5 Hz, 1H), 7.65–7.58 (m, 3H), 7.35–7.28 (m, 2H), 7.27–7.23 (m, 2H), 6.77–6.72 (m, 1H), 1.42 (s, 9H).

^{13}C NMR (100 MHz, $CDCl_3$) δ [ppm] = 161.9, 151.8, 139.5, 135.6, 134.1, 132.9, 129.2, 129.1, 128.5, 128.2, 127.3, 126.1, 123.1, 122.7, 121.9, 119.2, 117.3, 35.0, 31.6.

HRMS for $C_{23}H_{21}NO$ (ESI+) $[M+H]^+$: calc.: 328.1696, found: 328.1695.

MP: 178.7–180.2 °C (cyclohexane/ethylacetate).

***N*-(2,4-Difluorophenyl)-phenanthredin-6-one (2c)**

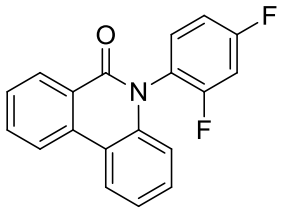

According to protocol D1, 62 mg (0.20 mmol, 1 equiv.) of **1c** and 5 mg NBu_4PF_6 in 5 mL HFIP were electrolyzed in a 5 mL screening cell. An amount of 2.2 F of electric charge was applied to afford 50 mg (yield: 80%; 0.16 mmol) of colorless crystalline solid.

^{1}H NMR (400 MHz, $CDCl_3$) δ [ppm] = 8.55 (dd, *J* = 8.0, 1.5 Hz, 1H), 8.33 (m, 2H), 7.83 (m, H), 7.62 (m, 1H), 7.41–7.29 (m, 3H), 7.16–7.08 (m, 2H), 6.73 (m, 1H).

^{13}C NMR (100 MHz, $CDCl_3$) δ [ppm] = 163.2 (d, *J* = 250 Hz), 161.5, 159.1 (d, *J* = 250 Hz), 138.5, 134.3, 133.3, 132.0 (dd, *J* = 10.0, 3.0 Hz), 129.6, 129.2, 128.4, 125.6, 123.5, 123.3, 122.1, 121.9 (d, *J* = 3.0 Hz), 119.4, 116.1, 112.8 (dd, *J* = 20.0, 3.0 Hz),105.9 (t, *J* = 24.0 Hz).

^{19}F NMR (377 MHz, $CDCl_3$) δ [ppm] = -108.73, -116.46.

HRMS for $C_{19}H_{11}F_2NO$ (ESI+) $[M+H]^+$: calc.: 308.0881, found: 308.0883.

MP: 248.2–249.5 °C (cyclohexane/ethylacetate).

***N*-(3-Cyano-4-methylphenyl)-phenanthredin-6-one (2d)**

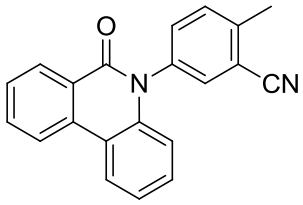

According to protocol D1, 62 mg (0.20 mmol, 1 equiv.) of **1d** and 5 mg NBu_4PF_6 in 5 mL HFIP were electrolyzed in a 5 mL screening cell. An amount of 2.2 F of electric charge was applied to afford 45 mg (yield: 72%; 0.15 mmol) of colorless crystalline solid.

^{1}H NMR (400 MHz, $CDCl_3$) δ [ppm] = 8.52 (dd, *J* = 8.1, 2.2 Hz, 1H), 8.37–8.27 (m, 2H), 7.83 (m, 1H), 7.65–7.56 (m, 3H), 7.48 (dd, *J* = 8.1, 2.2 Hz, 1H), 7.37–7.27 (m, 2H), 6.67–6.60 (m, 1H), 2.68 (s, 3H).

^{13}C NMR (100 MHz, $CDCl_3$) δ [ppm] = 161.8, 142.9, 138.6, 136.6, 134.0, 133.3, 133.3, 132.4, 129.4, 129.1, 128.4, 125.5, 123.4, 123.2, 122.0, 119.2, 117.2, 116.6, 114.9, 20.5.

HRMS for $C_{21}H_{14}N_2O$ (ESI+) $[M+H]^+$: calc.: 311.1179, found: 311.1181.

MP: 190.5–192.8 °C (cyclohexane/ethylacetate).

***N*-(3-Bromophenyl)-phenanthredin-6-one (2e)**

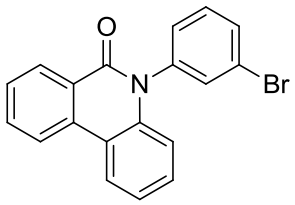

According to protocol D1, 70 mg (0.20 mmol, 1 equiv.) of **1e** and 5 mg NBu_4PF_6 in 5 mL HFIP were electrolyzed in a 5 mL screening cell. An amount of 2.2 F of electric charge was applied to afford 52 mg (yield: 74%; 0.15 mmol) of colorless crystalline solid.

^{1}H NMR (400 MHz, $CDCl_3$) δ [ppm] = 8.55 (dd, *J* = 7.9, 1.4 Hz, 1H), 8.35–8.26 (m, 2H), 7.82 (m, 1H), 7.68 (m, 1H), 7.62 (m, 1H), 7.54–7.46 (m, 2H), 7.32 (m, 3H), 6.69 (m, 1H).

^{13}C NMR (100 MHz, $CDCl_3$) δ [ppm] = 161.6, 139.6, 138.8, 134.1, 133.1, 132.5, 132.2, 131.5, 129.4, 129.1, 128.3, 128.2, 125.7, 123.6, 123.2, 123.0, 122.0, 119.1, 116.9.

HRMS for $C_{19}H_{12}{}^{78}BrNO$ (ESI+) $[M+H]^+$: calc.: 350.0175, found: 350.0171.

MP: 132.0–133.1 °C (cyclohexane/ethylacetate).

***N*-(2-Iodophenyl)-phenanthredin-6-one (2f)**

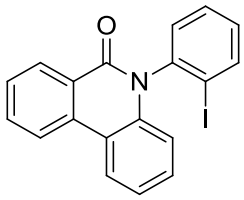

According to protocol D1, 80 mg (0.20 mmol, 1 equiv.) of **1f** and 5 mg NBu_4PF_6 in 5 mL HFIP were electrolyzed in a 5 mL screening cell. An amount of 2.2 F of electric charge was applied to afford 62 mg (yield: 78%; 0.16 mmol) of colorless crystalline solid.

^{1}H NMR (400 MHz, $CDCl_3$) δ [ppm] = 8.59 (dd, *J* = 8.0, 1.4 Hz, 1H), 8.39–8.31 (m, 2H), 8.09 (dd, *J* = 8.0, 1.4 Hz, 1H), 7.84 (ddd, *J* = 8.0, 7.2, 1.4 Hz, 1H), 7.66–7.57 (m, 2H), 7.41–7.29 (m, 3H), 7.28–7.23 (m, 1H), 6.57–6.51 (m, 1H).

^{13}C NMR (100 MHz, $CDCl_3$) δ [ppm] = 161.0, 141.2, 140.7, 138.0, 134.3, 133.2, 130.5, 130.4, 130.3, 129.5, 129.3, 128.3, 125.9, 123.4, 123.1, 122.0, 119.3, 116.5, 99.7.

HRMS for $C_{19}H_{12}INO$ (ESI+) $[M+H]^+$: calc.: 398.0036, found: 398.0034.

MP: 199.2–200.4 °C (cyclohexane/ethylacetate).

***N*-Phenyl-phenanthredin-6-one (2g)**

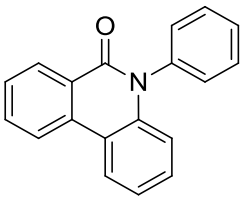

According to protocol D1, 54 mg (0.20 mmol, 1 equiv.) of **1g** and 5 mg NBu_4PF_6 in 5 mL HFIP were electrolyzed in a 5 mL screening cell. An amount of 2.2 F of electric charge was applied to afford 24 mg (yield: 44%; 0.09 mmol) of colorless crystalline solid.

^{1}H NMR (400 MHz, $CDCl_3$) δ [ppm] = 8.57 (dd, *J* = 8.0, 1.4 Hz, 1H), 8.38–8.29 (m, 2H), 7.82 (ddd, *J* = 8.0, 7.1, 1.4 Hz, 1H), 7.66–7.60 (m, 3H), 7.57–7.51 (m, 1H), 7.38–7.26 (m, 4H), 6.73–6.68 (m, 1H).

^{13}C NMR (100 MHz, $CDCl_3$) δ [ppm] = 161.8, 139.3, 138.4, 134.1, 133.0, 130.3, 129.3, 129.2, 129.1, 128.9, 128.3, 126.0, 123.1, 122.8, 121.9, 119.1, 117.1.

HRMS for $C_{19}H_{13}NO$ (ESI+) $[M+H]^+$: calc.: 272.1071, found: 272.1068.

MP: 118.2–119.7 °C (cyclohexane/ethylacetate).

The analytical data match the reported data.[9]

***N*-(2-Acetylphenyl)-phenanthredin-6-one (2h)**

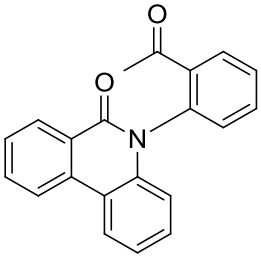

According to protocol D1, 63 mg (0.20 mmol, 1 equiv.) of **1h** and 5 mg NBu_4PF_6 in 5 mL HFIP were electrolyzed in a 5 mL screening cell. An amount of 2.2 F of electric charge was applied to afford 24 mg (yield: 40%; 0.08 mmol) of colorless oil.

^{1}H NMR (300 MHz, $CDCl_3$) δ [ppm] = 8.53 (dd, *J* = 8.0, 1.5 Hz, 1H), 8.38–8.29 (m, 2H), 8.03–7.98 (m, 1H), 7.82 (m, 1H), 7.74 (m, 1H), 7.68–7.58 (m, 2H), 7.36–7.27 (m, 3H), 6.62–6.54 (m, 1H), 2.35 (s, 3H).

^{13}C NMR (75 MHz, $CDCl_3$) δ [ppm] = 198.3, 161.9, 139.1, 137.6, 136.6, 134.3, 133.7, 133.1, 131.0, 130.6, 129.4, 129.4, 129.1, 128.3, 125.8, 123.3, 123.0, 122.1, 119.3, 116.7, 28.9.

HRMS for $C_{21}H_{15}NO_2$ (ESI+) $[M+Na]^+$: calc.: 336.0995, found: 336.0998.

***N*-(2-Ethyl benzoate-2-yl)-phenanthredin-6-one (2i)**

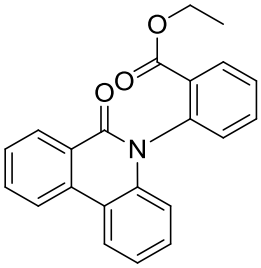

According to protocol D1, 69 mg (0.20 mmol, 1 equiv.) of **1i** and 5 mg NBu_4PF_6 in 5 mL HFIP were electrolyzed in a 5 mL screening cell. An amount of 2.2 F of electric charge was applied to afford 42 mg (yield: 61%; 0.12 mmol) of slightly colorless oil.

^{1}H NMR (400 MHz, $CDCl_3$) δ [ppm] = 8.55 (dd, *J* = 8.0, 1.5 Hz, 1H), 8.38–8.28 (m, 3H), 7.80 (m, 2H), 7.68–7.57 (m, 2H), 7.38 (m, 1H), 7.31–7.25 (m, 2H), 6.55 (m, 1H), 3.93 (q, *J* = 7.3 Hz, 2H), 0.71 (t, *J* = 7.2 Hz, 3H).

^{13}C NMR (100 MHz, $CDCl_3$) δ [ppm] = 164.8, 162.0, 139.3, 138.4, 134.2, 133.0, 132.9, 131.1, 129.7, 129.3, 129.2, 129.1, 128.2, 128.1, 125.9, 123.1, 122.7, 121.9, 119.1, 116.4, 61.2, 13.4.

HRMS for $C_{22}H_{17}NO_3$ (ESI+) $[M+H]^+$: calc.: 344.1281, found: 344.1283.

***N*-(3-Nitrophenyl)-phenanthredin-6-one (2j)**

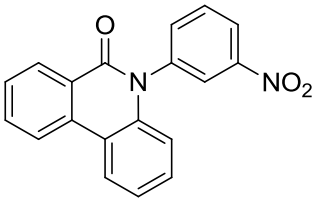

According to protocol D1, 64 mg (0.20 mmol, 1 equiv.) of **1j** and 5 mg NBu_4PF_6 in 5 mL HFIP were electrolyzed in a 5 mL screening cell. An amount of 2.2 F of electric charge was applied to afford 46 mg (yield: 73%; 0.15 mmol) of colourless crystalline solid.

^{1}H NMR (300 MHz, $CDCl_3$) δ [ppm] = 8.53 (dd, *J* = 8.0, 1.5 Hz, 1H), 8.43 (m, 1H), 8.38–8.30 (m, 2H), 8.27 (m, 1H), 7.90–7.79 (m, 2H), 7.73 (m, 1H), 7.64 (m, 1H), 7.38–7.30 (m, 2H), 6.66–6.58 (m, 1H).

^{13}C NMR (75 MHz, $CDCl_3$) δ [ppm] = 161.8, 149.6, 139.5, 138.5, 136.1, 134.1, 133.5, 131.2, 129.6, 129.1, 128.6, 125.5, 125.2, 124.0, 123.6, 123.4, 122.1, 119.3, 116.5.

HRMS for $C_{19}H_{12}N_2O_3$ (ESI+) $[M+H]^+$: calc.: 317.0921, found: 317.0924.

MP: 173.0–174.5 °C (cyclohexane/ethylacetate).

***N*-(4-Chlorophenyl)-3-trifluoromethylphenanthredin-6-one (2k)**

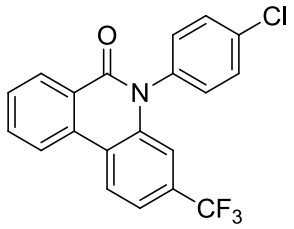

According to protocol D1, 75 mg (0.20 mmol, 1 equiv.) of **1k** and 5 mg NBu_4PF_6 in 5 mL HFIP were electrolyzed in a 5 mL screening cell. An amount of 2.2 F of electric charge was applied to afford 30 mg (yield: 40%; 0.08 mmol) of colorless crystalline solid.

^{1}H NMR (400 MHz, $CDCl_3$) δ [ppm] = 8.58–8.52 (m, 2H), 8.36 (d, *J* = 8.2 Hz, 1H), 7.88 (m, 1H), 7.69 (m, 1H), 7.64 – 7.59 (m, 2H), 7.54 (dd, *J* = 8.8, 2.0 Hz, 1H), 7.31–7.26 (m, 2H), 6.81 (d, *J* = 8.8 Hz, 1H).

^{13}C NMR (100 MHz, $CDCl_3$) δ [ppm] = 161.7, 141.2, 136.3, 135.4, 133.6, 133.2, 130.9, 130.5, 129.3, 126.0, 125.8 (m), 125.2 (q, *J* = 30 Hz), 124.3 (q, *J* = 270 Hz), 122.1, 120.8 (m), 119.2, 117.3.

^{19}F NMR (377 MHz, $CDCl_3$) δ = -63.00.

HRMS for $C_{20}H_{11}{}^{35}ClF_3NO$ (ESI+) $[M+H]^+$: calc.: 374.0554, found: 374.0558.

MP: 243.9–245.6 °C (cyclohexane/ethylacetate).

***N*-(4-Chlorophenyl)-3-chlorophenanthredin-6-one (2l)**

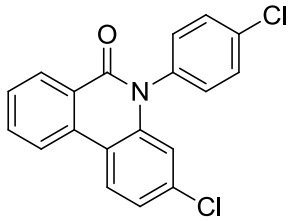

According to protocol D1, 68 mg (0.20 mmol, 1 equiv.) of **1l** and 5 mg NBu_4PF_6 in 5 mL HFIP were electrolyzed in a 5 mL screening cell. An amount of 2.2 F of electric charge was applied to afford 40 mg (yield: 59%; 1.18 mmol) of colorless crystalline solid.

^{1}H NMR (300 MHz, $CDCl_3$) δ [ppm] = 8.54 (dd, *J* = 8.0, 1.5 Hz, 1H), 8.31–8.22 (m, 2H), 7.89–7.80 (m, 1H), 7.70–7.56 (m, 3H), 7.27 (m, 3H), 6.64 (d, *J* = 9.0 Hz, 1H).

^{13}C NMR (75 MHz, $CDCl_3$) δ [ppm] = 161.5, 137.6, 136.5, 135.2, 133.4, 133.0, 130.8, 130.6, 129.3, 129.2, 129.1, 128.8, 126.0, 123.1, 122.1, 120.6, 118.3.

HRMS for $C_{19}H_{11}{}^{35}Cl_2NO$ (ESI+) $[M+H]^+$: calc.: 340.0296, found: 340.0288.

MP: 295.1–297.4 °C (cyclohexane/ethylacetate).

3-*tert*-Butyl-*N*-(4-chlorophenyl)-phenanthredin-6-one (2m)

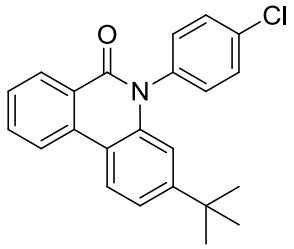

According to protocol D1, 73 mg (0.20 mmol, 1 equiv.) of **1m** and 5 mg NBu_4PF_6 in 5 mL HFIP were electrolyzed in a 5 mL screening cell. An amount of 2.2 F of electric charge was applied to afford 58 mg (yield: 80%; 1.6 mmol) of colorless oil.

^{1}H NMR (600 MHz, $CDCl_3$) δ [ppm] = 8.54 (dd, *J* = 8.0, 1.4 Hz, 1H), 8.38 (d, *J* = 8.0 Hz, 1H), 8.31 (d, *J* = 2.2 Hz, 1H), 7.83 (m, 1H), 7.64–7.56 (m, 3H), 7.38 (dd, *J* = 8.8, 2.2 Hz, 1H), 7.31–7.27 (m, 2H), 6.64 (d, *J* = 8.0 Hz, 1H), 1.41 (s, 9H).

^{13}C NMR (150 MHz, $CDCl_3$) δ [ppm] = 161.8, 145.8, 137.0, 136.8, 134.8, 134.4, 133.0, 130.7, 130.6, 129.2, 128.2, 127.0, 125.8, 121.9, 119.4, 118.6, 116.7, 34.7, 31.6.

HRMS for $C_{23}H_{20}{}^{35}ClNO$ (ESI+) $[M+H]^+$: calc.: 362.1306, found: 362.1301.

Crystallographic data

Crystal structure determination of **2a** (CCDC 1866675): $C_{19}H_{12}ClNO$, M_r = 305.8 g/mol, colorless needle (0.04 x 0.14 x 1.07 mm^3), P $2_1/c$ (monoklin), a = 5.4622 Å, b = 25.5595 Å, c = 10.5965 Å, V = 1447.4 $Å^3$, Z = 4, F(000) = 632, ρ = 1.403 g/cm^3, μ = 0.26 mm^{-1}, Mo-Kα graphite monochromator, -80 °C, 7572 reflections, 3631 independent reflections, wR_2 = 0.1329, R_1 = 0.0579, 0.29 e/$Å^3$, –0.29 e/$Å^3$, GoF = 1.104

Single crystals for structure determination were obtained by recrystallization from ethyl acetate at room temperature.

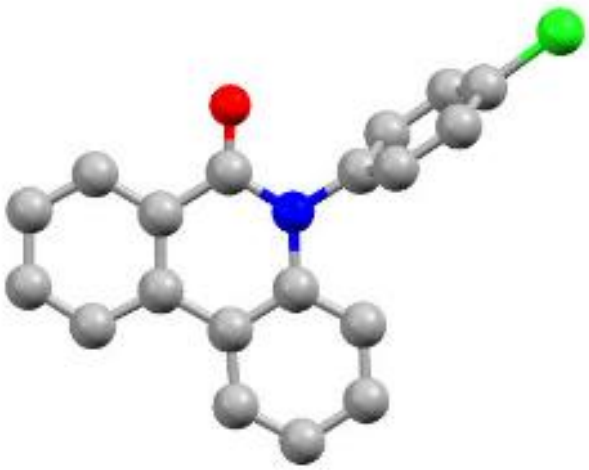

Figure 2: Molecular structure of derivative 2a by X-ray analysis.

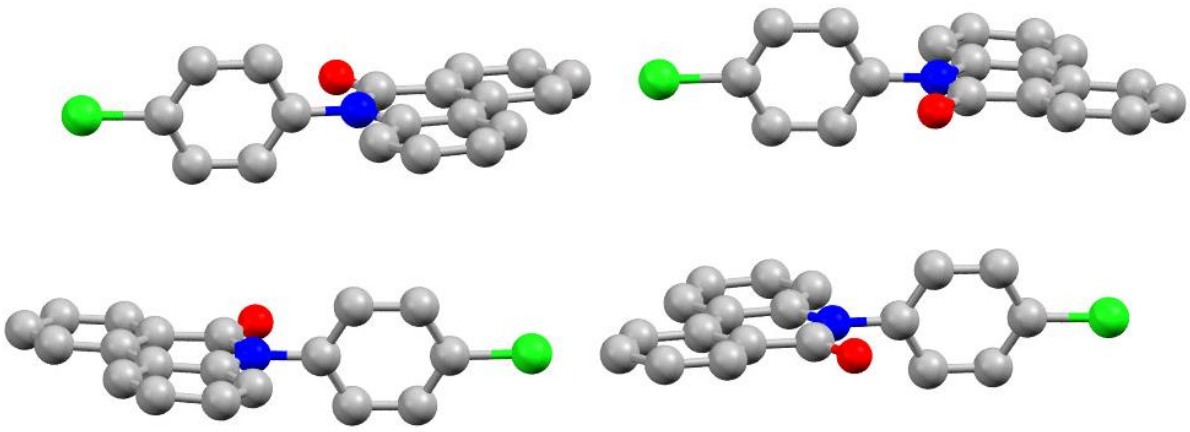

Figure 3: Packing of 2a in the solid state.

Cyclovoltammetric data

The individual oxidation potentials reveal that over-oxidation is possible, depending on the substrate-product pair. In the following some examples are provided:

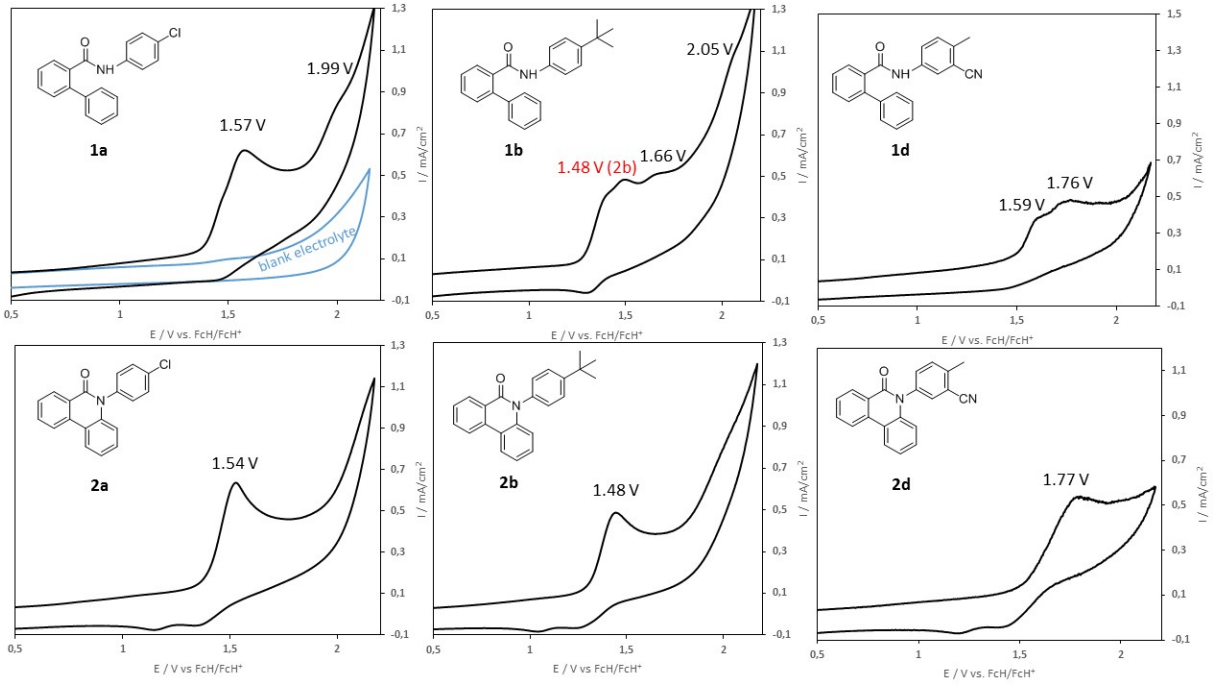

Figure 4: Cyclic voltammogramms of 6 selected examples in HFIP; 1 mM compound, 0.1 M NBu_4PF_6 in 5 mL HFIP, scan rate: 200 mV/s, working electrode: GC, counter electrode: GC, reference electrode: Ag/AgCl in sat. LiCl/EtOH, referenced vs. FcH/FcH^+.

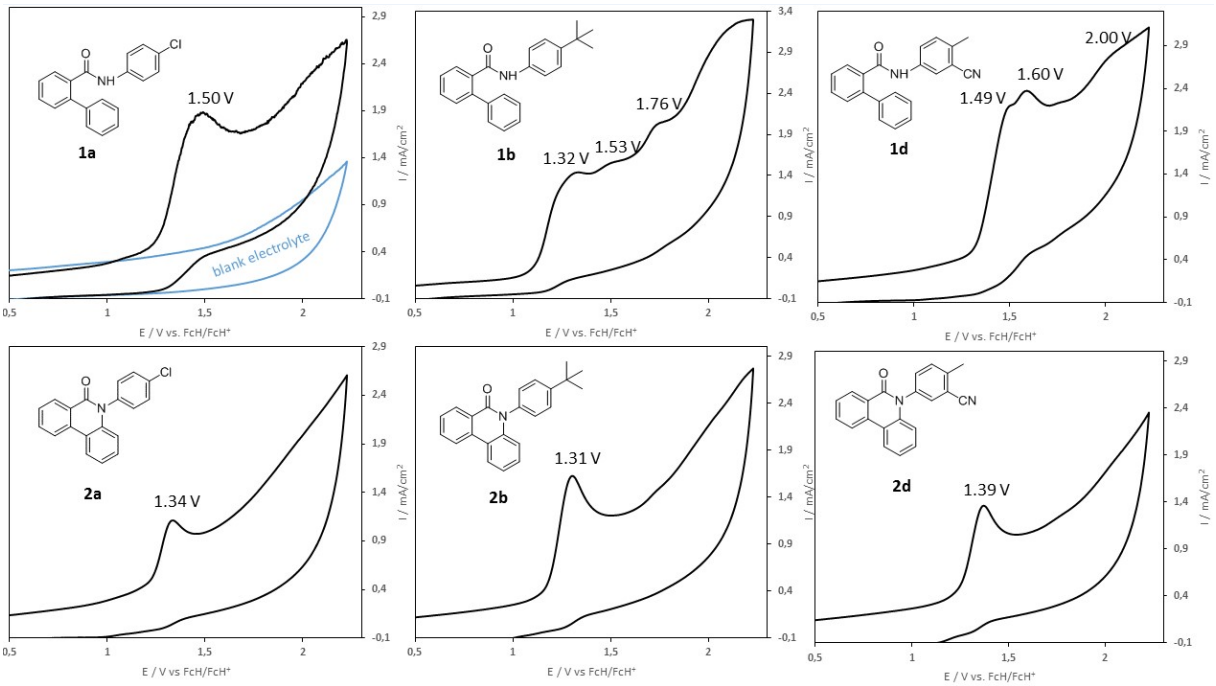

Figure 5: Cyclic voltammogramms of 6 selected examples in MeCN; 1 mM compound, 0.1 M NBu_4PF_6 in 5 mL MeCN, scan rate: 200 mV/s, working electrode: GC, counter electrode: GC, reference electrode: $Ag/AgNO_3$ (0.01 M) in 0.2 M NEt_4BF_4/MeCN, referenced vs. FcH/FcH^+.

NMR spectra

N-(4-Chlorophenyl)-biphenyl-2-carboxamide (1a)

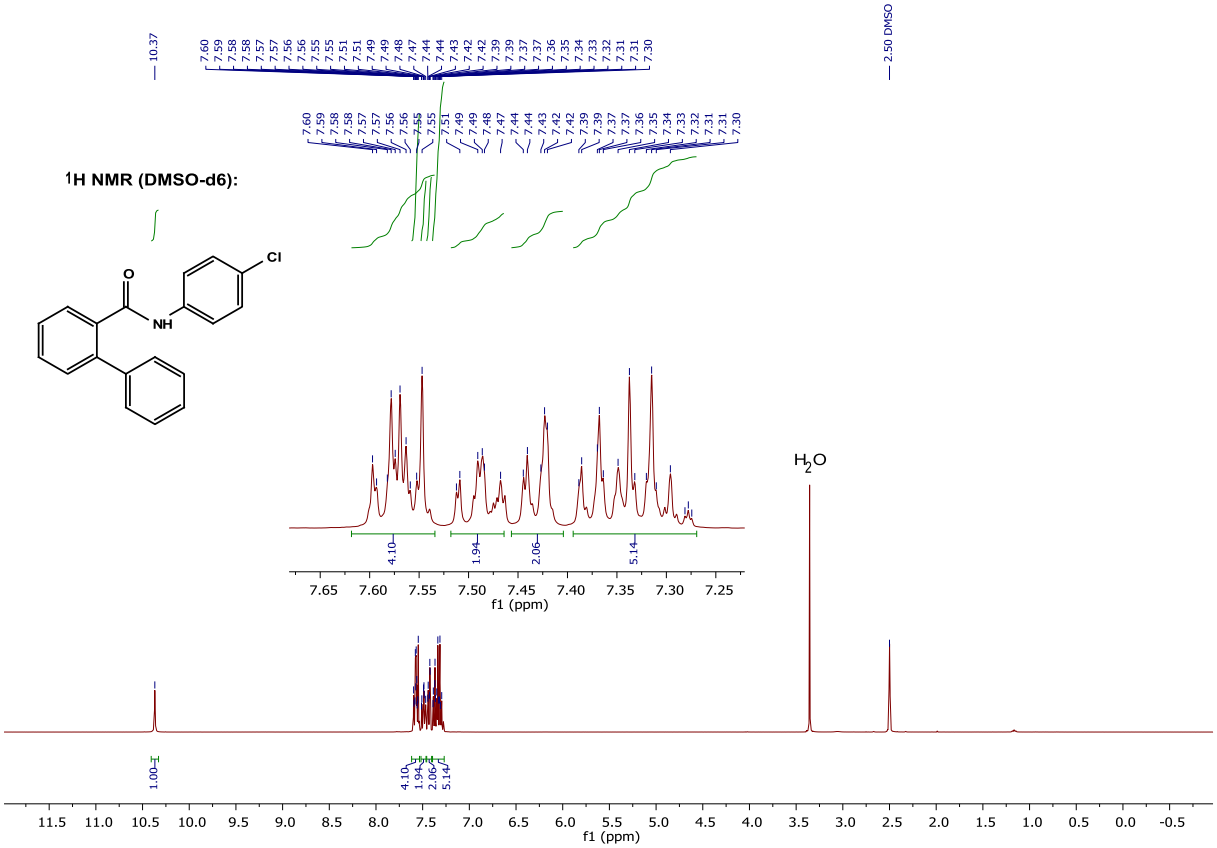

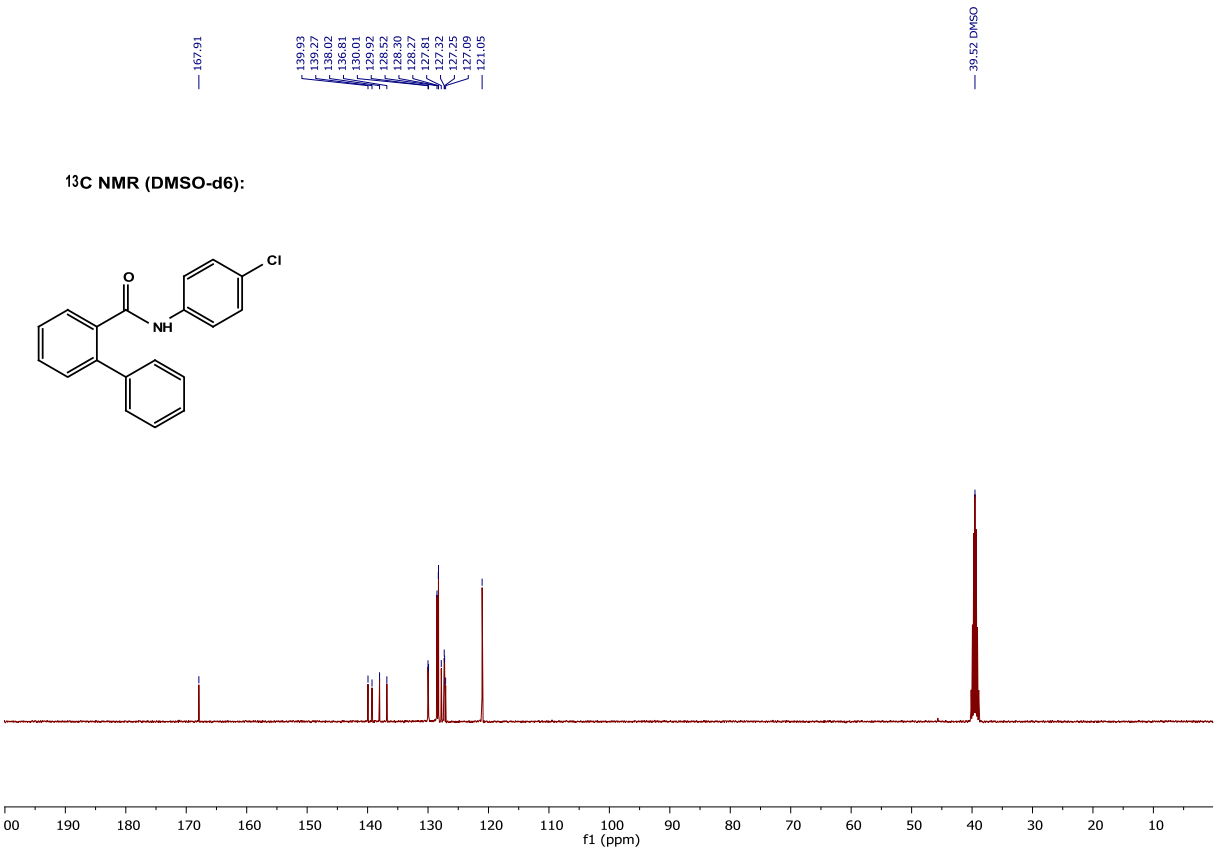

N-(4-*tert*-Butylphenyl)-biphenyl-2-carboxamide (1b)

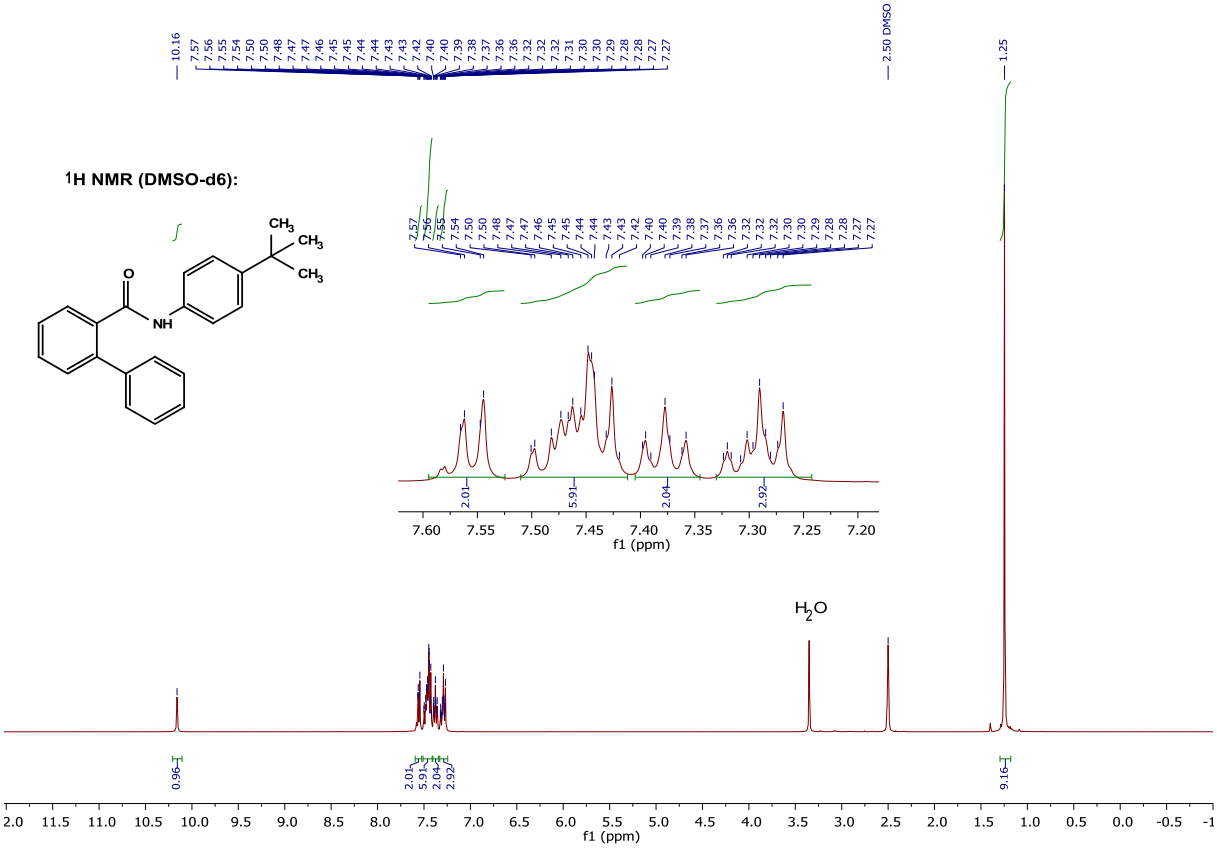

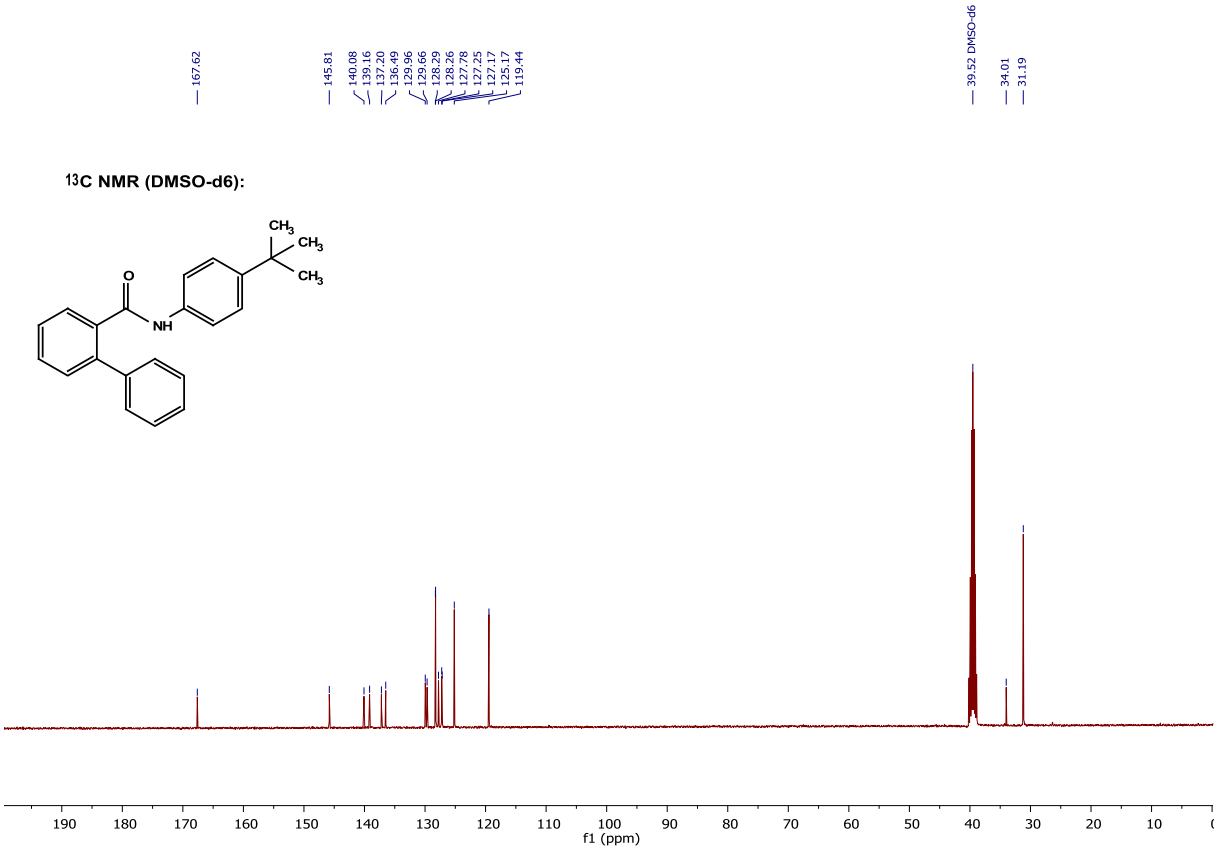

N-(2,4-Difluorophenyl)-biphenyl-2-carboxamide (1c)

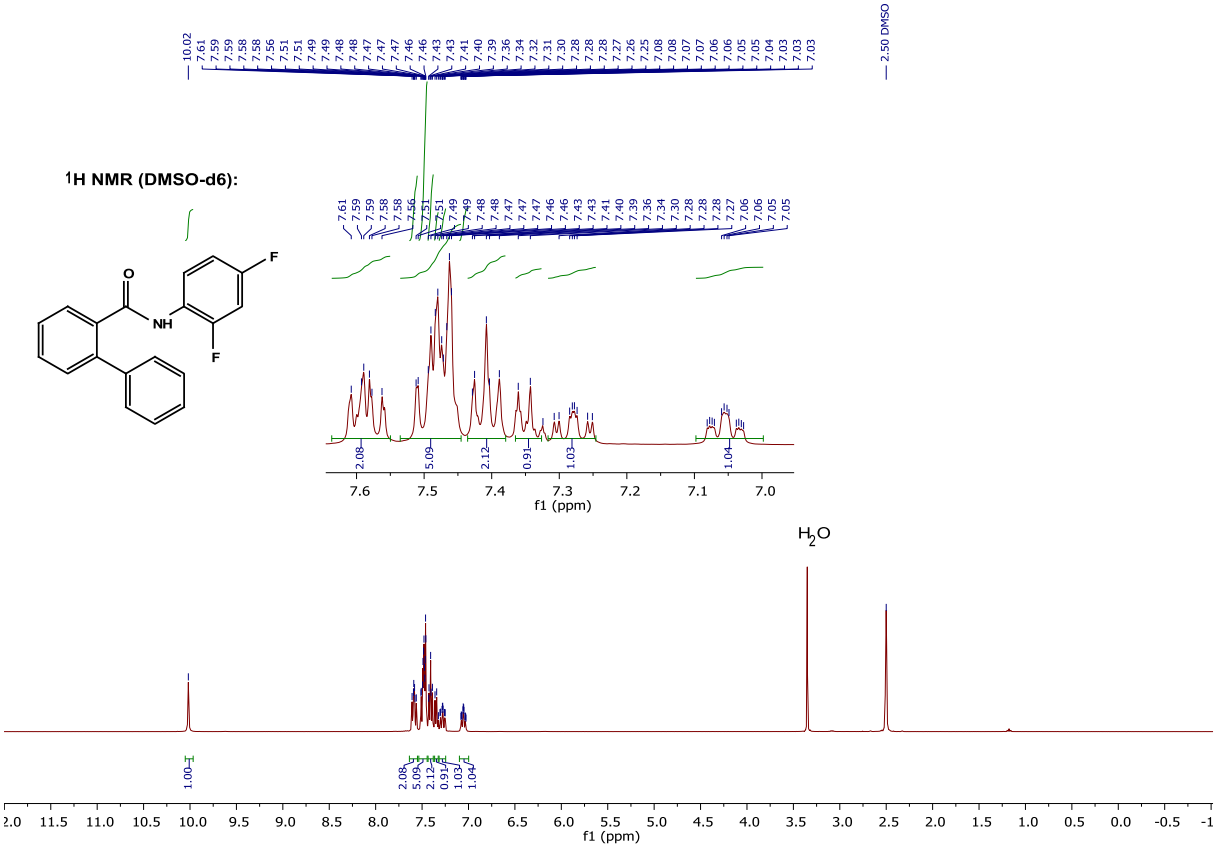

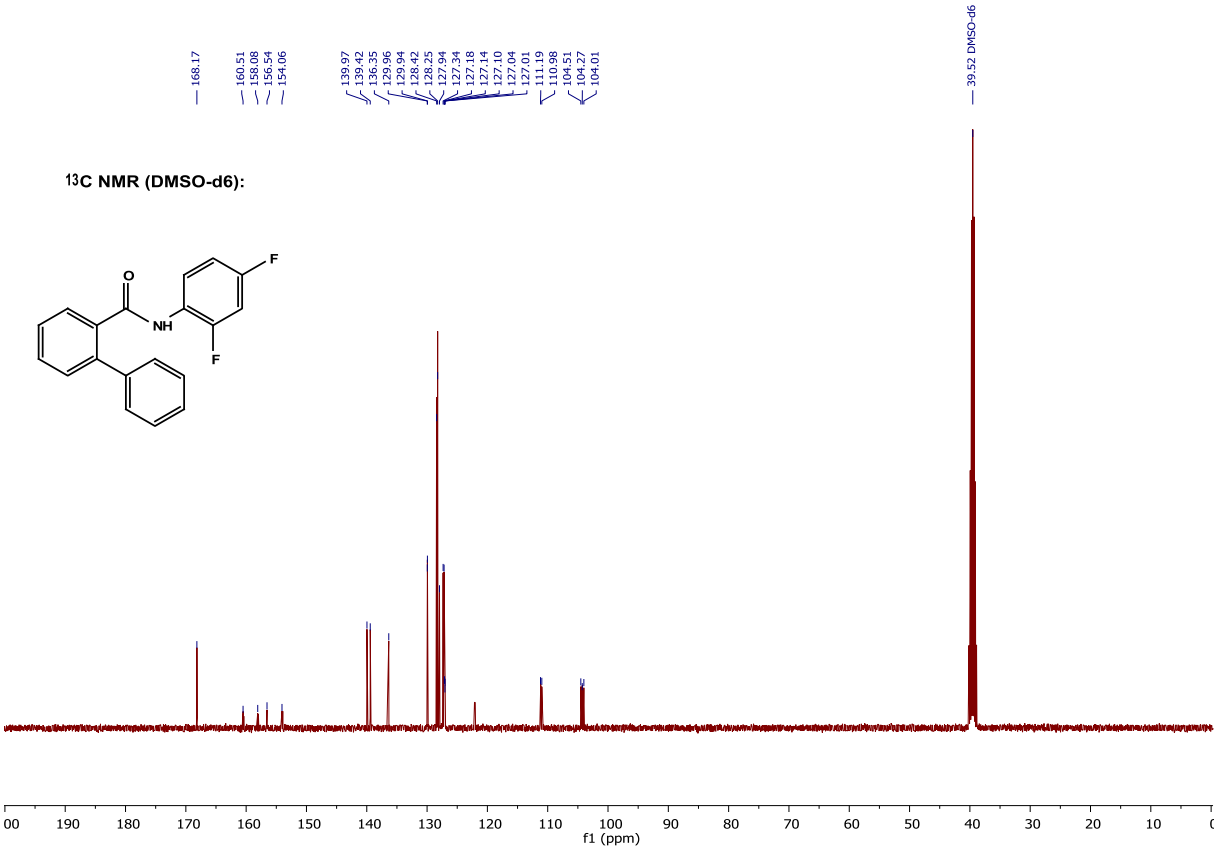

^{19}F NMR (DMSO-d6):

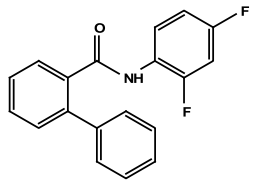

N-(3-Cyano-4-methylphenyl)-biphenyl-2-carboxamide (1d)

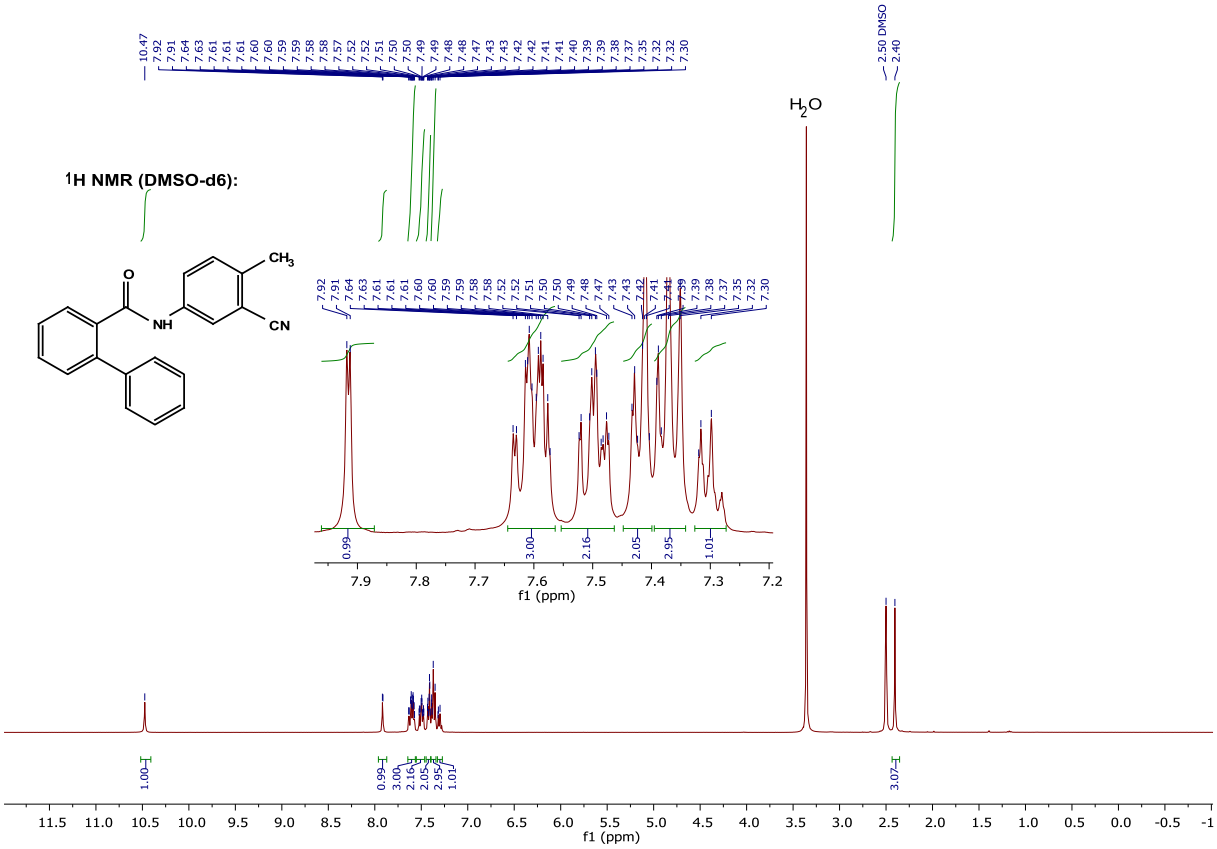

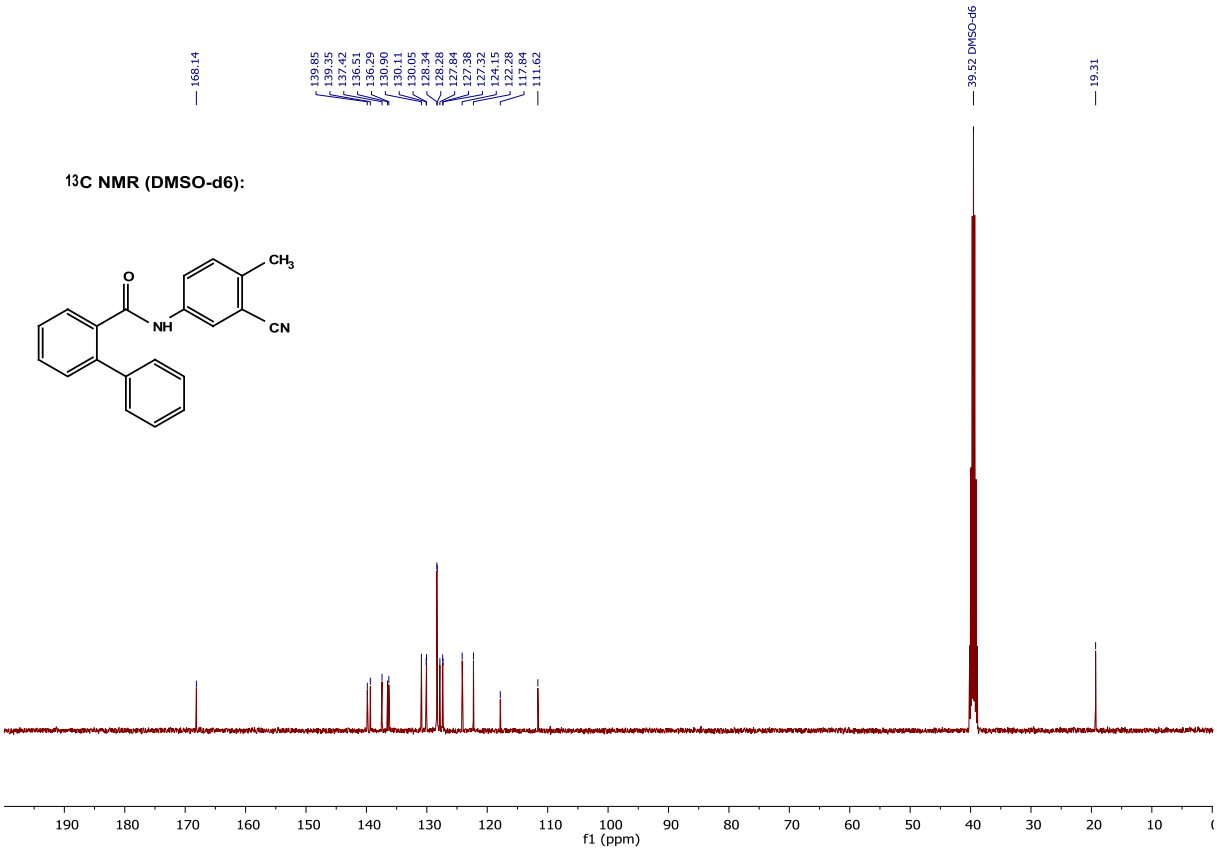

N-(3-Bromophenyl)-biphenyl-2-carboxamide (1e)

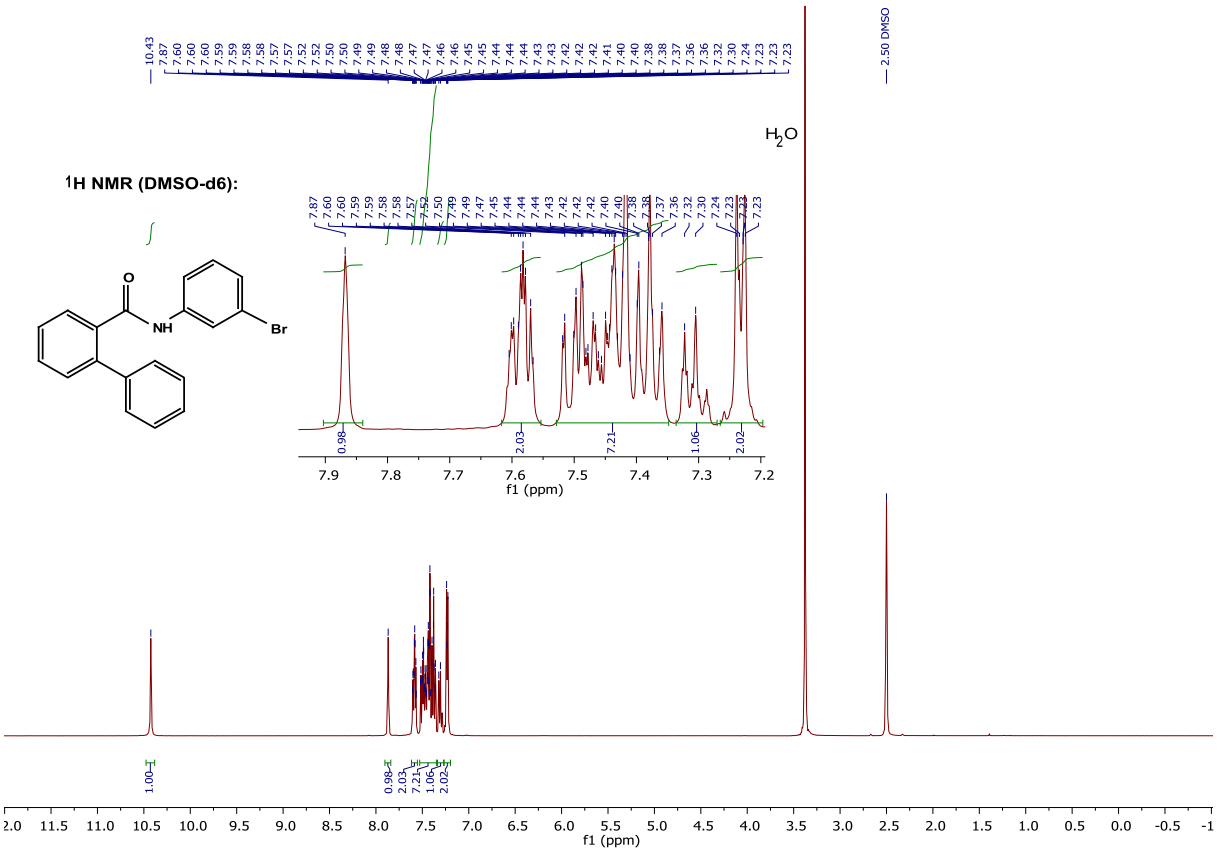

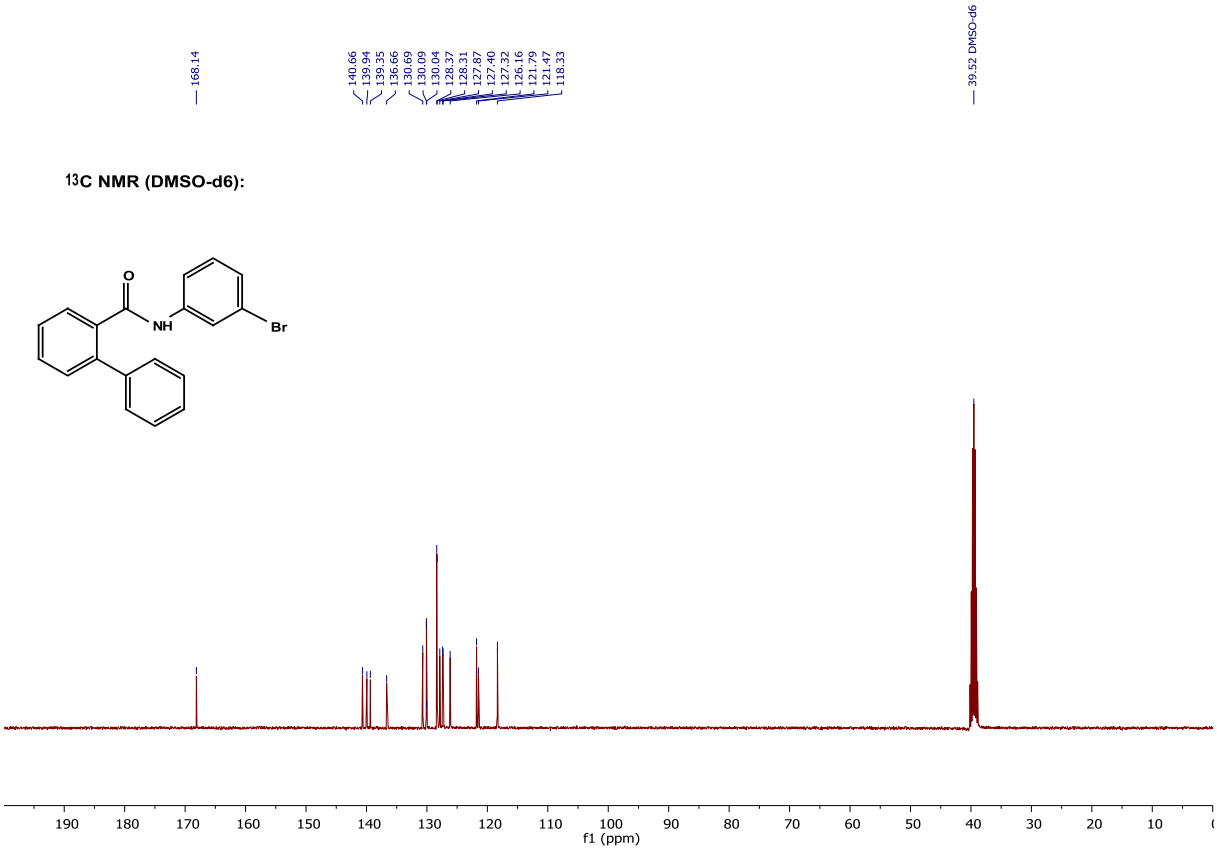

N-(2-Iodophenyl)-biphenyl-2-carboxamide (1f)

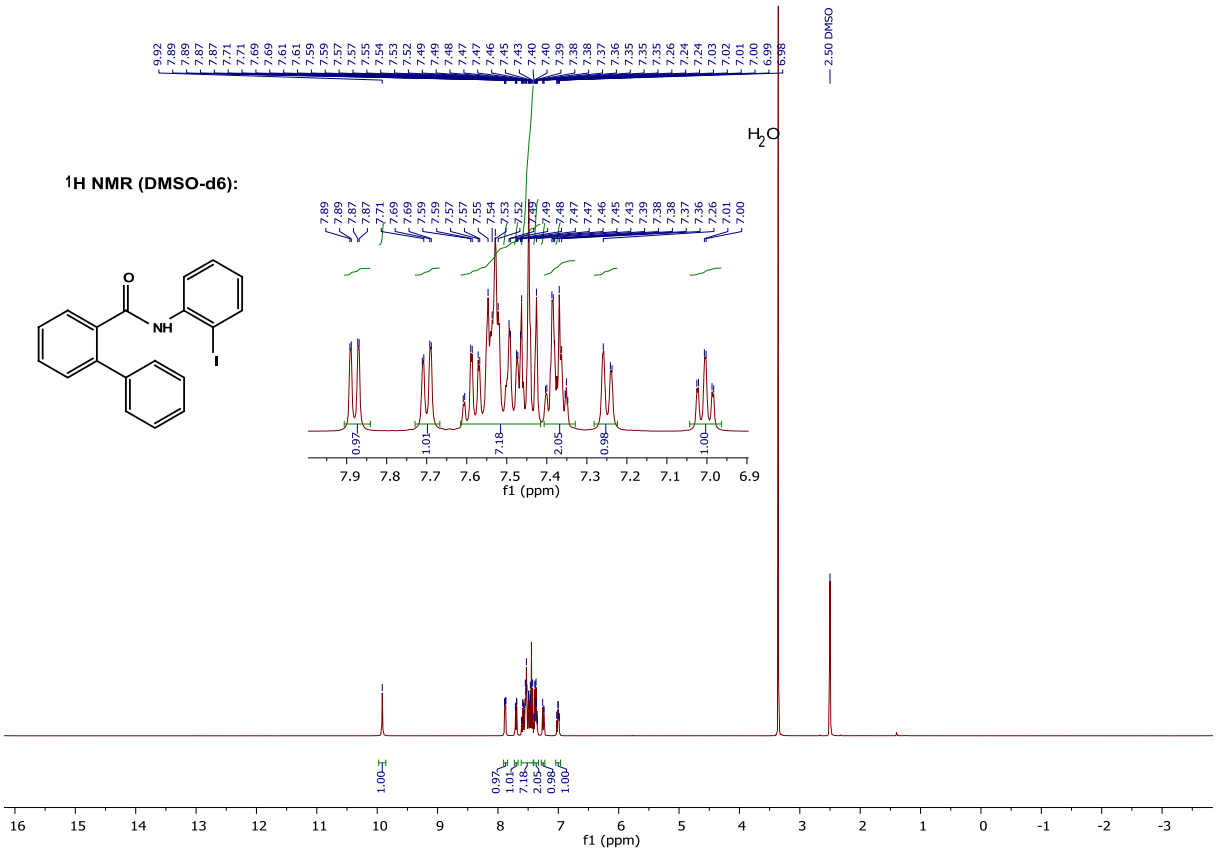

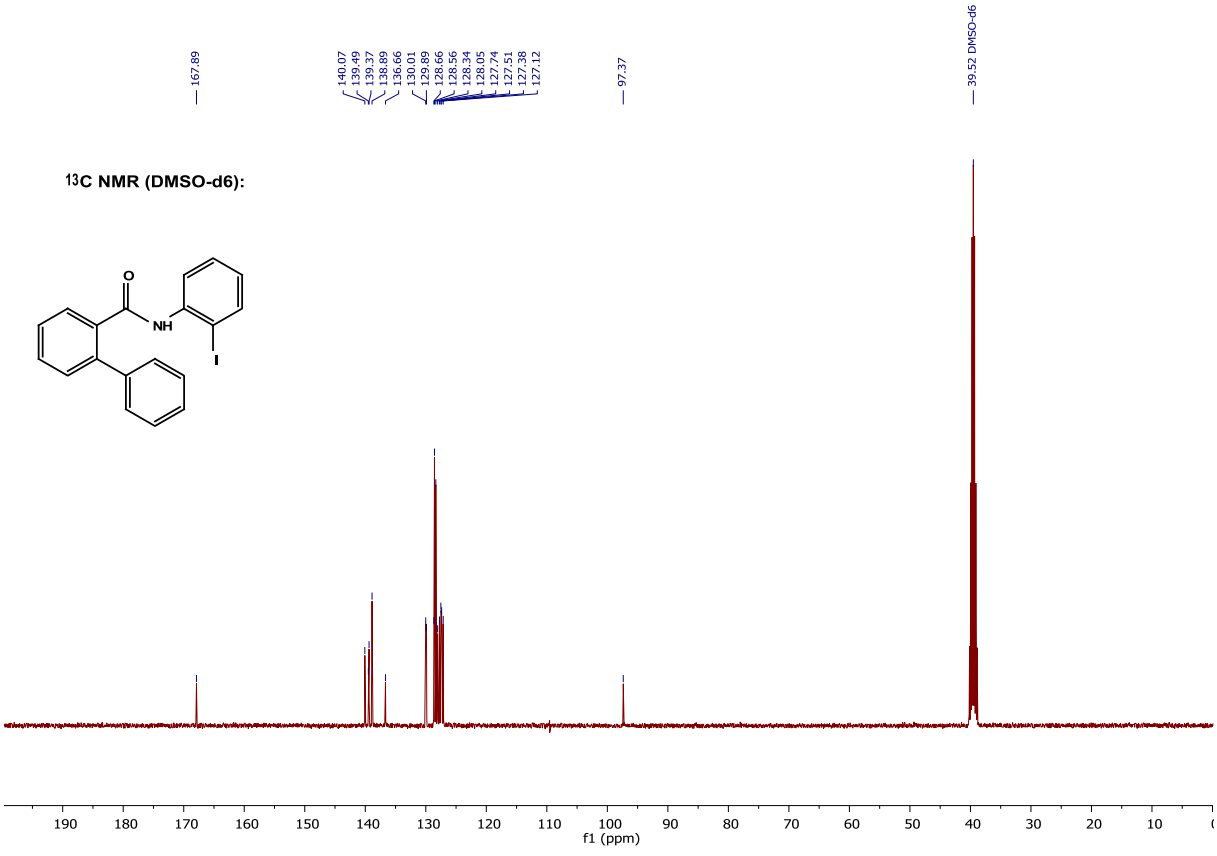

N-Phenyl-biphenyl-2-carboxamide (1g)

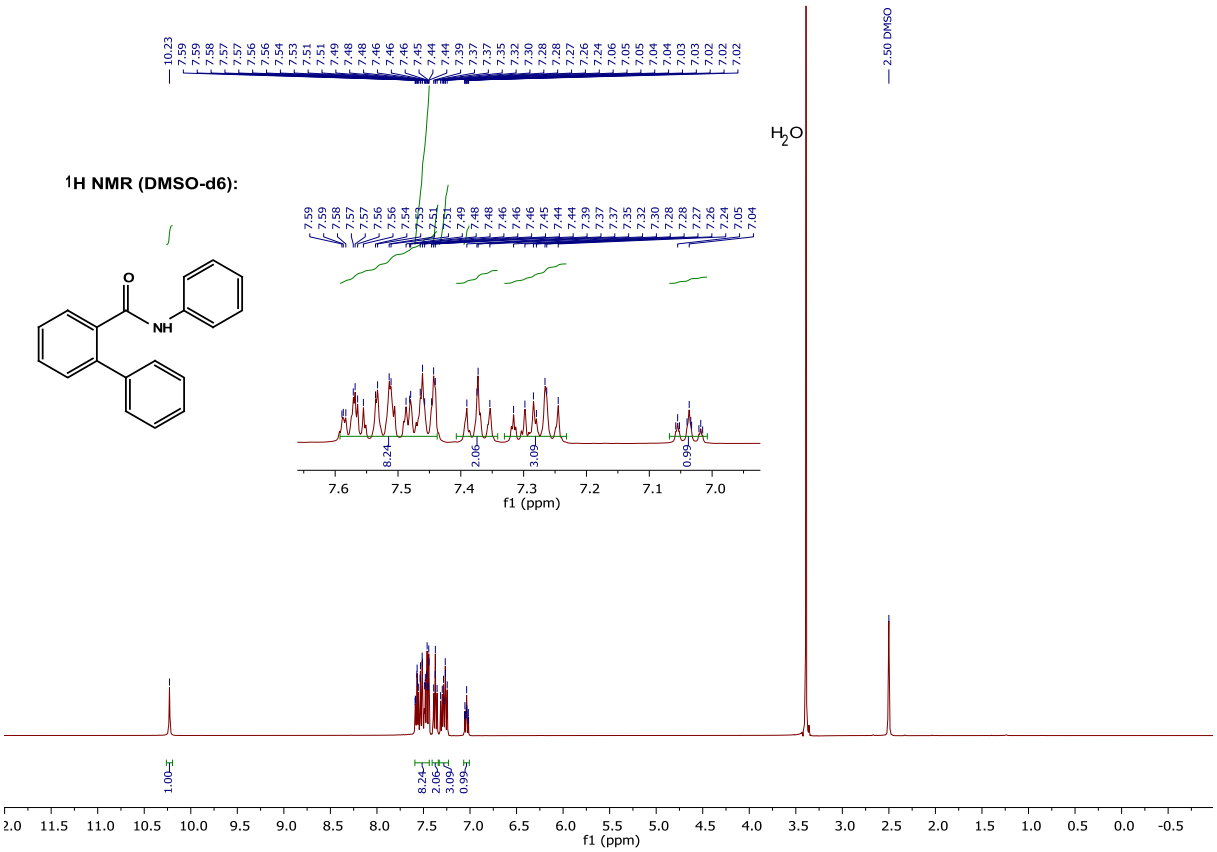

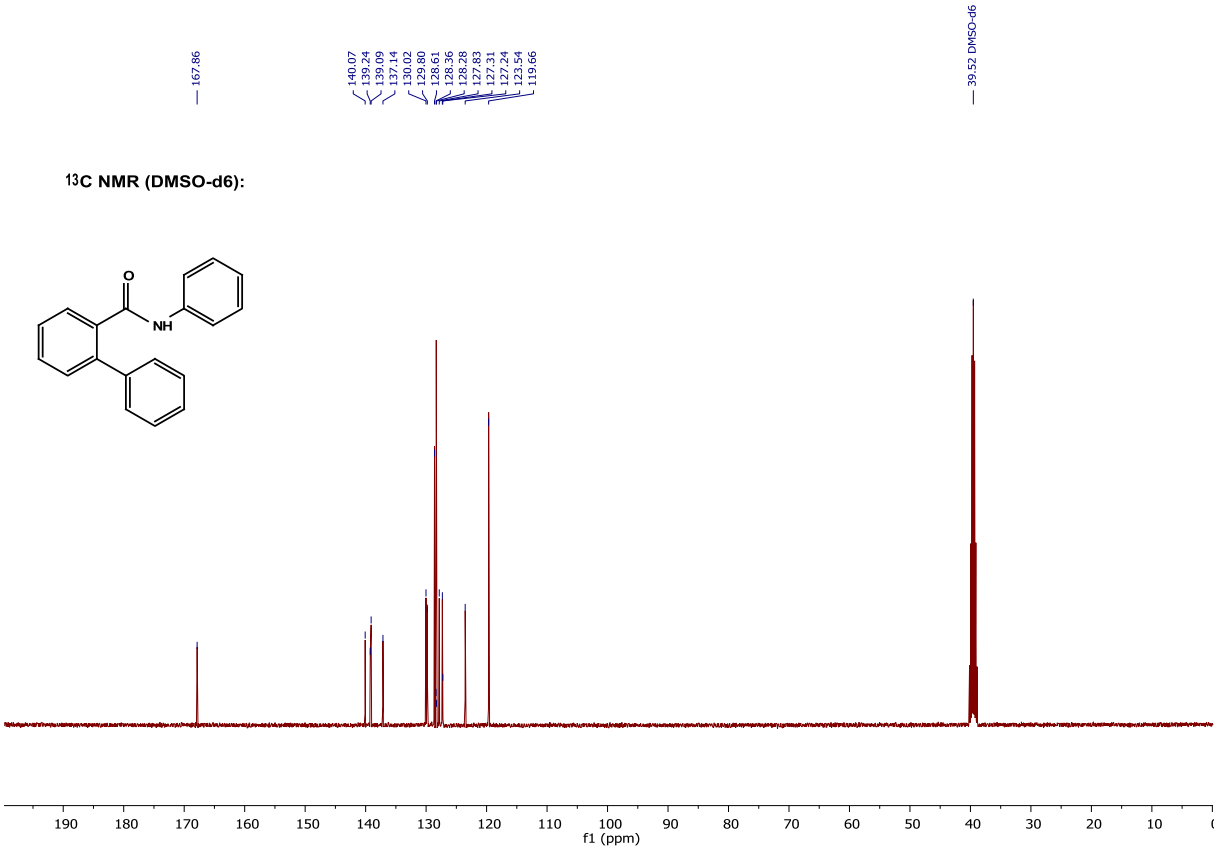

N-(2-Acetylphenyl)-biphenyl-2-carboxamide (1h)

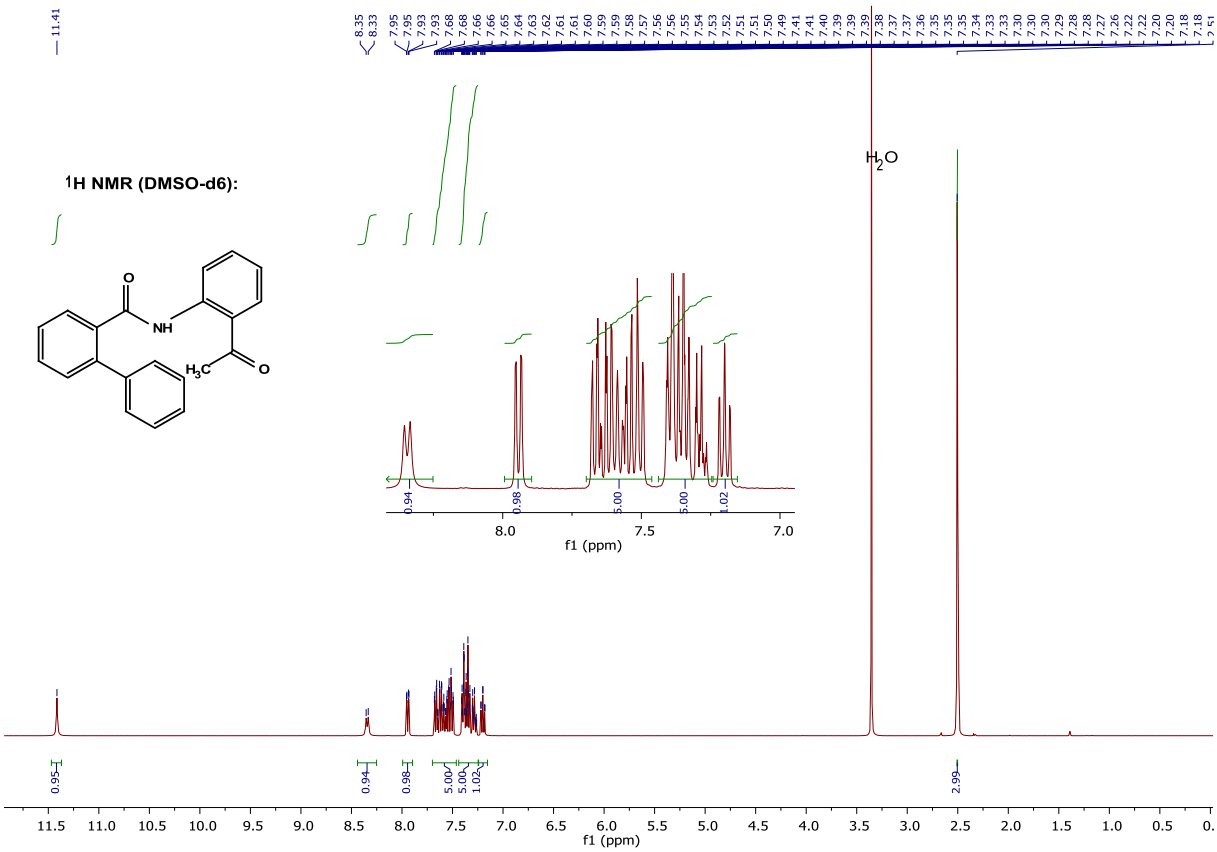

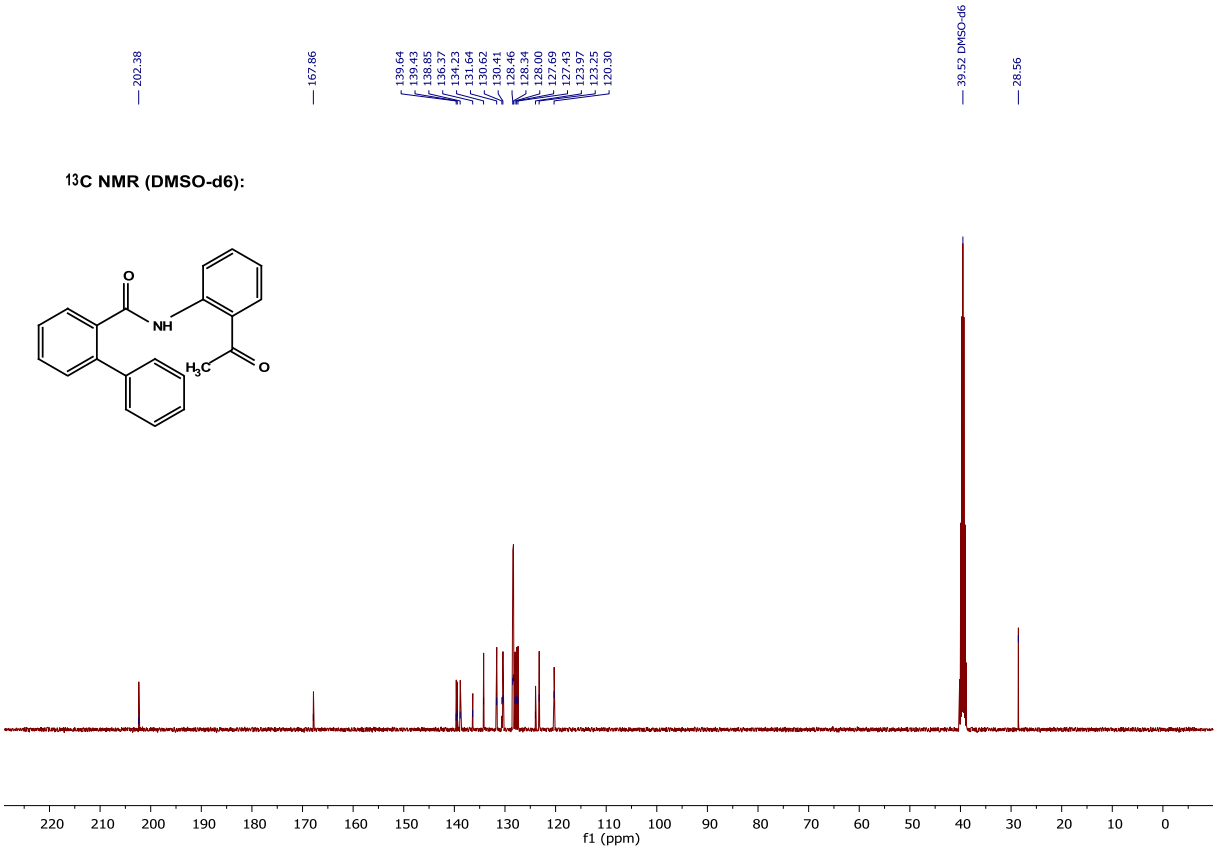

Ethyl 2-((1,1’-biphenyl)-2-ylcarboxamido)benzoate (1i)

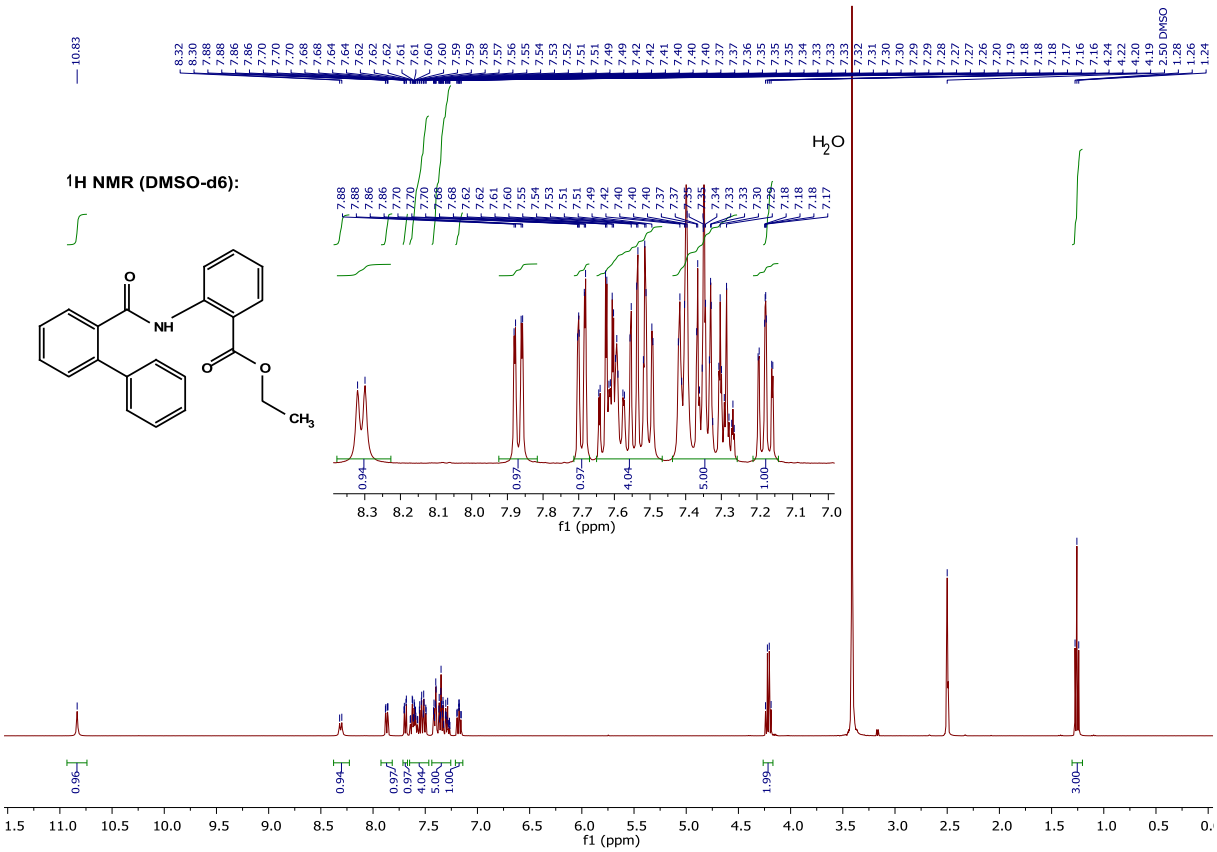

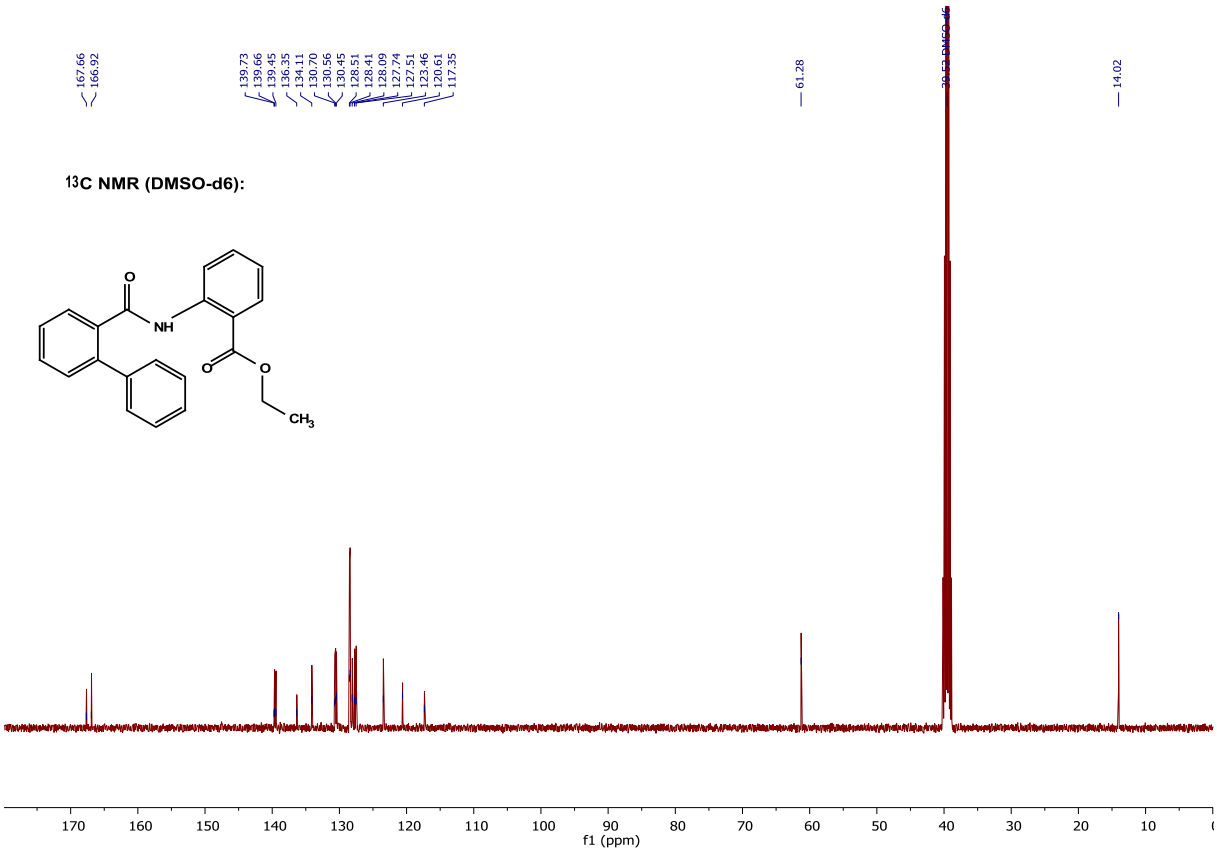

N-(3-Nitrophenyl)-biphenyl-2-carboxamide (1j)

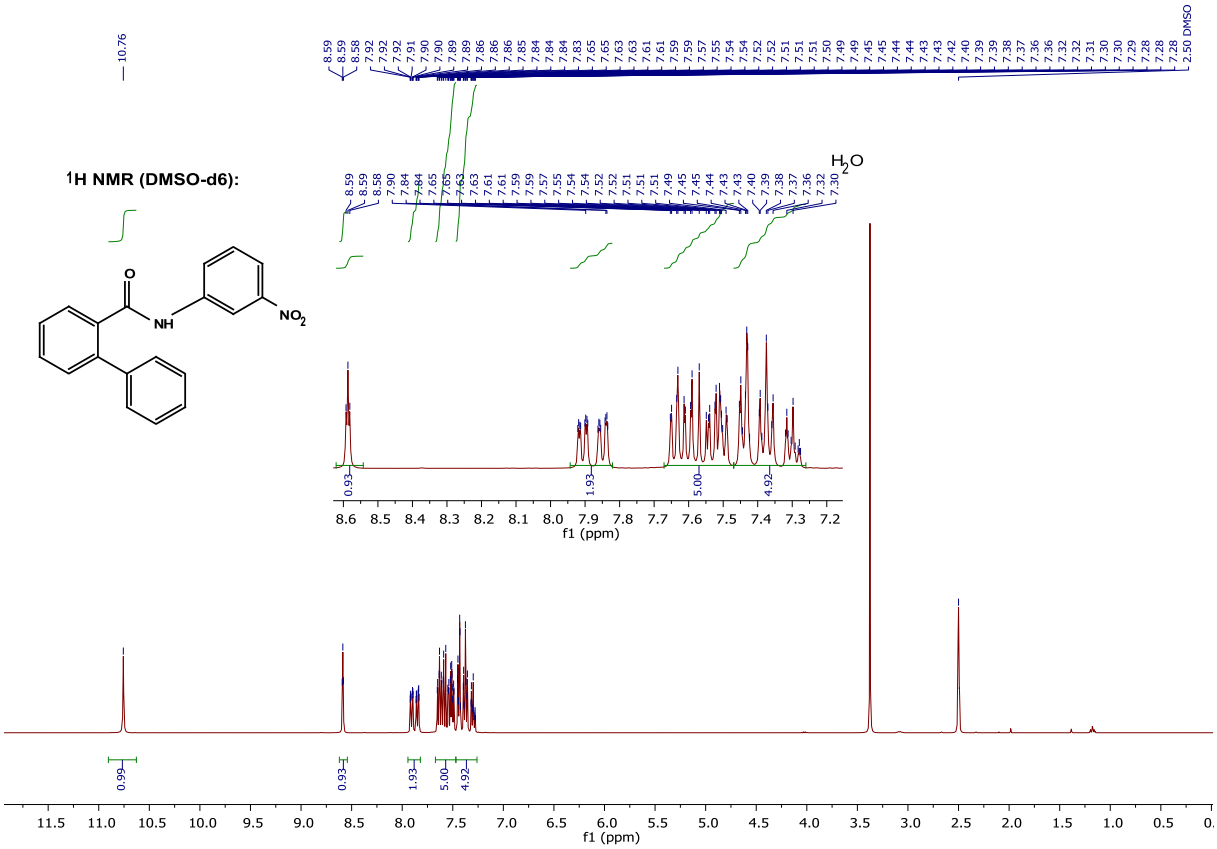

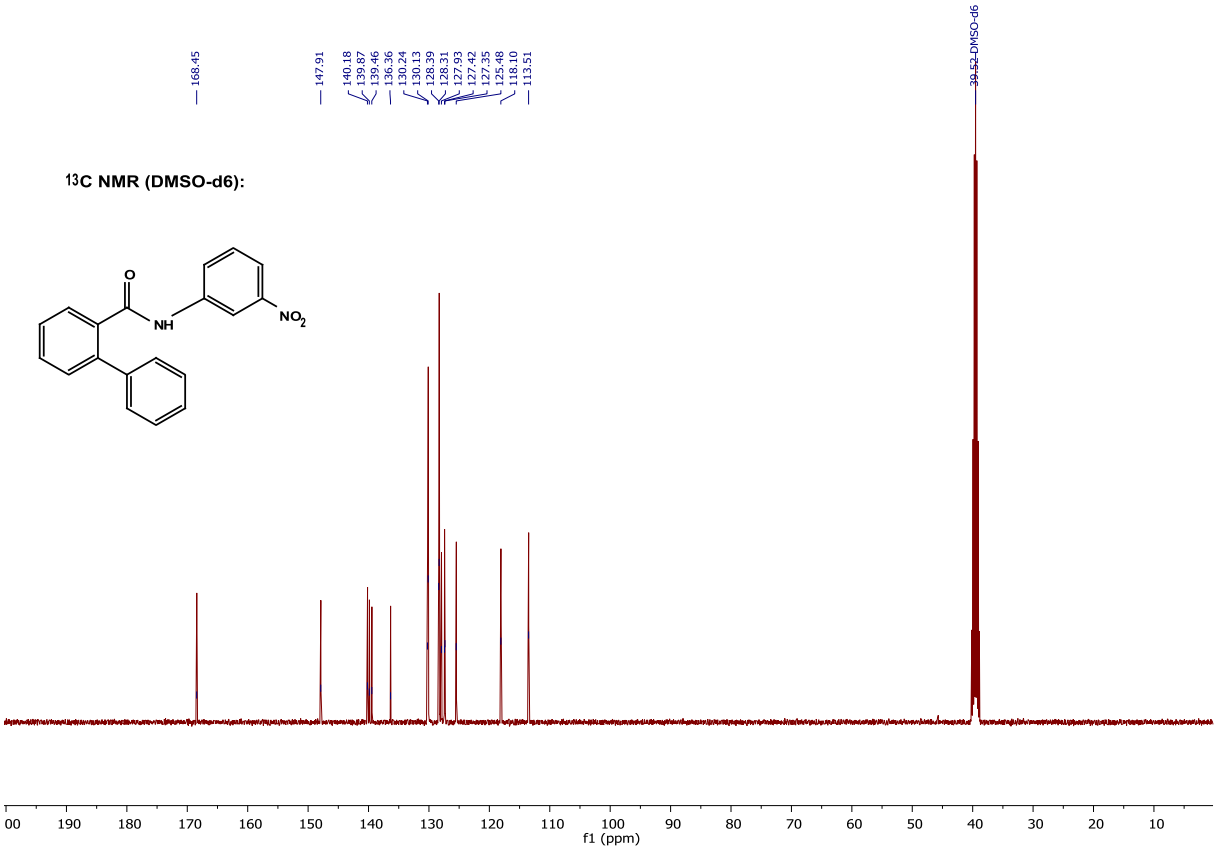

N-(4-Chlorophenyl)-4’-trifluoromethylbiphenyl-2-carboxamide (1k)

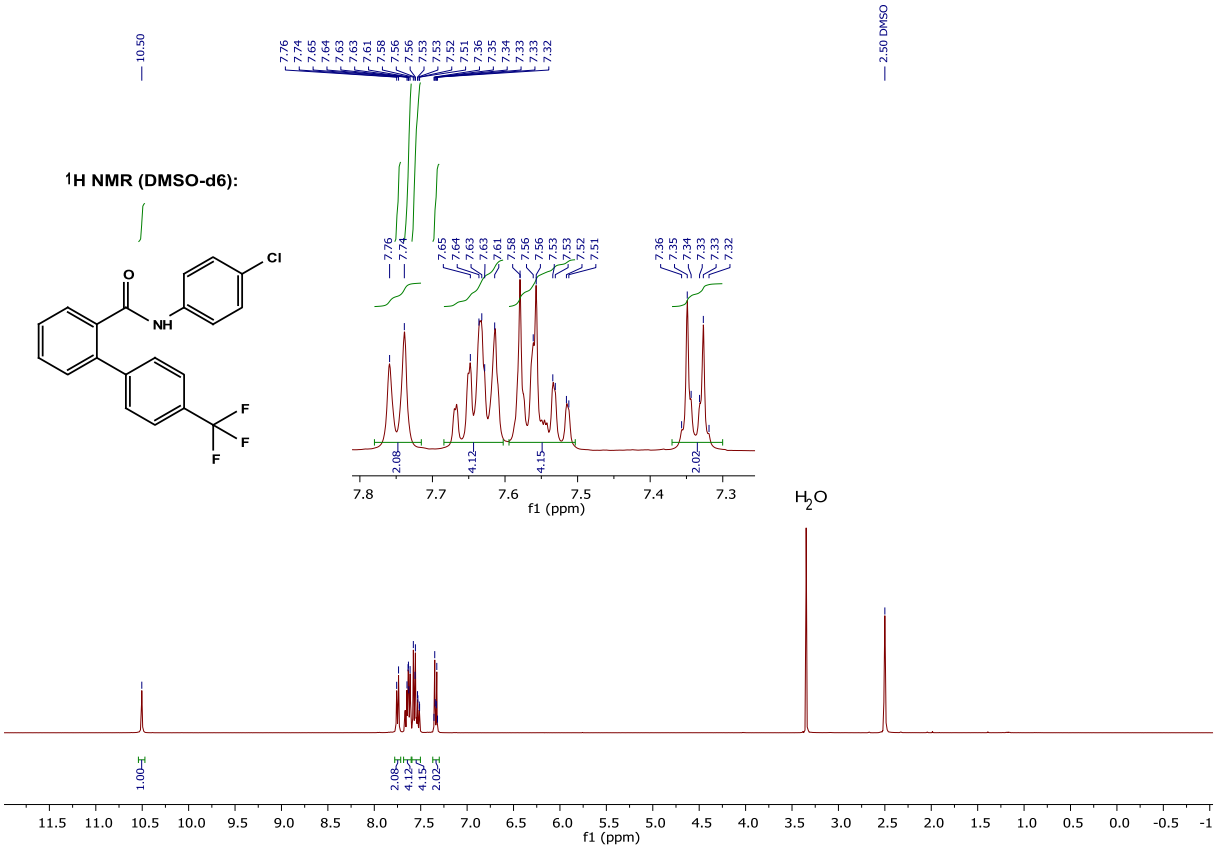

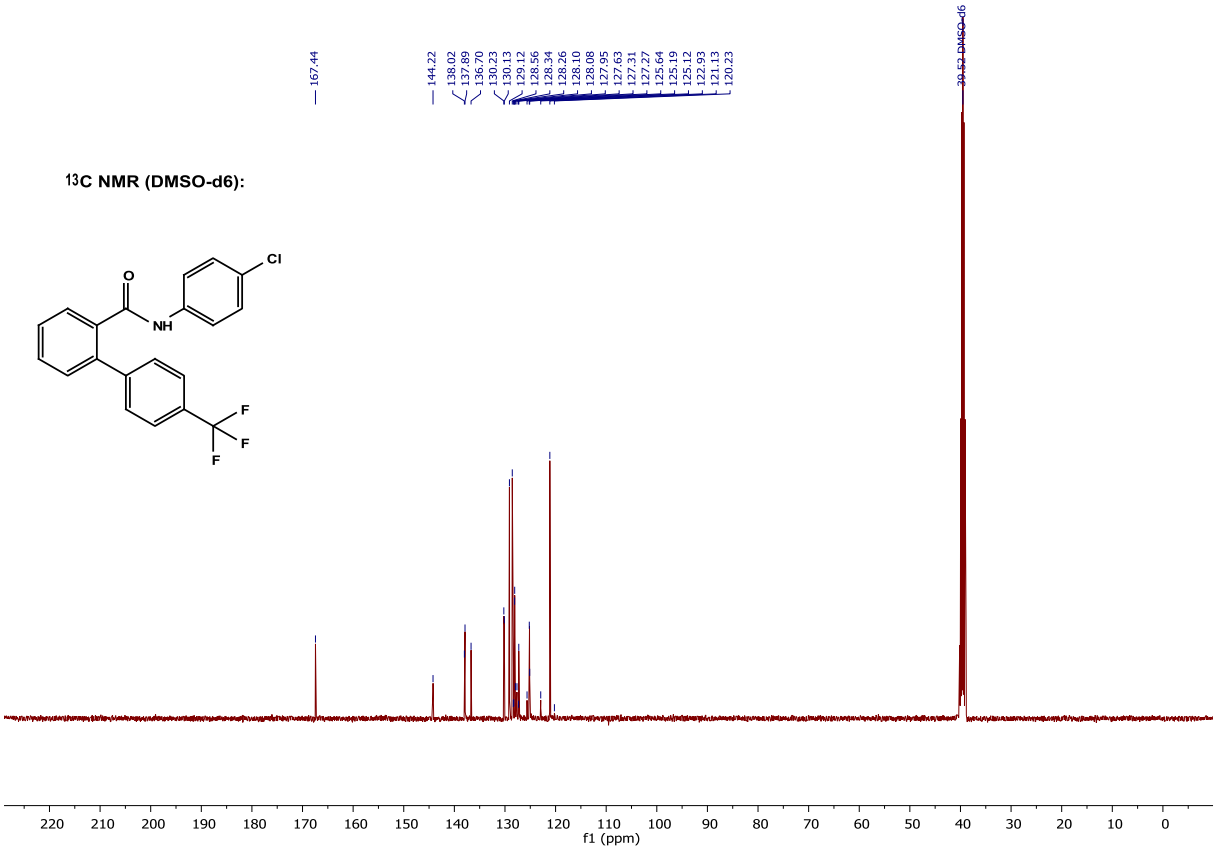

^{19}F NMR (DMSO-d6):

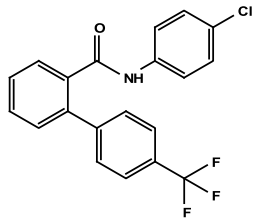

N-(4-Chlorophenyl)-4’-chlorobiphenyl-2-carboxamide (1l)

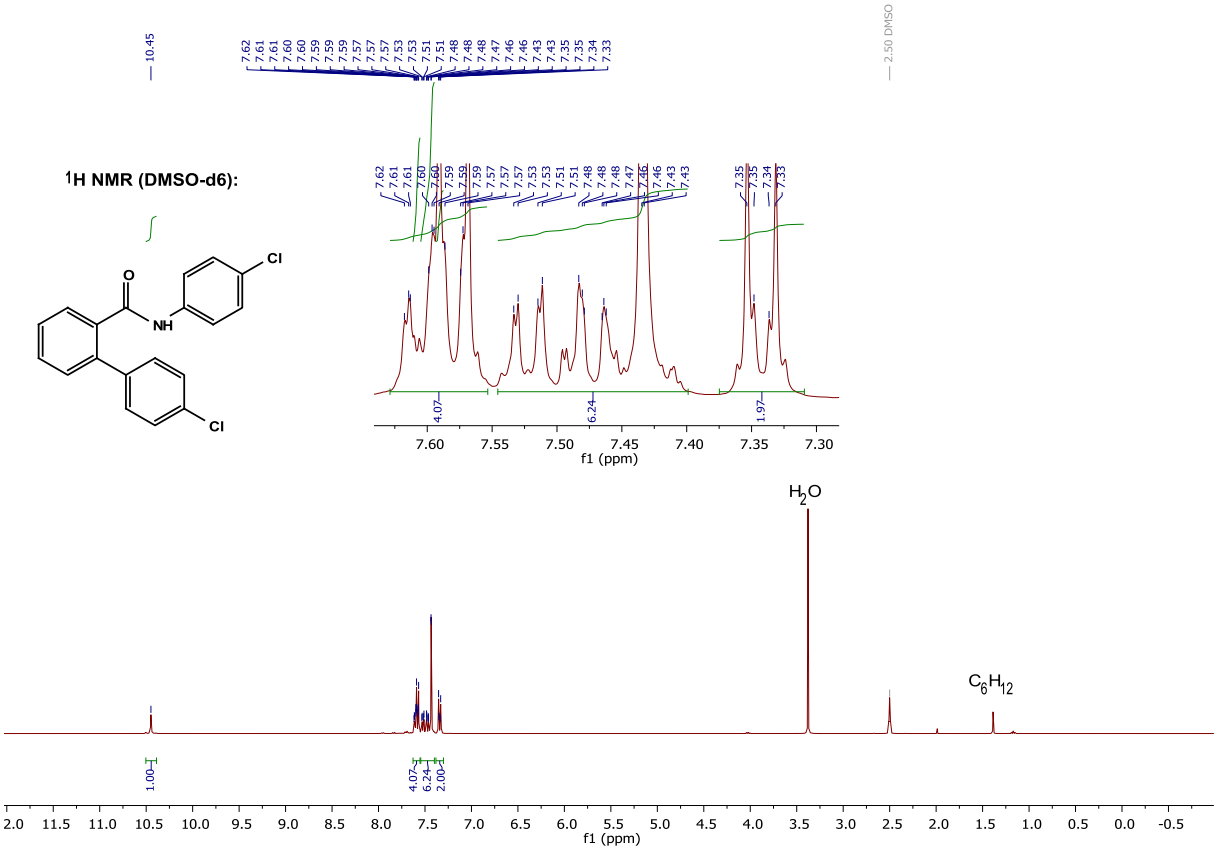

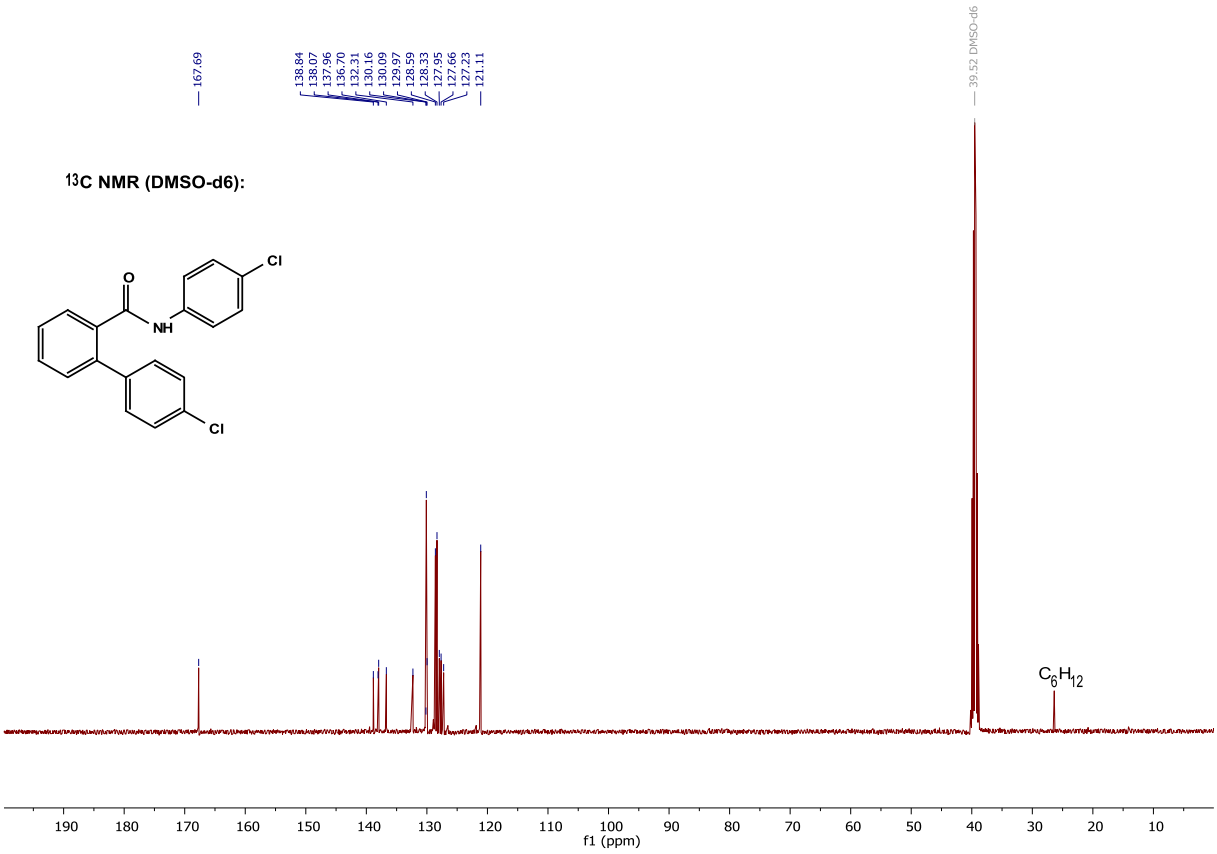

4’-*tert*-Butyl-*N*-(4-chlorophenyl)-biphenyl-2-carboxamide (1m)

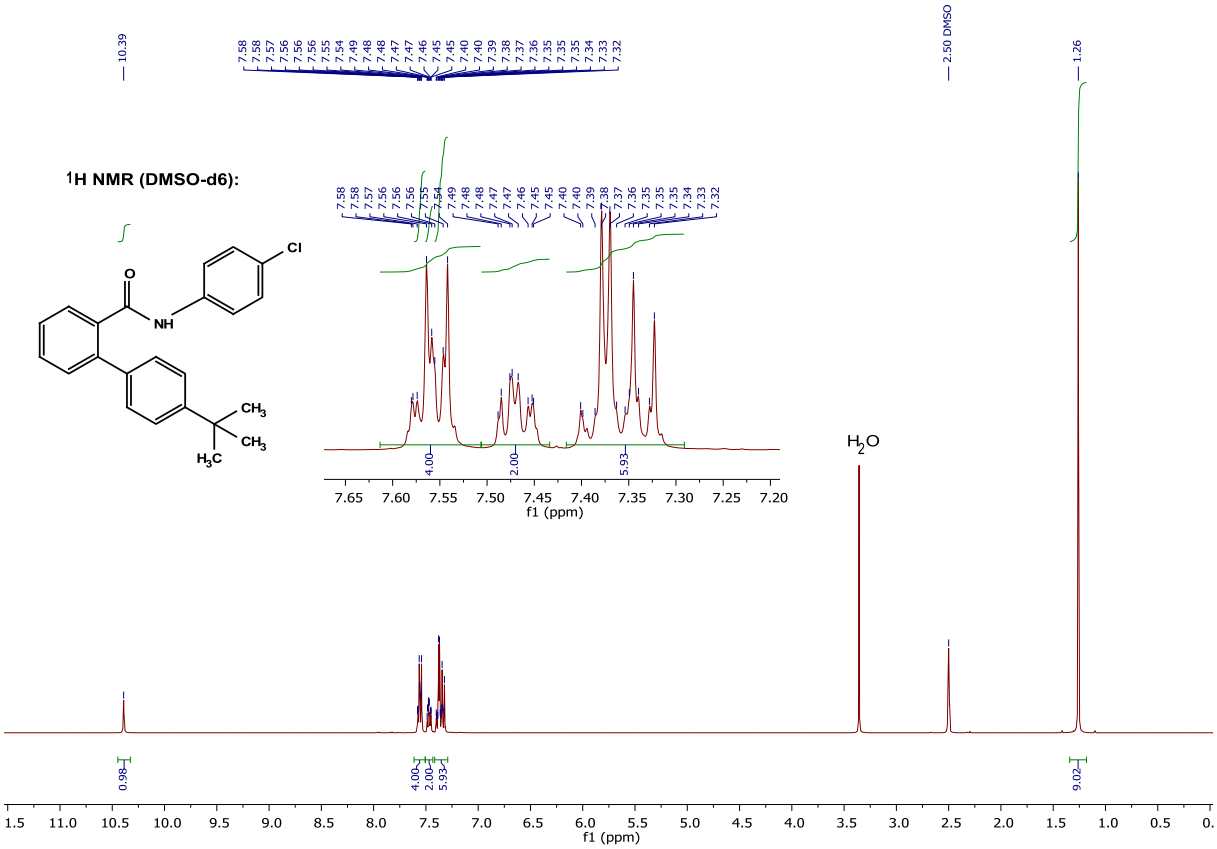

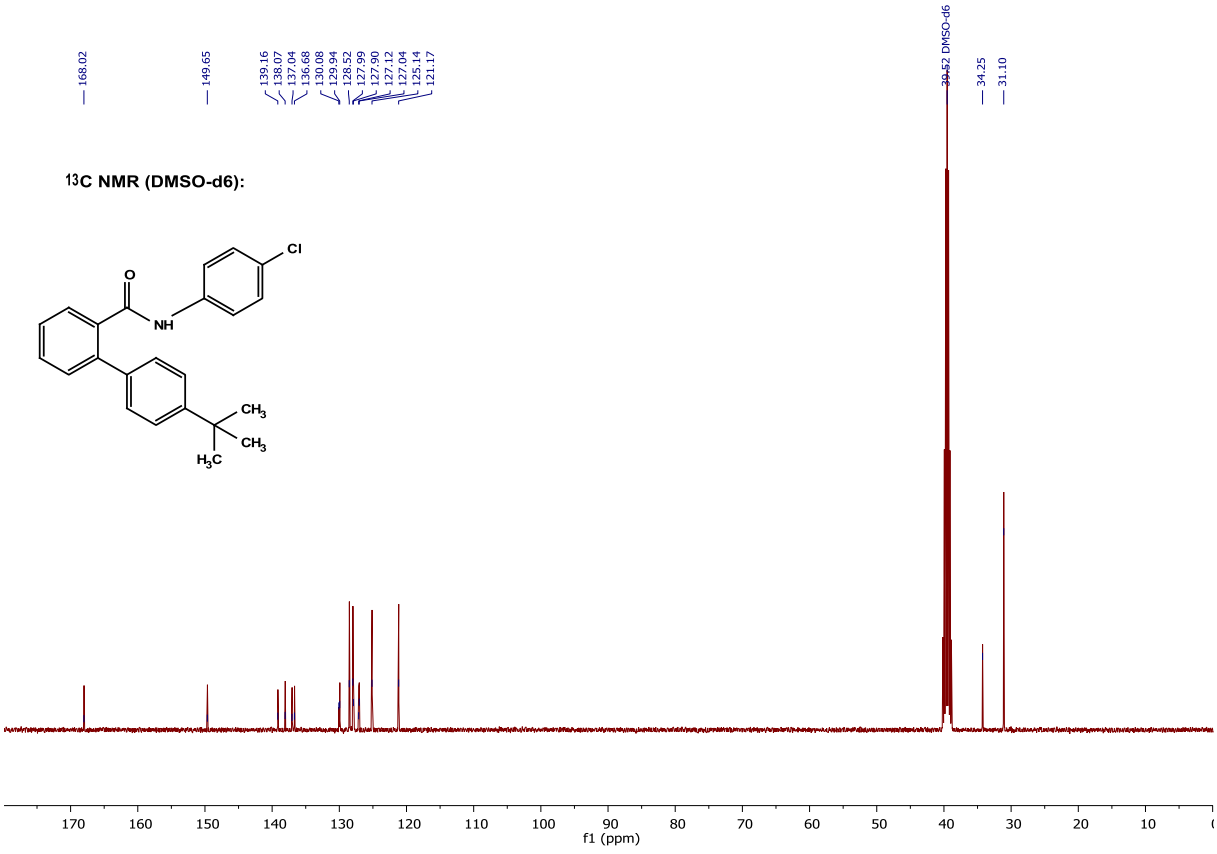

N-(4-Chlorophenyl)-phenanthredin-6-one (2a)

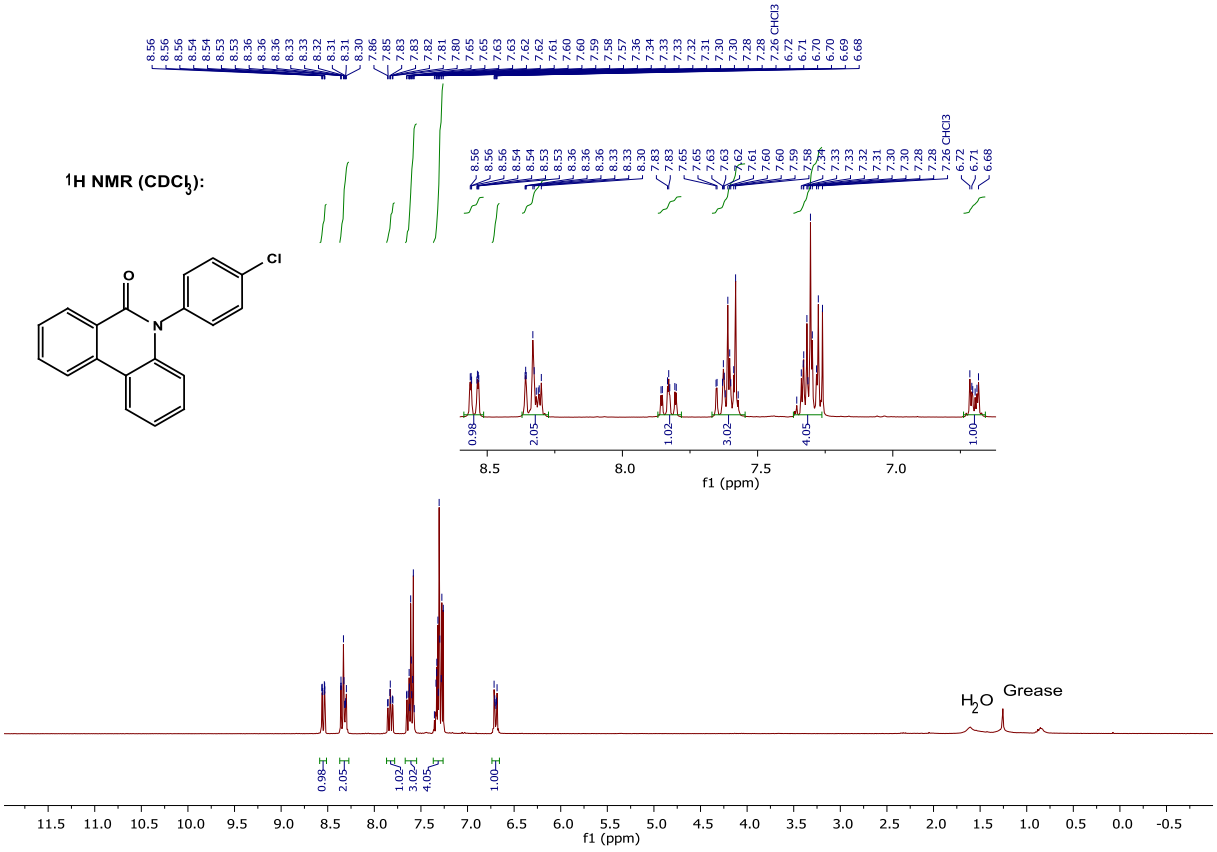

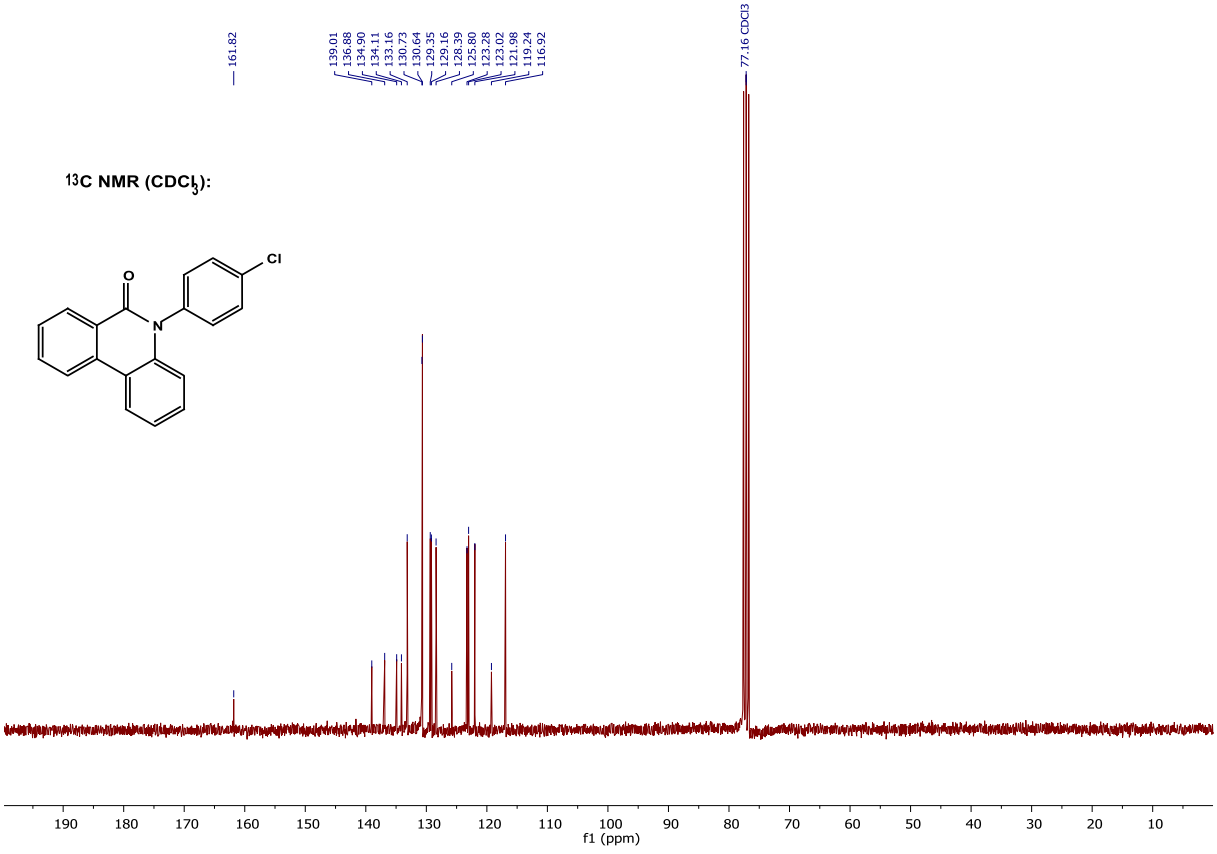

N-(4-*tert*-Butylphenyl)-phenanthredin-6-one (2b)

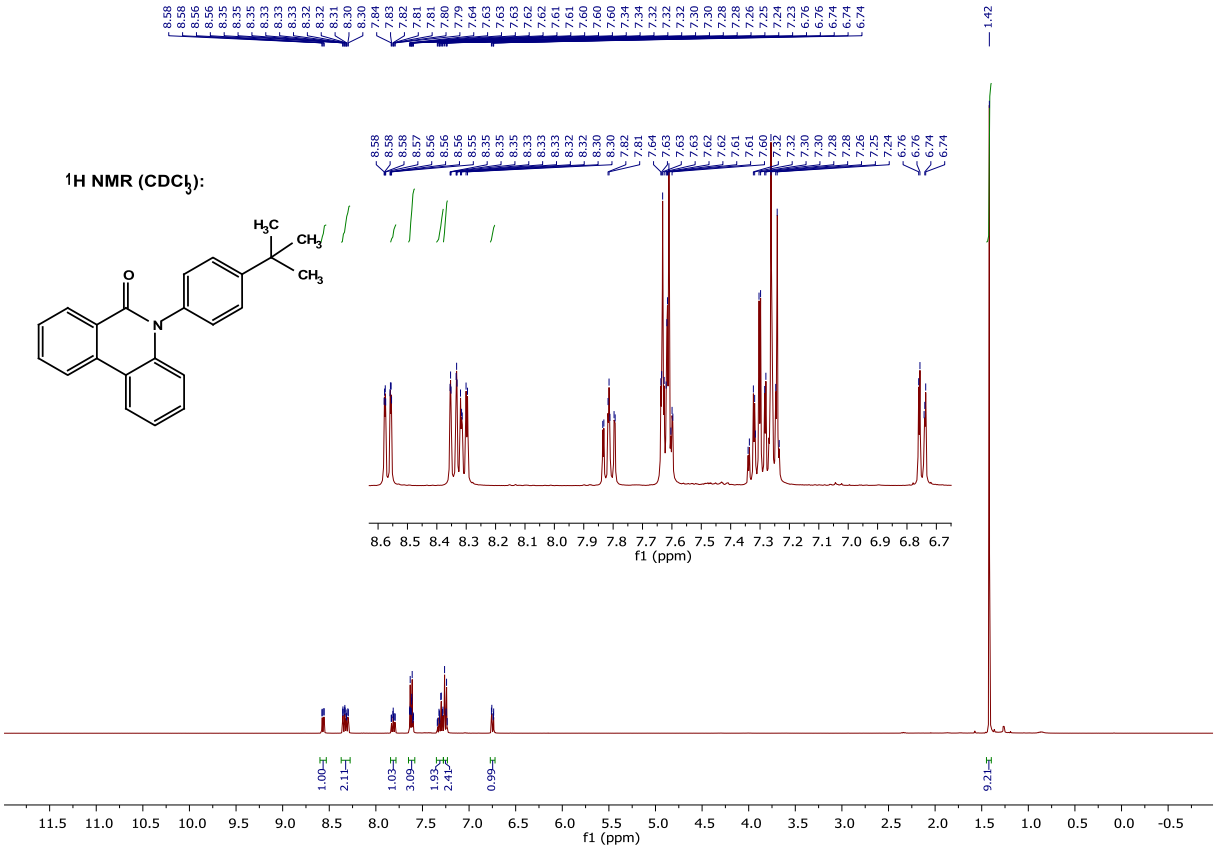

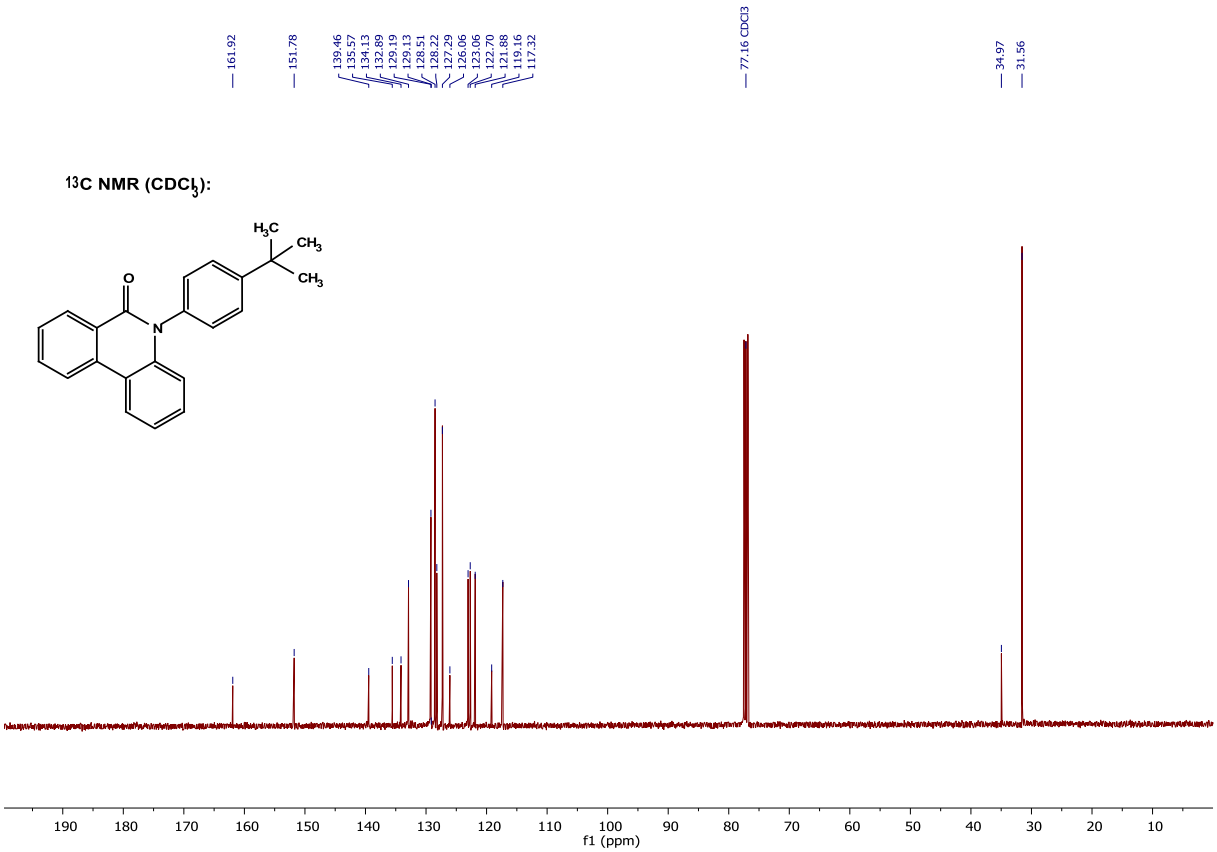

N-(2,4-Difluorophenyl)-phenanthredin-6-one (2c)

^{1}H NMR ($CDCl_3$):

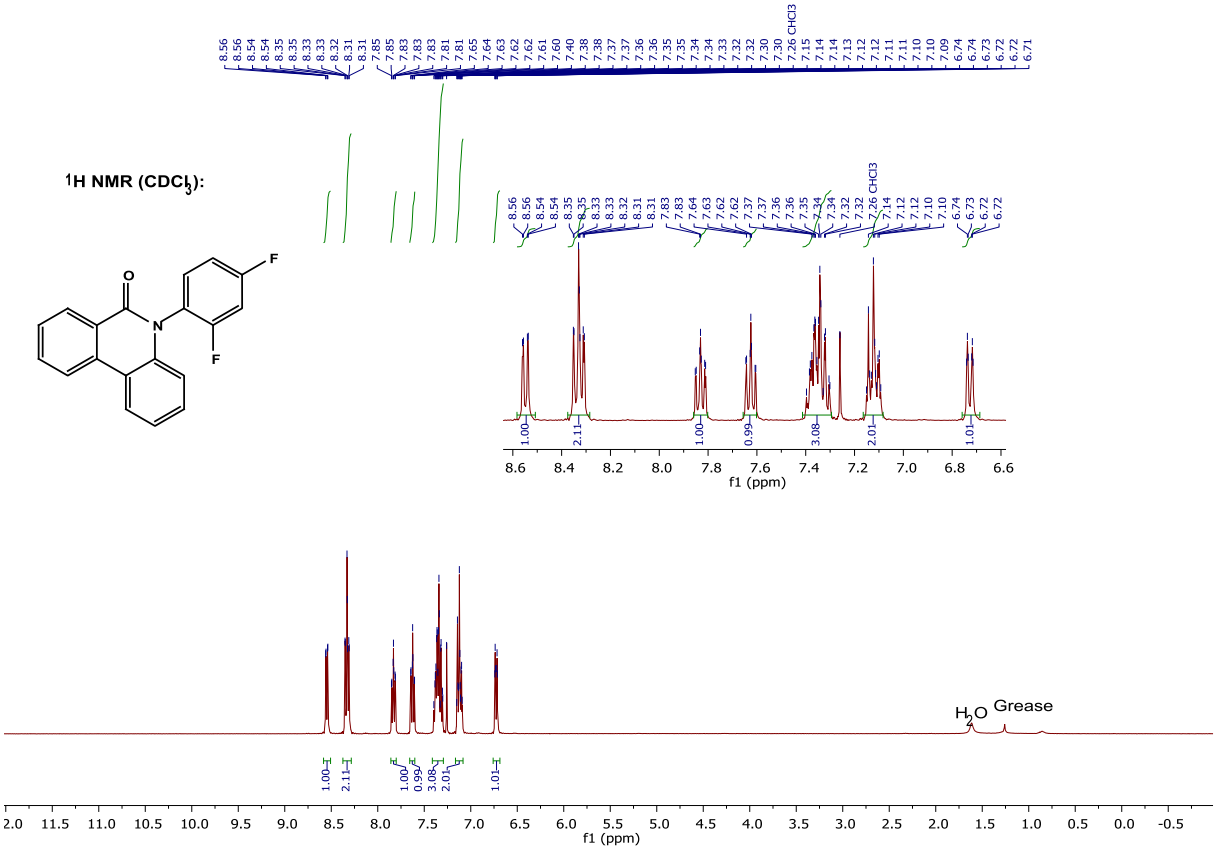

^{13}C NMR ($CDCl_3$):

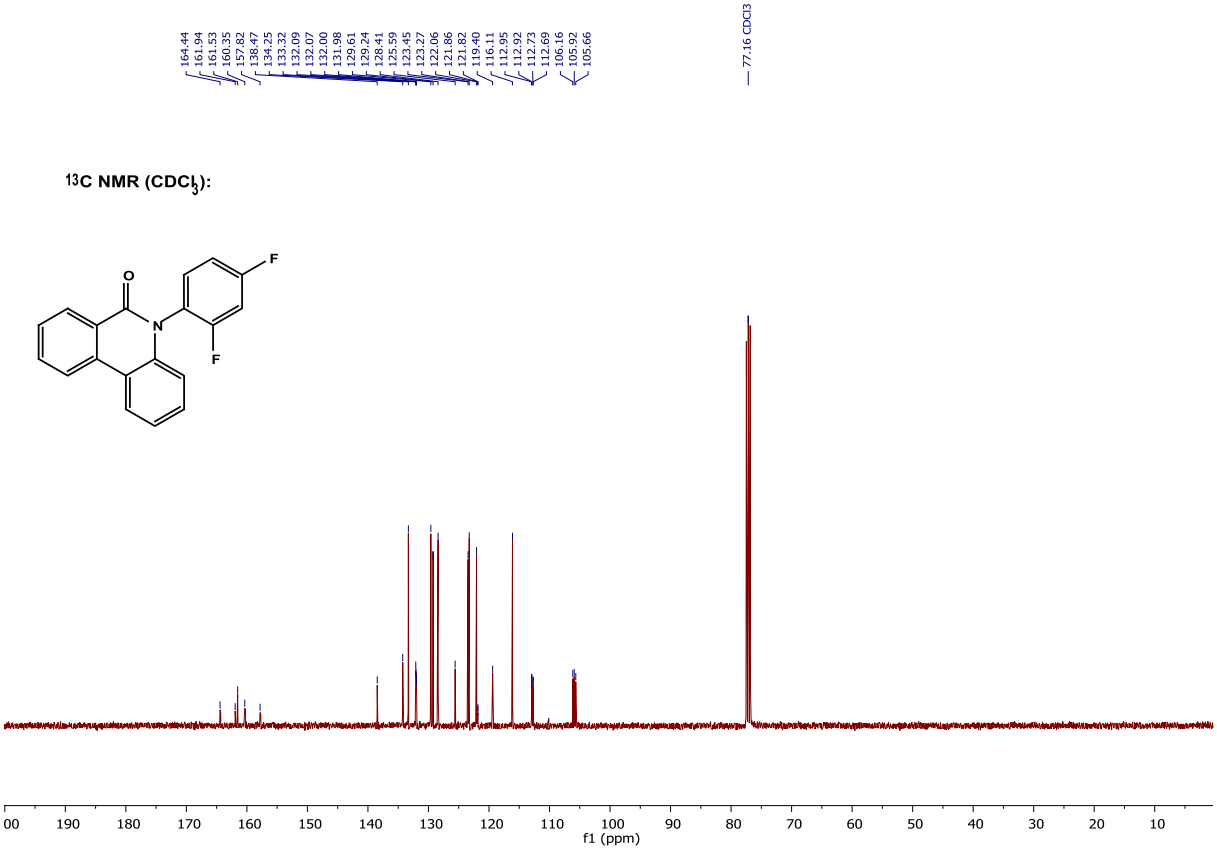

^{19}F NMR ($CDCl_3$):

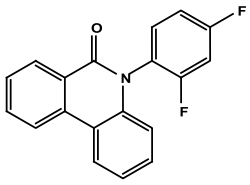

N-(3-Cyano-4-methylphenyl)-phenanthredin-6-one (2d)

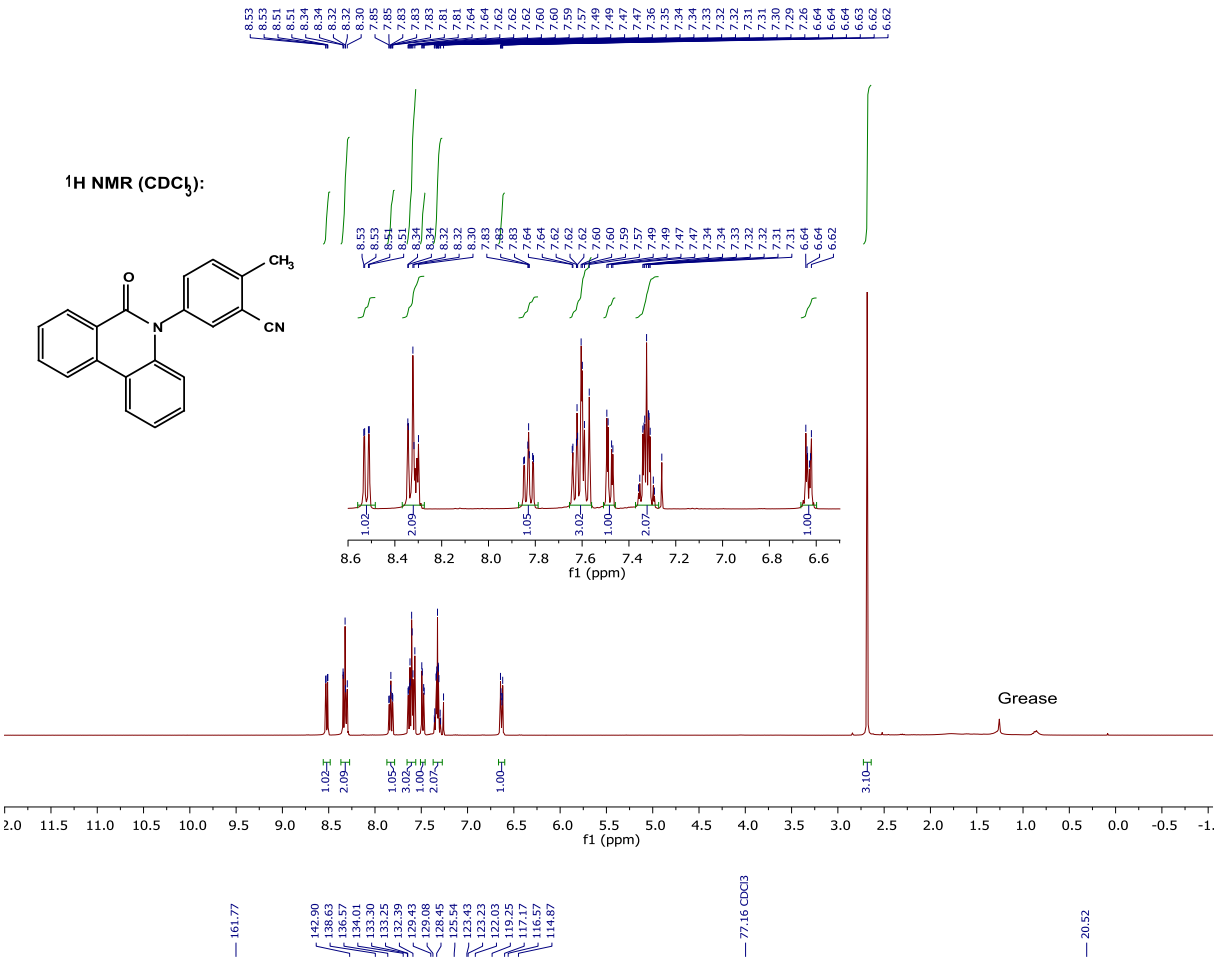

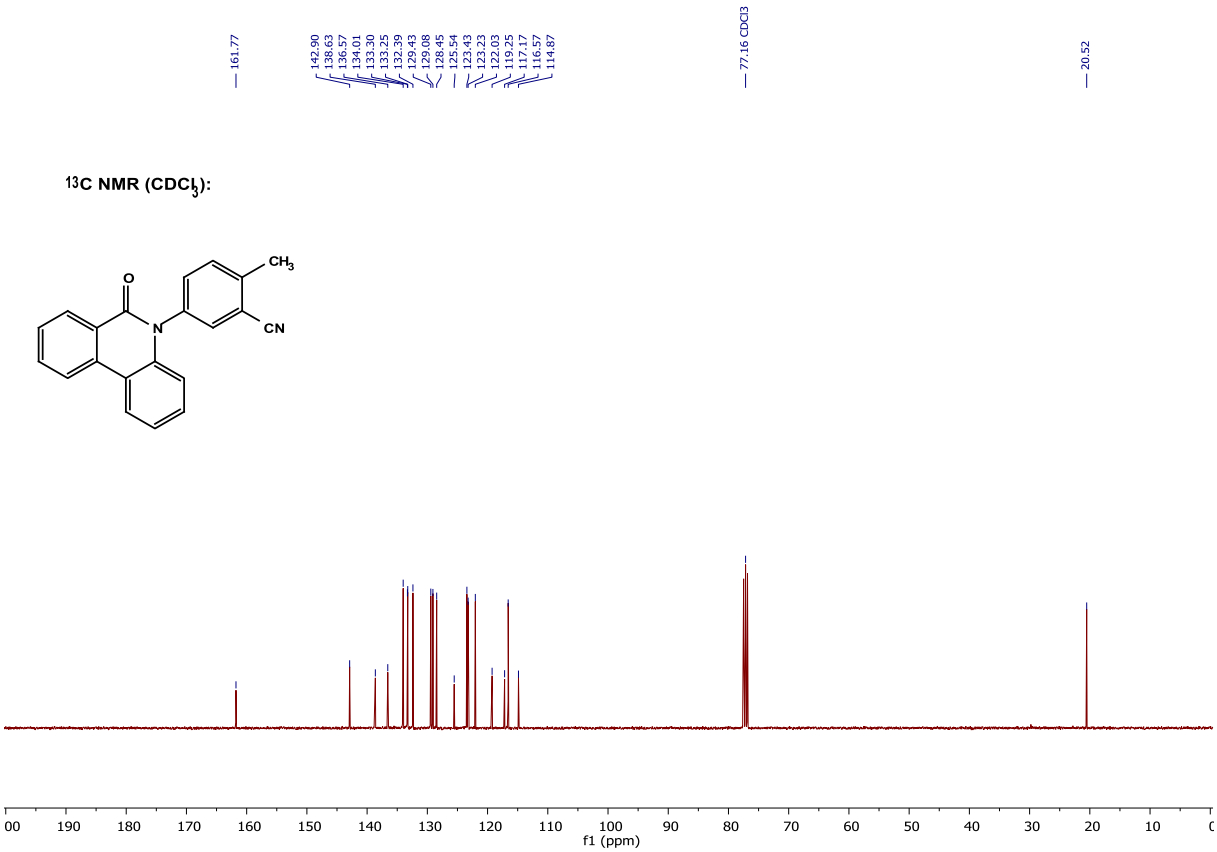

N-(3-Bromophenyl)-phenanthredin-6-one (2e)

^{1}H NMR ($CDCl_3$):

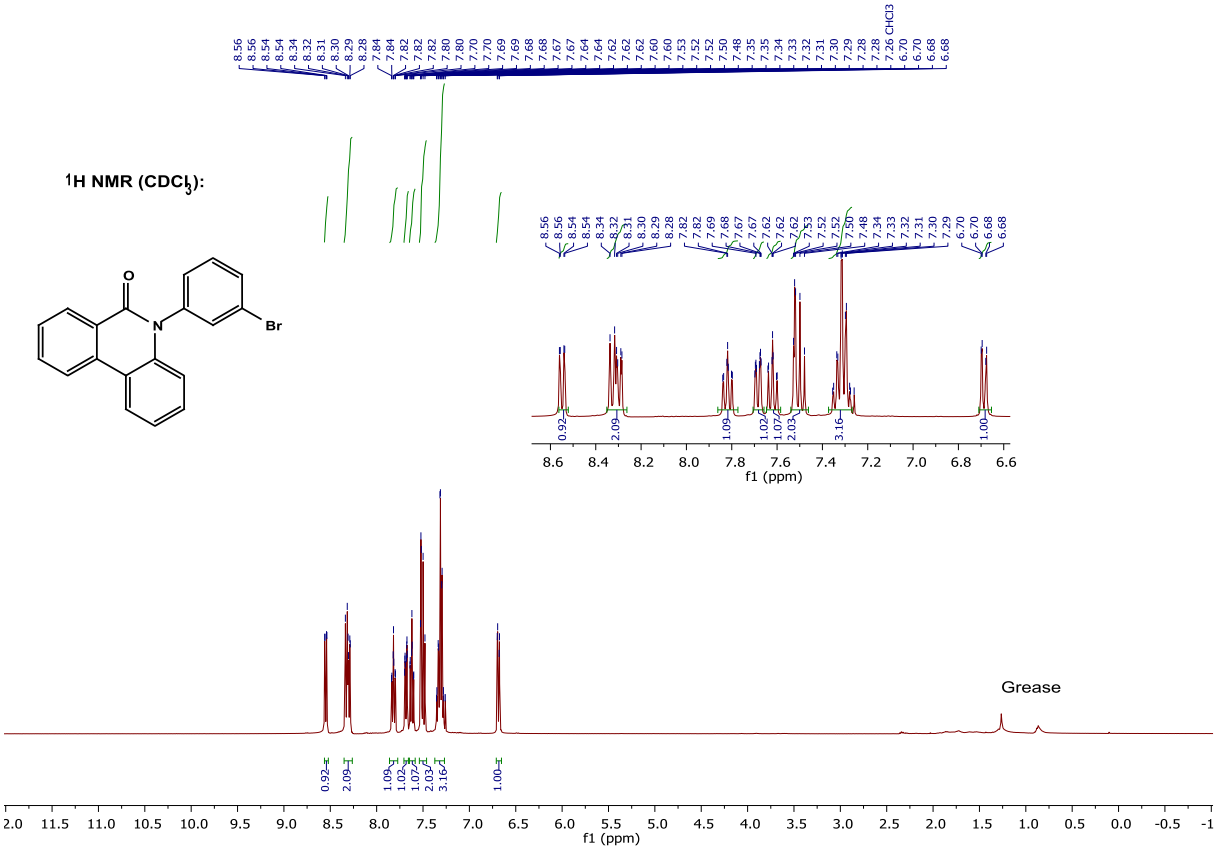

^{13}C NMR ($CDCl_3$):

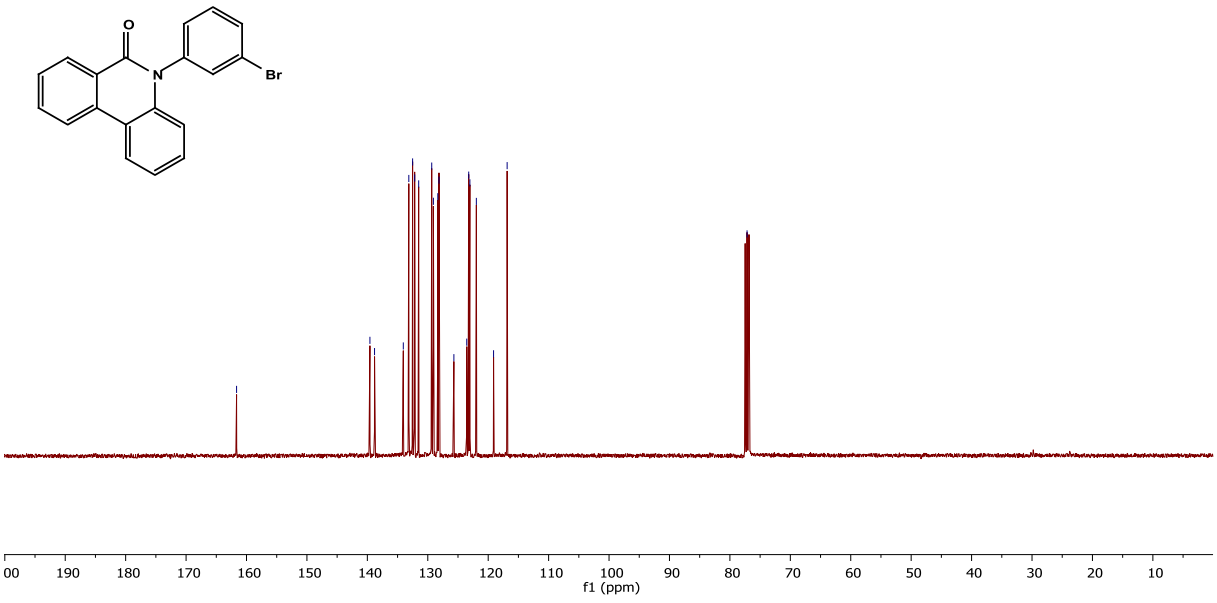

N-(2-Iodophenyl)-phenanthredin-6-one (2f)

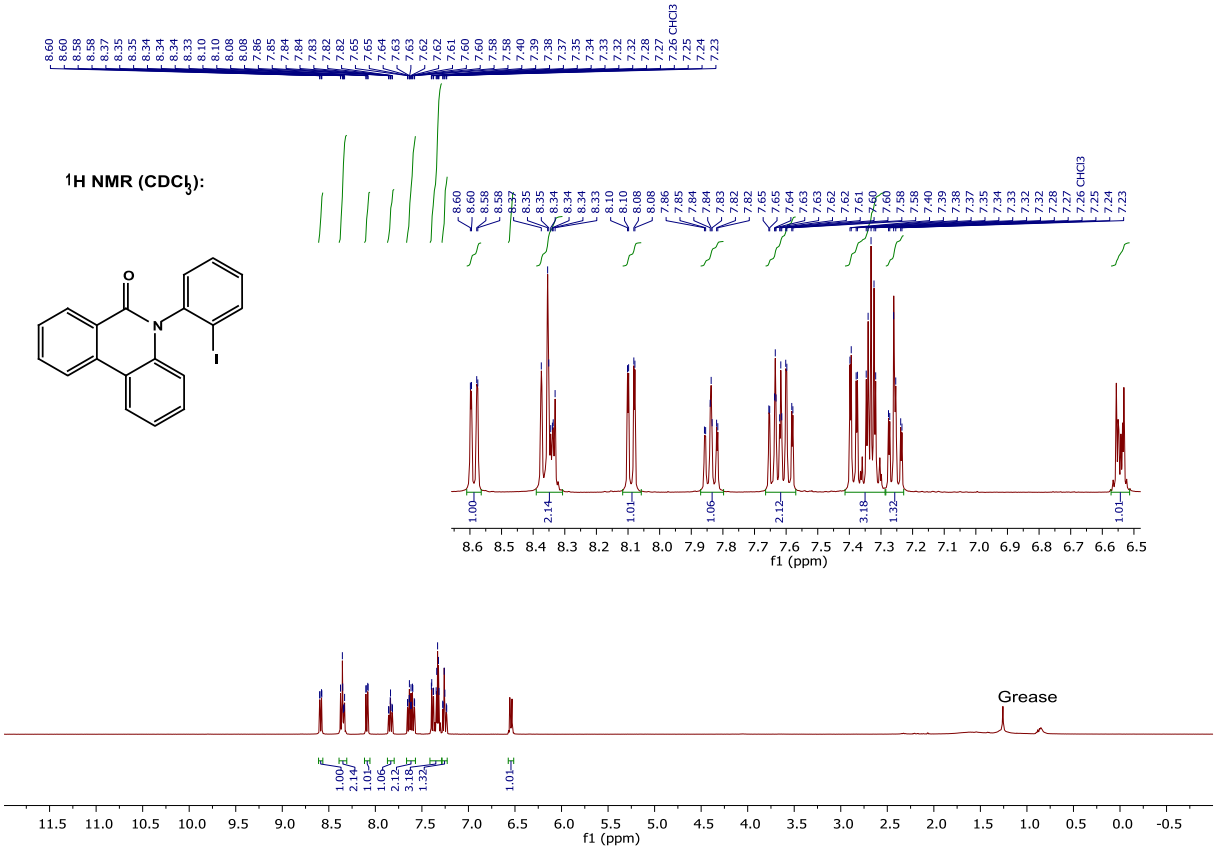

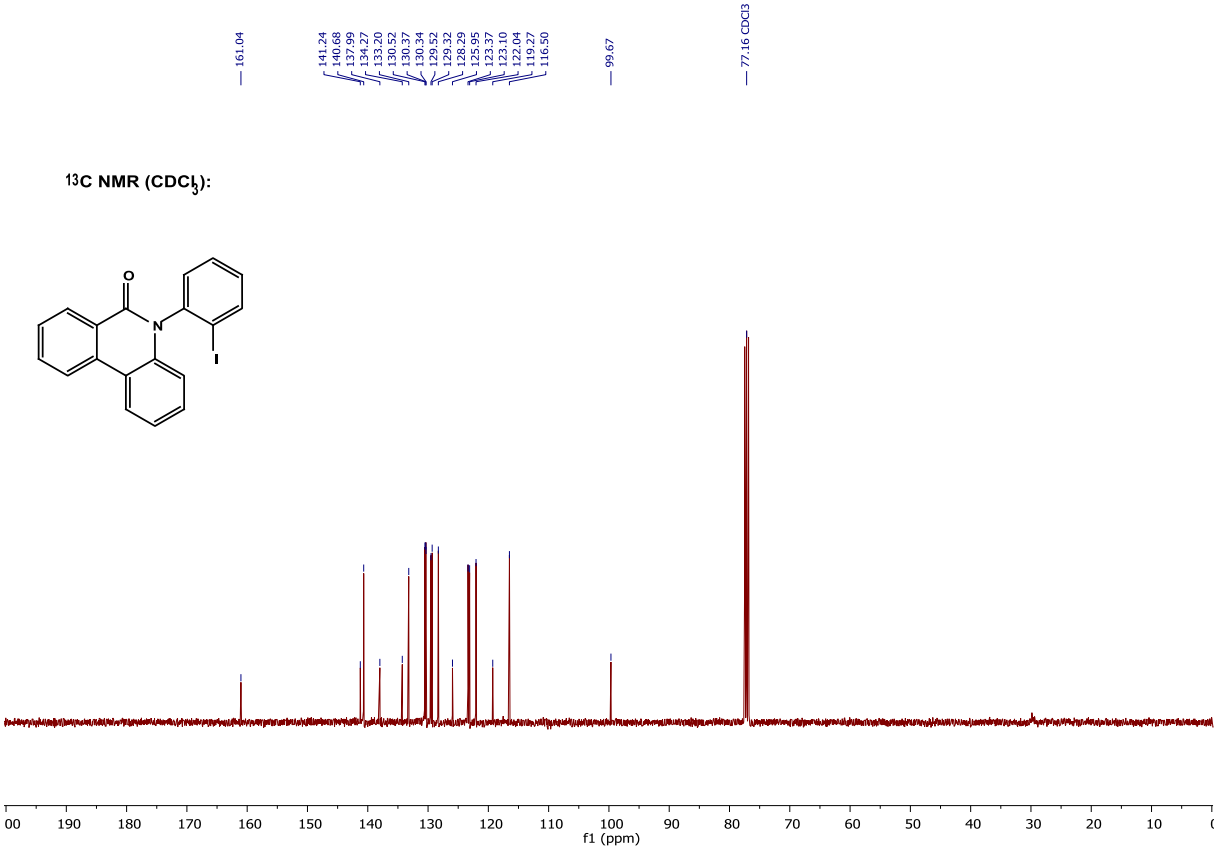

N-Phenyl-phenanthredin-6-one (2g)

^{1}H NMR ($CDCl_3$):

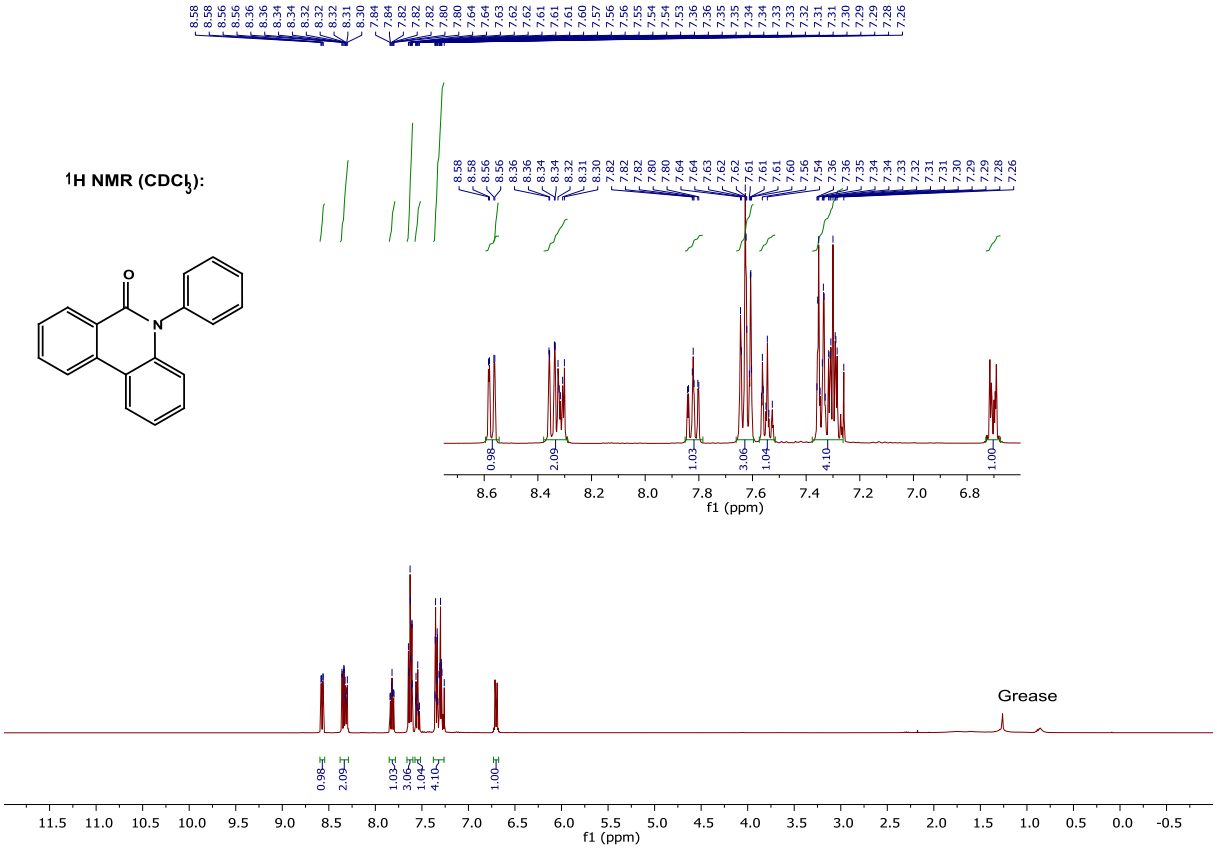

^{13}C NMR ($CDCl_3$):

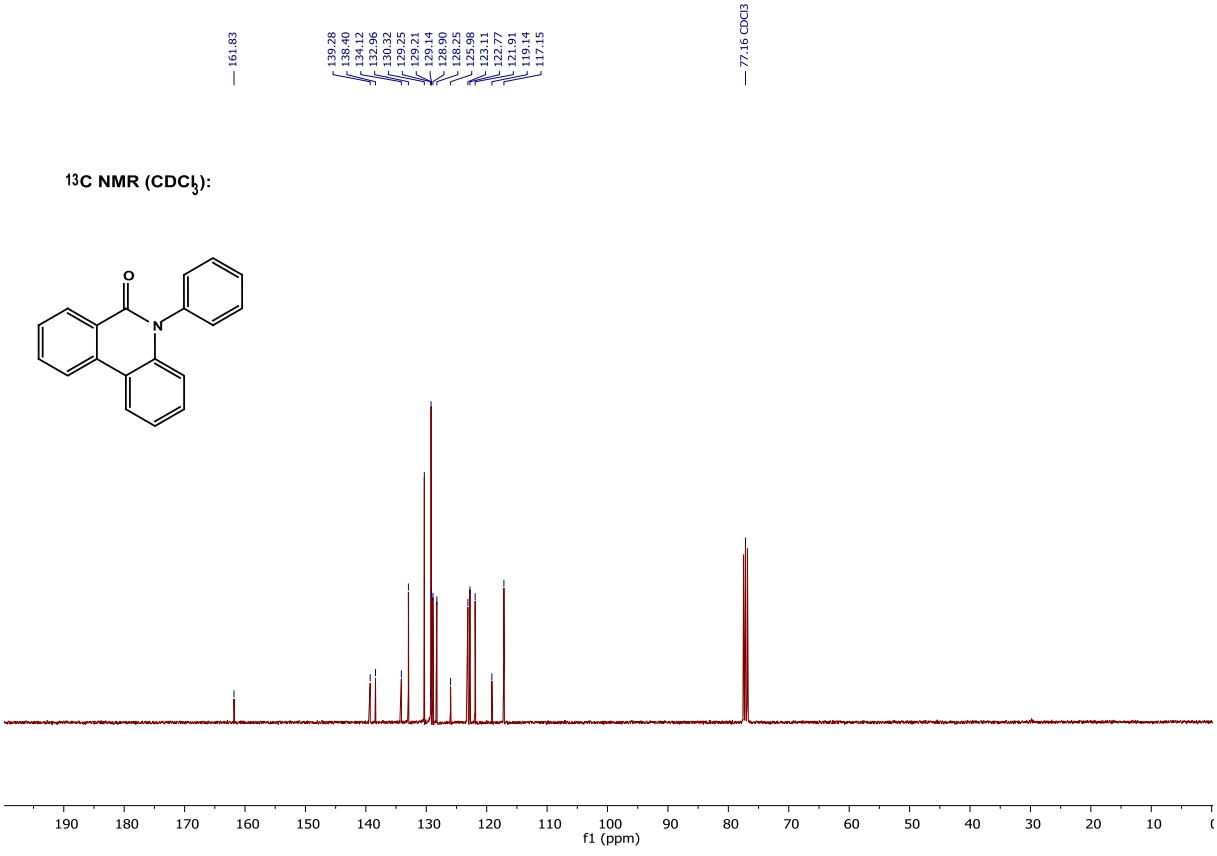

N-(2-Acetylphenyl)-phenanthredin-6-one (2h)

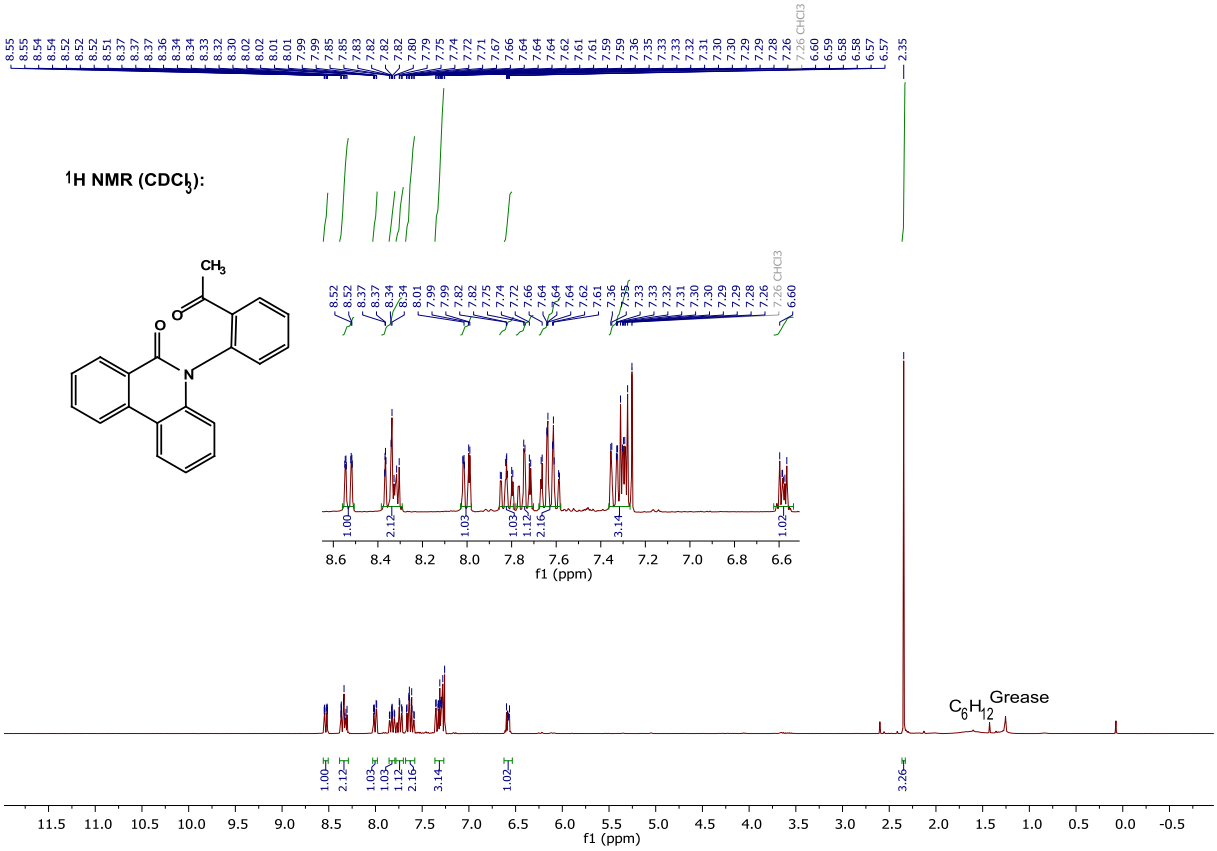

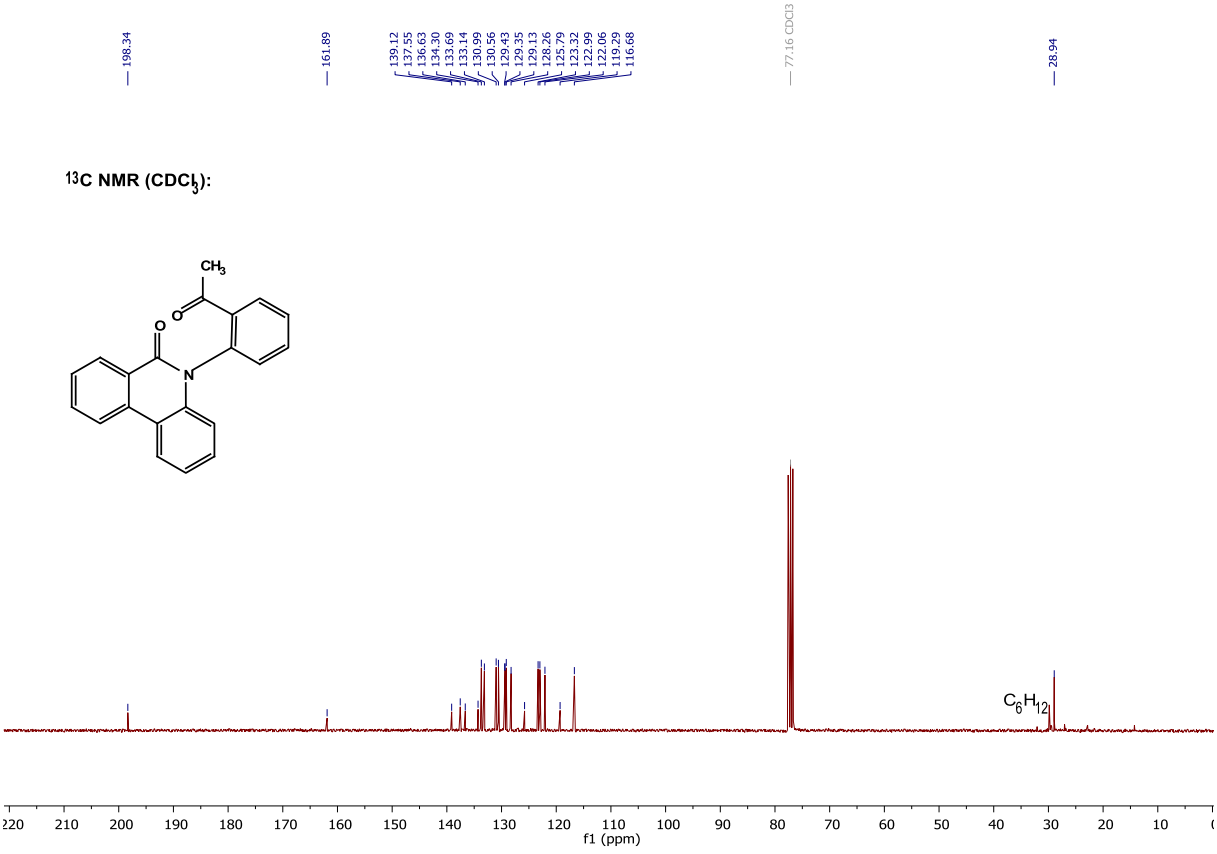

N-(2-Ethyl benzoate-2-yl)-phenanthredin-6-one (2i)

^{1}H NMR ($CDCl_3$):

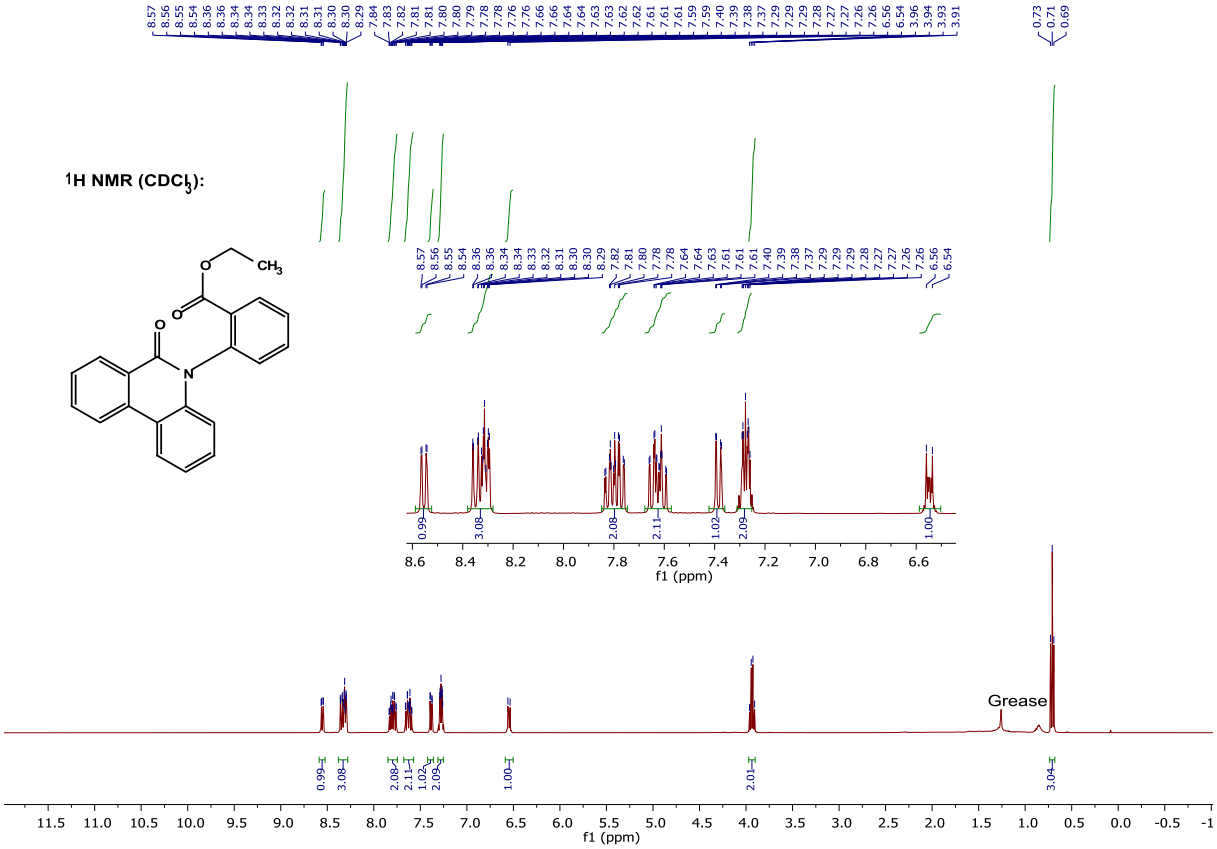

^{13}C NMR ($CDCl_3$):

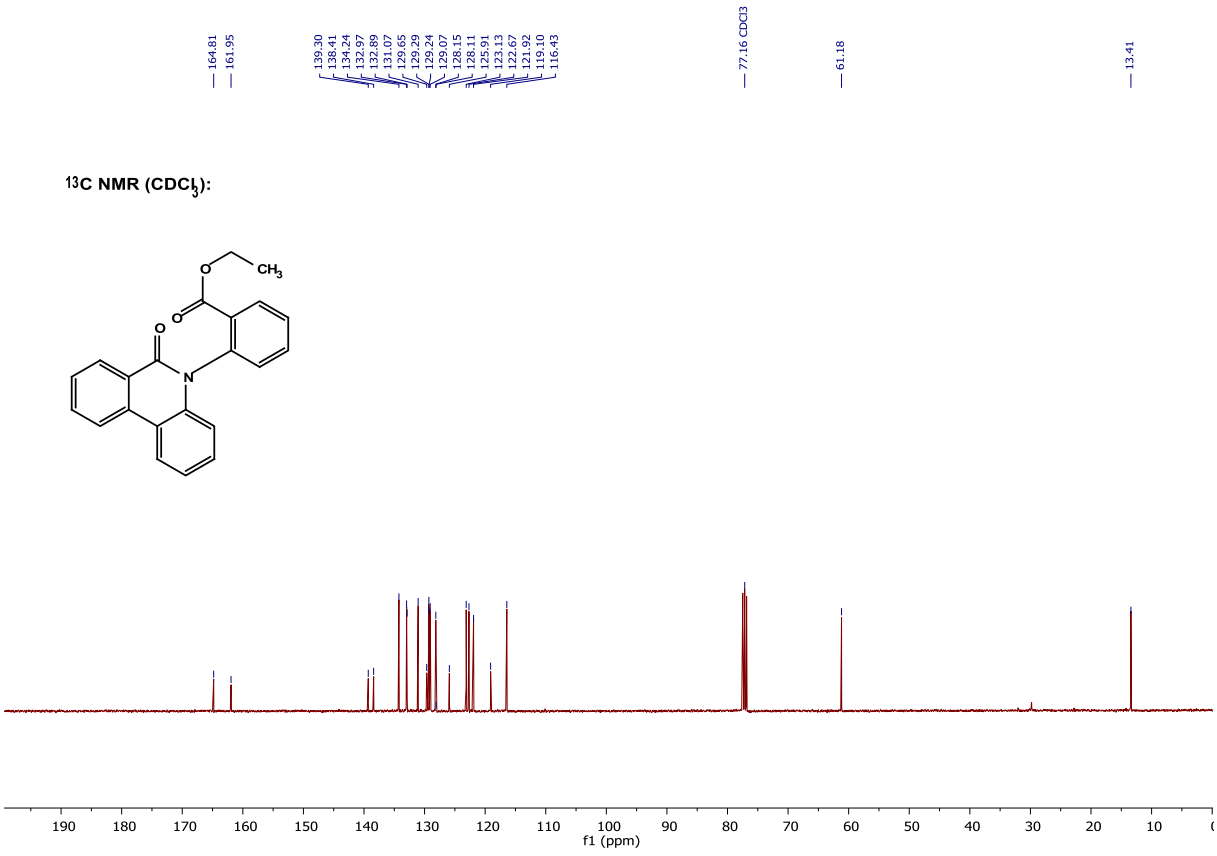

N-(3-Nitrophenyl)-phenanthredin-6-one (2j)

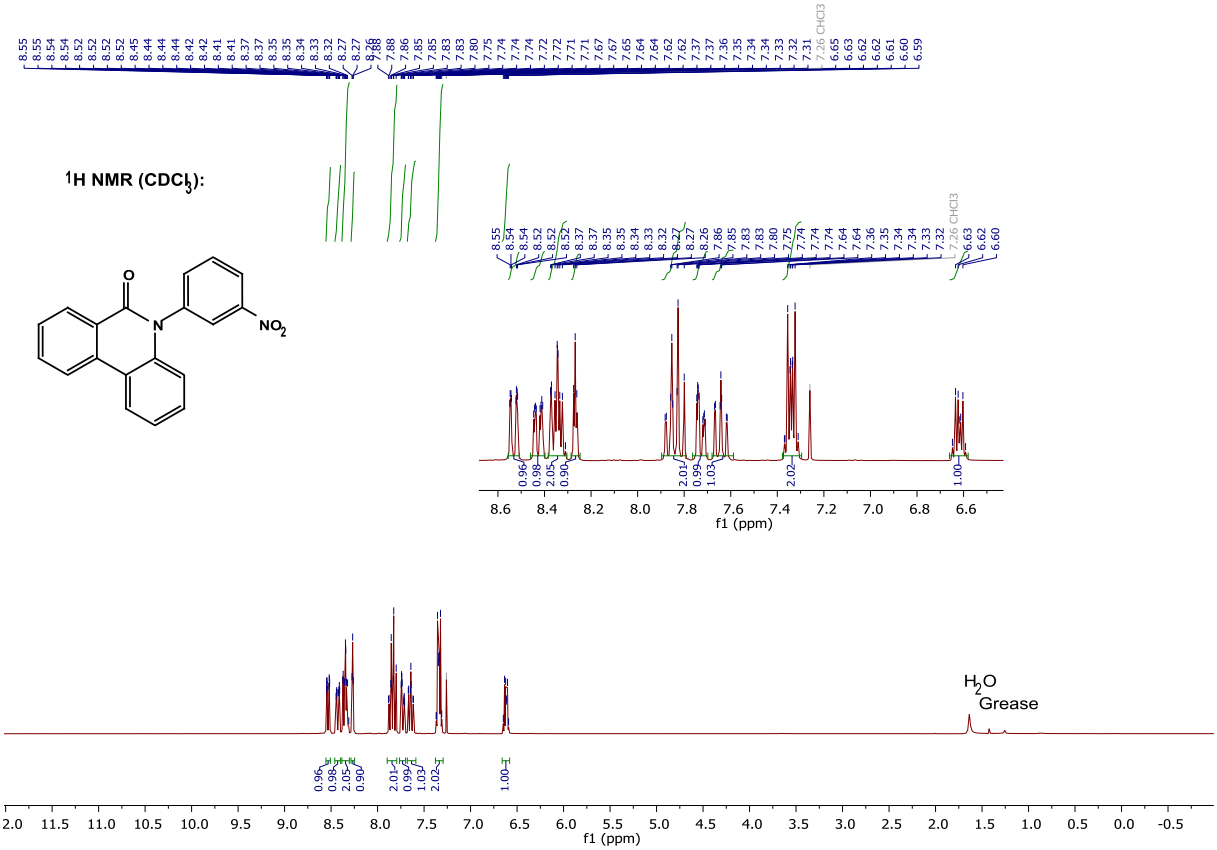

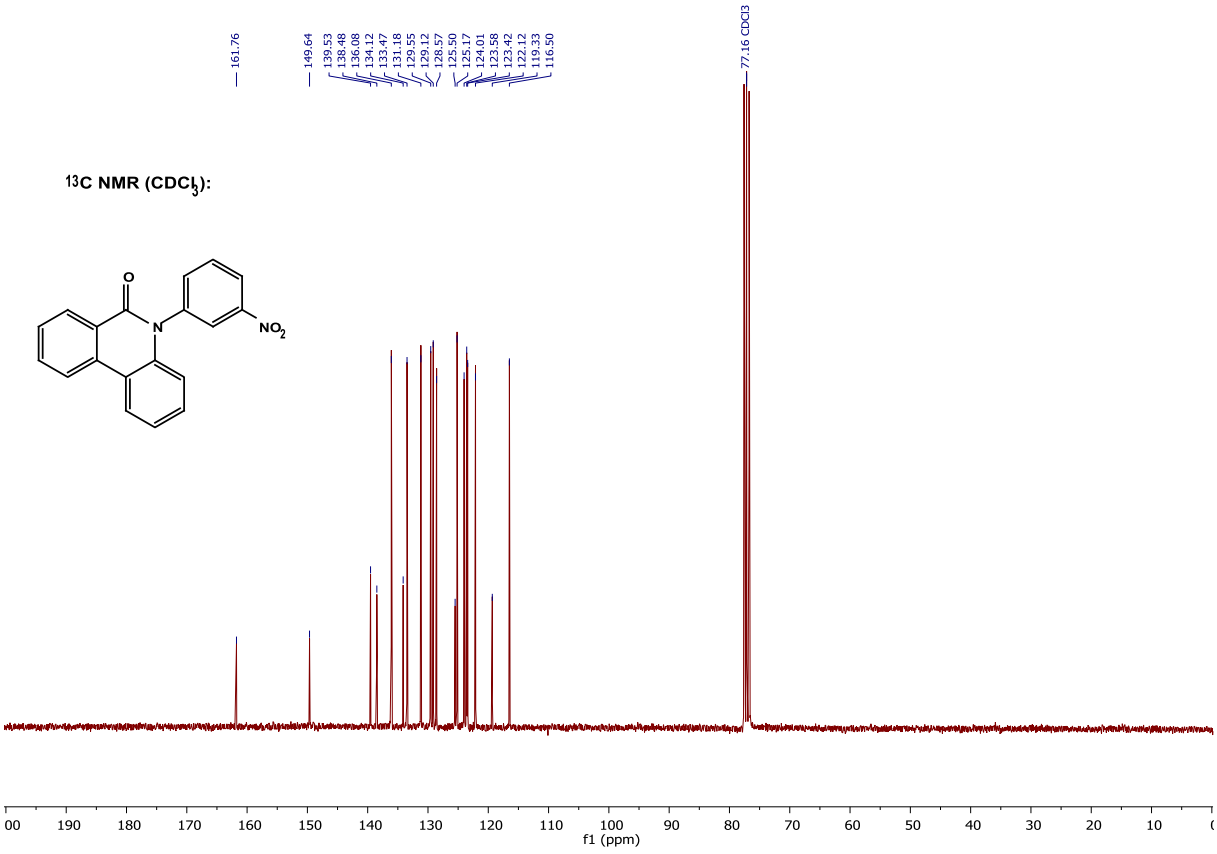

N-(4-Chlorophenyl)-3-trifluoromethylphenanthredin-6-one (2k)

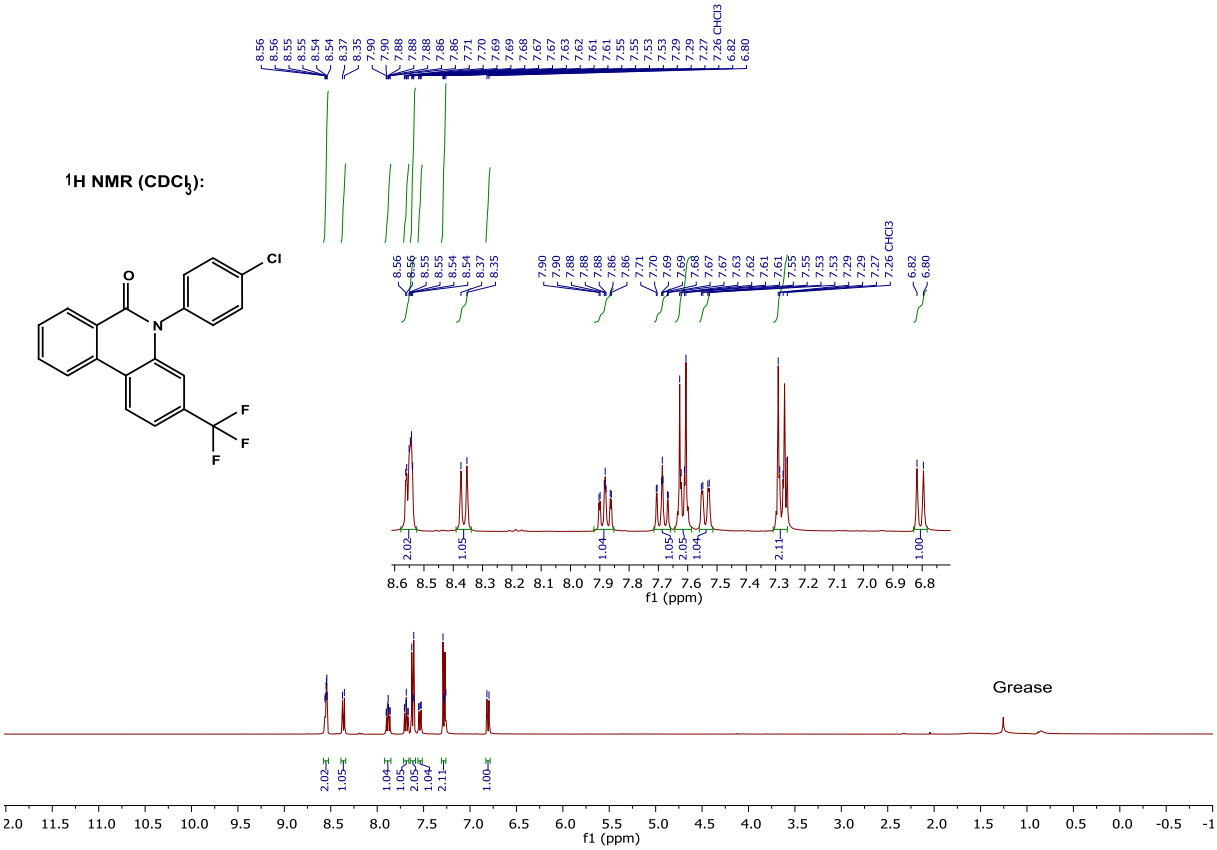

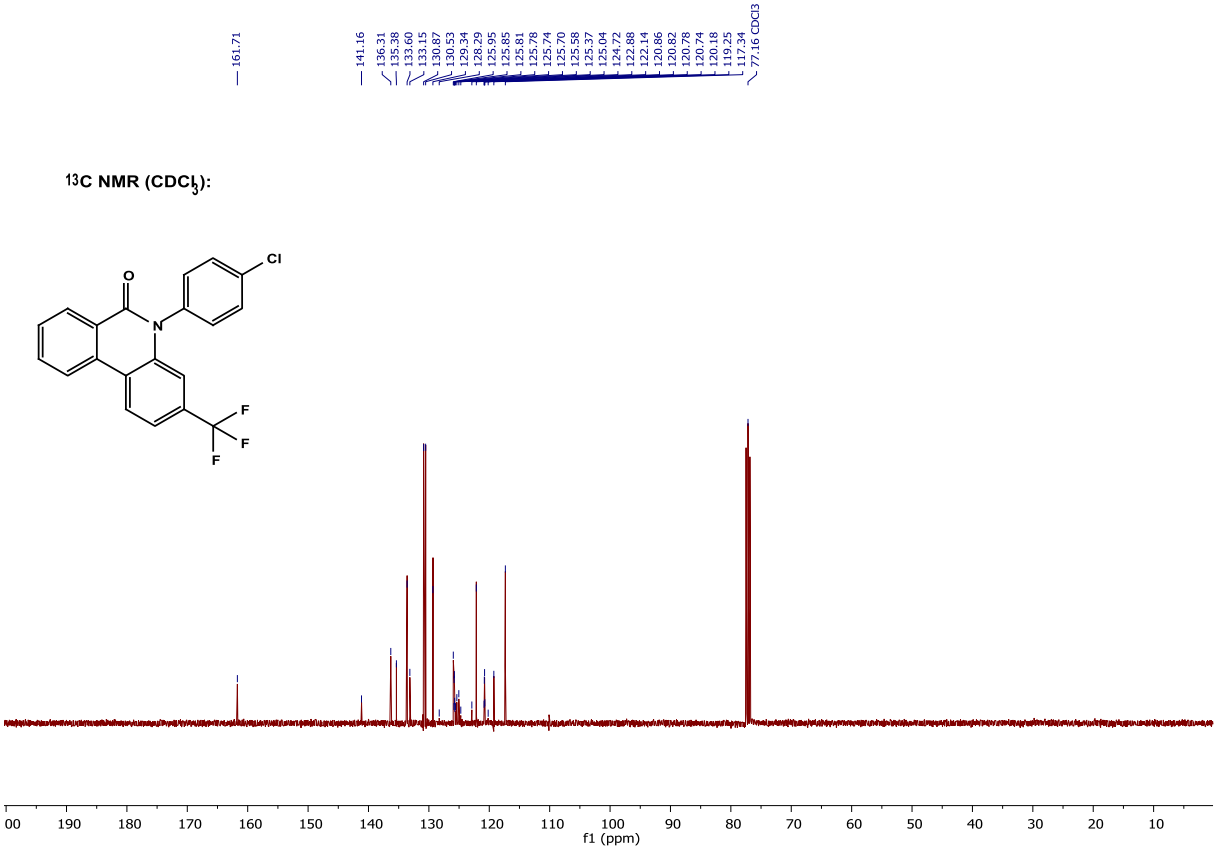

^{19}F NMR ($CDCl_3$):

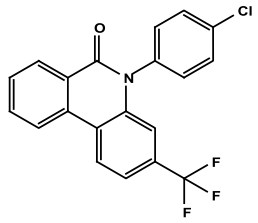

N-(4-Chlorophenyl)-3-chlorophenanthredin-6-one (2l)

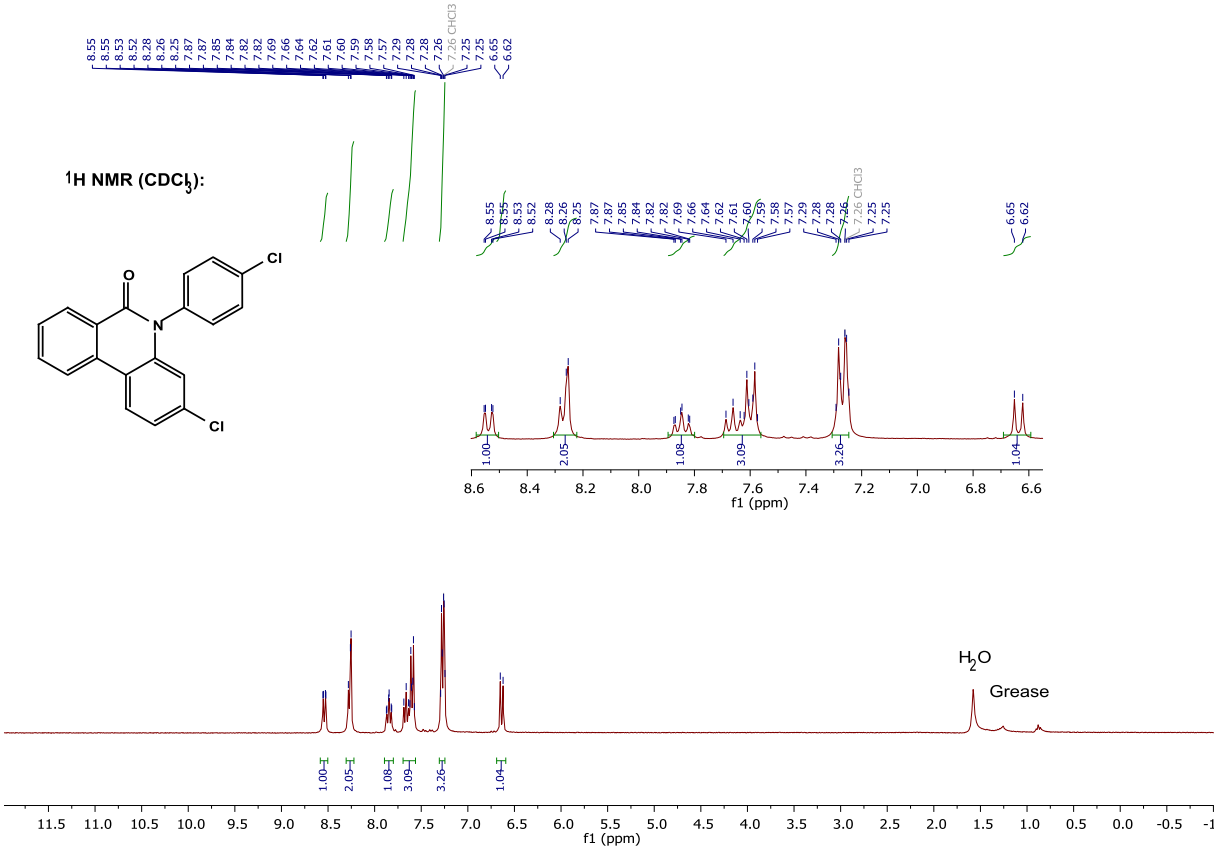

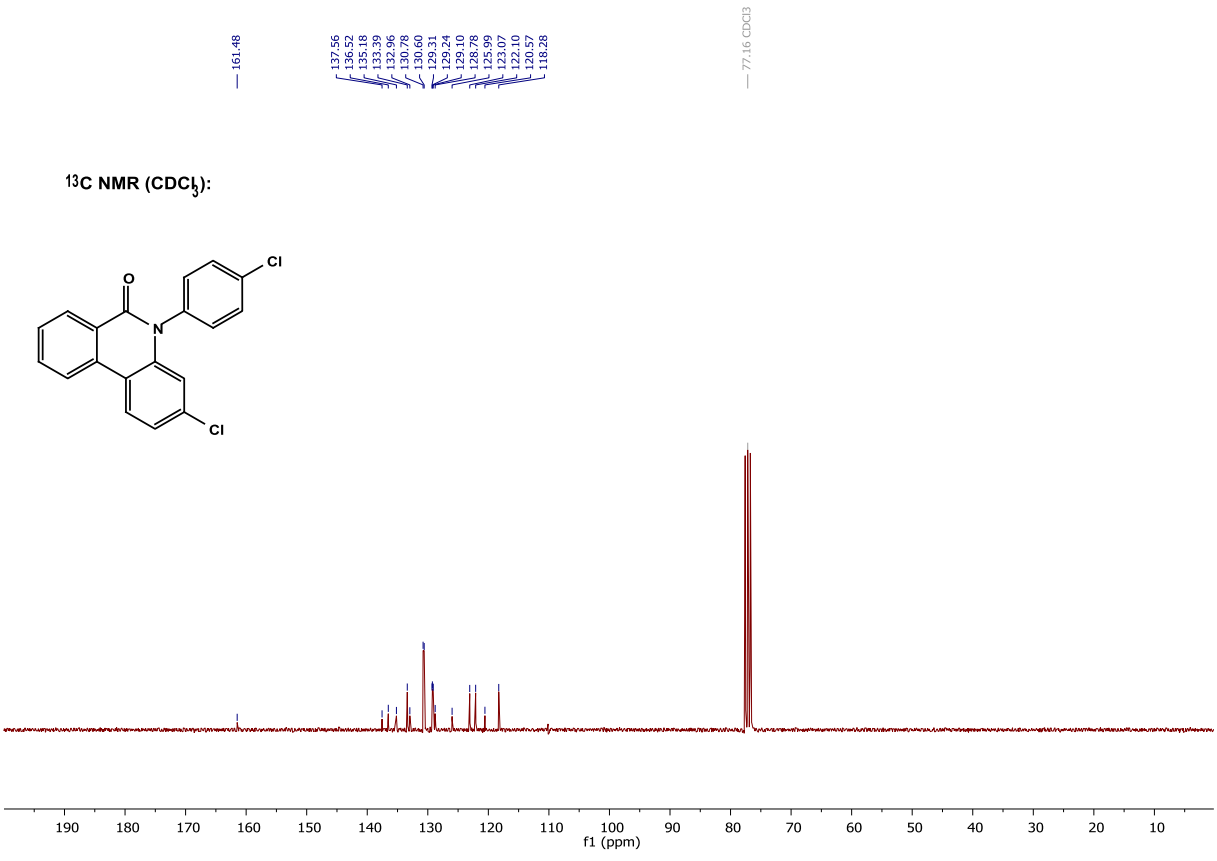

3-*tert*-Butyl *N*-(4-chlorophenyl)- phenanthredin-6-one (2m)

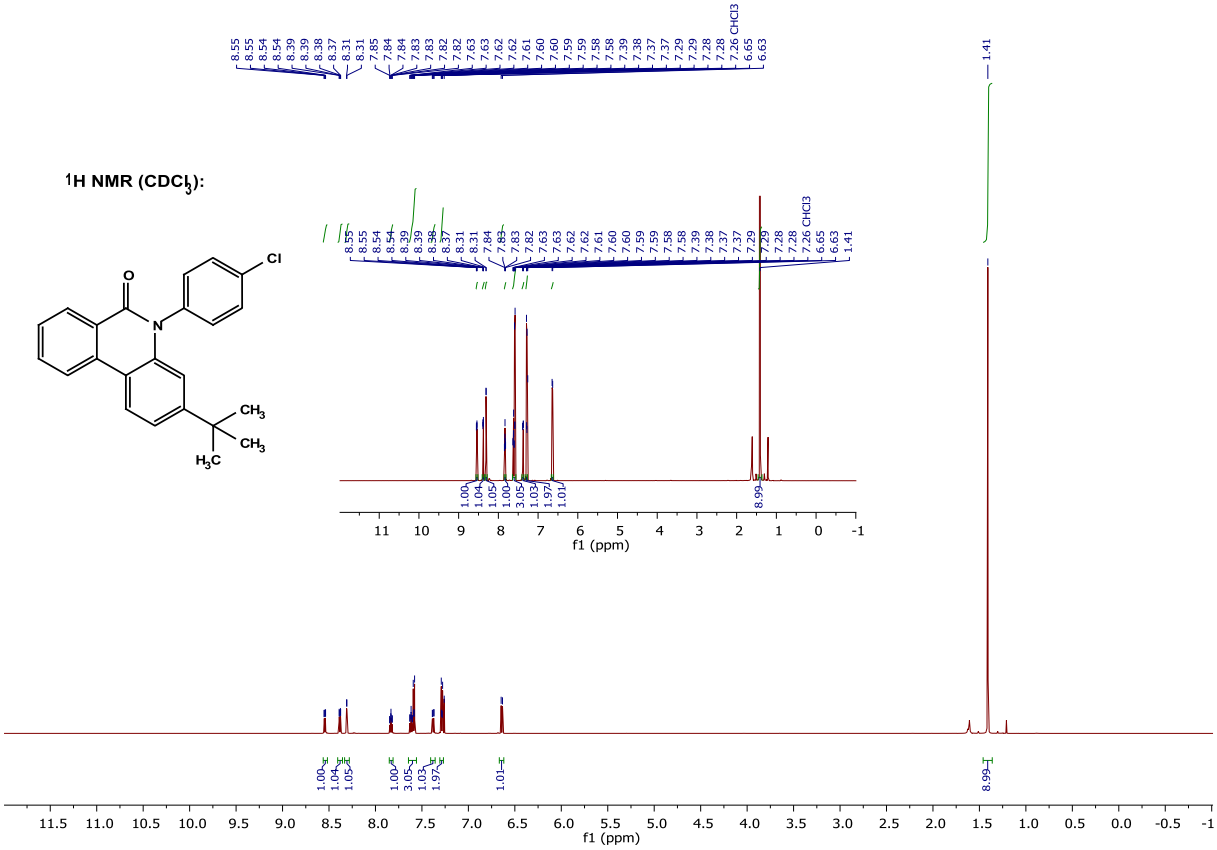

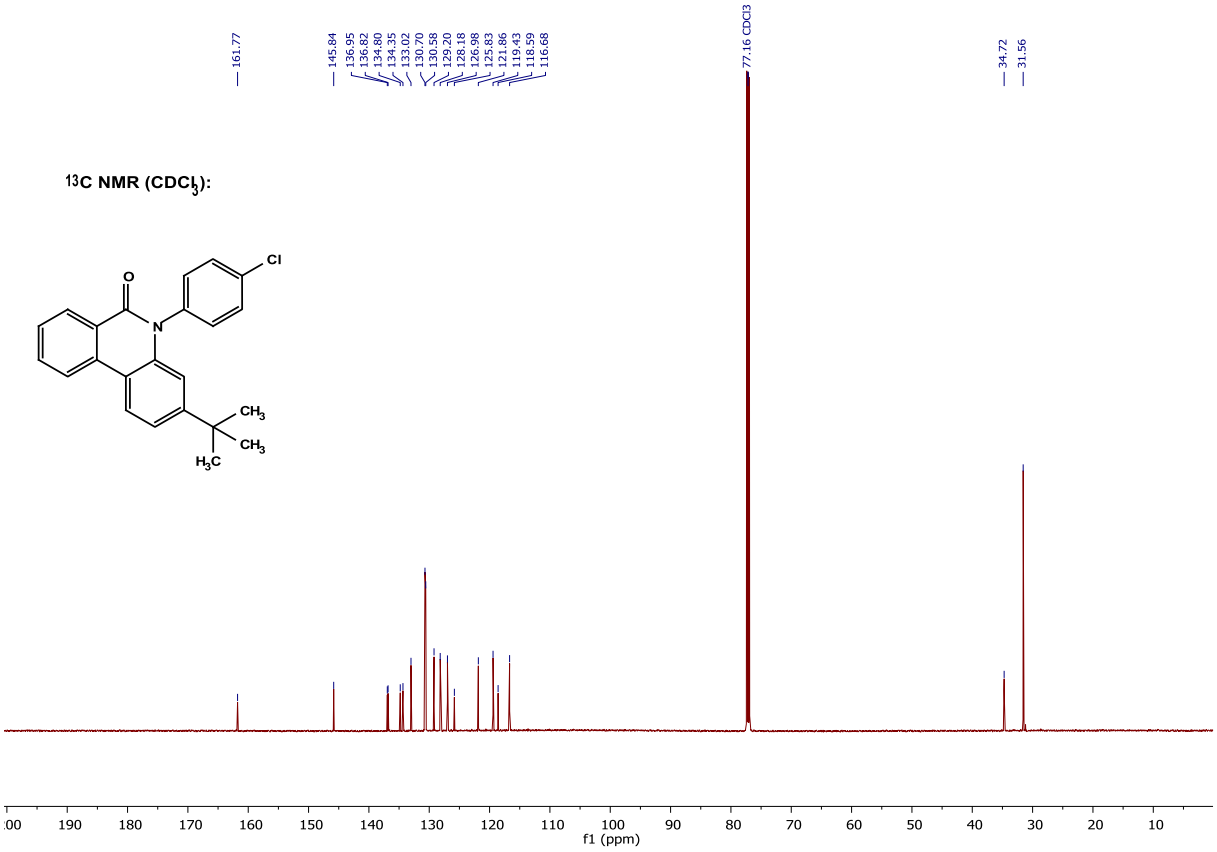

References

[1] W. L. F. Armarego, C. Chai Li Lin, *Purification of laboratory chemicals*, BH Butterworth-Heinemann/Elsevier, Amsterdam, **2013**.

[2] S. Berger, S. Braun, H.-O. Kalinowski, *NMR-Spektroskopie von Nichtmetallen*, Thieme, Stuttgart, **1994**.

[3] G. M. Sheldrick, *SHELXS97* and *SHELXL97: Programm for the Refinement of Crystal Structures;* Dept. of Structural Chemistry, University of Göttingen: Germany, **1997**

[4] A. R. Blaazer, J. H. M. Lange, M. A. W. van der Neut, A. Mulder, F. S. den Boon, T. R. Werkman, C. G. Kruse, W. J. Wadman, *Eur. J. Med. Chem.* **2011**, *46*, 5086–5098.

[5] T. Xiong, Y. Li, X. Bi, Y.-H. Lv, Q. Zhang, *Angew. Chem. Int. Ed.***2011**, *50*, 7140–7143.

[6] C. Gütz, B. Klöckner, S. R. Waldvogel, *Org. Process Res. Dev.* **2016**, *20*, 26–32.

[7] A. Wiebe, D. Schollmeyer, K. M. Dyballa, R. Franke, S. R. Waldvogel, *Angew. Chem. Int. Ed.* **2016**, *55*, 11801–11805; *Angew. Chem.* **2016**, *128*, 11979–11983.

[8] P. A. S. Smith, *J. Am. Chem. Soc.* **1954**, *76*, 431–436.

[9] a)T. Furuta, Y. Kitamura, A. Hashimoto, S. Fujii, K. Tanaka, T. Kan, *Org. Lett.* **2007**, *9*, 183–186; b) L. P. Walls, *J. Chem. Soc.* **1934**, 104–109.

Electrochemical Synthesis of Carbazoles by Dehydrogenative Coupling Reaction

Anton Kehl,[a] Niclas Schupp,[a] Valentina M. Breising,[a] Dieter Schollmeyer,[a] and Siegfried R. Waldvogel[a] *

In the memory of Prof. Dr. Kilian Muñiz

Abstract: A constant current protocol, employing undivided cells, a remarkably low supporting electrolyte concentration, inexpensive electrode materials, and a straightforward precursor synthesis enabling a novel access to N-protected carbazoles by anodic N,C bond formation using directly generated amidyl radicals is reported. Scalability of the reaction is demonstrated and an easy deblocking of the benzoyl protecting group is presented.

Carbazole was first isolated and characterized by Graebe and Glaser, which employed a high-boiling coal tar distillate, in 1872.[1] In the same year, Braun and Greiff reported a synthesis using aniline as starting material and intense heating in the course of a distillation process,[2] which was confirmed by Graebe and additionally refined employing diphenylamine as substrate in order to achieve higher yields.[3] The relevance of this compound class can be perceived when its potential use in the pharmaceutical sector[4] due to their anti-Alzheimer,[5] antibacterial,[6] fungicidal,[7] antitubercular,[8] antitumor properties,[9] or in the technical assignment[10] is taken into account.

Since the discovery of carbazole, reams of methods tackling different moieties in order to build up this particular scaffold were reported.[11] One convenient and straightforward access is by a cyclization reaction via a C,N bond formation. Classical strategies utilizing this approach are usually in demand of metal catalysis (Pd,[12] Cu,[13,14] Ir,[15] Rh[16]), oxidizers,[13] pre-functionalization,[17] or strongly elevated temperatures[18] which result in several drawbacks. On the one hand, leastwise stoichiometric amounts of oxidizers, toxic and partially expensive metal complexes, and essential leaving groups evoke reagent waste on an unfavorable scale. On the other hand, harsh conditions can narrow down the operational area, if the preservation of labile functionalities is targeted. Hence, improvements with regards to atom economy and ecology are highly desired.

Electrochemistry, which can be considered as a 'green' alternative,[19] representing a synthetic tool with inherent safety and extraordinary reaction pathways.[20] By solely employing electric current as inexpensive and sustainable reducing or oxidizing agent, amounts of waste are tremendously diminished and thus toxic reagents can be superseded. Two noteworthy approaches in the past decade considered the application of electrochemical means in order to generate a reactive species which facilitated the conversion in an ex-cell protocol. Nishiyama et al. reported the access to a hypervalent iodine species which was generated at constant current conditions (scheme 1).[21] After electrolysis, mostly substrates with electron releasing substituents were added to accomplish the reaction. Francke et al. refined this approach in elegantly combining the reagent and the supporting electrolyte. A few carbazoles were made with the newly designed reagent.[22] Recently, Powers et al. reported an in-cell approach with a broader scope (scheme 1).[23] However, that method relies also on hypervalent iodine species (25 mol% of 4-iodoanisole or substrate-dependent the more sophisticated 2,2'-diiodo-4,4',6,6'-tetramethyl-1,1'-biphenyl) two supporting electrolytes at once and constant potential conditions with a sophisticated three-electrode-setup. The unfortunate inconvenience of those three features evoked by the effort to separate the recyclable reagent and the ex-cell conditions or the constant potential setup are not optimal if a process with scaleup potential is desired.

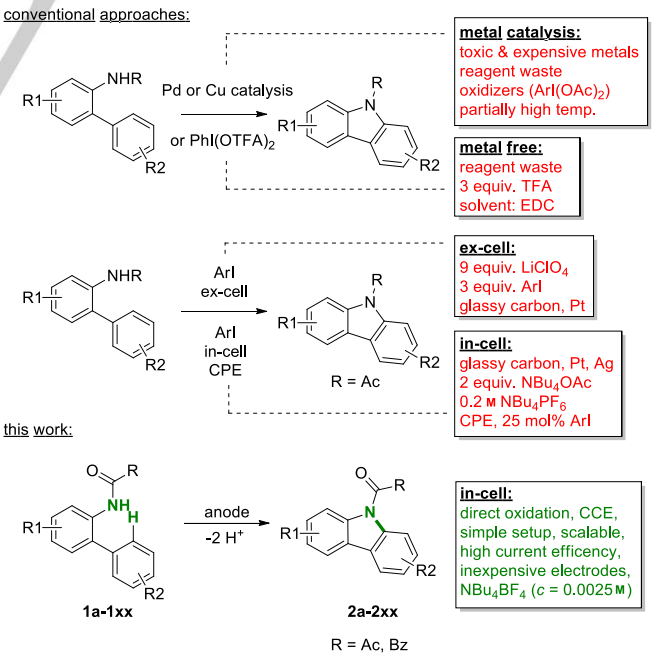

Scheme 1. Conventional approaches and our electrochemical access to N-protected carbazoles. TFA = trifluoroacetic acid; EDC = 1,2-dichloroethane; CPE = constant potential electrolysis; CCE = constant current electrolysis.

[a] A. Kehl, N. Schupp, V. M. Breising, Dr. D. Schollmeyer, Prof. Dr. S. R. Waldvogel
Johannes Gutenberg University Mainz, Department of Chemistry
Duesbergweg 10-14, 55128 Mainz, Germany
Homepage: www.aksw.uni-mainz.de
E-mail: waldvogel@uni-mainz.de

The electrochemistry of carbazoles and their predominant sensitivity towards side reactions are well-known and impede a progress in this direction.[24] Powers et al. addressed this issue by applying a mediated constant potential protocol. The employment of amidyl radicals as reactive intermediates was well explored in the last two decades and is associated with cyclization reactions[25] including rearrangements,[26] hydroaminations.[27] We reported a resources and user friendly methodology to afford amidyl radicals by direct oxidation in order to construct 5- and/or 6-membered heterocycles by dehydrogenative N,N,[28–30] N,C,[31] or O,C[32] coupling reactions. Herein we describe a new synthetic approach for N-protected carbazoles (scheme 1). With a straightforward synthesis to N-protected aminobiphenyl precursors, common electrode materials and a simple two-electrode arrangement utilizing a constant current protocol, this setup provides a general applicable access to this compound class.

The precursor synthesis was facilitated by treating a 2-aminobiphenyl with benzoyl chloride or acetic anhydride. If more elaborated derivatives are desired, an ordinary Suzuki reaction can be employed which involves 2-bromo- or 2-iodoaniline derivatives and the corresponding arylboronic acids. A subsequent protection of the amino function provides the precursor with this approach in two easy to perform steps (see Supporting Information).

The electrolytic conditions for the direct N,C coupling reaction were scrutinized within screening studies. Most of the applied conditions of the previously reported protocol for the synthesis of *N*-aryl-phenanthredin-6-ones served as indication for further investigation. The optimization was performed in undivided 5 mL Teflon® cells, which provide a time-efficient and straightforward screening approach.[33] 2-(4-Methylbenz)amido-5-chlorobiphenyl (**1a**) served as test substrate, since this particular aniline moiety has proven as a suitable candidate for the imminent electrochemical conditions.[30,31] Tested solvents such as methanol and ethanol resulted in a low conversion and alkoxylated byproducts. Acetonitrile and dimethyl sulfoxide displayed almost no conversion (see Supporting Information for additional data). 2,2,2-Trifluoroethanol yielded only a complex mixture of largely unidentified compounds according to gaschromatographic data. 1,1,1,3,3,3-Hexafluoroisopropanol (HFIP) exclusively enables an selective conversion due to its radical stabilizing properties.[34] However, the conversion was still incomplete. Further optimization efforts revealed that tetrabutylammonium tetrafluoroborate (NBu_4BF_4) allowed superior conversion compared to the default supporting electrolyte tetrabutylammonium hexafluorophosphate (NBu_4PF_6). The remarkably low concentration of supporting electrolyte (0.0025 M) enables sufficient conductivity for the electrotransformation. In order to ensure full conversion an addition of 15% of water is recommended. Higher (>20%) or lower (<5%) contents of water are significantly counterproductive. After accomplished electrolysis HFIP is almost entirely recovered by distillation, thus a small fluorine footprint can be retained.[35] As table 1 indicates, we tested a small set of common electrode materials. However, boron-doped diamond (BDD) and isostatic graphite offer a full conversion of the starting material and the highest yields of 73% and 65%, respectively. The amount of applied charge of 2.1 F is slightly higher than the theoretical amount needed of 2.0 F. Glassy carbon on the other hand revealed a rather low conversion and yield of 28%. Application of closely the theoretical amount of charge is necessary to keep over-oxidation products on a low level. Since isostatic graphite is the least expensive material, we decided to stick to it in order to provide a cost-efficient protocol as far as possible. Furthermore, the impact onto the yield of cathode materials were explored. Steel exhibited a performance inferior to the established nickel cathode. As far as platinum and graphite are concerned, a result similar to the nickel electrode was determined. Nevertheless, nickel was chosen for the final protocol. However, an application of this protocol is suitable for pharmaceutically active ingredients, since traces of toxic metals can be avoided by the choice of the electrode material. The last aspect of the optimization (Table 2) was the determination of a suitable current density, which is a key parameter in the organic electrosynthesis. The outcome of this study clearly indicates that best results (65%) are achieved with a current density of 1 mA/cm^2. Higher current densities decrease the conversion of the substrate and yield due to rising degradation reactions. Additionally, we replaced the 4-methylbenzoyl protecting group (**1a**) by the less expensive benzoyl group (**1b**).

Table 1. Influence of electrode materials onto the yield of **2a**.

Entry	anode	cathode	conversion [%][a]	yield [%][b]
1	**graphite[c]**	**nickel**	**>99**	**65**
2	BDD	nickel	>99	73
3	glassy carbon	nickel	41	28
4	graphite[c]	graphite[c]	>99	62
5	graphite[c]	steel[d]	70	42
6	graphite[c]	platinum	>99	68

0.2 mmol substrate **1a**, 0.0025 M NBu_4BF_4 in 4.25 mL/0.75 mL HFIP/H_2O, charge: 2.1 F, undivided cell; current density: 1 mA/cm^2; [a] based on recovered starting material; [b] isolated yield; [c] highly isostatic graphite; [d] stainless steel (VA 1.4571).

Table 2. Influence of current density onto the yield of **2a**.

Entry	current density [mA/cm^2]	conversion [%][a]	Yield [%][a]
1	0.5	>99	52
2	**1.0**	**>99**	**65**
3	2.0	85	50
4	3.0	69	42
5	4.0	65	40
6	5.0	62	33

0.2 mmol substrate **1a**, 0.0025 M NBu_4BF_4 in in 4.25 mL/0.75 mL HFIP/H_2O, anode: highly isostatic graphite, cathode: nickel, charge: 2.1 F, undivided Teflon® cell; [a] based on recovered starting material; [b] isolated yield.

Once the optimization was completed, we were able to establish a broad scope of N-protected carbazoles with various and valuable functional groups (Figure 1). The majority of compounds was synthesized in good to excellent yields. The formation of the N,C coupled product was verified via X-ray structure analysis of **2d** (Supporting Information). Apart from benzoyl protecting groups, 4-methyl-substituted benzoyl- (**2a**) and acetyl groups (**2c**) were demonstrated to point out the versatility of compatible protecting groups for this transformation. In the given case, the benzoyl groups afforded a slightly higher yield compared to the acetyl protected derivative. The impact of the substituted benzoyl group is insignificant (**2a** and **2b**). Both aryl moieties can contain different substitution patterns (e.g. **2j-o**, **2q**) to ensure a broad scope of compounds. Valuable functional groups such as chloro- (**2a-c**, **2j-n, 2q**), bromo- (**2g**), nitro- (**2m**), keto- (**2l**), ester- (**2i**, **2q**), or cyano- (**2h**), which allow subsequent reactions, are tolerated. Derivatives with electron withdrawing substituents such as **2h** and **2i** work excellent under the applied conditions. The highest yield of 86% was achieved by generation of compound **2h**, which contains a valuable cyano functionality. Additionally, this compound was successfully synthesized on gram scale and with the doubled concentration (0.08 M) in order to demonstrate the scalability of this method. The moderate yields of compounds **2d**, **2e**, **2k**, and the N-protected natural product glycozoline (**2o**) can be explained due to the fact that a free *para*-position or benzylic-position of the anilide moiety results in an elevated probability for side reactions.[28–31] Compounds with electron releasing moieties as represented by **2n** and **2o** performed moderately owing to an incomplete conversion of the starting material, which also could be observed in the synthesis of **2d**, **2e**, and **2k**. A further application of additional charge was counterproductive and resulted in lower yields. In terms of over-oxidation of the product during the electrolysis, its occurrence is likely due to a low potential difference or even a lower potential compared to the precursors (cyclic voltammograms in Supporting Information). Thus, employing too much applied charge above the theoretical amount is not always expedient. Generally, the applied charge ranged between 2.1 F and 2.8 F depending on the starting material. In some cases (**2e**, **2f**, **2j-m**) the addition of 15% water was counterproductive and resulted in a very low conversion of the starting material. In those cases, omission of water provided an increased conversion.

As far as the formation of regioisomers in the case of a non-symmetrical substitution pattern of the second aryl moiety is concerned, solely the compounds with the substituent in 6-position were found as **2l**, **2n**, and **2o** indicate. In order to elucidate the application-related nature of our method, we synthesized a protected carprofen (**2q)** in good yields, which can be deblocked easily, as depicted in scheme 2.

Mechanistically, transformation most likely proceeds via a radical pathway. The generation of an amidyl radical through a direct oxidation of the starting material at the anode and a subsequent deprotonation. The latter can be accomplished by an in situ generated anion of HFIP. The amidyl radical might be stabilized by the π system and solvent HFIP. Cyclization establishes a novel N,C bond with the other moiety of the biphenyl scaffold resulting in a rather stabilized radical species.

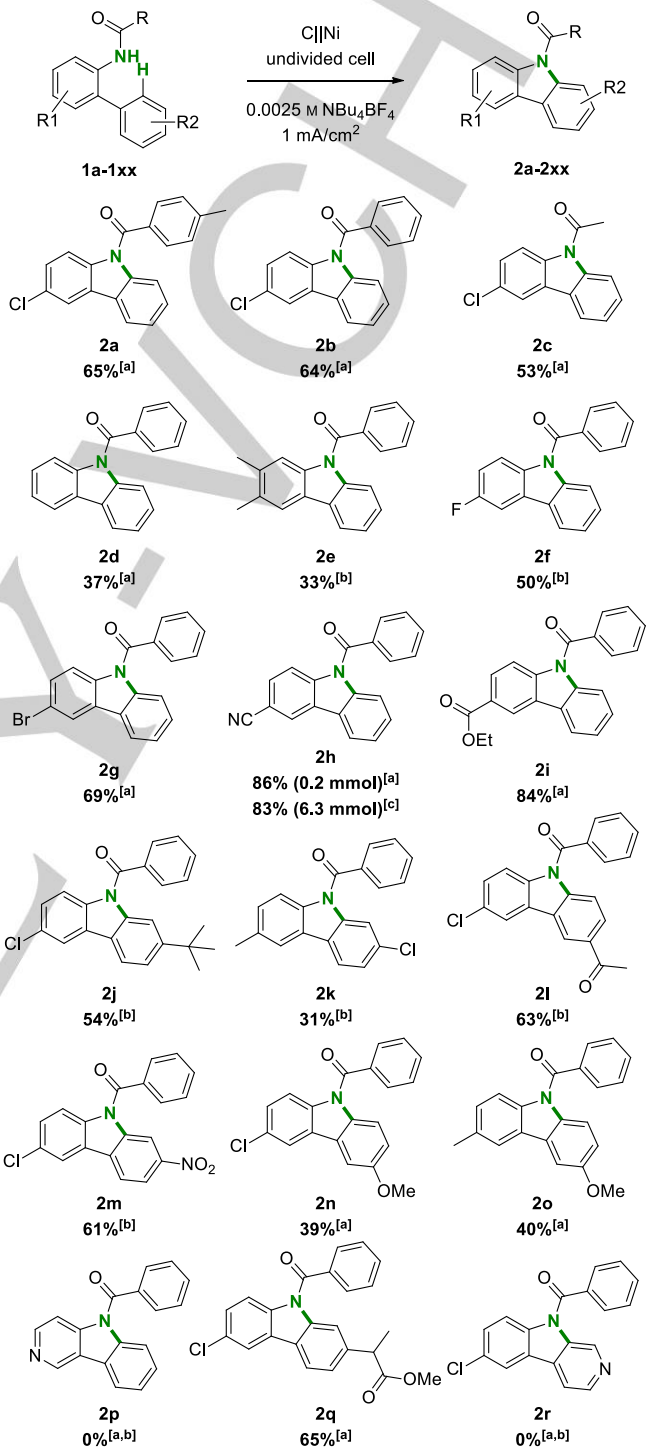

[a] 5 mL Teflon® cell, 0.2 mmol substrate, solvent: HFIP/H_2O(15%)
[b] 5 mL Teflon® cell, 0.2 mmol substrate, solvent: HFIP
[c] 80 mL beaker-type cell, 6.3 mmol substrate, solvent: HFIP/H_2O(15%), applied charge: 2.8 F

Figure 1. Scope of direct electrochemical carbazole synthesis by dehydrogenative N,C cyclization reaction.

A second oxidation step paired with a subsequent rearomatization by extrusion of a proton results in the final product (Supporting Information). We intended to demonstrate that the formation of the amidyl radical is a crucial step in the formation of the carbazoles. Therefore, we implemented a heterocyclic motif in the benzamido moiety (**1p**). Highly electron withdrawing moieties such as pyridine, exhibit a good resistance to oxidation which resulted in a nondetectable conversion and an almost whole starting material recovery (**1p**). Hence, the necessary oxidation potential is not addressed within the applied conditions. Thus, no amidyl radical can be formed (also see cyclic voltammograms in supporting information). The same strategy was utilized to equip the other side of the biphenyl scaffold with a pyridine moiety (**1r**) to see whether the impact on the oxidation of the starting material would match with **1p**. In that case, the oxidation of the starting material is possible, resulting in a complex mixture but no product. This circumstance leads to the conclusion that the oxidation of the amide moiety is crucial for a successful conversion.

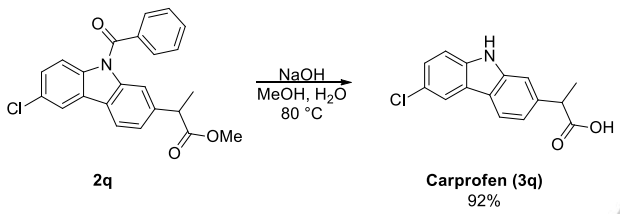

Scheme 2. Deblocking of **2q** to obtain Carprofen (**3q**).

With this method a new and sustainable access to N-protected carbazoles in overall good yields by direct oxidation was accomplished. This valuable alternative to the conventional synthetic routes provides the advantage of a very simple in-cell setup, mediator-, metal catalyst-, and organic oxidizer-free conditions as well as inexpensive and long-lasting electrode materials. Furthermore, reagent waste is minimized, minimal supporting electrolyte concentrations are required, and a high current efficiency is provided. Apart from a broad scope, valuable functionalities, which enable subsequent reactions, are accessible. Besides, this protocol features a route to precursors of a natural product (**2o**) and an active pharmaceutical ingredient (**2q**), which can be easily deblocked in high yields (92%). A scale-up of this reaction on a gram scale is possible as demonstrated for **2h**.

Acknowledgements

The support by the Deutsche Forschungsgemeinschaft (WA 1276/17-2) is highly appreciated.

Keywords: electrochemistry • N,C coupling • heterocyclic chemistry • green chemistry • carbazoles

[1] C. Graebe, C. Glaser, *Liebigs Ann. Chem.* **1872**, *162*, 343–360.
[2] R. Braun, P. Greiff, *Ber. Dtsch. Chem. Ges.* **1872**, *5*, 276–277.
[3] C. Graebe, *Ber. Dtsch. Chem. Ges.* **1872**, *5*, 376–378.
[4] S. Sellamuthu, G. Gutti, D. Kumar, S. Kumar Singh, *Mini-Rev. Org. Chem.* **2018**, *15*, 498–507.
[5] a) A. Zall, D. Kieser, N. Höttecke, E. C. Naumann, B. Thomaszewski, K. Schneider, D. T. Steinbacher, R. Schubenel, S. Masur, K. Baumann et al., *Bioorg. Med. Chem.* **2011**, *19*, 4903–4909; b) S. Thiratmatrakul, C. Yenjai, P. Waiwut, O. Vajragupta, P. Reubroycharoen, M. Tohda, C. Boonyarat, *Eur. J. Med. Chem.* **2014**, *75*, 21–30.
[6] a) F.-F. Zhang, L.-L. Gan, C.-H. Zhou, *Bioorg. Med. Chem. Lett.* **2010**, *20*, 1881–1884; b) P. Rajakumar, K. Sekar, V. Shanmugaiah, N. Mathivanan, *Eur. J. Med. Chem.* **2009**, *44*, 3040–3045.
[7] M. Saravanabhavan, K. Sathya, V. G. Puranik, M. Sekar, *Spectrochim. Acta A* **2014**, *118*, 399–406.
[8] a) G. Surineni, P. Yogeeswari, D. Sriram, S. Kantevari, *Med. Chem. Res.* **2015**, *24*, 1298–1309; b) C. Börger, C. Brütting, K. K. Julich-Gruner, R. Hesse, V. P. Kumar, S. K. Kutz, M. Rönnefahrt, C. Thomas, B. Wan, S. G. Franzblau et al., *Bioorg. Med. Chem.* **2017**, *25*, 6167–6174.
[9] a) L. Sun, Y. Wu, Y. Liu, X. Chen, L. Hu, *Bioorg. Med. Chem. Lett.* **2017**, *27*, 261–265; b) A. Caruso, D. Iacopetta, F. Puoci, A. Rita Capallo, C. Saturnino, M. Stefania Sinicropi, *Mini-Rev. Med. Chem.* **2016**, *16*, 630–643.
[10] N. Blouin, A. Michaud, D. Gendron, S. Wakim, E. Blair, R. Neagu-Plesu, M. Belletête, G. Durocher, Y. Tao, M. Leclerc, *J. Am. Chem. Soc.* **2008**, *130*, 732–742.
[11] A. W. Schmidt, K. R. Reddy, H.-J. Knölker, *Chem. Rev.* **2012**, *112*, 3193–3328.
[12] a) J. A. Jordan-Hore, C. C. C. Johansson, E. M. Beck, M. J. Gaunt, *J. Am. Chem. Soc.* **2008**, *130*, 16184–16186; b) W. C. P. Tsang, N. Zheng, S. L. Buchwald, *J. Am. Chem. Soc.* **2005**, *127*, 14560–14561.
[13] S. H. Cho, J. Yoon, S. Chang, *J. Am. Chem. Soc.* **2011**, *133*, 5996–6005.
[14] K. Takamatsu, K. Hirano, T. Satoh, M. Miura, *Org. Lett.* **2014**, *16*, 2892–2895.
[15] C. Suzuki, K. Hirano, T. Satoh, M. Miura, *Org. Lett.* **2015**, *17*, 1597–1600.
[16] B. J. Stokes, B. Jovanović, H. Dong, K. J. Richert, R. D. Riell, T. G. Driver, *J. Org. Chem.* **2009**, *74*, 3225–3228.
[17] a) W. D. Guerra, R. A. Rossi, A. B. Pierini, S. M. Barolo, *J. Org. Chem.* **2015**, *80*, 928–941; b) C. P. Leslie, R. Di Fabio, F. Bonetti, M. Borriello, S. Braggio, G. Dal Forno, D. Donati, A. Falchi, D. Ghirlanda, R. Giovannini et al., *Bioorg. Med. Chem. Lett.* **2007**, *17*, 1043–1046; c) M. Iwao, H. Takehara, S. Furukawa, M. Watanabe, *Heterocycles* **1993**, *36*, 1483–1488.
[18] T. Horaguchi, T. Oyanagi, E. C. Creencia, K. Tanemura, T. Suzuki, *J. Heterocyclic Chem.* **2004**, *41*, 1–6.
[19] a) B. A. Frontana-Uribe, R. D. Little, J. G. Ibanez, A. Palma, R. Vasquez-Medrano, *Green Chem.* **2010**, *12*, 2099–2119; b) H. J. Schäfer, *C. R. Chim.* **2011**, *14*, 745–765.
[20] a) A. Wiebe, T. Gieshoff, S. Möhle, E. Rodrigo, M. Zirbes, S. R. Waldvogel, *Angew. Chem. Int. Ed.* **2018**, *57*, 5594–5619; *Angew. Chem.* **2018**, *130*, 5694–5721; b) A. Wiebe, D. Schollmeyer, K. M. Dyballa, R. Franke, S. R. Waldvogel, *Angew. Chem. Int. Ed.* **2016**, *55*, 11801–11805; *Angew. Chem.* **2016**, *128*, 11979–11983; c) C. Gütz, M. Selt, M. Bänziger, C. Bucher, C. Römelt, N. Hecken, F. Gallou, T. R. Galvão, S. R. Waldvogel, *Chem. Eur. J.* **2015**, *21*, 13878–13882; d) J. Chen, W.-Q. Yan, C. M. Lam, C.-C. Zeng, L.-M. Hu, R. D. Little, *Org. Lett.* **2015**, *17*, 986–989; e) S. Lips, A. Wiebe, B. Elsler, D. Schollmeyer, K. M. Dyballa, R. Franke, S. R. Waldvogel, *Angew. Chem. Int. Ed.* **2016**, *55*, 10872–10876; *Angew. Chem.* **2016**, *128*, 11031–11035; f) S. Herold, S. Moehle, M. Zirbes, F. Richter, H. Nefzger, S. R. Waldvogel, *Eur. J. Org. Chem.* **2016**, 1274–1278; g) R. Francke, R. D. Little, *J. Am. Chem. Soc.* **2014**, *136*, 427–435; h) S. R. Waldvogel, S. Möhle, *Angew. Chem. Int. Ed.* **2015**, *54*, 6398–6399; *Angew. Chem.* **2015**, *127*, 6496–6497.; i) S. R. Waldvogel, M. Selt, *Angew. Chem. Int. Ed.* **2016**, *55*, 12578–12580; *Angew. Chem.* **2016**, *128*, 12766–12768; j) S. Möhle, M.

Zirbes, E. Rodrigo, T. Gieshoff, A. Wiebe, S. R. Waldvogel, *Angew. Chem. Int. Ed.* **2018**, *57*, 6018–6041; *Angew. Chem.* **2018**, *130*, 6124–6149; k) S. R. Waldvogel, B. Janza, *Angew. Chem. Int. Ed.* **2014**, *53*, 7122–7123; *Angew. Chem.* **2014**, *126*, 7248–7249; l) S. R. Waldvogel, S. Lips, M. Selt, B. Riehl, C. J. Kampf, *Chem. Rev.* **2018**, *118*, 6706–6765; m) T. Morofuji, A. Shimizu, J.-i. Yoshida, *J. Am. Chem. Soc.* **2013**, *135*, 5000–5003; n) M. Yan, Y. Kawamata, P. S. Baran, *Chem. Rev.* **2017**, *117*, 13230–13319.

[21] D. Kajiyama, K. Inoue, Y. Ishikawa, S. Nishiyama, *Tetrahedron* **2010**, *66*, 9779–9784.

[22] T. Broese, R. Francke, *Org. Lett.* **2016**, *18*, 5896–5899.

[23] A. Maity, B. L. Frey, N. Hoskinson, D. Powers, *J. Am. Chem. Soc.* **2020**, accepted, [DOI: 10.1021/jacs.9b13918].

[24] a) J. F. Ambrose, R. F. Nelson, *J. Electrochem. Soc.* **1968**, *115*, 1159–1164; b) J. F. Ambrose, L. L. Carpenter, R. F. Nelson, *J. Electrochem. Soc.* **1975**, *122*, 876–894; c) K. Karon, M. Lapkowski, *J. Solid State Electr.* **2015**, *19*, 2601–2610.

[25] a) G. J. Choi, R. R. Knowles, *J. Am. Chem. Soc.* **2015**, *137*, 9226–9229; b) B. Janza, A. Studer, *J. Org. Chem.* **2005**, *70*, 6991–6994; c) H.-C. Xu, J. M. Campbell, K. D. Moeller, *J. Org. Chem.* **2014**, *79*, 379–391; d) C. Moutrille, S. Z. Zard, *Chem. Commun.* **2004**, 1848–1849; e) K. C. Nicolaou, P. S. Baran, Y.-L. Zhong, S. Barluenga, K. W. Hunt, R. Kranich, J. A. Vega, *J. Am. Chem. Soc.* **2002**, *124*, 2233–2244; f) L. Zhu, P. Xiong, Z.-Y. Mao, Y.-H. Wang, X. Yan, X. Lu, H.-C. Xu, *Angew. Chem. Int. Ed.* **2016**, *55*, 2226–2229.

[26] N. Fuentes, W. Kong, L. Fernández-Sánchez, E. Merino, C. Nevado, *J. Am. Chem. Soc.* **2015**, *137*, 964–973.

[27] S. Z. Zard, *Chem. Soc. Rev.* **2008**, *37*, 1603–1618.

[28] T. Gieshoff, D. Schollmeyer, S. R. Waldvogel, *Angew. Chem. Int. Ed.* **2016**, *55*, 9437–9440; *Angew. Chem.* **2016**, *128*, 9587–9590.

[29] T. Gieshoff, A. Kehl, D. Schollmeyer, K. D. Moeller, S. R. Waldvogel, *J. Am. Chem. Soc.* **2017**, *139*, 12317–12324.

[30] A. Kehl, T. Gieshoff, D. Schollmeyer, S. R. Waldvogel, *Chem. Eur. J.* **2018**, *24*, 590–593.

[31] A. Kehl, V. M. Breising, D. Schollmeyer, S. R. Waldvogel, *Chem. Eur. J.* **2018**, *24*, 17230–17233.

[32] T. Gieshoff, A. Kehl, D. Schollmeyer, K. D. Moeller, S. R. Waldvogel, *Chem. Commun.* **2017**, *53*, 2974–2977.

[33] C. Gütz, B. Klöckner, S.R. Waldvogel, *Org. Process Res. Dev.* **2016**, *20*, 26–32.

[34] a) A. Kirste, M. Nieger, I. M. Malkowsky, F. Stecker, A. Fischer, S. R. Waldvogel, *Chem. Eur. J.* **2009**, *15*, 2273–2277; b) A. Kirste, G. Schnakenburg, F. Stecker, A. Fischer, S. R. Waldvogel, *Angew. Chem. Int. Ed.* **2010**, *49*, 971–975; *Angew. Chem.* **2010**, *122*, 983–987; c) R. Francke, D. Cericola, R. Kötz, D. Weingarth, S. R. Waldvogel, *Electrochim. Acta* **2012**, *62*, 372–380; d) B. Elsler, D. Schollmeyer, K. M. Dyballa, R. Franke, S. R. Waldvogel, *Angew. Chem. Int. Ed.* **2014**, *53*, 5210–5213; *Angew. Chem.* **2014**, *126*, 5311–5314; e) B. Elsler, A. Wiebe, D. Schollmeyer, K. M. Dyballa, R. Franke, S. R. Waldvogel, *Chem. Eur. J.* **2015**, *21*, 12321–12325.

[35] I. Colomer, A. E. R. Chamberlain, M. B. Haughey, T. J. Donohoe, *Nat. Rev. Chem.* **2017**, *1*, 88.

Entry for the Table of Contents (Please choose one layout)

Layout 2:

COMMUNICATION

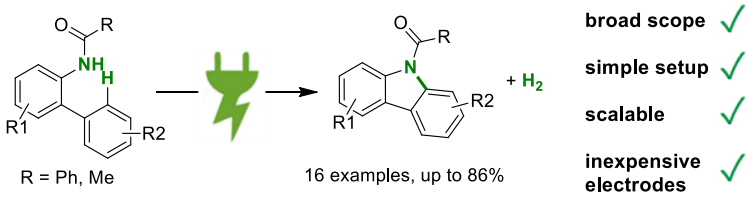

*A. Kehl, N. Schupp, V. M. Breising, D. Schollmeyer, S. R. Waldvogel**

Page No. – Page No.

Electrochemical Synthesis of Carbazoles by Dehydrogenative Coupling Reaction

Direct electrochemical synthesis of N-protected carbazoles in good yields by anodic N,C bond formation. Deblocking of the compounds is demonstrated. Inexpensive electrode materials and a simple, scalable electrolysis setup are employed. Many valuable substituents are tolerated. Access to valuable compounds such as Carprofen is demonstrated.

TABLE OF CONTENTS

General information

All reagents were used in analytical grades and were obtained from commercial sources. Solvents were purified by standard methods.[1]

Column chromatography was performed on silica gel 60 M (0.040-0.063 mm, Macherey-Nagel GmbH & Co, Düren, Germany) with a maximum pressure of 2.0 bar. A preparative chromatography system (Büchi Labortechnik GmbH, Essen, Germany) was used with a Büchi Control Unit C-620, an UV detector Büchi UV photometer C-635, Büchi fraction collector C-660 and two Pump Modules C-605 for adjusting the solvent mixtures. Mixtures of cyclohexane and ethyl acetate were used as eluents. Silica gel 60 sheets on aluminum (F254, Merck, Darmstadt, Germany) were employed for thin layer chromatography.

Gas chromatography was performed on a Shimadzu GC-2025 (Shimadzu, Japan) using a Zebron ZB-5MSi column (Phenomenex, USA; length: 30 m, inner diameter: 0.25 mm, film: 0.25 µm, pre-column: 5 m, carrier gas: hydrogen). GC-MS measurements were carried out on a Shimadzu GC-2010 (Shimadzu, Japan) using a Zebron ZB-5MSi column (Phenomenex, USA; length: 30 m, inner diameter: 0.25 mm, film: 0.25 µm, pre-column: 5 m, carrier gas: helium) combined with a GCMS-QP2010.

Melting points were determined by a M-565 (Büchi, Flawil, Switzerland) with a heating rate of 1 °C per minute and are uncorrected.

Spectroscopy and spectrometry: ^{1}H NMR, ^{13}C NMR and ^{19}F spectra were recorded at 25 °C by using a Bruker Avance II 400 or a Bruker Avance III HD 400 Bruker BioSpin GmbH, Rheinstetten, Germany). Chemical shifts (δ) are reported in parts per million (ppm) relative to TMS as internal standard or traces of $CHCl_3$ or DMSO-d_5 in the corresponding deuterated solvents. For the ^{19}F spectra, α-trifluorotoluene served as external standard (δ = –63.9 ppm).[2] Mass spectra and high-resolution mass spectra were obtained by using an Agilent 6545 QTOF-MS (Agilent, Santa Clara, USA) apparatus employing ESI+.

X-ray analysis: All data were collected on a STOE IPDS2T diffractometer (Oxford Cryostream 700er series, Oxford Cryosystems) using graphite monochromated Mo K_α radiation (λ= 0.71073 Å). Intensities were measured using fine-slicing ω and φ-scans and corrected for background, polarization and Lorentz effects. The structures were solved by direct methods and refined anisotropically by the least-squares procedure implemented in the SHELX program system.[3]

The supplementary crystallographic data for this paper can be obtained free of charge from The Cambridge Crystallographic Data Center via www.ccdc.cam.ac.uk/data_request/cif. Deposition numbers and further details are given with the individual characterization data.

Electrolysis setups

Electrolysis experiments as well as screening studies were conducted in a setup with electrodes in a parallel orientation in a 5 mL Teflon cell[6] (Figure 1, left). This screening setup is also commercially available as IKA Screenings System, IKA-Werke GmbH & Co. KG, Staufen, Germany.

Scale-up reactions were performed in a setup with electrodes in a parallel orientation in a 80 mL beaker-type glass cell[7] (Figure 1, right).

Terminal voltages in the 5 mL Teflon cell are typically around 4–6 V and around 12 V in the 80 mL glass beaker-type cell.

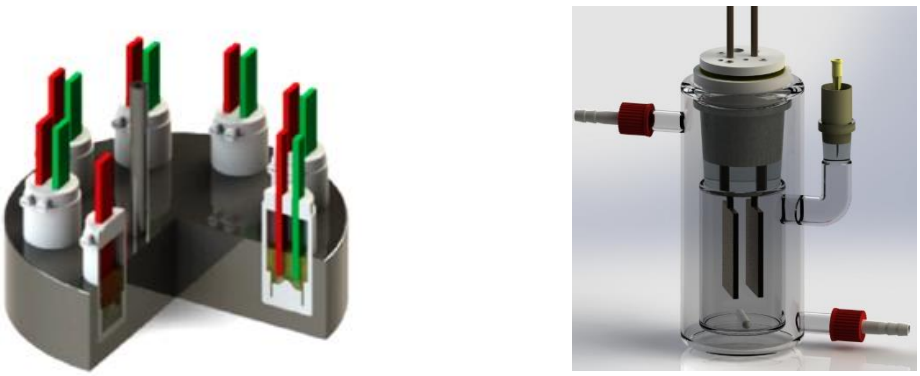

Figure 1: left: 5 mL Teflon cells; right: 80 mL glass beaker-type cell.

The corresponding dimensions of the electrodes are as follows:

For electrodes in the **5 mL Teflon cell**: 7 cm x 1 cm x 0.3 cm.

For electrodes in the **80 mL glass beaker-type cell:** 6 cm x 2 cm x 0.3 cm.

The electrode materials featured in our studies are enlisted in the following:

Isostatic graphite: Highly isostatic graphite Sigrafine™ V2100 was obtained from SGL Carbon, Bonn, Germany. The geometries were machined from a bigger piece.

Boron-doped diamond (BDD): BDD electrode with a 15 µm boron-doped diamond layer on silicon (DIACHEMTM quality) were obtained from CONDIAS GmbH, Itzehoe, Germany.

Glassy carbon: SIGRADUR® G, obtained from HTW Hochtemperatur Werkstoffe GmbH, Thierhaupten, Germany.

Steel: Stainless steel (VA 1.4571). The geometries were machined from a bigger piece.

Nickel: Obtained from IKA Werke GmbH & Co. KG, Staufen, Germany. The geometries were machined from a larger piece.

Platinum: Platinum sheets, 99.9% Pt (thickness: 0.1 mm) obtained from ÖGUSSA Ges.m.b.H., Liesinger-Flur-Gasse 4, 1230 Wien, Austria.

General protocols

Synthesis of starting materials

The required substituted anilines and benzanilides were prepared according to the literature.[4,5]

General protocol for the synthesis of 2-benzamido-biphenyl derivatives A

To a solution of 5.0 mmol (1.0 eqiuv.) of 2-aminobiphenyl and 5.0 mmol (1.0 equiv.) of triethylamine in 20 mL ethyl acetate and a solution of 5.0 mmol (1.0 equiv.) of benzoyl chloride in 10 mL ethyl acetate was added and stirred overnight (ca. 16 h) at room temperature, filtered and the solvent was evaporated at reduced pressure. If further purification was required, the solid was recrystallized from a suitable boiling solvent and was allowed to cool slowly to ambient temperature.

General protocol for the synthesis of 2-benzamido-biphenyl derivatives B

To a solution of 5 mmol (1 equiv.) of a 2-bromoaniline derivative in 25 mL acetonitrile 1 mol% of tetrakis(triphenylphosphine)palladium(0) was added and stirred for 15 minutes at room temperature. After adding 6 eq. of a 2 M potassium carbonate solution and 6 mmol (1.2 equiv.) of an arylboronic acid the solution was heated at 100 °C overnight (ca. 16 h). The solution was brought to room temperature, diluted with water, and extracted by dichloromethane. The combined organic fractions were washed with water, dried with anhydrous magnesium sulfate, filtered through silica, and the solvent was removed at reduced pressure. The residue was used without further purification. To a solution of the crude product in 50 mL ethyl acetate with 1.0 eqiuv. of trimethylamine a solution of 1.0 equiv. of benzoyl chloride in 10 mL ethyl acetate was added and stirred overnight (ca. 16 h) at room temperature, filtered and the solvent was evaporated at reduced pressure. The crude product was recrystallized from a suitable boiling solvent and was allowed to cool to ambient temperature or purified by column chromatography with the following gradient sequence: 5 minutes 100% cyclohexane; elevation of the ethyl acetate amount 0-10% within 30 minutes; if not stated otherwise.

General protocols for the electrochemical synthesis of N-protected carbazole derivatives C

C1: Application of undivided screening cells (5mL)

A solution of 0.2 mmol substrate (e.g., 2-*N*-benzoylamido-biphenyl) and 5 mg (0.0025 M) tetrabutylammonium tetrafluoroborate (NBu_4BF_4) in 4.25 mL 1,1,1,3,3,3-hexafluoro-isopropanol (HFIP) and 0.75 mL H_2O employing a graphite anode and a nickel cathode was electrolyzed. The electrolysis was performed at constant current conditions (current density j = 1 mA/cm^2, active surface 1.5 cm^2). After completion of the reaction according to TLC analysis, HFIP was recycled by distillation at reduced pressure (200-90 mbar, 50 °C). The purification of the product was conducted by column chromatography with the following gradient sequence: 5 minutes 100% cyclohexane; elevation of the ethyl acetate amount 0-1% within 30 minutes; if not stated otherwise.

C2: Application of undivided screening cells (5mL)

A solution of 0.2 mmol substrate (e.g., 2-benzamido-4-fluorobiphenyl) and 5 mg (0.0025 M) tetrabutylammonium tetrafluoroborate (NBu_4BF_4) in 5 mL 1,1,1,3,3,3-hexafluoro-isopropanol

(HFIP) employing a graphite anode and a nickel cathode was electrolyzed. The electrolysis was performed under constant current conditions (current density j = 1 mA/cm^2, active surface 1.5 cm^2). After completion of the reaction according to TLC analysis, HFIP was recycled by distillation at reduced pressure (200-90 mbar, 50 °C). The purification of the product was conducted by column chromatography with the following gradient sequence: 5 minutes 100% cyclohexane; elevation of the ethyl acetate amount 0-1% within 30 minutes; if not stated otherwise.

C3: Application of beaker-type glass cells (80 mL)

Protocol C3 is similar to protocol C1 with the following modifications: 6.3 mmol of substrate and 77 mg (0.0025 M) NBu_4PF_6 are dissolved in 68 mL HFIP and 12 mL of H_2O (current density j = 1 mA/cm^2 active surface 10.0 cm^2)

Additional Data

Optimization Data

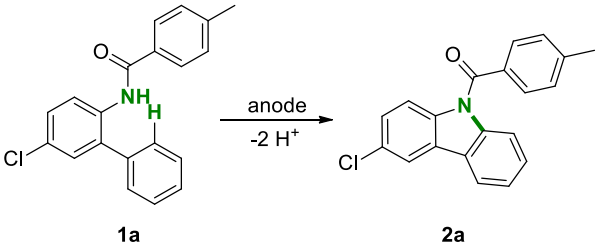

1a 2a

Scheme 1: General conversion strategy for the substrate 1a to the product 2a.

Table S1. Influence of the solvent onto the yield of **2a**.

entry	solvent	conversion [%][a]	yield [%][a]
1	Methanol	19	0
2	Ethanol	10	0
3	Acetonitrile	3	0
4	Dimethylsulfoxide	4	0
5	TFE	80	0
6	**HFIP**	**38**	**21**

0.2 mmol substrate **1a**, 0.0025 m NBu_4PF_6 in 5 mL solvent, anode: highly isostatic graphite, cathode: nickel, charge: 2.1 F, undivided Teflon® cell; [a] based on recovered starting material; [b] isolated yield.

Table S2. Influence of the supporting electrolyte onto the yield of **2a**.

entry	supporting electrolyte	conversion [%][a]	yield [%][a]
1	NBu_4PF_6	38	21
2	NBu_4BF_4	**49**	**30**

0.2 mmol substrate **1a**, in 5 mL HFIP, anode: highly isostatic graphite, cathode: nickel, charge: 2.1 F, undivided Teflon® cell; [a] based on recovered starting material; [b] isolated yield.

Table S3. Influence of water as additive onto the yield of **2a**.

entry	HFIP/H_2O ratio	conversion [%][a]	yield [%][a]
1	HFIP/H_2O(0%)	49	30
2	HFIP/H_2O(5%)	61	39
3	HFIP/H_2O(10%)	73	50
4	**HFIP/H_2O(15%)**	**99**	**65**
5	HFIP/H_2O(20%)	78	54
6	HFIP/H_2O(30%)	54	33
7	HFIP/H_2O(50%)	36	15

0.2 mmol substrate **1a**, 0.0025 m NBu_4BF_4 in 5 mL solvent, anode: highly isostatic graphite, cathode: nickel, charge: 2.1 F, undivided Teflon® cell; [a] based on recovered starting material; [b] isolated yield.

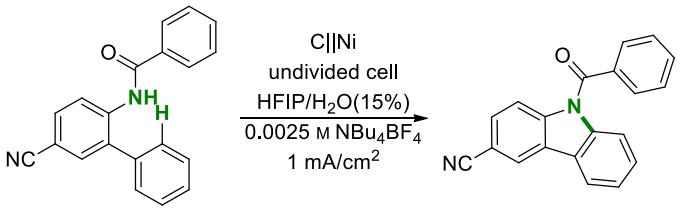

1h **2h**

Scheme 2: Conversion of the substrate 1h to the product 2h.

Table S4. Influence of the substrate concentration onto the yield of **2h**.

entry	substrate concentration [M]	conversion [%][a]	yield [%][a]
1	0.04	99	86
2	0.08	99	85

substrate **1h**, in 4.25 mL/0.75 mL HFIP/H_2O, anode: highly isostatic graphite, cathode: nickel, charge: 2.1 F, undivided Teflon® cell; [a] based on recovered starting material; [b] isolated yield.

Unsuccessful examples:

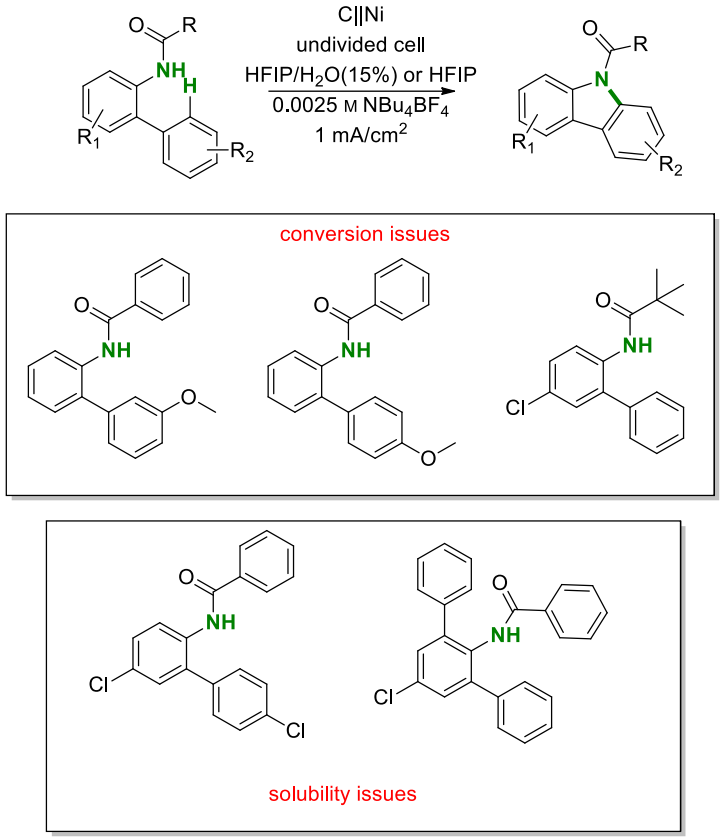

Scheme 3: Overview of all substrates that were unable to yield the desired product with the applied conditions.

Synthesis of 2-Benzamidobiphenyls

5-Chloro-2-(4-methylbenzamido)-biphenyl (1a)

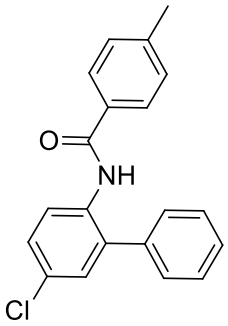

According to protocol B, 1.03 g (5.0 mmol, 1 equiv.) of 2-bromo-4-chloroaniline, 0.73 g (6.0 mmol, 1.2 equiv.) phenylboronic acid, and 0.66 mL (0.77 g, 5 mmol, 1 equiv.) *p*-toluoyl chloride yielded 1.38 g (overall yield: 86%; 4.3 mmol) of product in two steps as colorless crystalline solid after recrystallization from ethyl acetate (20 mL).

^{1}H NMR (400 MHz, $CDCl_3$) δ [ppm] = 8.52 (d, *J* = 8.2 Hz, 1H), 7.93 (s, 1H), 7.57–7.35 (m, 8H), 7.28 (d, *J* = 2.5 Hz, 1H), 7.19 (d, *J* = 8.2 Hz, 2H), 2.37 (s, 3H).

^{13}C NMR (100 MHz, $CDCl_3$) δ [ppm] = 165.0, 142.6, 136.9, 133.9, 133.8, 131.7, 129.8, 129.6, 129.5, 129.3, 129.2, 128.8, 128.6, 126.9, 122.4, 21.6.

HRMS for $C_{20}H_{16}{}^{35}ClNO$ (ESI+) $[M+H]^+$: calc.: 322.0999, found: 322.0987.

MP: 121.8–122.8 °C.

2-Benzamido-5-chlorobiphenyl (1b)

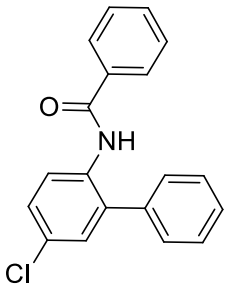

According to protocol B, 1.03 g (5.0 mmol, 1 equiv.) of 2-bromo-4-chloroaniline, 0.73 g (6.0 mmol, 1.2 equiv.) phenylboronic acid, and 0.58 mL (0.70 g, 5 mmol, 1 equiv.) benzoyl chloride yielded 1.23 g (overall yield: 80%; 4.0 mmol) of product in two steps as colorless crystalline solid after recrystallization from cyclohexane (30 mL).

^{1}H NMR (400 MHz, $CDCl_3$) δ [ppm] = 8.52 (d, *J* = 8.9 Hz, 1H), 7.96 (s, 1H), 7.60ff–7.35 (m, 11H), 7.29 (d, *J* = 2.5 Hz, 1H).

^{13}C NMR (100 MHz, $CDCl_3$) δ [ppm] = 164.9, 136.8, 134.4, 133.8, 133.6, 131.9, 129.8, 129.4, 129.3, 129.2, 128.8, 128.7, 128.5, 126.8, 122.3.

HRMS for $C_{19}H_{14}{}^{35}ClNO$ (ESI+) $[M+H]^+$: calc.: 308.0842, found: 308.0837.

MP: 140.3–142.5 °C.

2-Acetamido-5-chlorobiphenyl (1c)

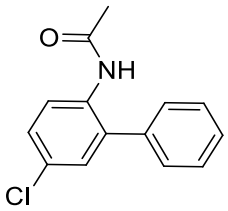

According to literature:[8] To a solution of 0.74 g (3.7 mmol, 1 equiv.) of 2-amino-5-chlorobiphenyl in 20 mL of dichloromethane 0.41 mL (0.45 g, 4.4 mmol, 1.2 equiv.) of acetic anhydride were added dropwise under argon atmosphere. After completion of the reaction (monitored by TLC) the solution was washed with 10 mL of sat. Na_2CO_3, dried with Na_2SO_4 and the solvent removed under at pressure. The reaction yielded 0.83 g (yield: 93%; 3.4 mmol) of product as colorless crystalline solid after recrystallization from n-heptane (20 mL).

^{1}H NMR (400 MHz, $CDCl_3$) δ [ppm] = 8.24 (d, *J* = 8.8 Hz, 1H), 7.53–7.41 (m, 3H), 7.37–7.31(m, 3H), 7.23 (d, *J* = 2.5 Hz, 1H), 7.10 (s, 1H), 2.01 (s, 3H).

^{13}C NMR (100 MHz, $CDCl_3$) δ [ppm] = 168.2, 136.8, 133.6, 133.4, 129.8, 129.3, 129.1, 129.0, 128.5, 128.3, 122.8, 24.6.

HRMS for $C_{14}H_{12}{}^{35}ClNO$ (ESI+) $[M+H]^+$: calc.: 246.0686, found: 246.0683.

MP: 125.8–127.0 °C.

The NMR data are in accordance with previously reported spectra.[9]

2-Benzamidobiphenyl (1d)

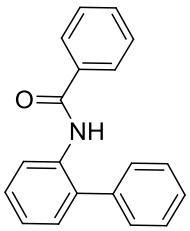

According to the protocol A, 0.85 g (5.0 mmol, 1 equiv.) of 2-aminobiphenyl, 0.69 mL (0.50 g, 2.5 mmol, 1 equiv.) of triethylamine, and 0.58 mL (0.70 g, 5 mmol, 1 equiv.) benzoyl chloride yielded 1.09 g (yield: 80%; 4.0 mmol) of product as colorless crystalline solid after recrystallization from cyclohexane (30 mL).

^{1}H NMR (400 MHz, $CDCl_3$) δ [ppm] = 8.55 (d, *J* = 8.0 Hz, 1H), 8.01 (s, 1H), 7.63–7.58 (m, 2H), 7.55–7.36 (m, 9H), 7.31 (dd, *J* = 8.0, 1.2 Hz, 1H), 7.23 (td, *J* = 8.0, 1.2 Hz, 1H).

^{13}C NMR (100 MHz, $CDCl_3$) δ [ppm] = 165.1, 138.2, 135.1, 134.9, 132.5, 131.9, 130.1, 129.5, 129.4, 128.9, 128.7, 128.3, 126.9, 124.5, 121.3.

HRMS for $C_{19}H_{15}NO$ (ESI+) $[M+H]^+$: calc.: 274.1232, found: 274.1224.

MP: 89.1–90.8 °C.

The NMR data are in accordance with previously reported spectra.[10]

2-Benzamido-4,5-dimethylbiphenyl (1e)

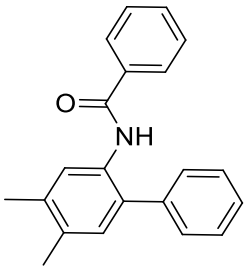

According to protocol A, 0.47 g (2.0 mmol, 1 equiv.) of 2-amino-4,5-dimethylbiphenyl hydrochloride, 0.55 mL (0.41 g, 4 mmol, 2 equiv.) of triethylamine, and 0.23 mL (0.28 g, 2.0 mmol, 1 equiv.) of benzoyl chloride yielded 0.50 g (yield: 83%; 1.6 mmol) of product as colorless crystalline solid after recrystallization from n-heptane (20 mL).

^{1}H NMR (400 MHz, $CDCl_3$) δ [ppm] = 8.29 (s, 1H), 7.90 (s, 1H), 7.65–7.58 (m, 2H), 7.54–7.34 (m, 8H), 7.09 (s, 1H), 2.36 (s, 3H), 2.29 (s, 3H).

^{13}C NMR (100 MHz, $CDCl_3$) δ [ppm] = 165.1, 138.3, 137.1, 135.0, 133.0, 132.5, 131.7, 131.2, 130.3, 129.5, 129.2, 128.8, 128.0, 126.9, 122.7, 20.0, 19.4.

HRMS for $C_{21}H_{19}NO$ (ESI+) $[M+Na]^+$: calc.: 324.1364, found: 324.1362.

MP: 140.1–142.2 °C.

2-Benzamido-5-fluorobiphenyl (1f)

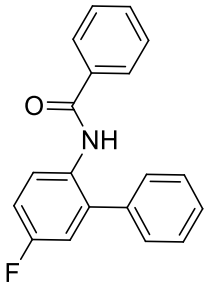

According to the protocol B, 0.57 mL (0.95 g, 5.0 mmol, 1 equiv.) of 2-bromo-4-fluoroaniline, 0.73 g (6.0 mmol, 1.2 equiv.) phenylboronic acid, and 0.58 mL (0.70 g, 5 mmol, 1 equiv.) benzoyl chloride yielded 1.39 g (overall yield: 95%; 4.8 mmol) of product in two steps as colorless crystalline solid after recrystallization from cyclohexane (40 mL).

^{1}H NMR (400 MHz, $CDCl_3$) δ [ppm] = 8.45 (dd, *J* = 9.0, 5.3 Hz, 1H), 7.88 (s, 1H), 7.63–7.57 (m, 2H), 7.57–7.34 (m, 8H), 7.13 (ddd, *J* = 9.0, 8.0, 3.0 Hz, 1H), 7.04 (dd, *J* = 9.0, 3.0 Hz, 1H)

^{13}C NMR (100 MHz, $CDCl_3$) δ [ppm] = 165.2, 159.36 (d, *J* = 244.7 Hz), 137.20 (d, *J* = 1.6 Hz), 134.7, 134.6, 132.0, 131.09 (d, *J* = 2.8 Hz), 129.5, 129.3, 128.9, 128.8, 126.9, 123.42 (d, *J* = 8.1 Hz), 116.79 (d, *J* = 21.8 Hz), 115.18 (d, *J* = 21.8 Hz).

^{19}F NMR (377 MHz, $CDCl_3$) δ [ppm] = -119.0.

HRMS for $C_{19}H_{14}FNO$ (ESI+) $[M+H]^+$: calc.: 292.1138, found: 292.1132.

MP: 113.2–115.0 °C.

2-Benzamido-5-bromobiphenyl (1g)

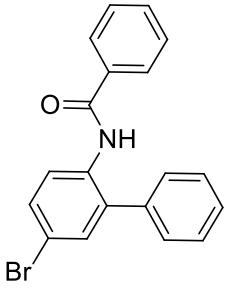

According to protocol A, 0.80 g (3.2 mmol, 1 equiv.) of 2-amino-5-bromobiphenyl and 0.37 mL (0.45 g, 3.2 mmol, 1 equiv.) of benzoyl chloride yielded 0.55 g (yield: 50%; 1.6 mmol) of product as colorless crystalline solid after recrystallization from cyclohexane (25 mL).

^{1}H NMR (400 MHz, $CDCl_3$) δ [ppm] = 8.48 (d, *J* = 8.8 Hz, 1H), 7.96 (s, 1H), 7.62–7.34 (m, 12H).

^{13}C NMR (100 MHz, $CDCl_3$) δ [ppm] = 165.0, 136.8, 134.6, 134.3, 134.2, 132.7, 132.1, 131.6, 129.6, 129.3, 129.0, 128.9, 126.9, 122.6, 117.1.

HRMS for $C_{19}H_{14}{}^{79}BrNO$ (ESI+) $[M+H]^+$: calc.: 352.0337, found: 352.0334.

MP: 159.3–161.0 °C.

2-Benzamido-5-cyanobiphenyl (1h)

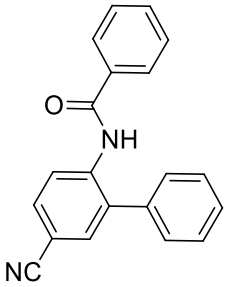

According to the protocol B, 0.99 g (5.0 mmol, 1 equiv.) of 3-bromo-4-aminobenzonitrile, 0.73 g (6.0 mmol, 1.2 equiv.) phenylboronic acid, and 0.58 mL (0.70 g, 5 mmol, 1 equiv.) benzoyl chloride yielded 1.17 g (overall yield: 84%; 3.9 mmol) of product in two steps as colorless crystalline solid after recrystallization from ethyl acetate (25 mL).

^{1}H NMR (400 MHz, $CDCl_3$) δ [ppm] = 8.81 (d, *J* = 8.7 Hz, 1H), 8.21 (s, 1H), 7.72 (dd, *J* = 8.7, 2.0 Hz, 1H), 7.61–7.49 (m, 7H), 7.45–7.37 (m, 4H).

^{13}C NMR (100 MHz, $CDCl_3$) δ [ppm] = 165.1, 139.3, 135.8, 134.1, 133.7, 132.9, 132.5, 132.5, 129.9, 129.4, 129.3, 129.1, 127.0, 120.7, 118.9, 107.3.

HRMS for $C_{20}H_{14}N_2O$ (ESI+) $[M+H]^+$: calc.: 299.1184, found: 299.1179.

MP: 140.4–142.1 °C.

Ethyl 6-benzamido-biphenyl-3-carboxylate (1i)

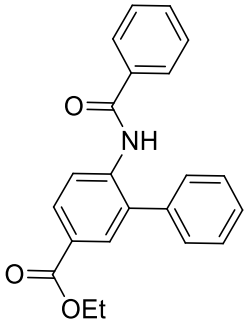

According to the protocol B, 1.22 g (5.0 mmol, 1 equiv.) of ethyl 3-bromo-4-aminobenzoate, 0.73 g (6.0 mmol, 1.2 equiv.) phenylboronic acid, and 0.58 mL (0.70 g, 5 mmol, 1 equiv.) benzoyl chloride yielded 1.42 g (overall yield: 82%; 4.1 mmol) of product in two steps as colorless crystalline solid after recrystallization from ethyl acetate (15 mL).

^{1}H NMR (400 MHz, $CDCl_3$) δ [ppm] = 8.75 (d, *J* = 8.7 Hz, 1H), 8.23 (s, 1H), 8.14 (dd, *J* = 8.7, 2.1 Hz, 1H), 8.02 (d, *J* = 2.1 Hz, 1H), 7.64–7.55 (m, 4H), 7.54–7.47 (m, 4H), 7.42 (dd, *J* = 8.7, 7.0 Hz, 2H), 4.41 (q, *J* = 7.0 Hz, 2H), 1.42 (t, *J* = 7.0 Hz, 3H).

^{13}C NMR (100 MHz, $CDCl_3$) δ [ppm] = 166.1, 164.9, 139.1, 137.1, 134.3, 132.1, 131.5, 131.3, 130.3, 129.5, 129.4, 128.9, 128.7, 126.8, 125.8, 119.8, 61.0, 14.4.

HRMS for $C_{22}H_{19}NO_3$ (ESI+) $[M+H]^+$: calc.: 346.1443, found: 346.1434.

MP: 136.3–138.2 °C.

2-Benzamido-4'-*tert*-butyl-5-chloro-biphenyl (1j)

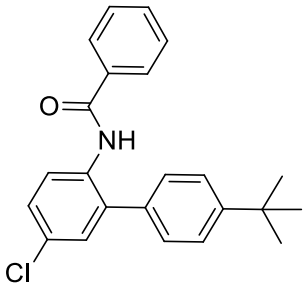

According to the protocol B, 1.03 g (5.0 mmol, 1 equiv.) of 2-bromo-4-chloroaniline, 1.07 g (6.0 mmol, 1.2 equiv.) 4-*tert*-butyl-phenylboronic acid, and 0.58 mL (0.70 g, 5 mmol, 1 equiv.) benzoyl chloride yielded 1.16 g (overall yield: 64%; 3.2 mmol) of product in two steps as colorless crystalline solid after purification by column chromatography.

^{1}H NMR (400 MHz, $CDCl_3$) δ [ppm] = 8.51 (d, *J* = 8.9 Hz, 1H), 7.99 (s, 1H), 7.62–7.52 (m, 4H), 7.52–7.45 (m, 1H), 7.42–7.33 (m, 5H), 7.30 (d, *J* = 2.5 Hz, 1H), 1.39 (s, 9H).

^{13}C NMR (100 MHz, $CDCl_3$) δ [ppm] = 165.0, 152.0, 134.7, 133.9, 133.8, 133.8, 132.0, 129.8, 129.3, 129.0, 128.9, 128.4, 127.0, 126.5, 122.2, 34.9, 31.4.

HRMS for $C_{23}H_{22}{}^{35}ClNO$ (ESI+) $[M+H]^+$: calc.: 364.1468, found: 364.1466.

MP: 117.1–119.8 °C.

2-Benzamido-4’-chloro-5-methyl-biphenyl (1k)

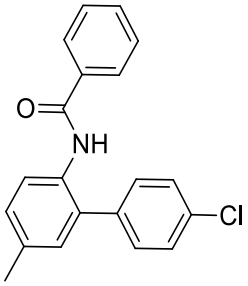

According to protocol B, 0.62 mL (0.93 g, 5.0 mmol, 1 equiv.) of 2-bromo-4-methylaniline, 0.94 g (6.0 mmol, 1.2 equiv.) 4-chloro-phenylboronic acid, and 0.58 mL (0.70 g, 2 mmol, 1 equiv.) benzoyl chloride yielded 1.28 g (overall yield: 80%; 4.0 mmol) of product in two steps as colorless crystalline solid after recrystallization from cyclohexane (30 mL).

^{1}H NMR (400 MHz, $CDCl_3$) δ [ppm] = 8.26 (d, *J* = 8.3 Hz, 1H), 7.78 (s, 1H), 7.67–7.59 (m, 2H), 7.55–7.34 (m, 7H), 7.28–7.21 (m, 1H), 7.09 (d, *J* = 2.1 Hz, 1H), 2.38 (s, 3H).

^{13}C NMR (100 MHz, $CDCl_3$) δ [ppm] = 165.3, 136.9, 134.8, 134.7, 134.2, 132.2, 131.9, 131.8, 130.8, 130.7, 129.6, 129.4, 128.9, 126.9, 122.4, 21.0.

HRMS for $C_{20}H_{16}{}^{35}ClNO$ (ESI+) $[M+H]^+$: calc.: 322.0999, found: 322.0994.

MP: 175.2–176.3 °C.

3’-Acetyl-2-benzamido-5-chloro-biphenyl (1l)

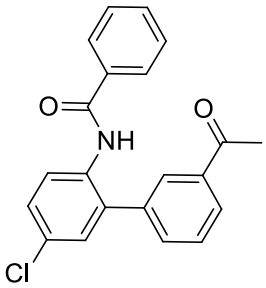

According to protocol B, 0.41 g (2.0 mmol, 1 equiv.) of 2-bromo-4-chloroaniline, 0.37 g (2.4 mmol, 1.2 equiv.) 3-acetyl-phenylboronic acid, and 0.23 mL (0.28 g, 2 mmol, 1 equiv.) benzoyl chloride yielded 0.59 g (overall yield: 85%; 1.7 mmol) of product in two steps as colorless crystalline solid after recrystallization from cyclohexane (20 mL).

^{1}H NMR (400 MHz, $CDCl_3$) δ [ppm] = 8.41 (d, *J* = 8.8 Hz, 1H), 8.05–7.99 (m, 2H), 7.83 (s, 1H), 7.66–7.56 (m, 4H), 7.53–7.45 (m, 1H), 7.45–7.33 (m, 3H), 7.31 (d, *J* = 2.5 Hz, 1H), 2.60 (s, 3H).

^{13}C NMR (100 MHz, $CDCl_3$) δ [ppm] = 197.5, 165.4, 138.2, 137.6, 134.4, 133.8, 133.6, 133.4, 132.2, 130.0, 129.9, 129.8, 129.1, 129.0, 128.5, 126.9, 126.8, 123.5, 26.8.

HRMS for $C_{21}H_{16}{}^{35}ClNO_2$ (ESI+) $[M+H]^+$: calc.: 372.0767, found: 372.0759.

MP: 139.2–140.4 °C.

2-Benzamido-5-chloro-4'-nitrobiphenyl (1m)

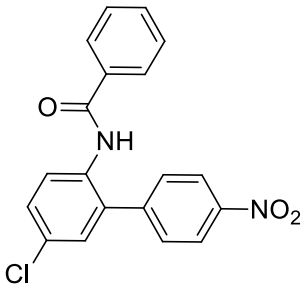

According to protocol B, 0.41 g (2.0 mmol, 1 equiv.) of 2-bromo-4-chloroaniline, 0.40 g (2.4 mmol, 1.2 equiv.) 4-nitro-phenylboronic acid, and 0.23 mL (0.28 g, 2 mmol, 1 equiv.) benzoyl chloride yielded 0.26 g (overall yield: 35%; 0.7 mmol) of product in two steps as yellow crystalline solid after purification by column chromatography (gradient 95:5 (cyclohexane:ethyl acetate)).

^{1}H NMR (400 MHz, $CDCl_3$) δ [ppm] = 8.39–8.35 (m, 2H), 8.29 (d, *J* = 8.8 Hz, 1H), 7.71 (s, 1H), 7.67–7.60 (m, 4H), 7.58–7.52 (m, 1H), 7.49–7.41 (m, 3H), 7.33 (d, *J* = 2.5 Hz, 1H).

^{13}C NMR (100 MHz, $CDCl_3$) δ [ppm] = 165.4, 147.8, 143.8, 133.9, 133.1, 132.8, 132.3, 130.6, 130.2, 129.7, 129.6, 129.0, 126.8, 124.6, 124.4.

HRMS for $C_{19}H_{13}{}^{35}ClN_2O_3$ (ESI+) $[M+H]^+$: calc.: 353.0693, found: 353.0686.

MP: 175.9–177.1 °C.

2-Benzamido-5-chloro-3'-methoxybiphenyl (1n)

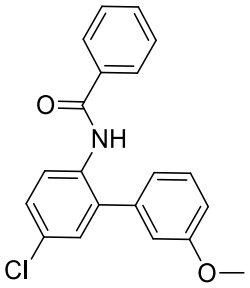

According to protocol B, 0.41 g (2.0 mmol, 1 equiv.) of 2-bromo-4-chloroaniline, 0.37 g (2.4 mmol, 1.2 equiv.) 3-methoxyphenylboronic acid, and 0.23 mL (0.28 g, 2 mmol, 1 equiv.) benzoyl chloride yielded 0.60 g (overall yield: 89%; 1.8 mmol) of product in two steps as colorless crystalline solid after recrystallization from n-heptane (70 mL).

^{1}H NMR (400 MHz, $CDCl_3$) δ [ppm] = 8.53 (d, *J* = 8.9 Hz, 1H), 8.06 (s, 1H), 7.64–7.57 (m, 2H), 7.52–7.36 (m, 5H), 7.30 (d, *J* = 2.5 Hz, 1H), 7.04–6.97 (m, 2H), 6.93 (t, *J* = 2.5 Hz, 1H), 3.82 (s, 3H).

^{13}C NMR (100 MHz, $CDCl_3$) δ [ppm] = 165.1, 160.5, 138.2, 134.6, 133.8, 133.7, 132.1, 130.6, 129.7, 129.3, 129.0, 128.6, 126.9, 122.3, 121.3, 114.7, 114.6, 55.5.

HRMS for $C_{20}H_{16}{}^{35}ClNO_2$ (ESI+) $[M+H]^+$: calc.: 338.0948, found: 338.0942.

MP: 112.6–114.1 °C.

2-Benzamido-3'-methoxy-5-methyl-biphenyl (1o)

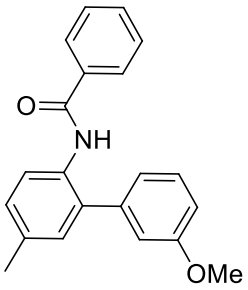

According to protocol B, 0.62 mL (0.93 g, 5.0 mmol, 1 equiv.) of 2-bromo-4-methylaniline, 0.91 g (6.0 mmol, 1.2 equiv.) 3-methoxyphenylboronic acid, and 0.58 mL (0.70 g, 2 mmol, 1 equiv.) benzoyl chloride yielded 0.86 g (overall yield: 54%; 2.7 mmol) of product in two steps as colorless crystalline solid after purification by column chromatography .

^{1}H NMR (400 MHz, $CDCl_3$) δ [ppm] = 8.42 (d, *J* = 8.3 Hz, 1H), 8.04 (s, 1H), 7.67–7.63 (m, 2H), 7.53–7.47 (m, 1H), 7.47–7.38 (m, 3H), 7.29–7.25 (m, 1H), 7.17–7.14 (m, 1H), 7.06–7.03 (m, 1H), 7.02–6.97 (m, 2H), 3.84 (s, 3H), 2.41 (s, 3H).

^{13}C NMR (100 MHz, $CDCl_3$) δ [ppm] = 164.9, 160.2, 139.6, 134.9, 134.0, 132.4, 132.2, 131.6, 130.4, 130.1, 129.1, 128.7, 126.8, 121.4, 121.3, 114.7, 113.9, 55.3, 20.9.

HRMS for $C_{21}H_{19}NO_2$ (ESI+) $[M+H]^+$: calc.: 318.1494, found: 318.1488.

MP: 95.1–96.6 °C.

4-Benzamido-3-phenylpyridine (1p)

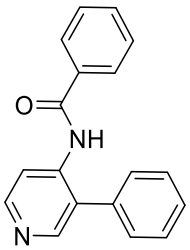

According to protocol B, 0.87 g (5.0 mmol, 1 equiv.) of 4-amino-3-bromopyridine, 0.73 g (6.0 mmol, 1.2 equiv.) phenylboronic acid, and 0.58 mL (0.70 g, 5 mmol, 1 equiv.) benzoyl chloride yielded 1.01 g (overall yield: 74%; 3.7 mmol) of product in two steps as slightly yellowish crystalline solid after column chromatography.

^{1}H NMR (400 MHz, $CDCl_3$) δ [ppm] = 8.64–8.56 (m, 2H), 8.48 (s, 1H), 8.23 (s, 1H), 7.64–7.56 (m, 4H), 7.55–7.50 (m, 2H), 7.48–7.39 (m, 4H).

^{13}C NMR (100 MHz, $CDCl_3$) δ [ppm] = 165.4, 150.5, 150.4, 142.2, 134.3, 134.0, 132.6, 129.9, 129.5, 129.2, 129.1, 127.0, 126.5, 113.7.

HRMS for $C_{18}H_{14}N_2O$ (ESI+) $[M+H]^+$: calc.: 275.1184, found: 275.1177.

MP: 125.1–126.6 °C.

Methyl 2-(2'-benzamido-5'-chloro-[1,1'-biphenyl]-4'-yl)propanoate (1q)

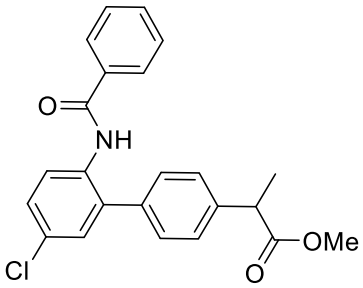

According to report:[11] In a dry 100 mL round bottom Schlenk flask, 0.25 g (1.1 mmol, 1.1 equiv.) 2-(4-(4,4,5,5-tetramethyl-1,3,2-dioxaborolan-2-yl)phenyl)-propanoate, 0.55 g (4.0 mmol, 4.0 equiv.) K_2CO_3, and 37 mg (5 mol%) $PdCl_2$(dppf) were dissolved in a solution containing 10 mL dioxane and 4 mL H_2O. 0.36 g (1.0 mmol, 1.0 equiv.) of *N*-(4-chloro-2-iodophenyl)benzamide were added, and the resulting mixture was heated at 80 °C for 1.5 hours. After cooling, the reaction solution was diluted with 10 mL of a 1.5 M NaOH solution and 30 mL of CH_2Cl_2. The aqueous layer was extracted with 3 × 30 mL of CH_2Cl_2. The combined organic fractions were dried over $MgSO_4$ and filtered through silica. The reaction yielded 0.37 g (yield: 93%; 0.9 mmol) of product as colorless highly viscous oil after purification by column chromatography (cyclohexane:ethyl acetate 7:3).

^{1}H NMR (400 MHz, $CDCl_3$) δ [ppm] = 8.50 (d, *J* = 8.8 Hz, 1H), 7.93 (s, 1H), 7.62–7.58 (m, 2H), 7.54–7.46 (m, 3H), 7.44–7.38 (m, 5H), 7.30 (d, *J* = 2.5 Hz, 1H), 3.84 (q, *J* = 7.2 Hz, 1H), 3.73 (s, 3H), 1.59 (d, *J* = 7.2 Hz, 3H).

^{13}C NMR (100 MHz, $CDCl_3$) δ [ppm] = 174.6, 164.9, 141.2, 135.6, 134.4, 133.6, 133.5, 131.9, 129.7, 129.5, 129.4, 128.8, 128.6, 128.5, 126.8, 122.4, 52.2, 45.2, 18.6.

HRMS for $C_{23}H_{20}{}^{35}ClNO_3$ (ESI+) $[M+H]^+$: calc.: 394.1210, found: 394.1201.

***N*-(4-Chloro-2-(pyridine-4-yl)phenyl)benzamide (1r)**

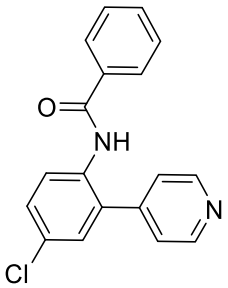

According to the same experimental protocol as for **1p**: 4-pyridineboronic acid 0.27 g (2.2 mmol, 1.3 equiv.), 1.11 g (8.0 mmol, 4.0 equiv.) K_2CO_3, and 73 mg (5 mol%) $PdCl_2$(dppf) were dissolved in a solution containing 20 mL dioxane and 8 mL H_2O. 0.72 g (1.7 mmol, 1.0 equiv.) *N*-(4-chloro-2-iodophenyl)benzamide were added, and the resulting mixture was heated at 80 °C for 1.5 hours. After cooling, the reaction solution was diluted with 10 mL of a 1.5 M NaOH solution and 30 mL of CH_2Cl_2. The aqueous layer was extracted by 3 × 30 mL of CH_2Cl_2. The combined organic fractions was dried over $MgSO_4$ and filtered through silica. The filtrate was concentrated under reduced pressure to afford a colorless crystalline solid. Washing with 15 mL cyclohexane yielded 0.48 g (yield: 81%; 1.4 mmol) of product.

^{1}H NMR (400 MHz, $CDCl_3$) δ [ppm] = 8.79–8.75 (m, 2H), 8.38 (d, *J* = 8.8 Hz, 1H), 7.79 (s, 1H), 7.66–7.61 (m, 2H), 7.57–7.52 (m, 1H), 7.50–7.41 (m, 3H), 7.41–7.38 (m, 2H), 7.32 (d, *J* = 2.5 Hz, 1H).

^{13}C NMR (100 MHz, $CDCl_3$) δ [ppm] = 165.2, 150.8, 145.1, 134.0, 133.1, 132.3, 131.8, 130.3, 129.7, 129.4, 129.0, 126.8, 124.0, 123.8.

HRMS for $C_{18}H_{13}{}^{35}ClN_2O$ (ESI+) $[M+H]^+$: calc.: 309.0795, found: 309.0786.

MP: 201.3–203.1 °C.

Synthesis of N-protected carbazoles

3-Chloro-9-(4-methylbenzoyl)-carbazole (2a)

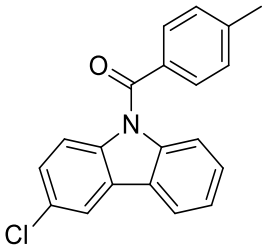

According to protocol C1, 64 mg (0.20 mmol, 1 equiv.) of **1a** and 5 mg NBu_4BF_4 in HFIP/H_2O (4.25/0.75 mL) were electrolyzed in a 5 mL screening cell. An amount of 2.1 F of electric charge was applied to afford 42 mg (yield: 65%; 0.13 mmol) of a colorless crystalline solid.

^{1}H NMR (300 MHz, $CDCl_3$) δ [ppm] = 8.01–7.96 (m, 2H), 7.64 (d, *J* = 8.2 Hz, 2H), 7.54 (d, *J* = 8.9 Hz, 1H), 7.51–7.45 (m, 1H), 7.40–7.30 (m, 5H), 2.52 (s, 3H).

^{13}C NMR (75 MHz, $CDCl_3$) δ [ppm] = 169.4, 143.5, 139.6, 137.6, 132.4, 129.6, 129.4, 128.8, 127.3, 127.2, 126.7, 124.8, 123.4, 120.0, 119.6, 116.8, 115.8, 21.8.

HRMS for $C_{20}H_{14}{}^{35}ClNO$ (ESI+) $[M+H]^+$: calc.: 320.0842, found: 320.0833.

MP: 150.9–151.6 °C (cyclohexane/ethyl acetate).

9-Benzoyl-3-chlorocarbazole (2b)

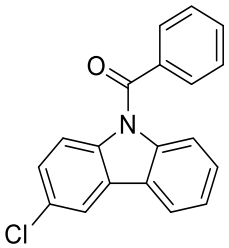

According to protocol C1, 62 mg (0.20 mmol, 1 equiv.) of **1b** and 5 mg NBu_4BF_4 in HFIP/H_2O (4.25/0.75 mL) were electrolyzed in a 5 mL screening cell. An amount of 2.1 F of electric charge was applied to afford 39 mg (yield: 64%; 0.13 mmol) of a colorless crystalline solid.

^{1}H NMR (400 MHz, $CDCl_3$) δ [ppm] = 8.01–7.96 (m, 2H), 7.75–7.66 (m, 3H), 7.59–7.51 (m, 3H), 7.46–7.42 (m, 1H), 7.40–7.33 (m, 2H), 7.33–7.29 (m, 1H).

^{13}C NMR (100 MHz, $CDCl_3$) δ [ppm] = 169.4, 139.5, 137.5, 135.4, 132.6, 129.1, 129.0, 128.9, 127.5, 127.4, 126.8, 125.0, 123.6, 120.0, 119.7, 116.9, 115.8.

HRMS for $C_{19}H_{12}{}^{35}ClNO$ (ESI+) $[M+H]^+$: calc.: 306.0686, found: 306.0681.

MP: 113.2–115.9 °C (cyclohexane/ethyl acetate).

9-Acetyl-3-chlorocarbazole (2c)

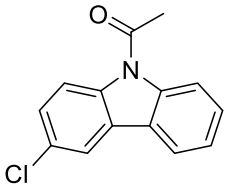

According to protocol C1, 49 mg (0.20 mmol, 1 equiv.) of **1c** and 5 mg NBu_4BF_4 in HFIP/H_2O (4.25/0.75 mL) were electrolyzed in a 5 mL screening cell. An amount of 2.1 F of electric charge was applied to afford 26 mg (yield: 53%; 0.11 mmol) of a colorless crystalline solid.

^{1}H NMR (400 MHz, $CDCl_3$) δ [ppm] = 8.24 (d, *J* = 8.6 Hz, 1H), 8.11 (d, *J* = 8.6 Hz, 1H), 7.96–7.93 (m, 1H), 7.92 (d, *J* = 1.4 Hz, 1H), 7.53 (ddd, *J* = 8.6, 7.3, 1.4 Hz, 1H), 7.45–7.39 (m, 2H), 2.88 (s, 3H).

^{13}C NMR (100 MHz, $CDCl_3$) δ [ppm] = 169.8, 138.8, 137.1, 129.3, 128.0, 127.7, 127.3, 125.4, 123.8, 120.2, 119.5, 117.6, 116.0, 27.7.

HRMS for $C_{14}H_{10}{}^{35}ClNO$ (ESI+) $[M+H]^+$: calc.: 244.0529, found: 244.0520.

MP: 124.8–125.9 °C (cyclohexane/ethyl acetate).

The NMR data are in accordance with previously reported spectra.[9]

9-Benzoylcarbazole (2d)

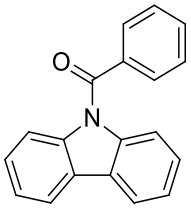

According to protocol C1, 55 mg (0.20 mmol, 1 equiv.) of **1d** and 5 mg NBu_4BF_4 in HFIP/H_2O (4.25/0.75 mL) were electrolyzed in a 5 mL screening cell. An amount of 2.1 F of electric charge was applied to afford 20 mg (yield: 37%; 0.07 mmol) of a colorless crystalline solid.

^{1}H NMR (400 MHz, $CDCl_3$) δ [ppm] = 8.07–8.01 (m, 2H), 7.78–7.73 (m, 2H), 7.71–7.65 (m, 1H), 7.58–7.52 (m, 4H), 7.41–7.32 (m, 4H).

^{13}C NMR (100 MHz, $CDCl_3$) δ [ppm] = 169.6, 139.2, 135.8, 132.4, 129.1, 128.9, 126.7, 126.0, 123.4, 119.8, 115.8.

HRMS for $C_{19}H_{13}NO$ (ESI+) $[M+H]^+$: calc.: 272.1075, found: 272.1072.

MP: 98.0–100.0 °C (cyclohexane/ethyl acetate).

The NMR data are in accordance with previously reported spectra.[10]

9-Benzoyl-2,3-dimethylcarbazole (2e)

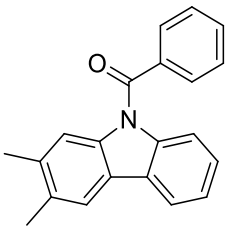

According to protocol C2, 60 mg (0.20 mmol, 1 equiv.) of **1e** and 5 mg NBu_4BF_4 in 5 mL of HFIP were electrolyzed in a 5 mL screening cell. An amount of 2.5 F of electric charge was applied to afford 20 mg (yield: 33%; 0.07 mmol) of a colorless crystalline solid.

^{1}H NMR (400 MHz, $CDCl_3$) δ [ppm] = 7.98–7.94 (m, 1H), 7.78 (s, 1H), 7.75–7.71 (m, 2H), 7.69–7.64 (m, 1H), 7.57–7.52 (m, 2H), 7.43–7.38 (m, 2H), 7.33 (td, *J* = 7.4, 1.2 Hz, 1H), 7.29–7.24 (m, 1H), 2.43 (s, 3H), 2.32 (s, 3H).

^{13}C NMR (100 MHz, $CDCl_3$) δ [ppm] = 169.6, 139.1, 137.9, 136.0, 135.9, 132.2, 132.1, 129.0, 128.8, 126.3, 126.0, 124.1, 123.3, 120.2, 119.4, 116.6, 115.8, 20.8, 20.0.

HRMS for $C_{21}H_{17}NO$ (ESI+) $[M+H]^+$: calc.: 300.1388, found: 300.1384.

MP: 111.2–112.8 °C (cyclohexane/ethyl acetate).

9-Benzoyl-3-fluorocarbazole (2f)

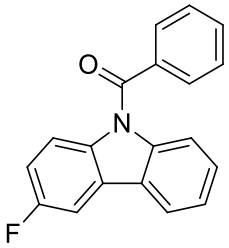

According to protocol C2, 58 mg (0.20 mmol, 1 equiv.) of **1f** and 5 mg NBu_4BF_4 in 5 mL of HFIP were electrolyzed in a 5 mL screening cell. An amount of 2.4 F of electric charge was applied to afford 29 mg (yield: 50%; 0.10 mmol) of a colorless crystalline solid.

^{1}H NMR (400 MHz, $CDCl_3$) δ [ppm] = 7.98–7.93 (m, 1H), 7.73–7.63 (m, 4H), 7.59 (dd, *J* = 9.0, 4.4 Hz, 1H), 7.56–7.51 (m, 2H), 7.39–7.29 (m, 3H), 7.06 (td, *J* = 9.0, 2.7 Hz, 1H).

^{13}C NMR (100 MHz, $CDCl_3$) δ [ppm] = 169.4, 159.5 (d, *J* = 244.0 Hz), 139.8, 135.6, 135.4, 132.5, 129.0, 127.4, 127.3, 127.2, 125.4 (d, *J* = 4.0 Hz), 123.5, 120.1, 117.0 (d, *J* = 9.0 Hz), 115.9, 114.2 (d, *J* = 24.0 Hz), 105.8 (d, *J* = 24.0 Hz).

^{19}F NMR (377 MHz, $CDCl_3$) δ [ppm] = -120.2.

HRMS for $C_{19}H_{12}FNO$ (ESI+) $[M+H]^+$: calc.: 290.0981, found: 290.0976.

MP: 130.5–131.9 °C (cyclohexane/ethyl acetate).

9-Benzoyl-3-bromocarbazole (2g)

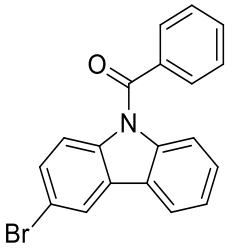

According to protocol C1, 70 mg (0.20 mmol, 1 equiv.) of **1g** and 5 mg NBu_4BF_4 in HFIP/H_2O (4.25/0.75 mL) were electrolyzed in a 5 mL screening cell. An amount of 2.1 F of electric charge was applied to afford 48 mg (yield: 69%; 0.14 mmol) of a colorless crystalline solid.

^{1}H NMR (400 MHz, $CDCl_3$) δ [ppm] = 8.13 (m, 1H), 7.99–7.94 (m, 1H), 7.75–7.66 (m, 3H), 7.58–7.53 (m, 2H), 7.48–7.41 (m, 3H), 7.40–7.32 (m, 2H).

^{13}C NMR (100 MHz, $CDCl_3$) δ [ppm] = 169.3, 139.4, 137.9, 135.4, 132.6, 129.5, 129.1, 129.0, 127.8, 127.4, 124.8, 123.7, 122.7, 120.0, 117.3, 116.6, 115.8.

HRMS for $C_{19}H_{12}{}^{79}BrNO$ (ESI+) $[M+H]^+$: calc.: 350.0181, found: 350.0172.

MP: 121.6–123.8 °C (cyclohexane/ethyl acetate).

The NMR data was in accordance with previously reported spectra.[12]

9-Benzoyl-3-cyanocarbazole (2h)

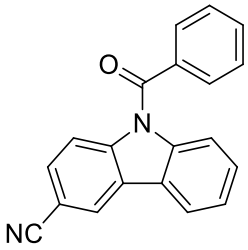

According to protocol C1, 60 mg (0.20 mmol, 1 equiv.) of **1h** and 5 mg NBu_4BF_4 in HFIP/H_2O (4.25/0.75 mL) were electrolyzed in a 5 mL screening cell. An amount of 2.8 F of electric charge was applied to afford 51 mg (yield: 86%; 0.17 mmol) of a colorless crystalline solid.

Large scale: According to protocol C3, 1.89 g (6.3 mmol, 1 equiv.) of **1h** and 77 mg NBu_4BF_4 in HFIP/H_2O (68 mL/12 mL) were electrolyzed in a 80 mL beaker-type cell. An amount of 2.8 F of electric charge was applied to afford 1.56 g (yield: 83%; 5.2 mmol) of a colorless crystalline solid.

^{1}H NMR (400 MHz, $CDCl_3$) δ [ppm] = 8.33 (dd, *J* = 1.6, 0.7 Hz, 1H), 8.07–8.03 (m, 1H), 7.77–7.68 (m, 4H), 7.64–7.55 (m, 3H), 7.46–7.39 (m, 3H).

^{13}C NMR (100 MHz, $CDCl_3$) δ [ppm] = 169.4, 141.3, 139.7, 134.8, 133.3, 130.1, 129.4, 129.3, 128.2, 126.4, 124.5, 124.4, 124.1, 120.4, 119.4, 116.5, 115.8, 106.7.

HRMS for $C_{20}H_{12}N_2O$ (ESI+) $[M+H]^+$: calc.: 297.1028, found: 297.1022.

MP: 164.8–166.4 °C (cyclohexane/ethyl acetate).

Ethyl 9-benzoylcarbazole-3-carboxylate (2i)

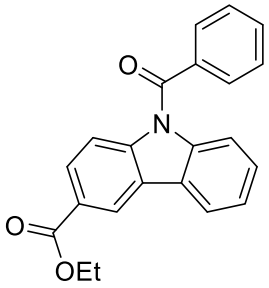

According to protocol C1, 69 mg (0.20 mmol, 1 equiv.) of **1i** and 5 mg NBu_4BF_4 in HFIP/H_2O (4.25/0.75 mL) were electrolyzed in a 5 mL screening cell. An amount of 2.1 F of electric charge was applied to afford 58 mg (yield: 84%; 0.07 mmol) of a colorless crystalline solid.

^{1}H NMR (400 MHz, $CDCl_3$) δ [ppm] = 8.73 (dd, *J* = 1.8, 0.6 Hz, 1H), 8.12–8.08 (m, 1H), 8.05 (dd, *J* = 8.7, 1.8 Hz, 1H), 7.77–7.73 (m, 2H), 7.72–7.67 (m, 1H), 7.59–7.50 (m, 4H), 7.43–7.35 (m, 2H), 4.46 (q, *J* = 7.0 Hz, 2H), 1.47 (t, *J* = 7.0 Hz, 3H).

^{13}C NMR (100 MHz, $CDCl_3$) δ [ppm] = 169.5, 166.6, 141.9, 139.7, 135.2, 132.8, 129.2, 129.0, 128.0, 127.3, 125.9, 125.6, 125.5, 123.8, 121.8, 120.2, 115.7, 115.2, 61.1, 14.5.

HRMS for $C_{22}H_{17}NO_3$ (ESI+) $[M+H]^+$: calc.: 344.1287, found: 344.1280.

MP: 122.2–123.8 °C (cyclohexane/ethyl acetate).

9-Benzoyl-7-*tert*-butyl-3-chlorocarbazole (2j)

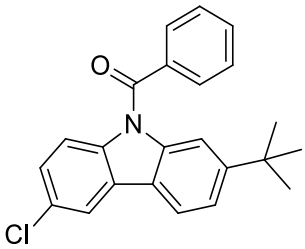

According to protocol C1, 72 mg (0.20 mmol, 1 equiv.) of **1j** and 5 mg NBu_4BF_4 in HFIP/H_2O (4.25/0.75 mL) were electrolyzed in a 5 mL screening cell. An amount of 2.2 F of electric charge was applied to afford 39 mg (yield: 54%; 0.11 mmol) of a colorless crystalline solid.

^{1}H NMR (400 MHz, $CDCl_3$) δ [ppm] = 7.94 (dd, *J* = 2.1, 0.6 Hz, 1H), 7.88 (dd, *J* = 8.2, 0.6 Hz, 1H), 7.75–7.65 (m, 4H), 7.60–7.53 (m, 2H), 7.42 (dd, *J* = 8.2, 2.1 Hz, 1H), 7.33–7.29 (m, 2H), 1.24 (s, 1H).

^{13}C NMR (100 MHz, $CDCl_3$) δ [ppm] = 169.5, 151.0, 139.7, 137.8, 135.7, 132.4, 129.1, 129.0, 128.9, 127.5, 126.4, 122.6, 121.3, 119.5, 119.4, 117.0, 112.9, 35.2, 31.4.

HRMS for $C_{23}H_{20}{}^{35}ClNO$ (ESI+) $[M+H]^+$: calc.: 362.1312, found: 362.1304.

MP: 119.0–121.8 °C (cyclohexane/ethyl acetate).

9-Benzoyl-2-chloro-6-methylcarbazole (2k)

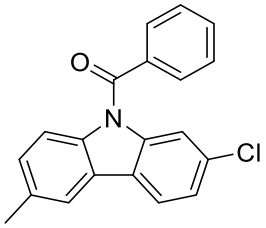

According to protocol C2, 64 mg (0.20 mmol, 1 equiv.) of **1k** and 5 mg NBu_4BF_4 in 5 mL of HFIP were electrolyzed in a 5 mL screening cell. An amount of 2.1 F of electric charge was applied to afford 20 mg (yield: 31%; 0.06 mmol) of a colorless crystalline solid.

^{1}H NMR (400 MHz, $CDCl_3$) δ [ppm] = 7.89 (d, *J* = 8.3 Hz, 1H), 7.78–7.66 (m, 5H), 7.59–7.53 (m, 2H), 7.35 (dd, *J* = 8.3, 1.8 Hz, 1H), 7.17–7.09 (m, 2H), 2.50 (s, 3H).

^{13}C NMR (100 MHz, $CDCl_3$) δ [ppm] = 169.3, 139.9, 137.4, 135.4, 133.4, 132.5, 132.4, 129.0, 128.9, 128.0, 125.5, 124.5, 123.9, 120.4, 119.9, 116.3, 115.4, 21.3.

HRMS for $C_{20}H_{14}{}^{35}ClNO$ (ESI+) $[M+H]^+$: calc.: 320.0842, found: 320.0832.

MP: 115.2–117.2 °C (cyclohexane/ethyl acetate).

6-Acetyl-9-benzoyl-3-chlorocarbazole (2l)

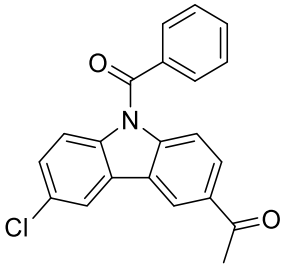

According to protocol C2, 70 mg (0.20 mmol, 1 equiv.) of **1l** and 5 mg NBu_4BF_4 in 5 mL of HFIP were electrolyzed in a 5 mL screening cell. An amount of 2.1 F of electric charge was applied to afford 44 mg (yield: 63%; 0.13 mmol) of a colorless crystalline solid. Purification by column chromatography (cyclohexane/ethyl acetate: 7:3)

^{1}H NMR (400 MHz, $CDCl_3$) δ [ppm] = 8.21 (dd, *J* = 8.1, 2.1 Hz, 1H), 8.04 (dd, *J* = 2.1, 0.5 Hz, 1H), 7.80 (ddd, *J* = 8.1, 2.1, 0.5 Hz, 3H), 7.69–7.63 (m, 1H), 7.55–7.45 (m, 3H), 7.31–7.27 (m, 1H), 7.14 (dd, *J* = 8.1, 0.5 Hz, 1H), 2.46 (s, 3H).

^{13}C NMR (100 MHz, $CDCl_3$) δ [ppm] = 199.4, 170.2, 138.7, 136.9, 134.8, 133.5, 130.1, 129.0, 128.3, 127.4, 127.3, 127.2, 126.4, 125.6, 124.2, 122.6, 119.9, 114.7, 27.7.

HRMS for $C_{21}H_{14}{}^{35}ClNO_2$ (ESI+) $[M+H]^+$: calc.: 348.0791, found: 348.0783.

MP: 147.6–150.0 °C (cyclohexane/ethyl acetate).

9-Benzoyl-3-chloro-7-nitrocarbazole (2m)

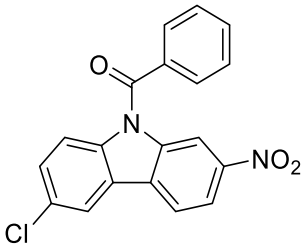

According to protocol C2, 71 mg (0.20 mmol, 1 equiv.) of **1m** and 5 mg NBu_4BF_4 in 5 mL of HFIP were electrolyzed in a 5 mL screening cell. An amount of 2.1 F of electric charge was applied to afford 43 mg (yield: 61%; 0.12 mmol) of a pale yellow crystalline solid.

^{1}H NMR (400 MHz, $CDCl_3$) δ [ppm] = 8.43–8.38 (m, 2H), 8.32–8.23 (m, 4H), 7.67 (d, *J* = 1.9 Hz, 1H), 7.63–7.53 (m, 4H).

^{13}C NMR (100 MHz, $CDCl_3$) δ [ppm] = 164.2, 151.6, 147.5, 142.3, 139.1, 132.2, 131.0, 130.8, 129.7, 129.1, 129.0, 127.9, 126.4, 124.2, 124.0, 123.9, 111.5.

HRMS for $C_{19}H_{11}{}^{35}ClN_2O_3$ (ESI+) $[M+H]^+$: calc.: 351.0536, found: 351.0528.

MP: 222.0–223.5 °C (cyclohexane/ethyl acetate).

9-Benzoyl-3-chloro-6-methoxycarbazole (2n)

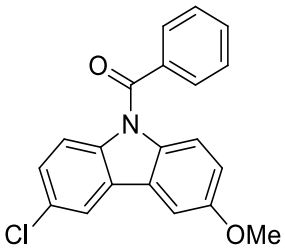

According to protocol C1, 68 mg (0.20 mmol, 1 equiv.) of **1n** and 5 mg NBu_4BF_4 in HFIP/H_2O (4.25/0.75 mL) were electrolyzed in a 5 mL screening cell. An amount of 2.4 F of electric charge was applied to afford 26 mg (yield: 39%; 0.08 mmol) of a pale orange crystalline solid.

^{1}H NMR (400 MHz, $CDCl_3$) δ [ppm] = 7.92 (d, *J* = 2.5 Hz, 1H), 7.72–7.62 (m, 3H), 7.58–7.50 (m, 2H), 7.51–7.43 (m, 1H), 7.40 (d, *J* = 2.5 Hz, 1H), 7.35 (d, *J* = 8.9 Hz, 1H), 7.27 (dd, *J* = 8.9, 2.5 Hz, 1H), 6.94 (dd, *J* = 8.9, 2.5 Hz, 1H), 3.92 (s, 3H).

^{13}C NMR (100 MHz, $CDCl_3$) δ [ppm] = 169.0, 156.5, 137.9, 135.6, 133.9, 132.4, 129.0, 128.9, 128.8, 127.4, 126.8, 125.9, 119.6, 117.1, 116.9, 115.5, 102.9, 55.8.

HRMS for $C_{20}H_{14}{}^{35}ClNO_2$ (ESI+) $[M+H]^+$: calc.: 336.0791, found: 336.0786.

MP: 113.2–115.1 °C (cyclohexane/ethyl acetate).

9-Benzoyl-3-methoxy-6-methylcarbazole (2o)

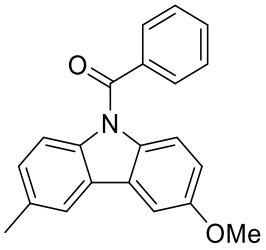

According to protocol C1, 63 mg (0.20 mmol, 1 equiv.) of **1o** and 5 mg NBu_4BF_4 in HFIP/H_2O (4.25/0.75 mL) were electrolyzed in a 5 mL screening cell. An amount of 2.5 F of electric charge was applied to afford 25 mg (yield: 40%; 0.08 mmol) of a colorless crystalline solid.

^{1}H NMR (400 MHz, $CDCl_3$) δ [ppm] = 7.78–7.76 (m, 1H), 7.73–7.69 (m, 2H), 7.68–7.63 (m, 1H), 7.57–7.47 (m, 3H), 7.45 (d, *J* = 2.6 Hz, 1H), 7.32 (d, *J* = 8.5 Hz, 1H), 7.13 (dd, *J* = 8.5, 2.6, 0.7 Hz, 1H), 6.93 (dd, *J* = 9.1, 2.6 Hz, 1H), 3.94 (s, 3H), 2.51 (s, 3H).

^{13}C NMR (100 MHz, $CDCl_3$) δ [ppm] = 169.2, 156.4, 137.8, 136.1, 133.8, 133.0, 132.0, 128.9, 128.8, 128.0, 127.1, 126.3, 119.8, 116.9, 115.7, 114.4, 103.0, 55.8, 21.3.

HRMS for $C_{21}H_{17}NO_2$ (ESI+) $[M+H]^+$: calc.: 316.1338, found: 316.1328.

MP: 86.7–88.9 °C.

Methyl 9-benzoyl-2-(6-chlorocarbazol-2-yl)propanoate (2q)

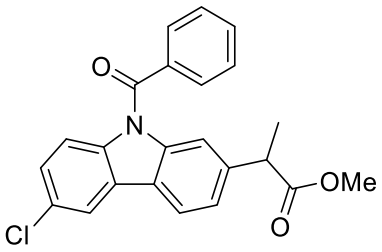

According to protocol C1, 79 mg (0.20 mmol, 1 equiv.) of **1q** and 5 mg NBu_4BF_4 in HFIP/H_2O (4.25/0.75 mL) were electrolyzed in a 5 mL screening cell. An amount of 2.1 F of electric charge was applied to afford 48 mg (yield: 62%; 0.13 mmol) of a colorless oil. Purification by column chromatography (cyclohexane/ethyl acetate: 9:1).

^{1}H NMR (400 MHz, $CDCl_3$) δ [ppm] = 7.95–7.88 (m, 2H), 7.74–7.67 (m, 3H), 7.59–7.53 (m, 2H), 7.47–7.41 (m, 2H), 7.32 (m, 1H), 7.27 (dd, *J* = 8.1, 1.5 Hz, 1H), 3.78 (q, *J* = 7.2 Hz, 1H), 3.66 (s, 3H), 1.46 (d, *J* = 7.2 Hz, 3H).

^{13}C NMR (100 MHz, $CDCl_3$) δ [ppm] = 174.6, 169.3, 140.2, 139.8, 137.7, 135.3, 132.6, 129.1, 129.0, 128.9, 127.1, 126.7, 124.0, 123.3, 120.1, 119.6, 116.8, 115.0, 52.1, 45.8, 18.6.

HRMS for $C_{23}H_{18}{}^{35}ClNO_3$ (ESI+) $[M+H]^+$: calc.: 392.1053, found: 392.1045.

Carprofen: (2-(6-chlorocarbazol-2-yl)propanoic acid) (3q)

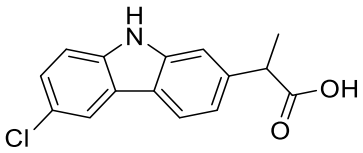

In a round bottom flask 70 mg (0.18 mmol, 1 equiv.) of **2q** were dissolved in 15 mL of MeOH. After addition of 2 mL of a 2.5 M NaOH solution the resulting mixture was heated to 80 °C for 1.5 h. After addition of 50 mL of H_2O and adjusting the pH to 5-6, 15 mL of CH_2Cl_2 were added. Once the organic layer was separated, the water phase was extracted with 3x20 mL of CH_2Cl_2, the combined organic phases were washed with 2x30 mL of H_2O, dried with $MgSO_4$ and the solvent was evaporated under reduced pressure to afford a colorless solid. The solid was recrystallization from $CHCl_3$ (3 mL) to afford 45 mg (0.17 mmol; 92%) of product as colorless crystalline solid. The NMR data are in accordance with previously reported spectra.[13]

Crystallographic data

Crystal structure determination of **2d** (CCDC 1986341): $C_{19}H_{13}NO$, M_r = 271.3 g/mol, colorless needle (0.06 x 0.08 x 0.45 mm^3), P 2_1 2_1 2_1 (orthorhombic), a = 4.9649 Å, b = 14.7991 Å, c = 18.2260 Å, V = 1339.17 $Å^3$, Z = 4, F(000) = 568, ρ = 1.346 g/cm^3, μ = 0.083 mm^{-1}, Mo-Kα graphite monochromator, -153 °C, 13226 reflections, 3217 independent reflections, wR_2 = 0.1224, R_1 = 0.0477, 0.17 e/$Å^3$, –0.22 e/$Å^3$, GoF = 1.047.

Single crystals for structure determination were obtained by recrystallization from ethyl acetate at room temperature.

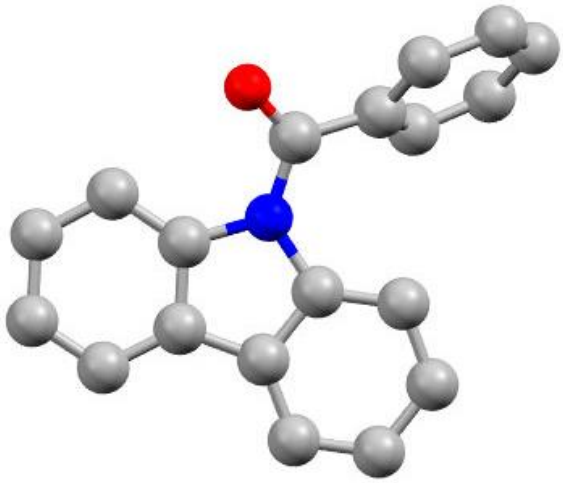

Figure 2: Molecular structure of derivative 2d by X-ray analysis.

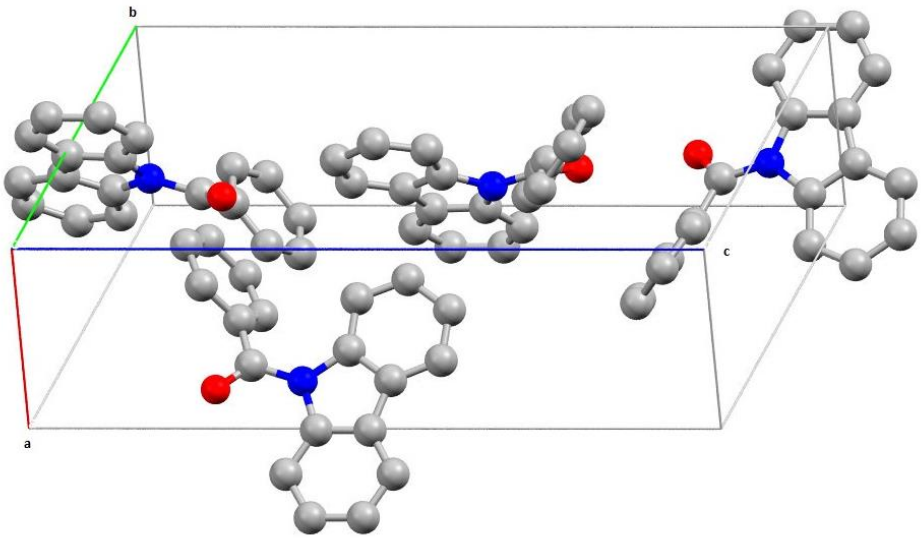

Figure 3: Packing of 2d in the solid state.

Cyclovoltammetric data

The cyclic voltammograms of six selected examples were measured in HFIP/H_2O(15%) (figure 4) and in HFIP (figure 5). Since these two electrolyte systems are employed to ensure a high conversion for all presented examples (see manuscript, scheme 2), we chose **1h** (figure 4 A) that worked well in HFIP/H_2O(15%) and **1f** (figure 4 C & figure 5 A) which worked well in HFIP. Additionally, **1p** (figure 4 E & 5 E) & **1r** (figure 4 F & 5 F) were chosen to elucidate the impact of highly electron withdrawing moieties on the reaction in both electrolyte systems. The corresponding products, if existing, were added in order to display their potential stability/instability in the electrochemical environment. In most cases, it is hard to tell whether the second oxidation peak is located within the potential limit wave or nearby the first oxidation peak. However, judging from our previous work with anilide compounds, [14] it is likely that the second oxidation peak is buried under the potential limit wave due to a strong electron withdrawing nature of the compounds. Therefore, we added **1j** (figure 5 C) which exhibits both oxidation steps visible within the potential frame.

We employed cyclovoltammetric measurements in order to investigate the following issues:

a) *Is the occurrence of over-oxidation of the product during electrolysis likely?*
   The individual oxidation potentials, which are depicted in figure 4 and 5, reveal that over-oxidation is a likely threat to the formed product, since a low potential gap (in figure 4: C (**1f**; 1.37 V) & D (**2f**; 1.44 V); ΔE = 0.07 V) or even a lower potential (in figure 4: A (**1h**; 1.58 V) & B (**2h**;1.53 V); in figure 5: A (**1f**;1.50 V) & B (**2f**;1.33 V), C (**1j**;1.53 V) & D (**2j**;1.40 V)) compared to the precursors are present.
b) *In some cases, the conversion of the starting material is favored in HFIP as solvent. Is there a difference in the oxidation potentials of the starting material in HFIP and HFIP/H_2O(15%) which can explain the compatibility of substrate and electrolyte (e.g. a dramatical shift of the oxidation potential)?*
   The low conversion of **1f** in HFIP/H_2O(15%) cannot be explained by the cyclic voltammograms (figure 4 C & 5 A). Although both electrolytes enable an oxidation within an acceptable range (HFIP/H_2O(15%): 1.37 V & HFIP: 1.50 V) only HFIP provides a full conversion of the starting material after 2.4 F.
c) *Is the generation of amidyl radicals the key step to conversion and/or formation of carbazoles?*
   We could confirm via cyclic voltammograms of **1p** in both electrolytes (figure 4 E & 5 E) the lack of oxidation activity and the recovery of almost the whole starting material. As already mentioned in the manuscript, **1r** can be oxidized in both electrolytes, indicated by a small shoulder in figure 4 F (1.76 V) and figure 5 F (1.77 V). Thus, the generation of amidyl radicals is possible unlike in the case of **1p**. Regardless, a complex mixture –among others small amounts of benzoxazole and HFIP adducts (verified by GCMS)– and no formation of the product in the case of **1r** were observed.

In the following, the cyclic voltammograms are provided:

Solvent HFIP/H_2O(15%):

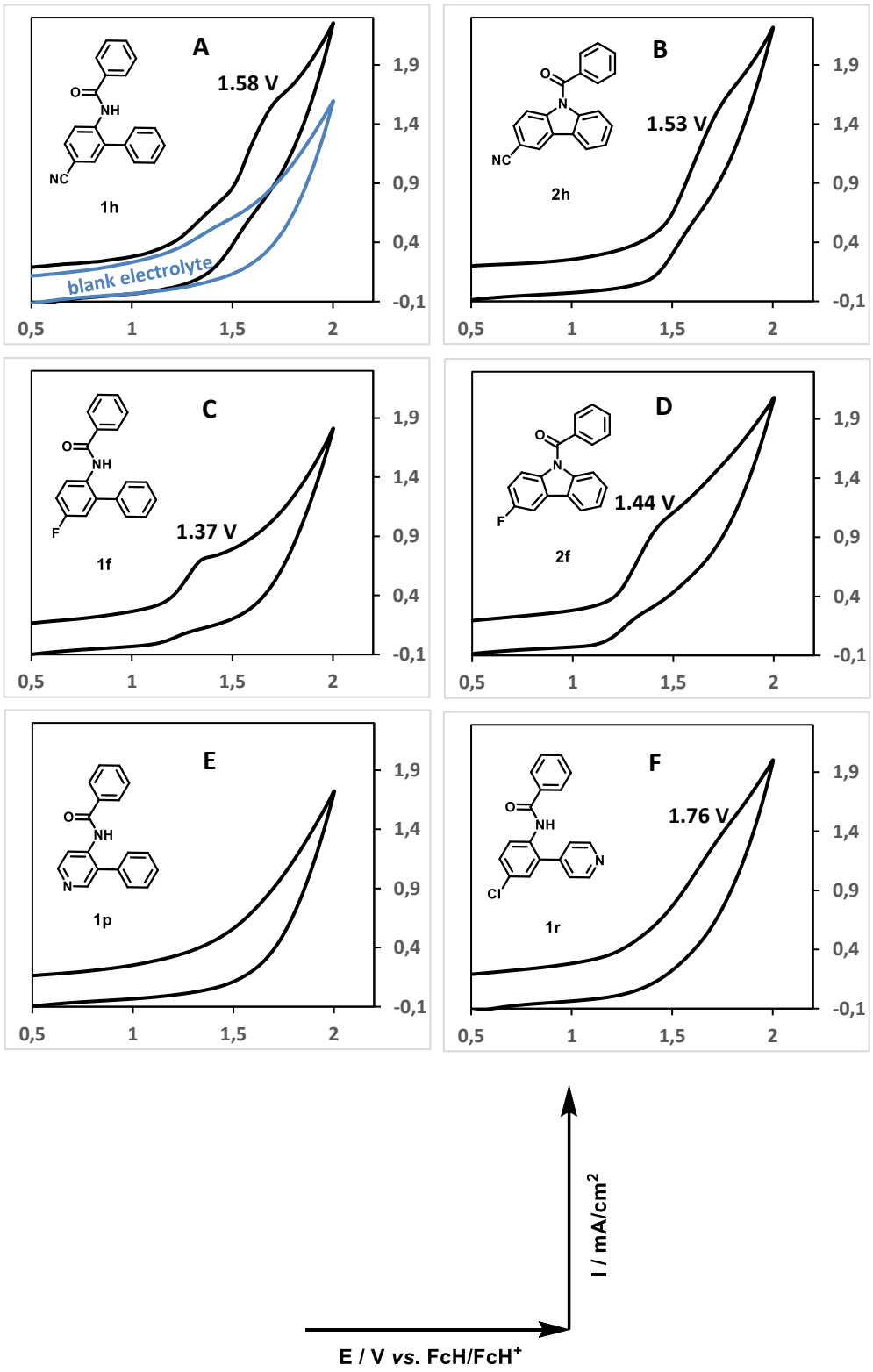

Figure 4: Cyclic voltammograms of 6 selected examples in HFIP/H_2O(15%); 1 mM compound, 0.1 M NBu_4BF_4 in 4.25 mL HFIP and 0.75 mL H_2O, scan rate: 200 mV/s, working electrode: GC, counter electrode: GC, reference electrode: Ag/AgCl in sat. LiCl/EtOH, referenced vs. FcH/FcH^+; top: substrate 1h (A) & product 2h (B); mid: substrate 1f (C) & product 2f (D); bottom: substrate 1p (E) & substrate 1r (F).

Solvent HFIP:

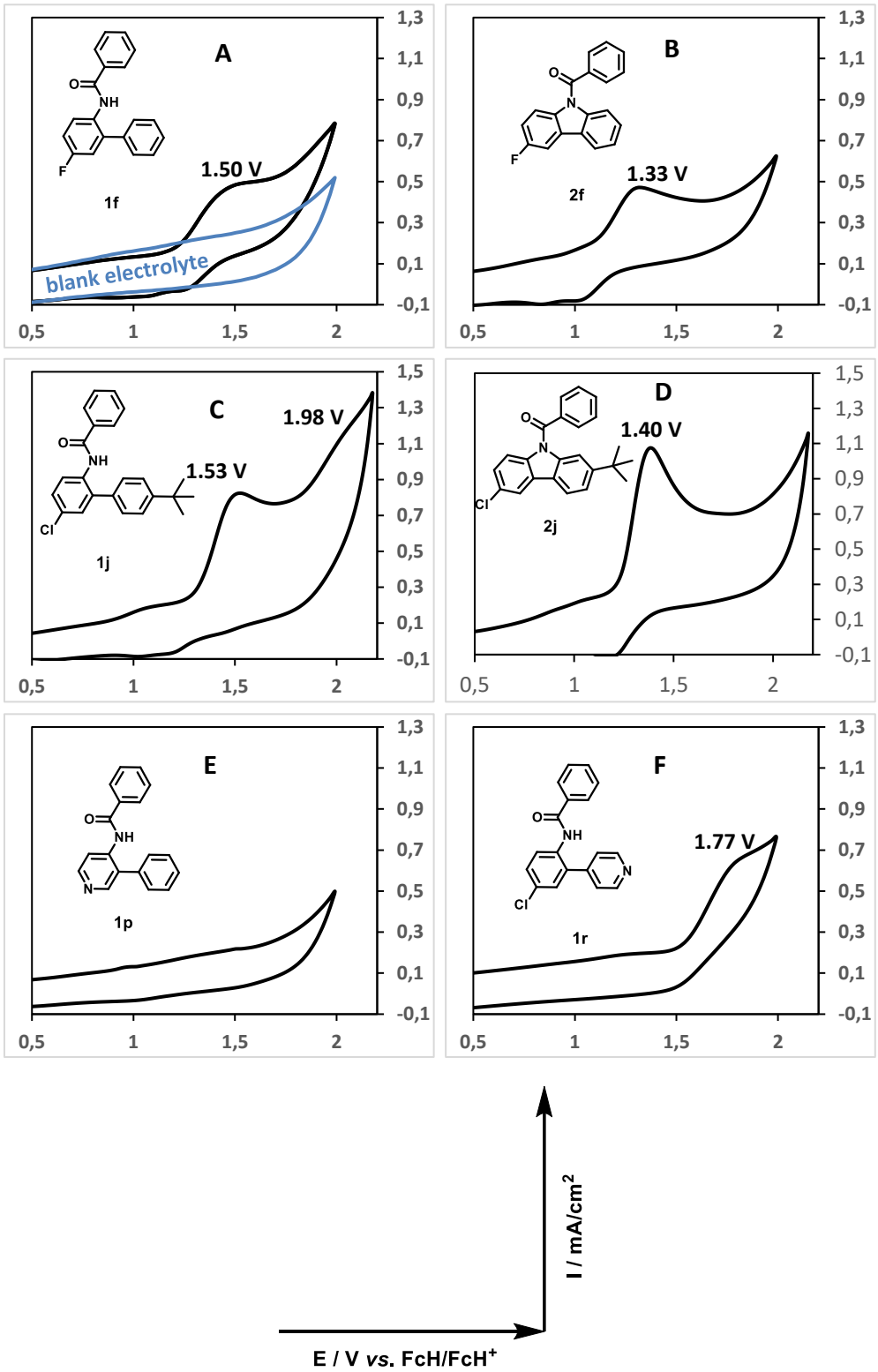

Figure 5: Cyclic voltammograms of 6 selected examples in HFIP; 1 mM compound, 0.1 M NBu_4BF_4 in 5 mL HFIP, scan rate: 200 mV/s, working electrode: GC, counter electrode: GC, reference electrode: Ag/AgCl in sat. LiCl/EtOH, referenced vs. FcH/FcH^+; top: substrate 1f (A) & product 2f (B); mid: substrate 1j (C) & product 2j (D); bottom: substrate 1p (E) & substrate 1r (F).

Proposed mechanism

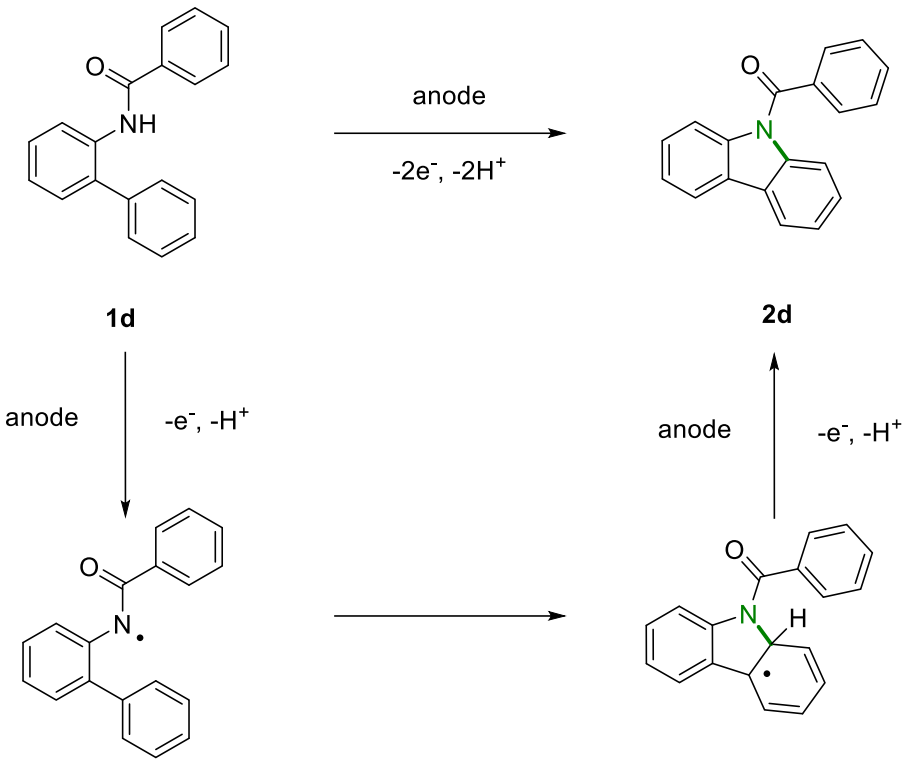

Figure 6: Proposed mechanism of the carbazole formation involving a direct oxidation at the anode and a radical intermediate.

NMR spectra

5-Chloro-2-(4-methylbenzamido)biphenyl (1a)

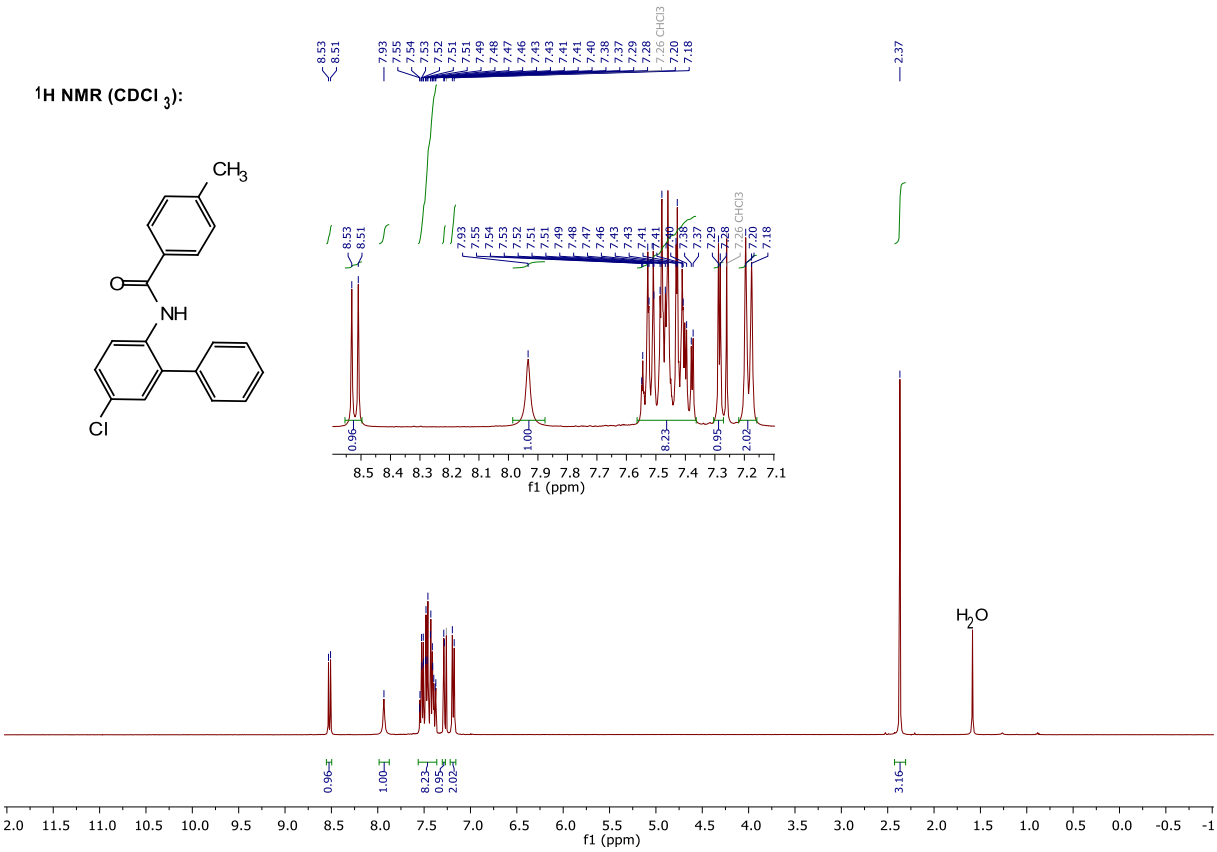

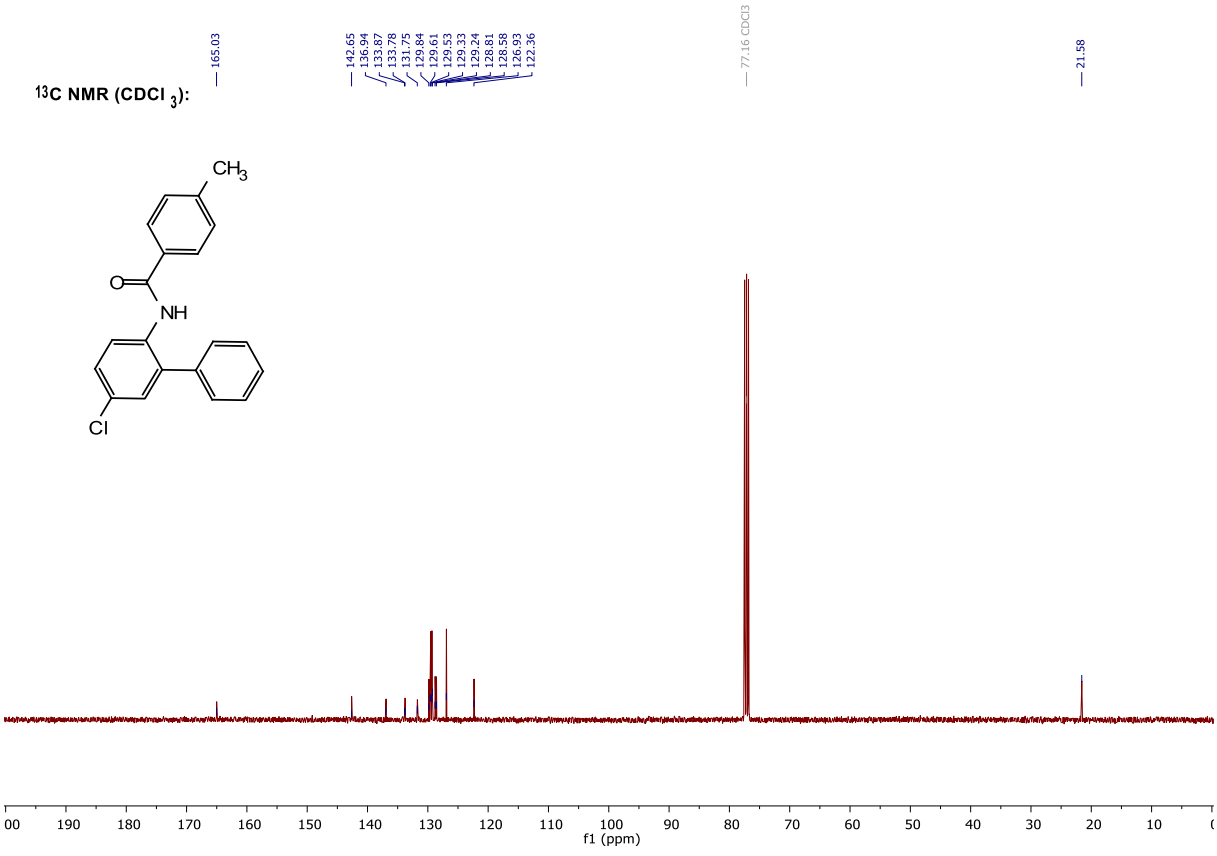

2-Benzamido-5-chlorobiphenyl (1b)

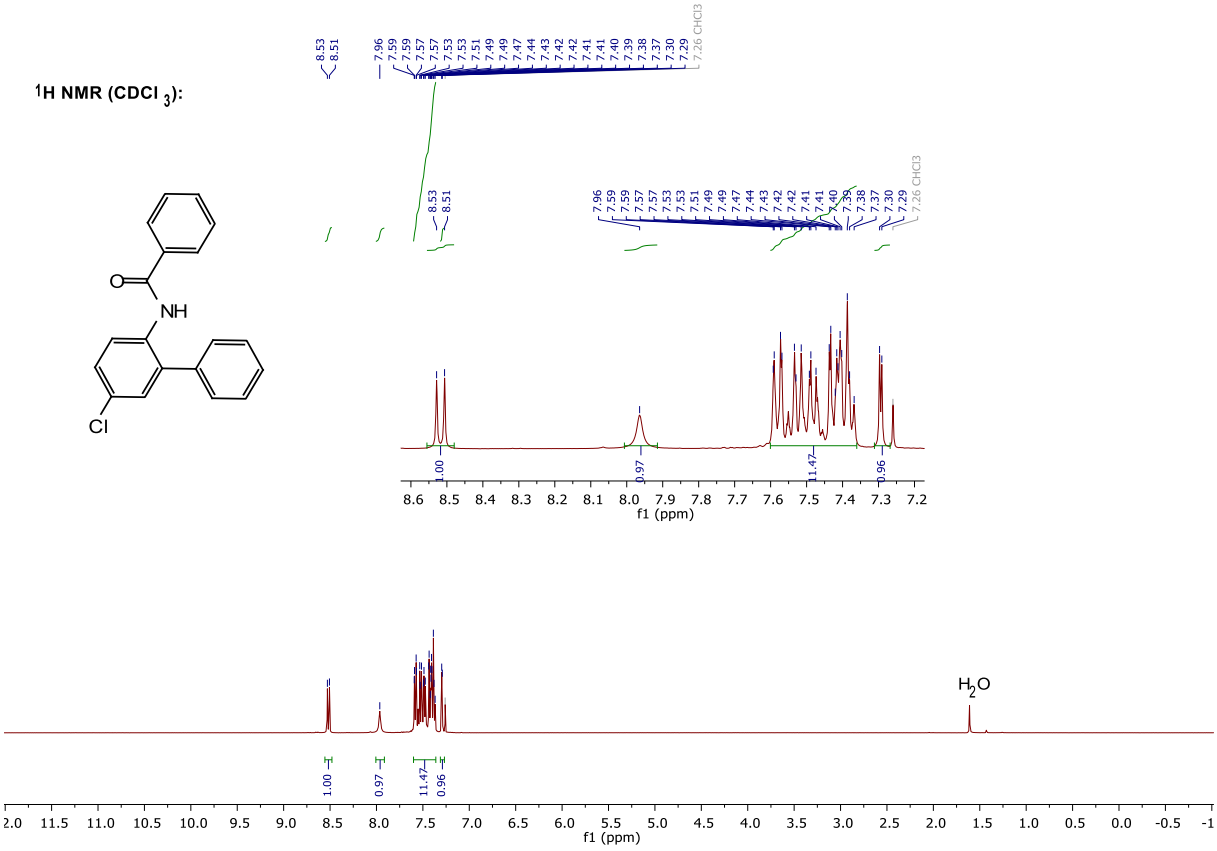

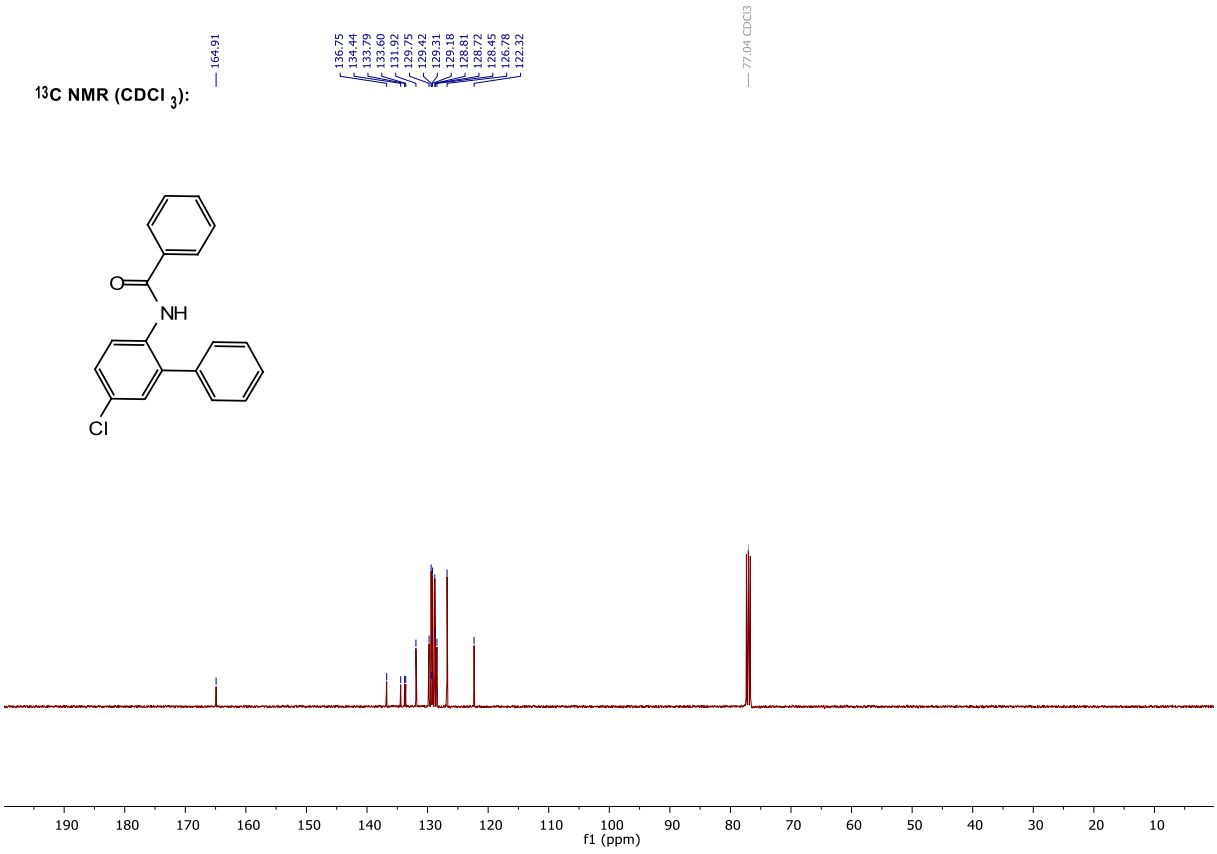

2-Acetamido-5-chlorobiphenyl (1c)

^{1}H NMR (CDCl$_3$):

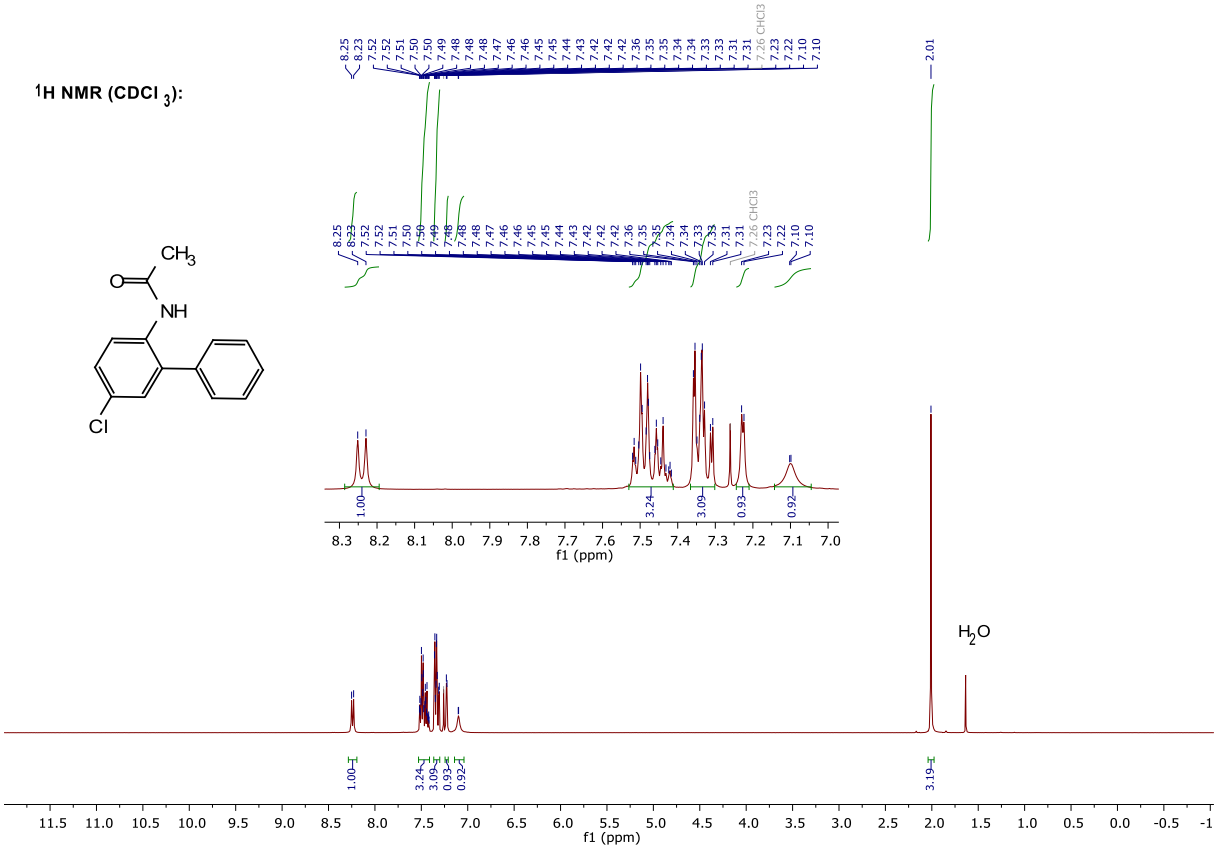

^{13}C NMR (CDCl$_3$):

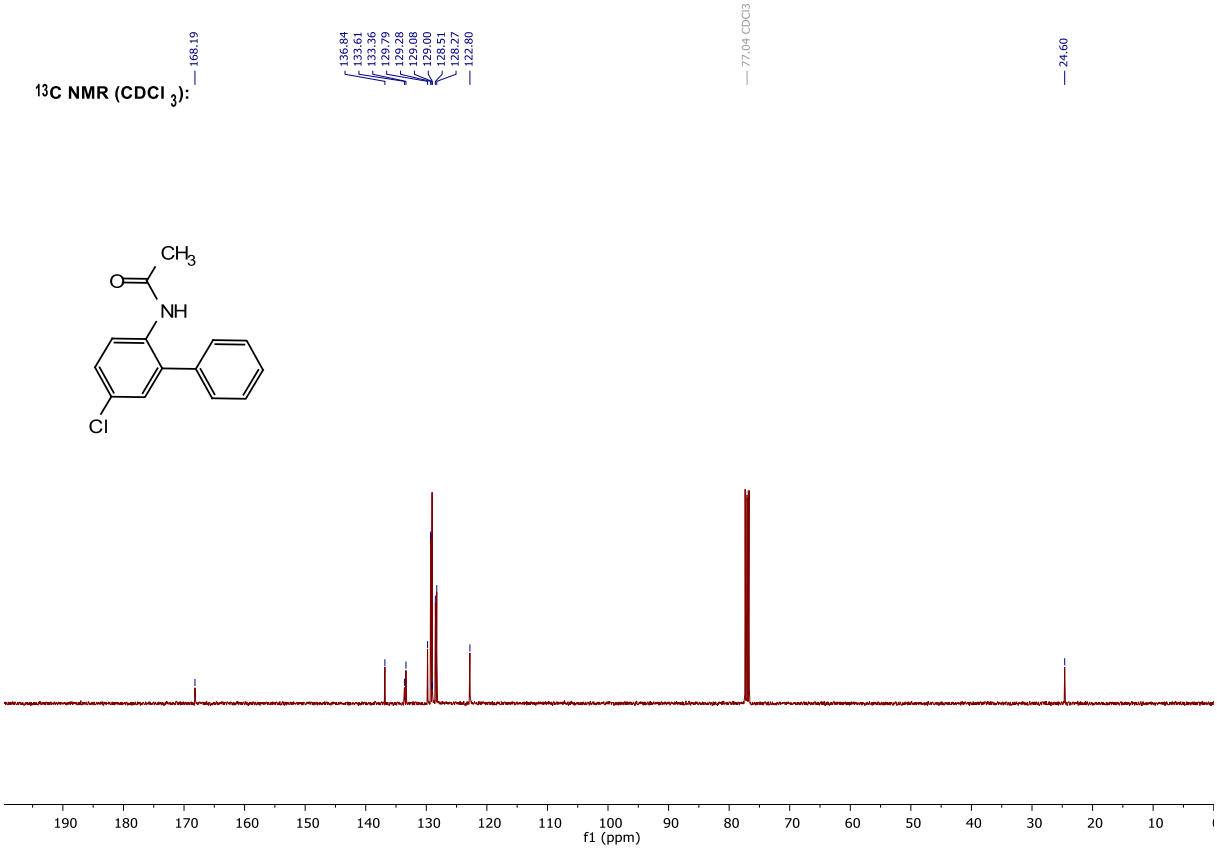

2-Benzamidobiphenyl (1d)

^{1}H NMR (CDCl$_3$):

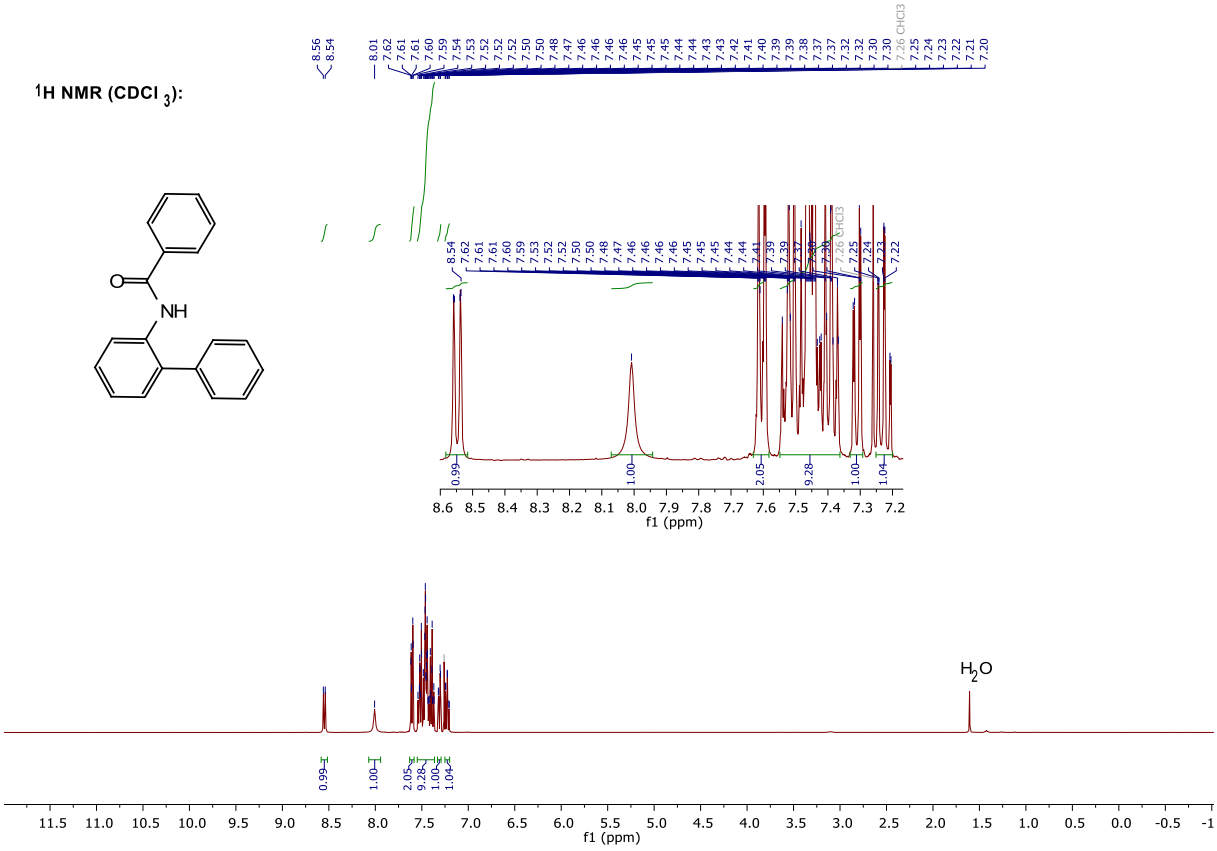

^{13}C NMR (CDCl$_3$):

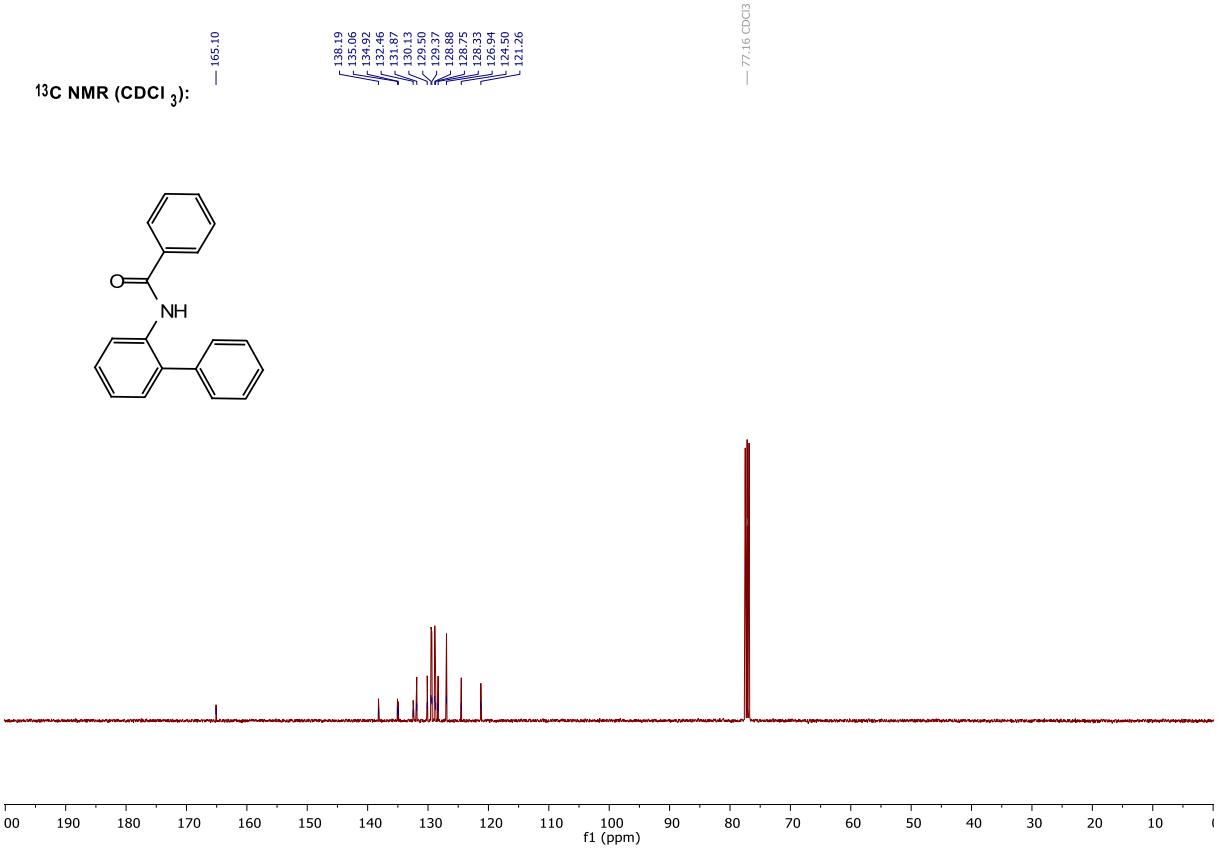

2-Benzamido-4,5-dimethylbiphenyl (1e)

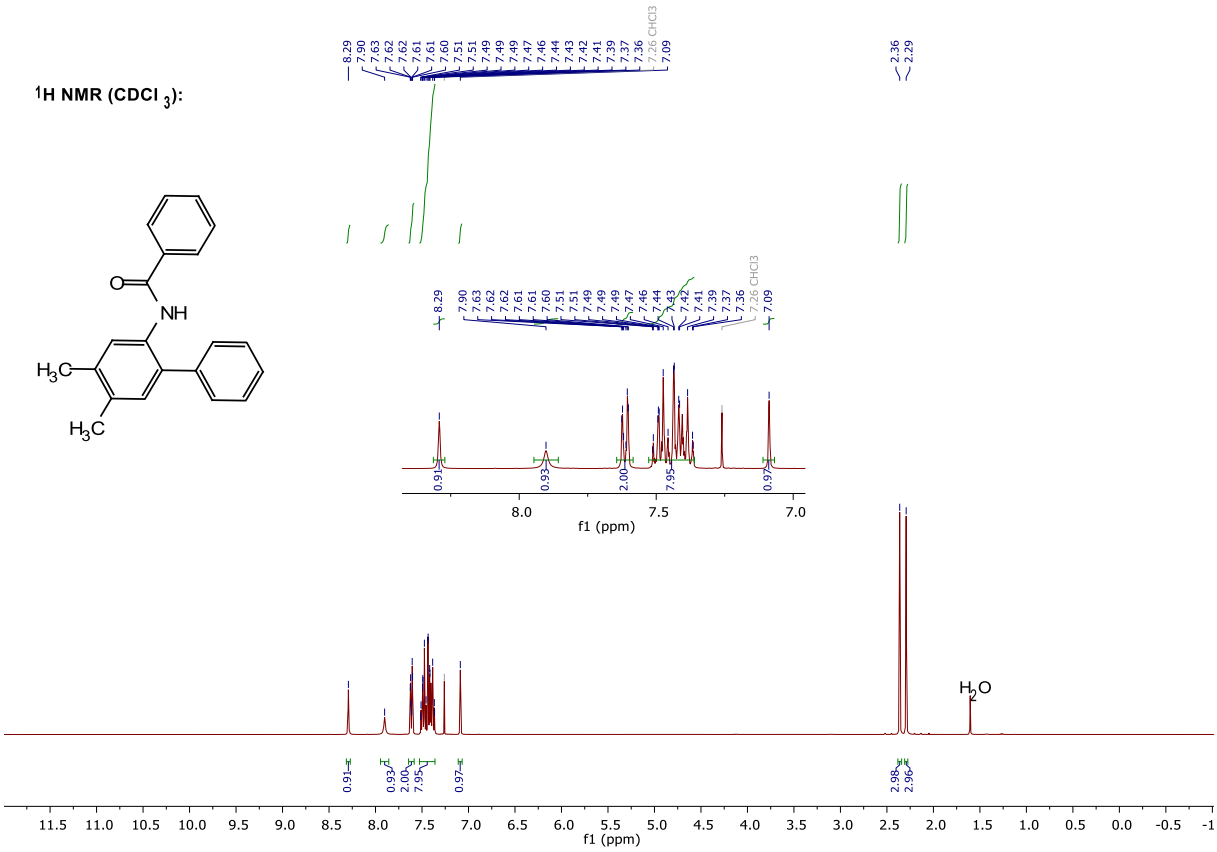

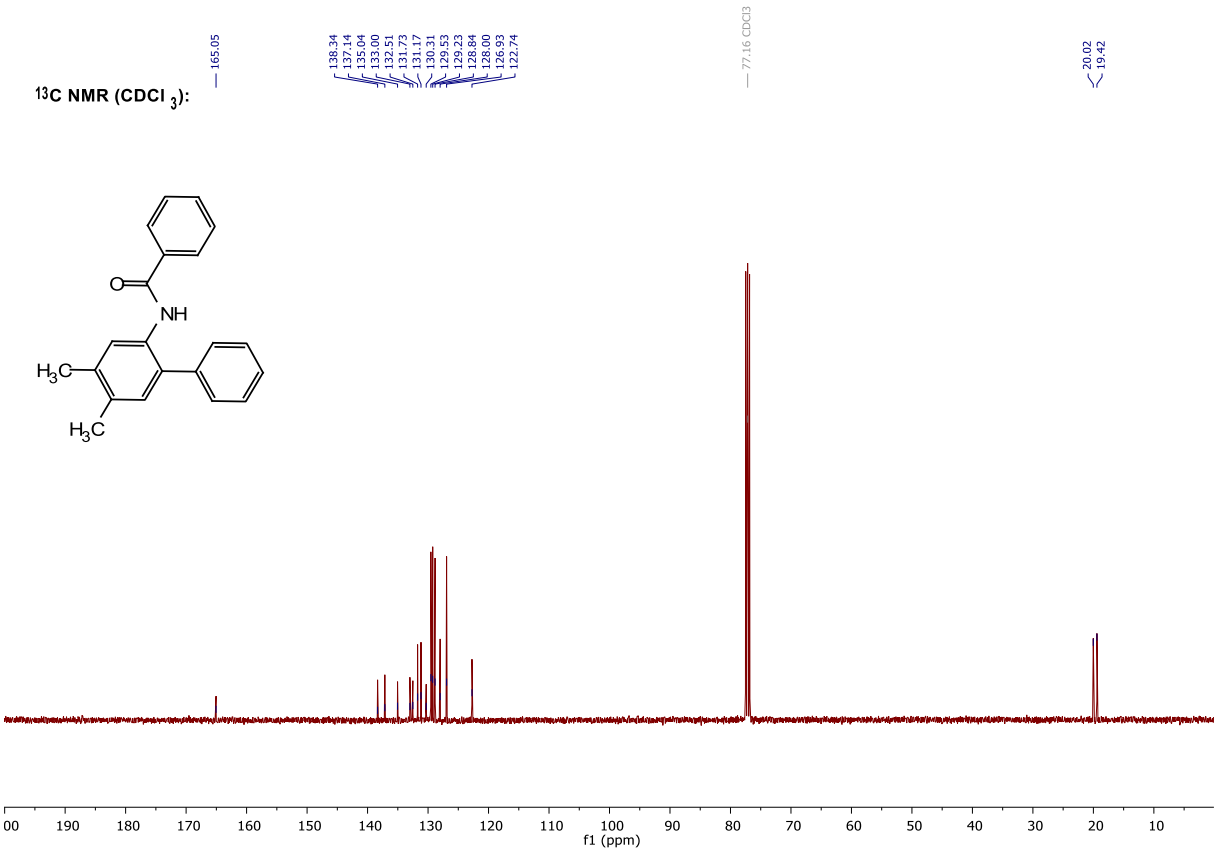

2-Benzamido-5-fluorobiphenyl (1f)

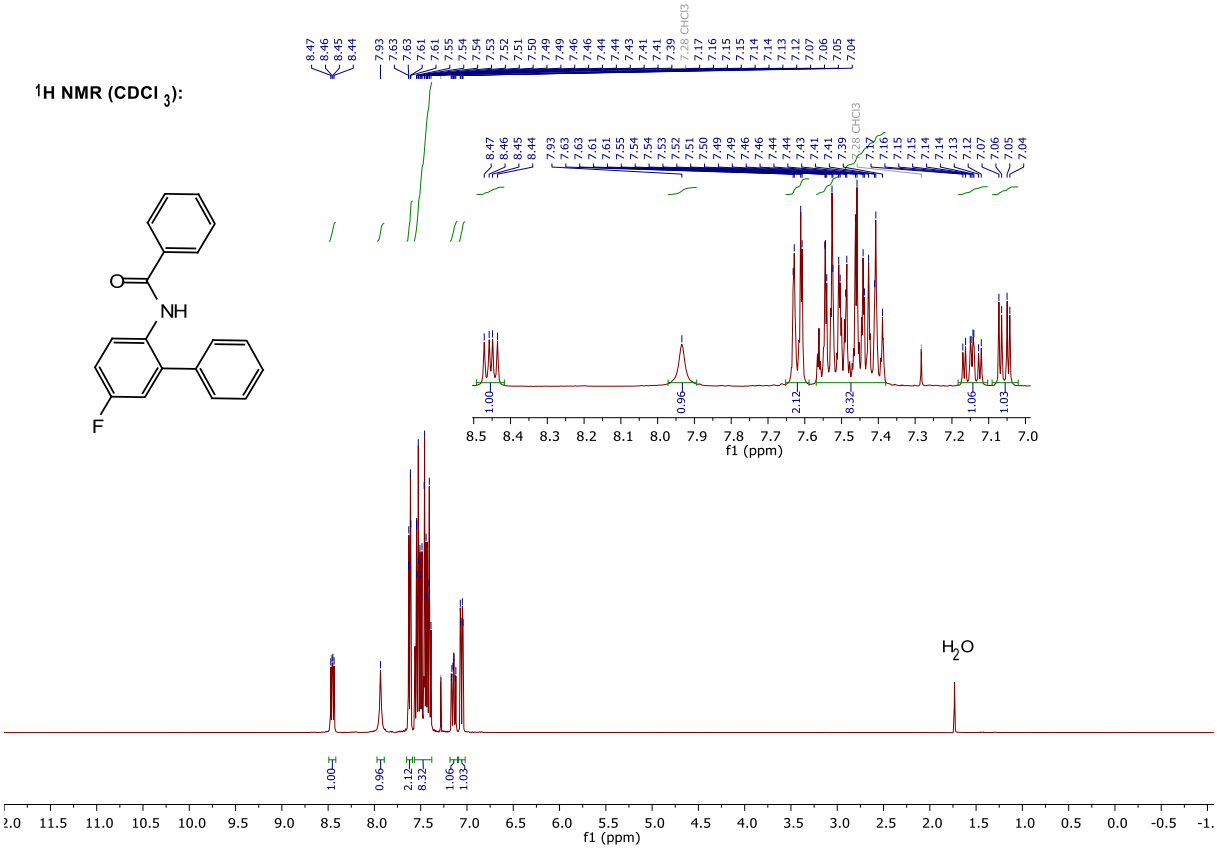

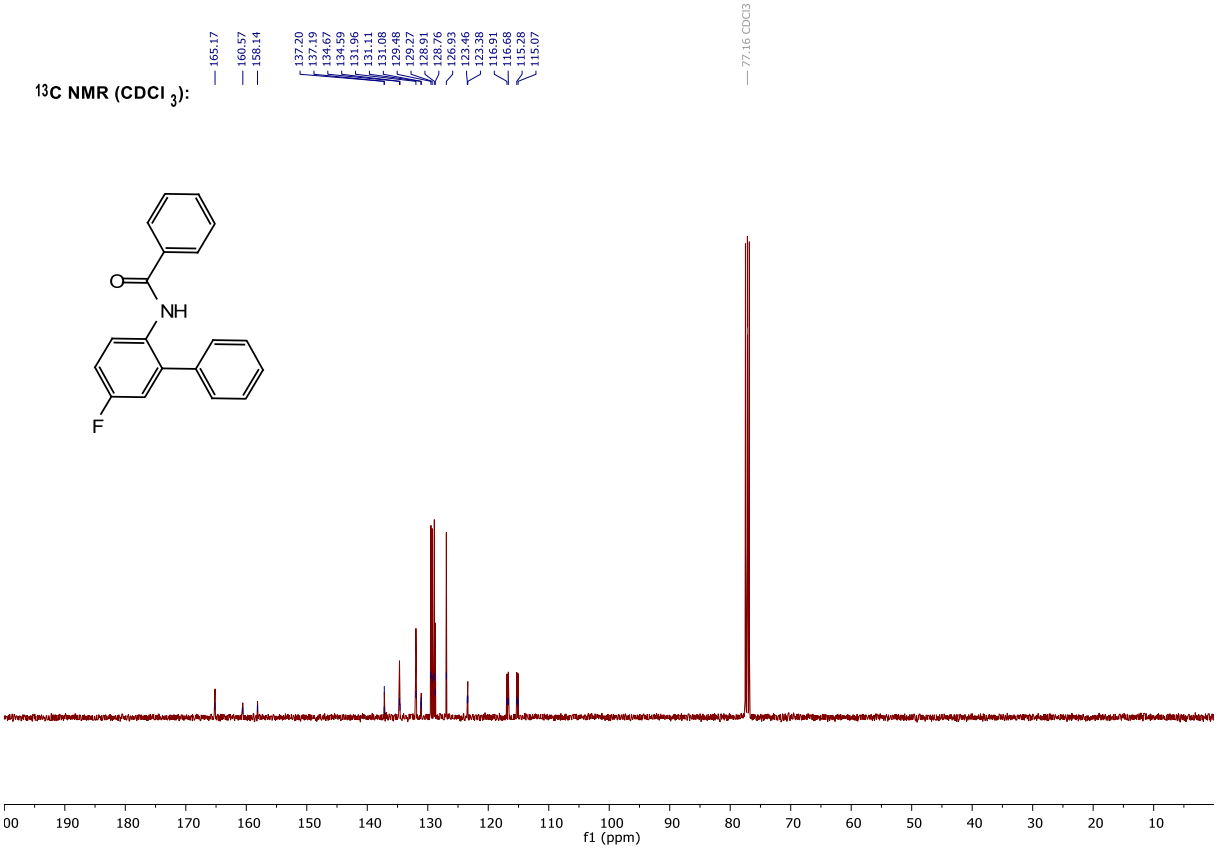

^{19}F NMR ($CDCl_3$):

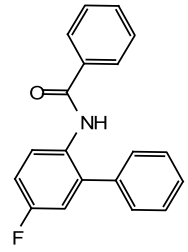

2-Benzamido-5-bromobiphenyl (1g)

^{1}H NMR ($CDCl_3$):

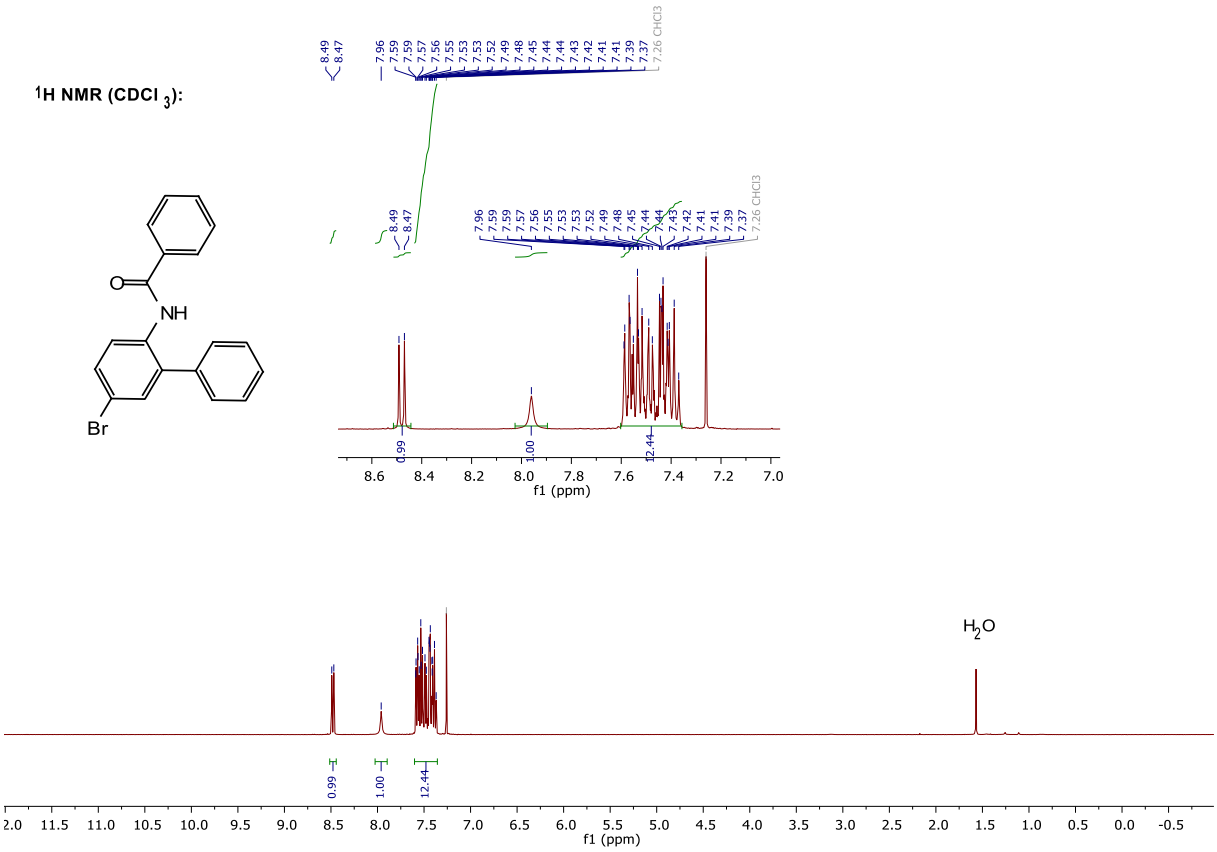

^{13}C NMR ($CDCl_3$):

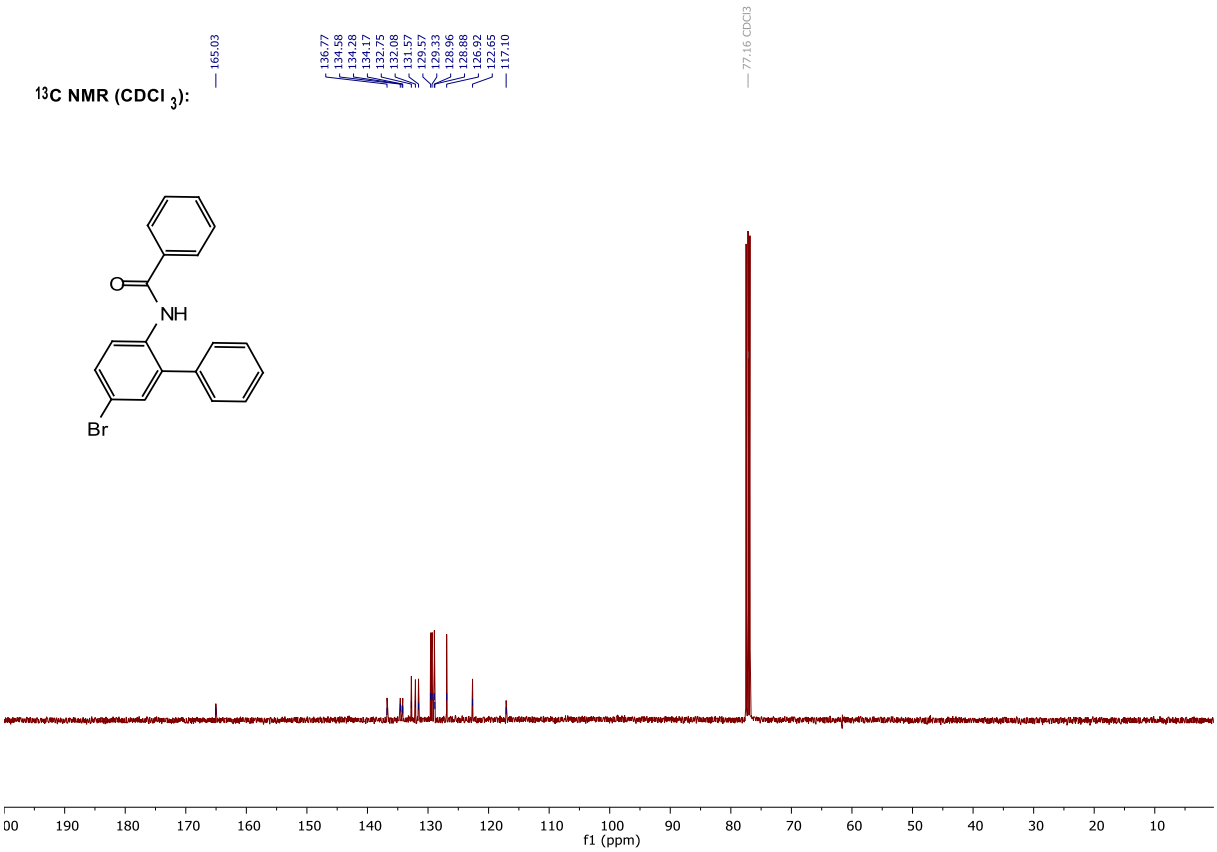

2-Benzamido-5-cyanobiphenyl (1h)

^{1}H NMR ($CDCl_3$):

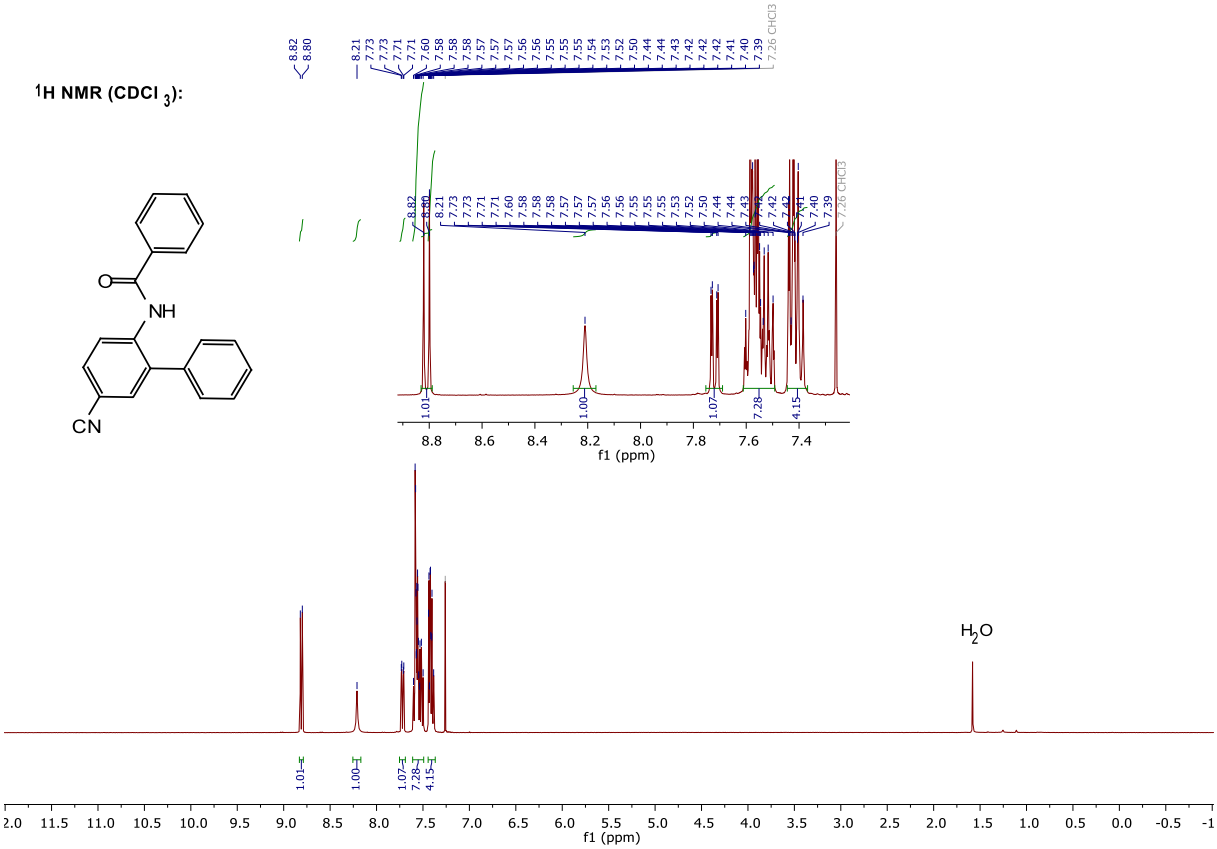

^{13}C NMR ($CDCl_3$):

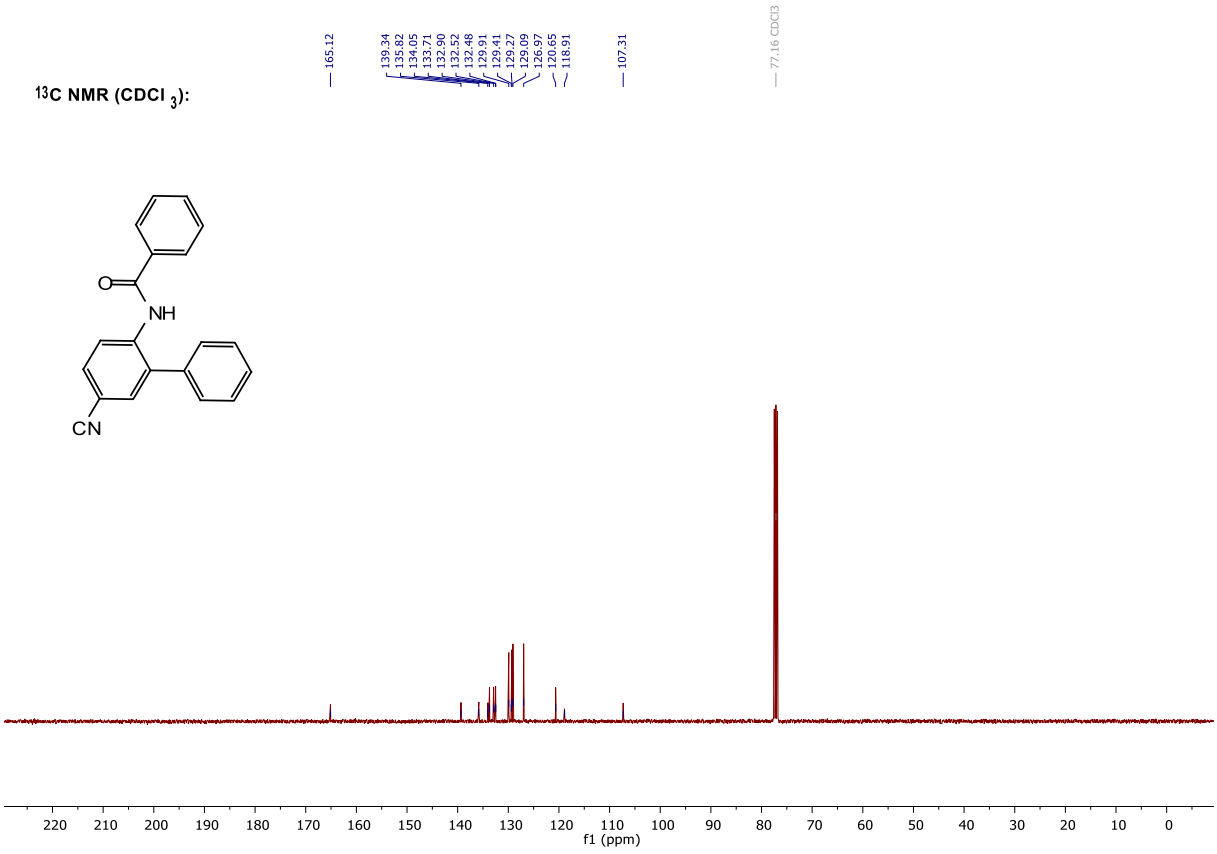

Ethyl 6-benzamido-biphenyl-3-carboxylate (1i)

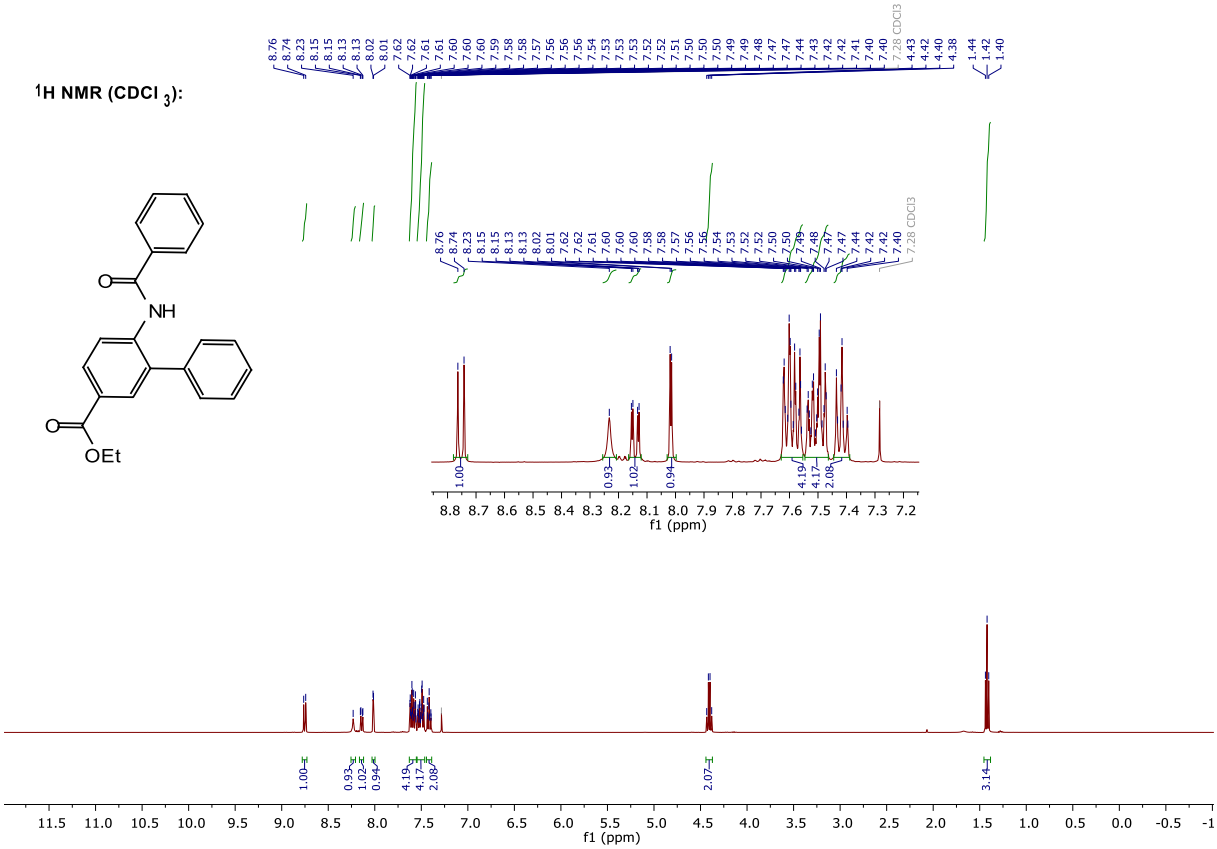

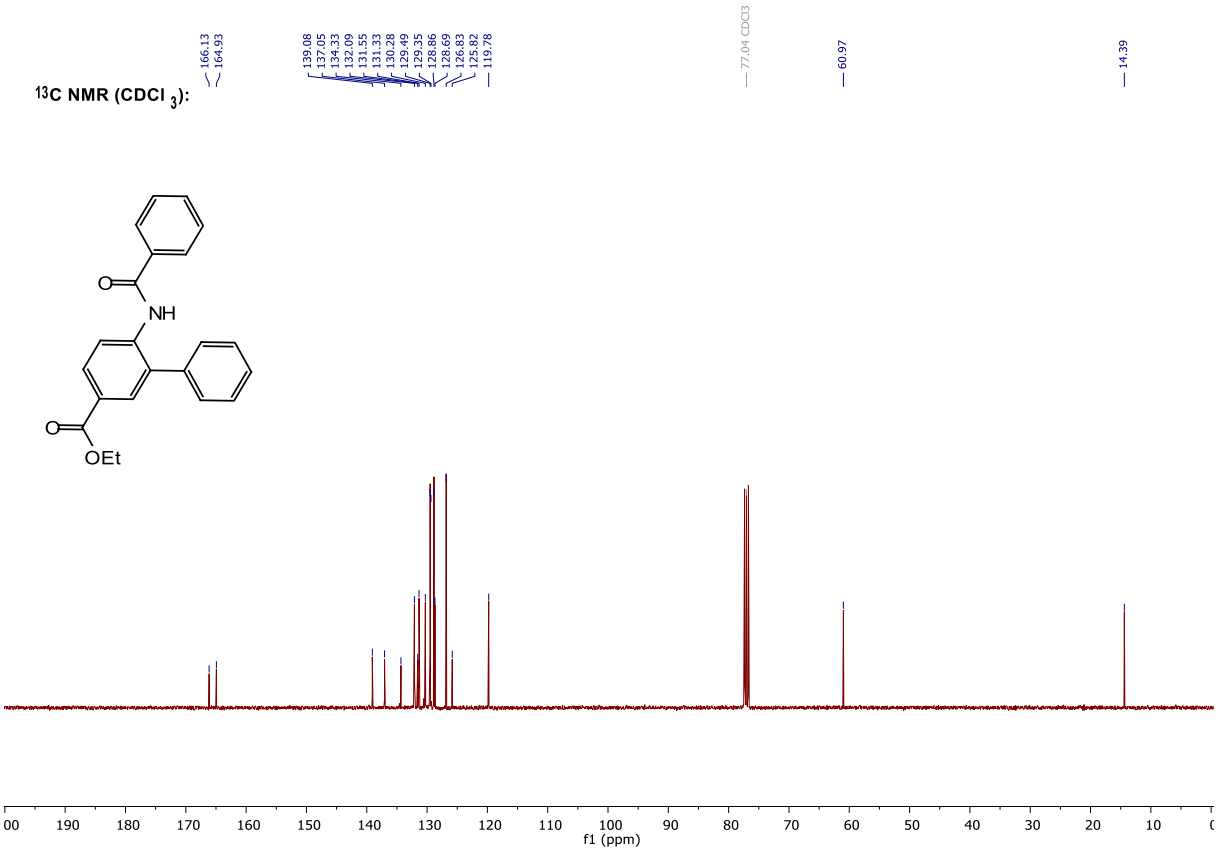

2-Benzamido-4'-*tert*-butyl-5-chloro-biphenyl (1j)

^{1}H NMR (CDCl$_3$):

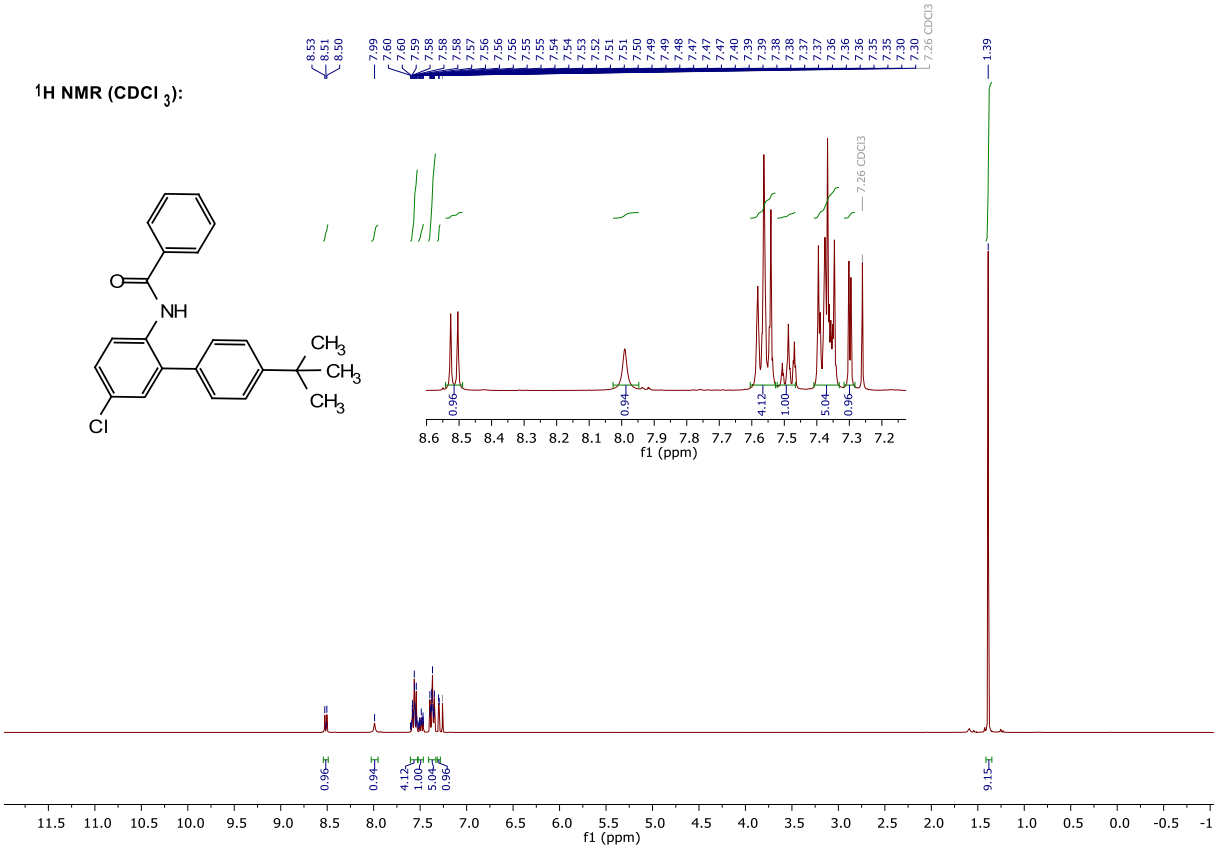

^{13}C NMR (CDCl$_3$):

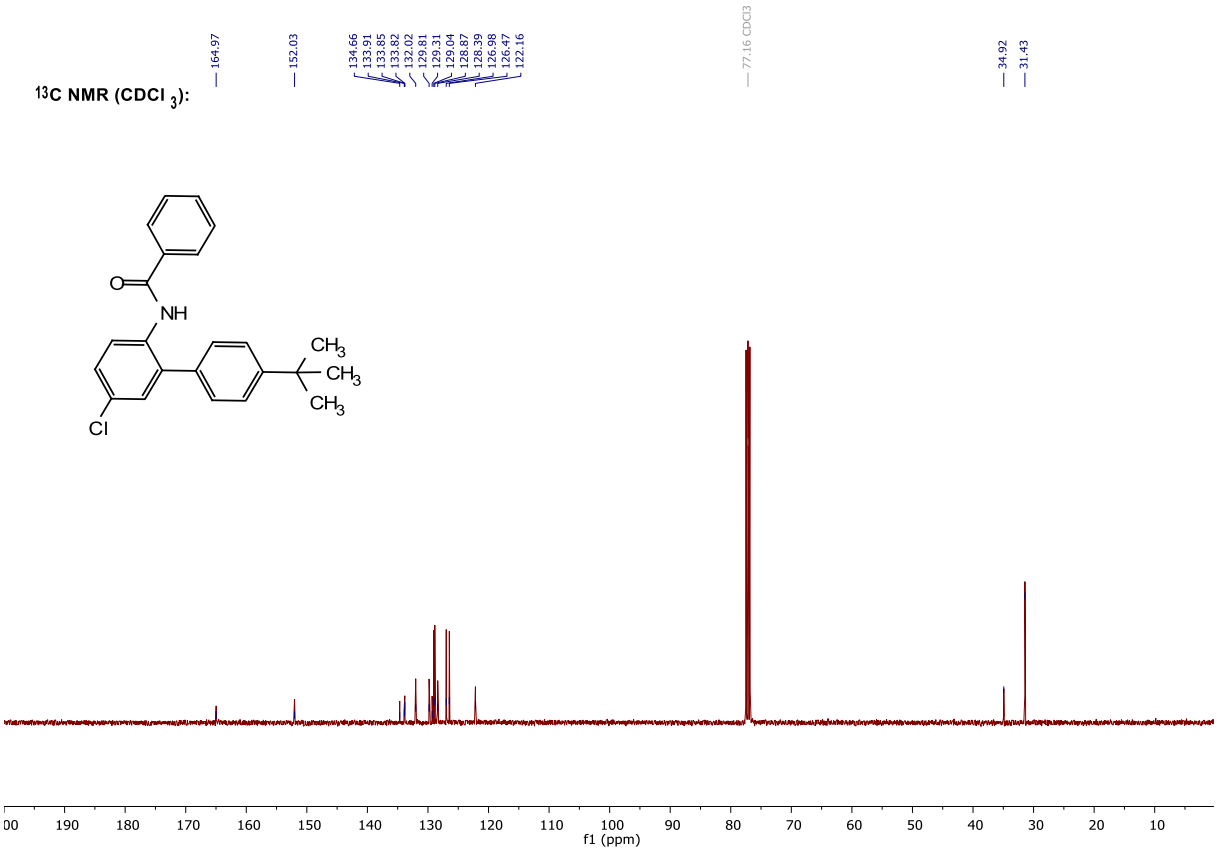

2-Benzamido-4’-chloro-5-methyl-biphenyl (1k)

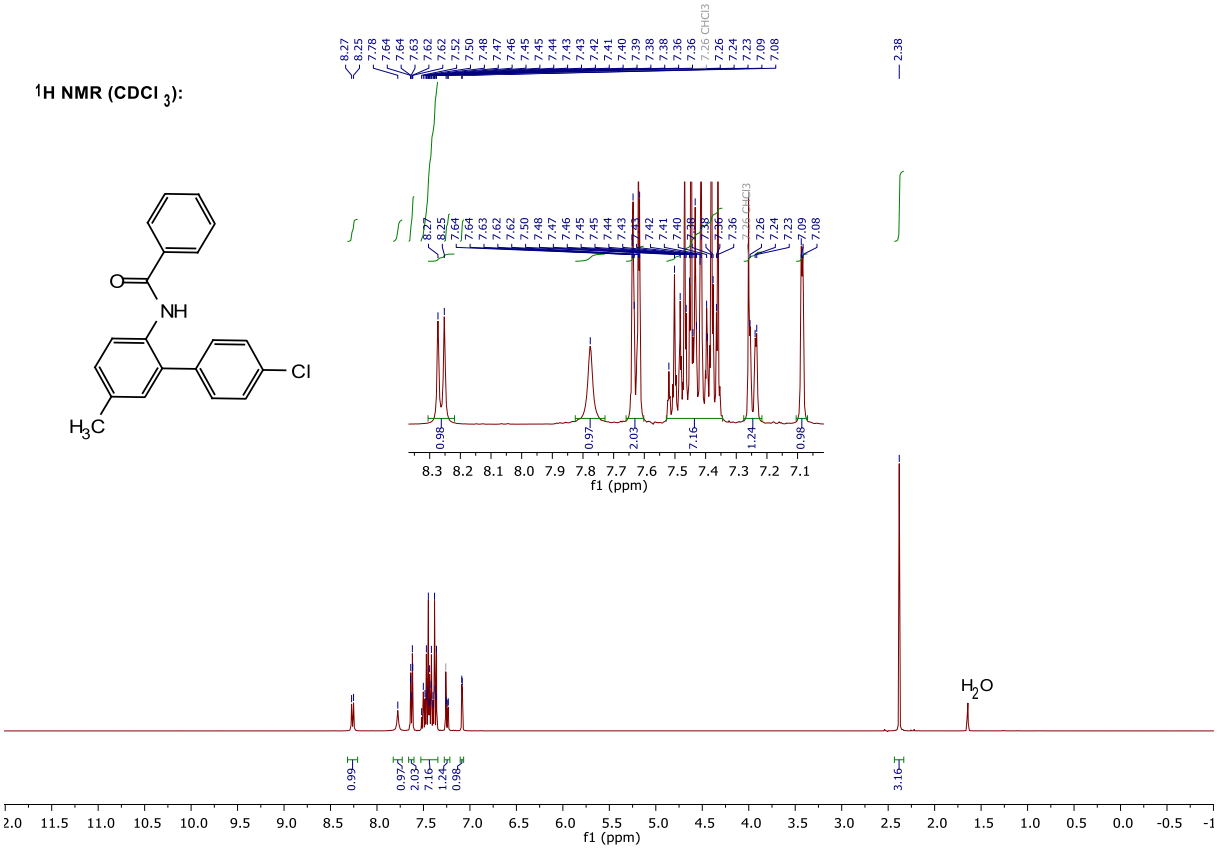

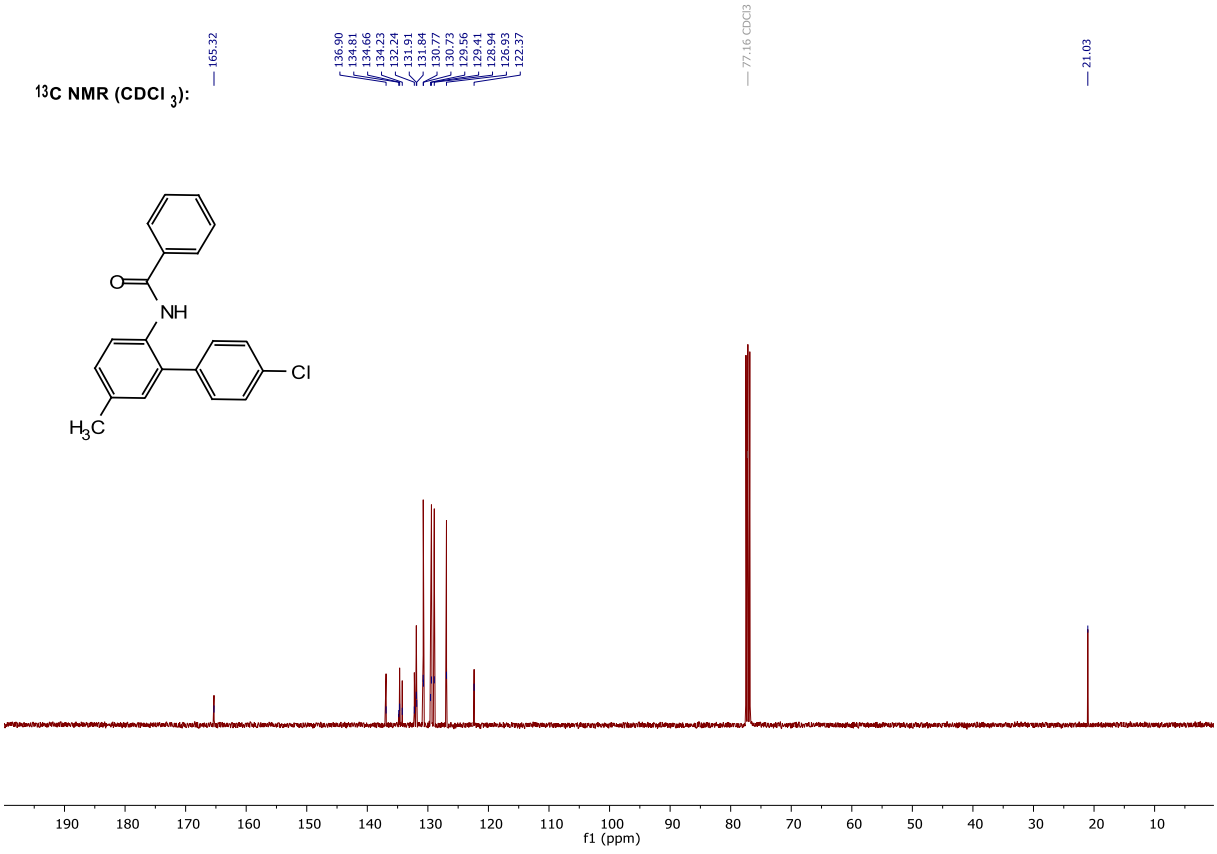

3’-Acetyl-2-benzamido-5-chloro-biphenyl (1l)

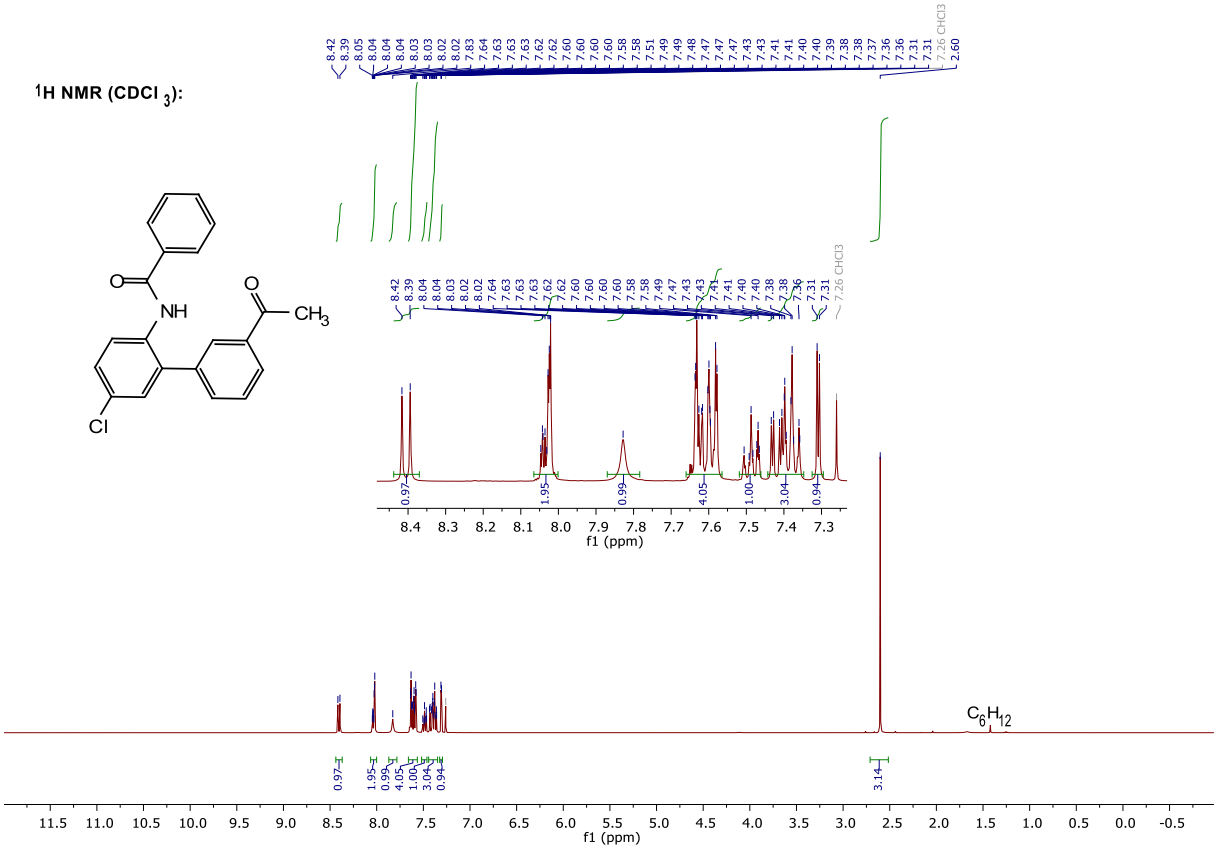

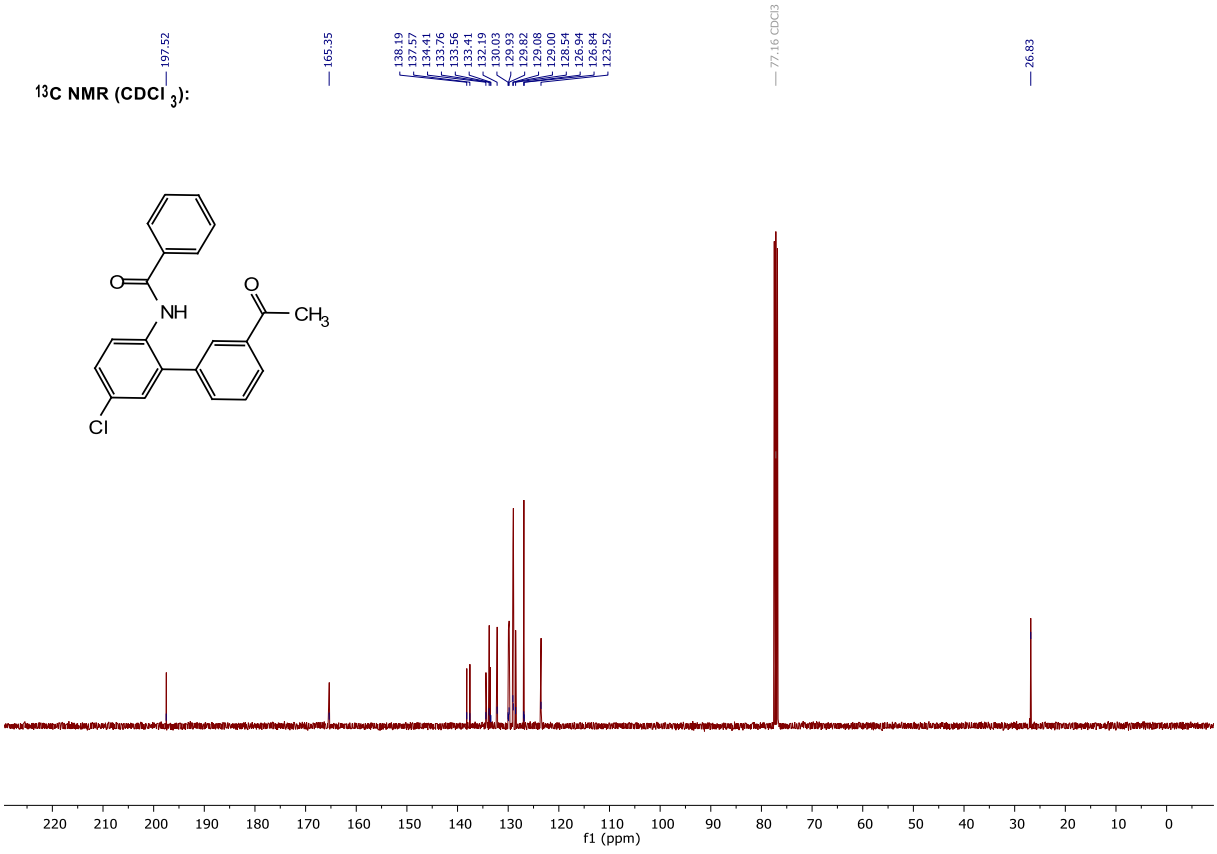

2-Benzamido-5-chloro-4’-nitrobiphenyl (1m)

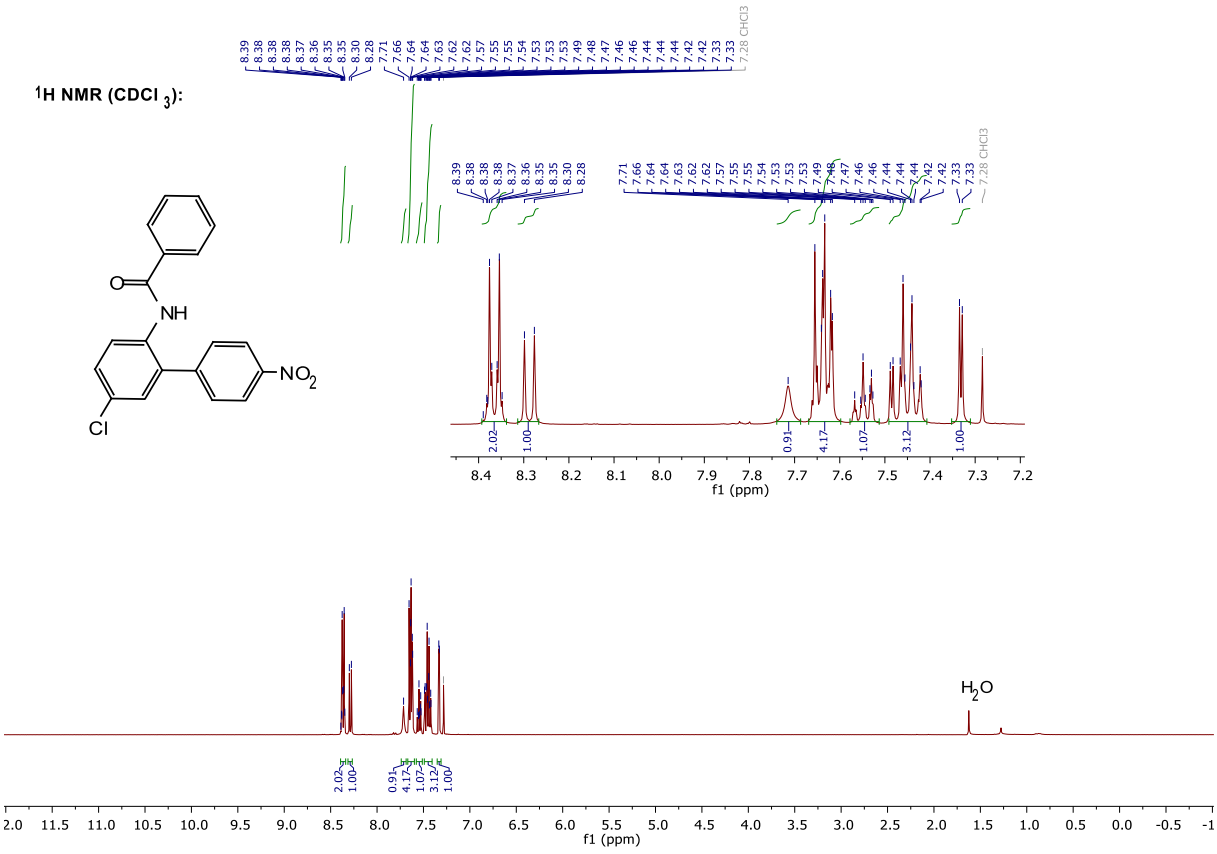

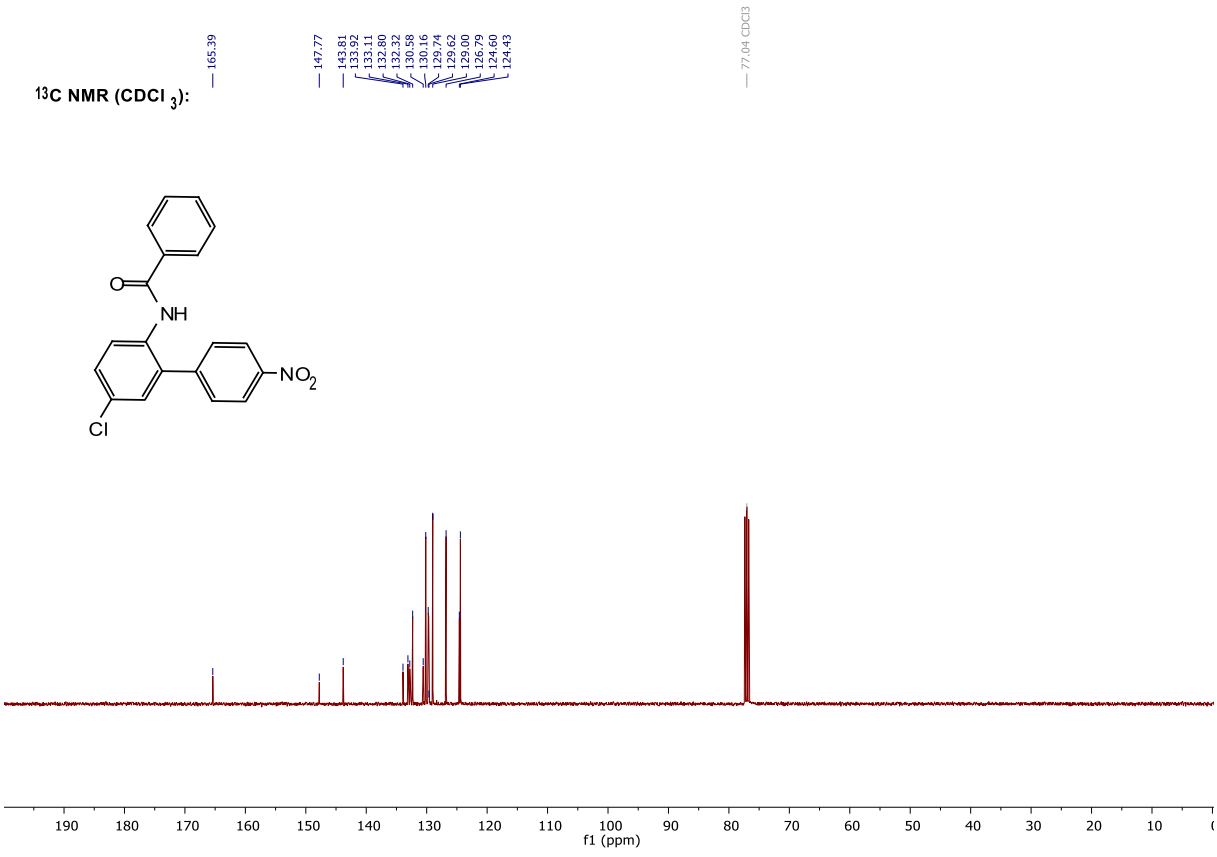

2-Benzamido-5-chloro-3’-methoxybiphenyl (1n)

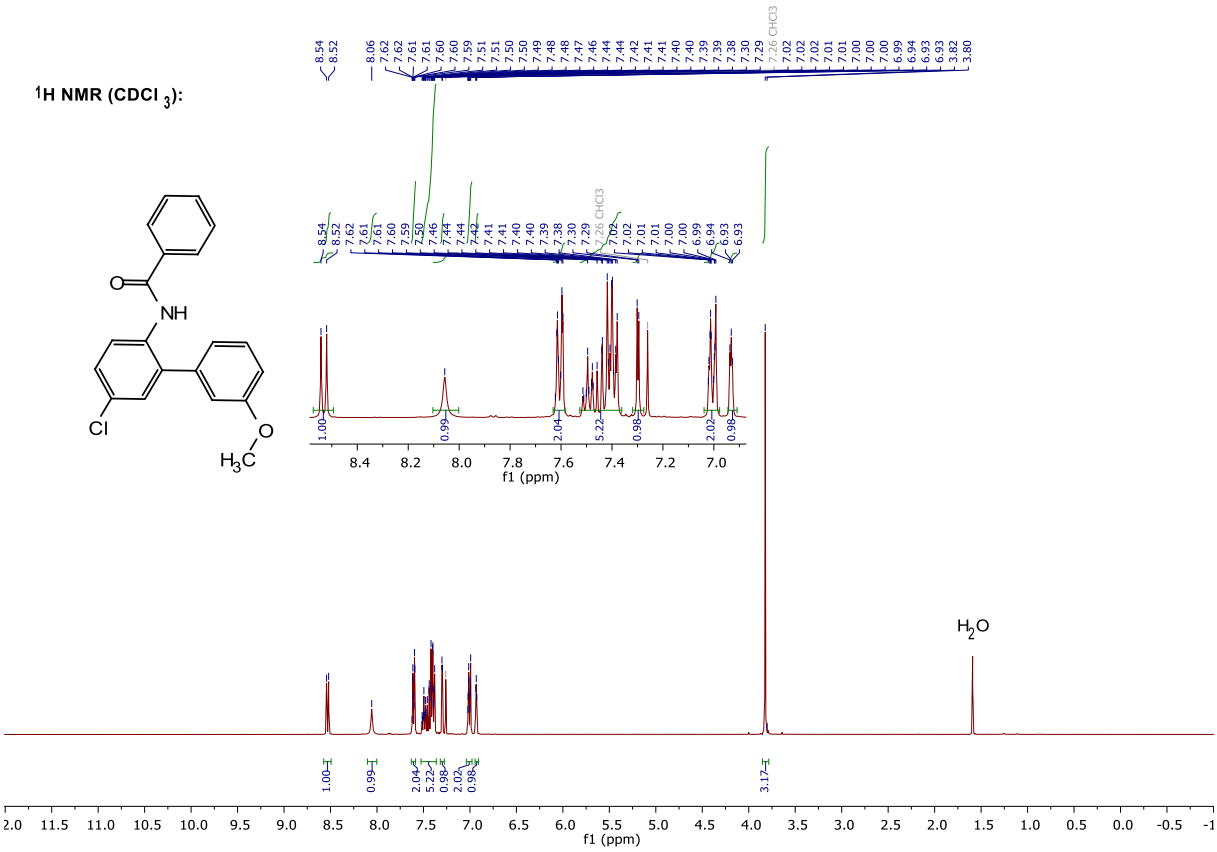

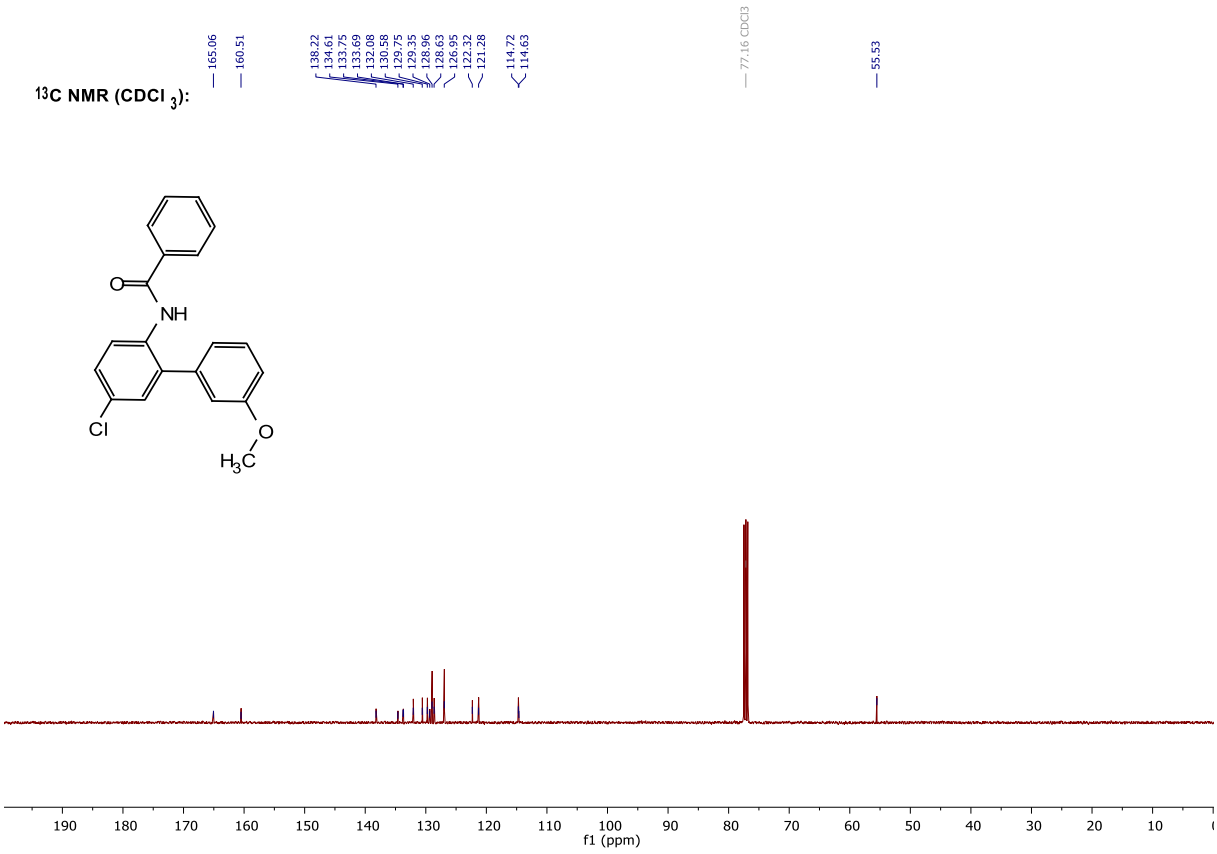

2-Benzamido-3’-methoxy 5-methyl-biphenyl (1o)

^{1}H NMR (CDCl $_3$):

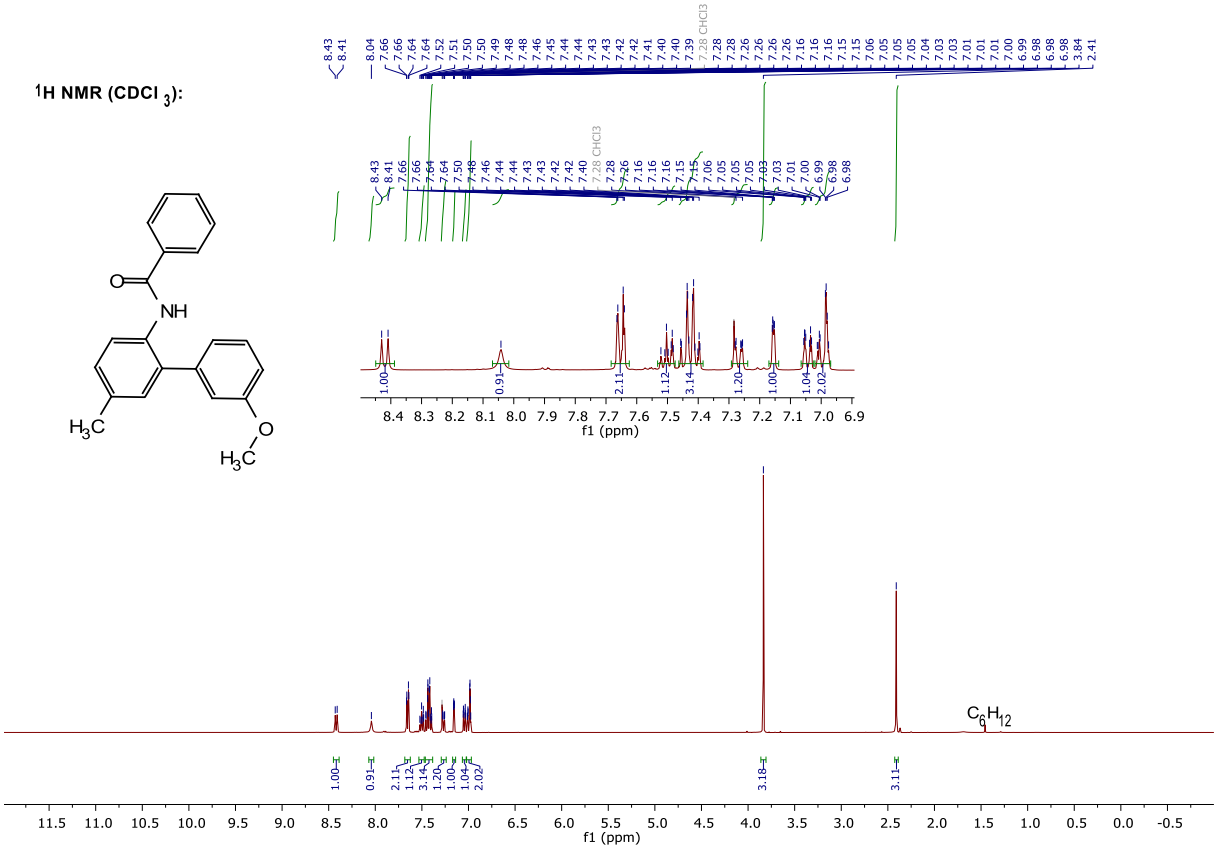

^{13}C NMR (CDCl $_3$):

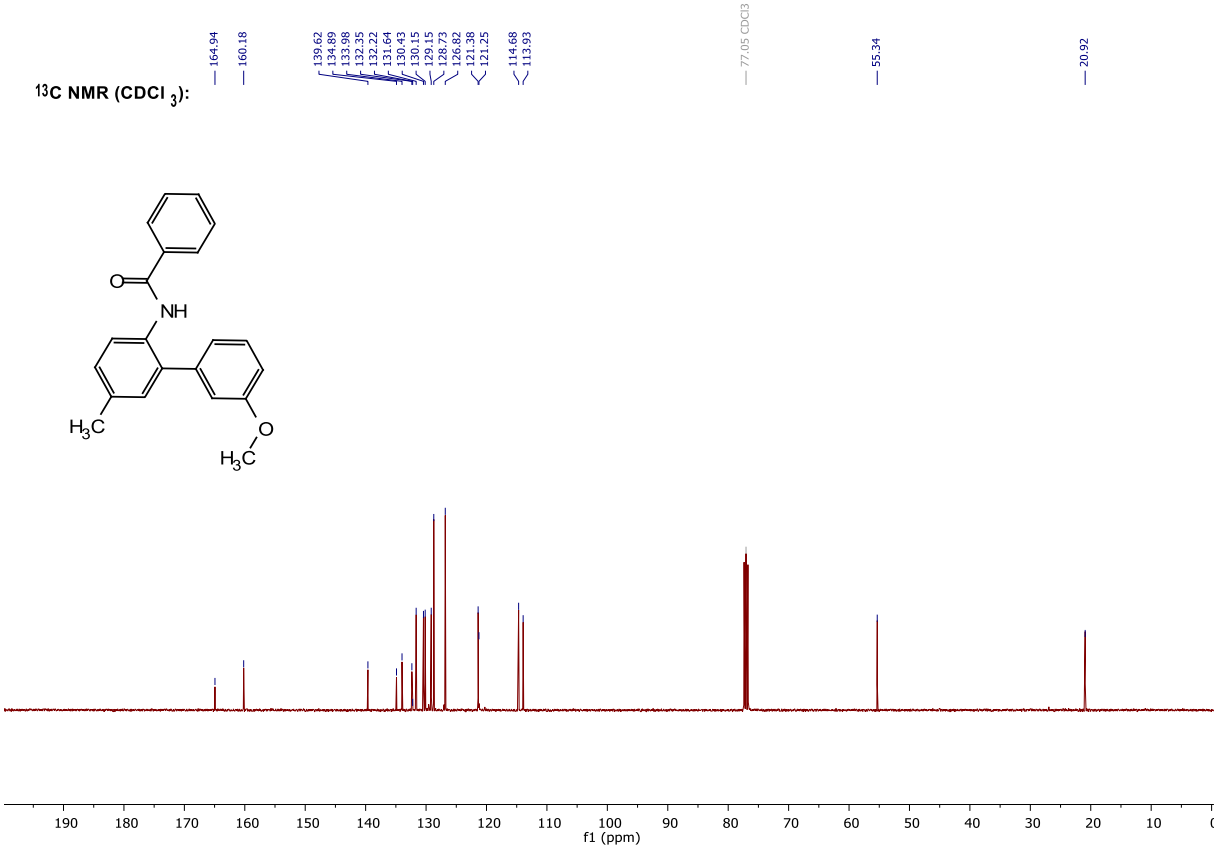

4-Benzamido-3-phenylpyridine (1p)

^{1}H NMR (CDCl$_3$):

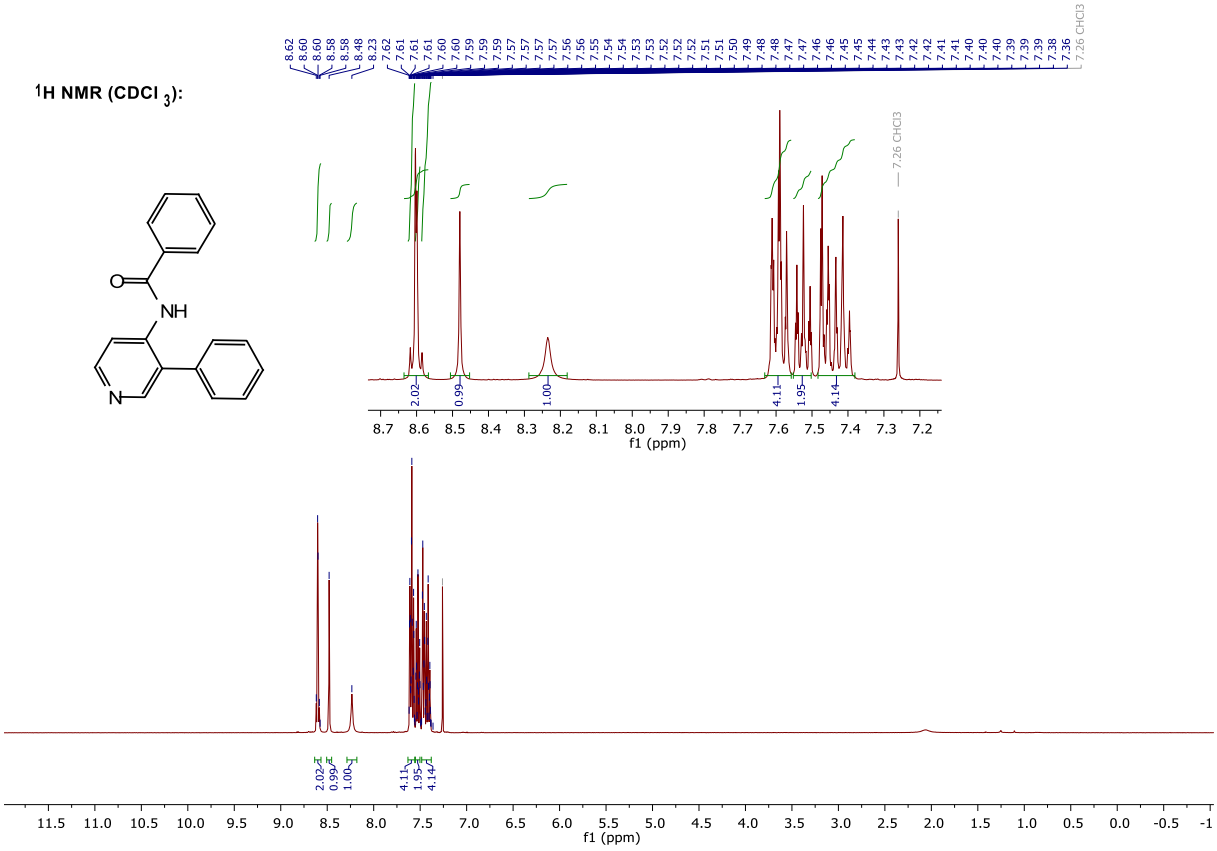

^{13}C NMR (CDCl$_3$):

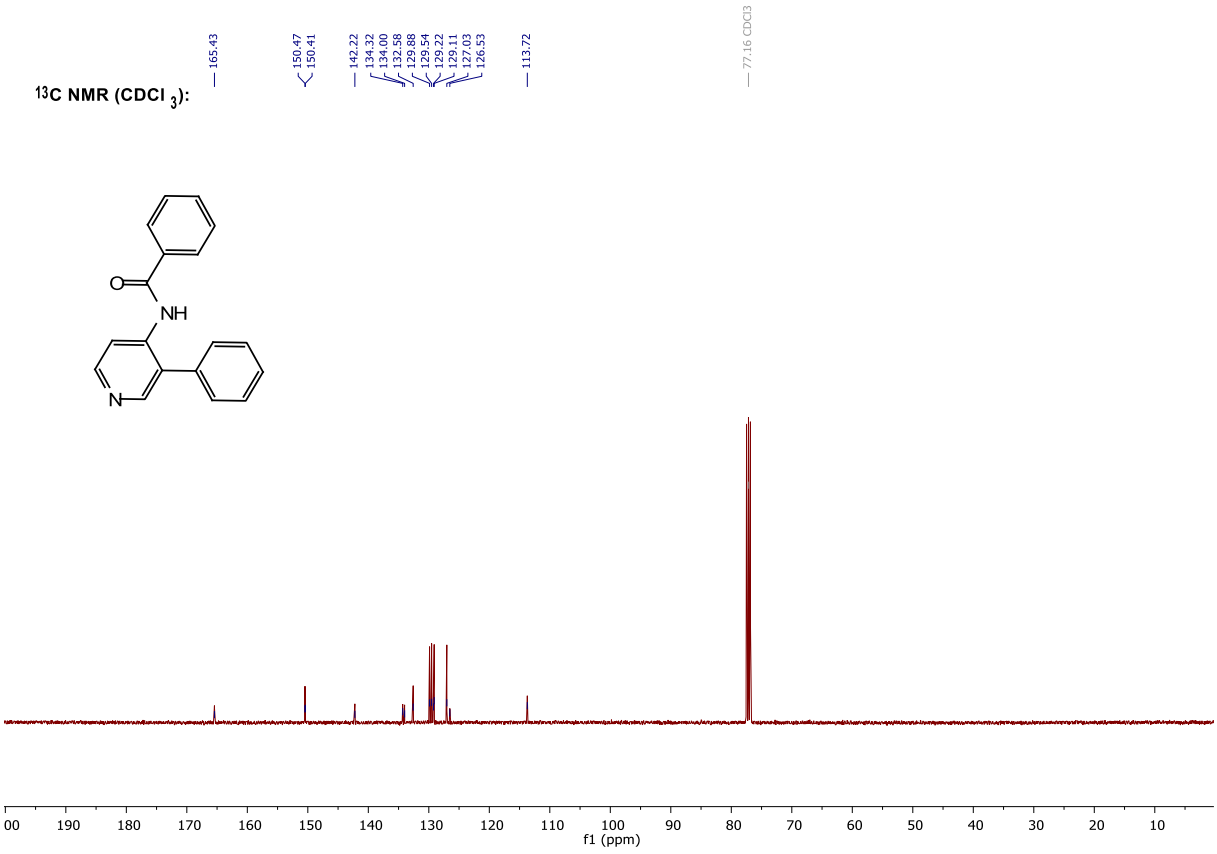

Methyl 2-(2’-benzamido-5’-chloro-[1,1’-biphenyl]-4’-yl)propanoate (1q)

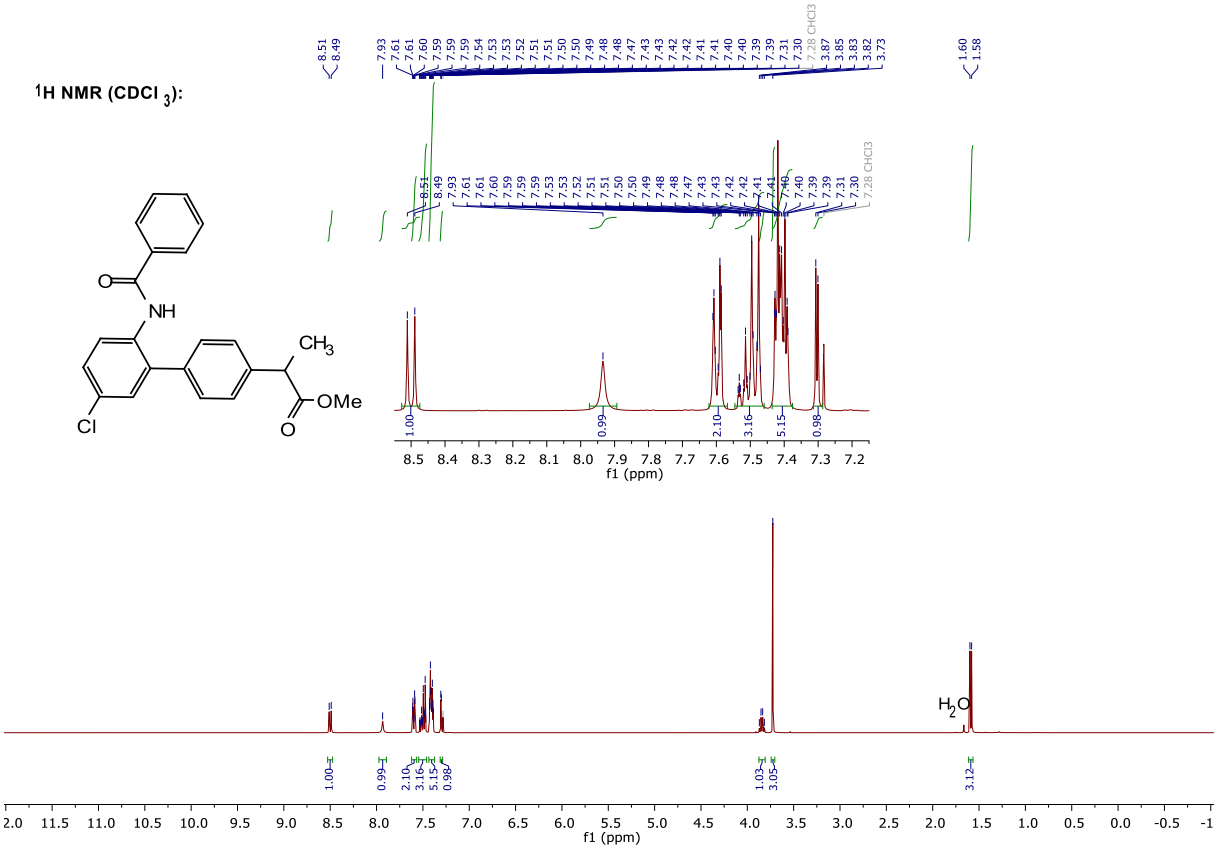

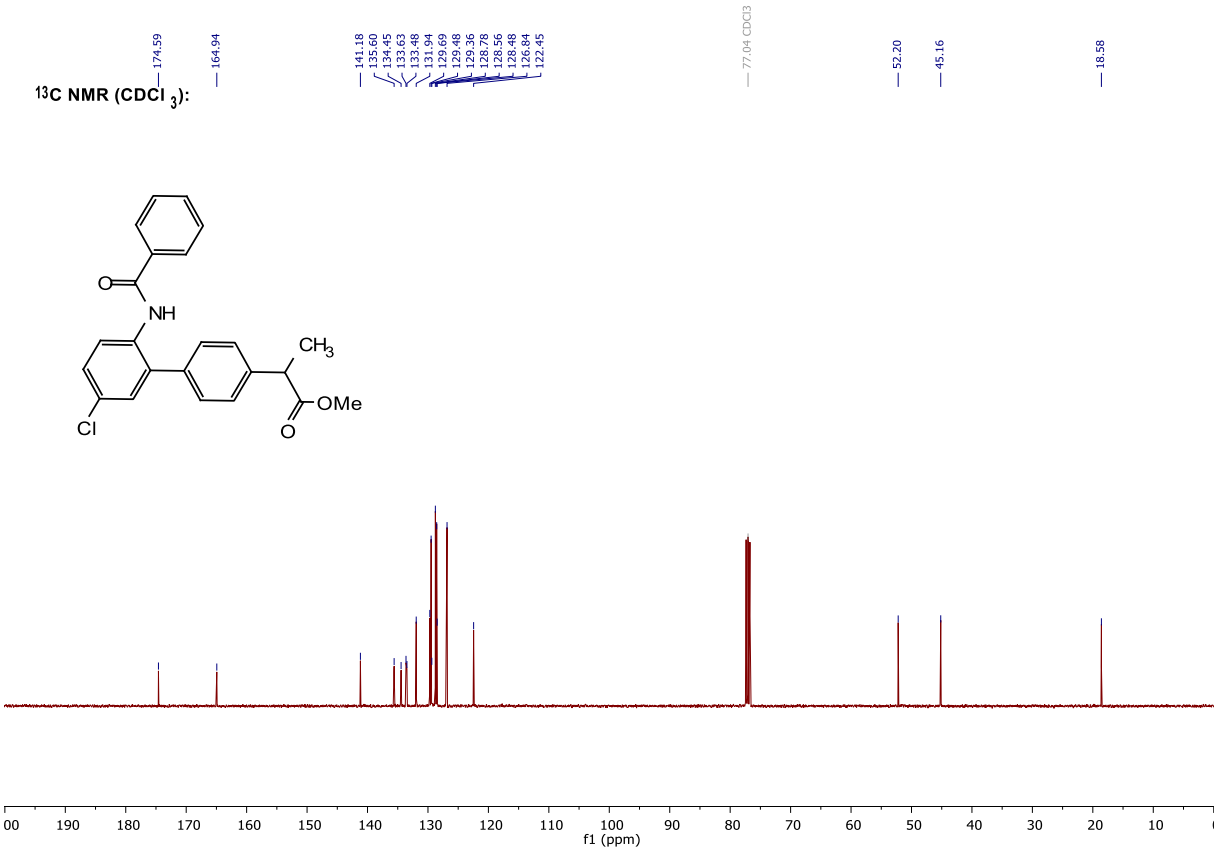

N-(4-Chloro-2-(pyridine-4-yl)phenyl)benzamide (1r)

^{1}H NMR (CDCl $_3$):

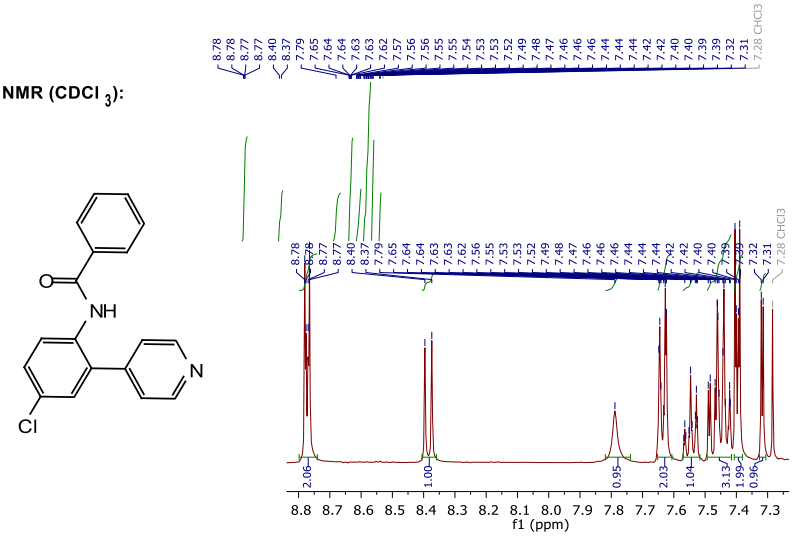

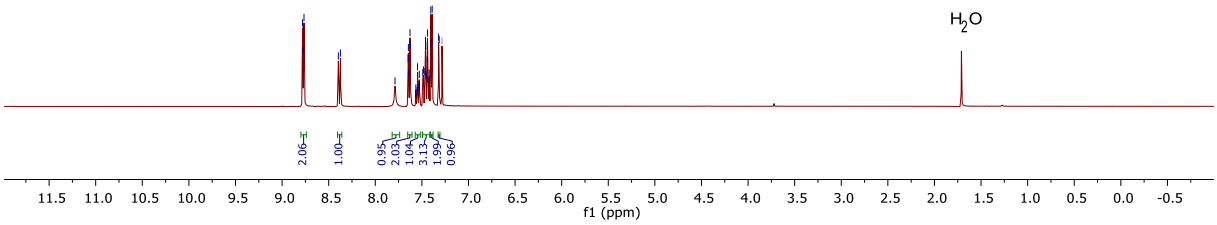

^{13}C NMR (CDCl $_3$):

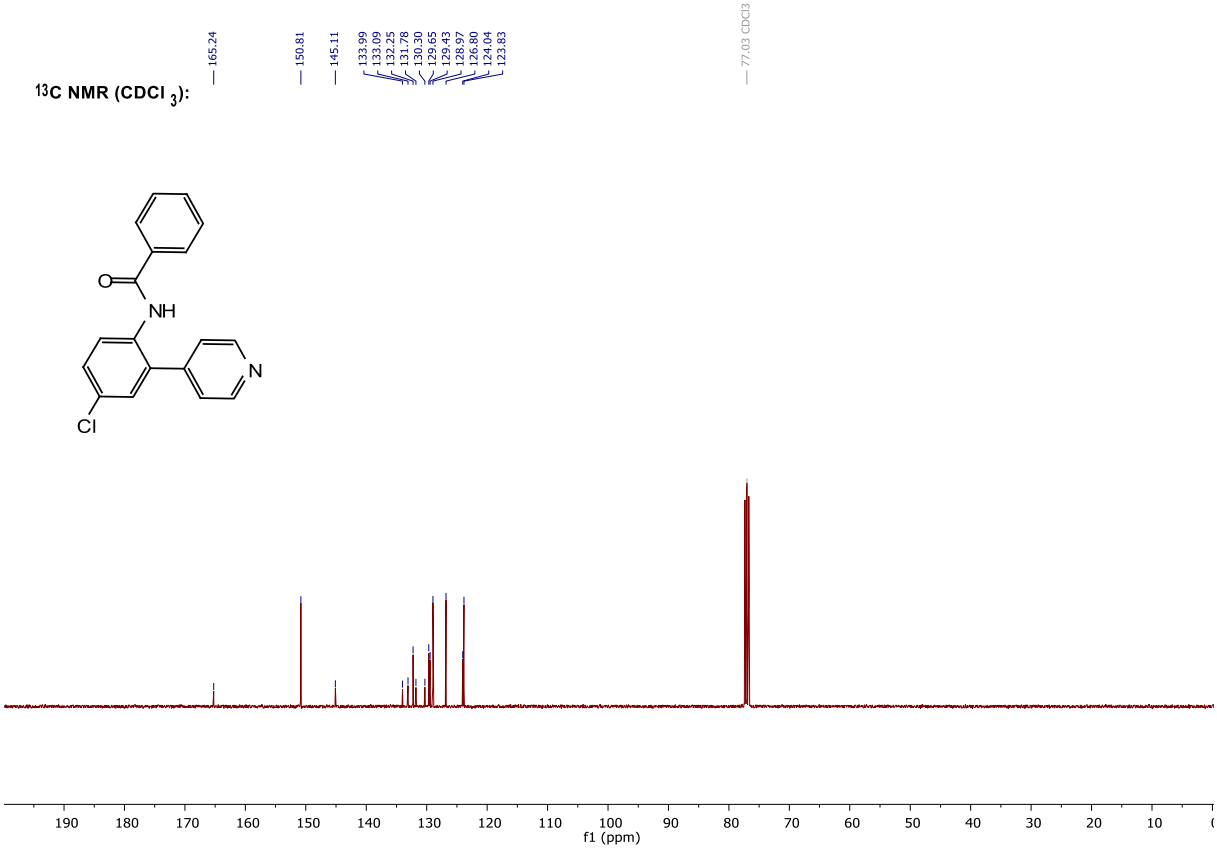

3-Chloro-9-(4-methylbenzoyl)-carbazole (2a)

^{1}H NMR ($CDCl_3$):

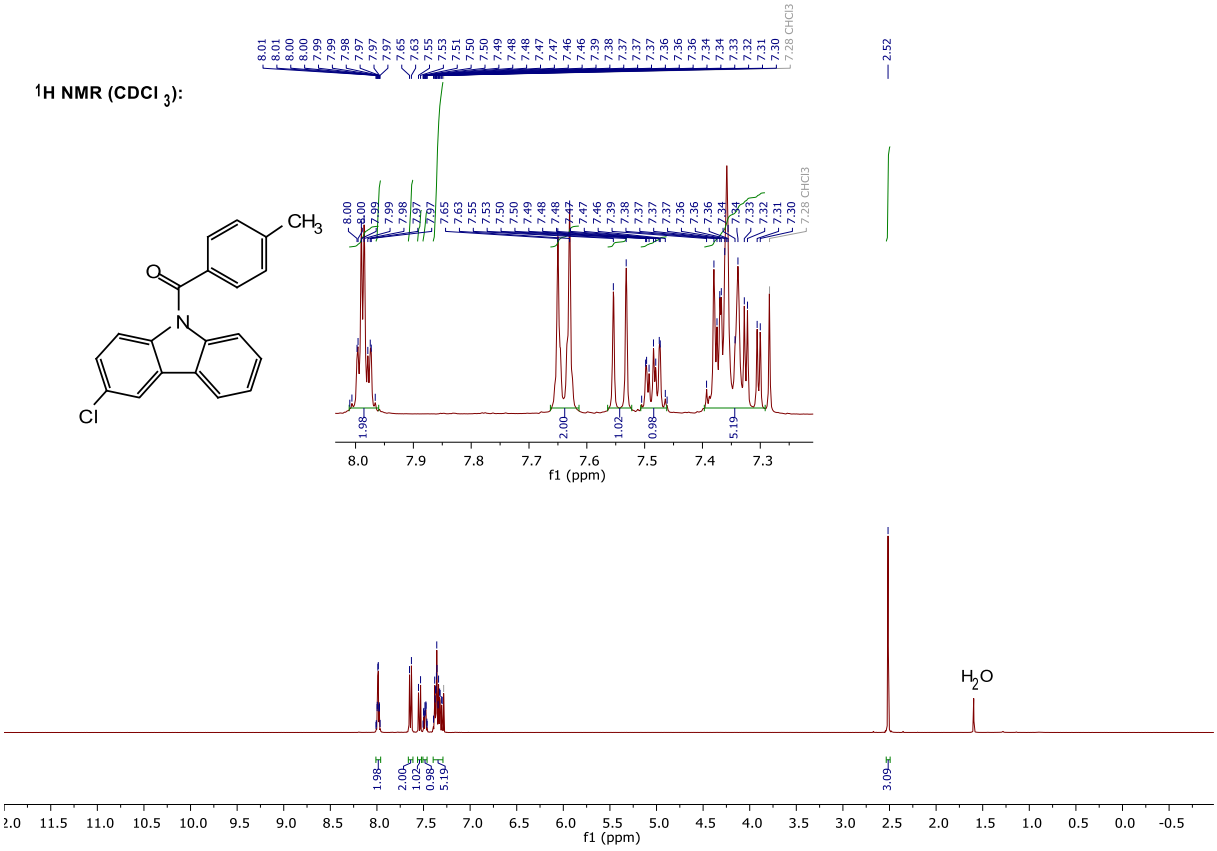

^{13}C NMR ($CDCl_3$):

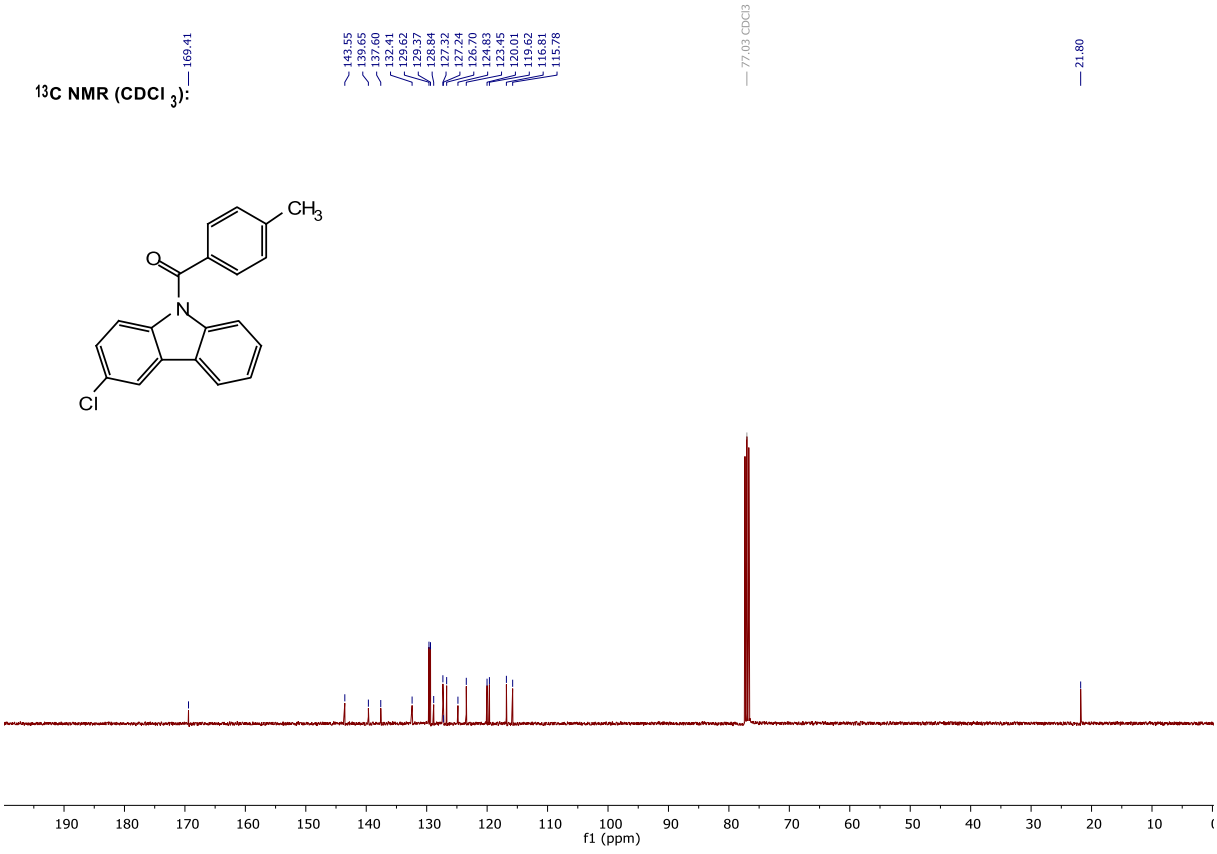

9-Benzoyl-3-chlorocarbazole (2b)

^{1}H NMR ($CDCl_3$):

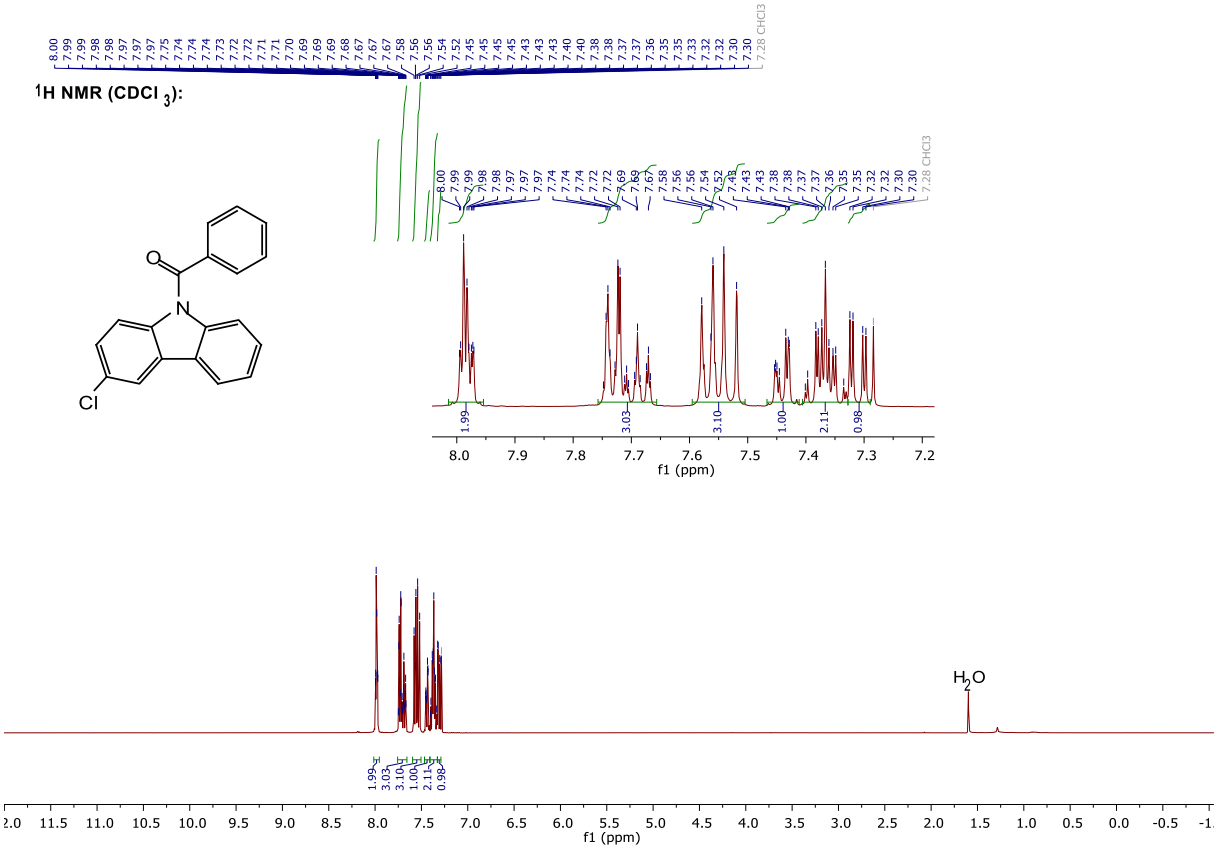

^{13}C NMR ($CDCl_3$):

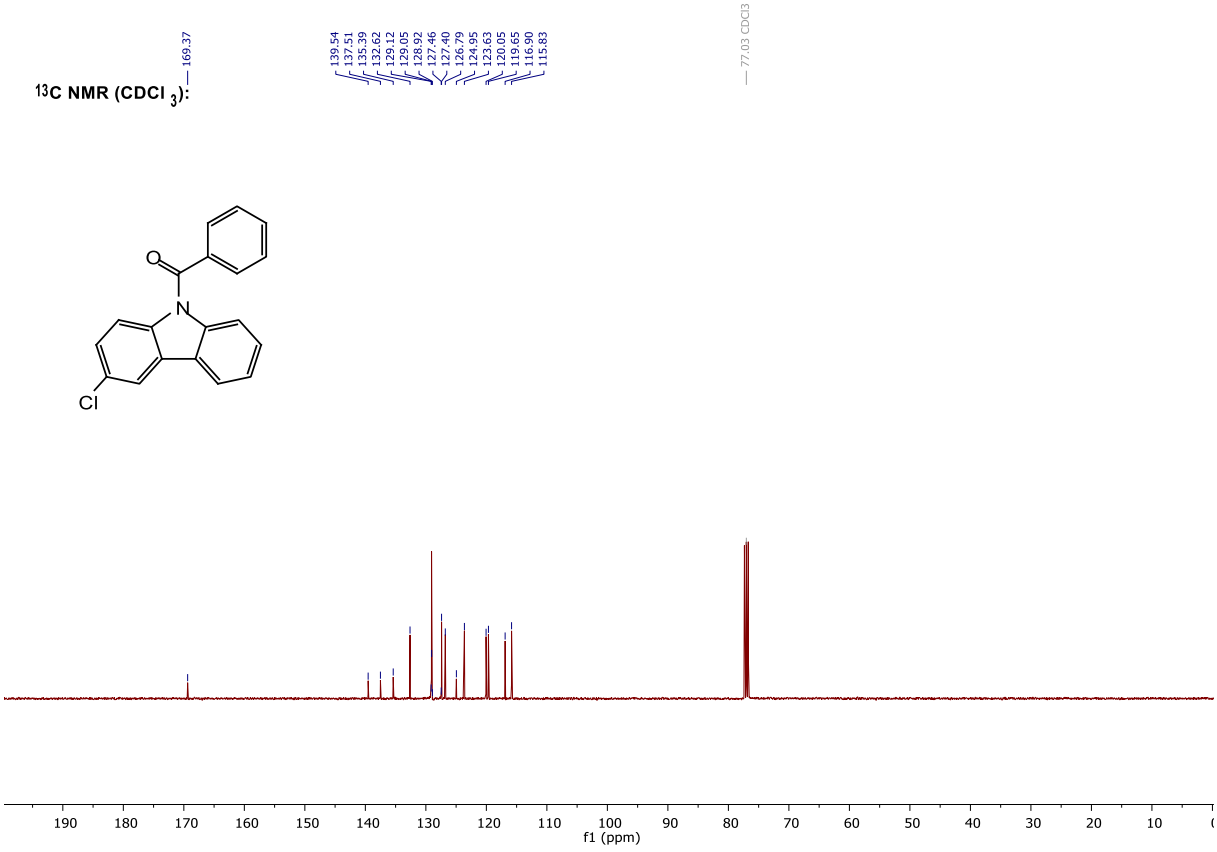

9-Acetyl-3-chlorocarbazole (2c)

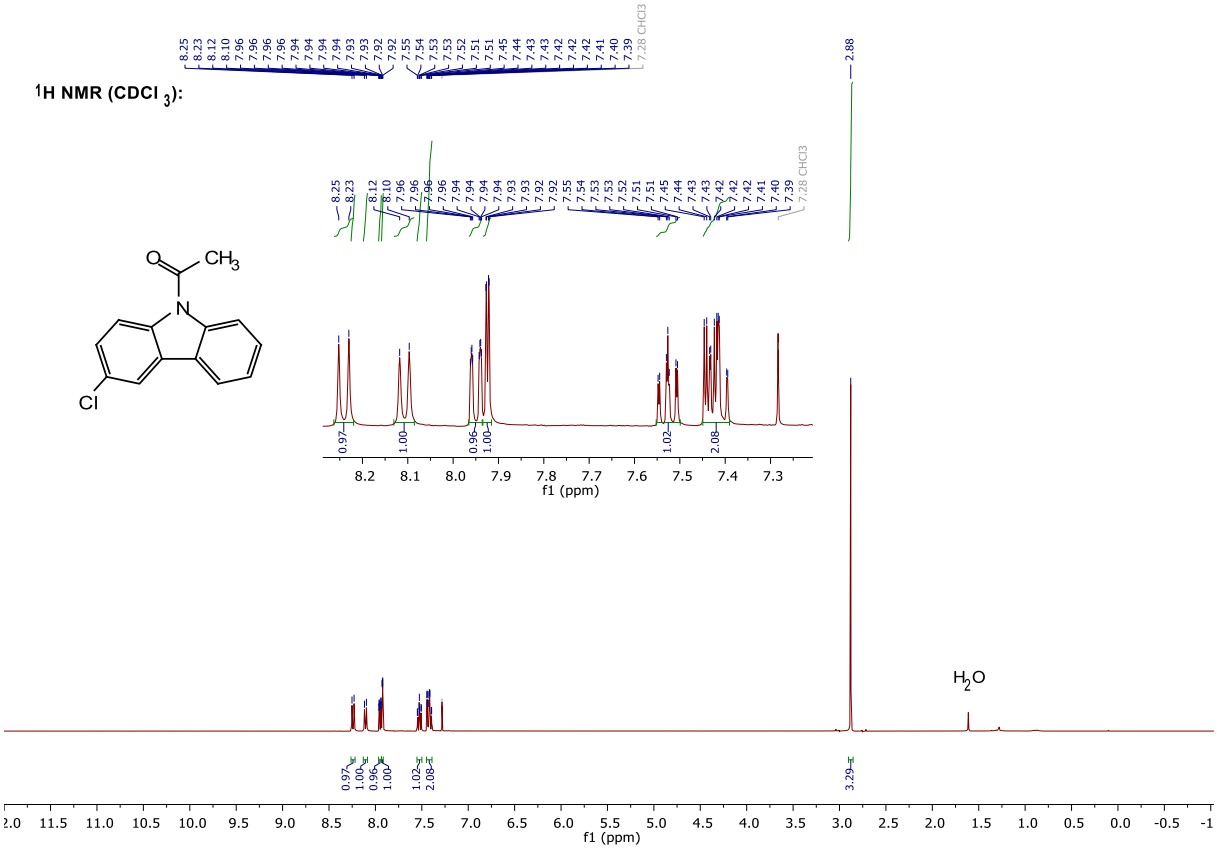

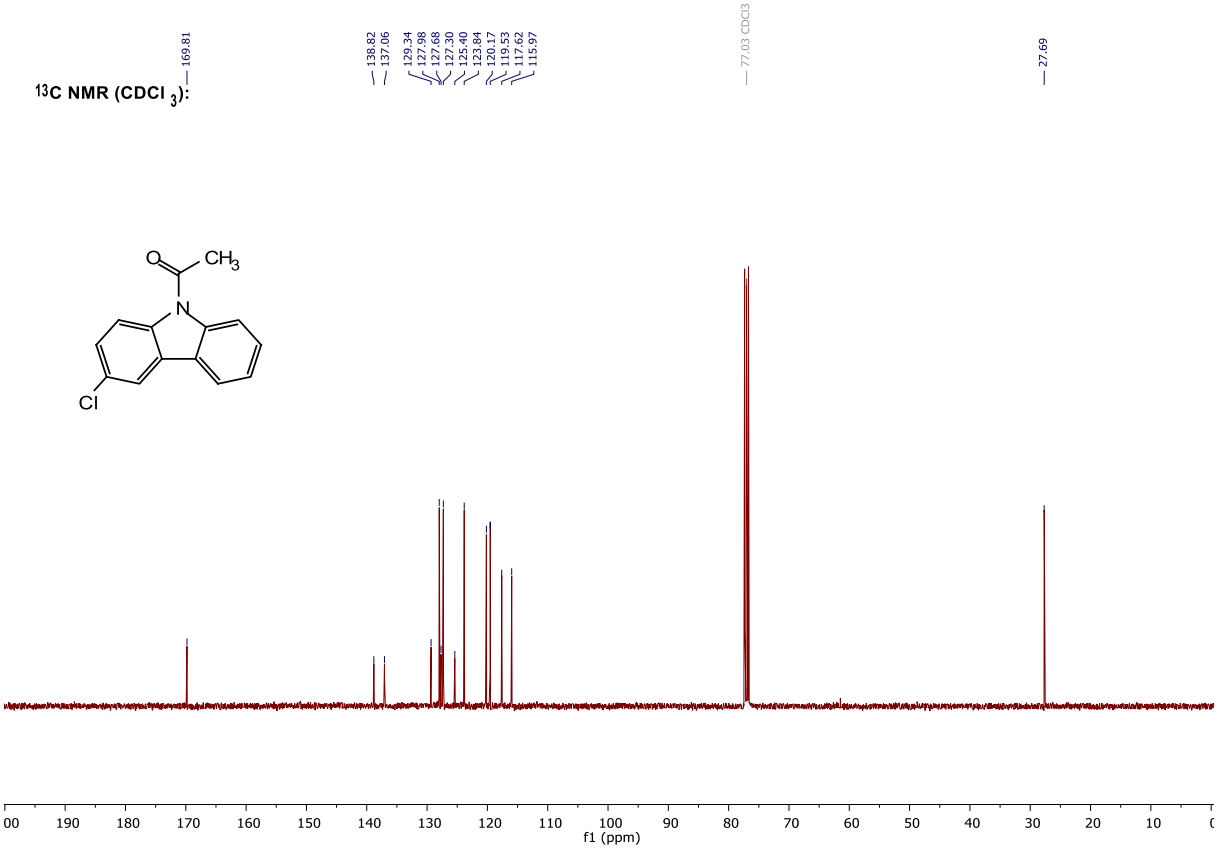

9-Benzoylcarbazole (2d)

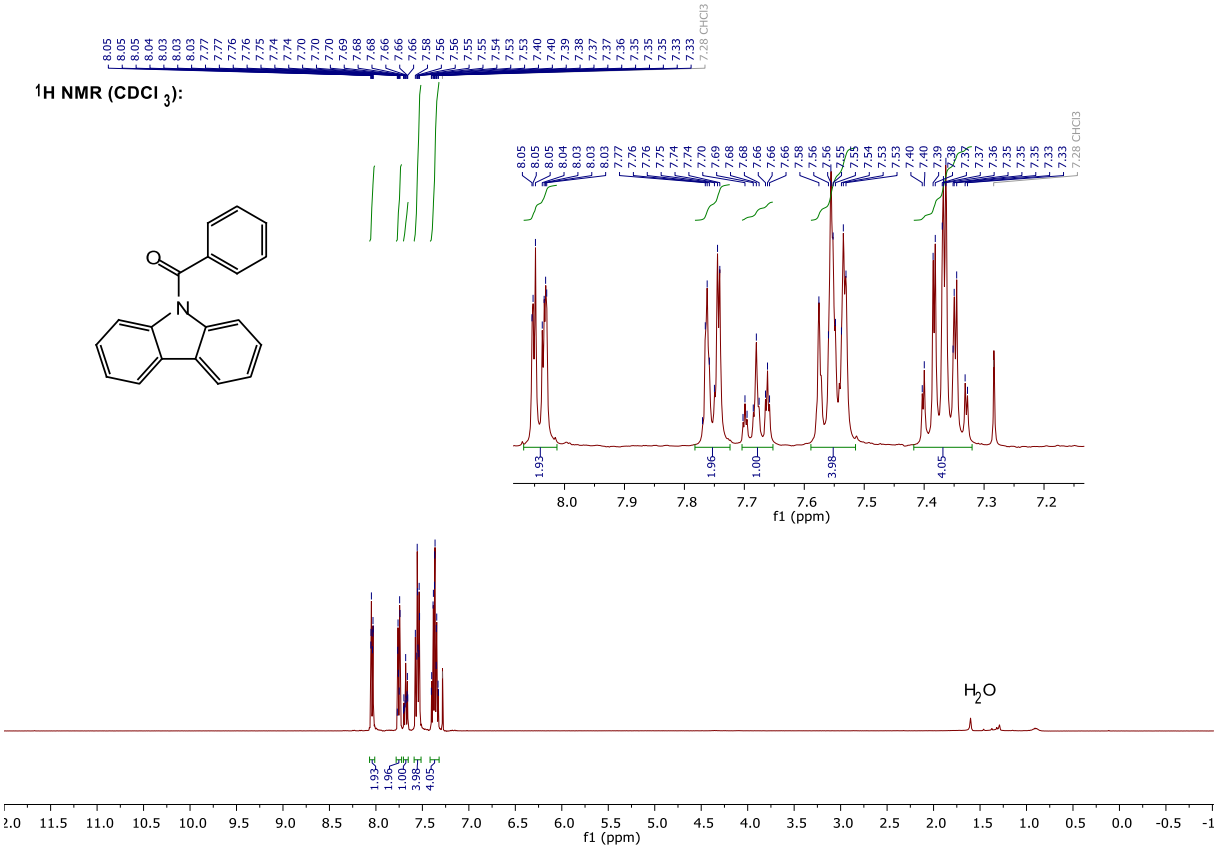

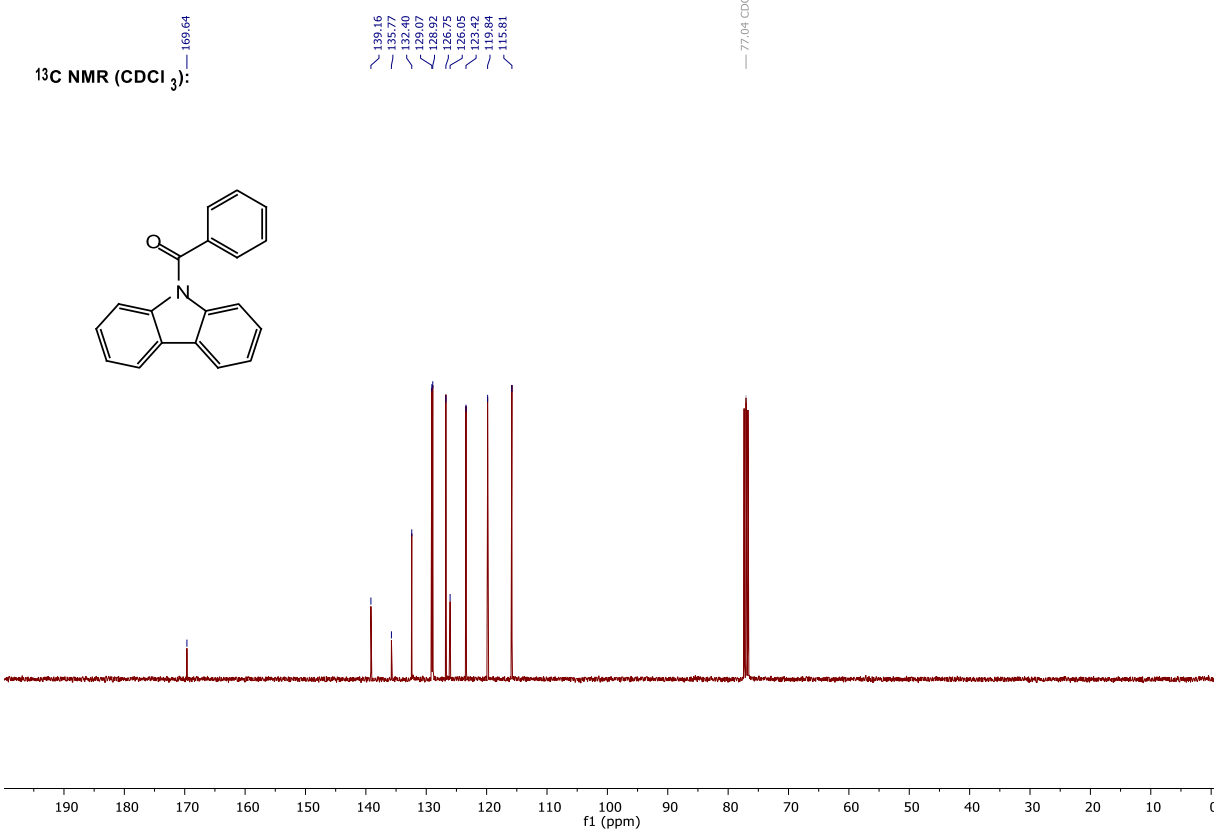

9-Benzoyl-2,3-dimethylcarbazole (2e)

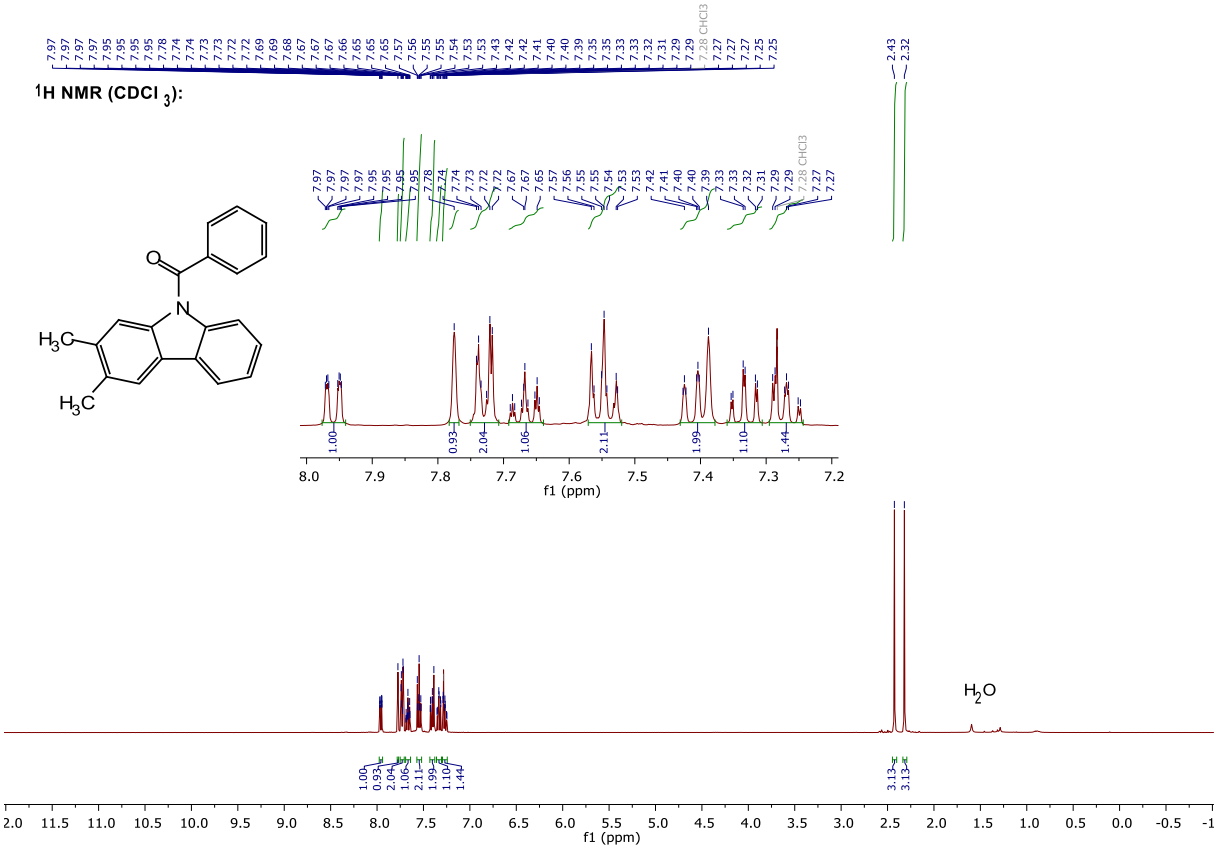

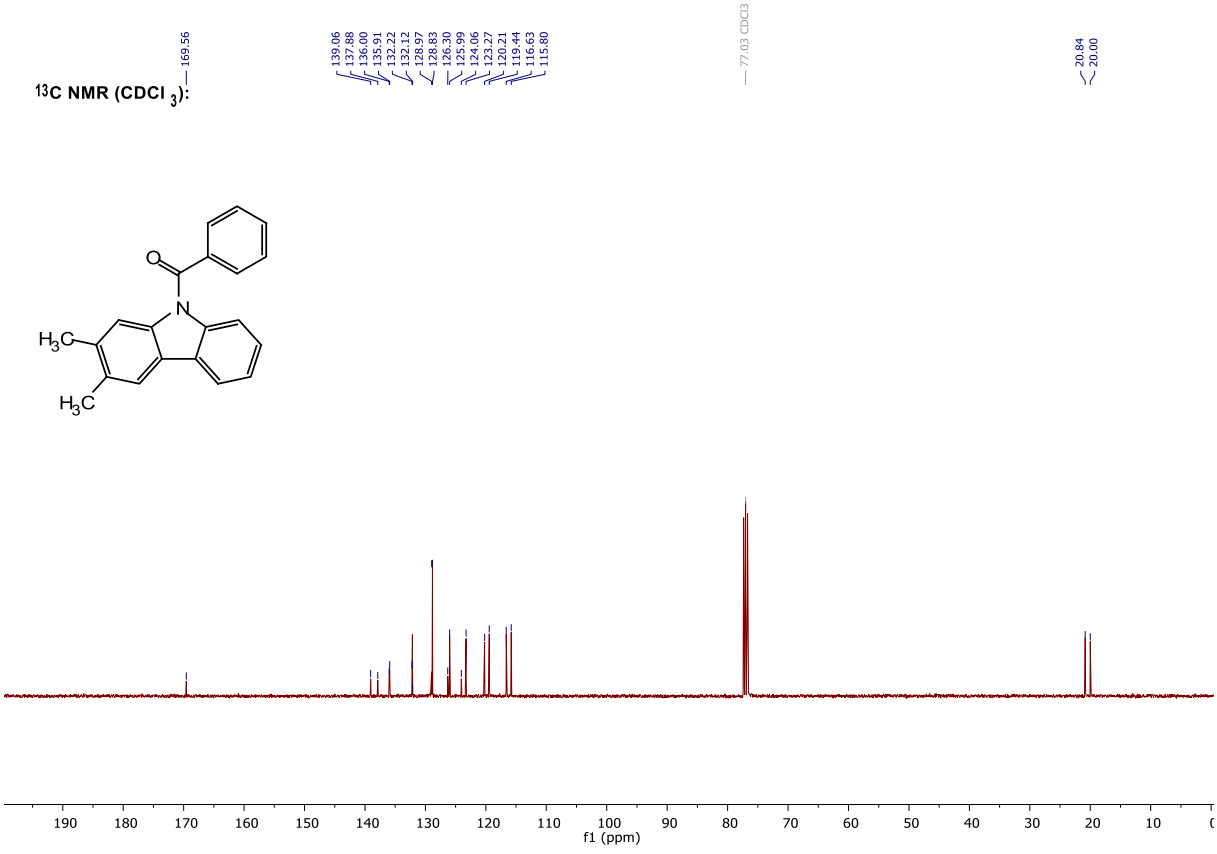

9-Benzoyl-3-fluorocarbazole (2f)

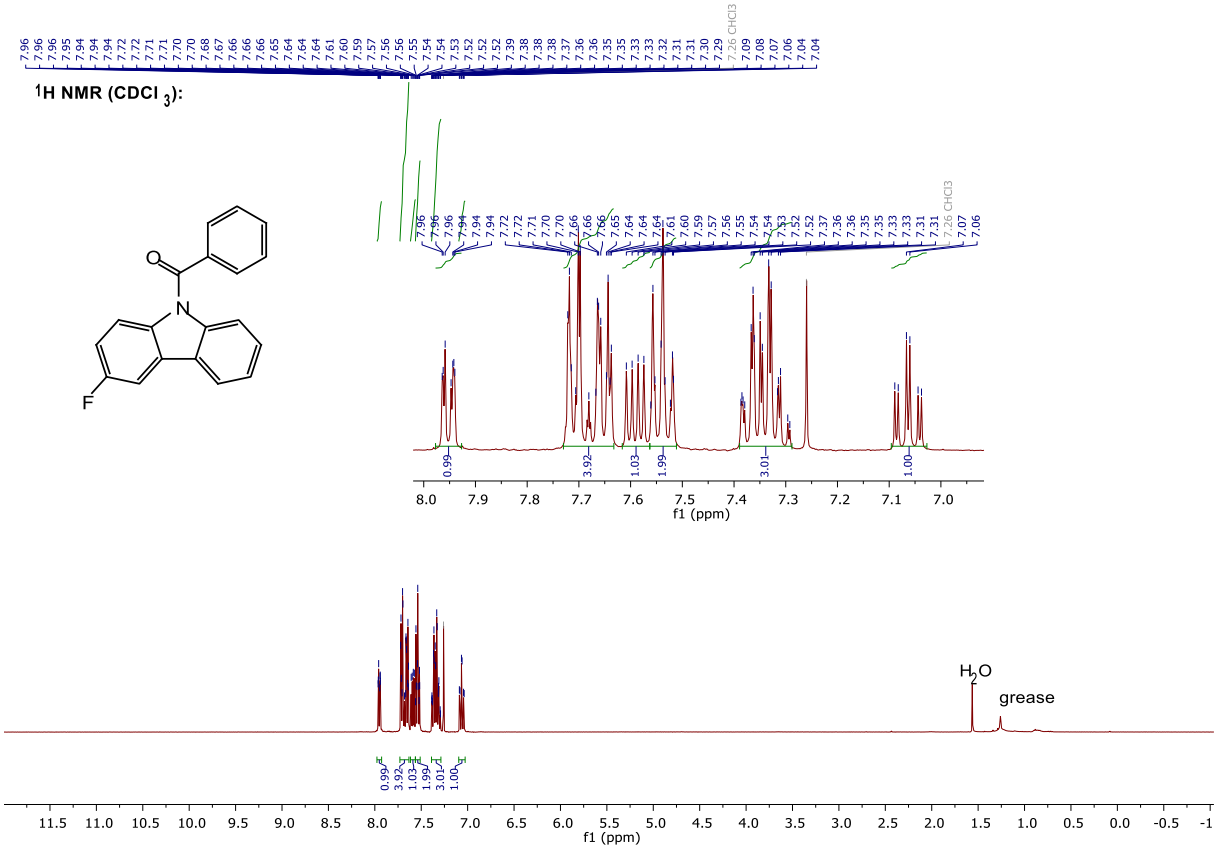

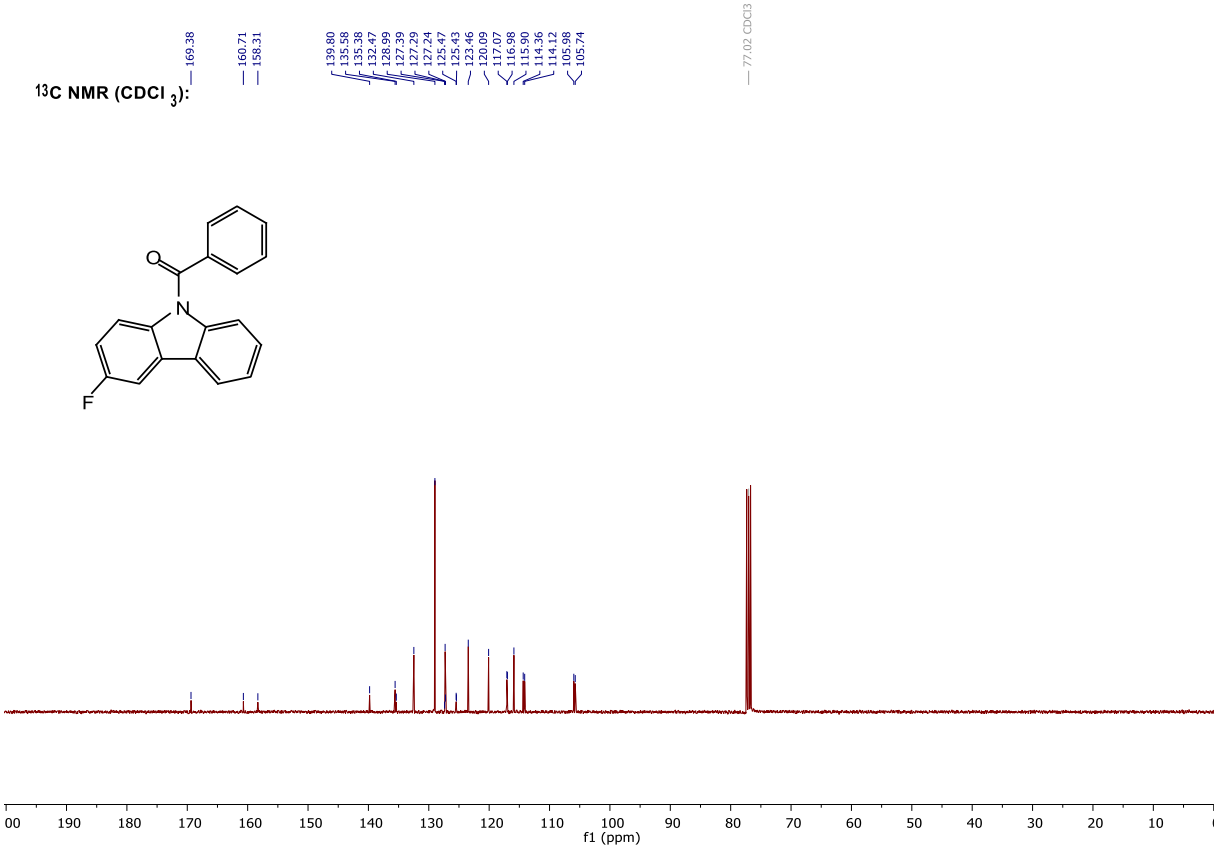

^{19}F NMR ($CDCl_3$):

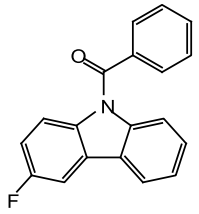

9-Benzoyl-3-bromocarbazole (2g)

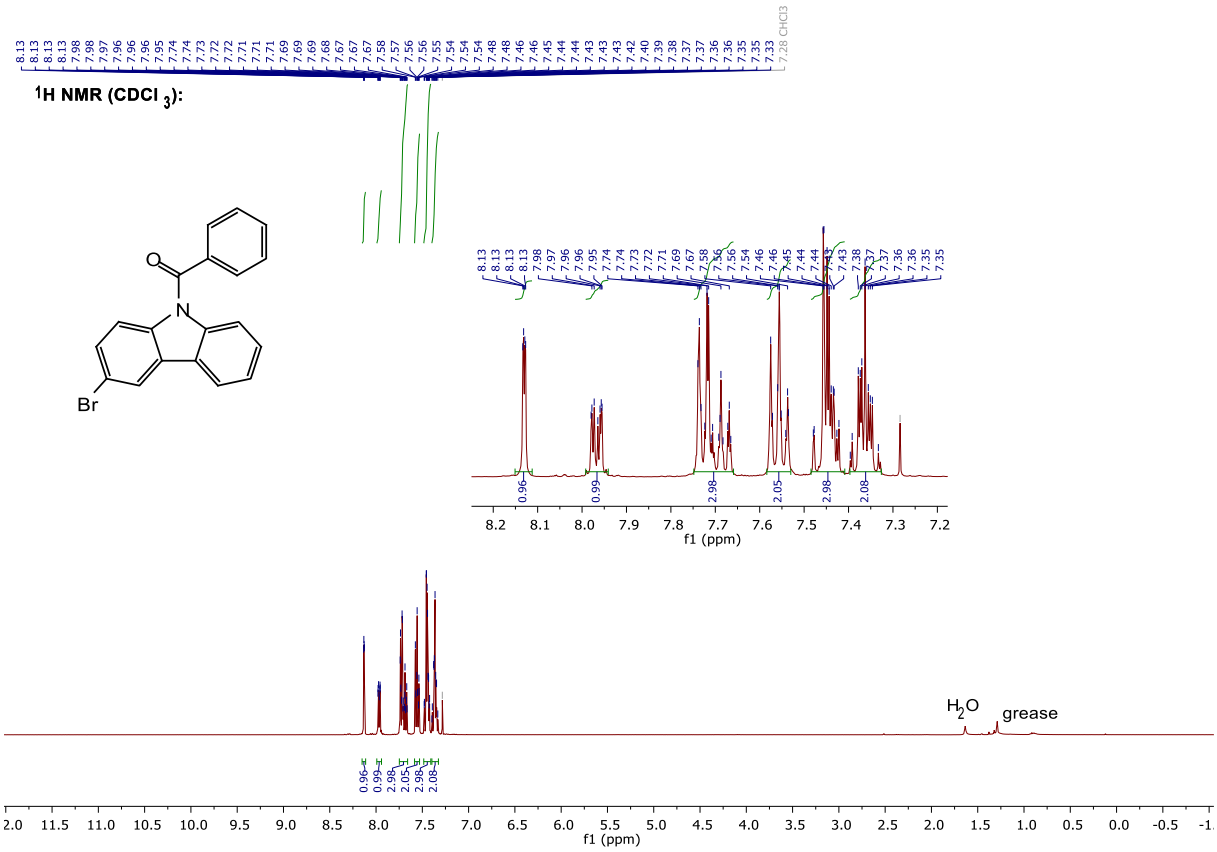

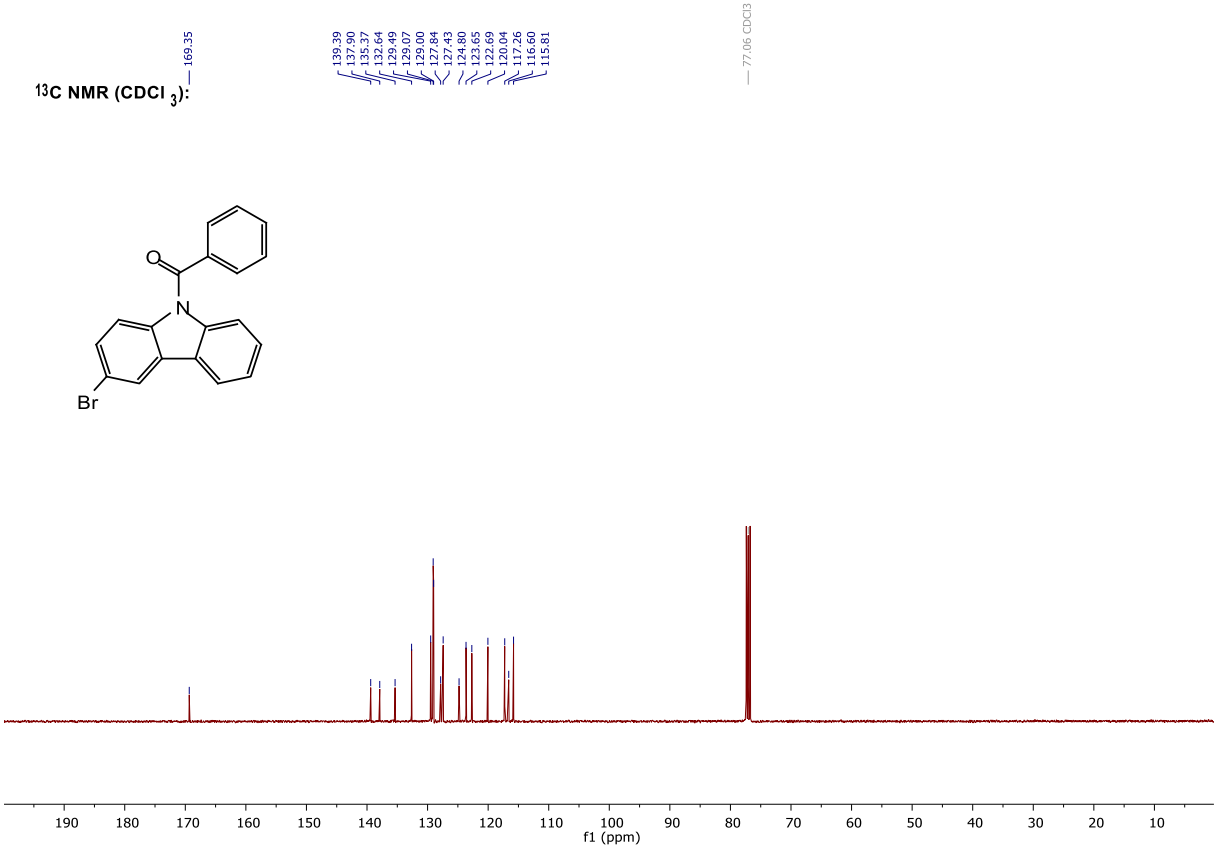

9-Benzoyl-3-cyanocarbazole (2h)

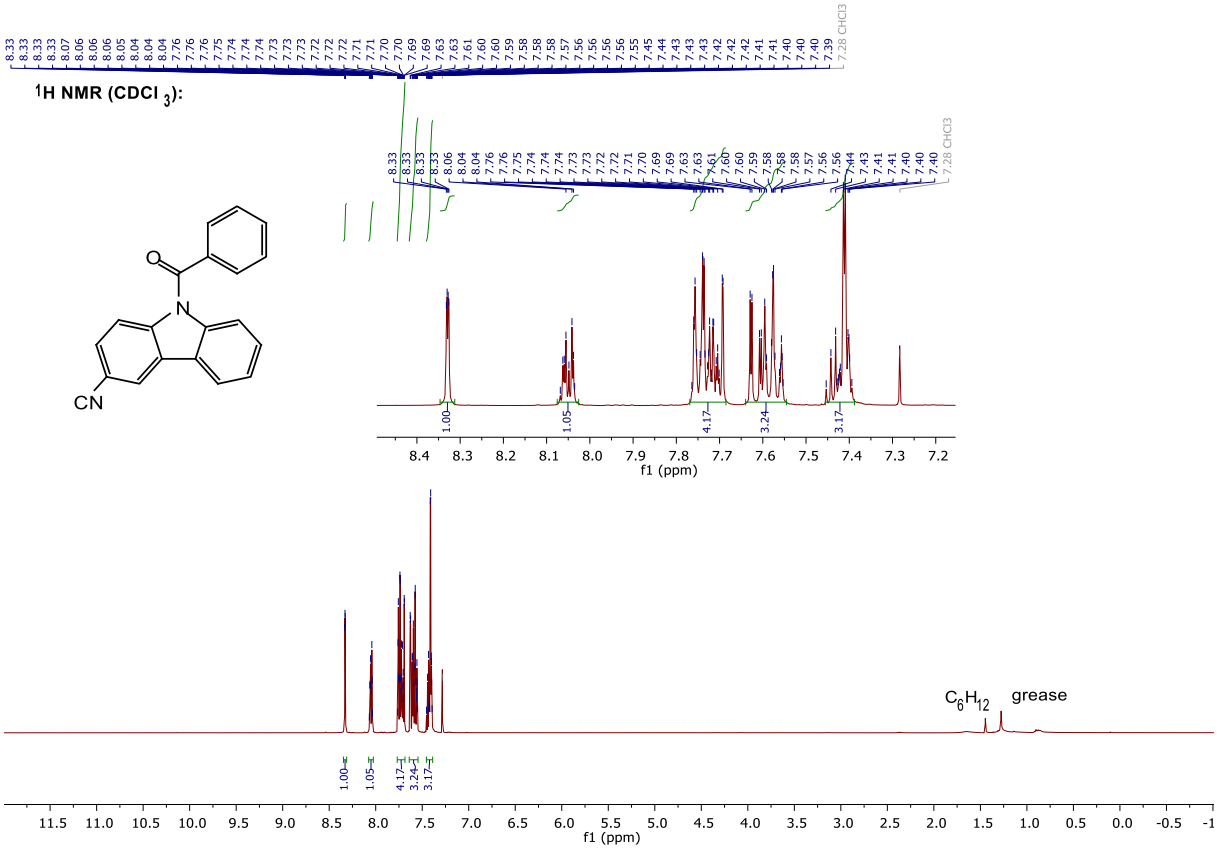

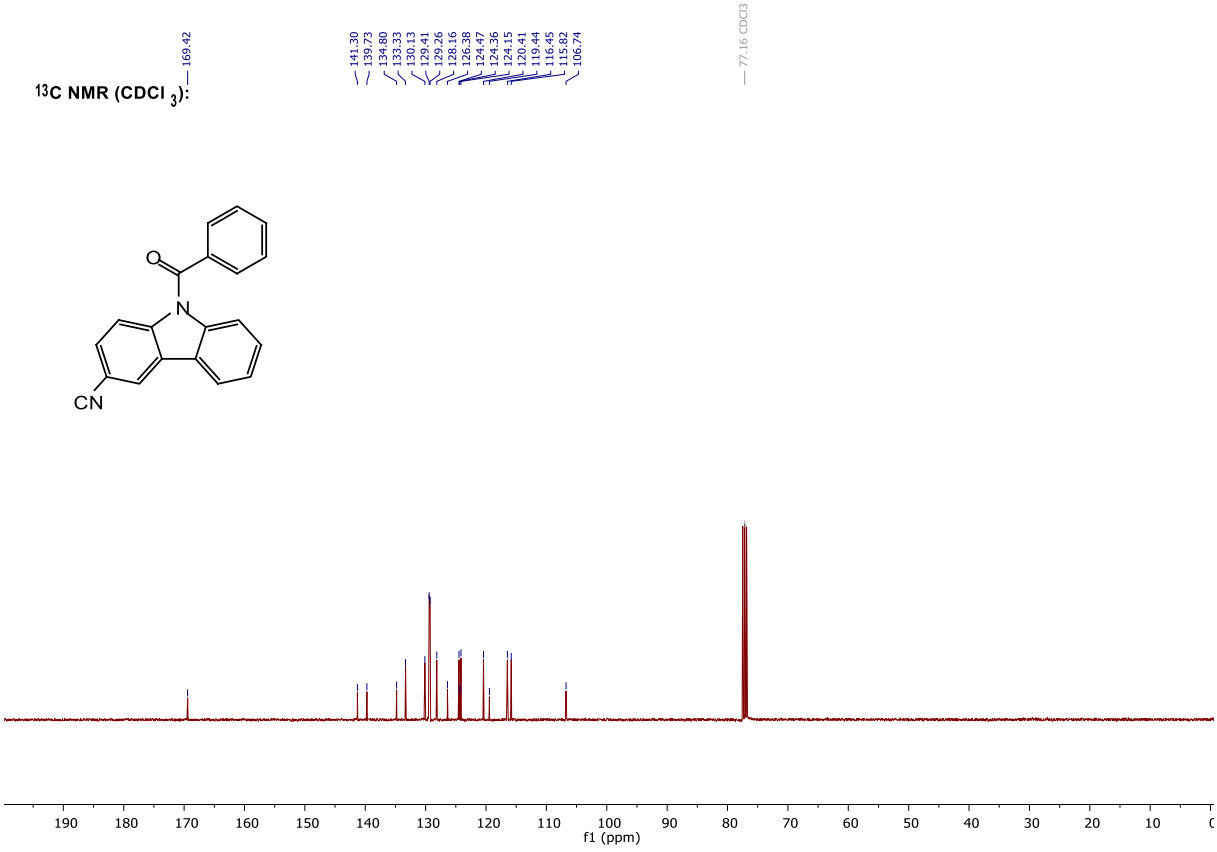

Ethyl 9-benzoylcarbazole-3-carboxylate (2i)

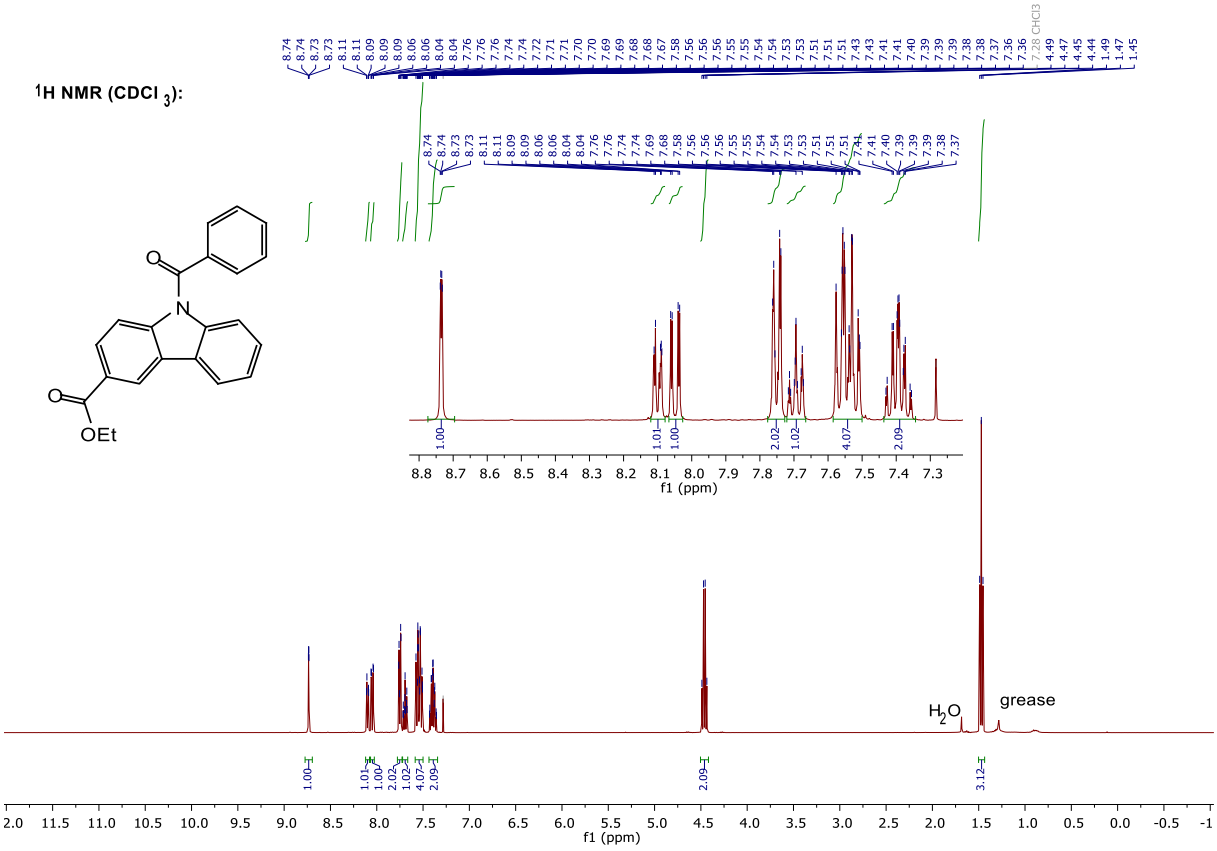

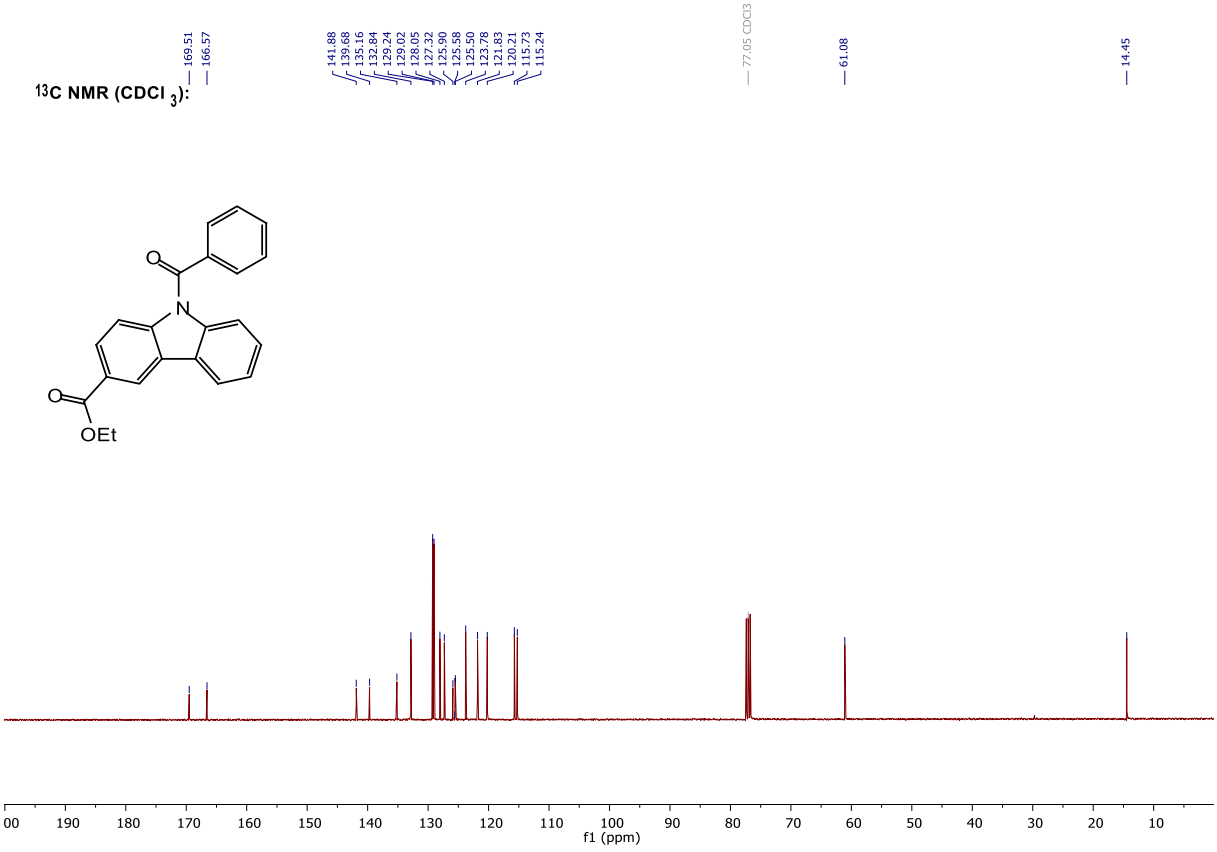

9-Benzoyl-7-*tert*-butyl-3-chloro-carbazole (2j)

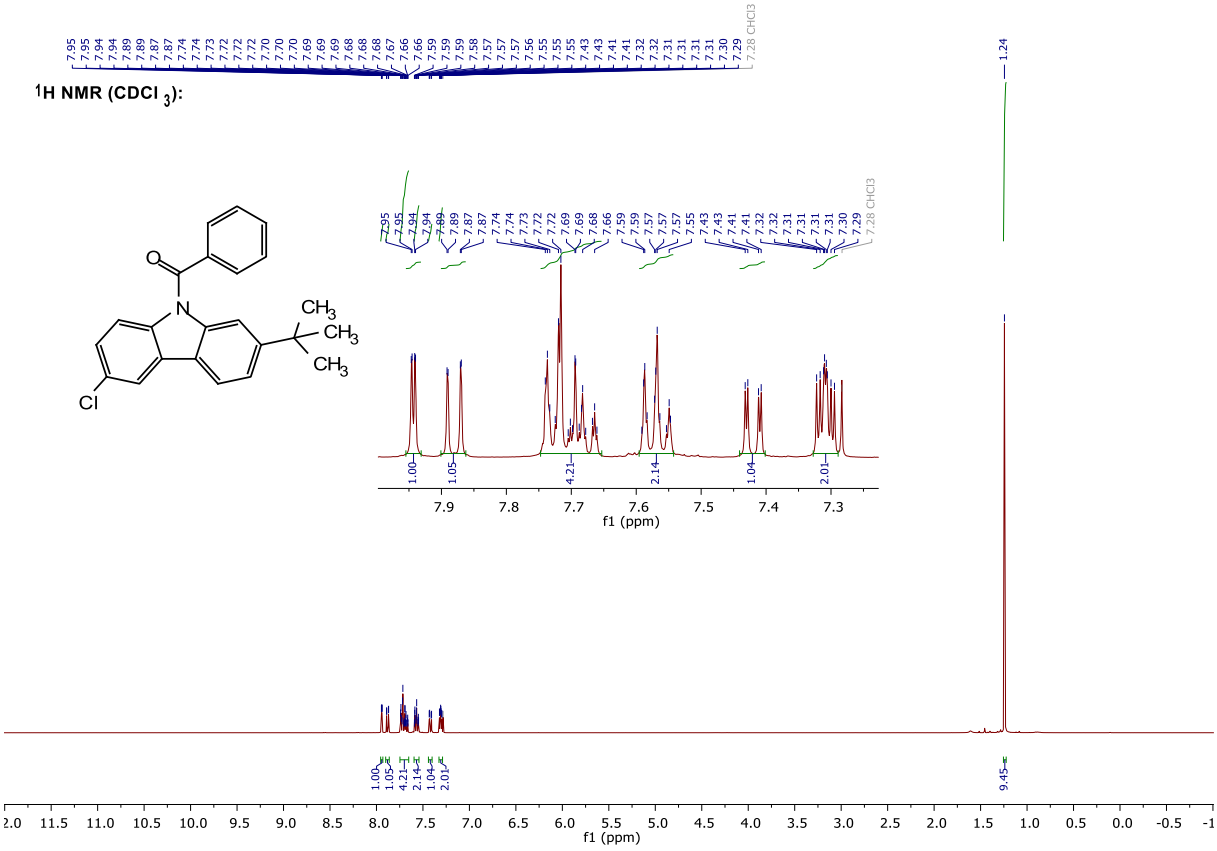

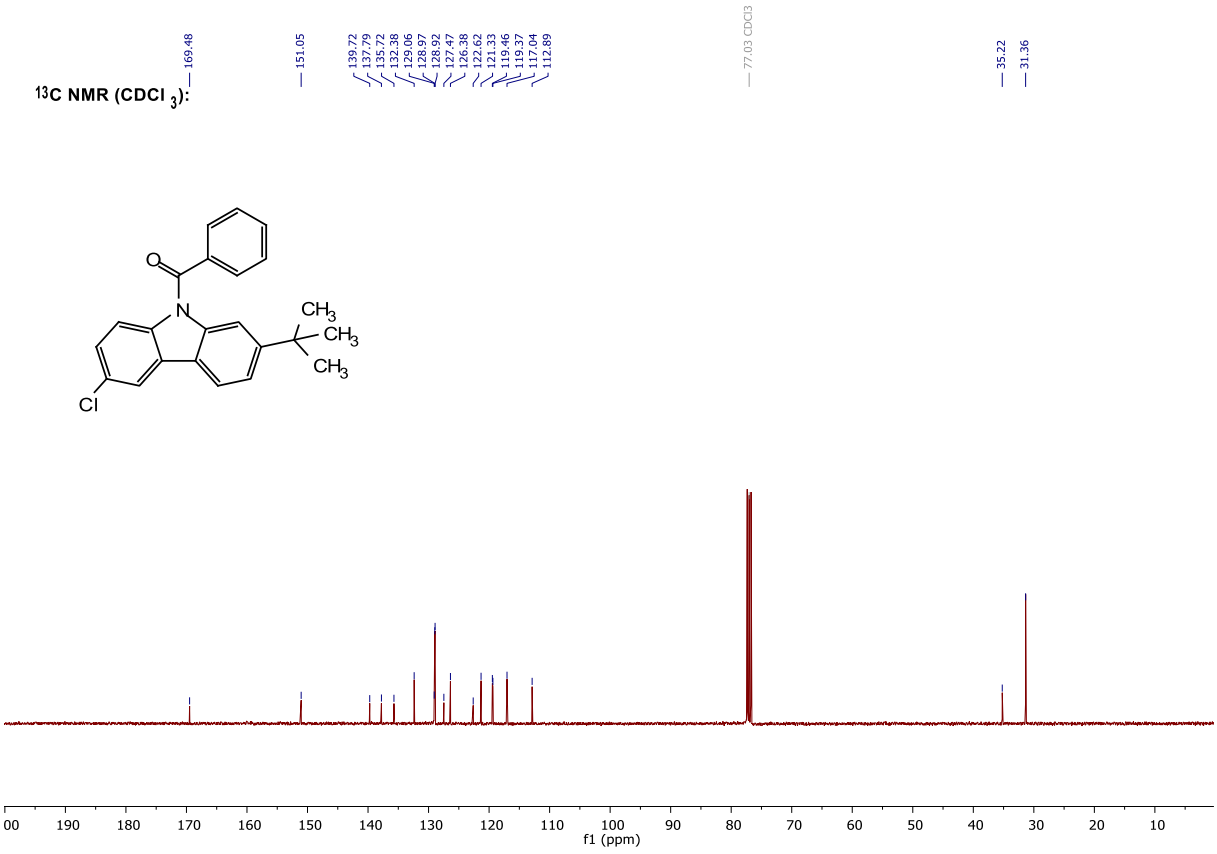

9-Benzoyl-2-chloro-6-methylcarbazole (2k)

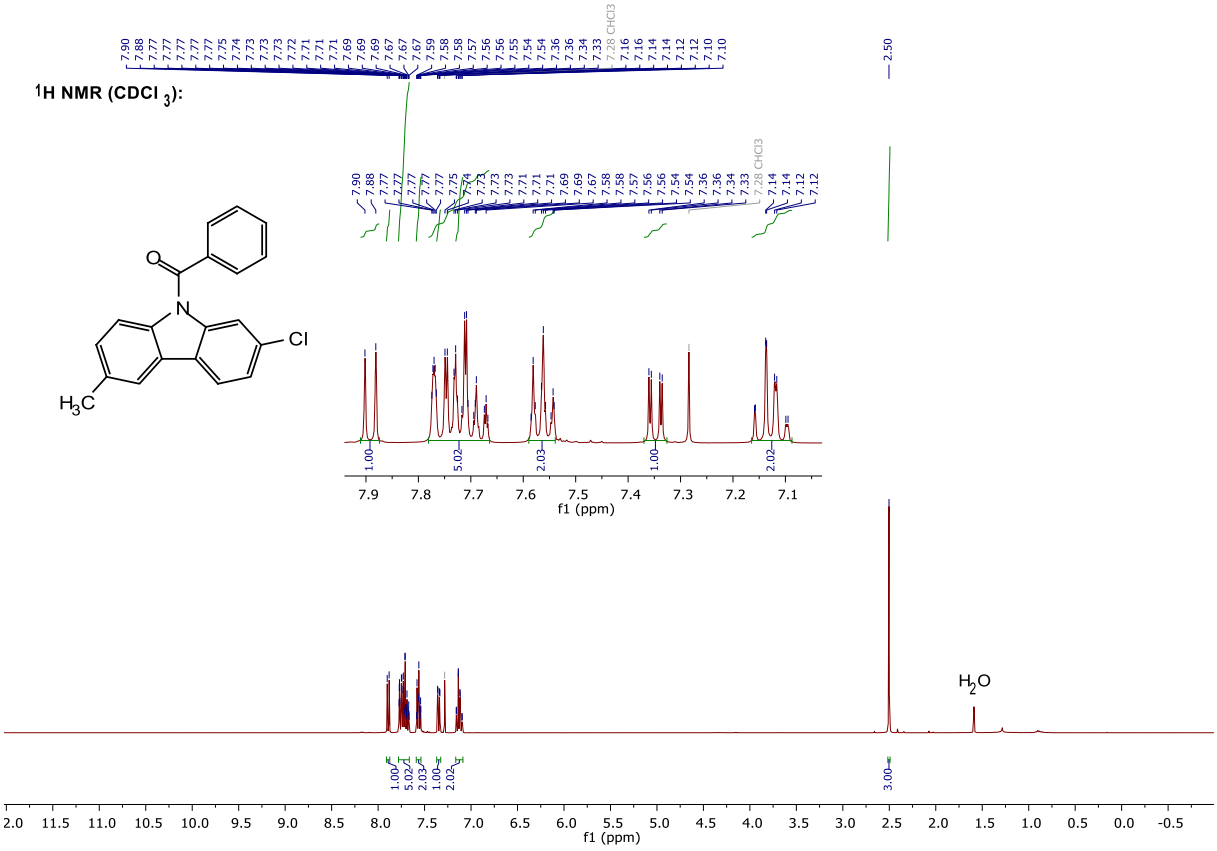

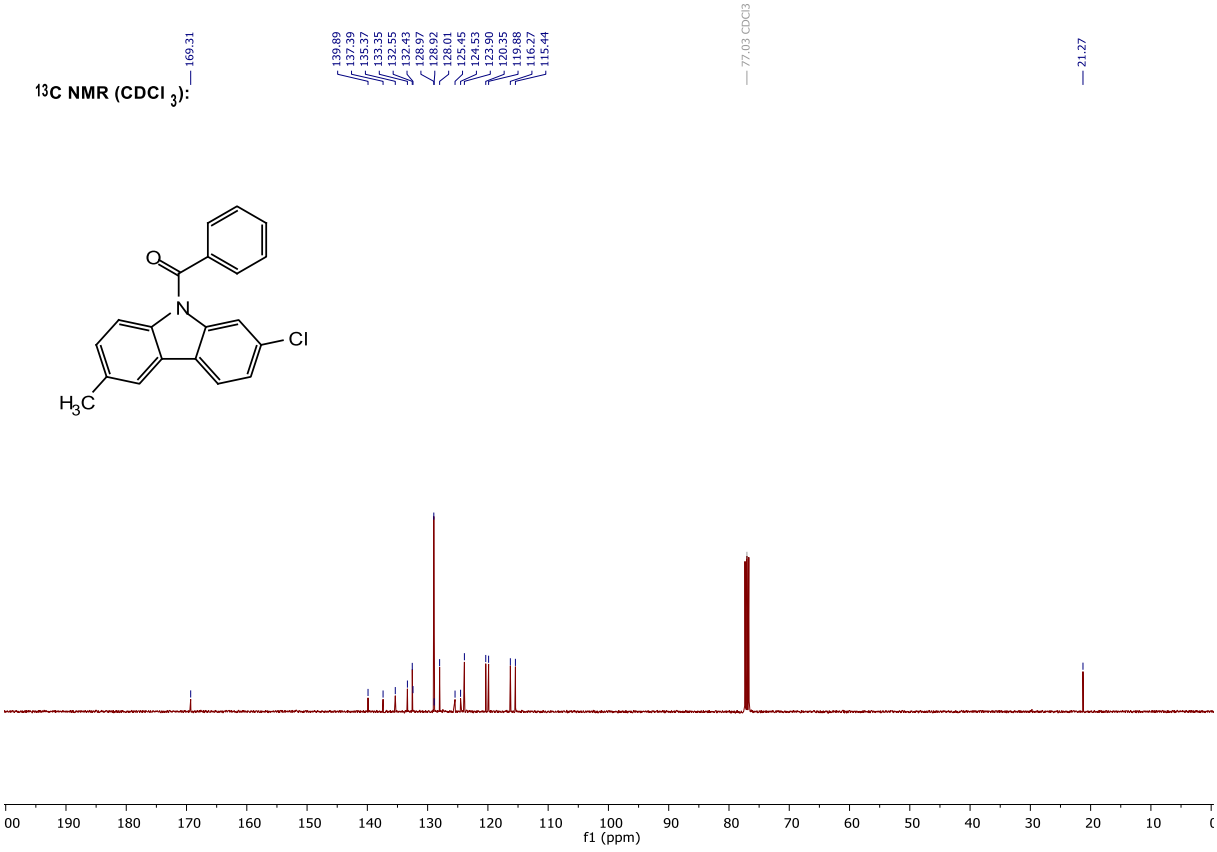

6-Acetyl-9-benzoyl-3-chlorocarbazole (2l)

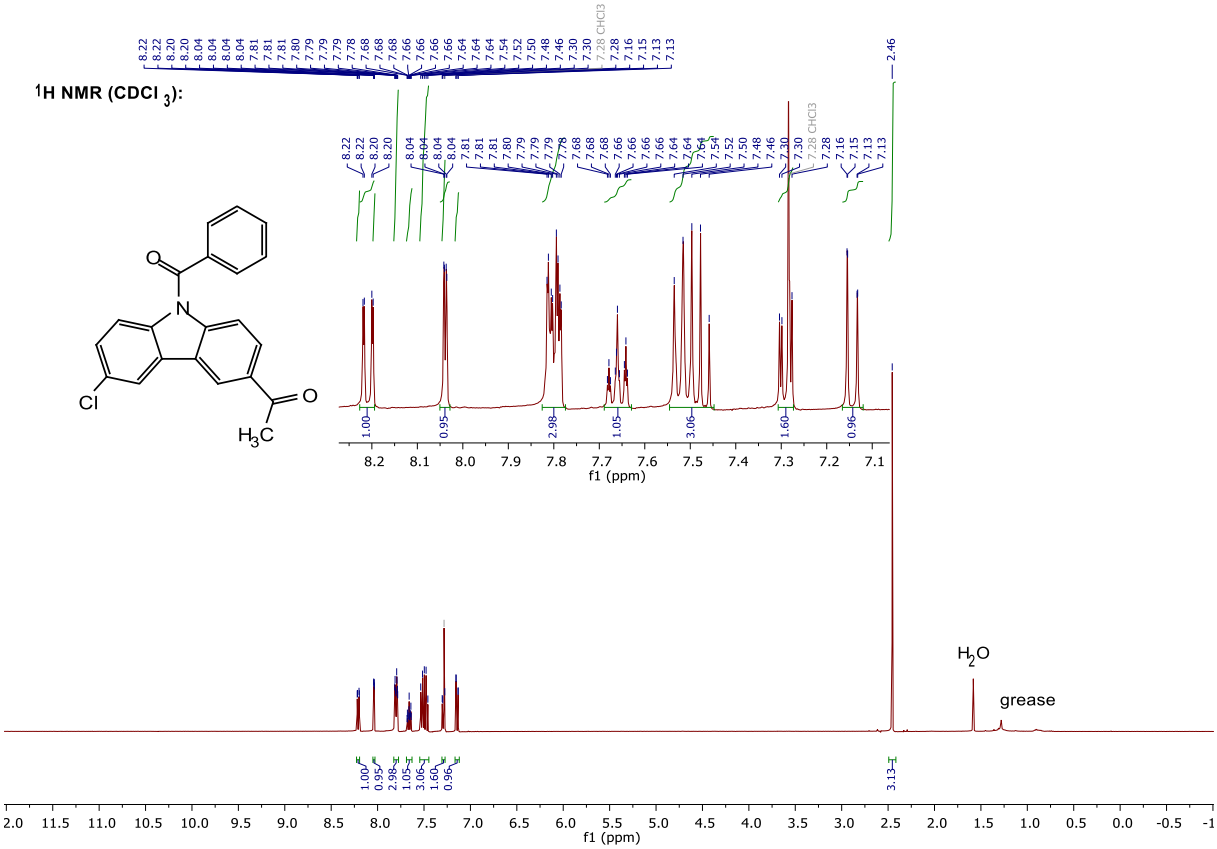

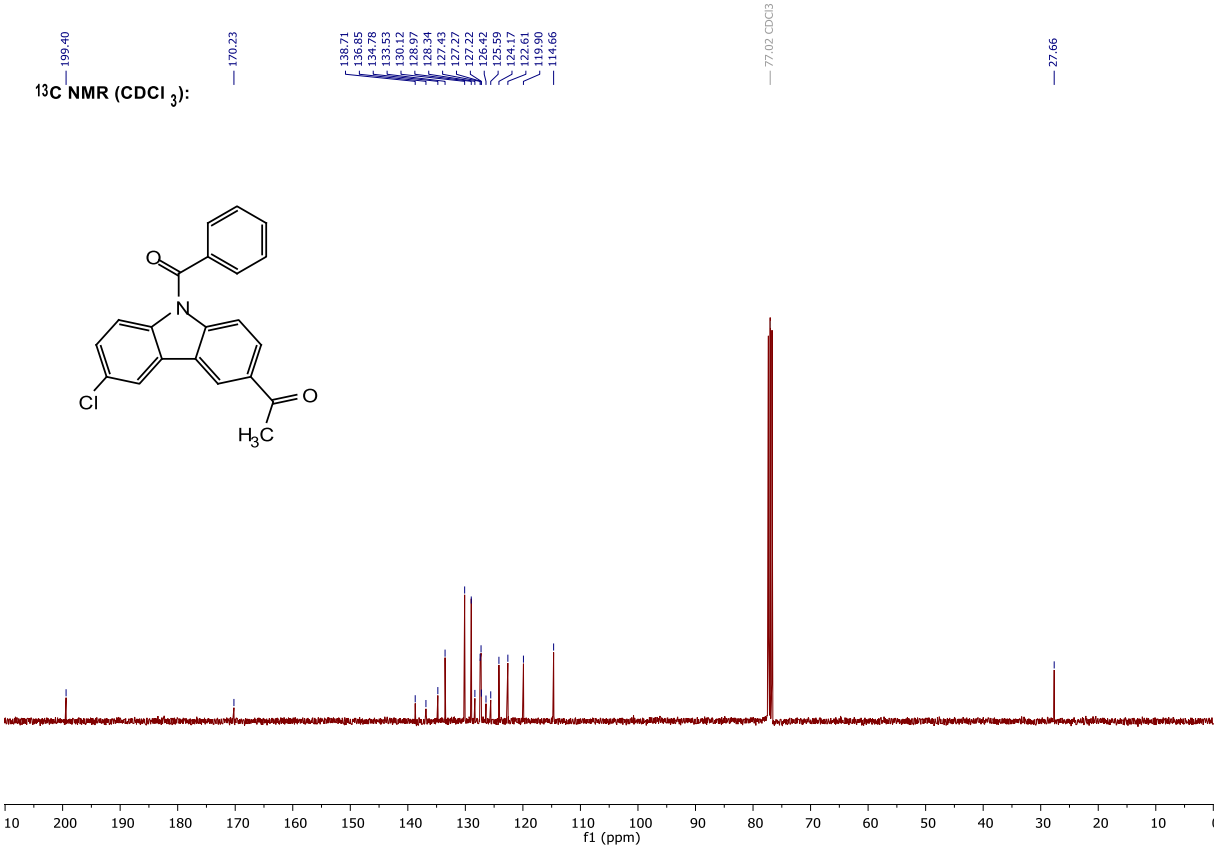

9-Benzoyl-3-chloro-7-nitrocarbazole (2m)

^{1}H NMR (CDCl $_3$):

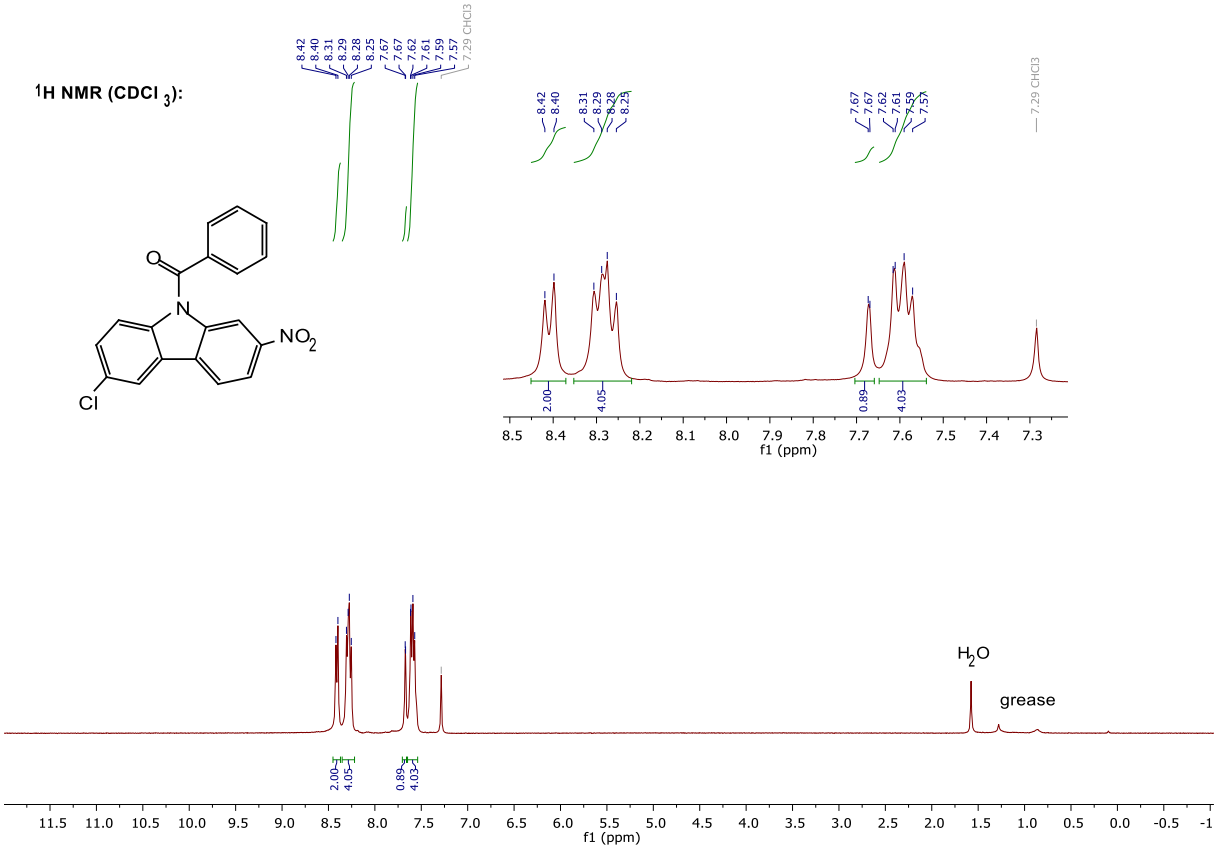

^{13}C NMR (CDCl $_3$):

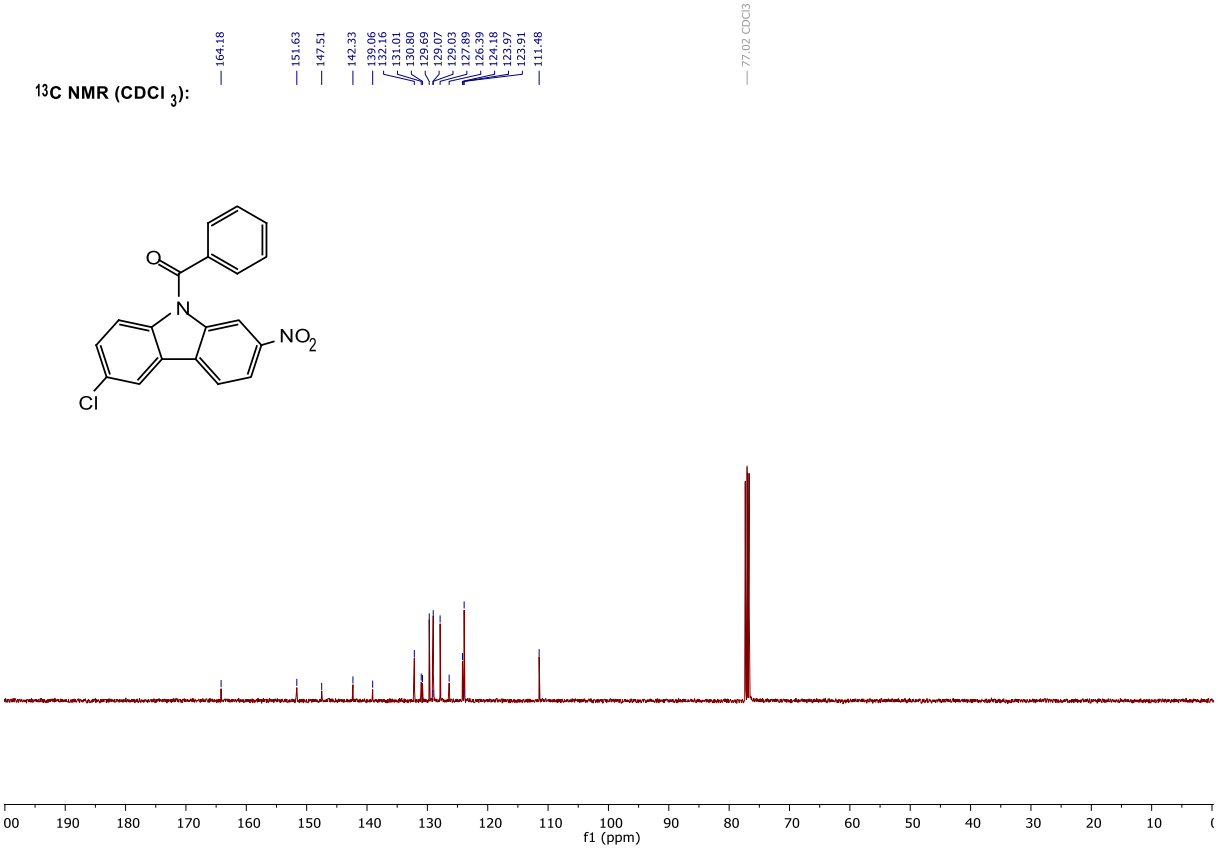

9-Benzoyl-3-chloro-6-methoxycarbazole (2n)

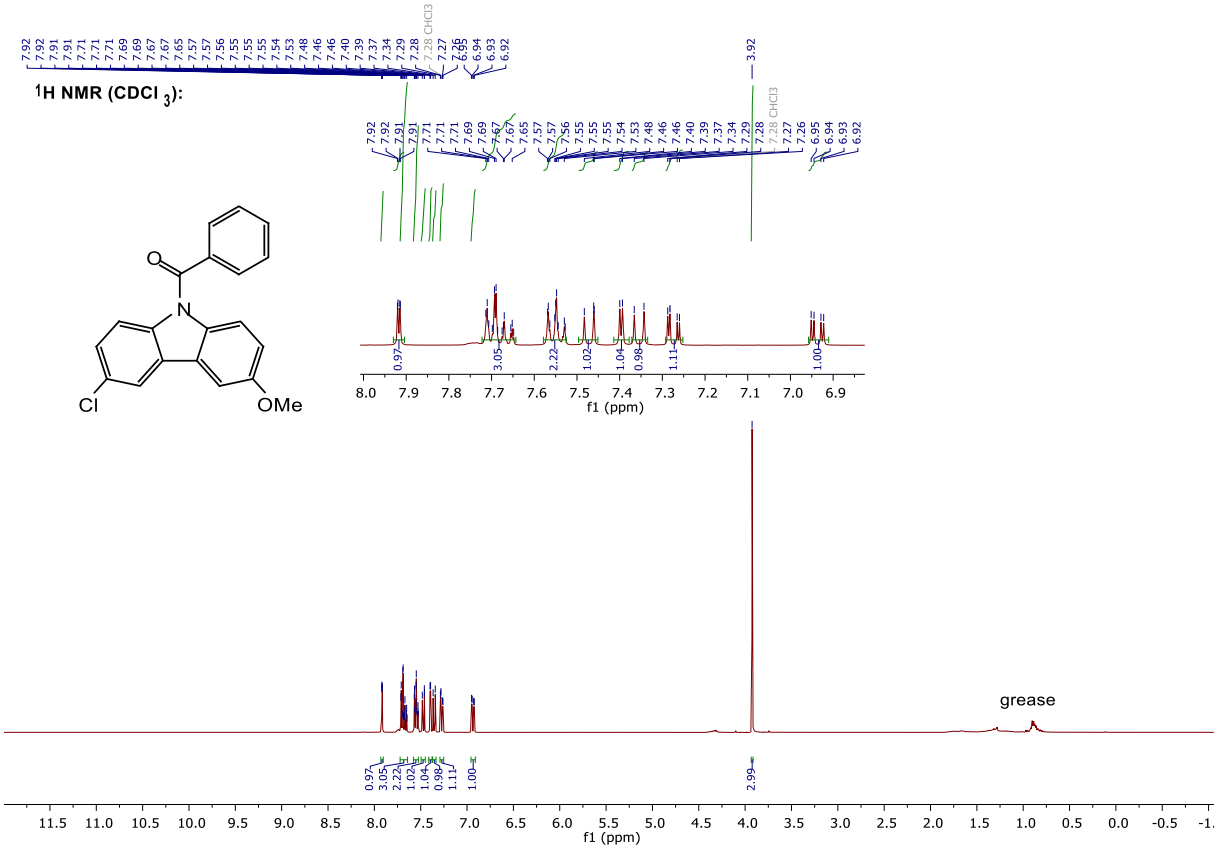

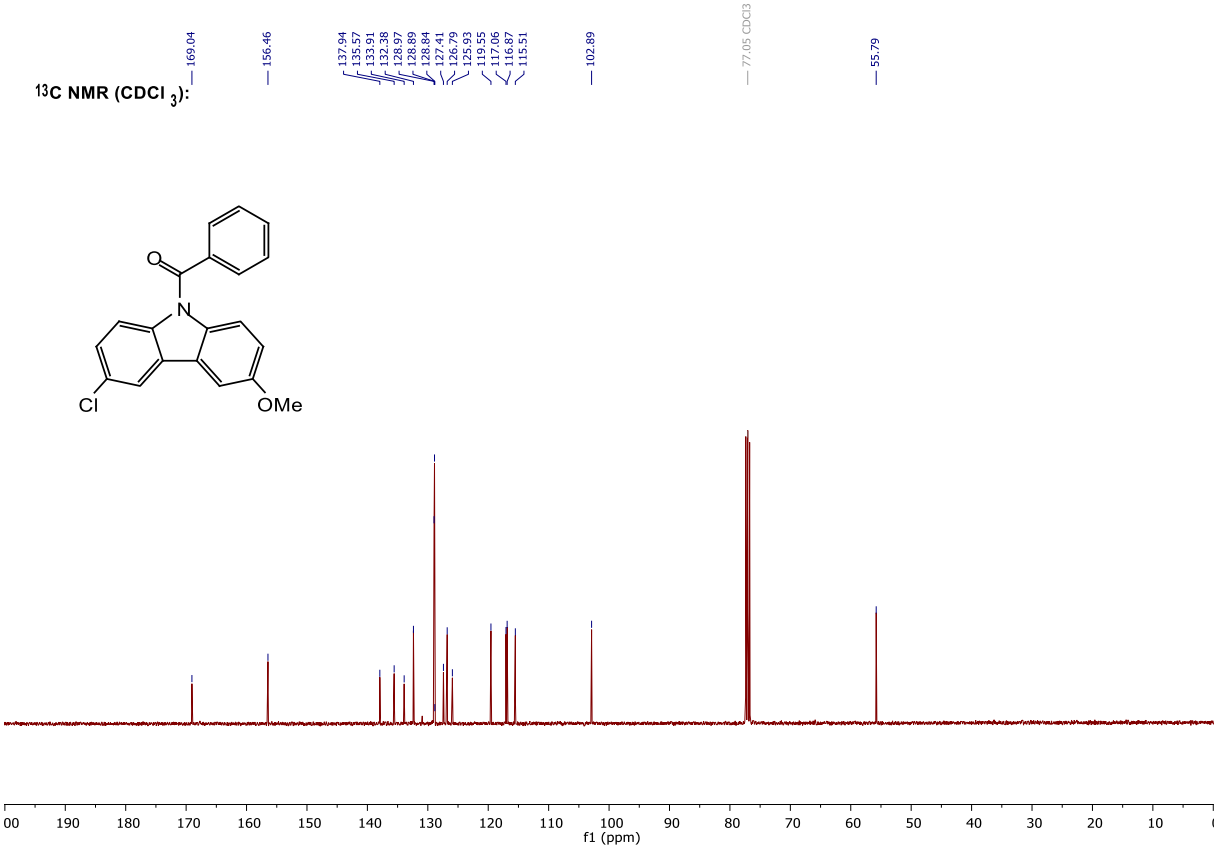

9-Benzoyl-3-methoxy-6-methylcarbazole (2o)

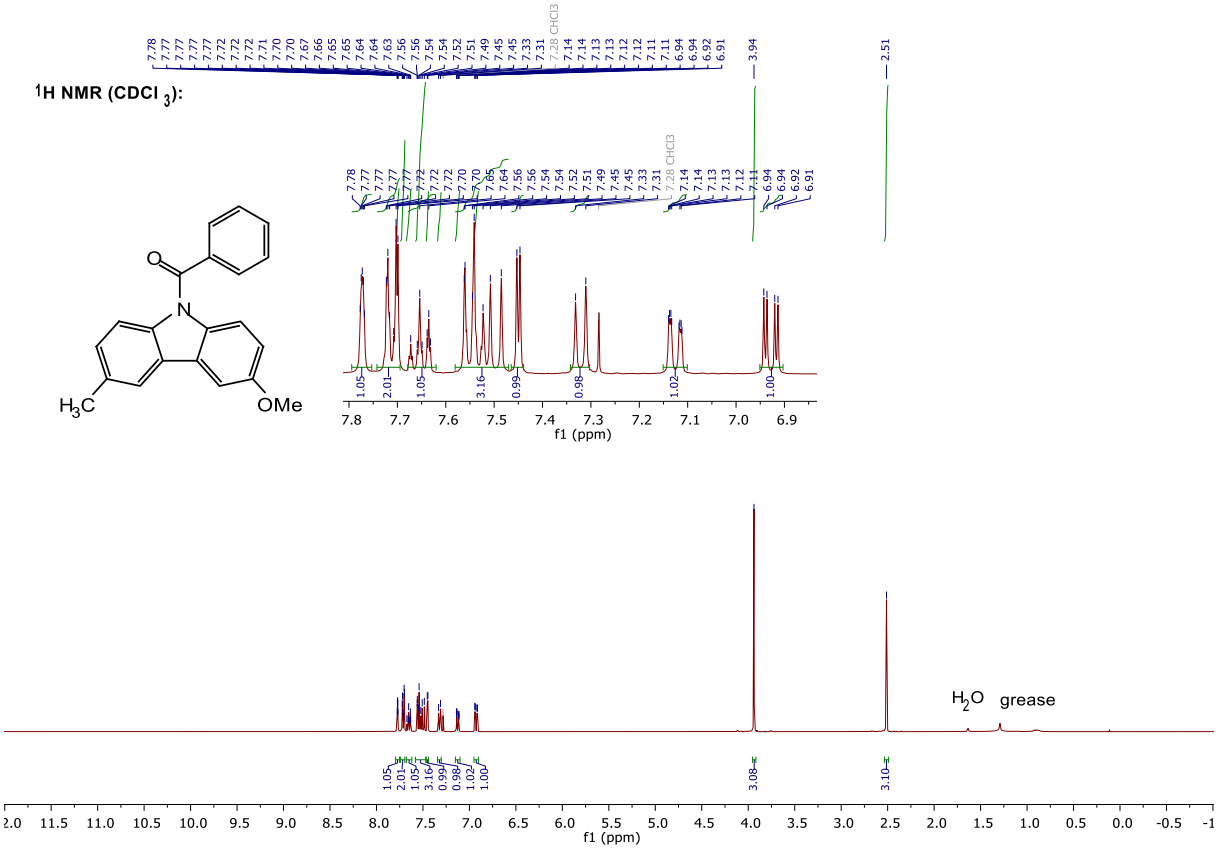

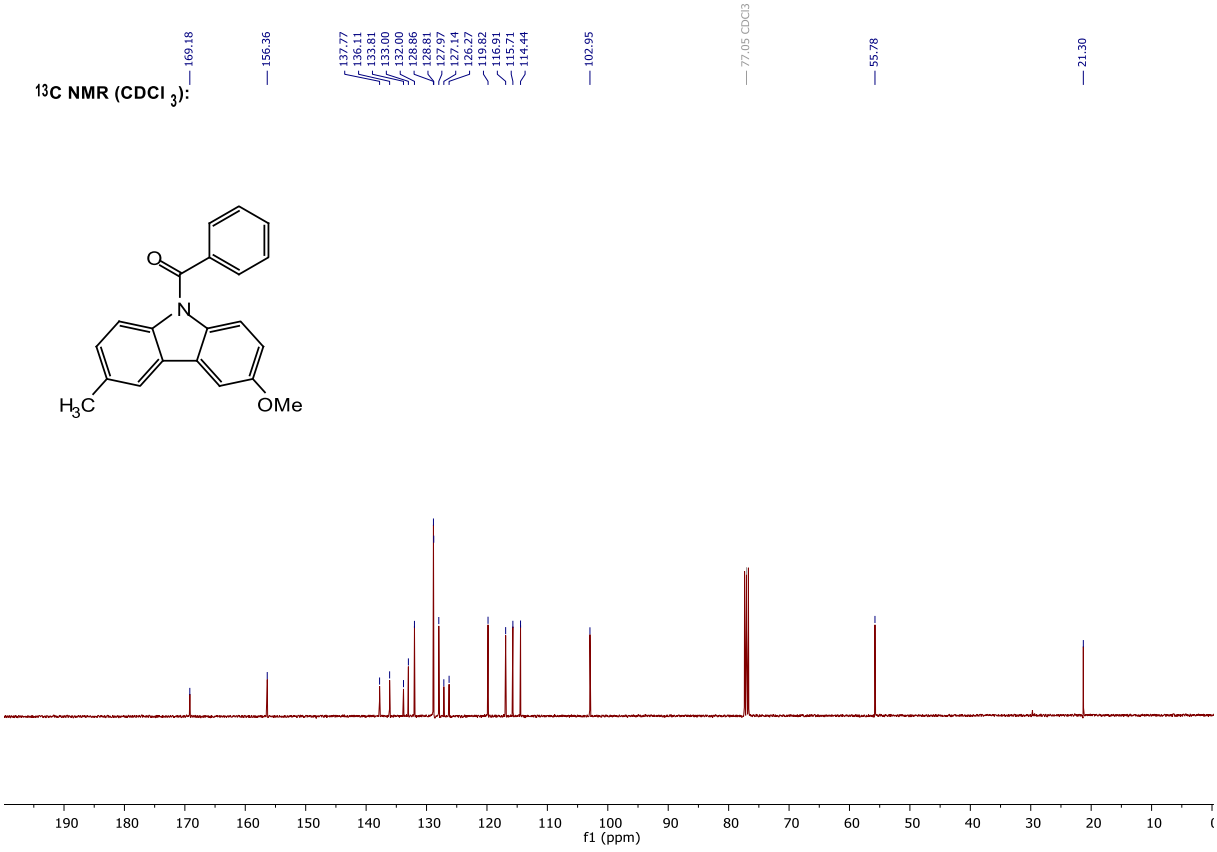

Methyl 9-benzoyl-2-(6-chlorocarbazol-2-yl)propanoate (2q)

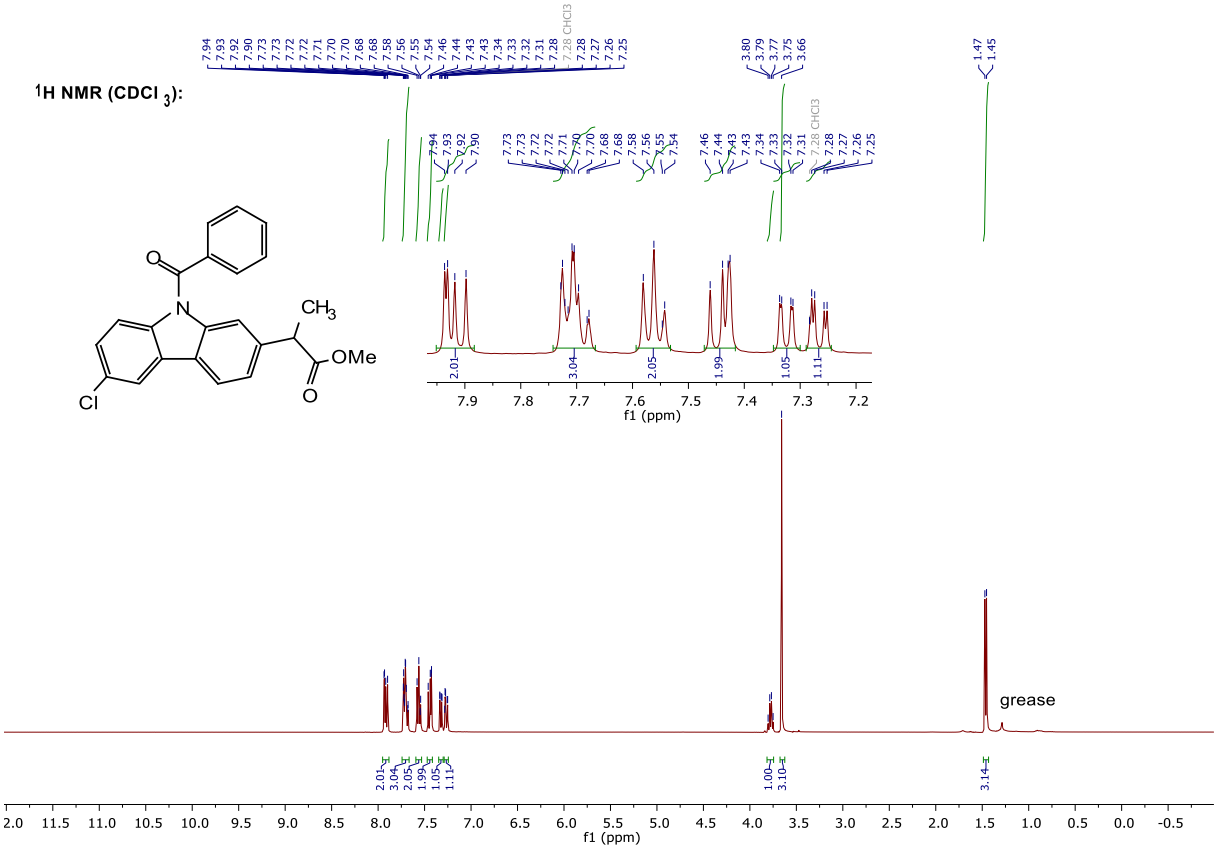

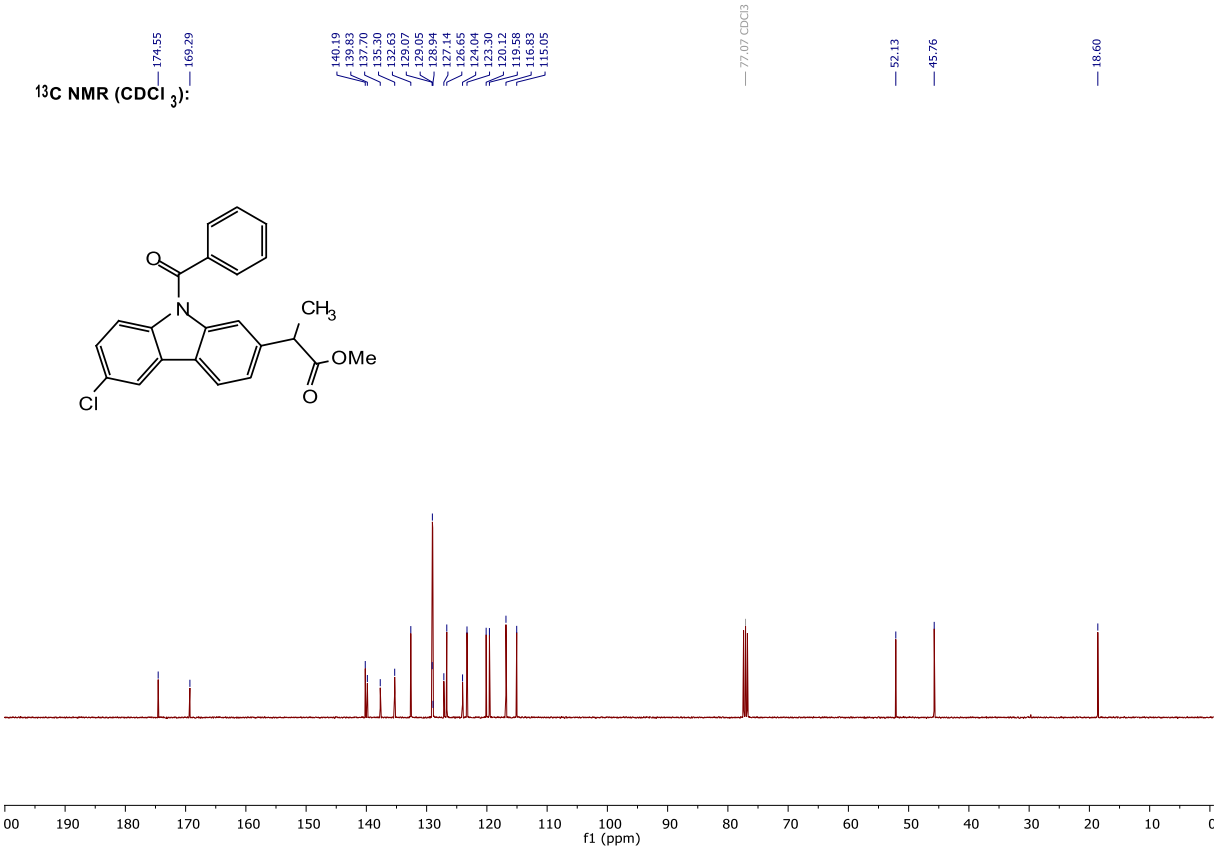

References

[1] W. L. F. Armarego, C. Chai Li Lin, *Purification of laboratory chemicals*, BH Butterworth-Heinemann/Elsevier, Amsterdam, **2013**.

[2] S. Berger, S. Braun, H.-O. Kalinowski, *NMR-Spektroskopie von Nichtmetallen*, Thieme, Stuttgart, **1994**.

[3] G. M. Sheldrick, *SHELXS97* and *SHELXL97: Programm for the Refinement of Crystal Structures;* Dept. of Structural Chemistry, University of Göttingen: Germany, **1997**

[4] a) P. P. Sharp, M. G. Banwell, J. Renner, K. Lohmann, A. C. Willis, *Org. Lett.* **2013**, *15*, 2616–2619; b) K. Venkateswarlu, K. Suneel, B. Das, K. N. Reddy, T. S. Reddy, *Synth. Commun.* **2008**, *39*, 215–219.

[5] F. Buckingham, S. Calderwood, B. Checa, T. Keller, M. Tredwell, T. L. Collier, I. M. Newington, R. Bhalla, M. Glaser, V. Gouverneur, *J. Fluorine Chem.* **2015**, *180*, 33–39.

[6] C. Gütz, B. Klöckner, S. R. Waldvogel, *Org. Process Res. Dev.* **2016**, *20*, 26–32.

[7] A. Wiebe, D. Schollmeyer, K. M. Dyballa, R. Franke, S. R. Waldvogel, *Angew. Chem. Int. Ed.* **2016**, *55*, 11801–11805; *Angew. Chem.* **2016**, *128*, 11979–11983.

[8] D. R. Stuart, M. Bertrand-Laperle, K. M. N. Burgess, K. Fagnou, *J. Am. Chem. Soc.* **2008**, *130*, 16474–16475.

[9] S. H. Cho, J. Yoon, S. Chang, *J. Am. Chem. Soc.* **2011**, *133*, 5996–6005.

[10] G. Li, C.-L. Ji, X. Hong, M. Szostak, *J. Am. Chem. Soc.* **2019**, *141*, 11161–11172.

[11] A. L. Pumphrey, H. Dong. T. G. Driver, *Angew. Chem. Int. Ed.* **2012**, *51*, 5920–5923.

[12] S. K. Kolli, B. Prasad, P. V. Babu, M. A. Ashfaq, N. Z. Ehtesham, R. R. Raju, M. Palb, *Org. Biomol. Chem.* **2014**, *12*, 6080–6084.

[13] J. Shi, H. Xu, D. Qiu, J. He, Y. Li, *J. Am. Chem. Soc.* **2017**, *139*, 623–626.

[14] a) T. Gieshoff, A. Kehl, D. Schollmeyer, K. Moeller, S. R. Waldvogel, *J. Am. Chem. Soc.* **2017**, *139*, 12317–12324; b) A. Kehl, V. M. Breising, D. Schollmeyer, S. R. Waldvogel, *Chem.- Eur. J.* **2018**, *24*, 17230–17233.

Curriculum Vitae

Personenbezogene Daten